NASA Contractor Report 2971

Static Aerodynamic Characteristics of a Typical Single-Engine Low-Wing General Aviation Design for an Angle-of-Attack Range of -8° to 90°

William Bihrle, Jr., Billy Barnhart,
and Paul Pantason

CONTRACT NAS1-14849
JULY 1978

NASA

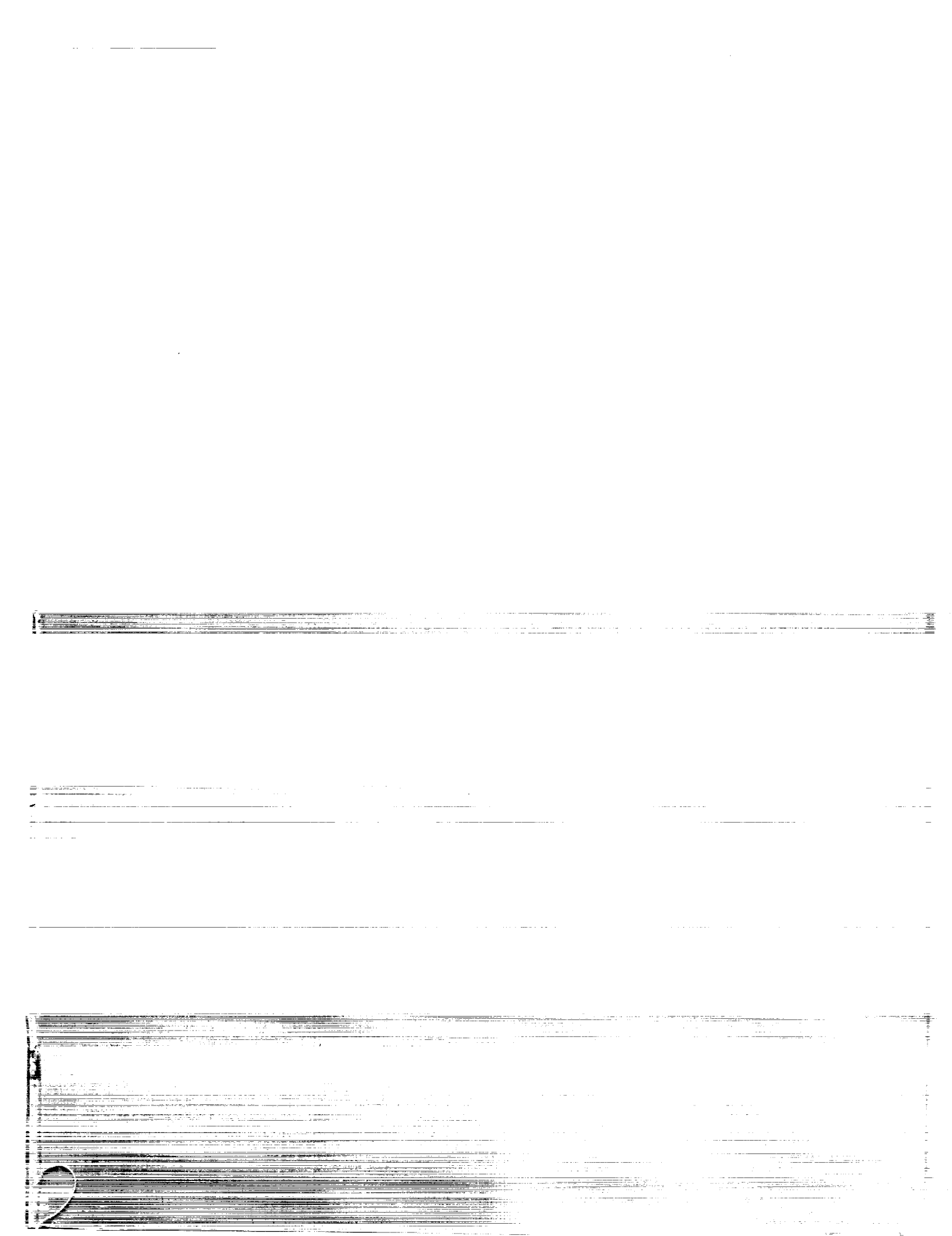

NASA Contractor Report 2971

Static Aerodynamic Characteristics of a Typical Single-Engine Low-Wing General Aviation Design for an Angle-of-Attack Range of -8° to 90°

William Bihrle, Jr., Billy Barnhart,
and Paul Pantason
Bihrle Applied Research, Inc.
Jericho, New York

Prepared for
Langley Research Center
under Contract NAS1-14849

National Aeronautics
and Space Administration

**Scientific and Technical
Information Office**

1978

SUMMARY

Static force data obtained at the NASA Ames Research Center 12-foot Pressure Tunnel are presented in plotted form for a 1/7-scale, single-engine, low-wing general aviation airplane model. The configurations tested included the basic airplane, various airfoil shapes, tail designs, fuselage strakes and fuselage modifications as well as airplane components. The test conditions included an angle-of-attack and sideslip range of -8 to 90 and -10 to 30 degrees, respectively, at a Mach number of 0.2 for Reynolds numbers of 0.288×10^6 and 3.45×10^6. The data are presented without analysis.

INTRODUCTION

The NASA Langley Research Center has initiated a broad general aviation stall/spin research program which includes spin-tunnel and free-flight radio control model tests, as well as full-scale flight tests for a number of configurations typical of light general aviation designs. As a supporting part of this effort, a series of static and rotary balance wind tunnel force tests covering these same configurations will be conducted to establish a data base for analysis of model and full-scale flight results, and to be used in the development of design charts for desirable stall/spin characteristics.

The first force test program, reported herein, involved static wind tunnel tests of a typical single-engine, low-wing, general aviation airplane configuration in the Ames Research Center 12-foot Pressure Tunnel. During these tests, data were obtained for the basic configuration and for modifications previously investigated during spin tunnel tests of a 1/11-scale model (ref. 1). These modifications consisted of different airfoil shapes, tail designs, fuselage strakes, and fuselage shapes. In addition, airplane component (i.e., fuselage alone, fuselage-wing, etc.) data were acquired. The data are presented in this report, and a subsequent report will present an analysis of the data.

The data obtained in a spinning flow environment with a rotary balance located in the Langley spin tunnel is presented in reference 2 for the configurations presented herein.

SYMBOLS

The units for physical quantities used herein are presented in the International System of Units (SI) and U.S. Customary Units. The measurements were made in the U.S. Customary Units, and equivalent dimensions were determined by using the conversion factors given in reference 3.

b wing span, m (ft)

$\bar{c}$ mean aerodynamic chord, cm (in.)

C_D drag coefficient, $\frac{\text{Drag}}{qS}$

C_L lift coefficient, $\frac{\text{Lift}}{qS}$

C_A axial-force coefficient, $\frac{\text{Axial force}}{qS}$

C_N normal-force coefficient, $\frac{\text{Normal force}}{qS}$

C_Y side-force coefficient, $\frac{\text{Side force}}{qS}$

C_ℓ rolling-moment coefficient, $\frac{\text{Rolling moment}}{qSb}$

C_m pitching-moment coefficient, $\frac{\text{Pitching moment}}{qS\bar{c}}$

C_n yawing-moment coefficient, $\frac{\text{Yawing moment}}{qSb}$

q free-stream dynamic pressure

R_E Reynolds number

S wing area, m^2 (ft^2)

α angle of attack of fuselage reference line, deg

β angle of sideslip, positive when nose is to left, deg

δ_a aileron deflection, positive when right aileron is down, $(\delta_{a_R} - \delta_{a_L})/2$, deg

δ_e elevator deflection, positive when trailing edge is down, deg

δ_r rudder deflection, positive when trailing edge is to left, deg

MODEL

A 1/7-scale steel model of a configuration considered to be a typical low-wing, single-engine, light general aviation airplane was tested. A three-view drawing of the model is shown in figure 1. The basic dimensional characteristics of the model are presented in Table I. Photographs and sketches of the model installed in the Ames Research Center 12-Foot Pressure Tunnel are presented in figures 2 and 3, respectively.

The model was fabricated such that various airplane components were removable for component build-up tests and for testing alternate wing airfoils and tail configurations. In addition, allowance was made for attaching various fuselage strakes and modifications.

The three wing airfoil sections tested were a modified NACA 64 series airfoil with and without leading-edge droop, and a NASA GA(W) -1 airfoil. Sketches of the airfoils are shown in figure 4. The three tail configurations tested involved different locations of the horizontal tail as shown in figure 5. The fuselage strakes and modifications tested are shown in figures 6 and 7, respectively. The dimensional characteristics of these fuselage additions are presented in Table II. A modification of the wing fillet trailing edge was also tested; this entailed rounding the sharp trailing edge as shown in figure 8.

The model control surfaces were constructed such that they could be set at any of three desired positions prior to the test

(zero and full throw in either direction from zero). The maximum deflections for the control surfaces were:

Rudder, deg	25 right, 25 left
Elevator, deg	25 up, 15 down
Aileron, deg	25 up, 20 down

TEST CONDITIONS

The tests were performed in the Ames 12-foot Pressure Tunnel. Two tunnel entries, during November 1976 and January 1977, were required to complete the program. The model was tested for an angle-of-attack range of -8 to 90 degrees and a sideslip angle range of -10 to 30 degrees. Two stings were required to cover the angle-of-attack range. The sting shown in figure 4a, which entered the model through the bottom of the fuselage, was used for testing at α = -8 to 50 degrees. The high angle-of-attack sting, shown in figure 4b, which entered the model through the canopy, was used for testing at α = 40 to 90 degrees. This arrangement allowed an overlap of the data in the 40 to 50 degree range.

The Mach number of the tests was 0.2, and measurements were taken for each configuration at Reynolds numbers of 0.288×10^6 and 3.45×10^6 based on model mean aerodynamic chord. The high Reynolds number data is representative of the full-scale airplane, whereas the low Reynolds number data more nearly represents free-spinning tunnel and free-flight radio-controlled models.

DATA PRESENTATION

Table III identifies the configurations tested as well as the figure and page numbers in which the corresponding data are plotted. Each figure consists of six parts:

a) Longitudinal coefficients vs α, stability axis
b) Longitudinal coefficients vs α, body axis
c) Lateral- directional coefficients at zero sideslip vs α, body axis

d) Lateral-directional coefficients vs α for various β values, body axis

e) Directional coefficients vs β, body axis

f) Lateral coefficients vs β, body axis

Table IV lists a key to the configuration nomenclature used in Table III and the data figures.

The data are arranged in two parts. The first part, figures 9 through 45, presents the data at $R_E = 3.45 \times 10^6$. The second part, figures 46 through 82, presents the $R_E = 0.288 \times 10^6$ data.

All moment data are presented for a center-of-gravity position of $0.255\bar{c}$.

An examination of the data indicates many instances in which the data measured with the low and high angle-of-attack stings are offset in the overlapping angle-of-attack range of 40 to 50 degrees. The angle of attack and sideslip value at which the measurements are compromised by sting and/or tunnel wall interference depends on the configuration tested, i.e., fuselage alone, tail off, complete configuration, etc. and the coefficient measured. However, all of the data appears valid at $\alpha = 40^\circ$ and below and $\alpha = 70^\circ$ and above for the low and high angle-of-attack stings, respectively. For the above reasons, the directional and lateral coefficients vs sideslip are not presented in figures (e) and (f), respectively, for angles of attack between 40 and 70 degrees.

REFERENCES

1. Burk, Sanger M., Jr.; Bowman, James S., Jr.; White, William: Spin-Tunnel Investigation of the Spinning Characteristics of Typical Single-Engine General Aviation Designs. I Low-Wing Model A: Effects of Tail Configurations. NASA TP 1009, Sept. 1977.

2. Bihrle, William, Jr.; Hultberg, Randy S.; Mulcay, William: Rotary Balance Data for a Typical Single-Engine Low-Wing General Aviation Design for an Angle-of-Attack Range of 30 to 90^{o}. NASA CR-2972, 1978.

3. Mechtly, E.A.: The International System of Units - Physical Constants and Conversion Factors. NASA SP-7012, 1973.

TABLE I.- DIMENSIONAL CHARACTERISTICS OF THE MODEL

Overall length with tail 3, m (ft)	.83 (2.73)
Wing:	
Span, m (ft)	1.07 (3.5)
Area, m^2 (ft^2)	.19 (2.00)
Root chord, cm (in.)	17.53 (6.87)
Tip chord, cm (in.)	17.53 (6.87)
Mean aerodynamic chord	17.53 (6.87)
Leading edge of $\bar{c}$, distance rearward of leading edge of root chord, cm (in.)	0
Aspect ratio	6.1
Dihedral, deg	5.0
Incidence:	
Root, deg	3.5
Tip, deg	3.5
Airfoil section	NACA 64_2-415 modified
Horizontal tail:	
Span, m (ft)	.33 (1.07)
Incidence, deg	-3.0
Airfoil section	NACA 65_1-012
Vertical tail:	
Airfoil section	NACA 65_1-012

TABLE II.- DIMENSIONAL CHARACTERISTICS OF FUSELAGE ADDITIONS

Rounded fuselage corners (C):	
Length, cm (in.)	13.84 (5.45)
Radius, cm (in.)	.95 (.38)
Strake, horizontal (SH):	
Length, cm (in.)	21.97 (8.65)
Width, cm (in.)	1.65 (.65)
Thickness, cm (in.)	.16 (.06)
Strake, vertical (SV):	
Length, cm (in.)	13.84 (5.45)
Width, cm (in.)	.94 (.37)
Thickness, cm (in.)	.16 (.06)
Strake, cowl (SC):	
Length, cm (in.)	12.37 (4.88)
Width, cm (in.)	.51 (.20)
Thickness, cm (in.)	.16 (.06)
Ventral fin (U):	
Length, cm (in.)	20.83 (8.20)
Maximum width, cm (in.)	3.18 (1.25)
Thickness, cm (in.)	.15 (.06)

TABLE III.- CONFIGURATIONS TESTED AND FIGURE INDEX

(Unless noted otherwise, all configs. tested through α = -8 to 90° and β = -10 to 30°)

REYNOLDS NO. 3.45 x 10^6 Figure No./Page	REYNOLDS NO. .288 x 10^6 Figure No./Page	CONFIGURATION		CONTROLS δ_e deg.	CONTROLS δ_a deg.	CONTROLS δ_r deg.	REMARKS
9/20	46/242	BW1H6V		0	0	0	
10/26	47/248	↓		-25	↓	↓	α= -8 to 45° only
11/32	48/254	↓		15	↓	↓	α= -8 to 45° only
12/38	49/260	BW1H4V		0	↓	↓	
13/44	50/266	↓		-25	↓	↓	α= -8 to 45° only
14/50	51/272	↓		15	↓	↓	α= -8 to 45° only
15/56	52/278	BW1H3V		0	↓	↓	
16/62	53/284	↓		-25	↓	↓	
17/68	54/290	↓		15	↓	↓	
18/74	55/296	BW2H3V		0	↓	↓	
19/80	56/302	BW3H3V		0	↓	↓	
20/86	57/308	↓		-25	↓	↓	α= -8 to 45° only
21/92	58/314	↓		15	↓	↓	α= -8 to 45° only
22/98	59/320	BW1H4V	+C	↓	↓	↓	
23/104	60/326	↓	+SH	↓	↓	↓	
24/110	61/332	↓	+SV	↓	↓	↓	
25/116	62/338	↓	+SC	↓	↓	↓	
26/122	63/344	↓	+U	↓	↓	↓	C_ℓ missing for α= 40 to 90° @ R_E= .288 x 10^6
27/128	64/350	↓	+D	↓	↓	↓	
28/134	65/356	↓	+ Wing fillet mod.	↓	↓	↓	
29/140	66/362	↓	+ Wing fillet off	↓	↓	↓	
30/146	67/368	↓	+E	↓	↓	↓	
31/152	68/374	BW1H4V		0	↓	-25	α= 40 to 90° only
32/158	69/380	BW1H3V		-25	22.5	↓	
33/164	70/386	↓		↓	-22.5	↓	
34/170	71/392	↓		↓	0	↓	
35/176	72/398	↓		↓	-22.5	0	α= -8 to 45° only
36/182	73/404	↓		0	0	-25	α= 40 to 90° only
37/188	74/410	BH3V		↓	↓	0	
38/194	75/416	BH4V		↓	↓	↓	
39/200	76/422	BH6V		↓	↓	↓	
40/206	77/428	BW1H3		↓	↓	↓	
41/212	78/434	BW1V		↓	↓	↓	
42/218	79/440	BW1		↓	↓	↓	
43/224	80/446	BH3		↓	↓	↓	
44/230	81/452	BV		↓	↓	↓	
45/236	82/458	B		↓	↓	↓	

TABLE IV.- CONFIGURATION NOTATION

B	Fuselage
V	Vertical tail
W1	Modified NACA 64_2 - 415 airfoil
W2	NASA GA(W) - 1 airfoil
W3	Modified NACA 64_2 - 415 airfoil with leading-edge droop
F	Wing fillet
FM	Wing fillet modification
H3	Horizontal tail #3
H4	Horizontal tail #4
H6	Horizontal tail #6
SH	Horizontal fuselage strakes
SC	Cowl strakes
SV	Vertical fuselage strakes
C	Rounded fuselage corners
U	Ventral fin
E	Extended fuselage
D	Deep rounded fuselage bottom

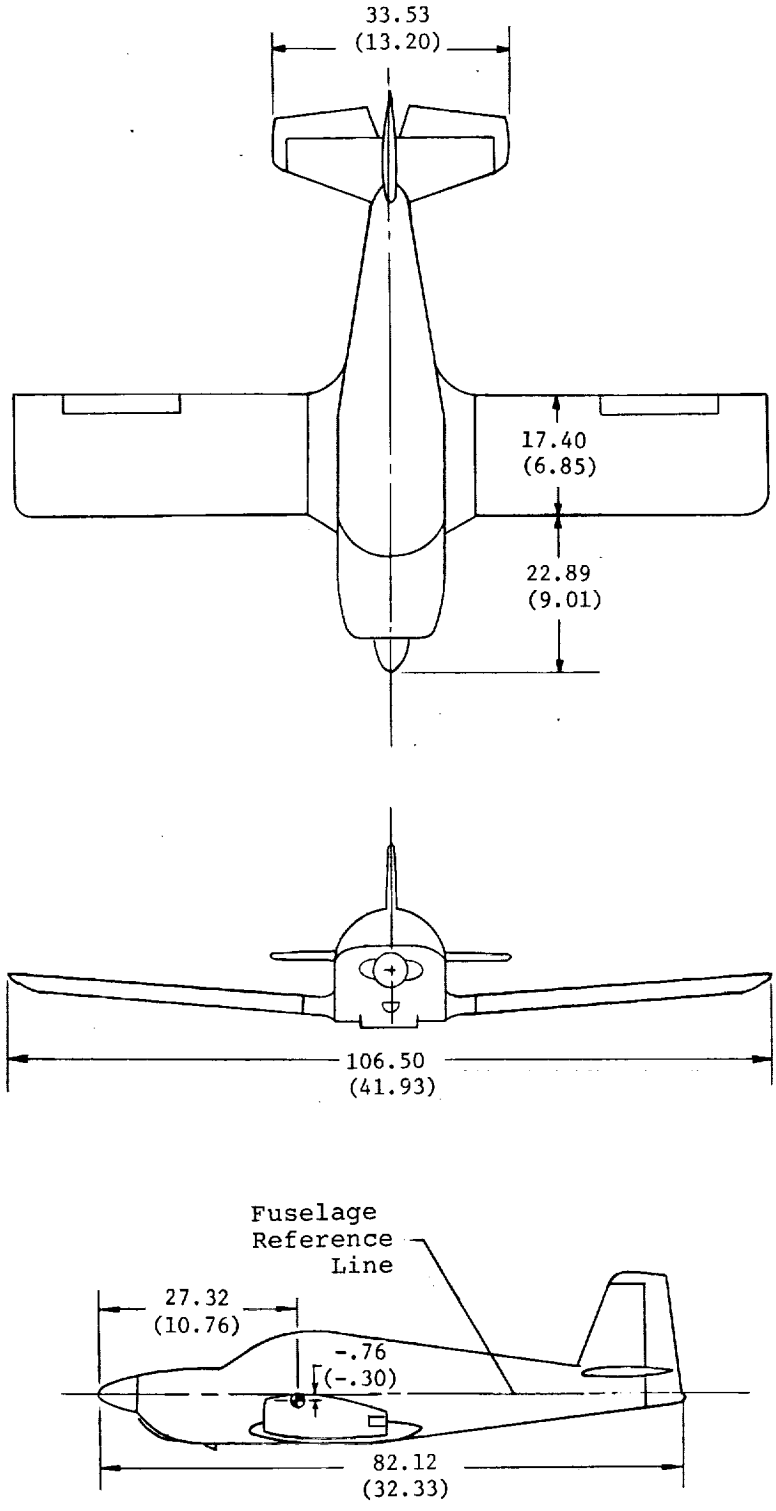

Figure 1.- Three-view drawing of 1/7-scale low-wing general aviation model with tail 3 illustrated. Center-of-gravity position at 0.255$\bar{c}$. Dimensions are given in centimeters (inches), model scale.

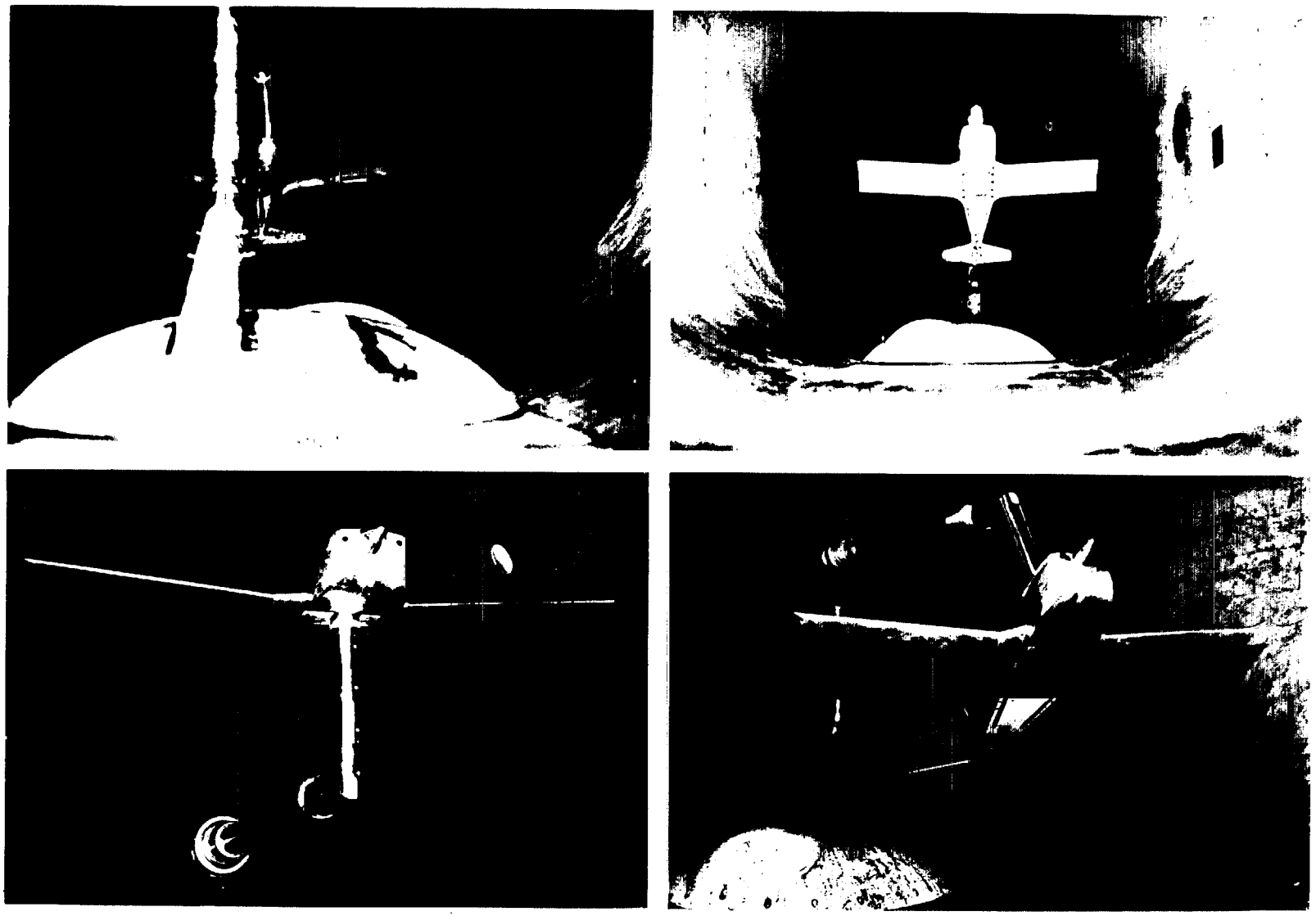

Figure 2.- Installation photographs of low-wing general aviation model in Ames 12-foot Pressure Tunnel, showing high and low alpha range sting configurations.

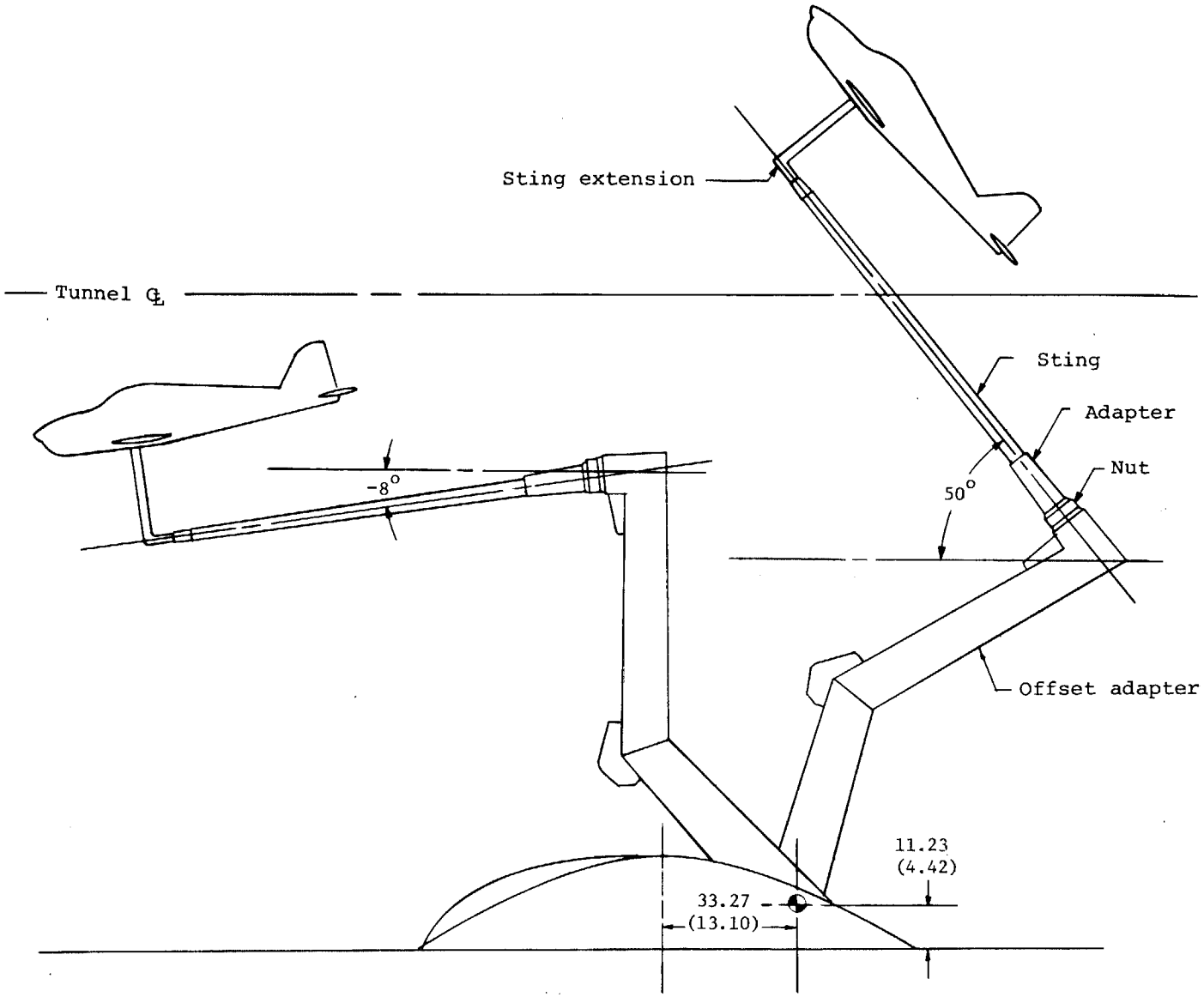

a) Sting configuration for $-8^{\circ} \leq \alpha \leq 50^{\circ}$.

Figure 3.- Sketch of model installation in Ames 12-foot Pressure Tunnel. Tunnel dimensions given in centimeters (inches).

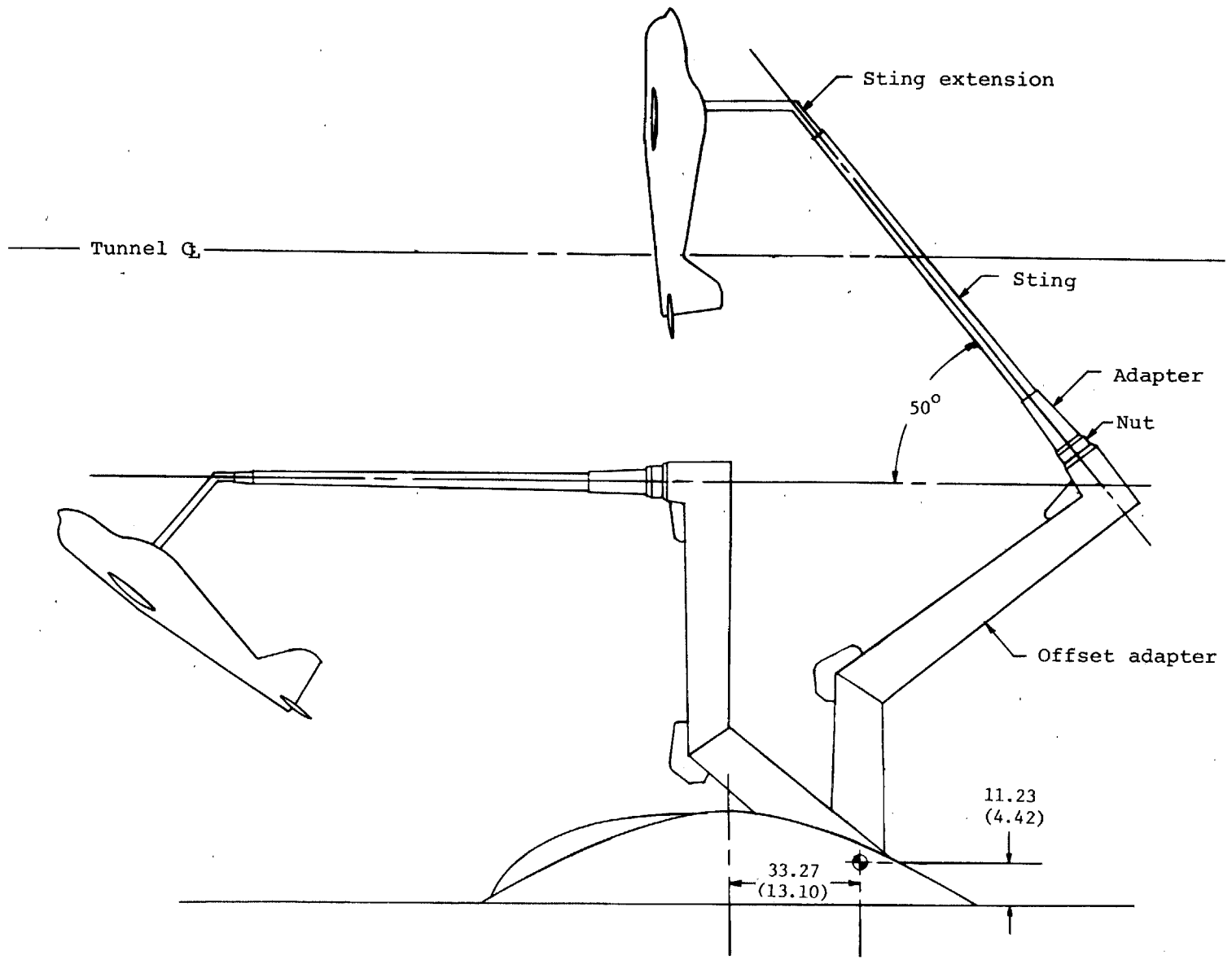

b) Sting configuration for $40^{\circ} \leq \alpha \leq 90^{\circ}$.

Figure 3.- Concluded.

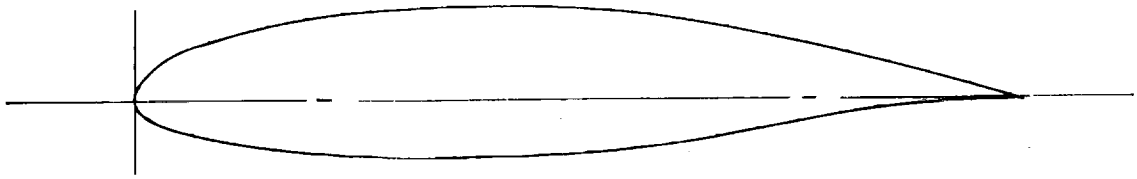

NASA GA(W) -1 airfoil.

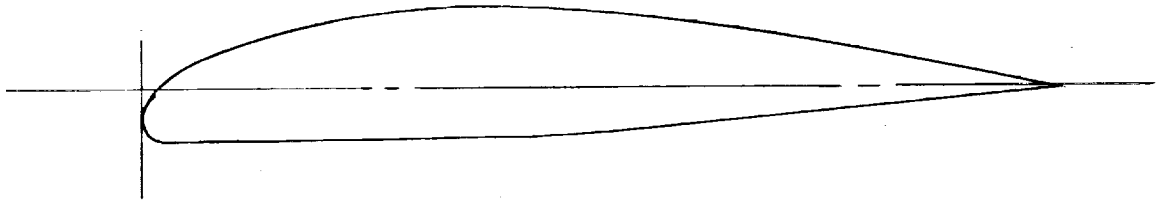

Modified NACA 64_2 - 415 airfoil with leading-edge droop.

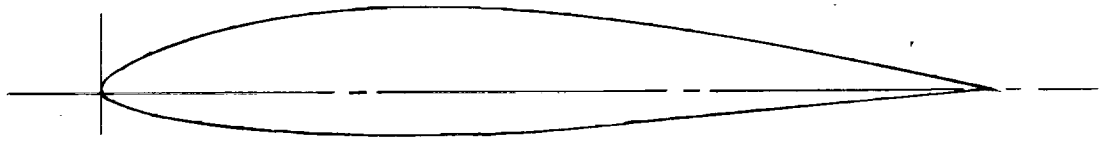

Modified NACA 64_2 - 415 airfoil.

Figure 4.- Wing airfoil sections tested on model.

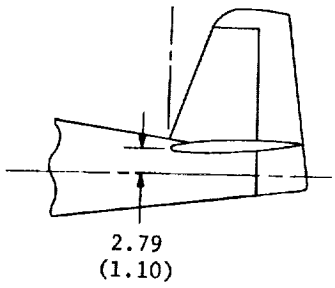

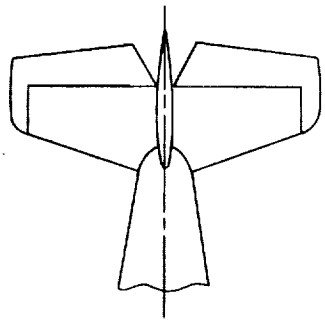

a) Tail 3.

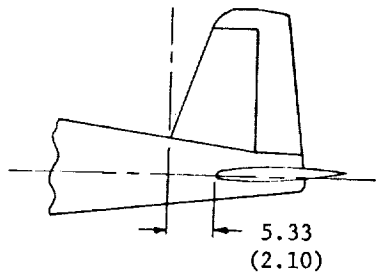

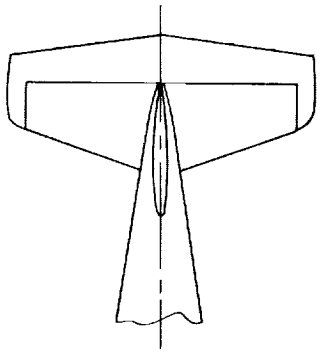

b) Tail 4.

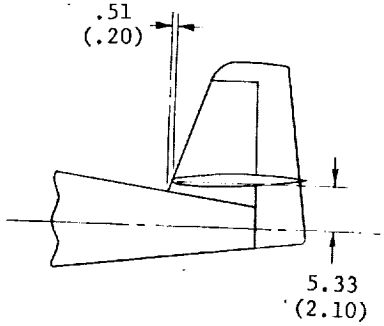

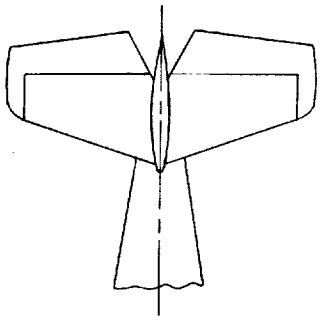

c) Tail 6.

Figure 5.- Tail configurations tested on model. Dimensions are given in centimeters (inches), model scale.

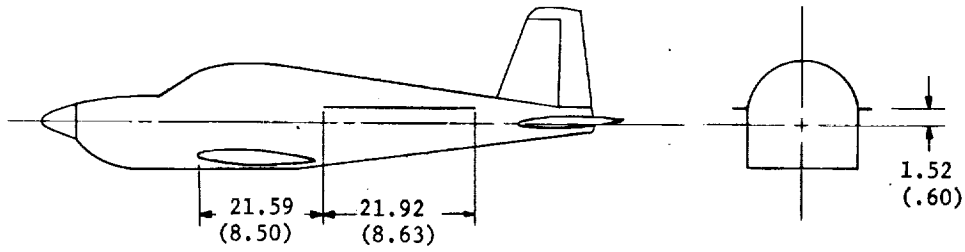

a) Horizontal strakes on fuselage sides.

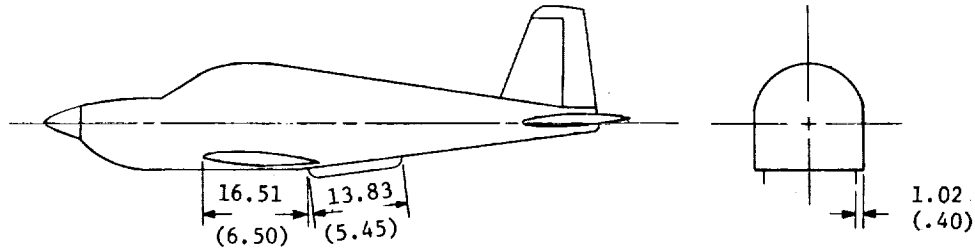

b) Vertical strakes on fuselage bottom.

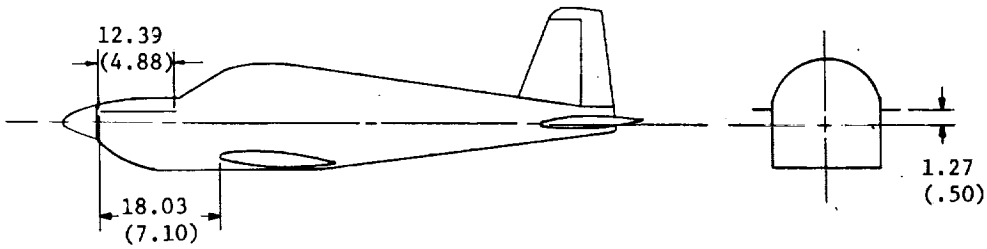

c) Cowl strakes on fuselage sides.

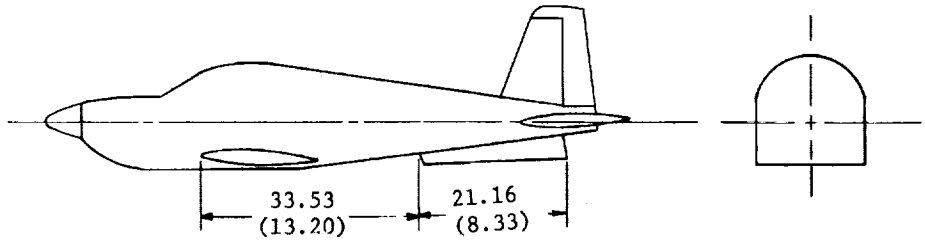

d) Ventral fin on fuselage bottom.

Figure 6.- Fuselage strakes and ventral fin tested on model. Dimensions are given in centimeters (inches), model scale.

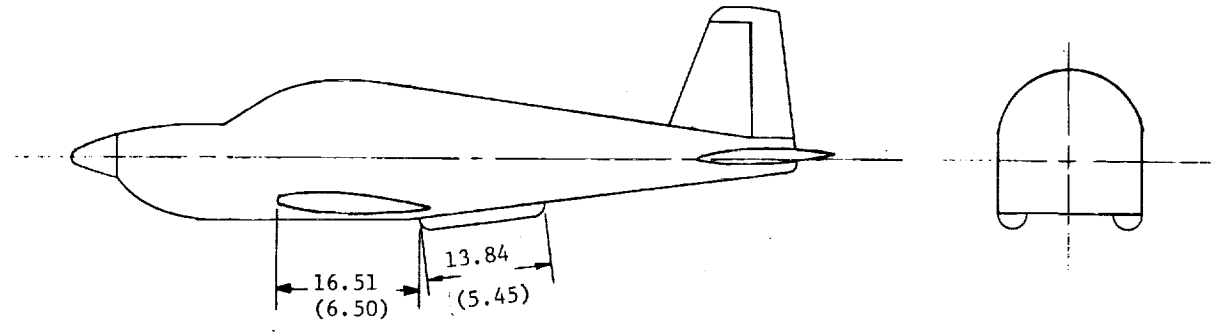

a) Rounded fuselage corners (cylinders).

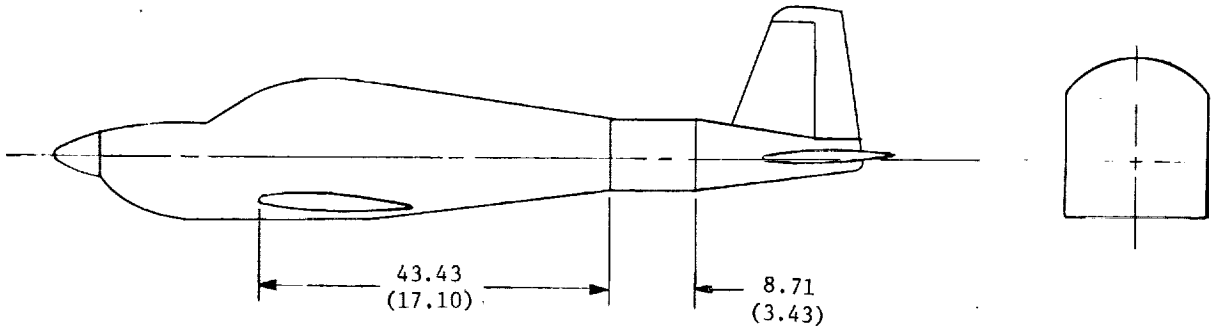

b) Extended fuselage.

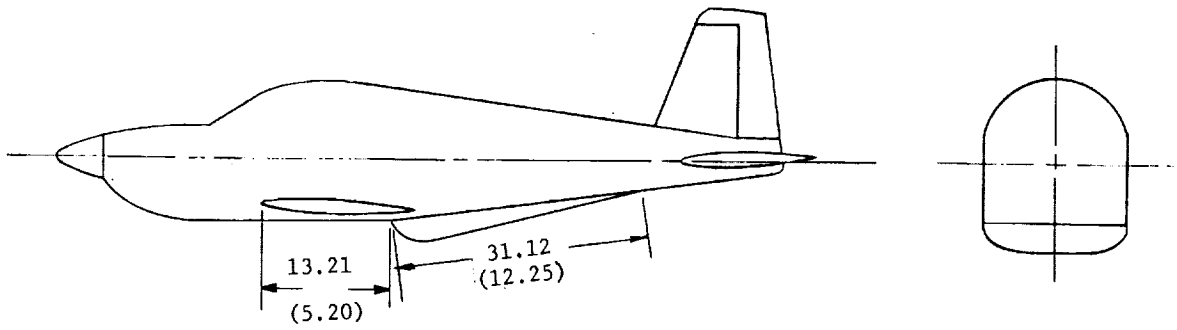

c) Deep rounded fuselage bottom.

Figure 7.- Fuselage modifications tested on model. Dimensions are given in centimeters (inches), model scale.

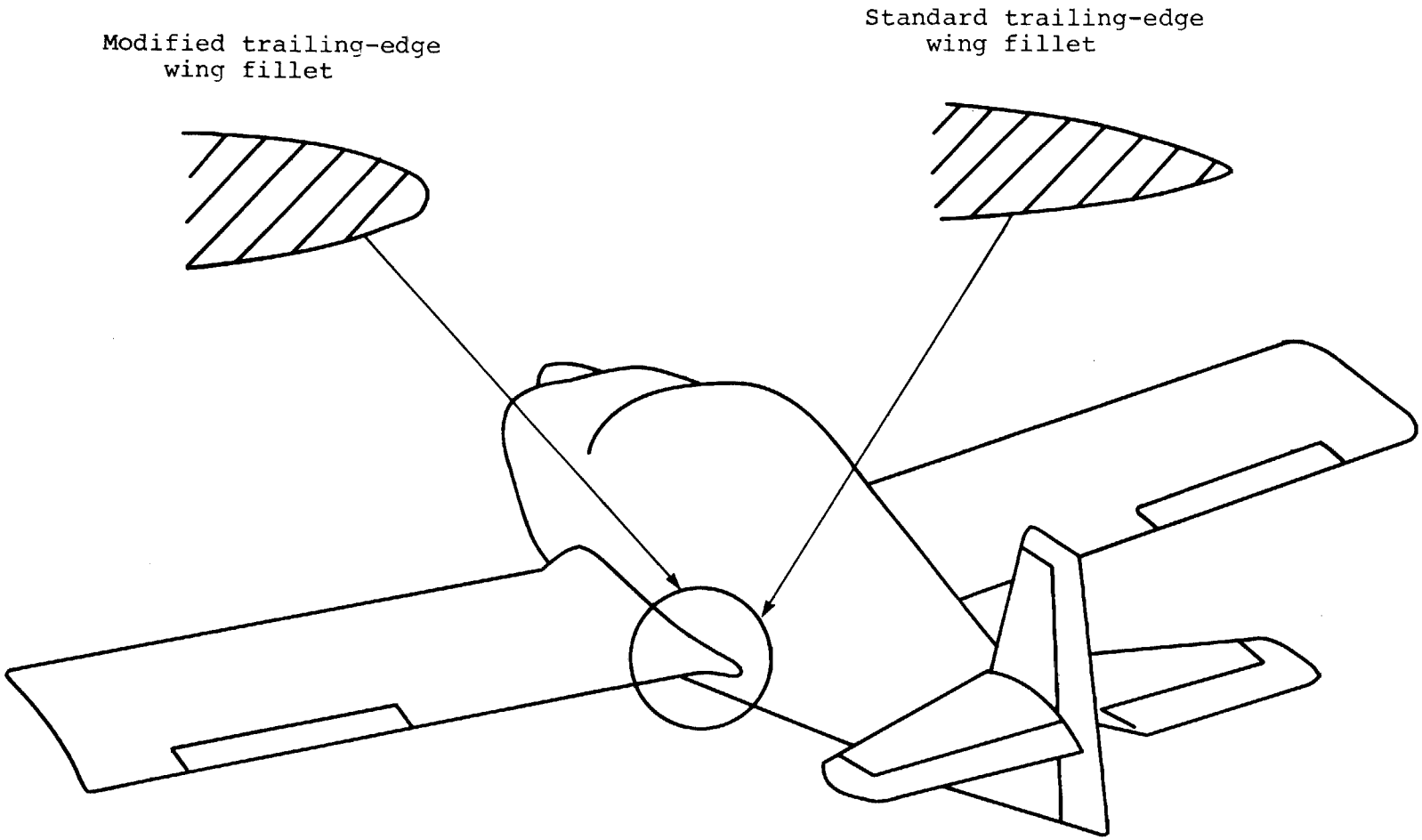

Figure 8.- Trailing-edge wing fillets tested on model.

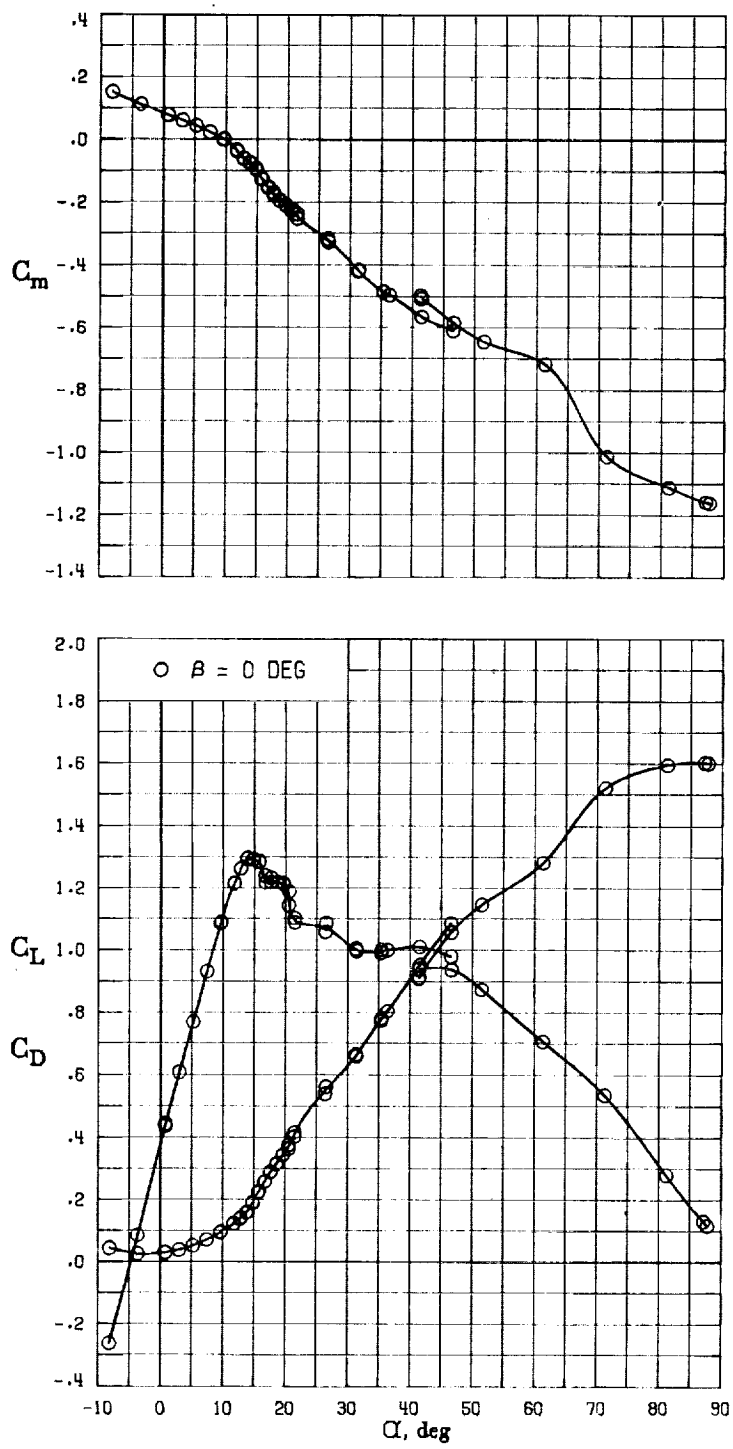

(A) LONGITUDINAL FORCE AND MOMENT COEFFICIENTS ABOUT STABILITY AXES.

FIGURE 9. - EFFECT OF ANGLE OF ATTACK AND SIDESLIP ANGLE ON AERODYNAMIC CHARACTERISTICS AT RE = 3.45 E+06 FOR CONFIGURATION B W1 H6 V. $\delta_E = 0°$, $\delta_A = 0°$, $\delta_R = 0°$.

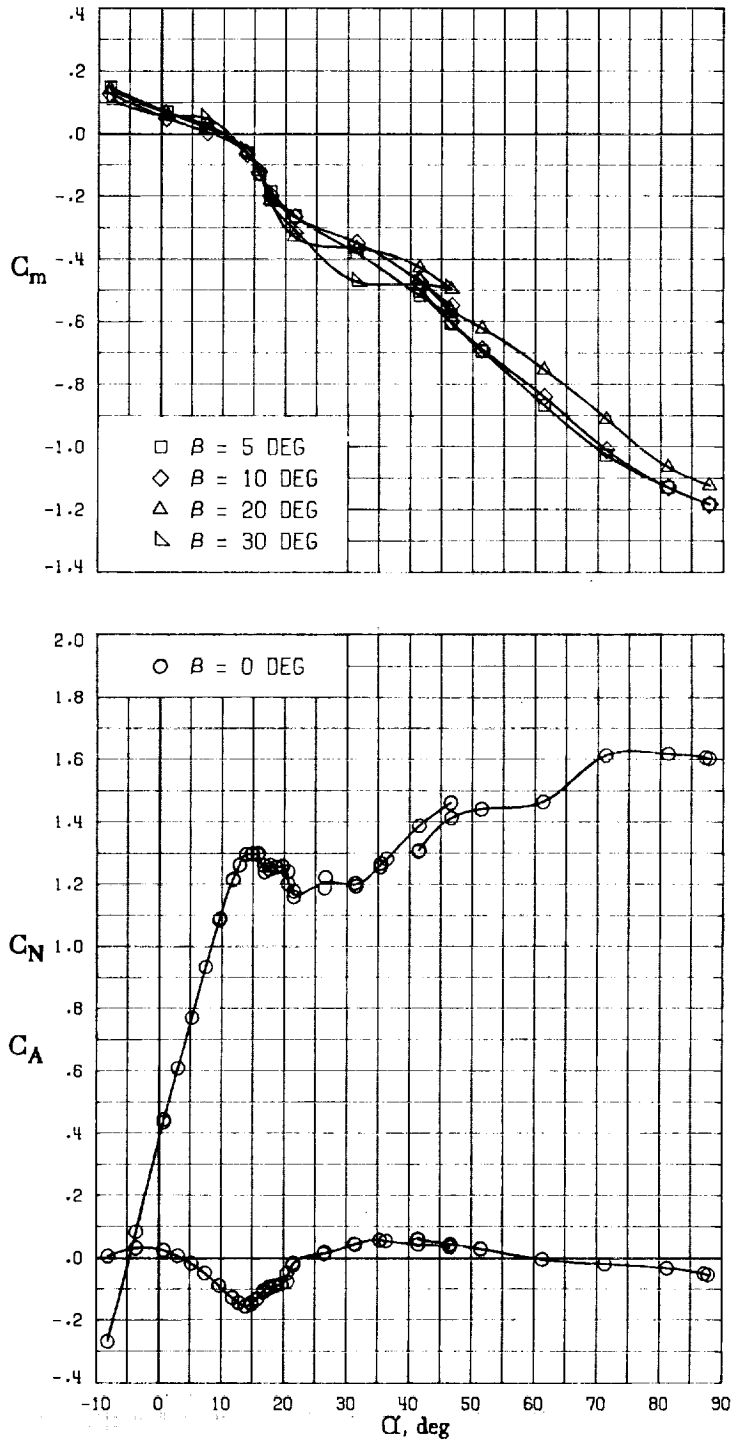

(B) LONGITUDINAL FORCE AND MOMENT COEFFICIENTS ABOUT BODY AXES.

FIGURE 9. - CONTINUED

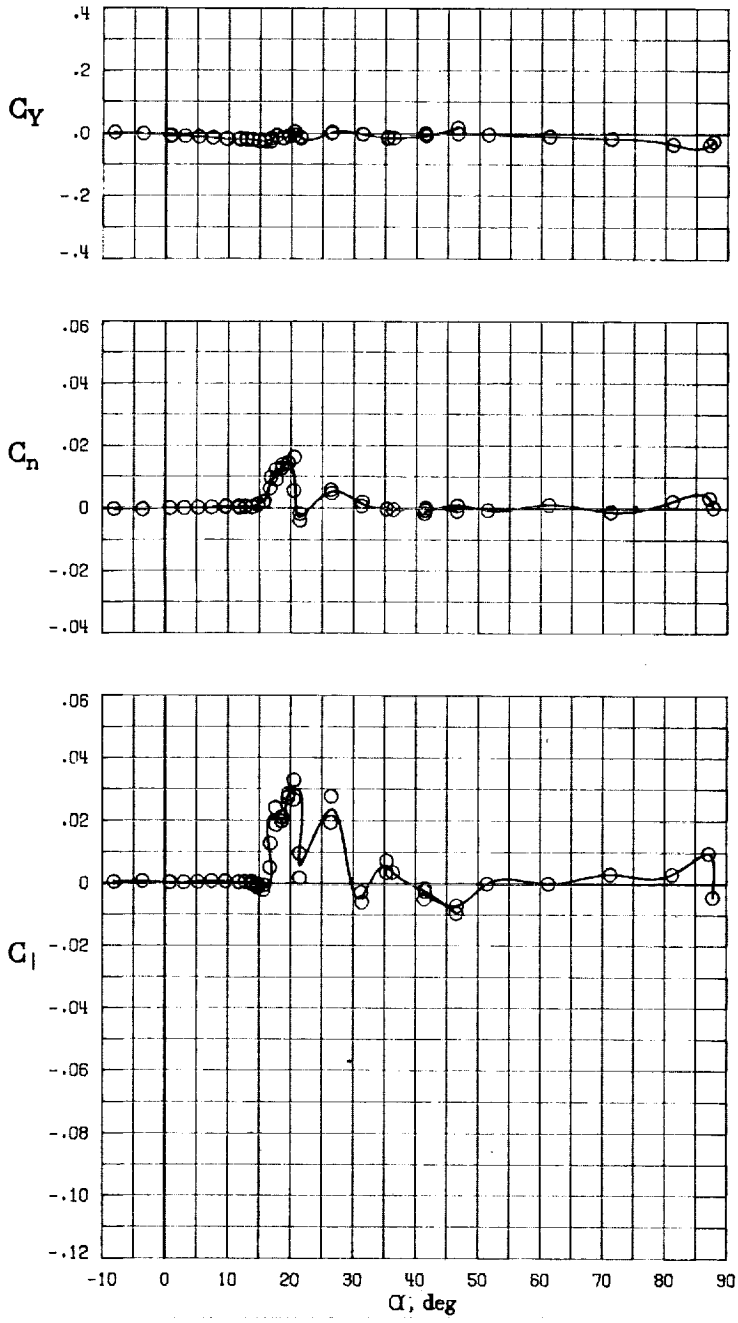

(C) LATERAL - DIRECTIONAL FORCE AND MOMENT COEFFICIENTS ABOUT BODY AXES AT ZERO SIDESLIP.

FIGURE 9. - CONTINUED

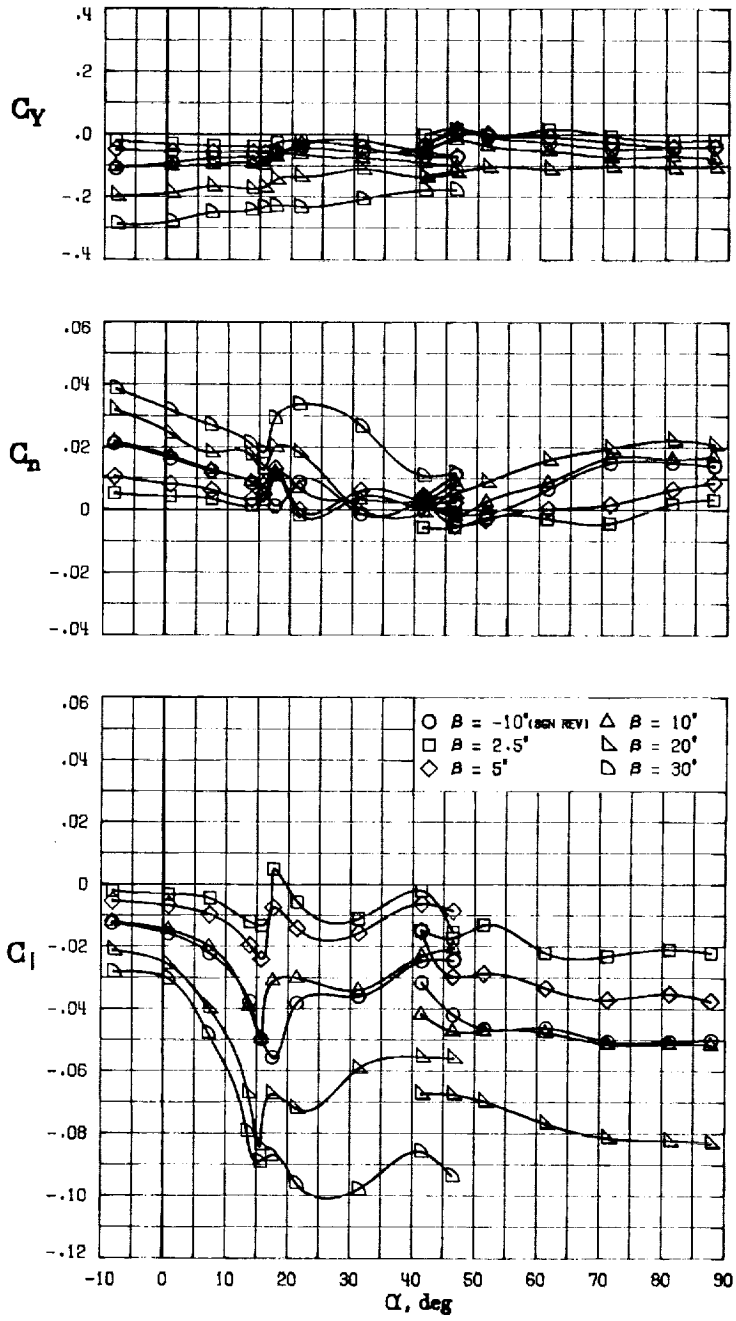

(D) LATERAL - DIRECTIONAL FORCE AND MOMENT COEFFICIENTS ABOUT BODY AXES.

FIGURE 9. - CONTINUED

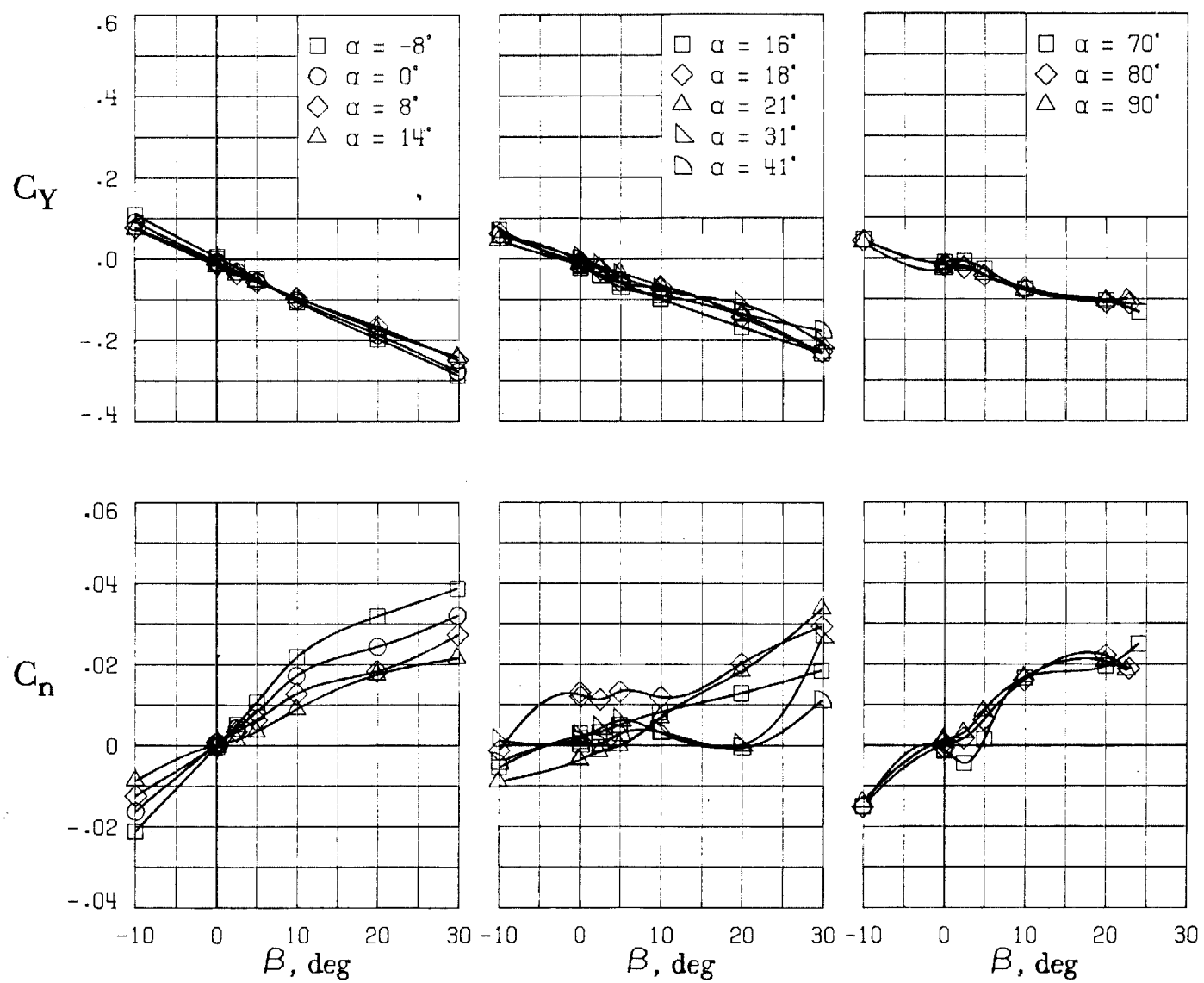

(E) DIRECTIONAL - STABILITY CHARACTERISTICS ABOUT BODY AXES AT VARIOUS ANGLES OF ATTACK.

FIGURE 9. - CONTINUED

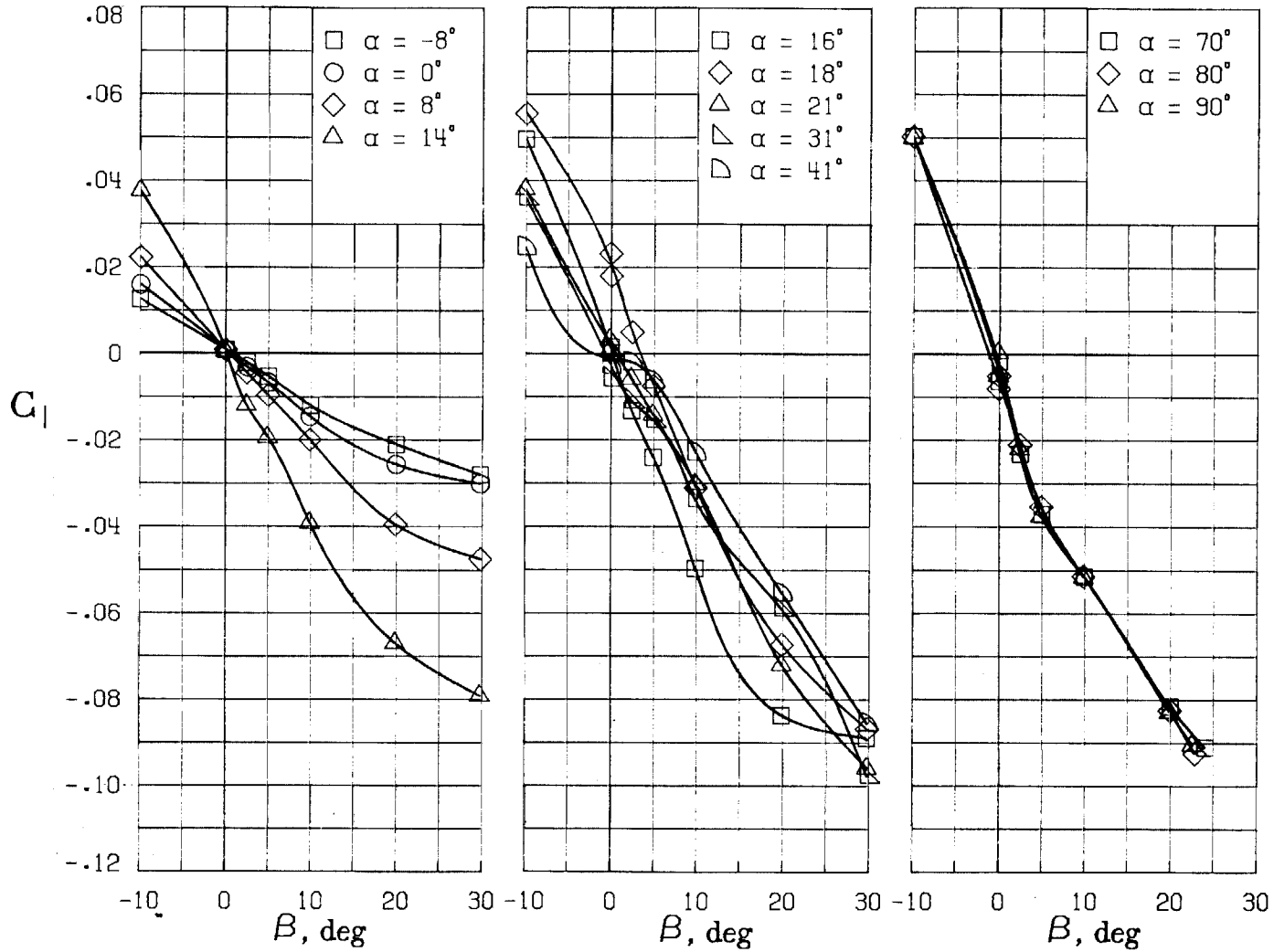

(F) LATERAL - STABILITY CHARACTERISTICS ABOUT BODY AXIS AT VARIOUS ANGLES OF ATTACK.

FIGURE 9. - CONCLUDED.

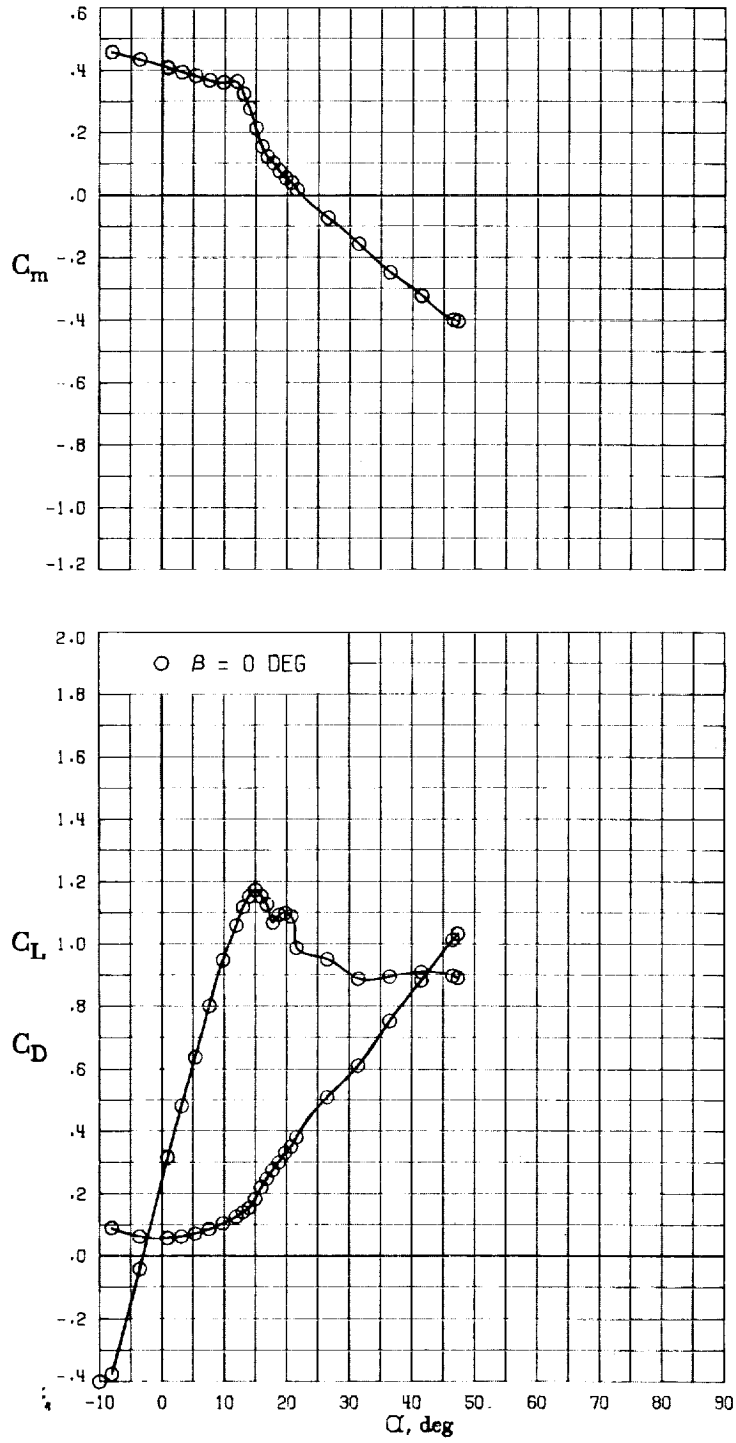

(A) LONGITUDINAL FORCE AND MOMENT COEFFICIENTS ABOUT STABILITY AXES.

FIGURE 10. - EFFECT OF ANGLE OF ATTACK AND SIDESLIP ANGLE ON AERODYNAMIC CHARACTERISTICS AT RE = 3.45 E+06 FOR CONFIGURATION B W1 H6 V. δ_E = -25°, δ_A = 0°, δ_R = 0°.

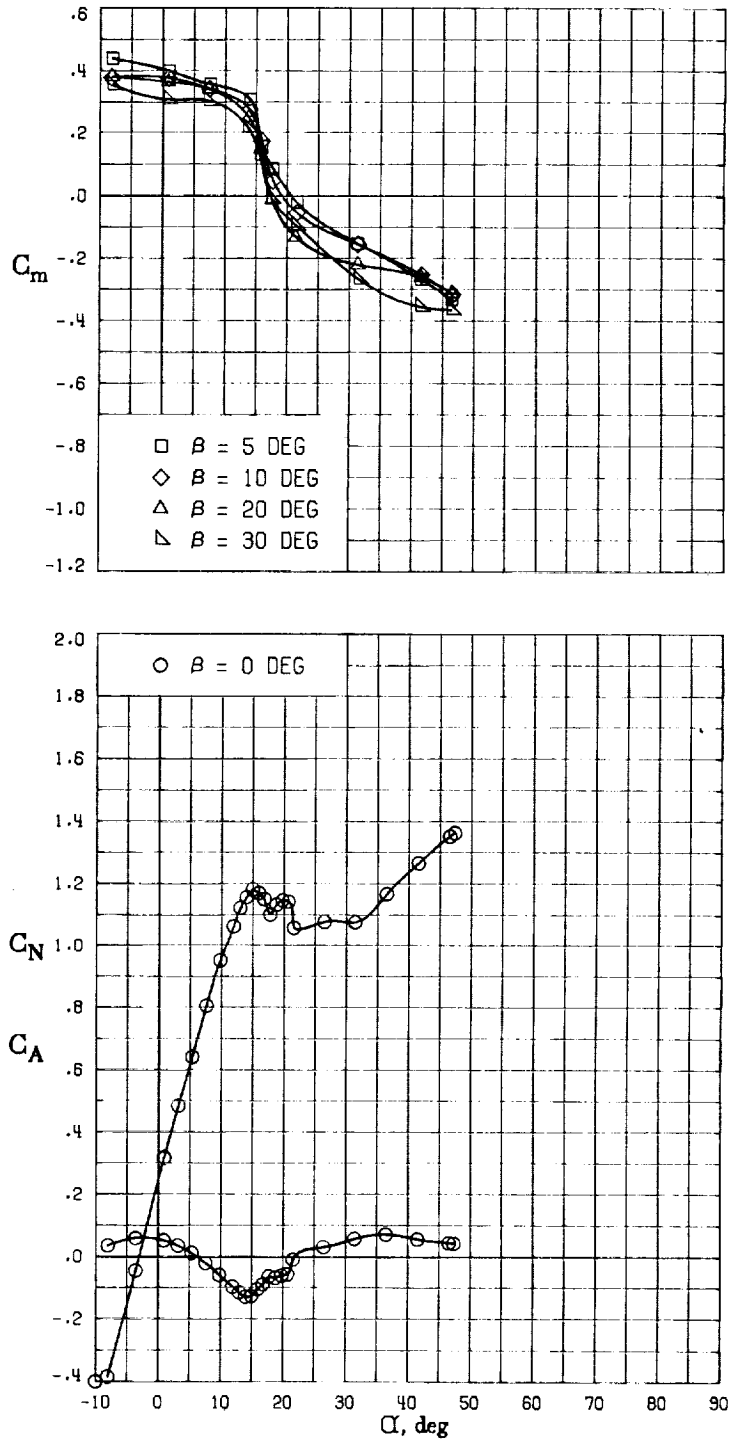

(B) LONGITUDINAL FORCE AND MOMENT COEFFICIENTS ABOUT BODY AXES.

FIGURE 10. - CONTINUED

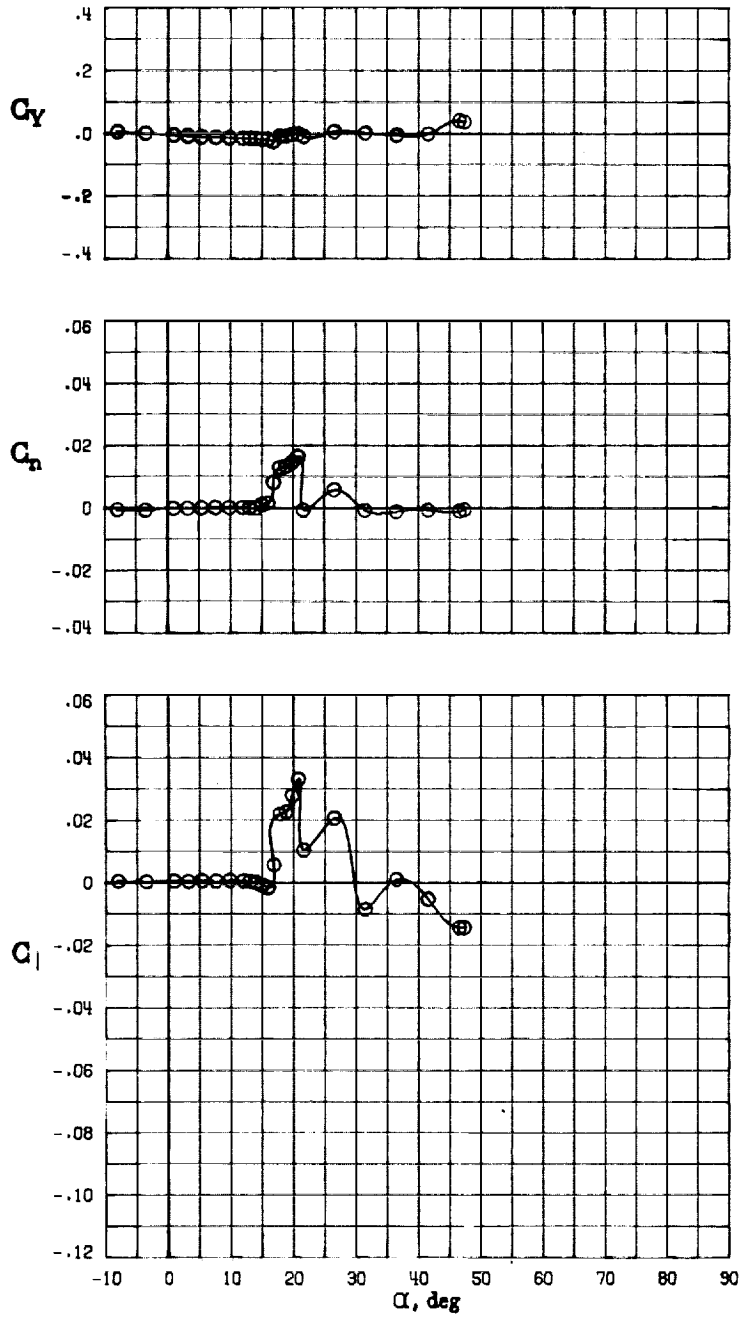

(C) LATERAL - DIRECTIONAL FORCE AND MOMENT COEFFICIENTS ABOUT BODY AXES AT ZERO SIDESLIP.

FIGURE 10. - CONTINUED

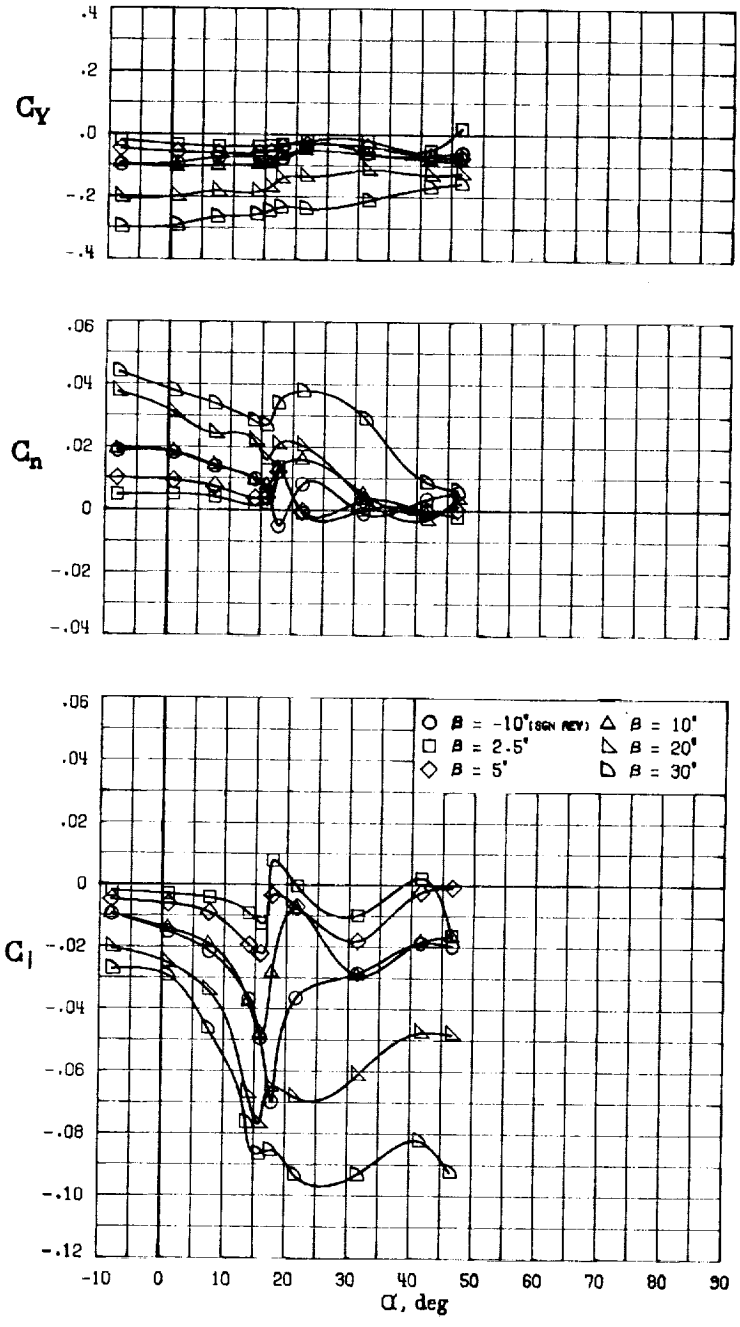

(D) LATERAL - DIRECTIONAL FORCE AND MOMENT COEFFICIENTS ABOUT BODY AXES.

FIGURE 10. - CONTINUED

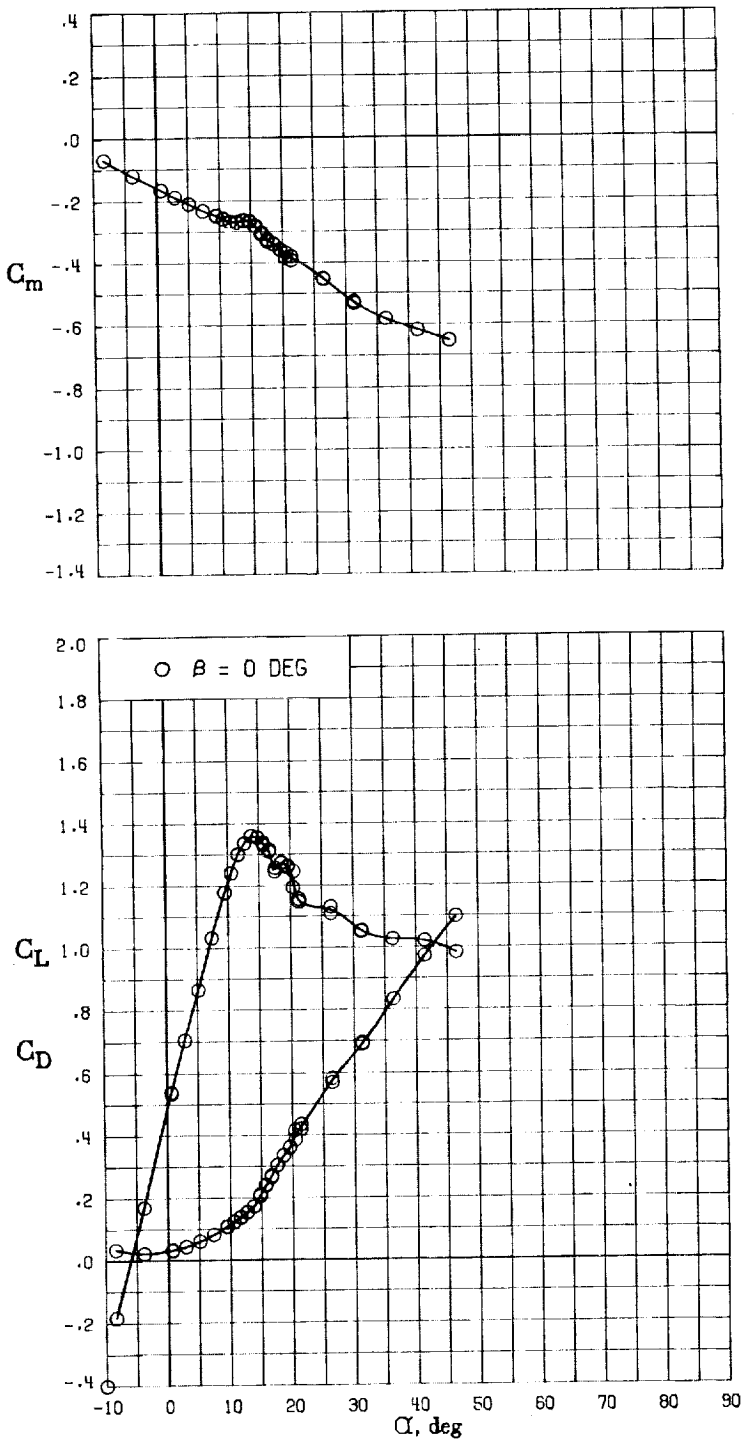

(A) LONGITUDINAL FORCE AND MOMENT COEFFICIENTS ABOUT STABILITY AXES.

FIGURE 11. - EFFECT OF ANGLE OF ATTACK AND SIDESLIP ANGLE ON AERODYNAMIC CHARACTERISTICS AT RE = 3.45 E+06 FOR CONFIGURATION B W1 H6 V. $\delta_E = 15°$, $\delta_A = 0°$, $\delta_R = 0°$.

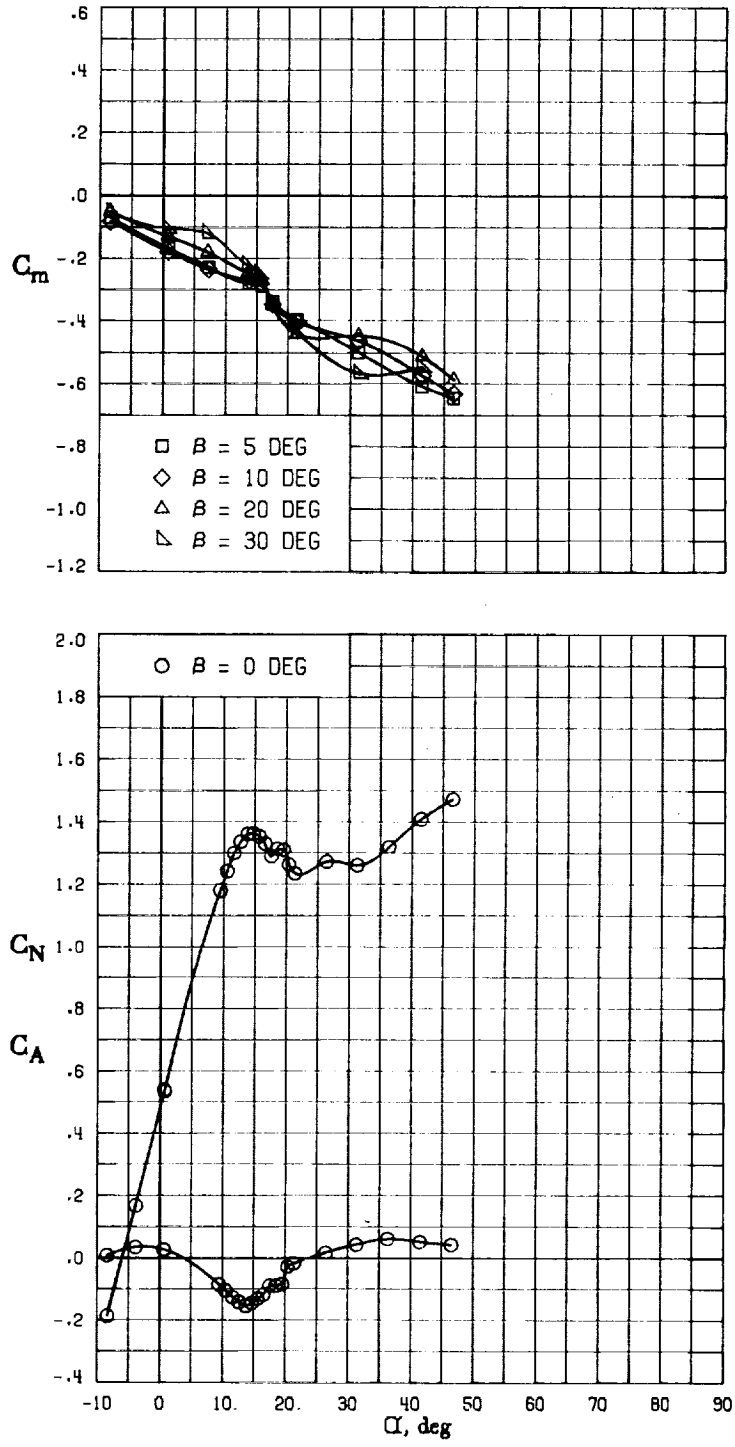

(B) LONGITUDINAL FORCE AND MOMENT COEFFICIENTS ABOUT BODY AXES.

FIGURE 11. - CONTINUED

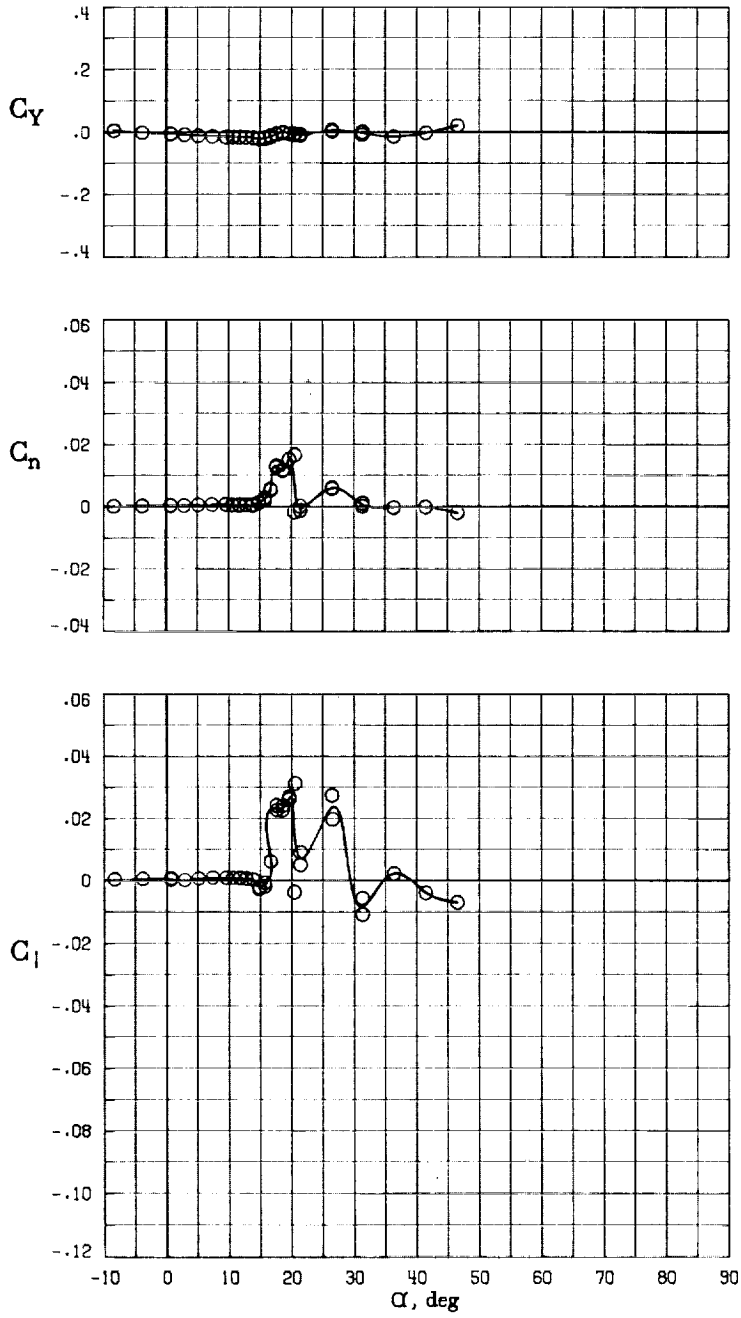

(C) LATERAL - DIRECTIONAL FORCE AND MOMENT COEFFICIENTS ABOUT BODY AXES AT ZERO SIDESLIP.

FIGURE 11. - CONTINUED

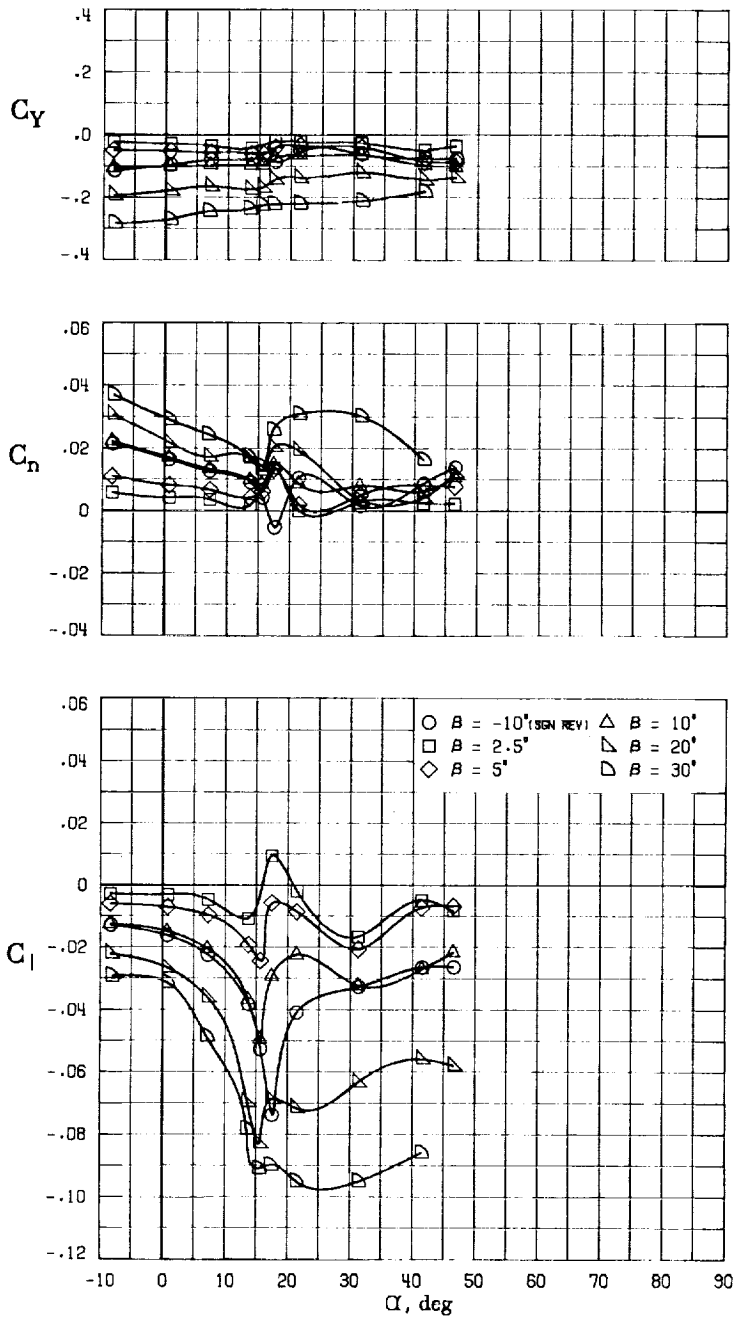

(D) LATERAL - DIRECTIONAL FORCE AND MOMENT COEFFICIENTS ABOUT BODY AXES.

FIGURE 11. - CONTINUED

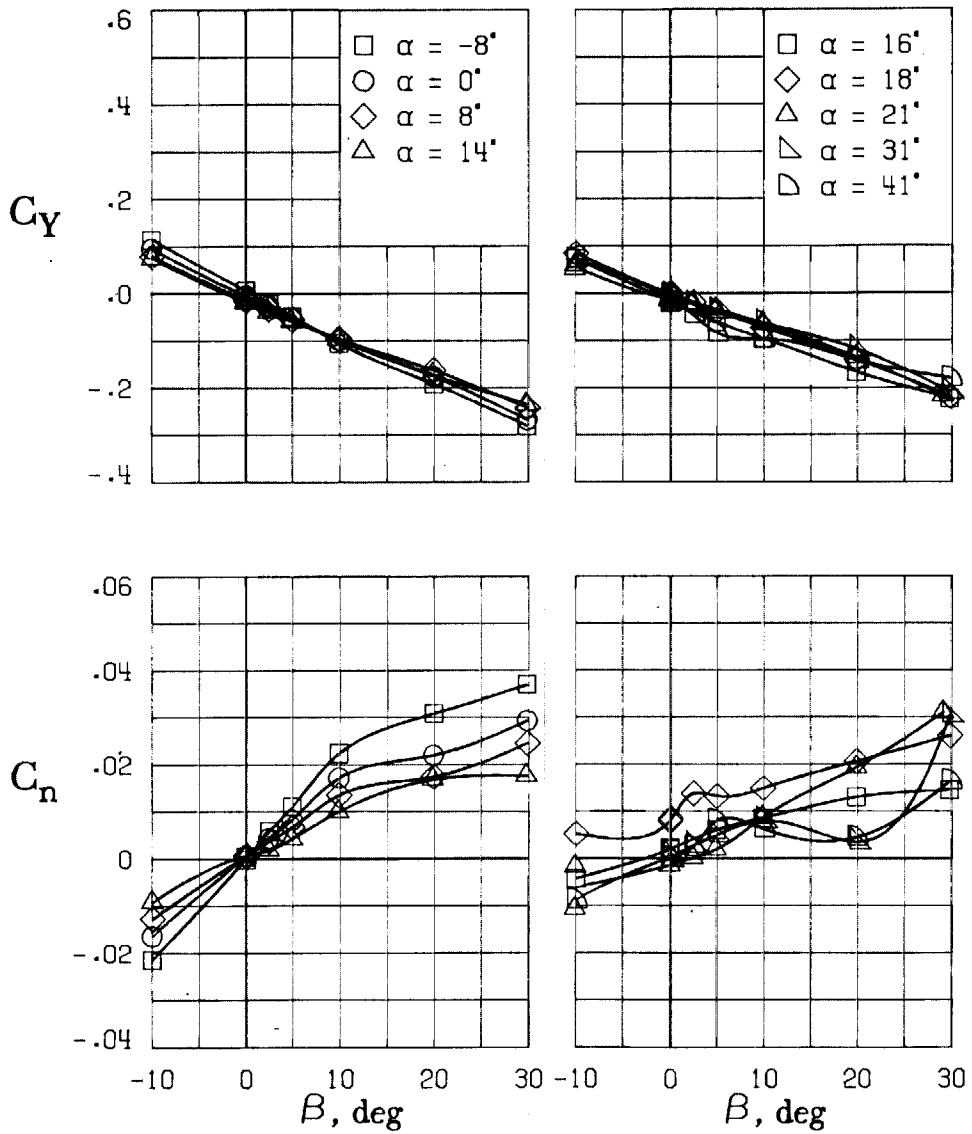

(E) DIRECTIONAL - STABILITY CHARACTERISTICS ABOUT BODY AXES AT VARIOUS ANGLES OF ATTACK.

FIGURE 11. - CONTINUED.

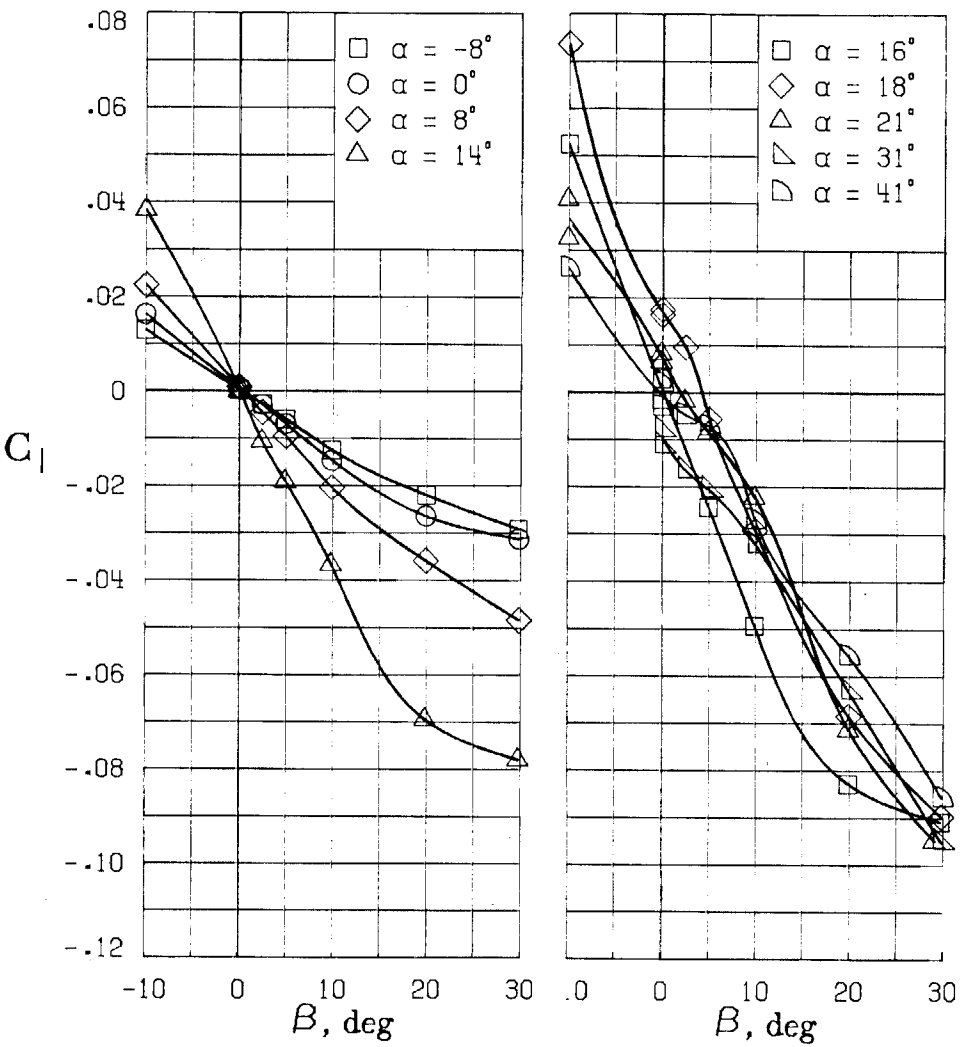

(F) LATERAL - STABILITY CHARACTERISTICS ABOUT BODY AXES AT VARIOUS ANGLES OF ATTACK.

FIGURE 11. - CONCLUDED.

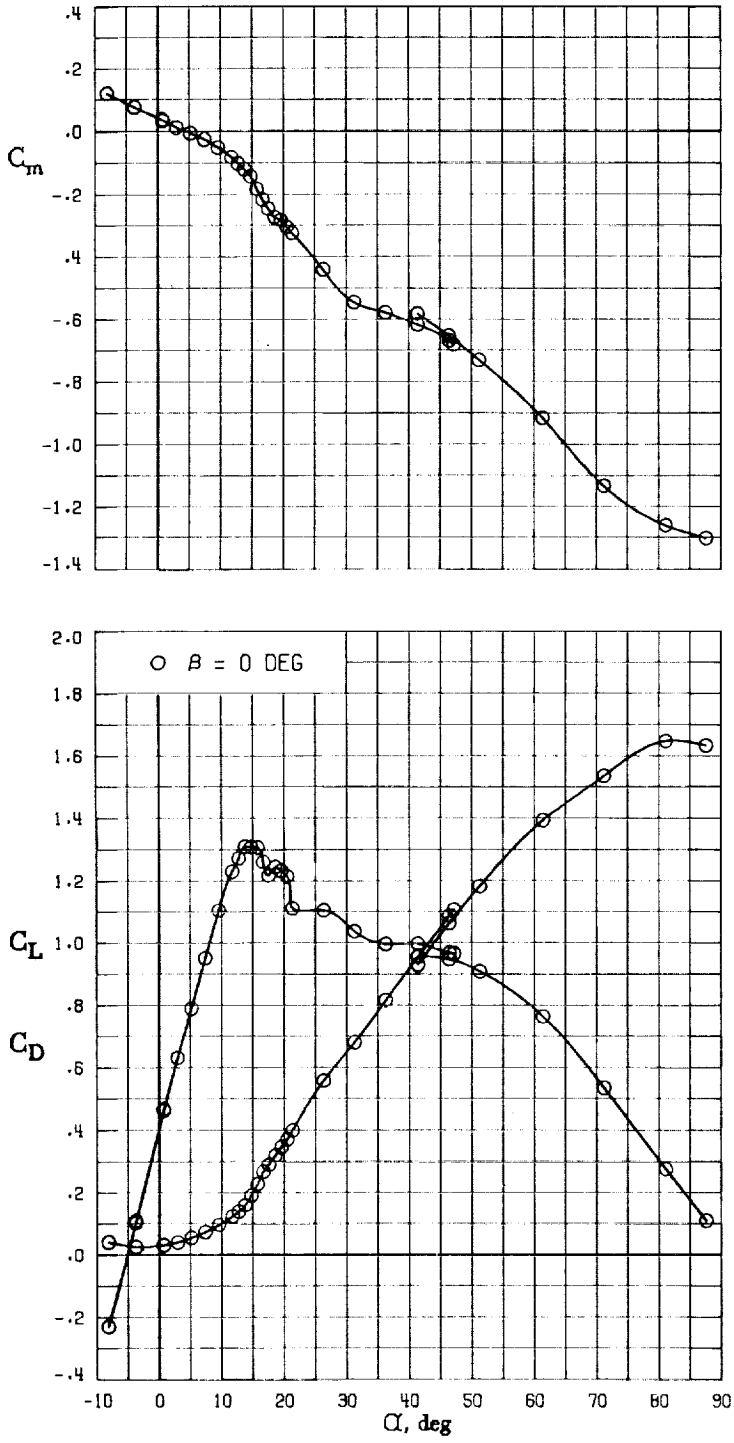

(A) LONGITUDINAL FORCE AND MOMENT COEFFICIENTS ABOUT STABILITY AXES.

FIGURE 12. - EFFECT OF ANGLE OF ATTACK AND SIDESLIP ANGLE ON AERODYNAMIC CHARACTERISTICS AT RE = 3.45 E+06 FOR CONFIGURATION B W1 H4 V. $\delta_E = 0°$, $\delta_A = 0°$, $\delta_R = 0°$.

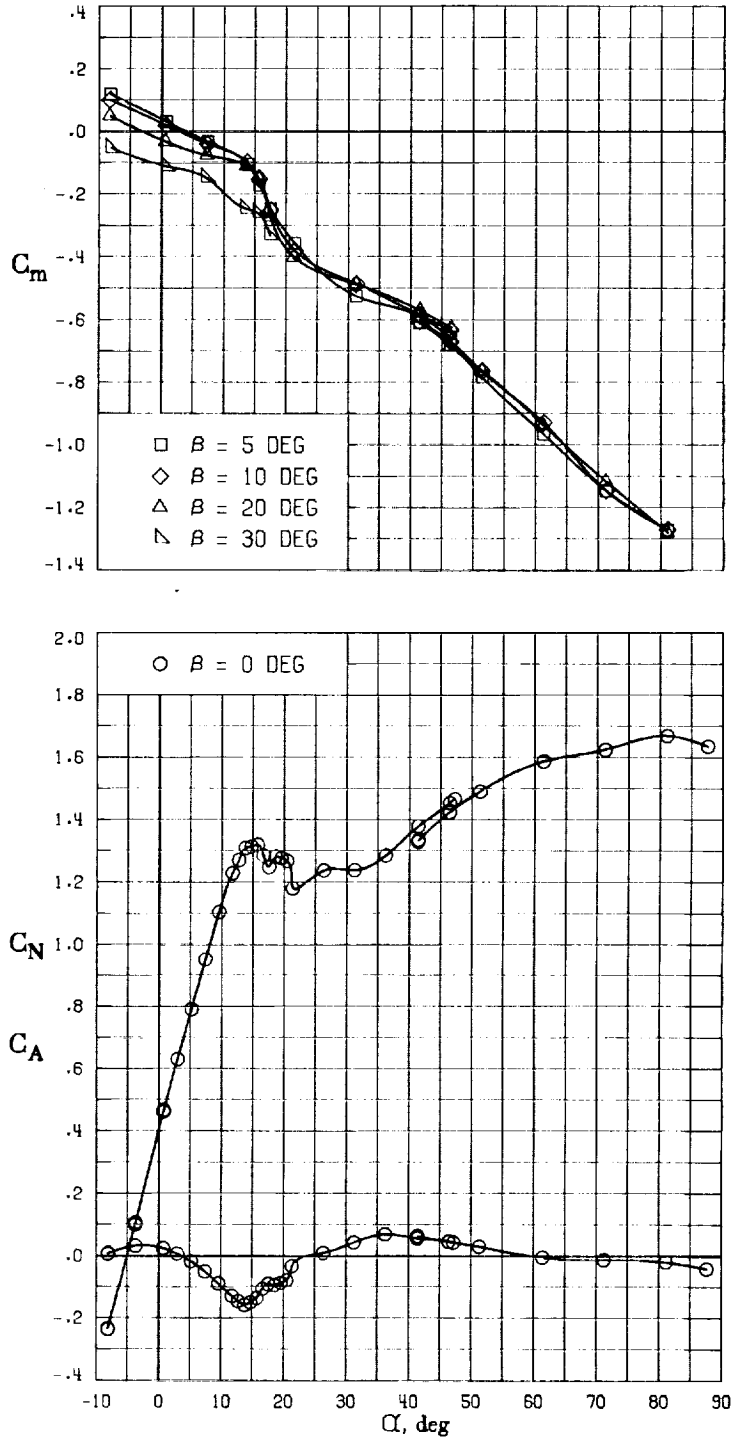

(B) LONGITUDINAL FORCE AND MOMENT COEFFICIENTS ABOUT BODY AXES.

FIGURE 12. - CONTINUED

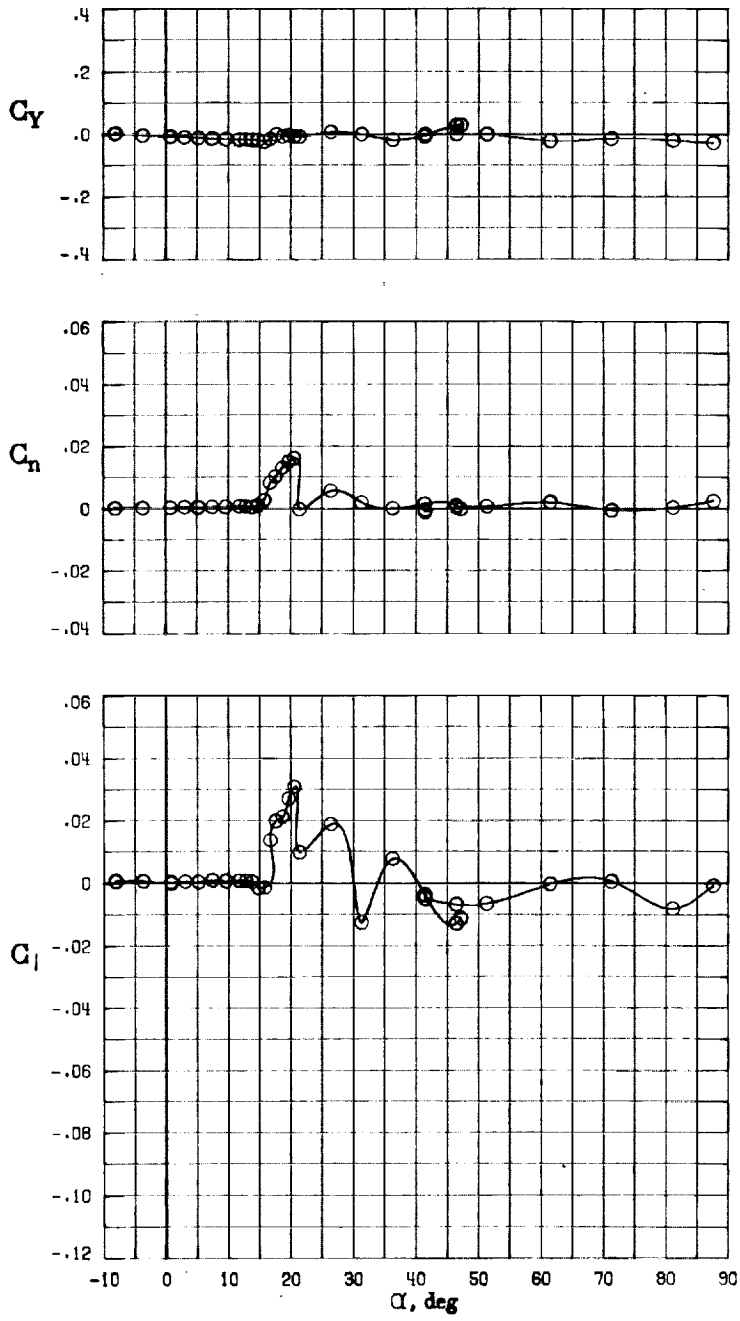

(C) LATERAL - DIRECTIONAL FORCE AND MOMENT COEFFICIENTS ABOUT BODY AXES AT ZERO SIDESLIP.

FIGURE 12. - CONTINUED

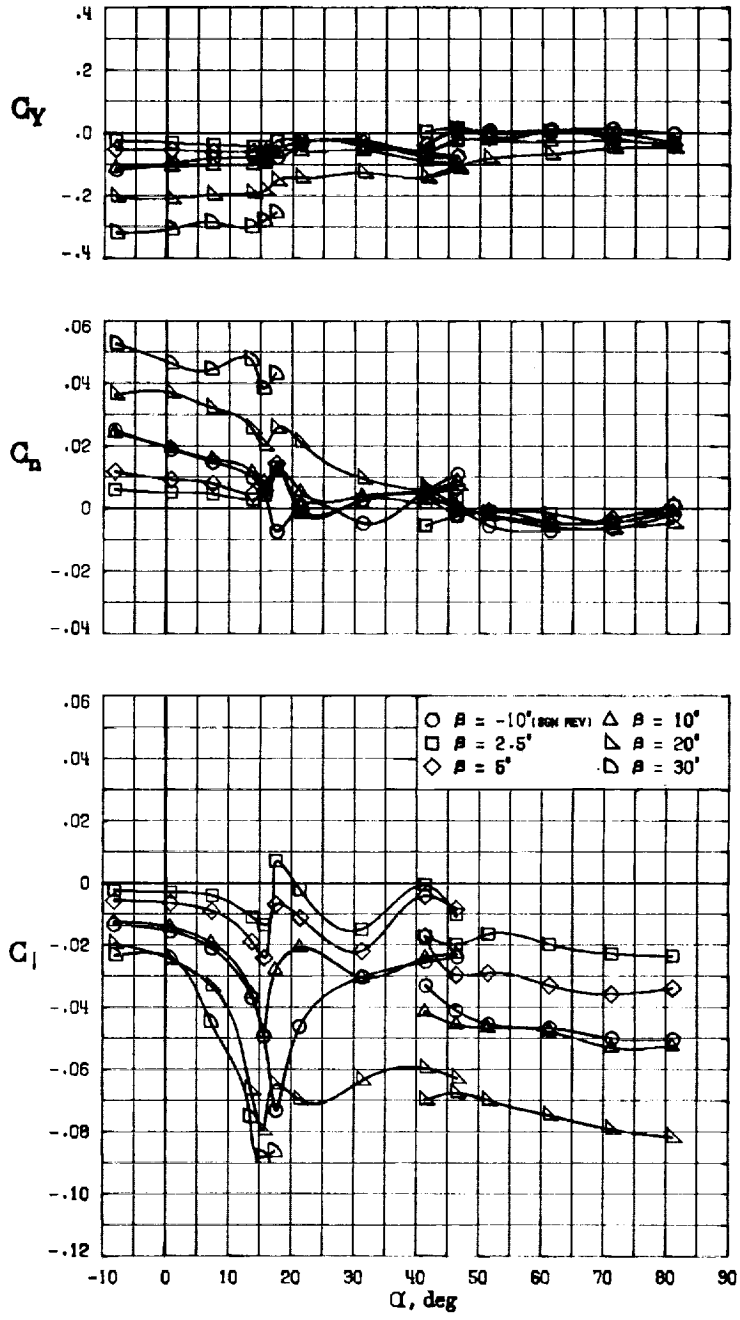

(D) LATERAL - DIRECTIONAL FORCE AND MOMENT COEFFICIENTS ABOUT BODY AXES.

FIGURE 12. - CONTINUED

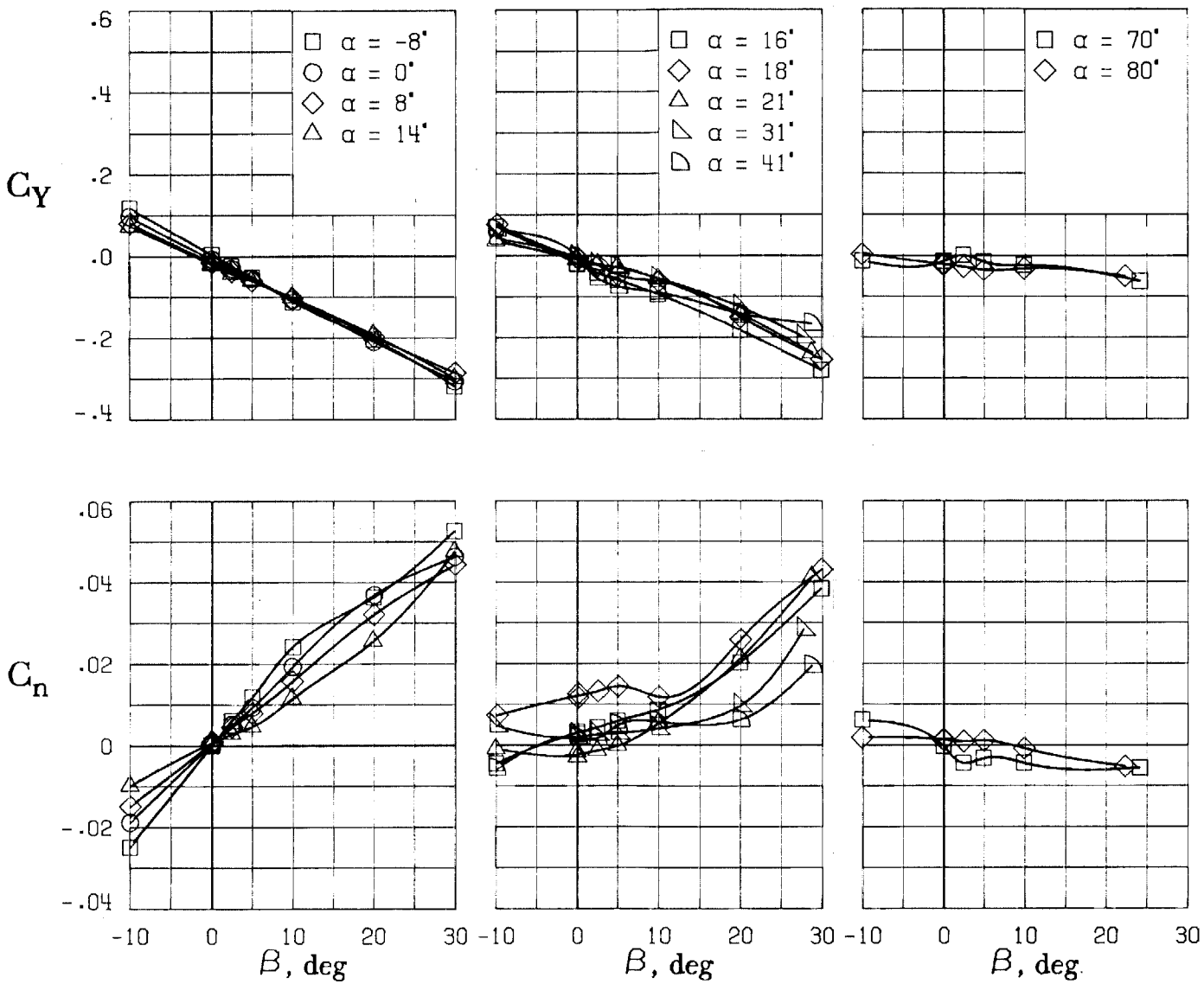

(E) DIRECTIONAL - STABILITY CHARACTERISTICS ABOUT BODY AXES AT VARIOUS ANGLES OF ATTACK.

FIGURE 12. - CONTINUED

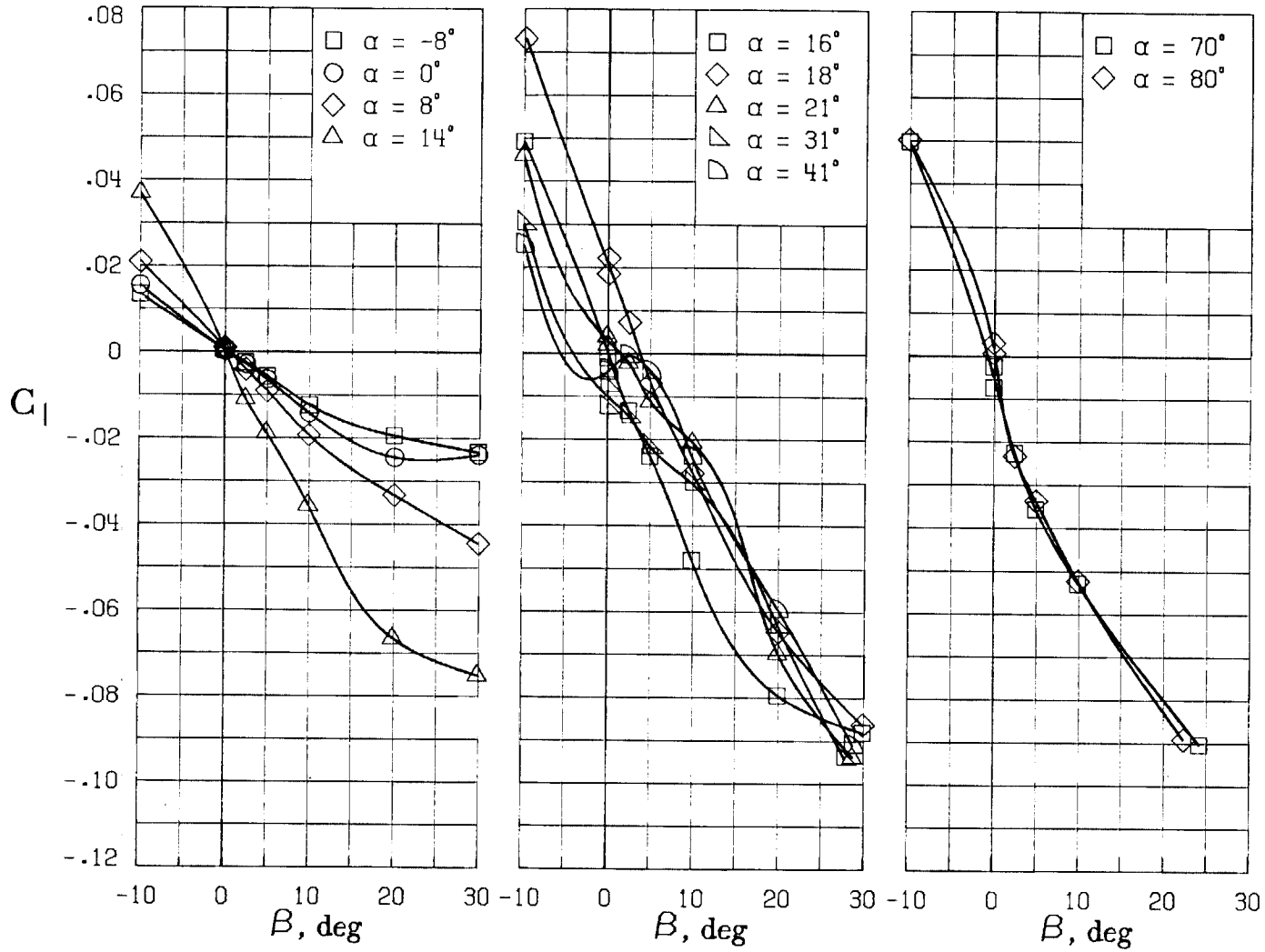

(F) LATERAL - STABILITY CHARACTERISTICS ABOUT BODY AXES AT VARIOUS ANGLES OF ATTACK.

FIGURE 12. - CONCLUDED.

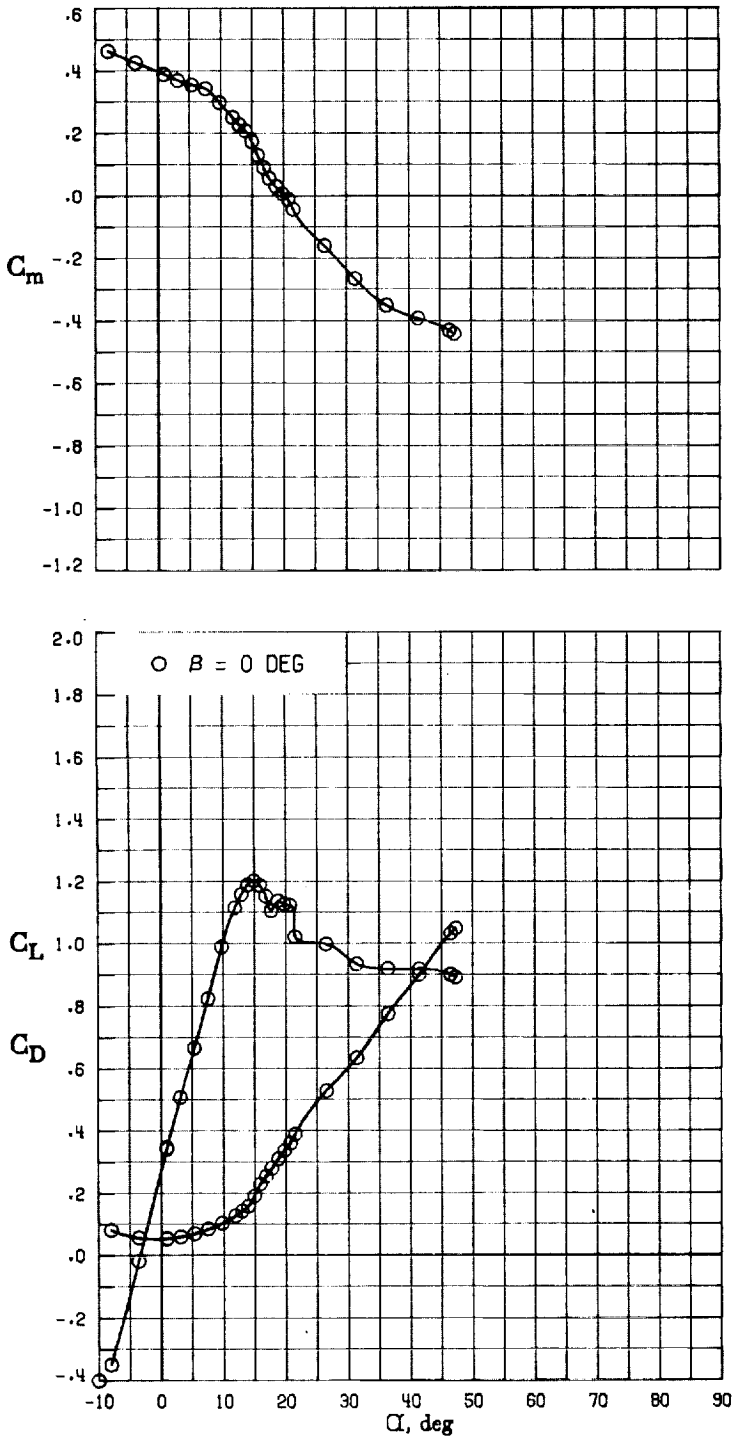

(A) LONGITUDINAL FORCE AND MOMENT COEFFICIENTS ABOUT STABILITY AXES.

FIGURE 13. - EFFECT OF ANGLE OF ATTACK AND SIDESLIP ANGLE ON AERODYNAMIC CHARACTERISTICS AT RE = 3.45 E+06 FOR CONFIGURATION B W1 H4 V. δ_E = -25°, δ_A = 0°, δ_R = 0°.

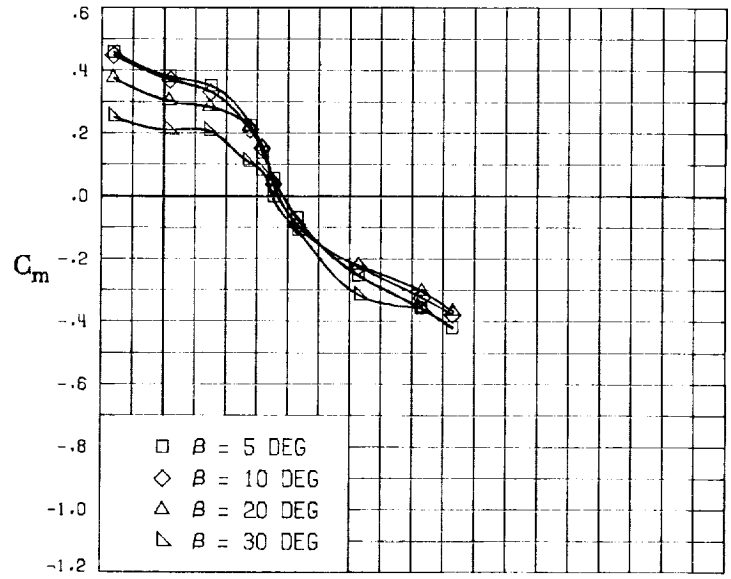

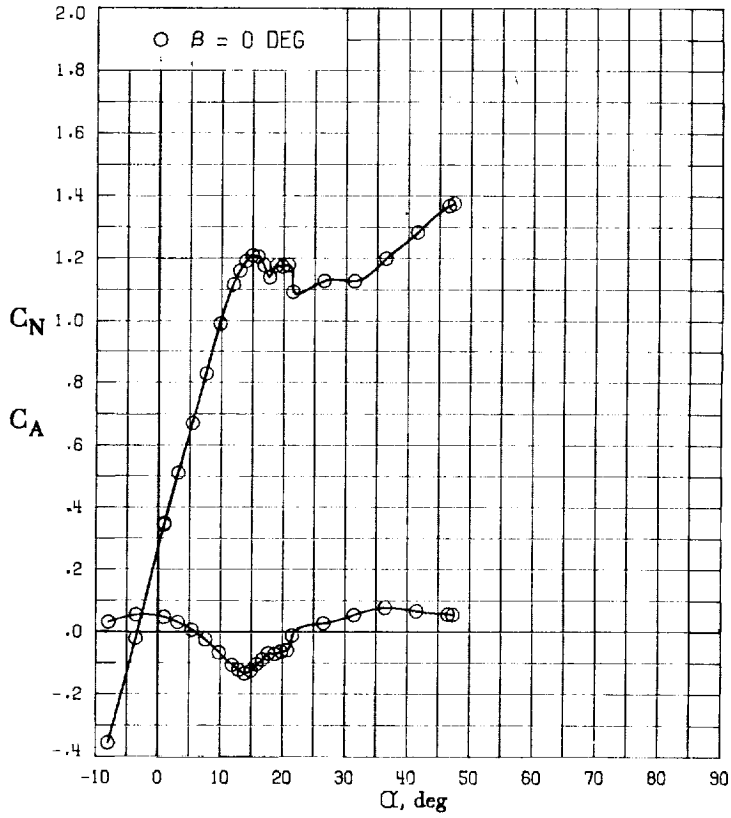

(B) LONGITUDINAL FORCE AND MOMENT COEFFICIENTS ABOUT BODY AXES.

FIGURE 13. - CONTINUED

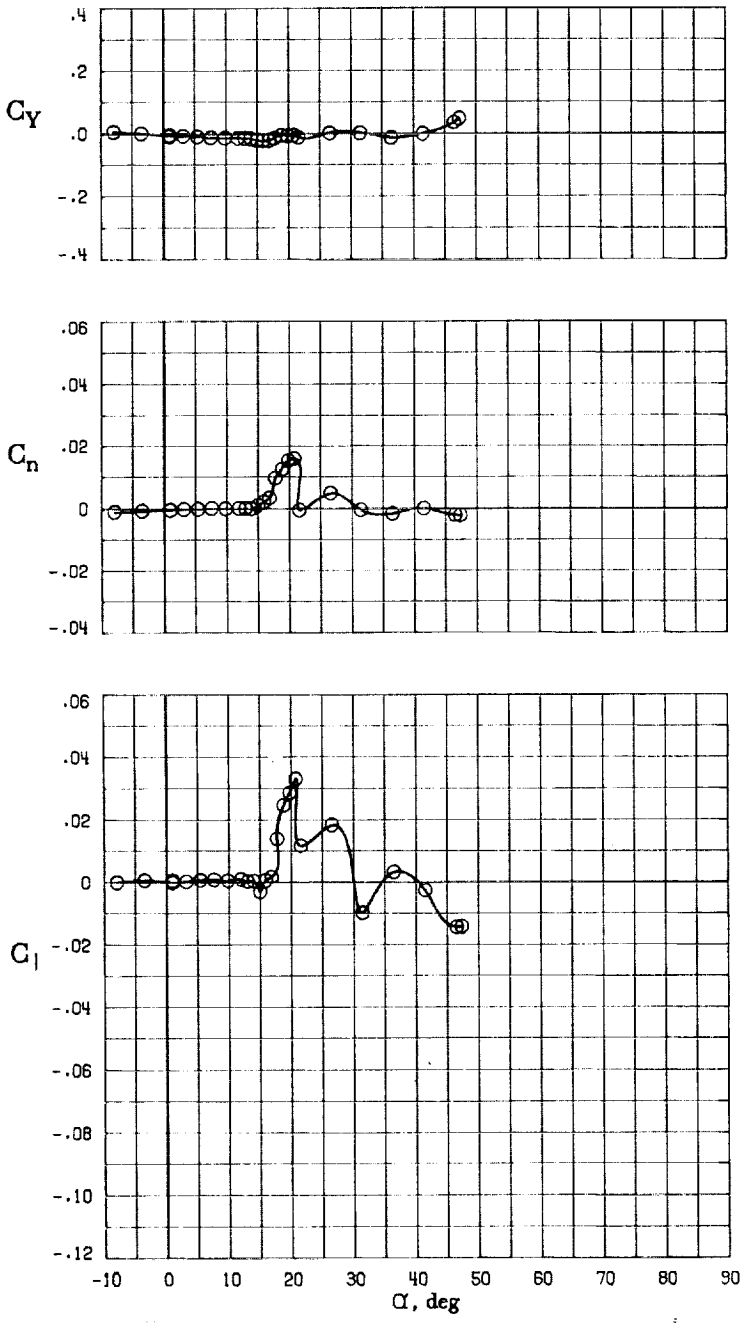

(C) LATERAL - DIRECTIONAL FORCE AND MOMENT COEFFICIENTS ABOUT BODY AXES AT ZERO SIDESLIP.

FIGURE 13. - CONTINUED

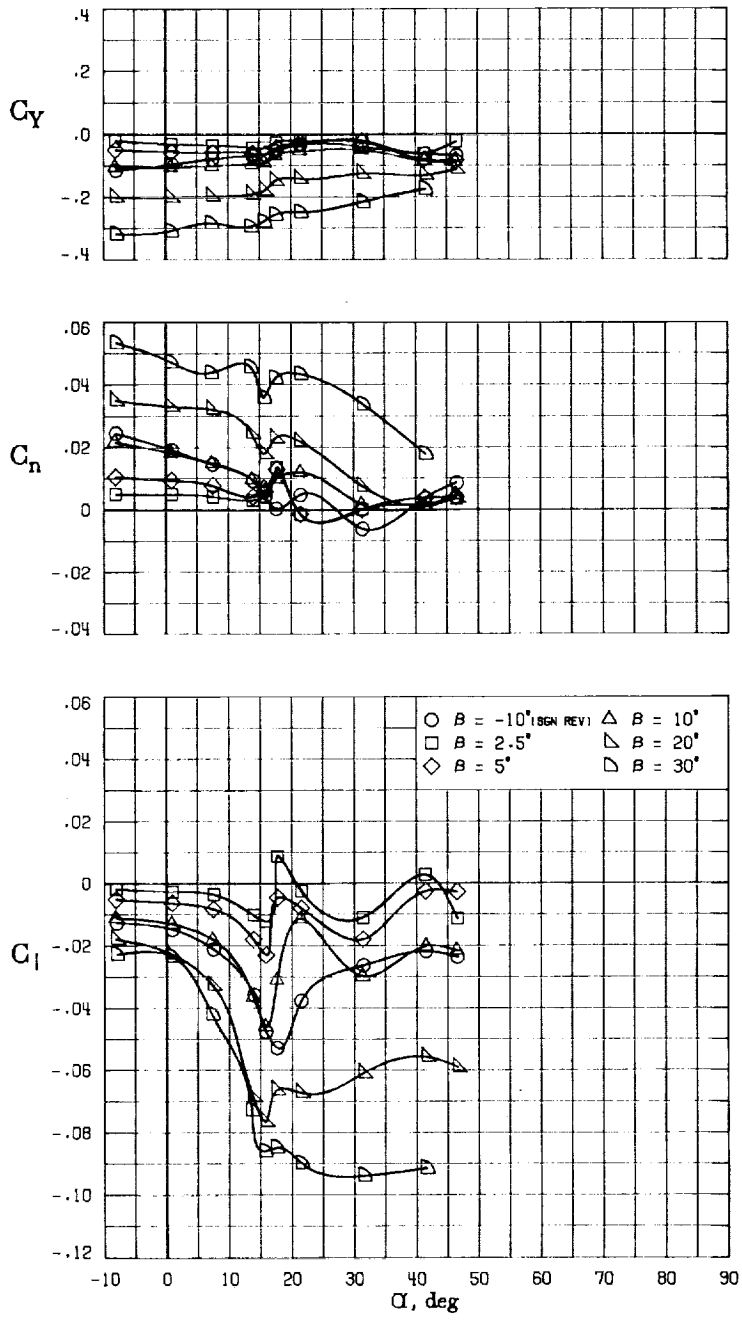

D) LATERAL - DIRECTIONAL FORCE AND MOMENT COEFFICIENTS ABOUT BODY AXES.

FIGURE 13. - CONTINUED

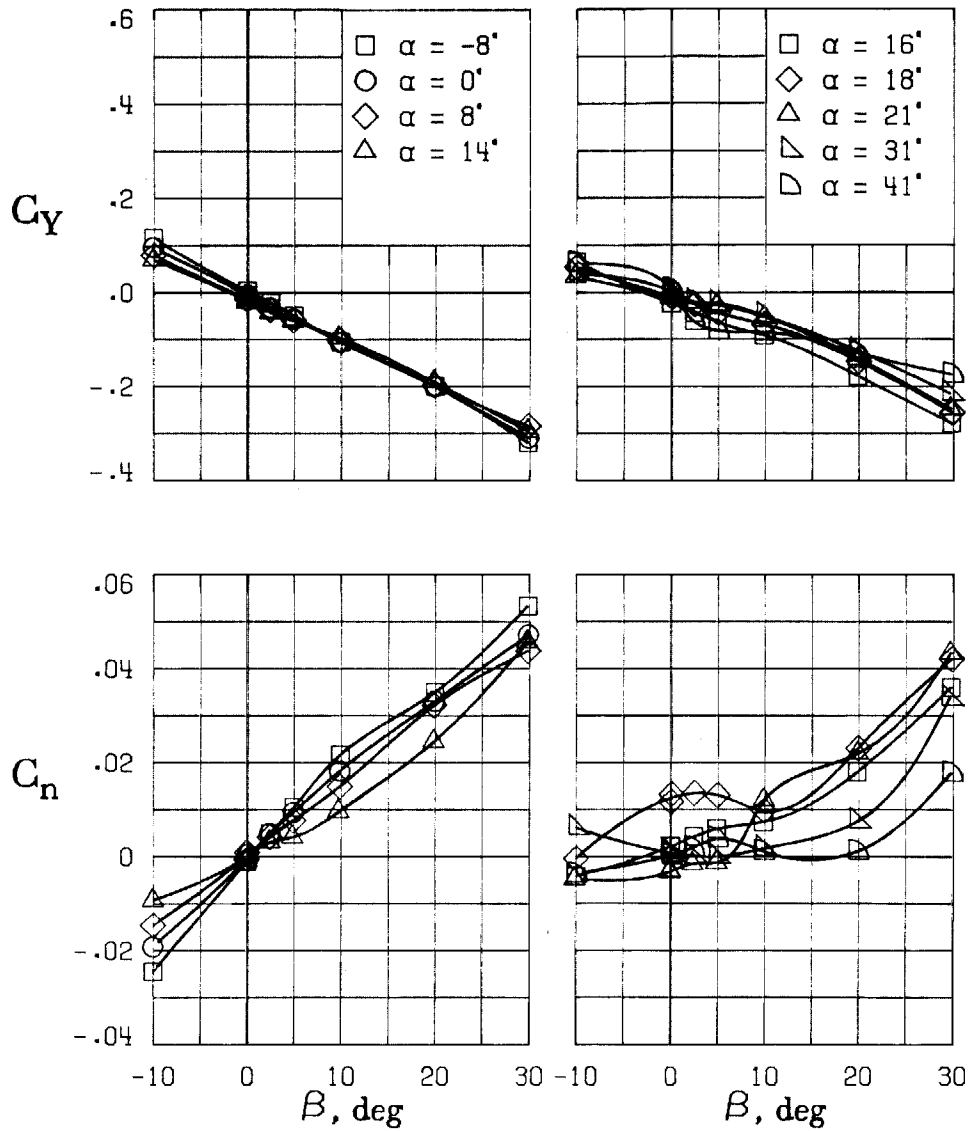

(E) DIRECTIONAL - STABILITY CHARACTERISTICS ABOUT BODY AXES AT VARIOUS ANGLES OF ATTACK.

FIGURE 13. - CONTINUED

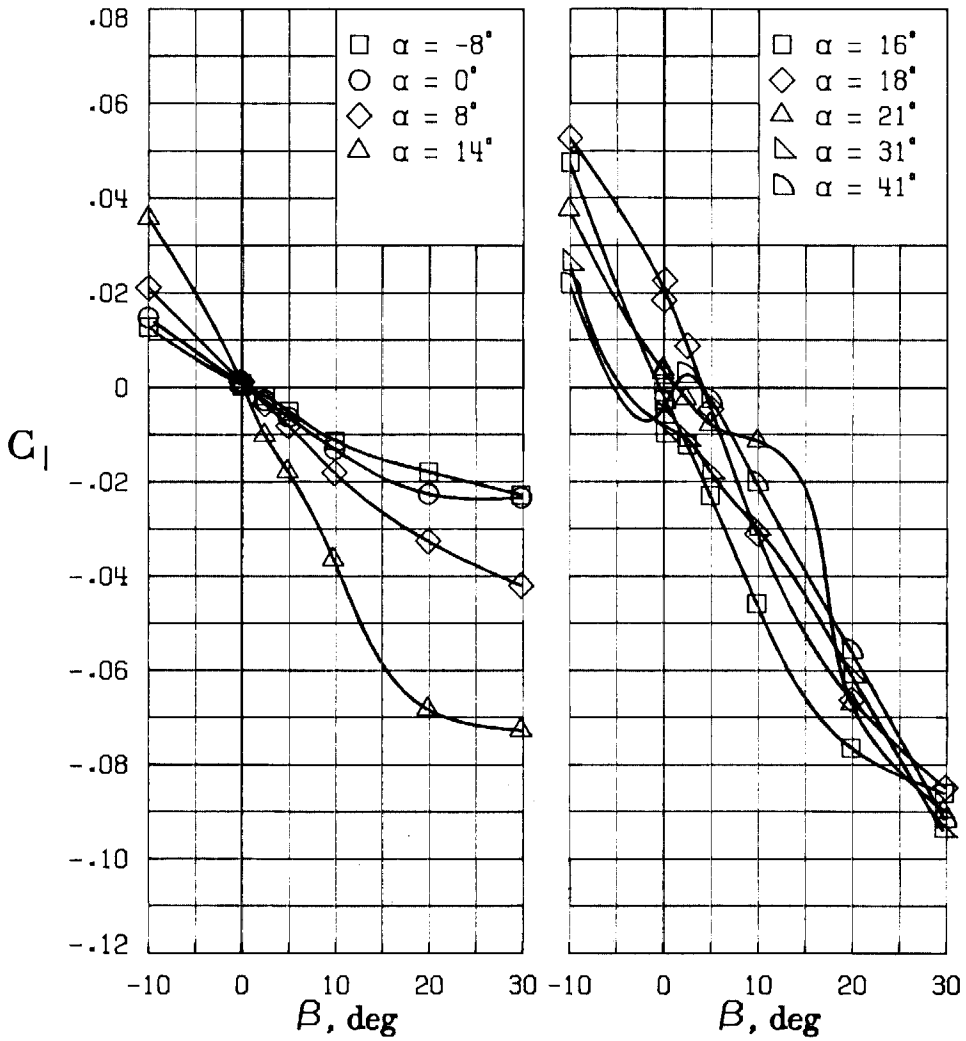

(F) LATERAL - STABILITY CHARACTERISTICS ABOUT BODY AXES AT VARIOUS ANGLES OF ATTACK.

FIGURE 13. - CONCLUDED.

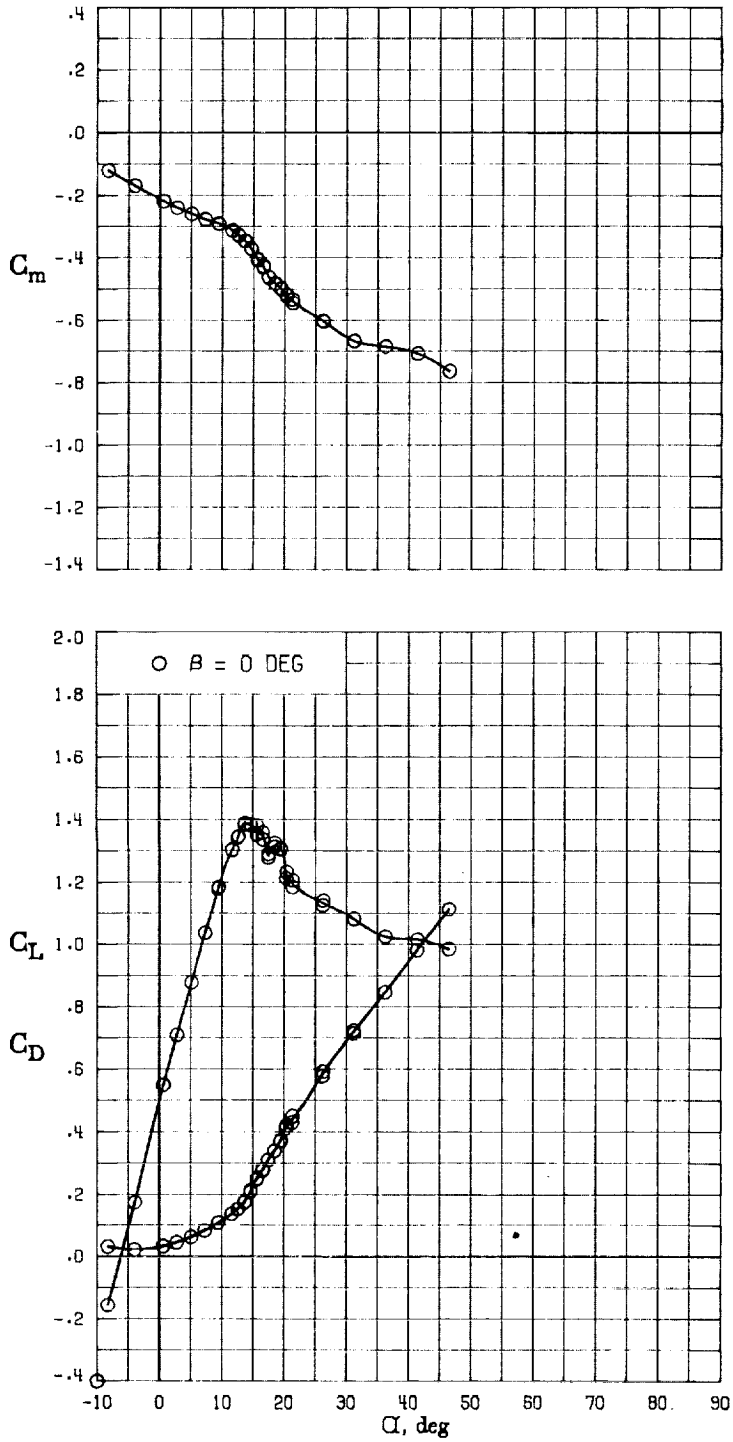

(A) LONGITUDINAL FORCE AND MOMENT COEFFICIENTS ABOUT STABILITY AXES.

FIGURE 14. - EFFECT OF ANGLE OF ATTACK AND SIDESLIP ANGLE ON AERODYNAMIC CHARACTERISTICS AT RE = 3.45 E+06 FOR CONFIGURATION B W1 H4 V. $\delta_E = 15°$, $\delta_A = 0°$, $\delta_R = 0°$.

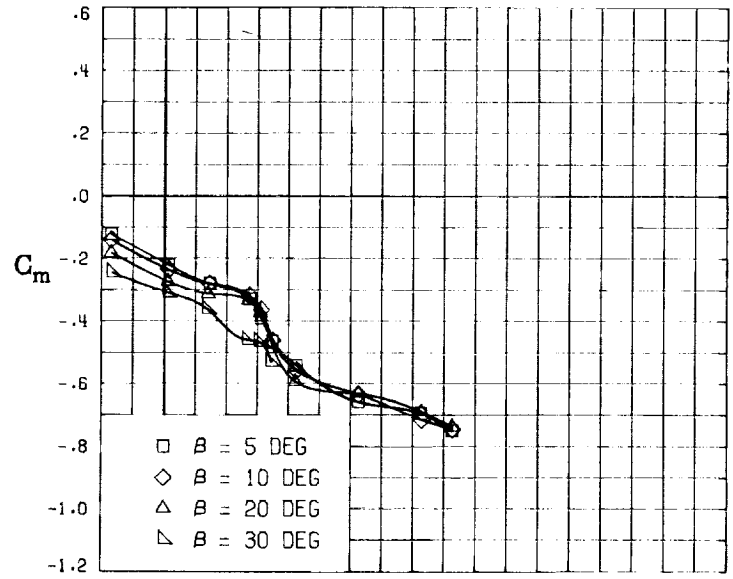

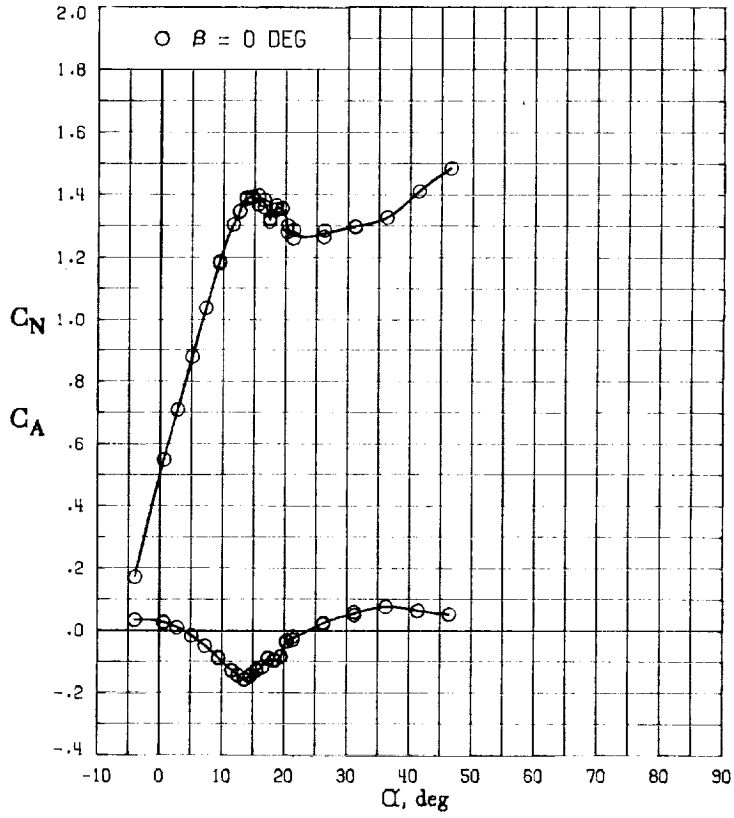

(B) LONGITUDINAL FORCE AND MOMENT COEFFICIENTS ABOUT BODY AXES.

FIGURE 14. - CONTINUED

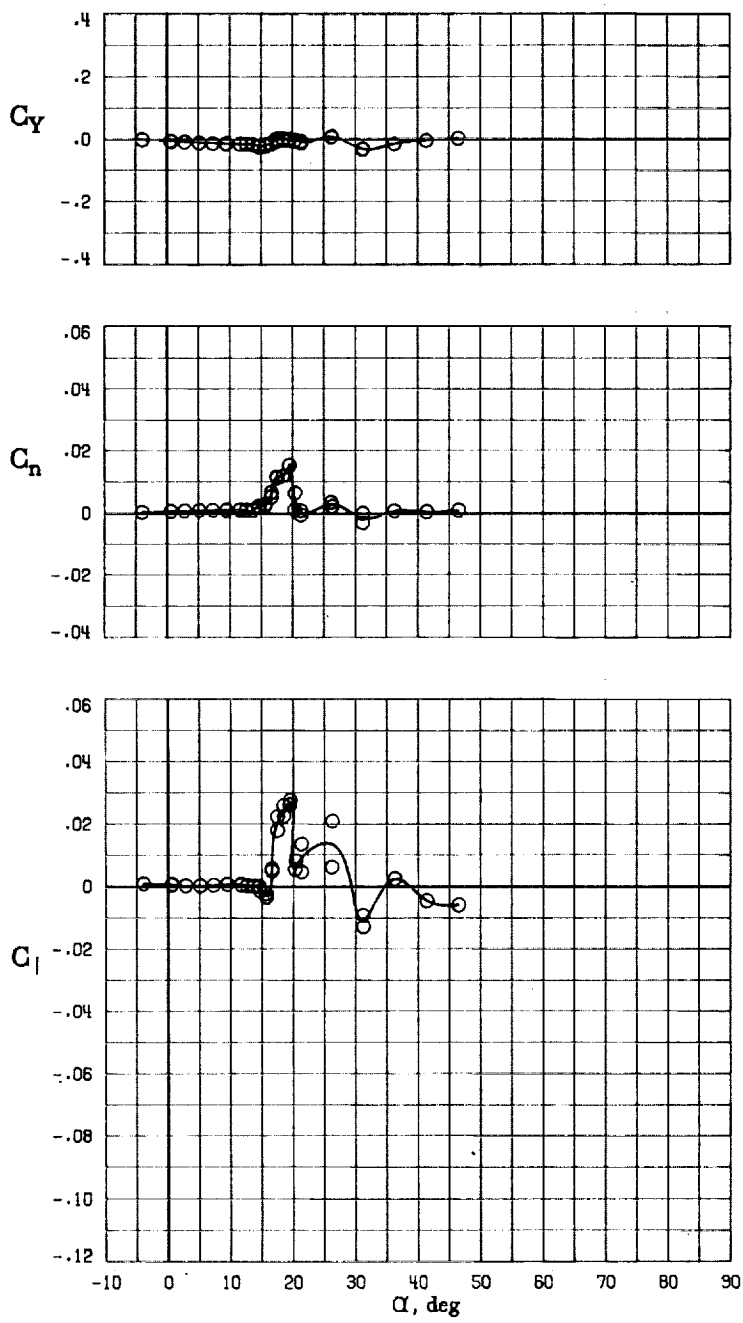

(C) LATERAL - DIRECTIONAL FORCE AND MOMENT COEFFICIENTS ABOUT BODY AXES AT ZERO SIDESLIP.

FIGURE 14. - CONTINUED

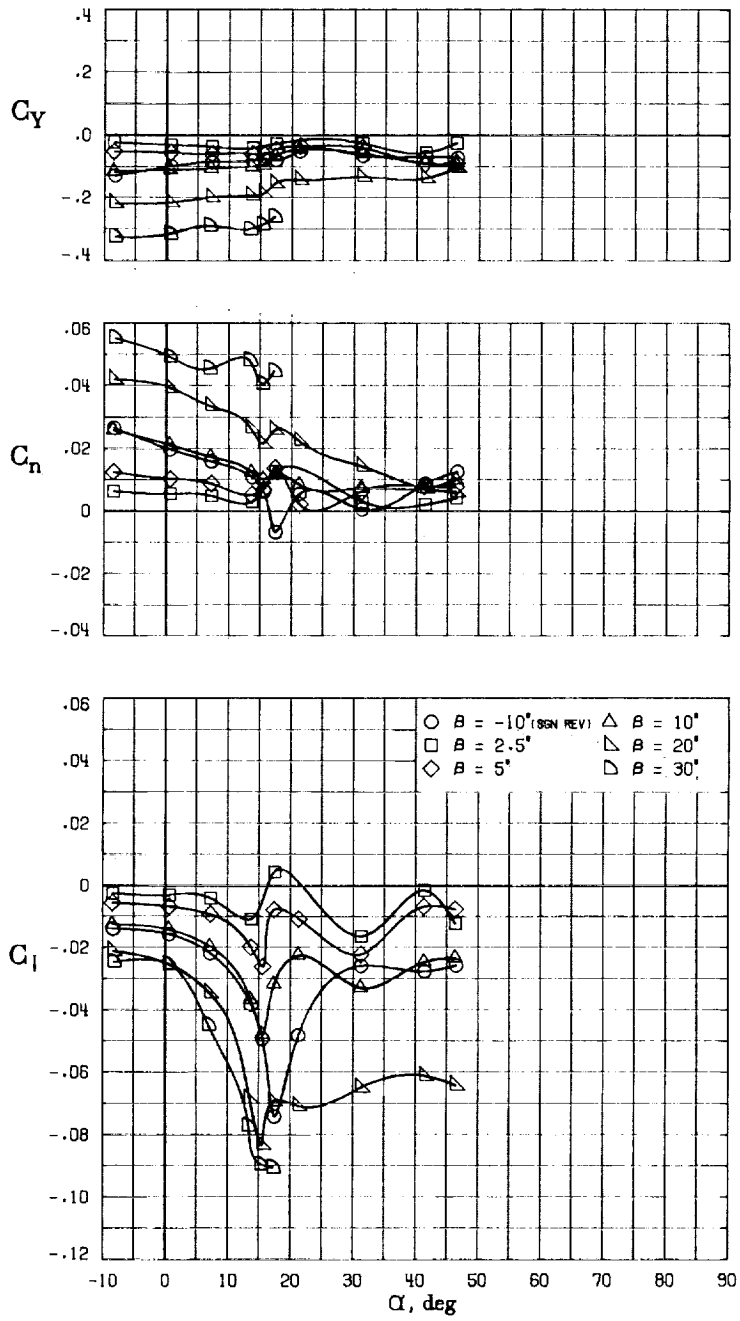

(D) LATERAL - DIRECTIONAL FORCE AND MOMENT COEFFICIENTS ABOUT BODY AXES.

FIGURE 14. - CONTINUED

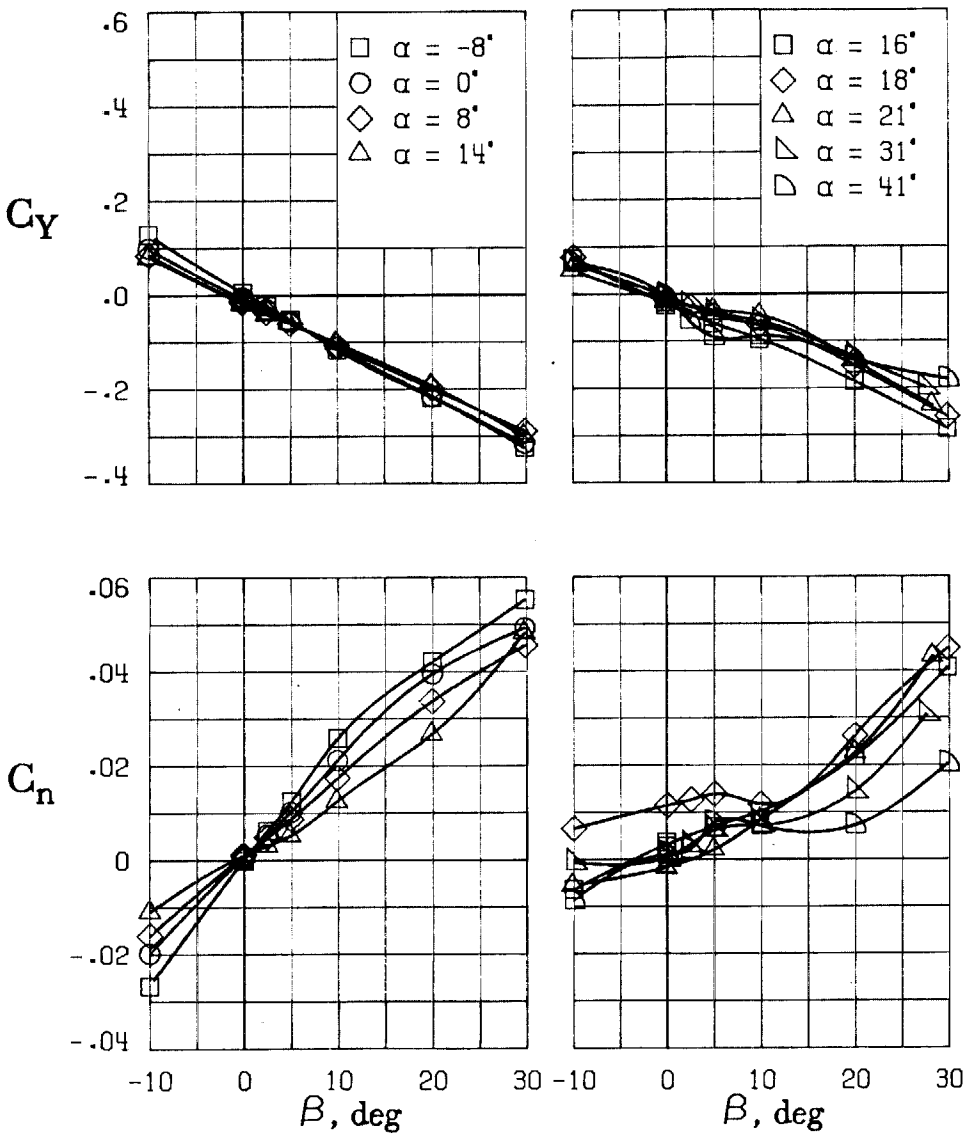

(E) DIRECTIONAL - STABILITY CHARACTERISTICS ABOUT BODY AXES AT VARIOUS ANGLES OF ATTACK.

FIGURE 14 CONTINUED

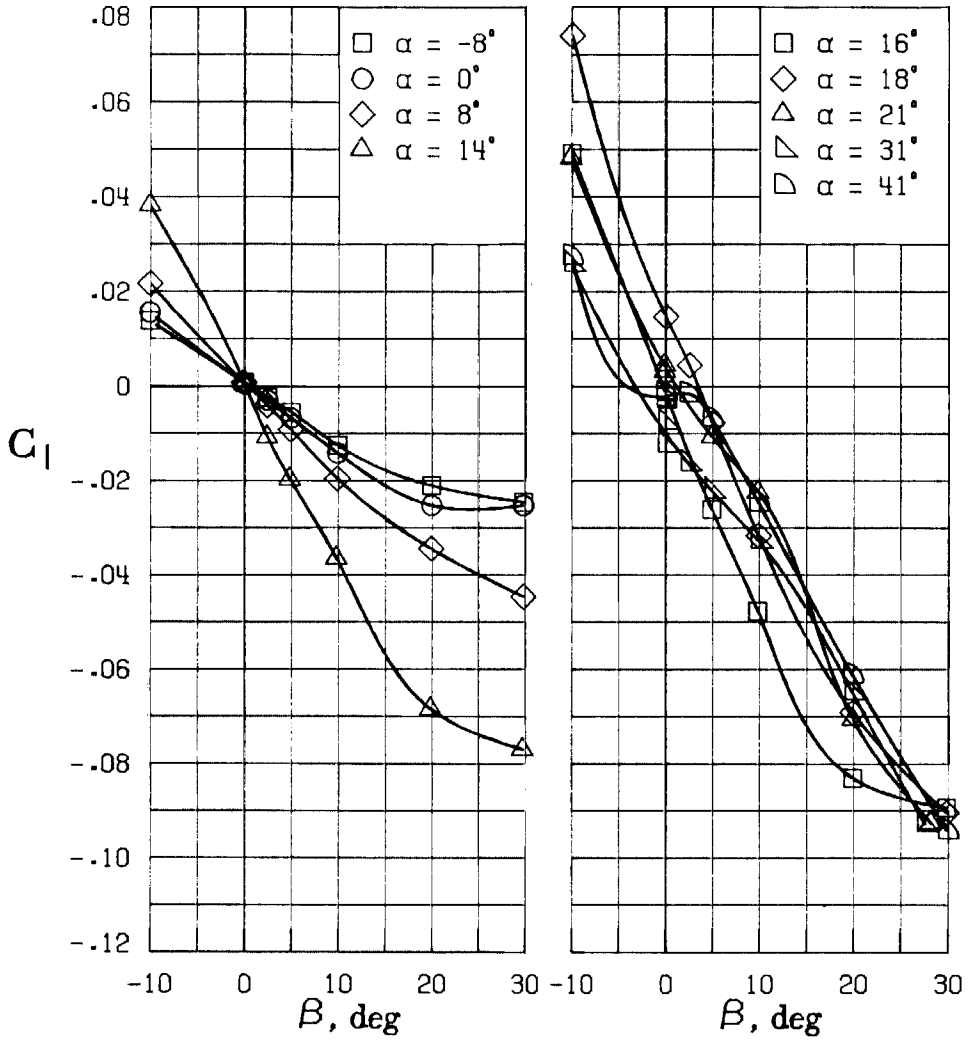

(F) LATERAL - STABILITY CHARACTERISTICS ABOUT BODY AXES AT VARIOUS ANGLES OF ATTACK.

FIGURE 14. - CONCLUDED.

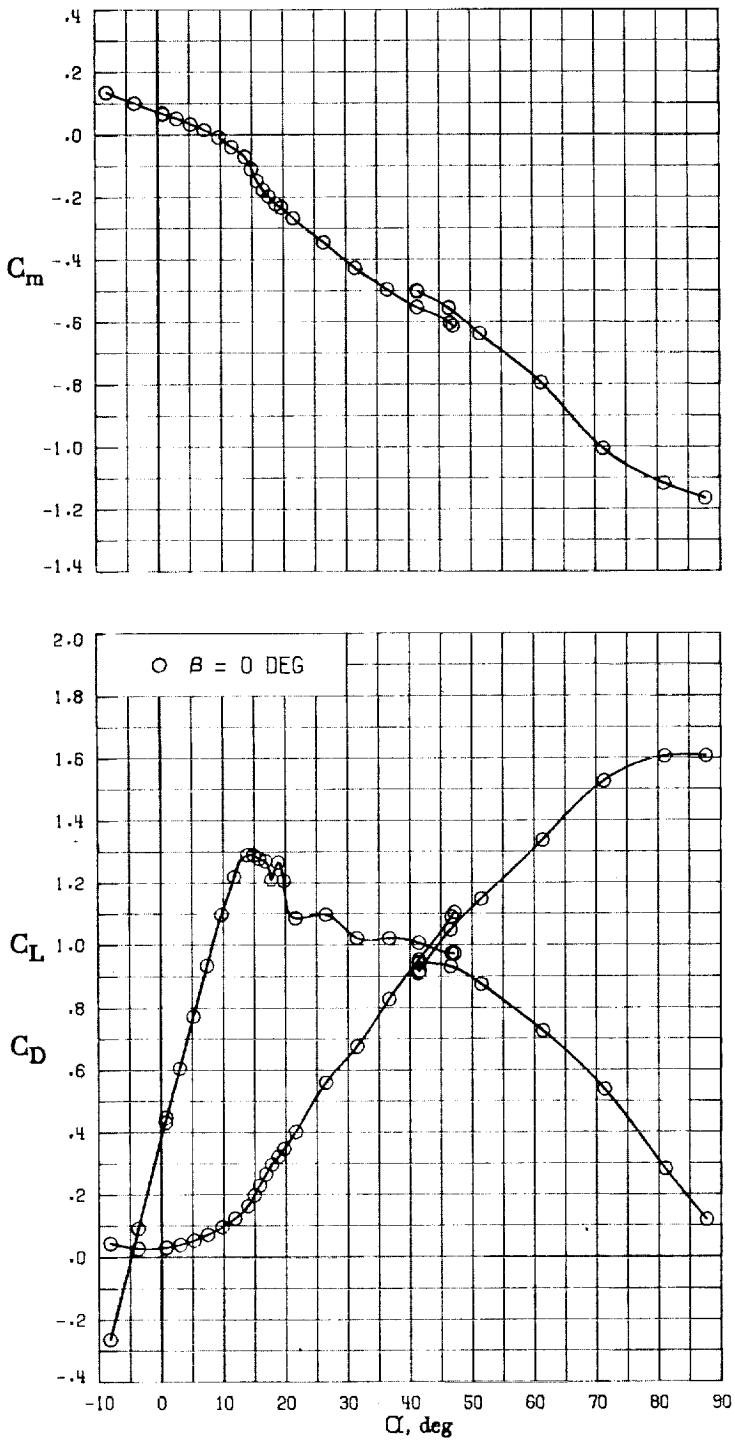

(A) LONGITUDINAL FORCE AND MOMENT COEFFICIENTS ABOUT STABILITY AXES.

FIGURE 15. - EFFECT OF ANGLE OF ATTACK AND SIDESLIP ANGLE ON AERODYNAMIC CHARACTERISTICS AT RE = 3.45 E+06 FOR CONFIGURATION B W1 H3 V. $\delta_E = 0°$, $\delta_A = 0°$, $\delta_R = 0°$.

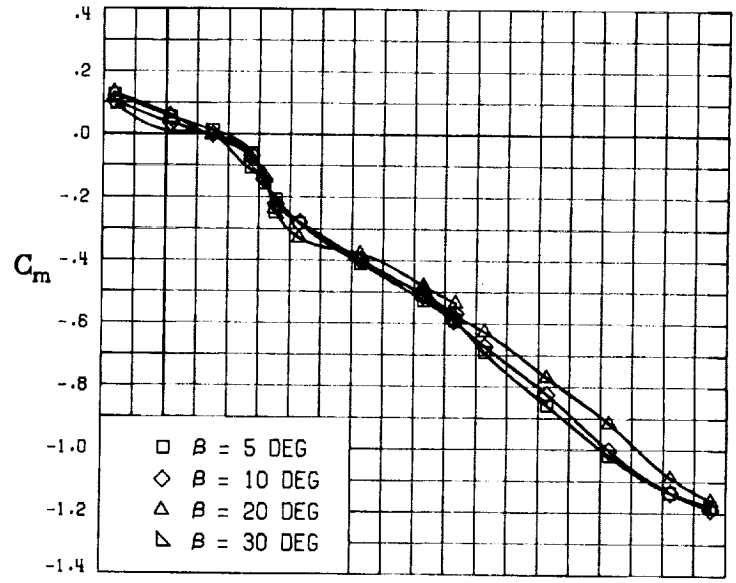

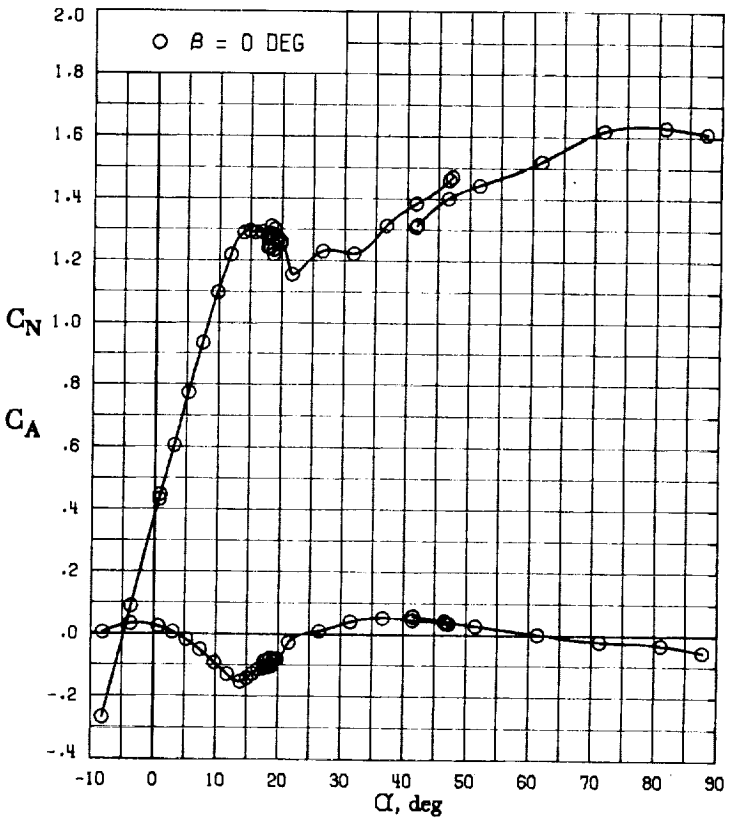

(B) LONGITUDINAL FORCE AND MOMENT COEFFICIENTS ABOUT BODY AXES.

FIGURE 15. - CONTINUED

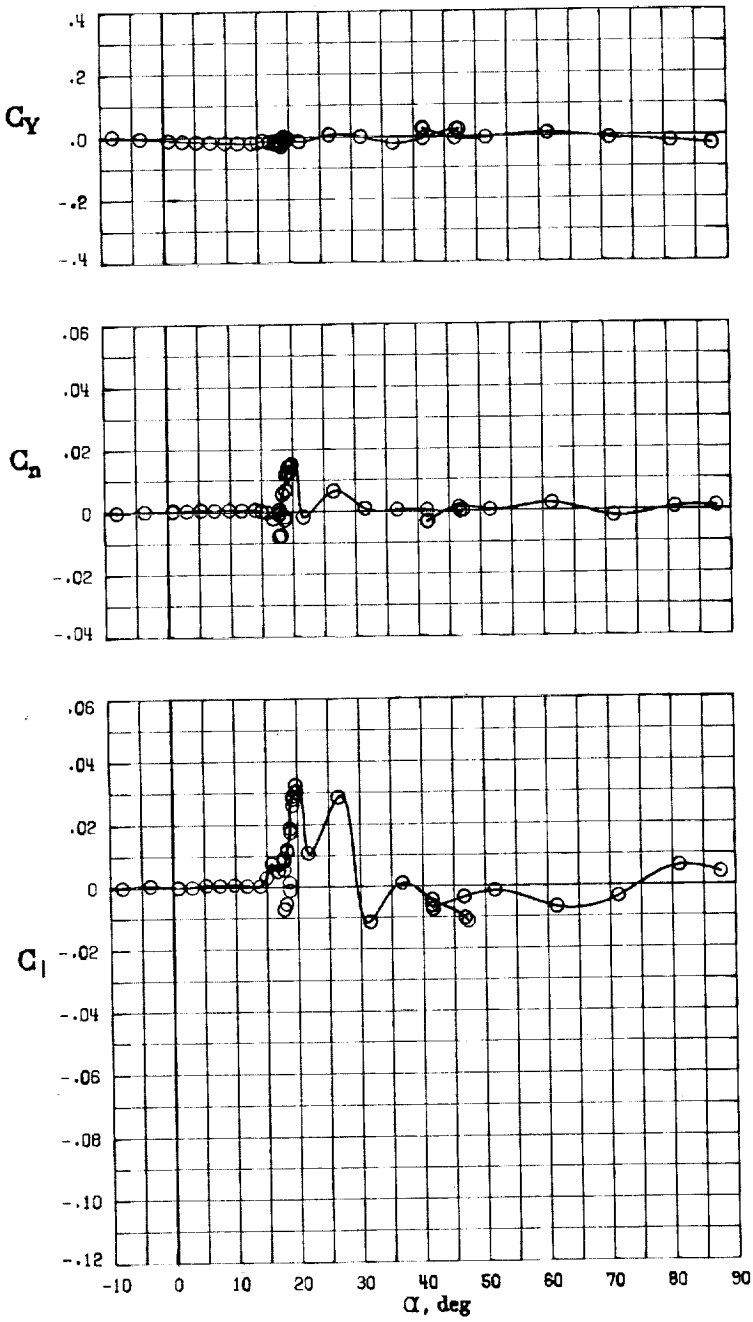

(C) LATERAL - DIRECTIONAL FORCE AND MOMENT COEFFICIENTS ABOUT BODY AXES AT ZERO SIDESLIP.

FIGURE 15. - CONTINUED

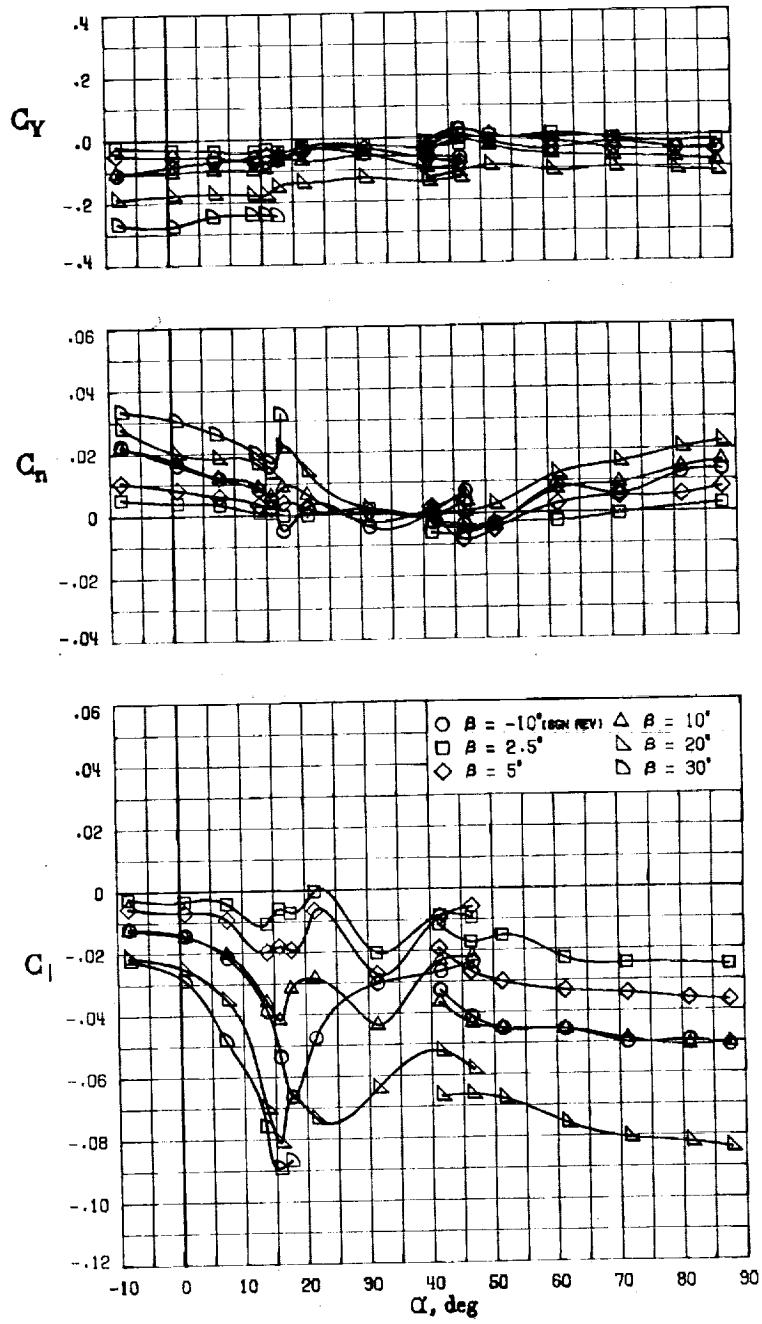

(D) LATERAL - DIRECTIONAL FORCE AND MOMENT COEFFICIENTS ABOUT BODY AXES.

FIGURE 15. - CONTINUED

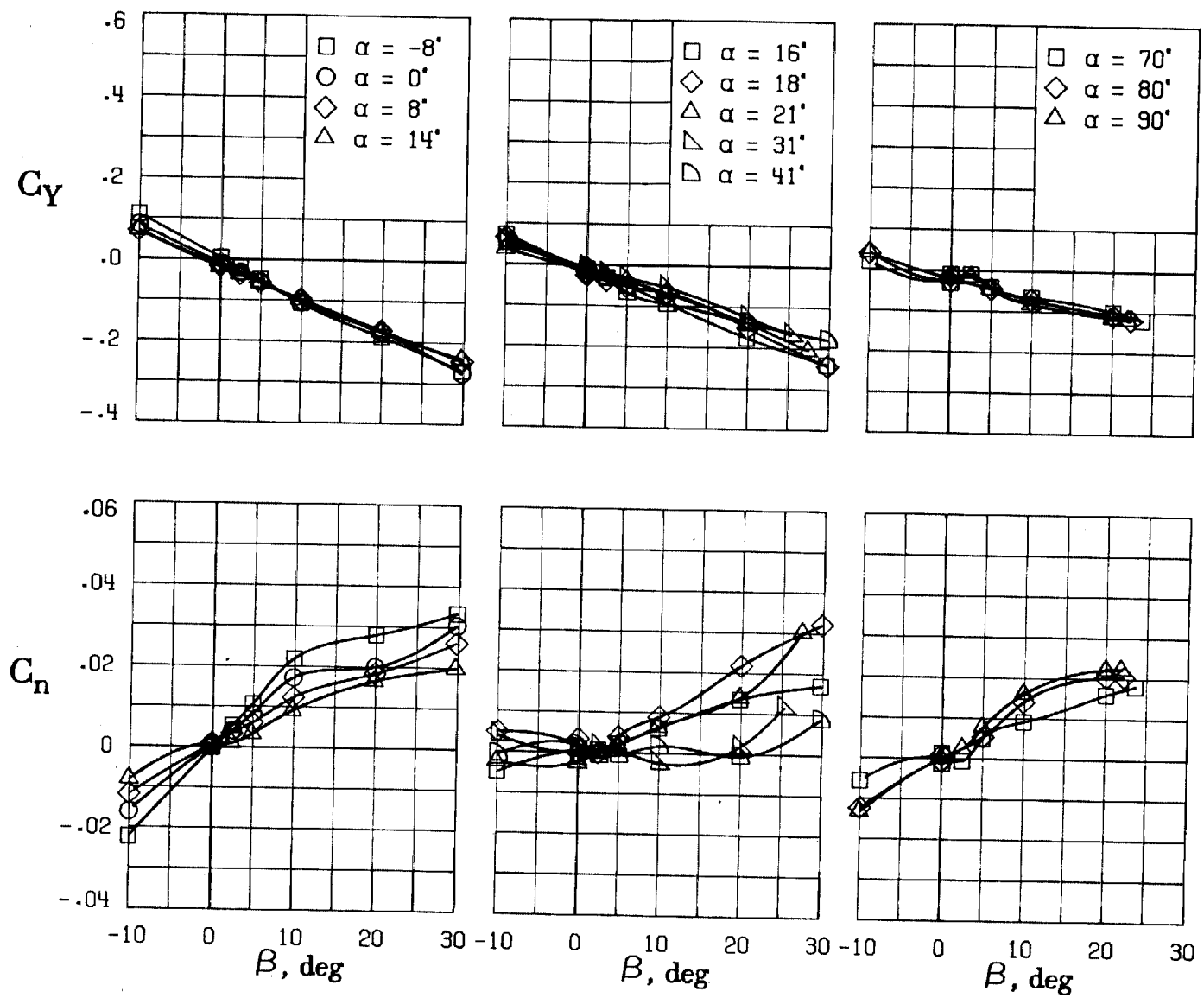

(E) DIRECTIONAL - STABILITY CHARACTERISTICS ABOUT BODY AXES AT VARIOUS ANGLES OF ATTACK.

FIGURE 15. - CONTINUED

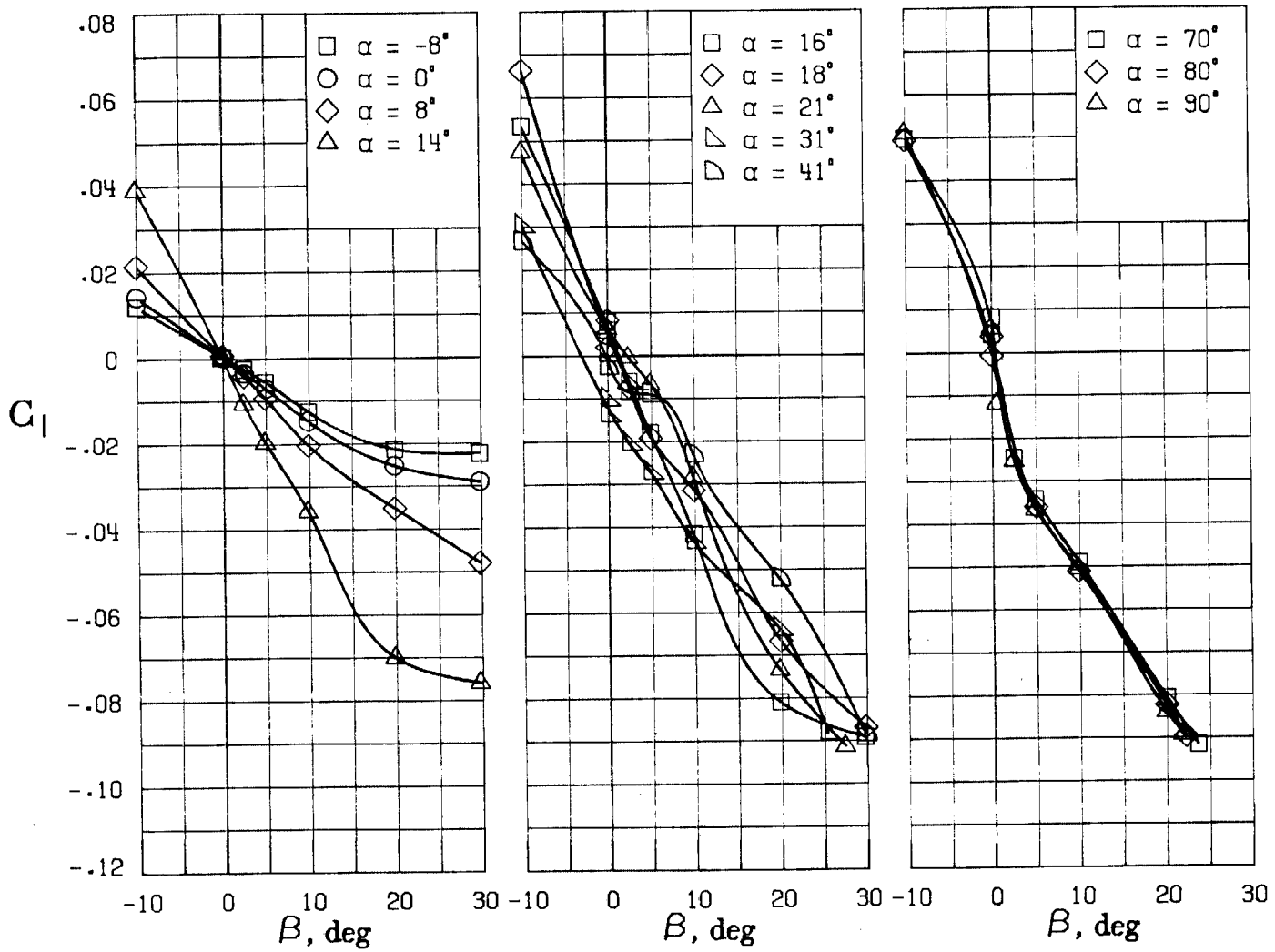

(F) LATERAL - STABILITY CHARACTERISTICS ABOUT BODY AXES AT VARIOUS ANGLES OF ATTACK.

FIGURE 15. - CONCLUDED.

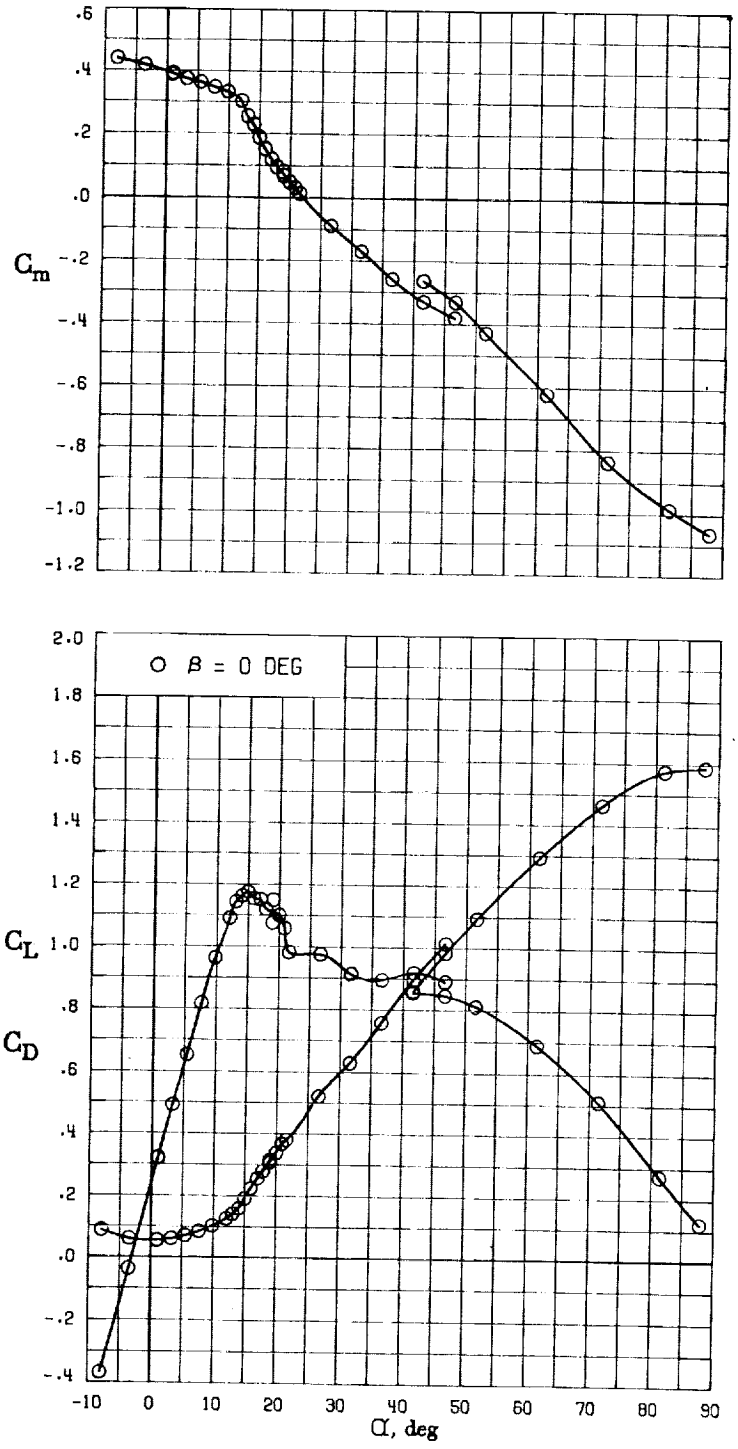

(A) LONGITUDINAL FORCE AND MOMENT COEFFICIENTS ABOUT STABILITY AXES.

FIGURE 16. - EFFECT OF ANGLE OF ATTACK AND SIDESLIP ANGLE ON AERODYNAMIC CHARACTERISTICS AT RE = 3.45 E+06 FOR CONFIGURATION B W1 H3 V. $\delta_E = -25°$, $\delta_A = 0°$, $\delta_R = 0°$.

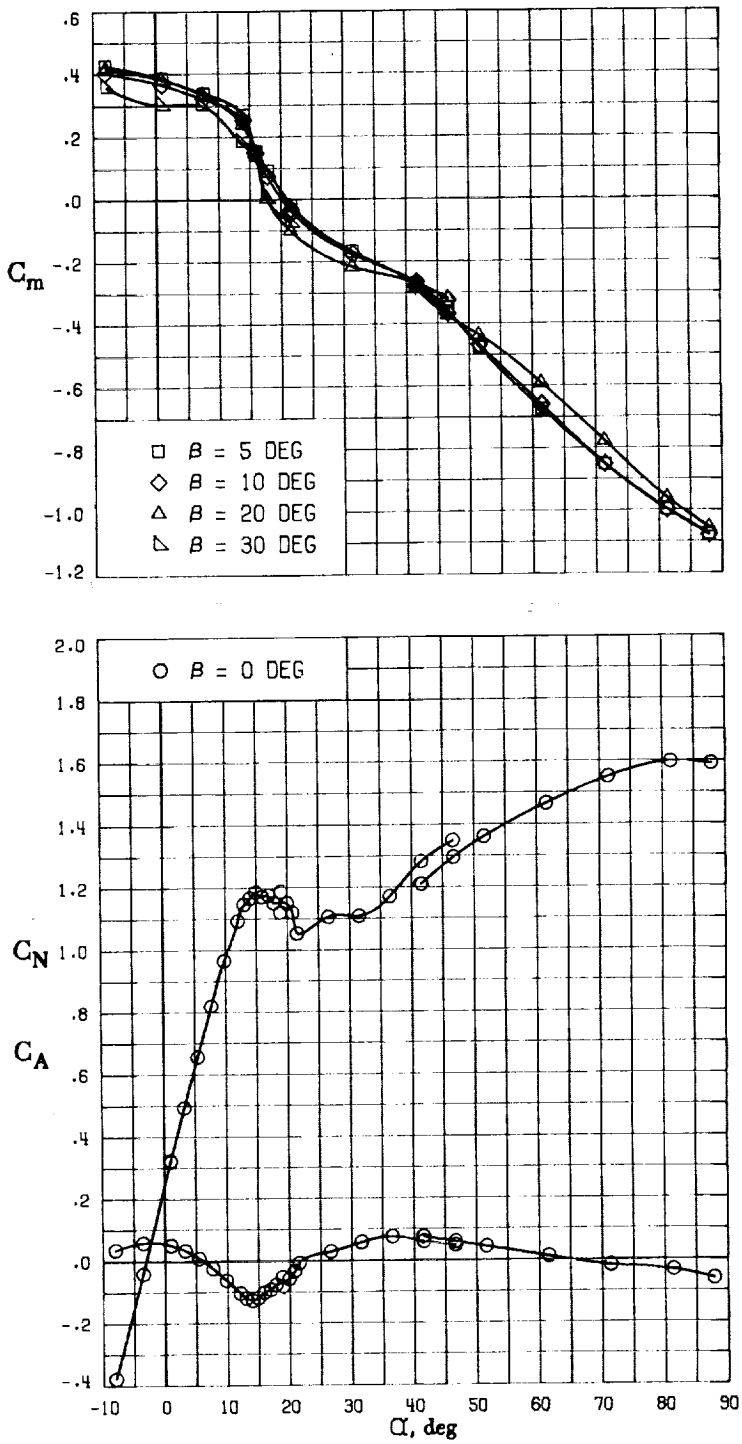

(B) LONGITUDINAL FORCE AND MOMENT COEFFICIENTS ABOUT BODY AXES.

FIGURE 16. - CONTINUED.

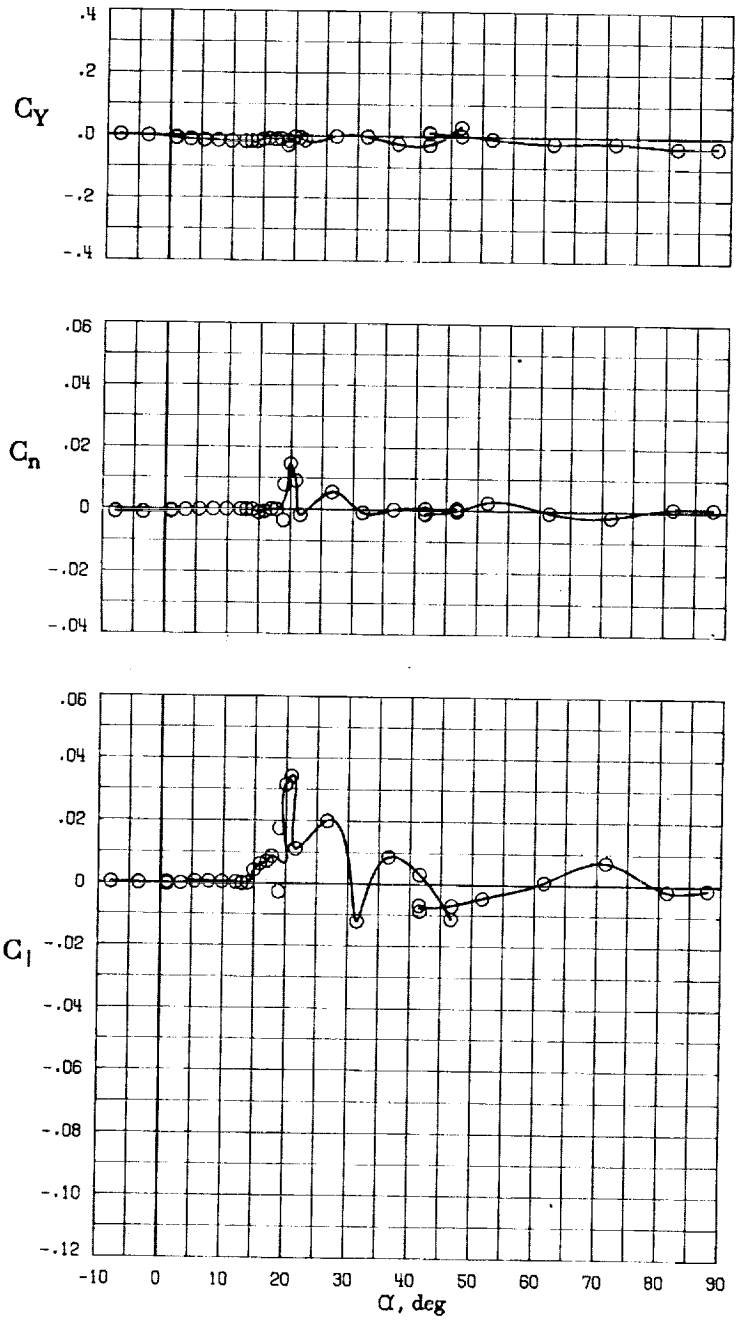

C) LATERAL - DIRECTIONAL FORCE AND MOMENT COEFFICIENTS ABOUT BODY AXES AT ZERO SIDESLIP.

FIGURE 16. - CONTINUED.

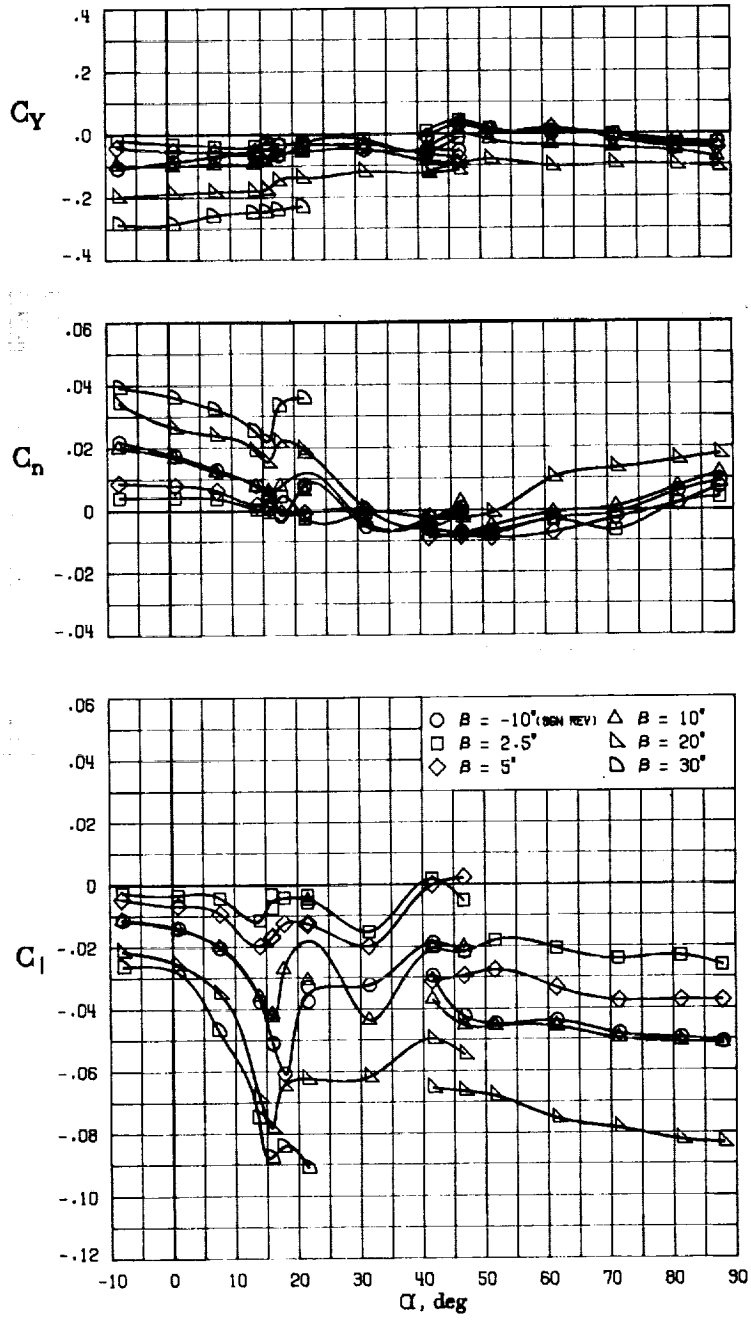

(D) LATERAL - DIRECTIONAL FORCE AND MOMENT COEFFICIENTS ABOUT BODY AXES.

FIGURE 16. - CONTINUED.

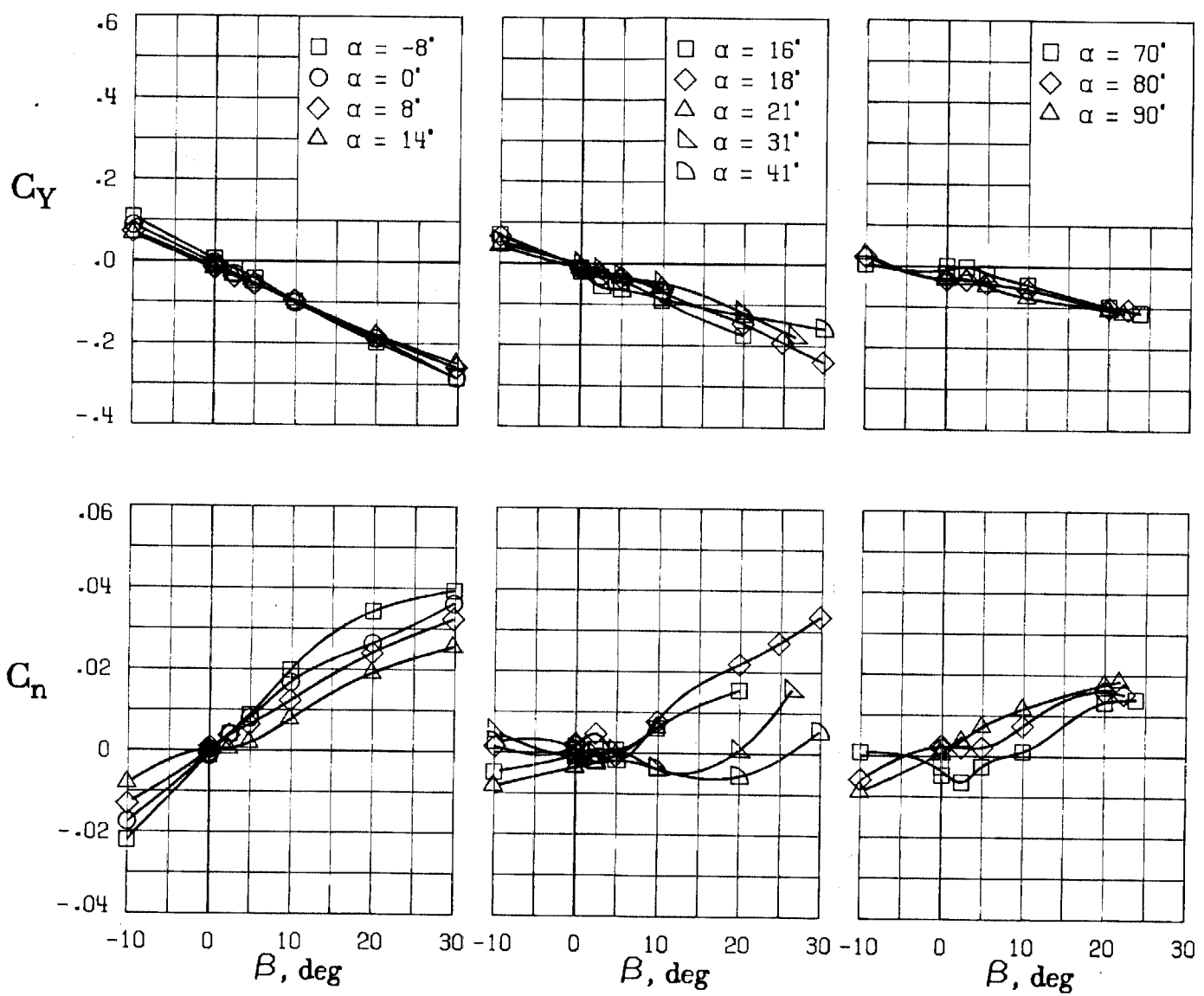

(E) DIRECTIONAL - STABILITY CHARACTERISTICS ABOUT BODY AXES AT VARIOUS ANGLES OF ATTACK.

FIGURE 16. - CONTINUED.

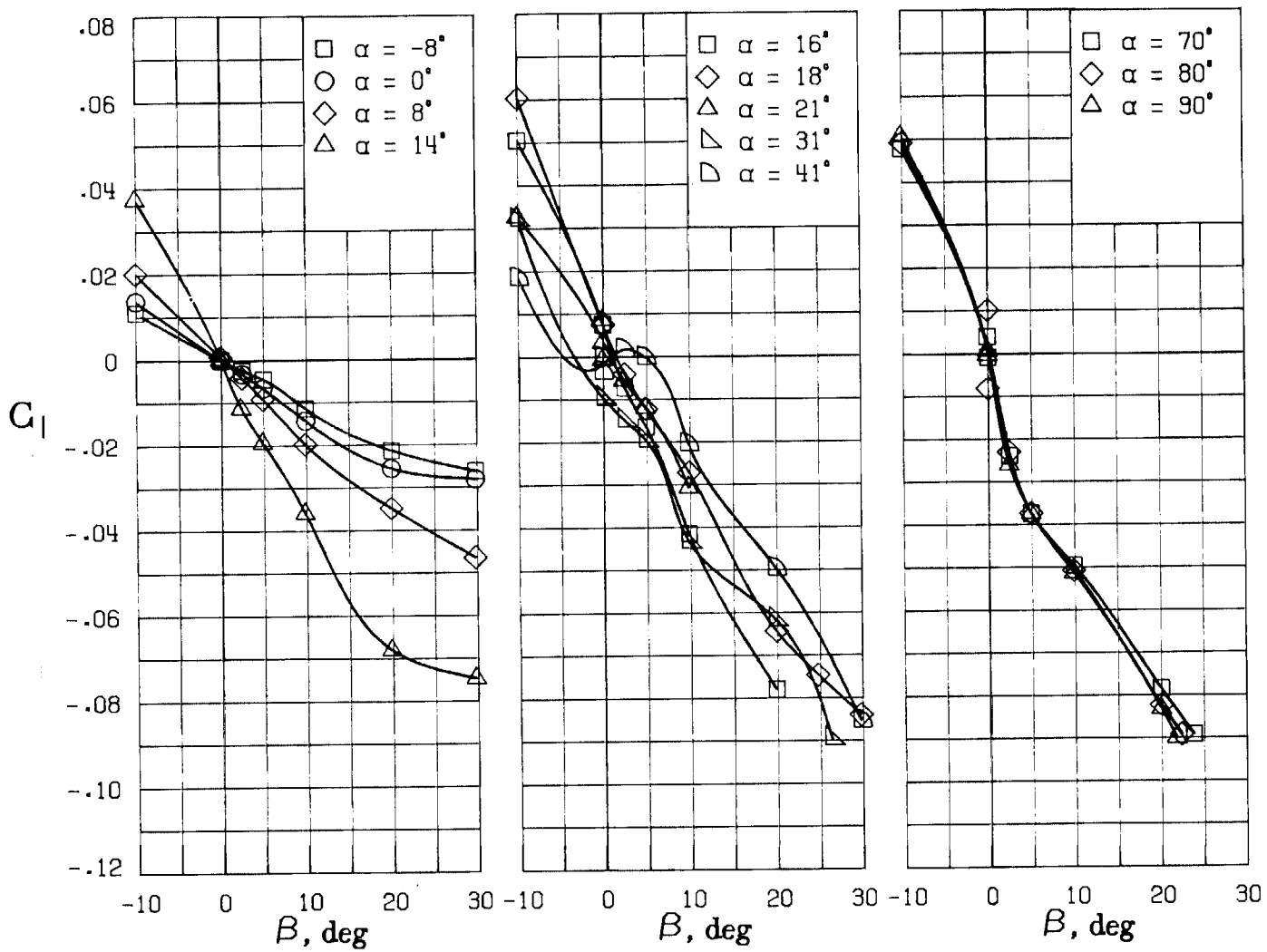

(F) LATERAL - STABILITY CHARACTERISTICS ABOUT BODY AXES AT VARIOUS ANGLES OF ATTACK.

FIGURE 16. - CONCLUDED.

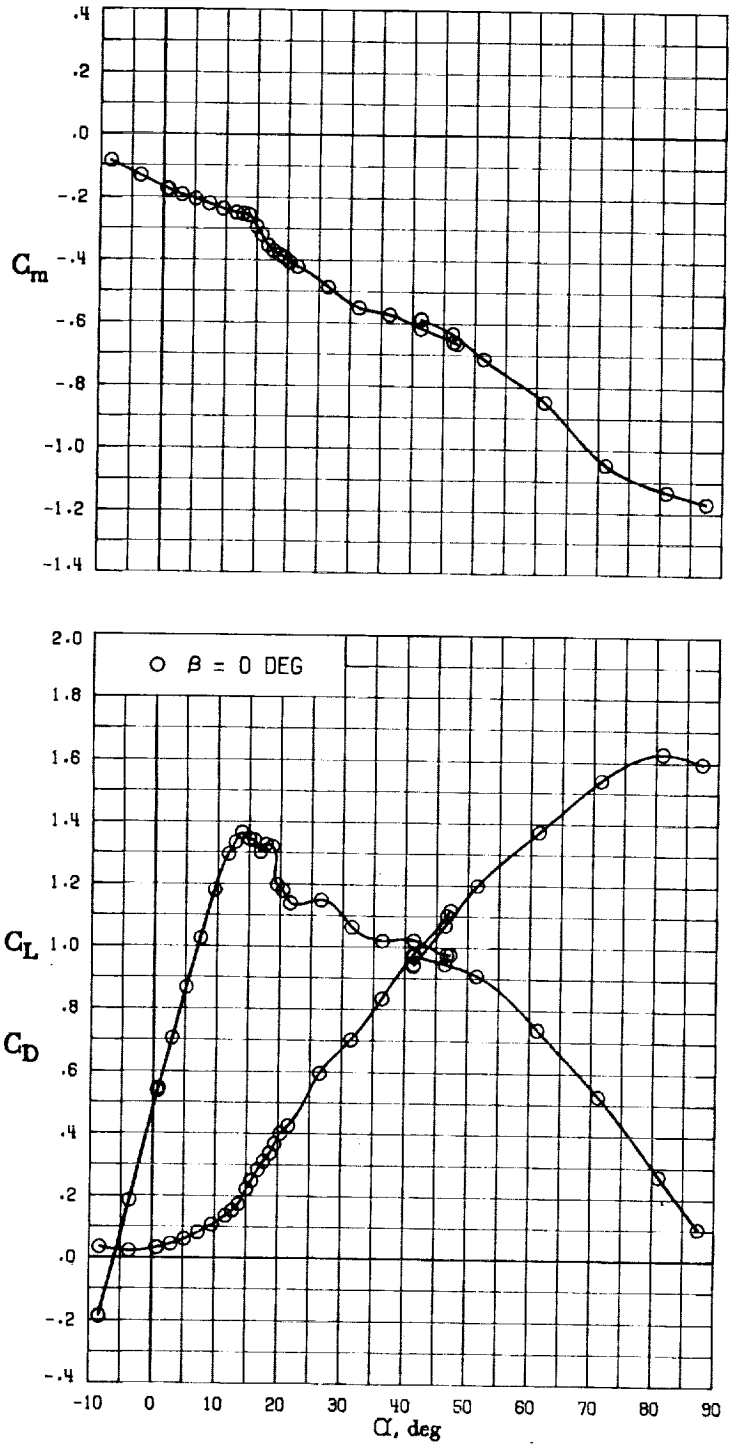

(A) LONGITUDINAL FORCE AND MOMENT COEFFICIENTS ABOUT STABILITY AXES.

FIGURE 17. - EFFECT OF ANGLE OF ATTACK AND SIDESLIP ANGLE ON AERODYNAMIC CHARACTERISTICS AT RE = 3.45 E+06 FOR CONFIGURATION B W1 H3 V. δ_E = 15°, δ_A = 0°, δ_R = 0°.

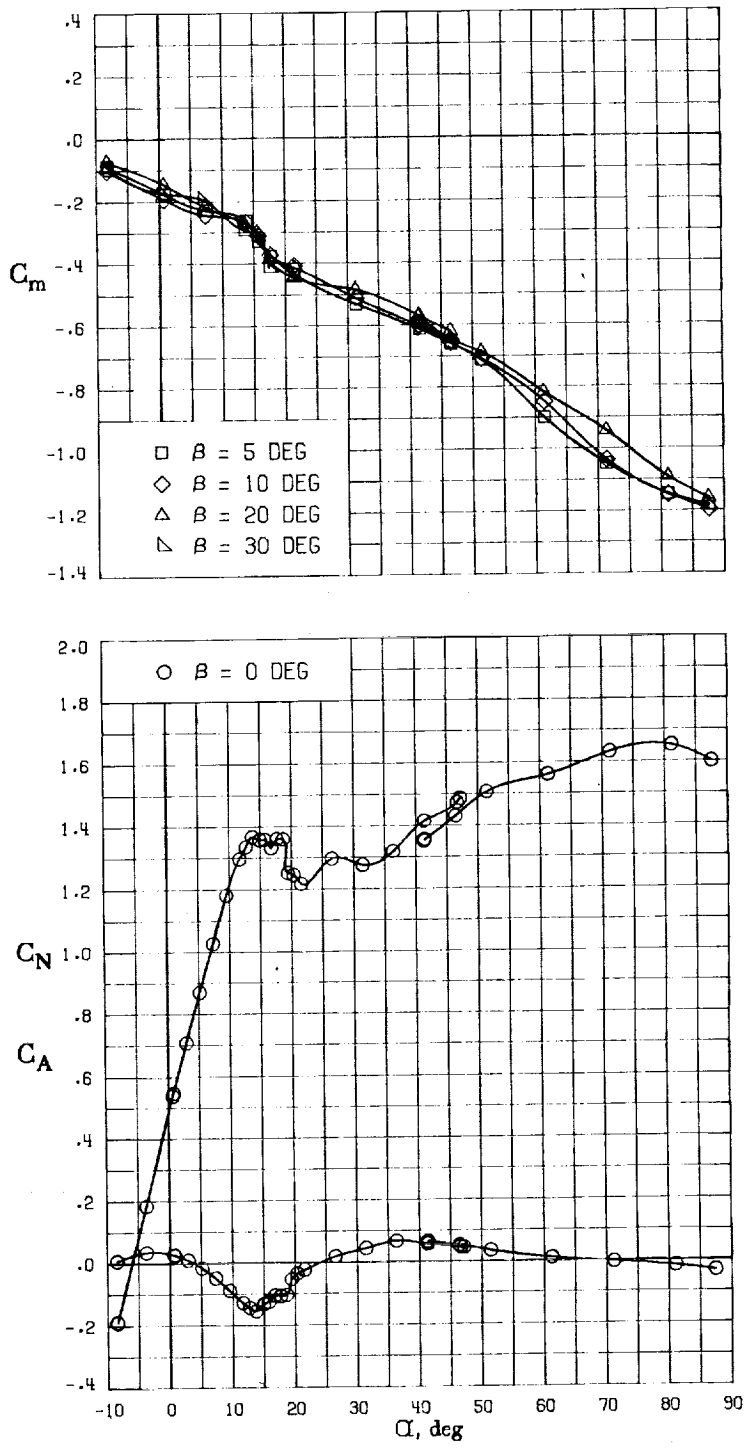

(B) LONGITUDINAL FORCE AND MOMENT COEFFICIENTS ABOUT BODY AXES.

FIGURE 17. - CONTINUED.

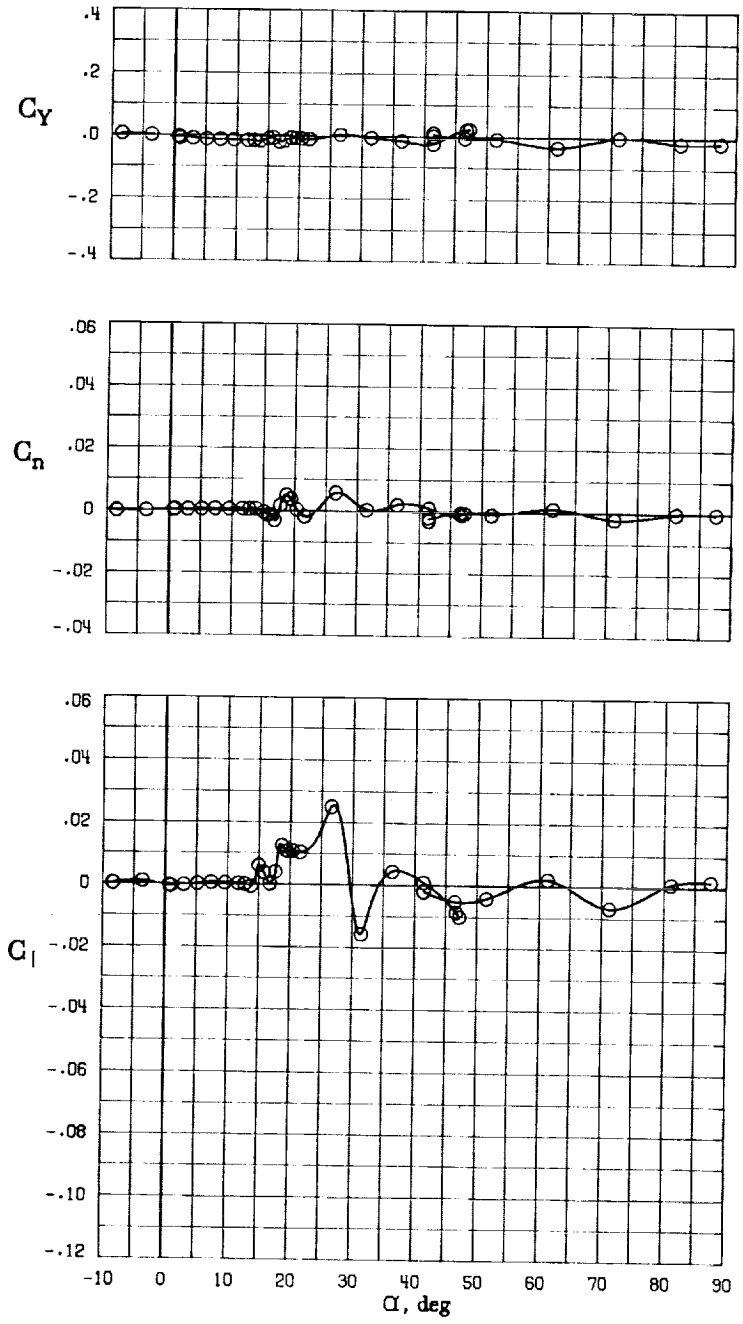

(C) LATERAL - DIRECTIONAL FORCE AND MOMENT COEFFICIENTS ABOUT BODY AXES AT ZERO SIDESLIP.

FIGURE 17. - CONTINUED.

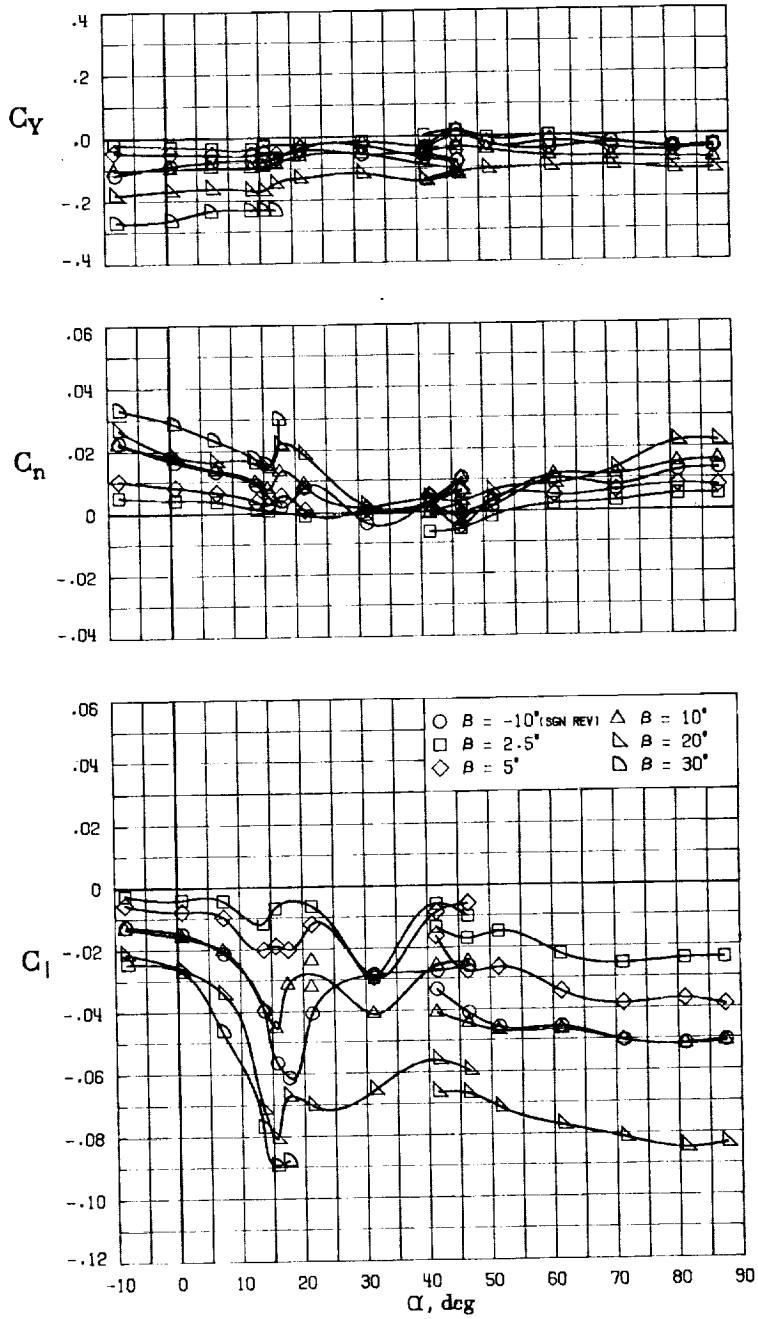

(D) LATERAL - DIRECTIONAL FORCE AND MOMENT COEFFICIENTS ABOUT BODY AXES.

FIGURE 17. - CONTINUED.

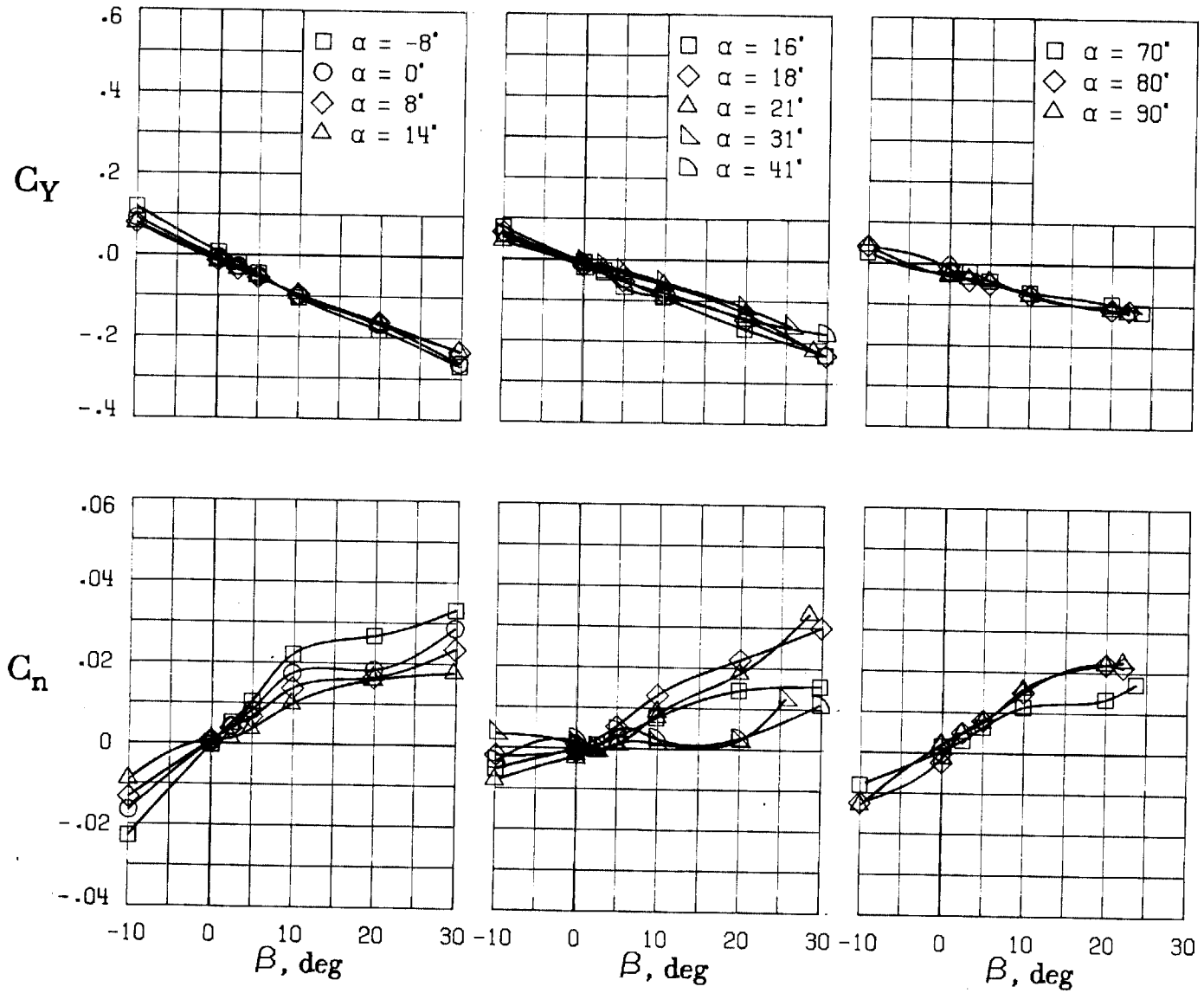

(E) DIRECTIONAL - STABILITY CHARACTERISTICS ABOUT BODY AXES AT VARIOUS ANGLES OF ATTACK.

FIGURE 17. - CONTINUED.

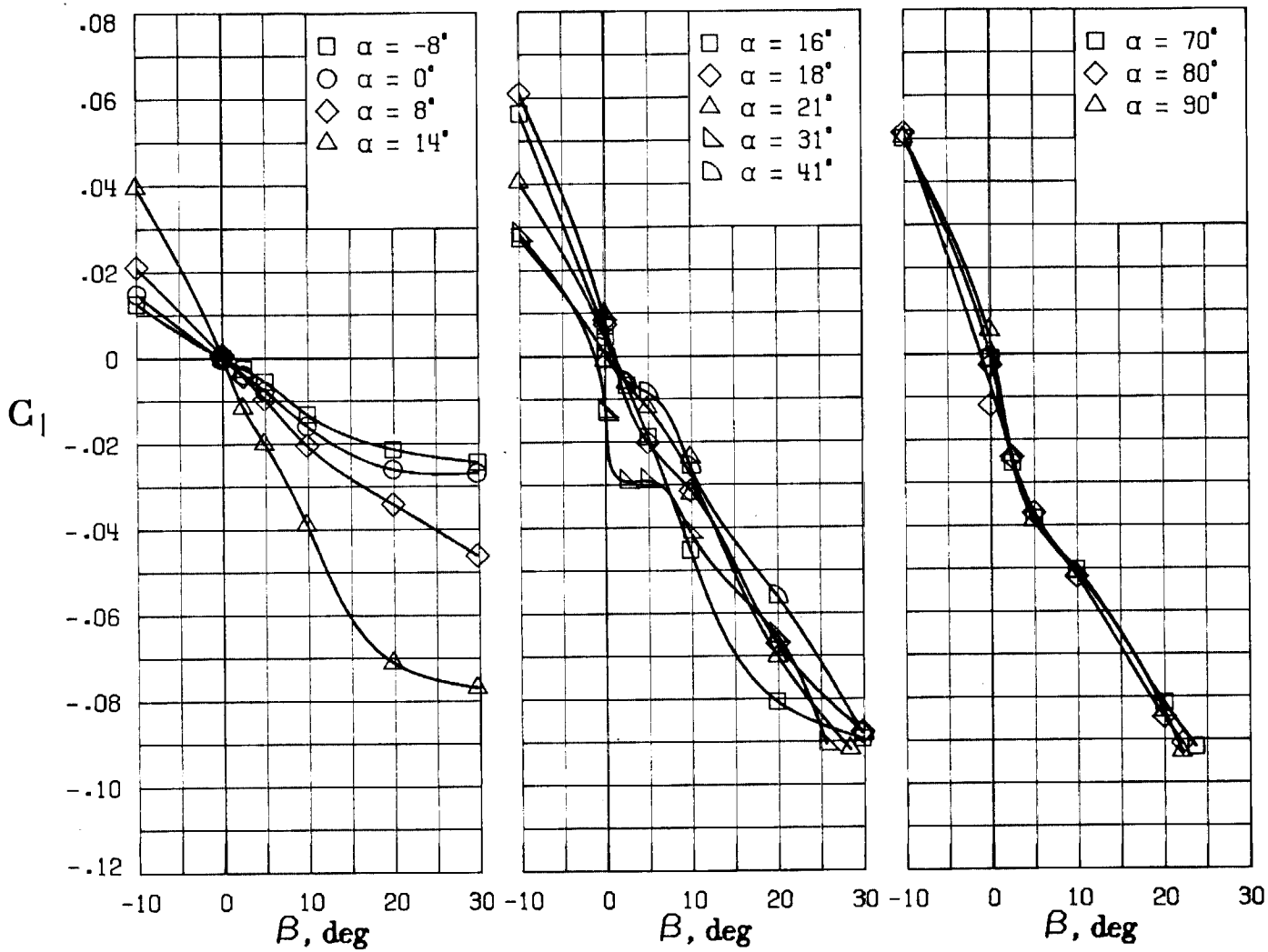

(F) LATERAL - STABILITY CHARACTERISTICS ABOUT BODY AXES AT VARIOUS ANGLES OF ATTACK.

FIGURE 17. - CONCLUDED.

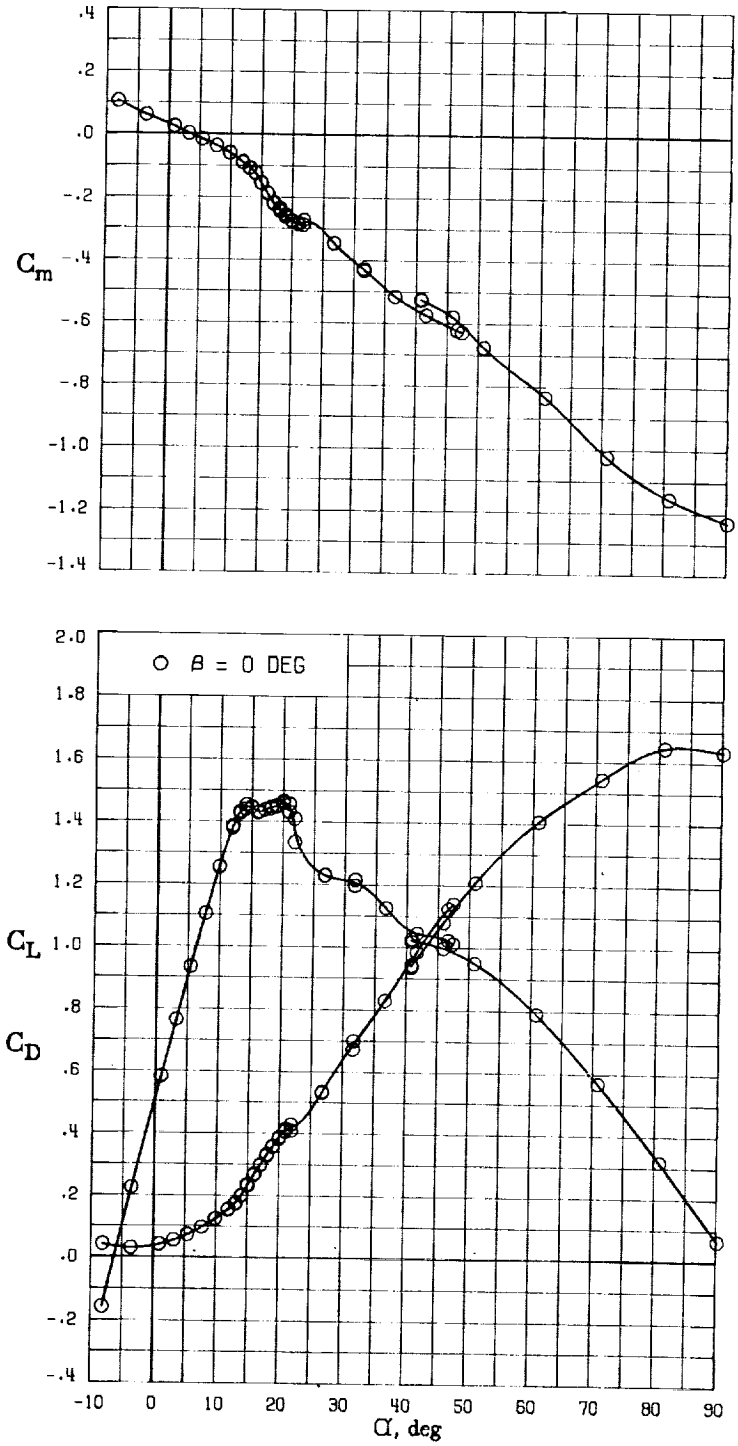

(A) LONGITUDINAL FORCE AND MOMENT COEFFICIENTS ABOUT STABILITY AXES.

FIGURE 18. - EFFECT OF ANGLE OF ATTACK AND SIDESLIP ANGLE ON AERODYNAMIC CHARACTERISTICS AT RE = 3.45 E+06 FOR CONFIGURATION B W2 H3 V. $\delta_E = 0°$, $\delta_A = 0°$, $\delta_R = 0°$.

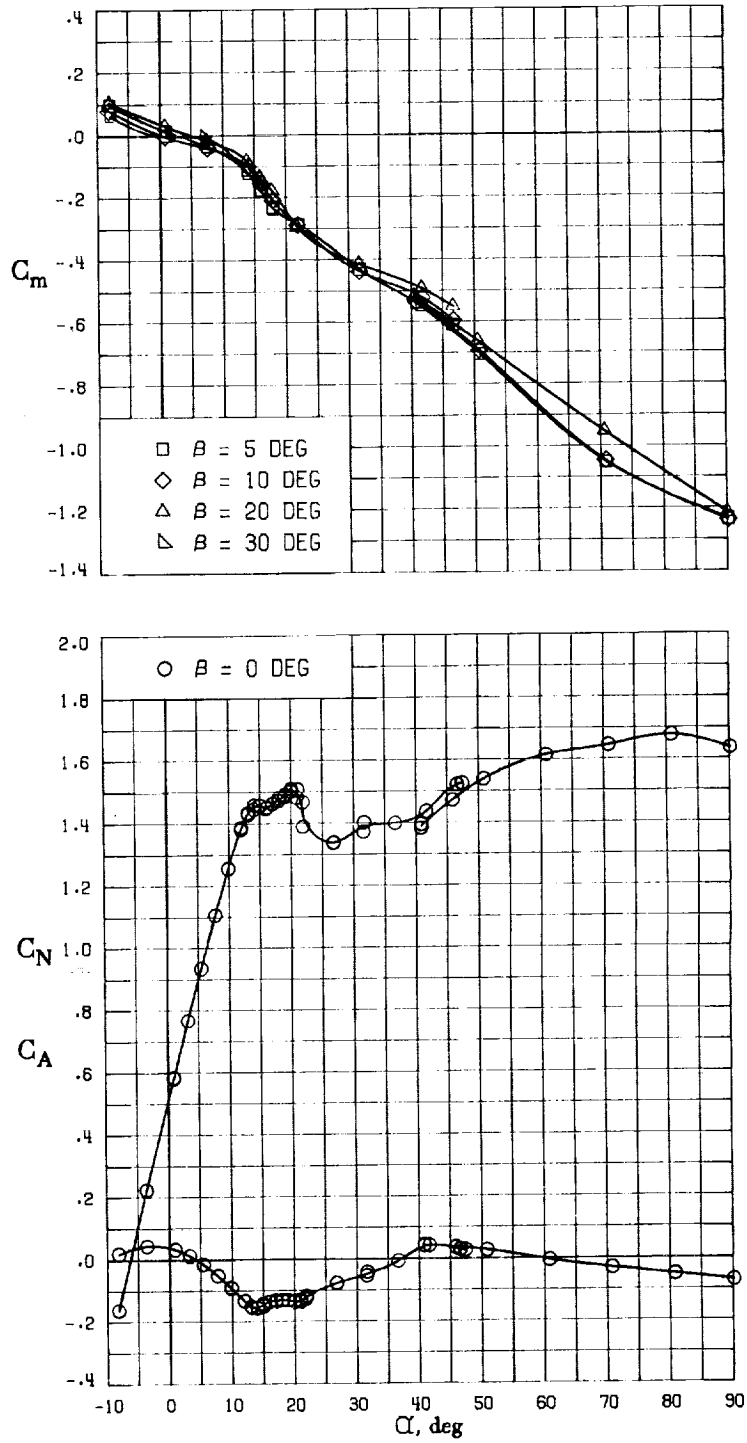

(B) LONGITUDINAL FORCE AND MOMENT COEFFICIENTS ABOUT BODY AXES.

FIGURE 18. - CONTINUED.

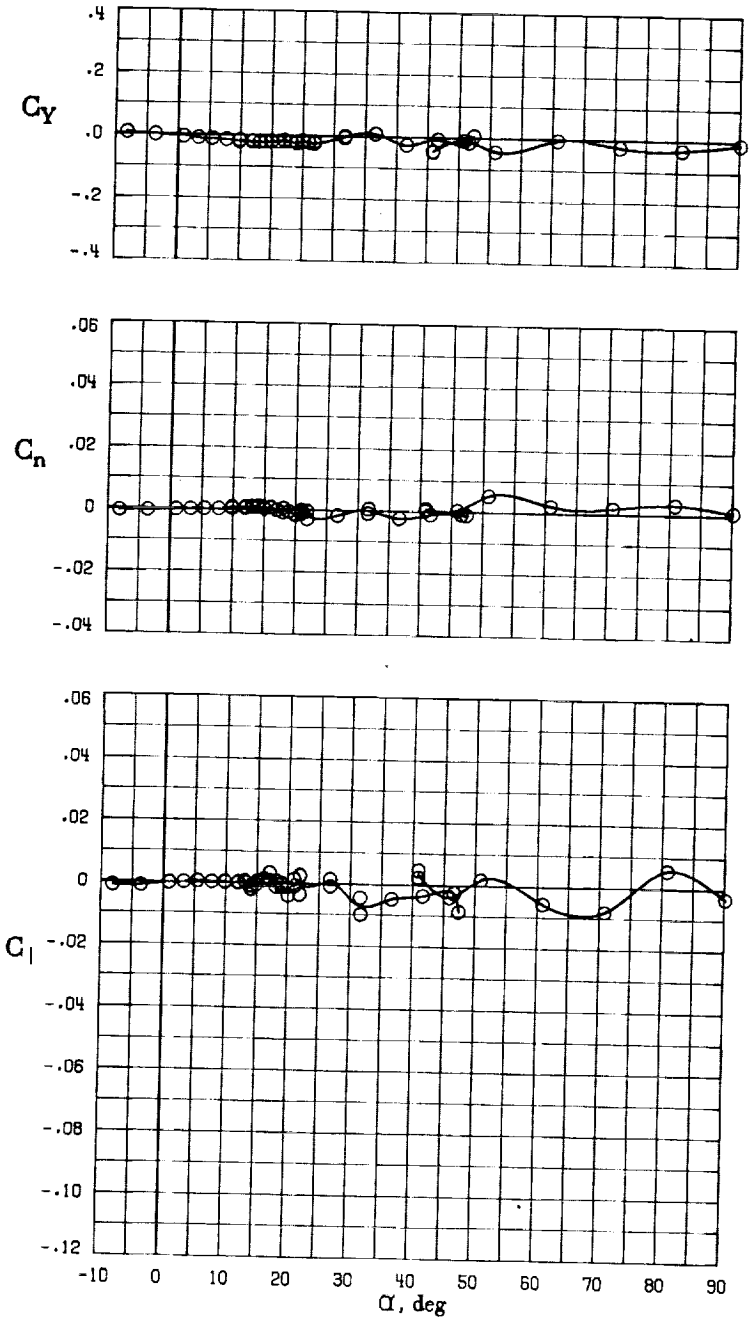

(C) LATERAL - DIRECTIONAL FORCE AND MOMENT COEFFICIENTS ABOUT BODY AXES AT ZERO SIDESLIP.

FIGURE 18. - CONTINUED.

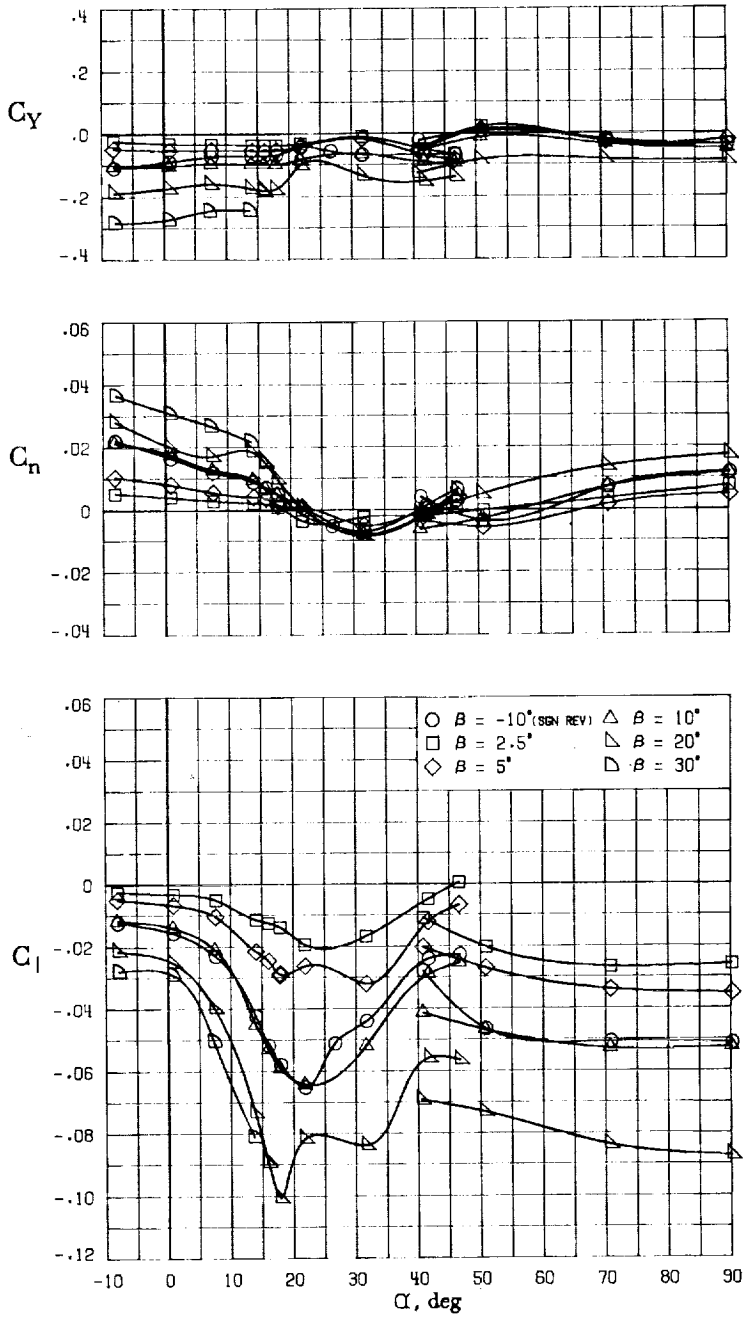

(D) LATERAL - DIRECTIONAL FORCE AND MOMENT COEFFICIENTS ABOUT BODY AXES.

FIGURE 18. - CONTINUED.

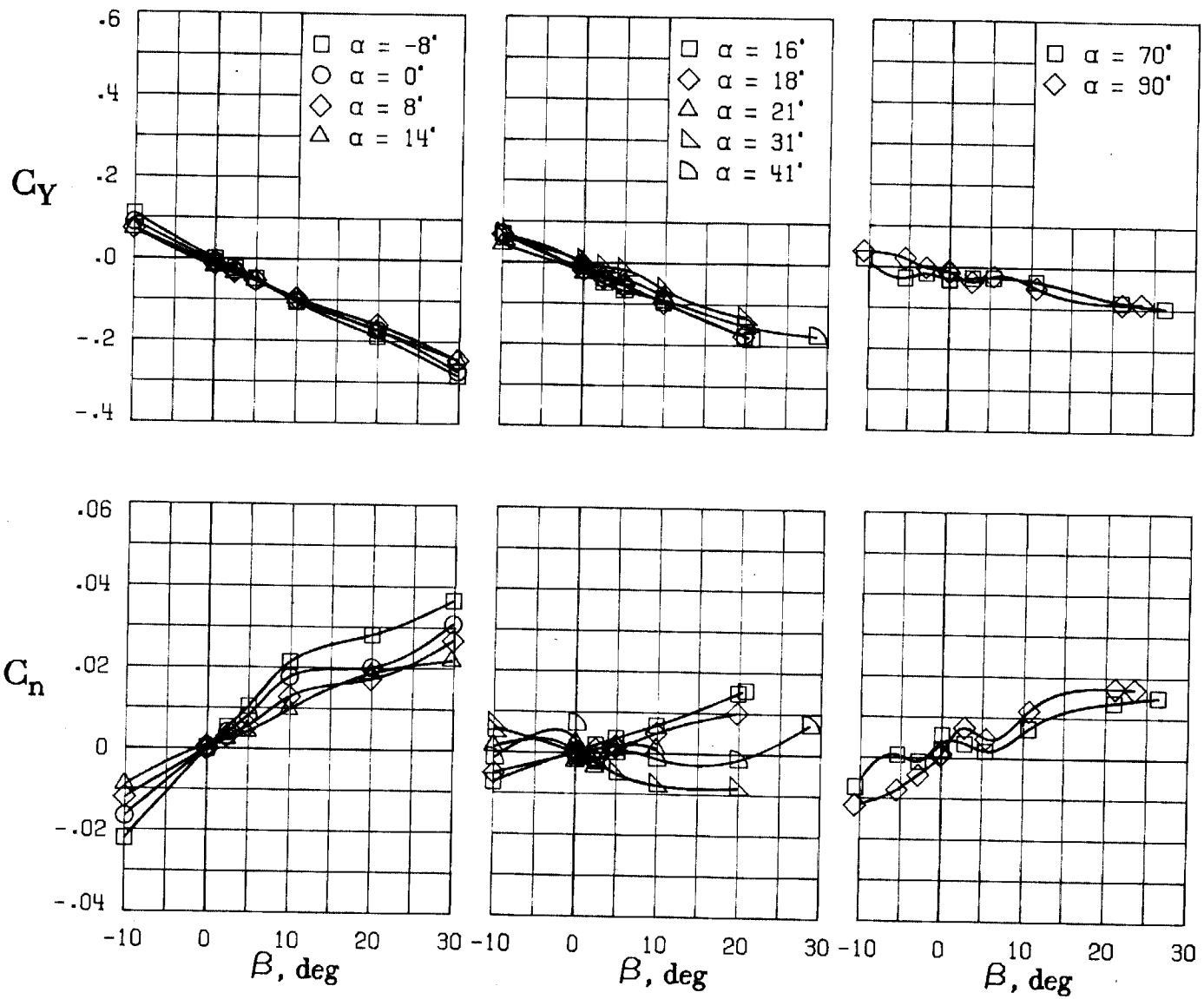

(E) DIRECTIONAL - STABILITY CHARACTERISTICS ABOUT BODY AXES AT VARIOUS ANGLES OF ATTACK.

FIGURE 18. - CONTINUED.

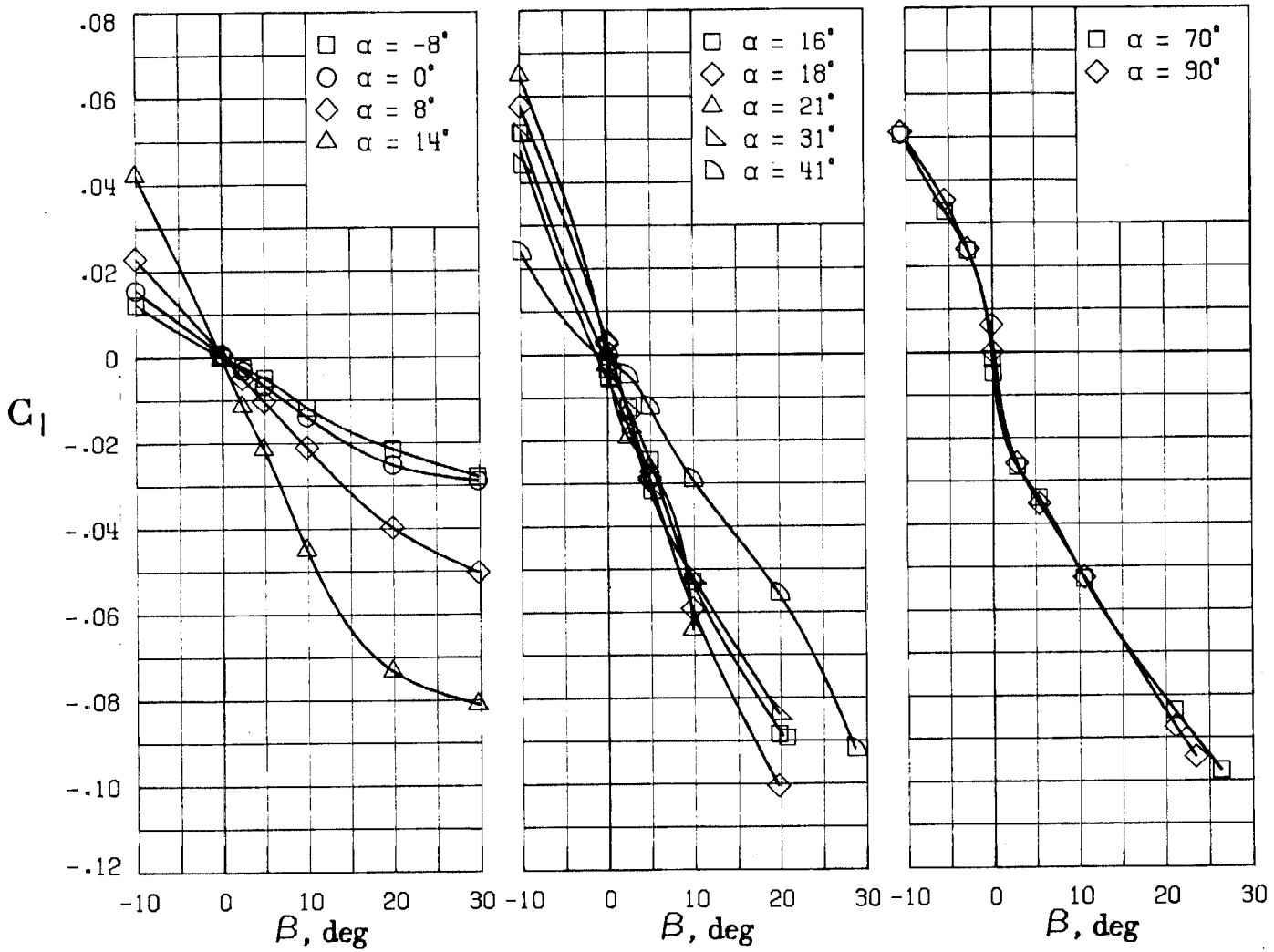

(F) LATERAL - STABILITY CHARACTERISTICS ABOUT BODY AXES AT VARIOUS ANGLES OF ATTACK.

FIGURE 18. - CONCLUDED.

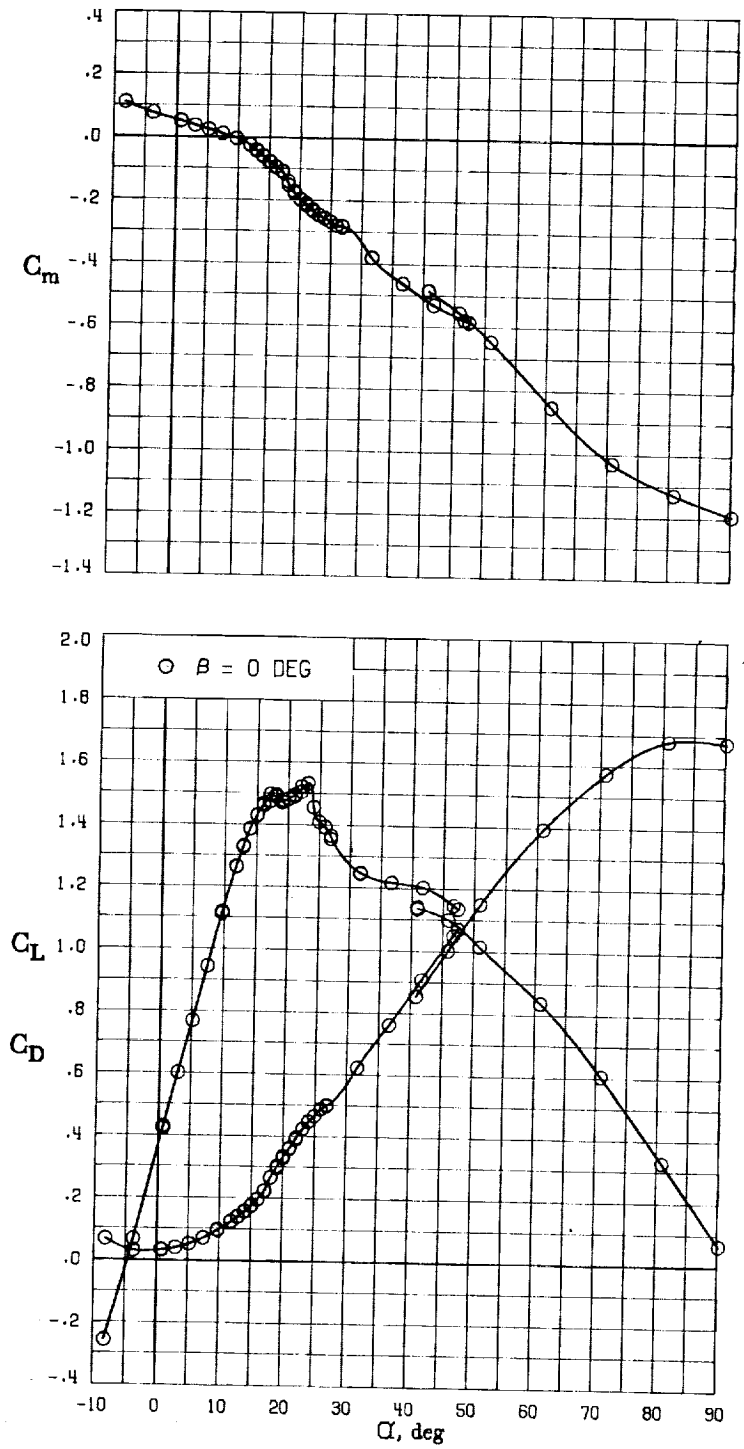

(A) LONGITUDINAL FORCE AND MOMENT COEFFICIENTS ABOUT STABILITY AXES.

FIGURE 19. - EFFECT OF ANGLE OF ATTACK AND SIDESLIP ANGLE ON AERODYNAMIC CHARACTERISTICS AT RE = 3.45 E+06 FOR CONFIGURATION B W3 H3 V. $\delta_E = 0°$, $\delta_A = 0°$, $\delta_R = 0°$.

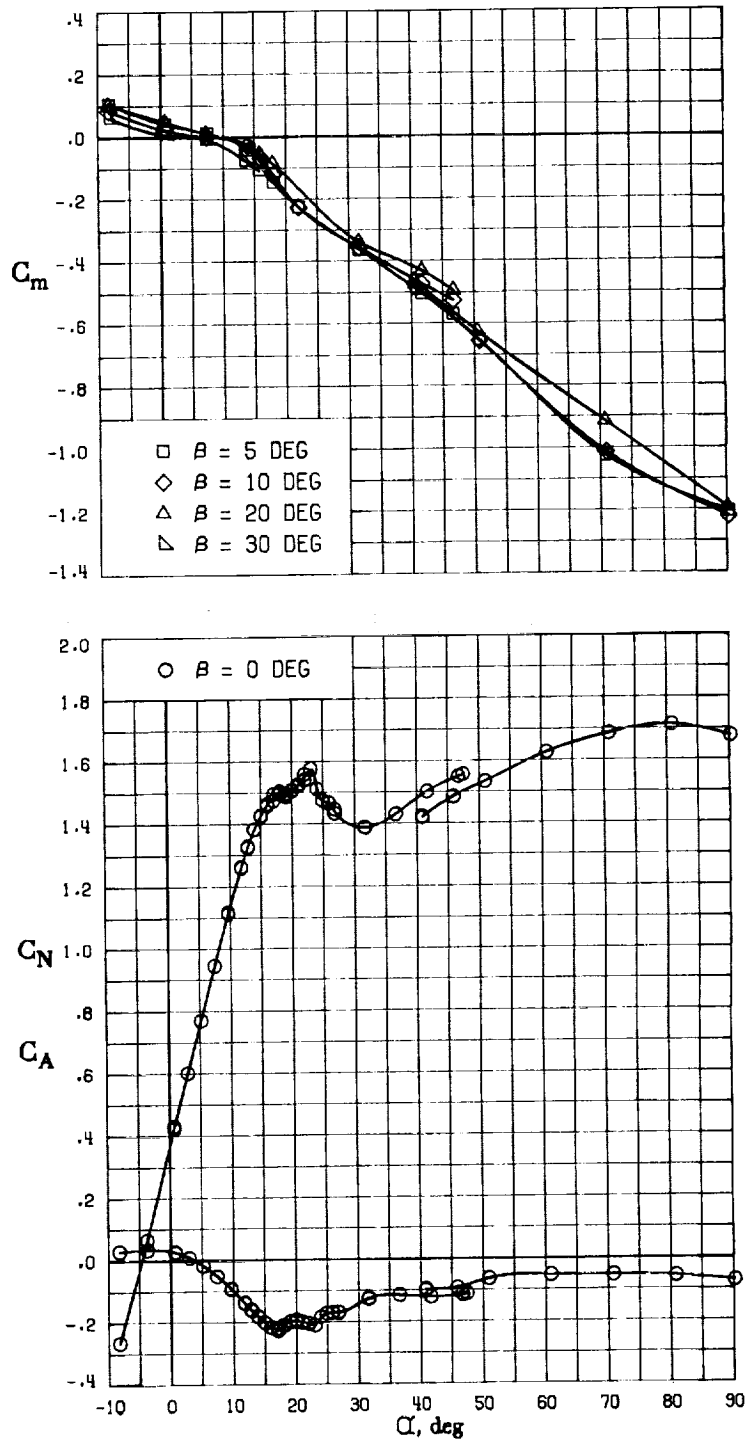

(B) LONGITUDINAL FORCE AND MOMENT COEFFICIENTS ABOUT BODY AXES.

FIGURE 19. - CONTINUED.

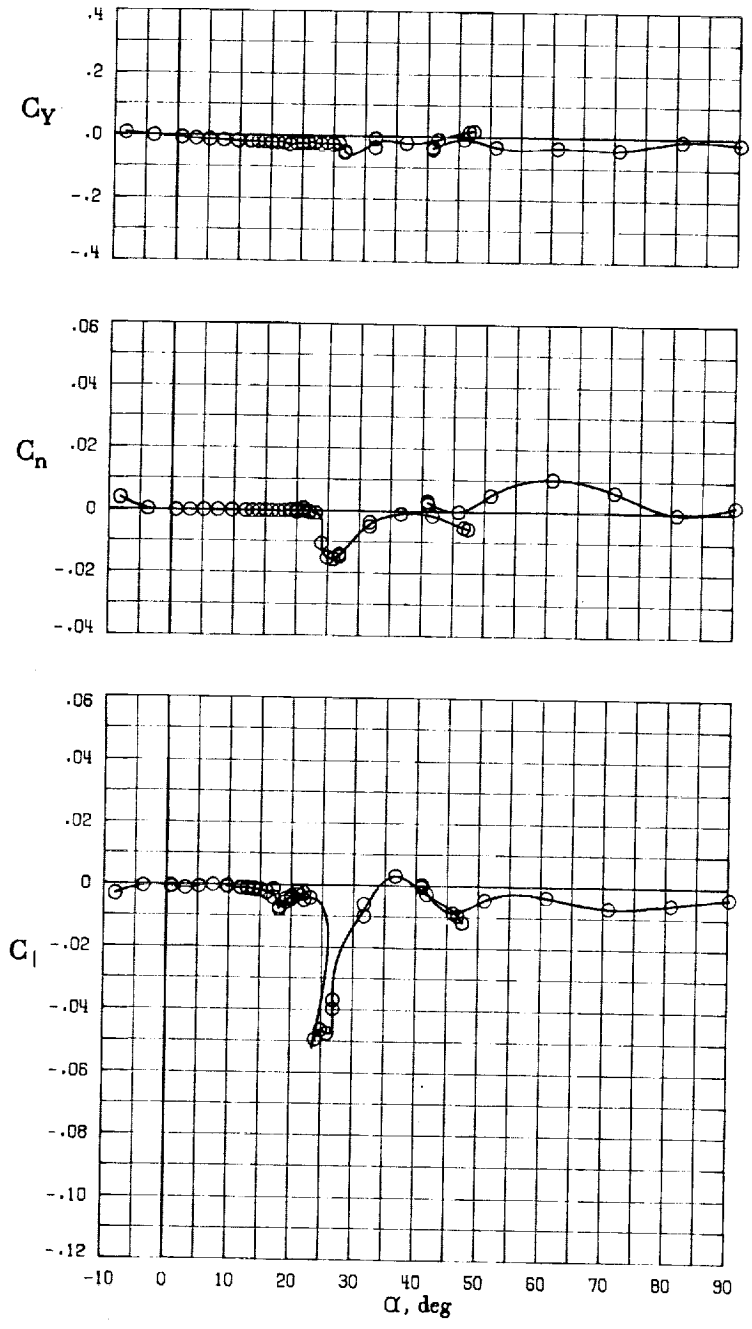

(C) LATERAL - DIRECTIONAL FORCE AND MOMENT COEFFICIENTS ABOUT BODY AXES AT ZERO SIDESLIP.

FIGURE 19. - CONTINUED.

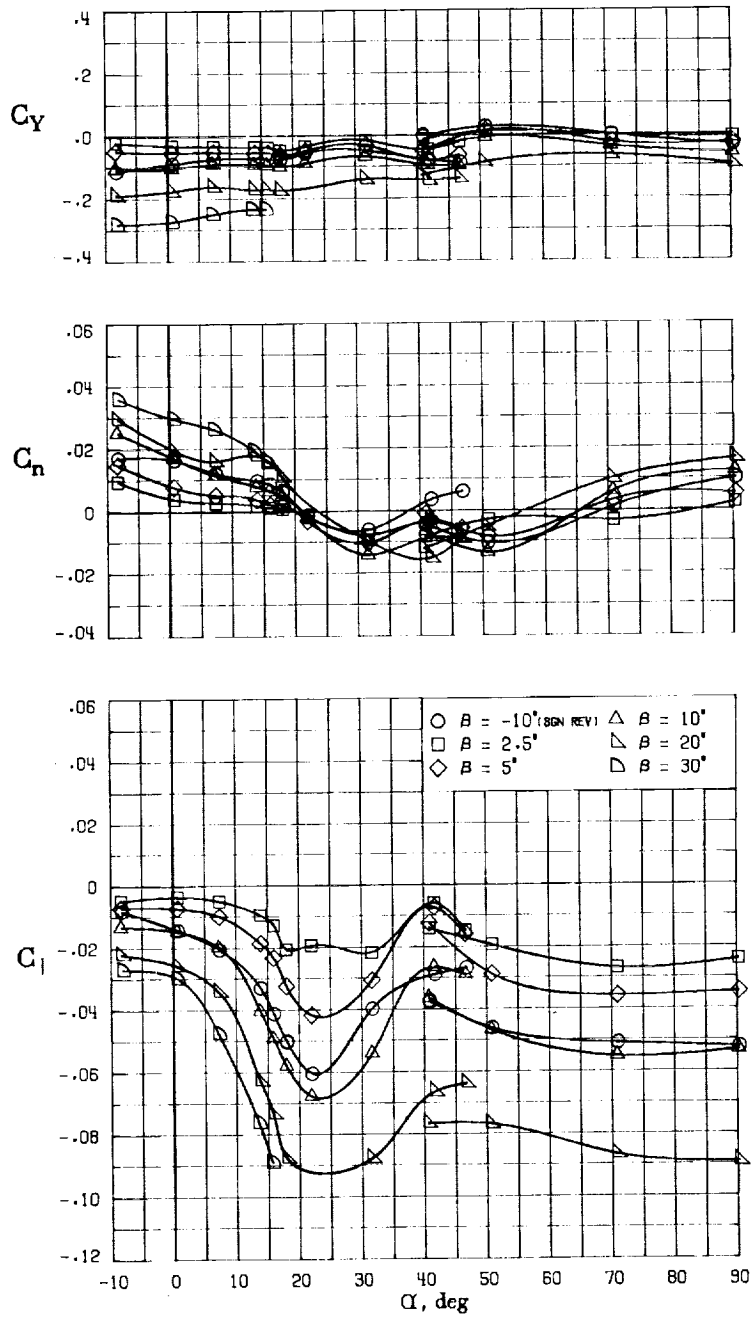

(D) LATERAL - DIRECTIONAL FORCE AND MOMENT COEFFICIENTS ABOUT BODY AXES.

FIGURE 19. - CONTINUED.

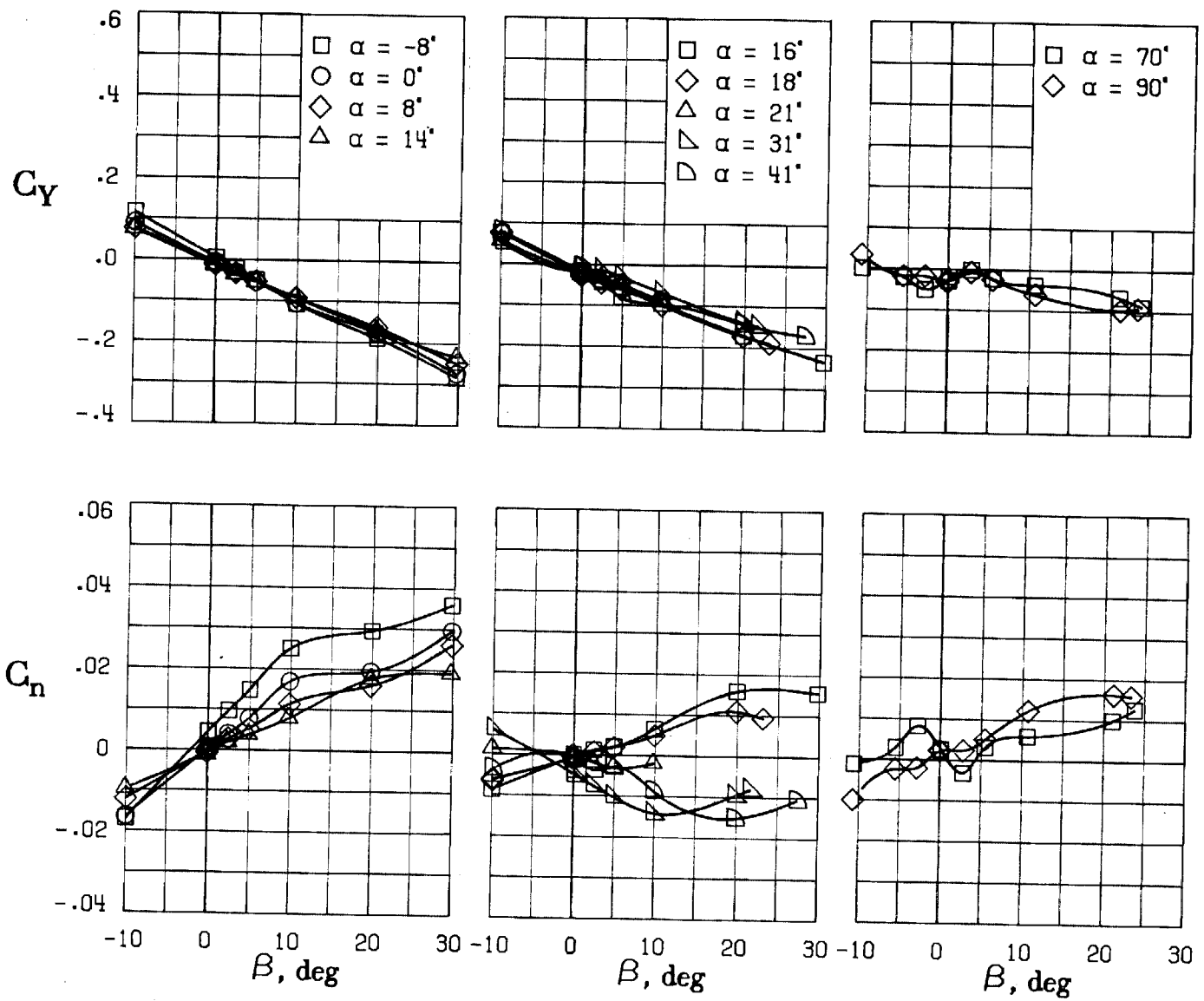

(E) DIRECTIONAL - STABILITY CHARACTERISTICS ABOUT BODY AXES AT VARIOUS ANGLES OF ATTACK.

FIGURE 19. - CONTINUED.

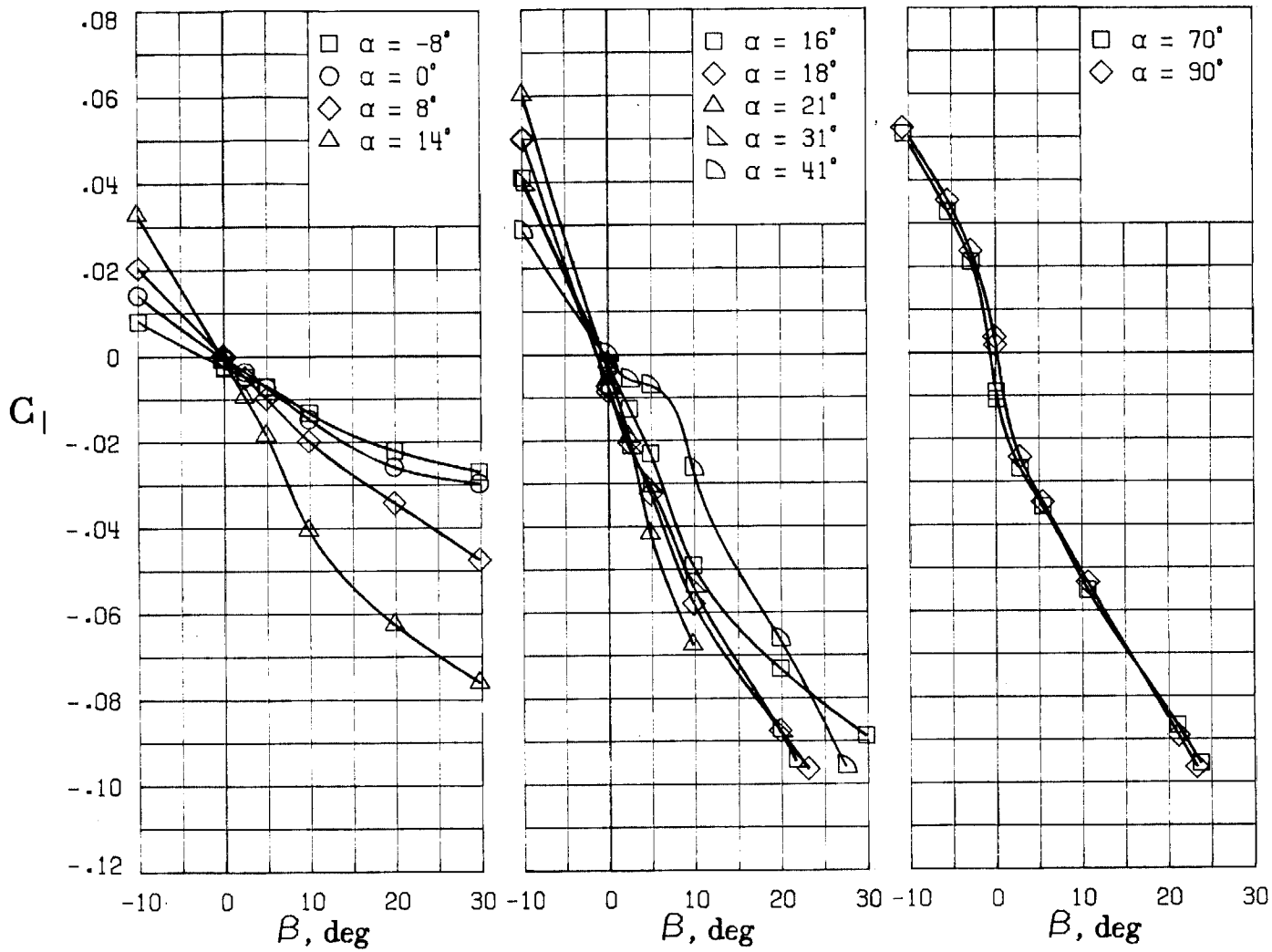

(F) LATERAL - STABILITY CHARACTERISTICS ABOUT BODY AXES AT VARIOUS ANGLES OF ATTACK.

FIGURE 19. - CONCLUDED.

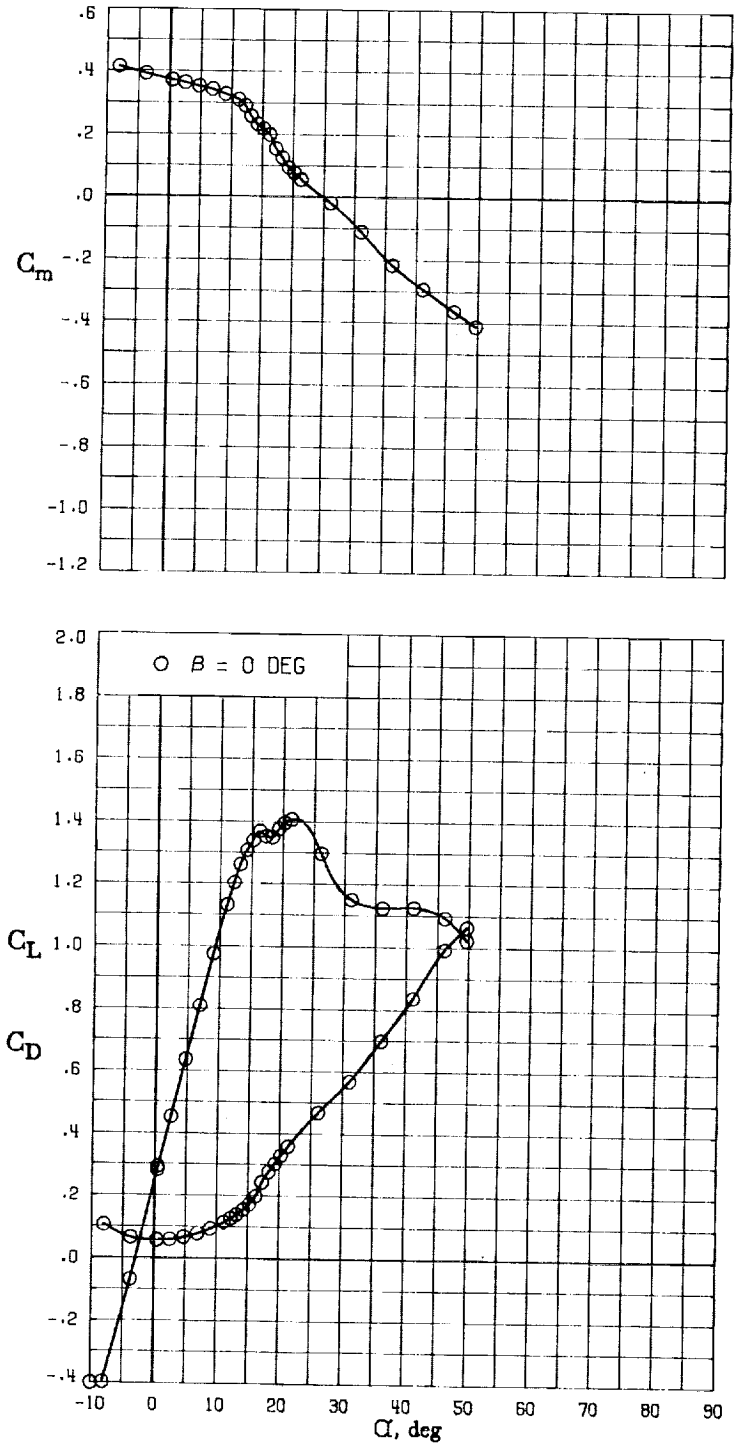

(A) LONGITUDINAL FORCE AND MOMENT COEFFICIENTS ABOUT STABILITY AXES.

FIGURE 20. - EFFECT OF ANGLE OF ATTACK AND SIDESLIP ANGLE ON AERODYNAMIC CHARACTERISTICS AT RE = 3.45 E+06 FOR CONFIGURATION B W3 H3 V. δ_E = -25°, δ_A = 0°, δ_R = 0°.

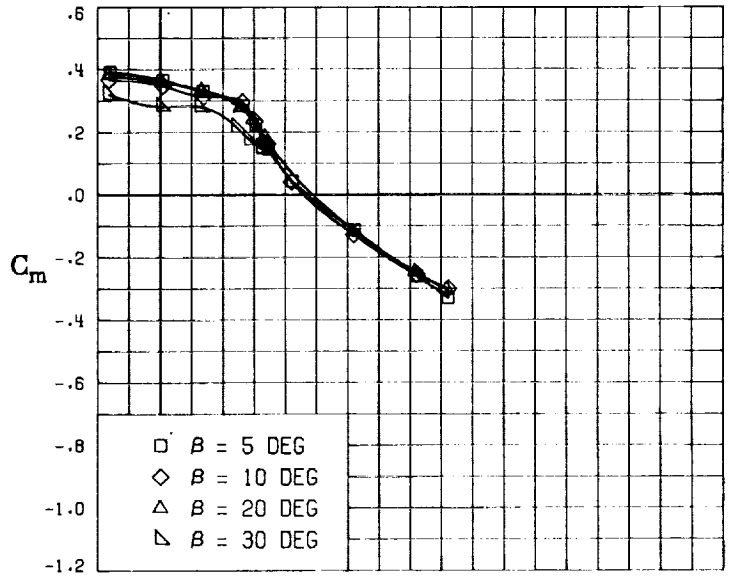

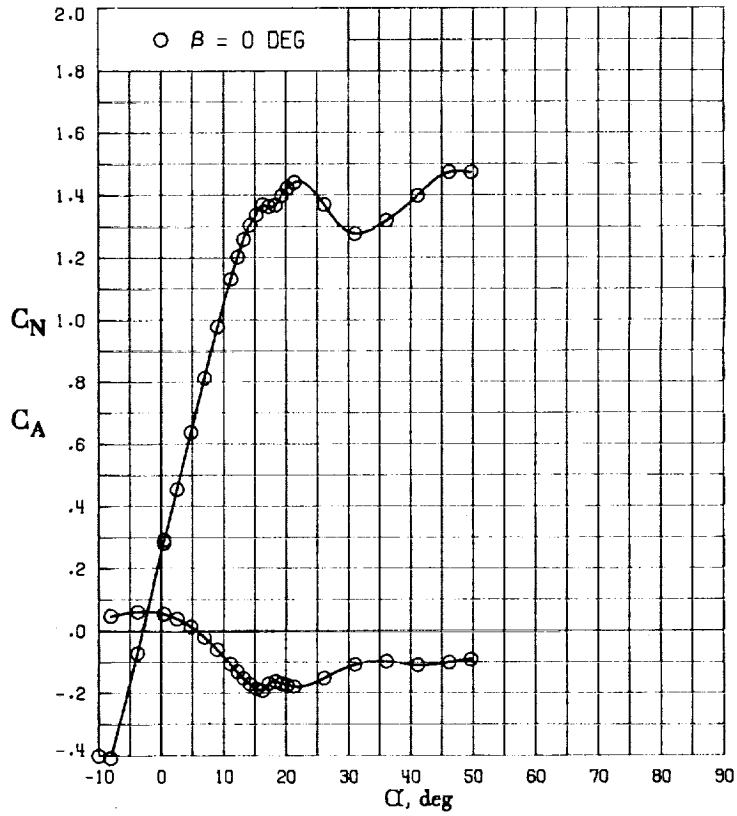

(B) LONGITUDINAL FORCE AND MOMENT COEFFICIENTS ABOUT BODY AXES.

FIGURE 20. - CONTINUED.

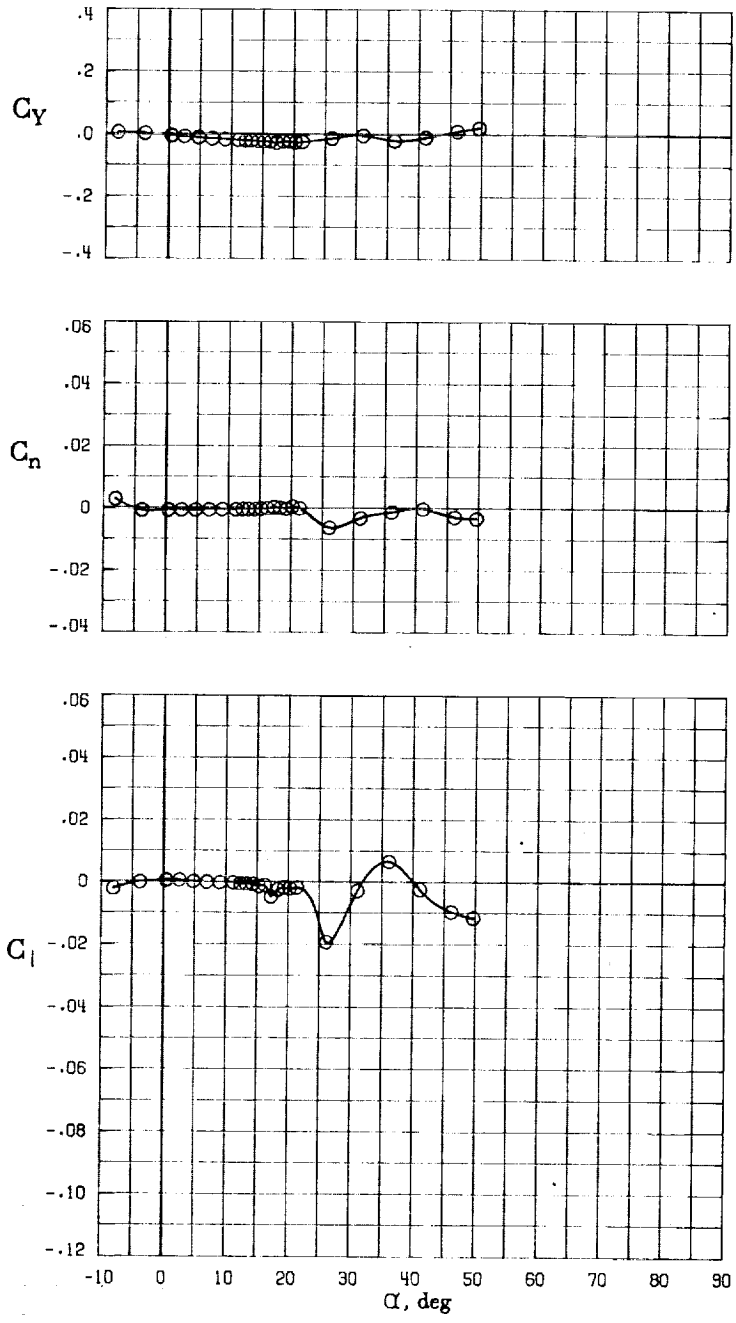

C) LATERAL - DIRECTIONAL FORCE AND MOMENT COEFFICIENTS ABOUT BODY AXES AT ZERO SIDESLIP.

FIGURE 20. - CONTINUED.

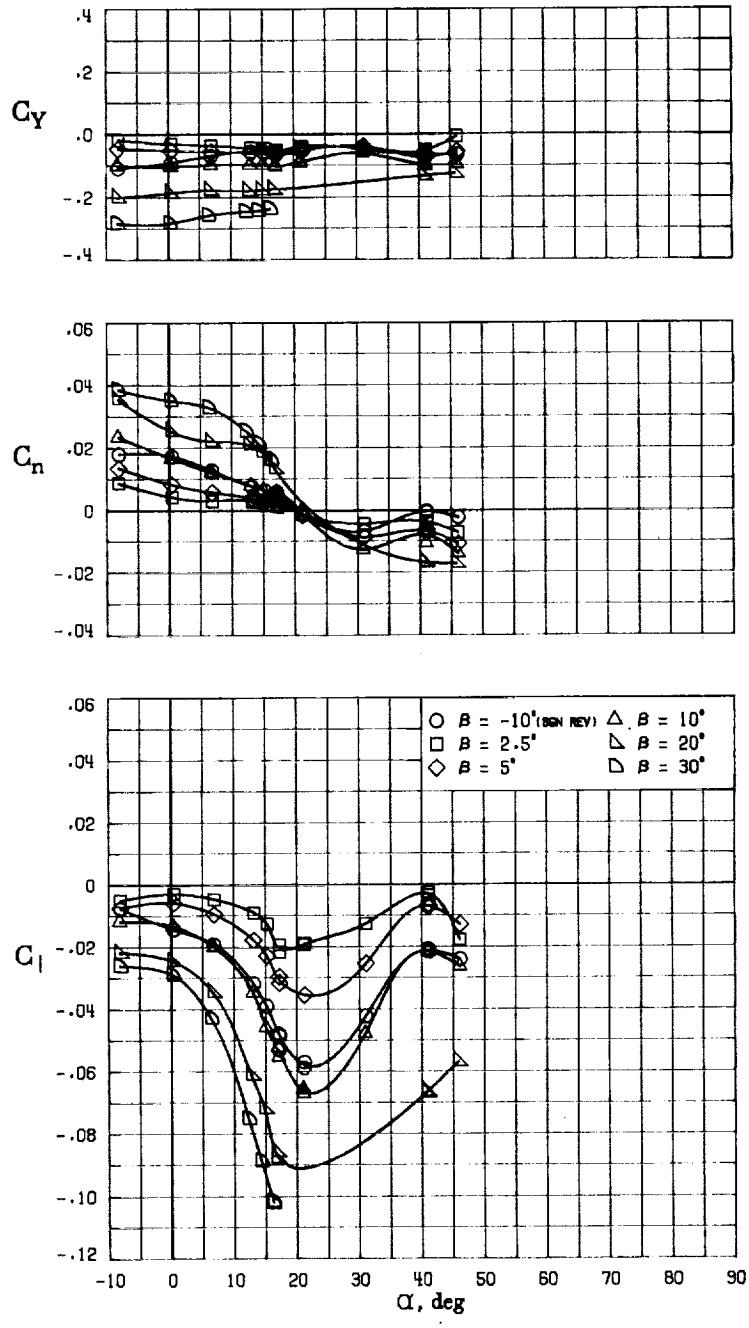

(D) LATERAL - DIRECTIONAL FORCE AND MOMENT COEFFICIENTS ABOUT BODY AXES.

FIGURE 20. - CONTINUED.

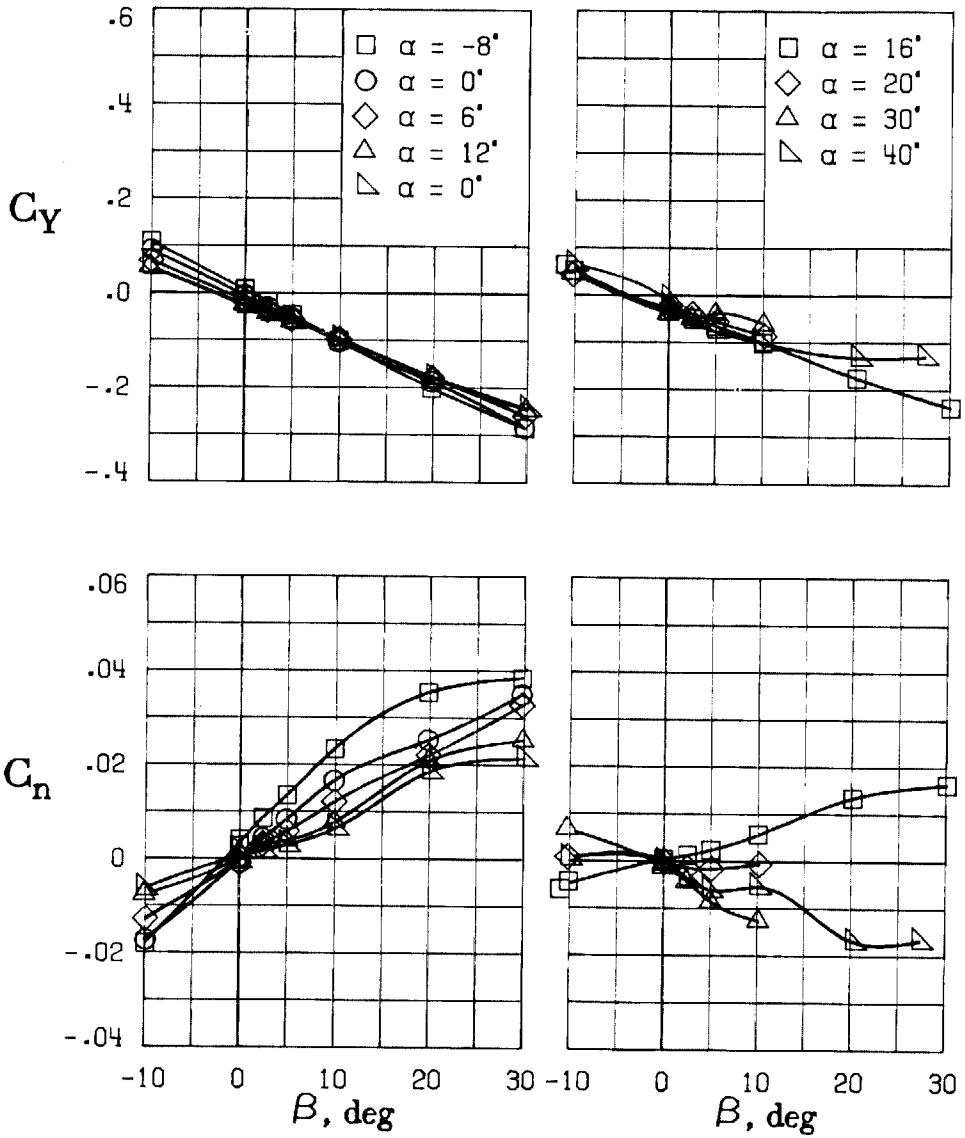

(E) DIRECTIONAL - STABILITY CHARACTERISTICS ABOUT BODY AXES AT VARIOUS ANGLES OF ATTACK.

FIGURE 20. - CONTINUED.

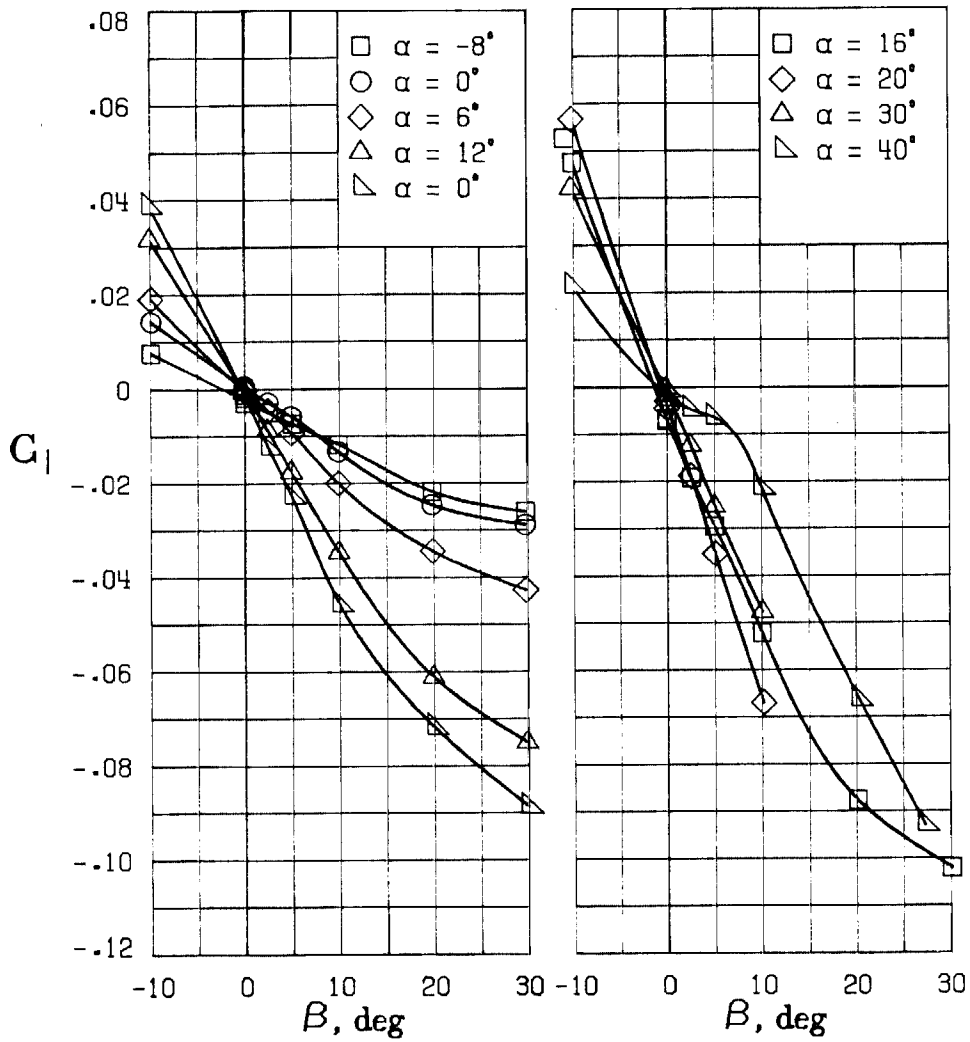

(F) LATERAL - STABILITY CHARACTERISTICS ABOUT BODY AXES AT VARIOUS ANGLES OF ATTACK.

FIGURE 20. - CONCLUDED.

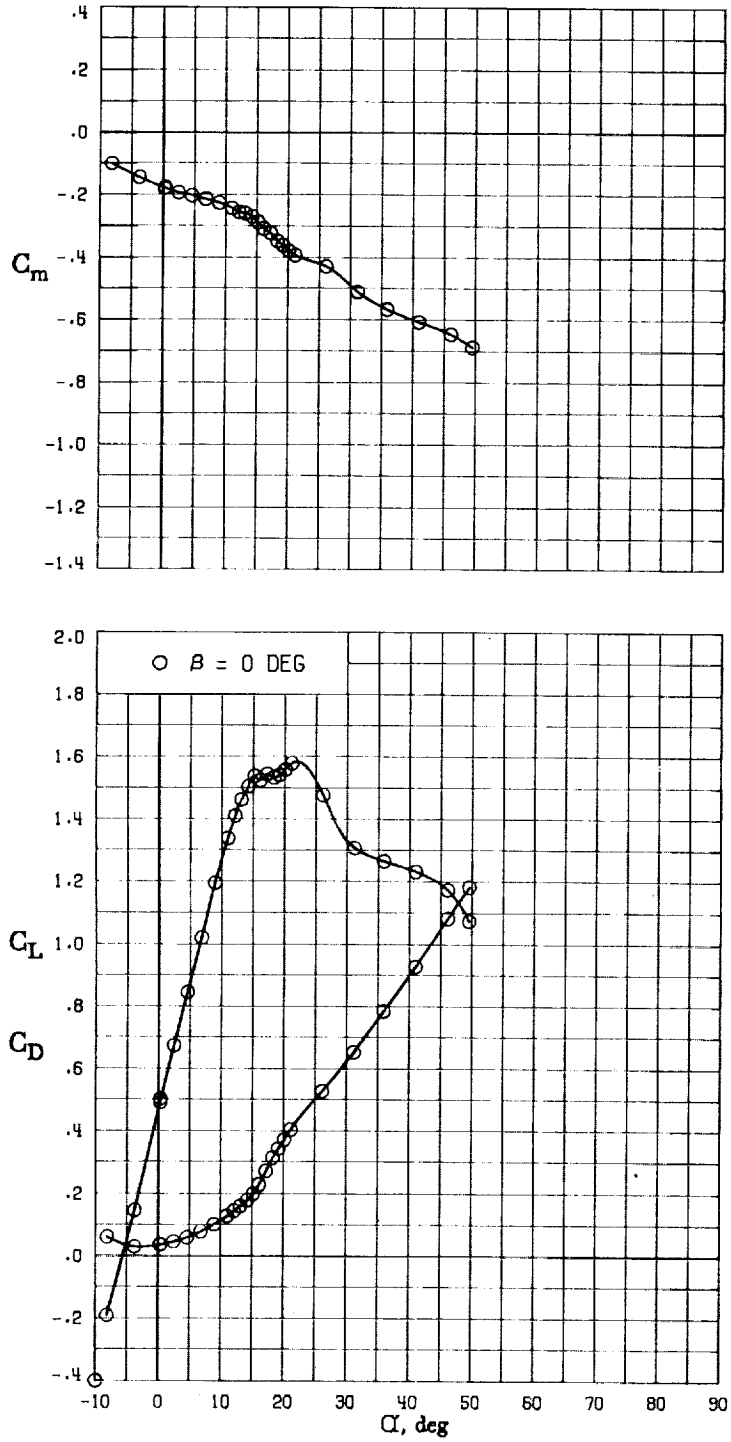

(A) LONGITUDINAL FORCE AND MOMENT COEFFICIENTS ABOUT STABILITY AXES.

FIGURE 21. - EFFECT OF ANGLE OF ATTACK AND SIDESLIP ANGLE ON AERODYNAMIC CHARACTERISTICS AT RE = 3.45 E+06 FOR CONFIGURATION B W3 H3 V. $\delta_E = 15°$, $\delta_A = 0°$, $\delta_R = 0°$.

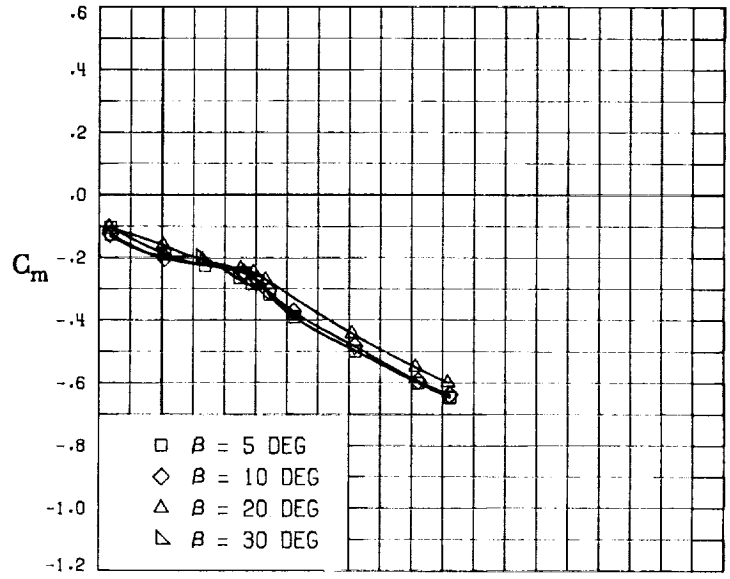

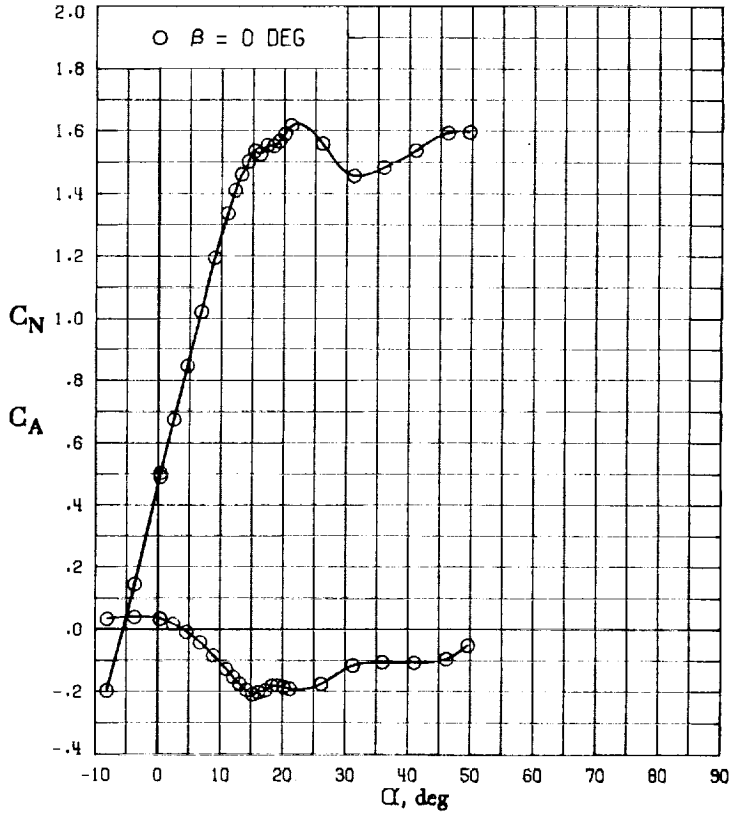

(B) LONGITUDINAL FORCE AND MOMENT COEFFICIENTS ABOUT BODY AXES.

FIGURE 21. - CONTINUED.

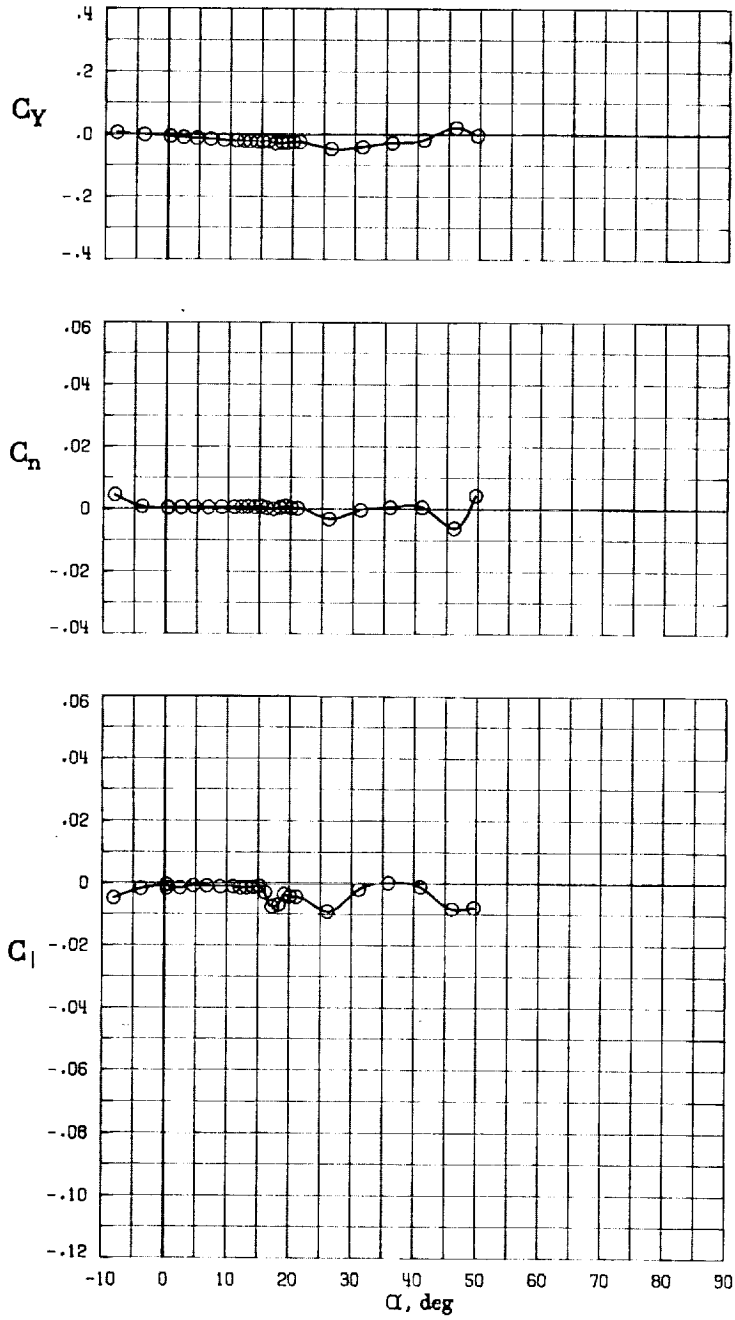

(C) LATERAL - DIRECTIONAL FORCE AND MOMENT COEFFICIENTS ABOUT BODY AXES AT ZERO SIDESLIP.

FIGURE 21. - CONTINUED.

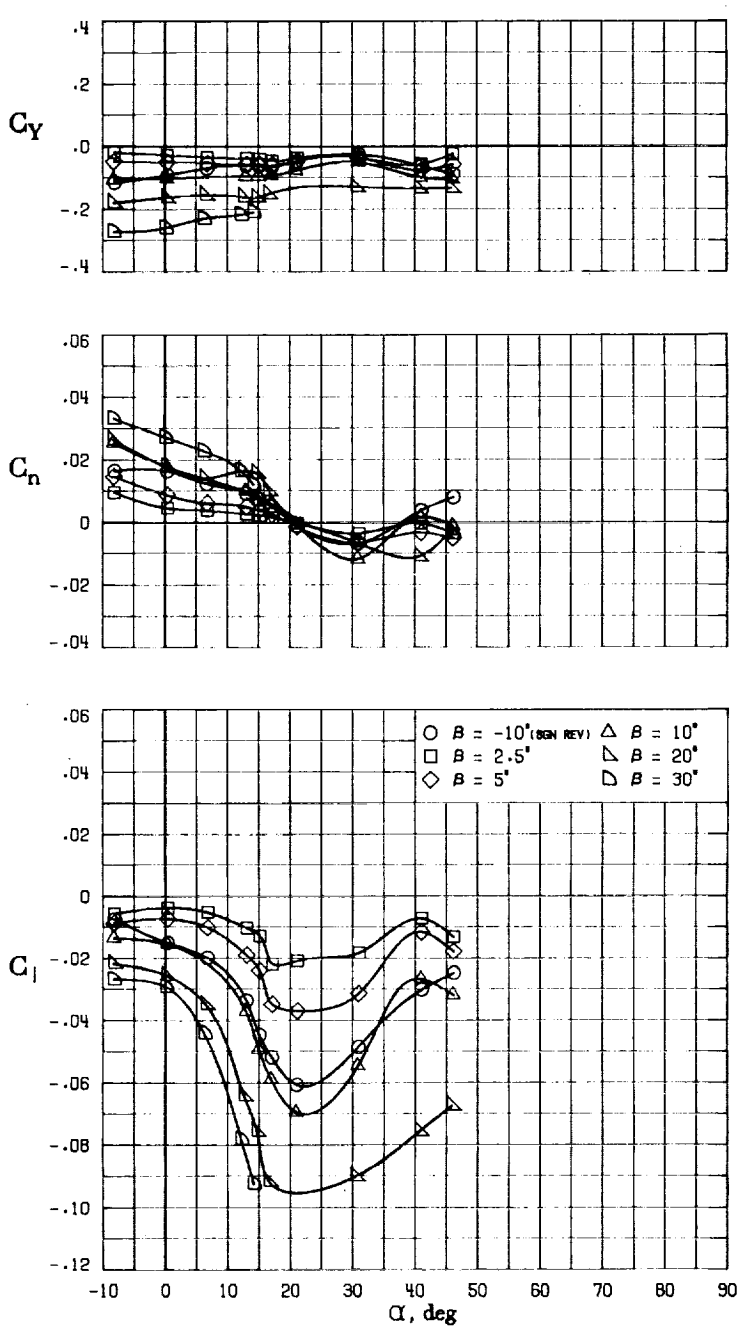

(D) LATERAL - DIRECTIONAL FORCE AND MOMENT COEFFICIENTS ABOUT BODY AXES.

FIGURE 21. - CONTINUED.

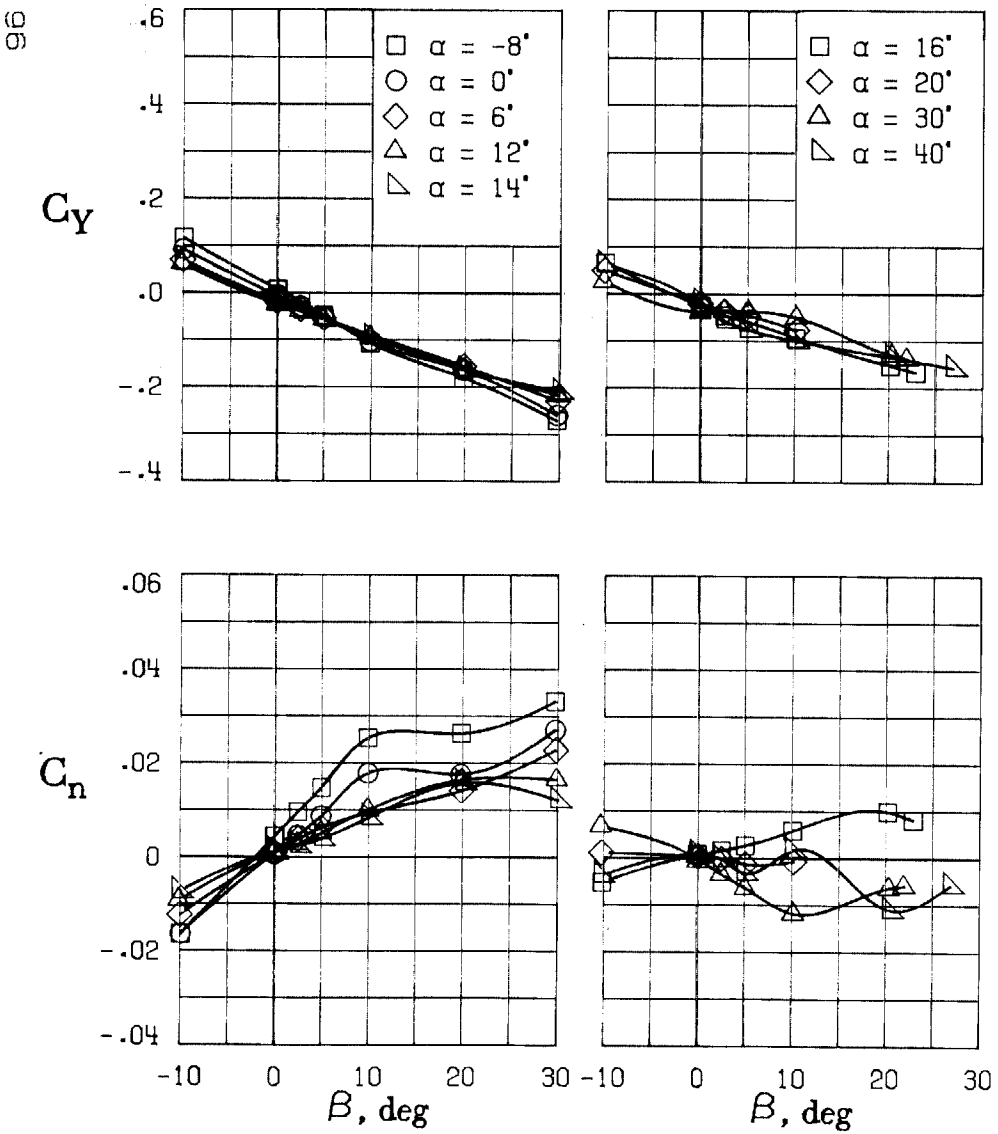

(E) DIRECTIONAL - STABILITY CHARACTERISTICS ABOUT BODY AXES AT VARIOUS ANGLES OF ATTACK.

FIGURE 21. - CONTINUED.

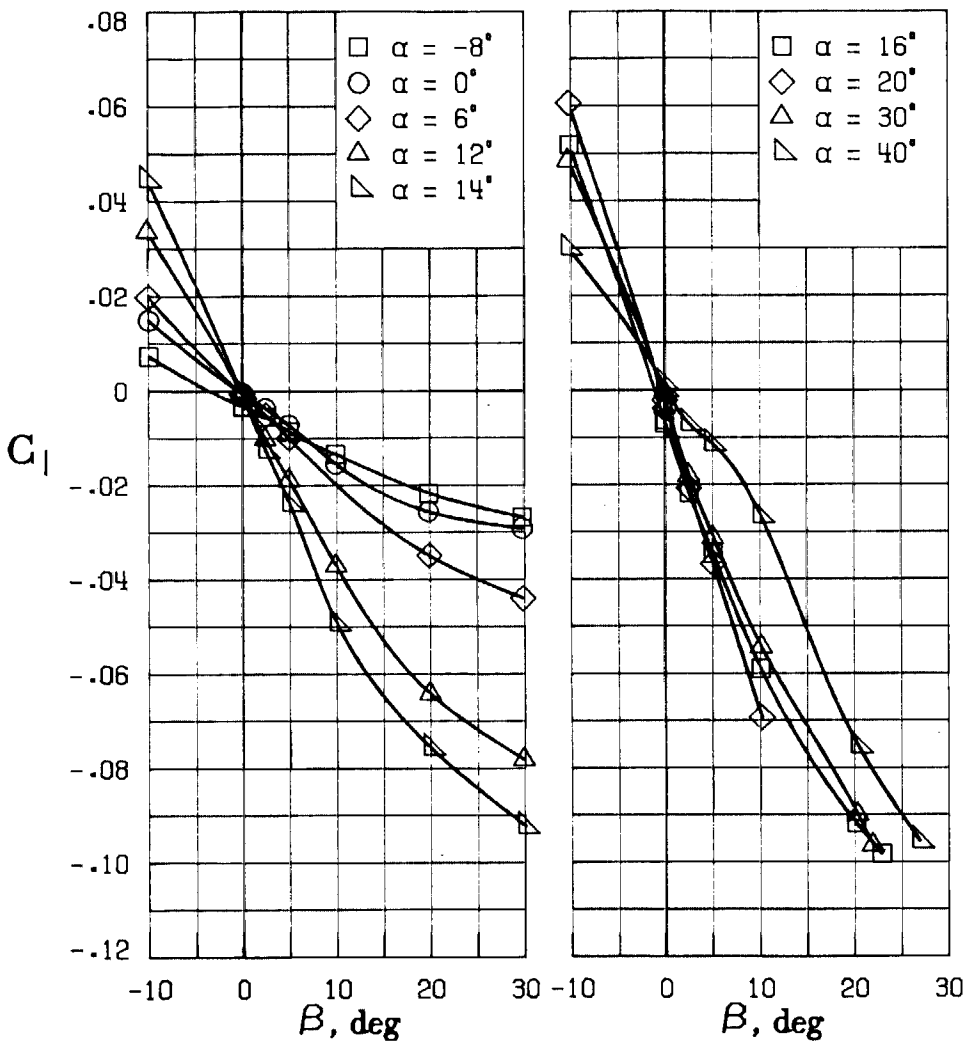

(F) LATERAL - STABILITY CHARACTERISTICS ABOUT BODY AXES AT VARIOUS ANGLES OF ATTACK.

FIGURE 21. - CONCLUDED.

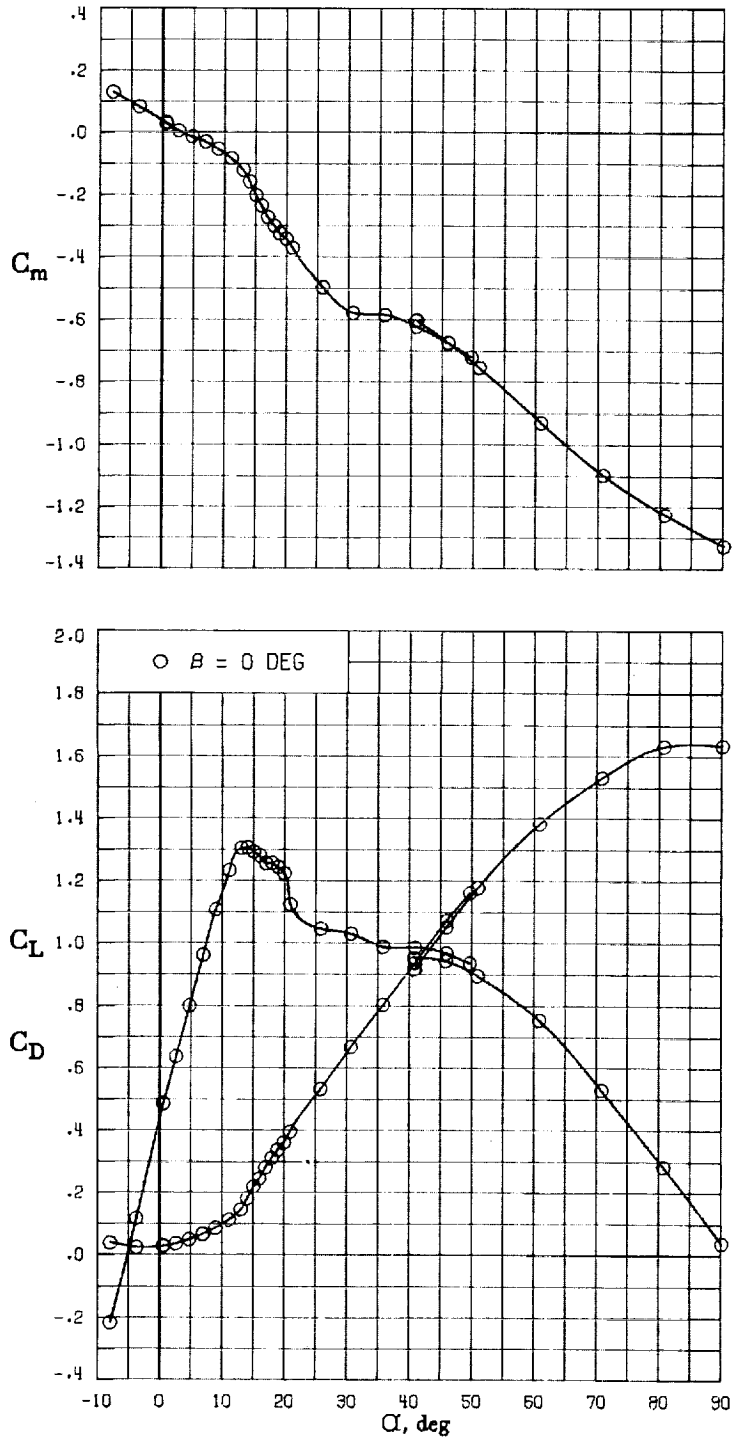

(A) LONGITUDINAL FORCE AND MOMENT COEFFICIENTS ABOUT STABILITY AXES.

FIGURE 22. - EFFECT OF ANGLE OF ATTACK AND SIDESLIP ANGLE ON AERODYNAMIC CHARACTERISTICS AT RE = 3.45 E+06 FOR CONFIGURATION B W1 H4 V C. $\delta_E = 0°$, $\delta_A = 0°$, $\delta_R = 0°$.

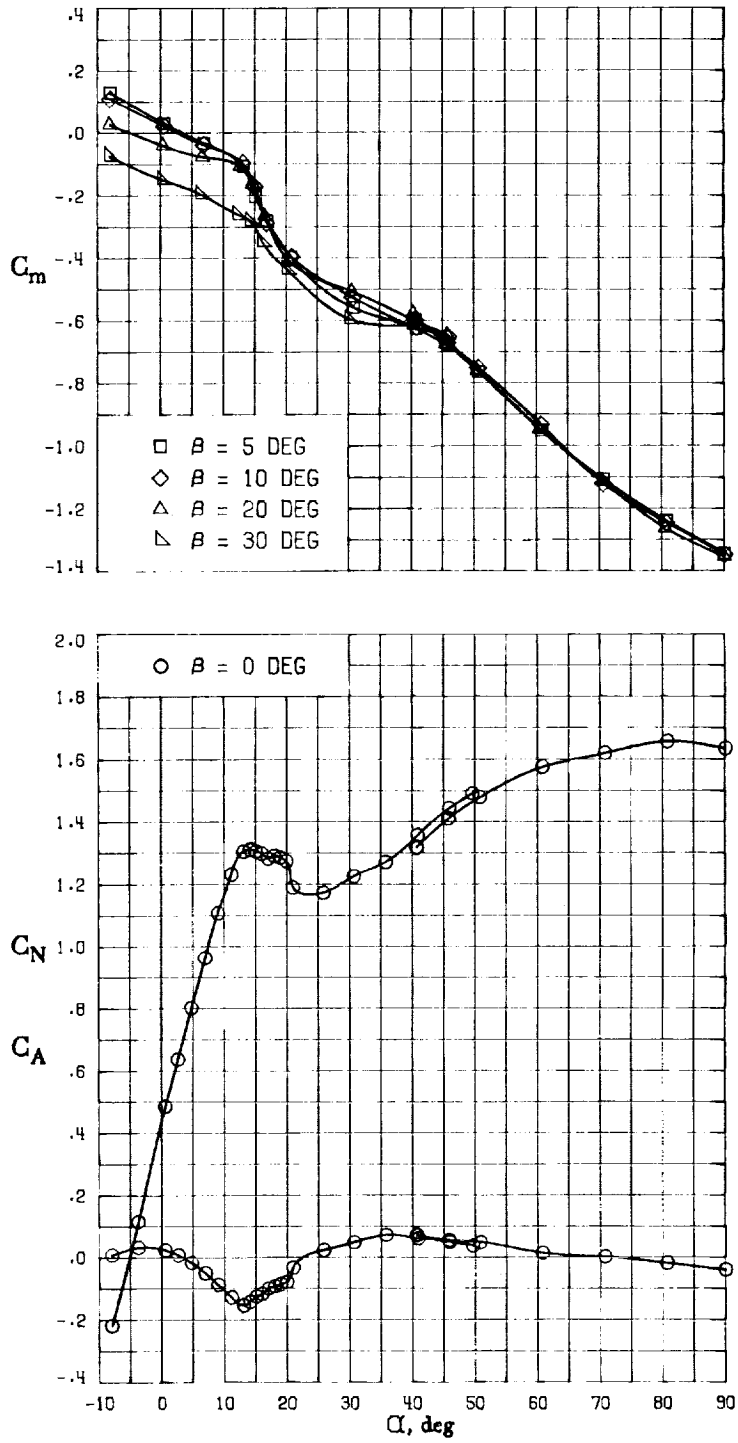

(B) LONGITUDINAL FORCE AND MOMENT COEFFICIENTS ABOUT BODY AXES.

FIGURE 22. - CONTINUED.

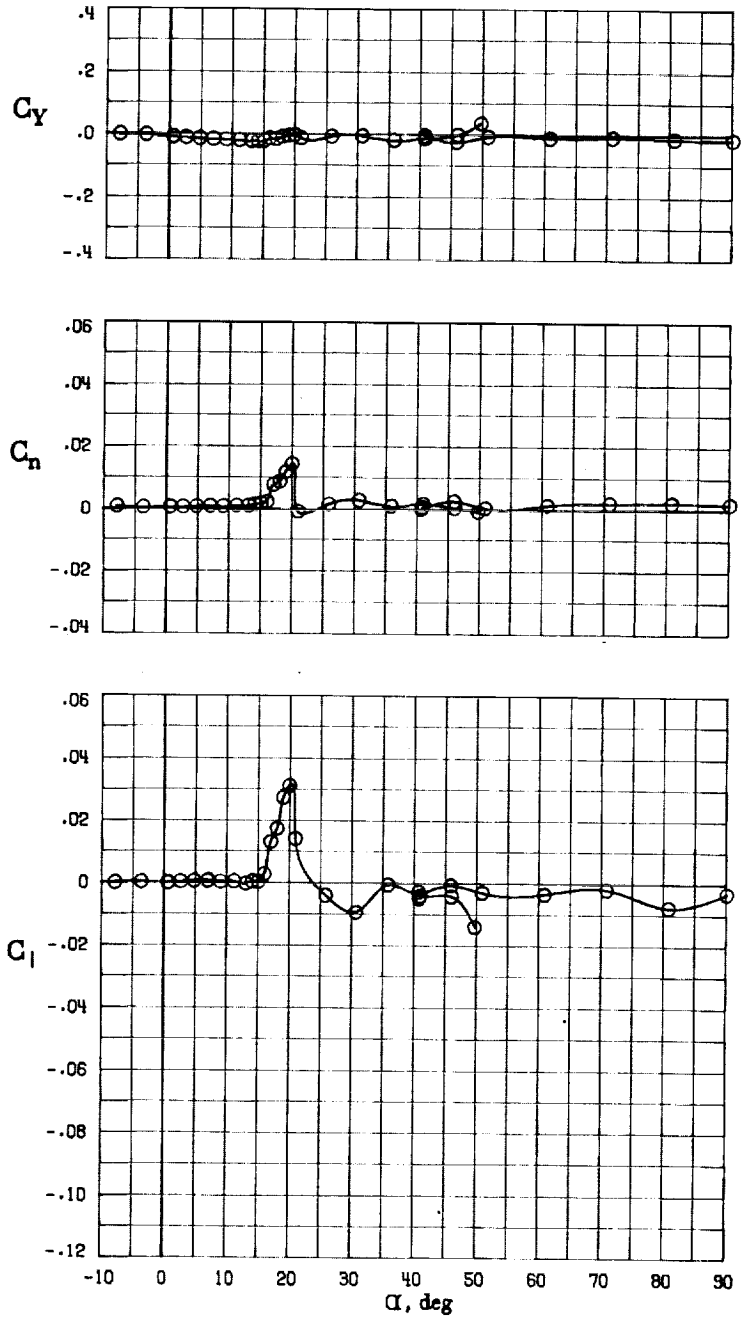

(C) LATERAL - DIRECTIONAL FORCE AND MOMENT COEFFICIENTS ABOUT BODY AXES AT ZERO SIDESLIP.

FIGURE 22. - CONTINUED.

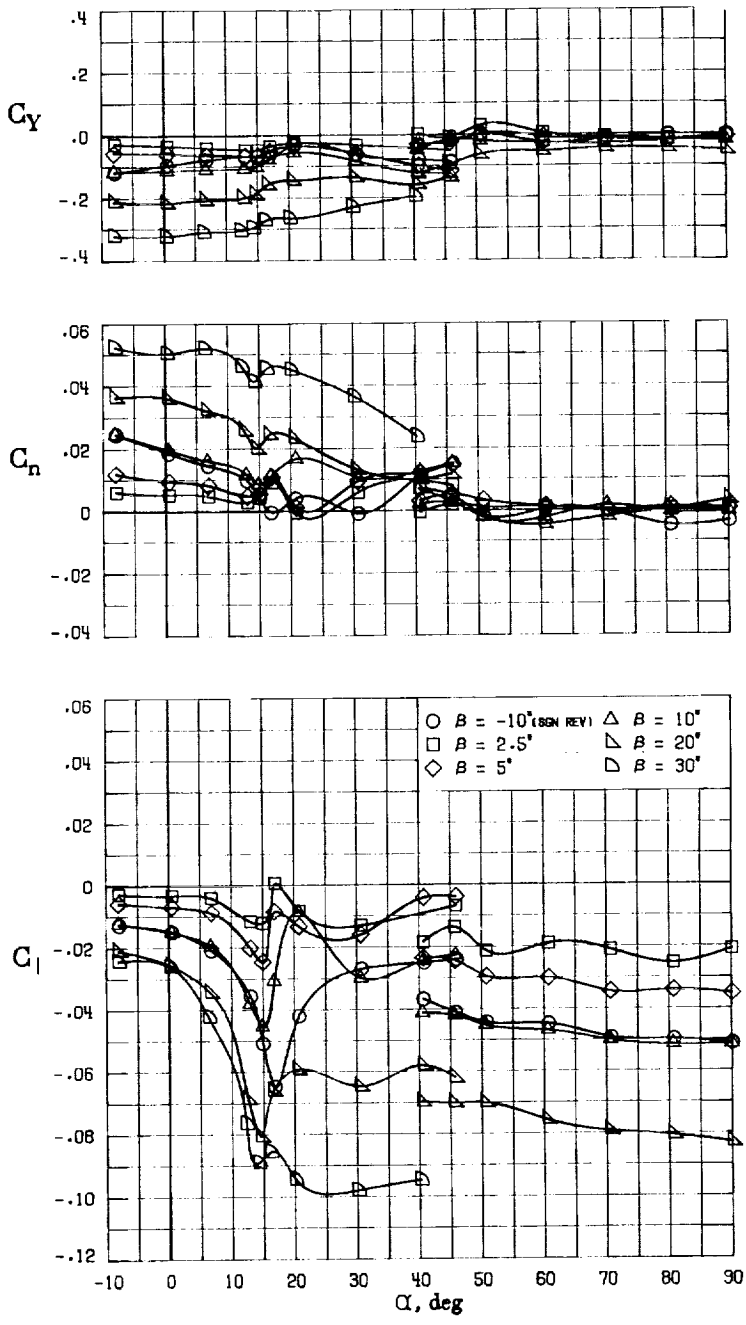

(D) LATERAL - DIRECTIONAL FORCE AND MOMENT COEFFICIENTS ABOUT BODY AXES.

FIGURE 22. - CONTINUED.

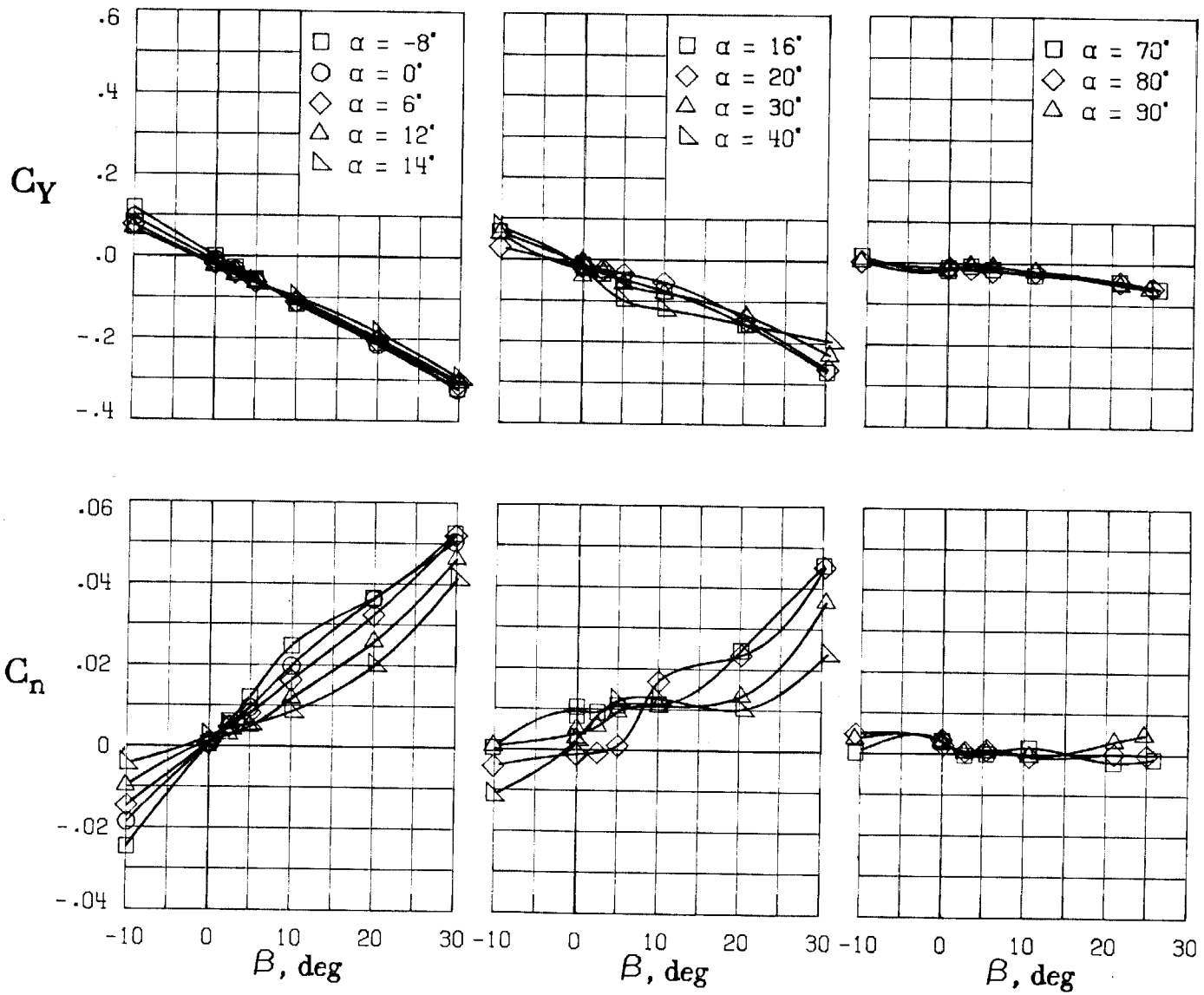

(E) DIRECTIONAL - STABILITY CHARACTERISTICS ABOUT BODY AXES AT VARIOUS ANGLES OF ATTACK.

FIGURE 22. - CONTINUED.

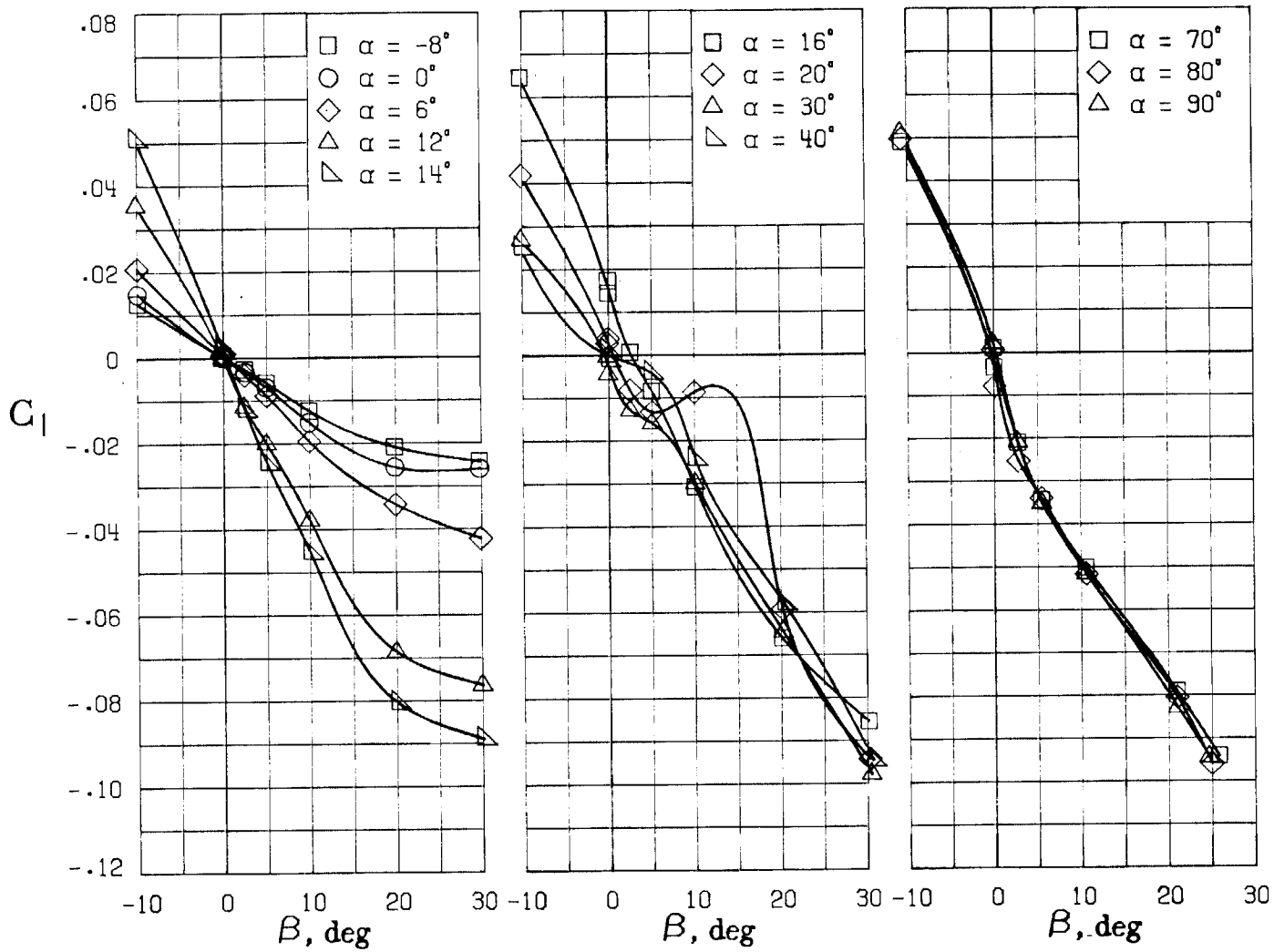

(F) LATERAL - STABILITY CHARACTERISTICS ABOUT BODY AXES AT VARIOUS ANGLES OF ATTACK.

FIGURE 22. - CONCLUDED.

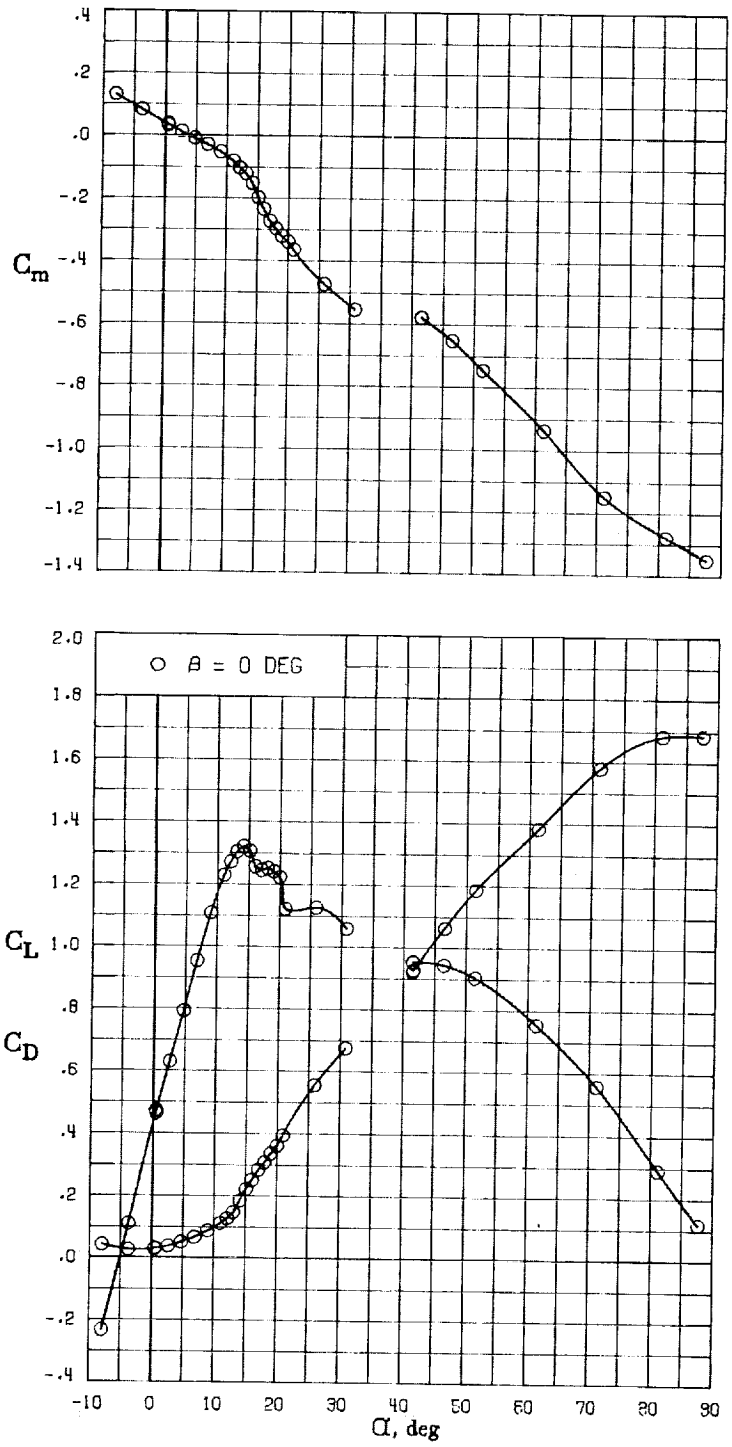

(A) LONGITUDINAL FORCE AND MOMENT COEFFICIENTS ABOUT STABILITY AXES.

FIGURE 23. - EFFECT OF ANGLE OF ATTACK AND SIDESLIP ANGLE ON AERODYNAMIC CHARACTERISTICS AT RE = 3.45 E+06 FOR CONFIGURATION B W1 H4 V SH. $\delta_E = 0°$, $\delta_A = 0°$, $\delta_R = 0°$.

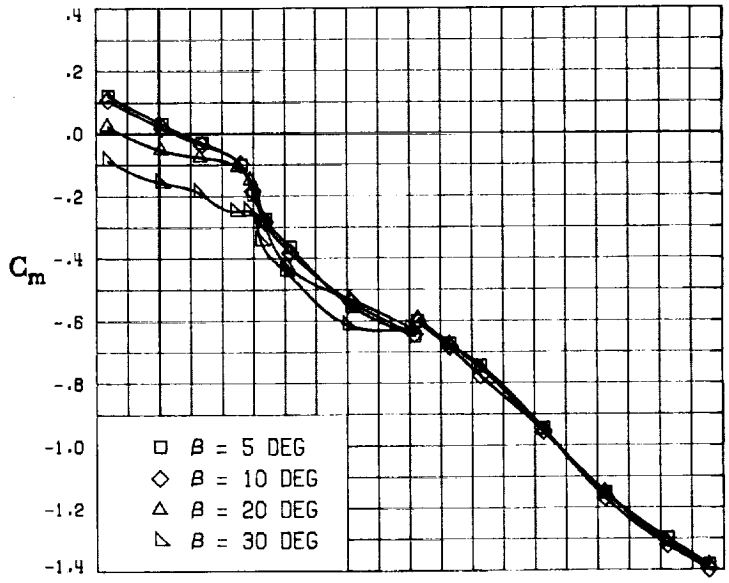

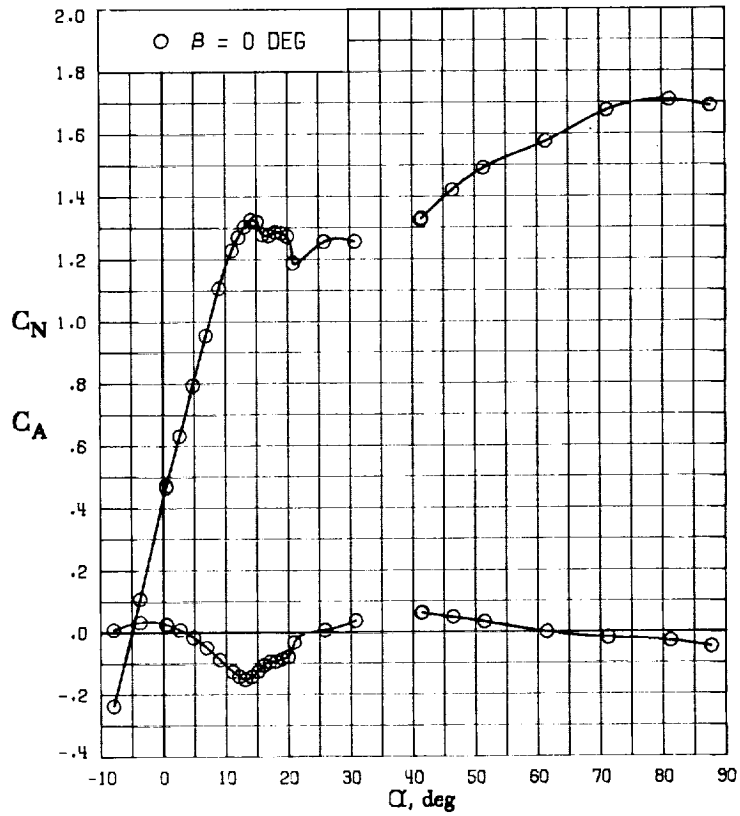

(B.) LONGITUDINAL FORCE AND MOMENT COEFFICIENTS ABOUT BODY AXES.

FIGURE 23. - CONTINUED.

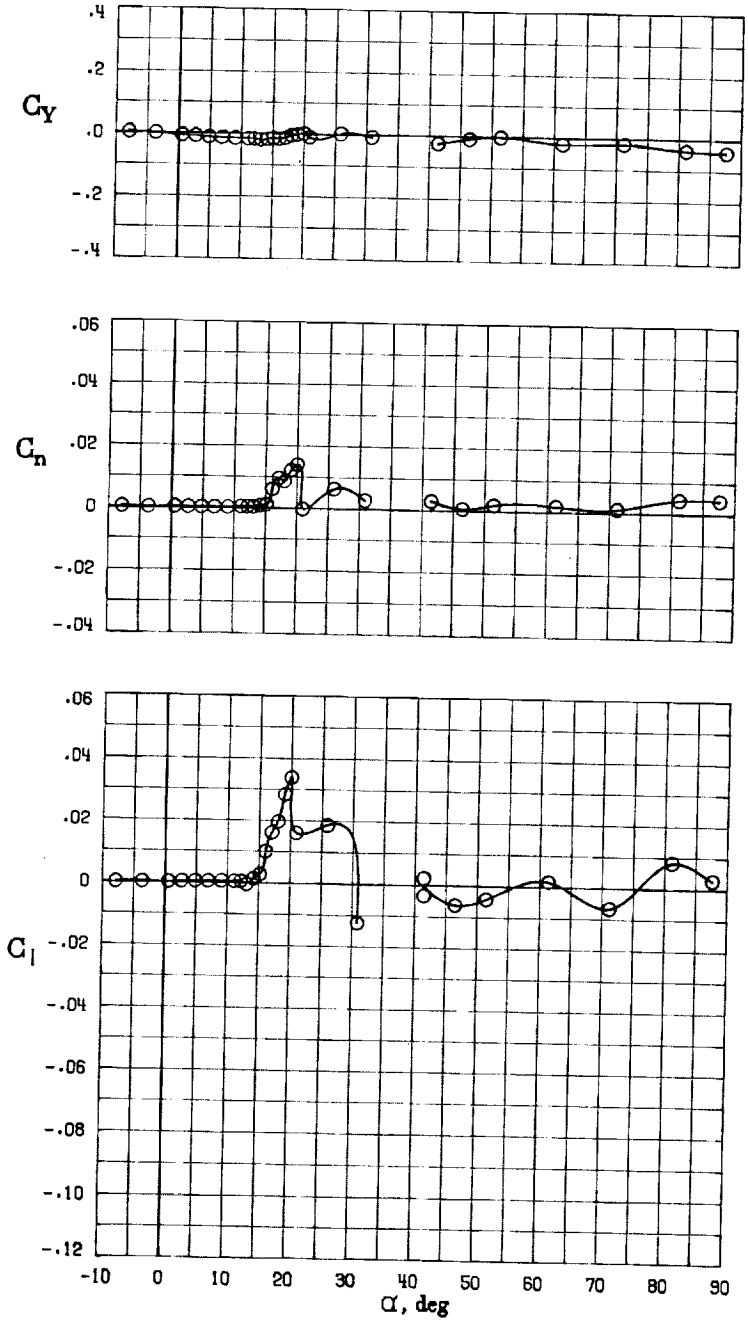

(C) LATERAL - DIRECTIONAL FORCE AND MOMENT COEFFICIENTS ABOUT BODY AXES AT ZERO SIDESLIP.

FIGURE 23. - CONTINUED.

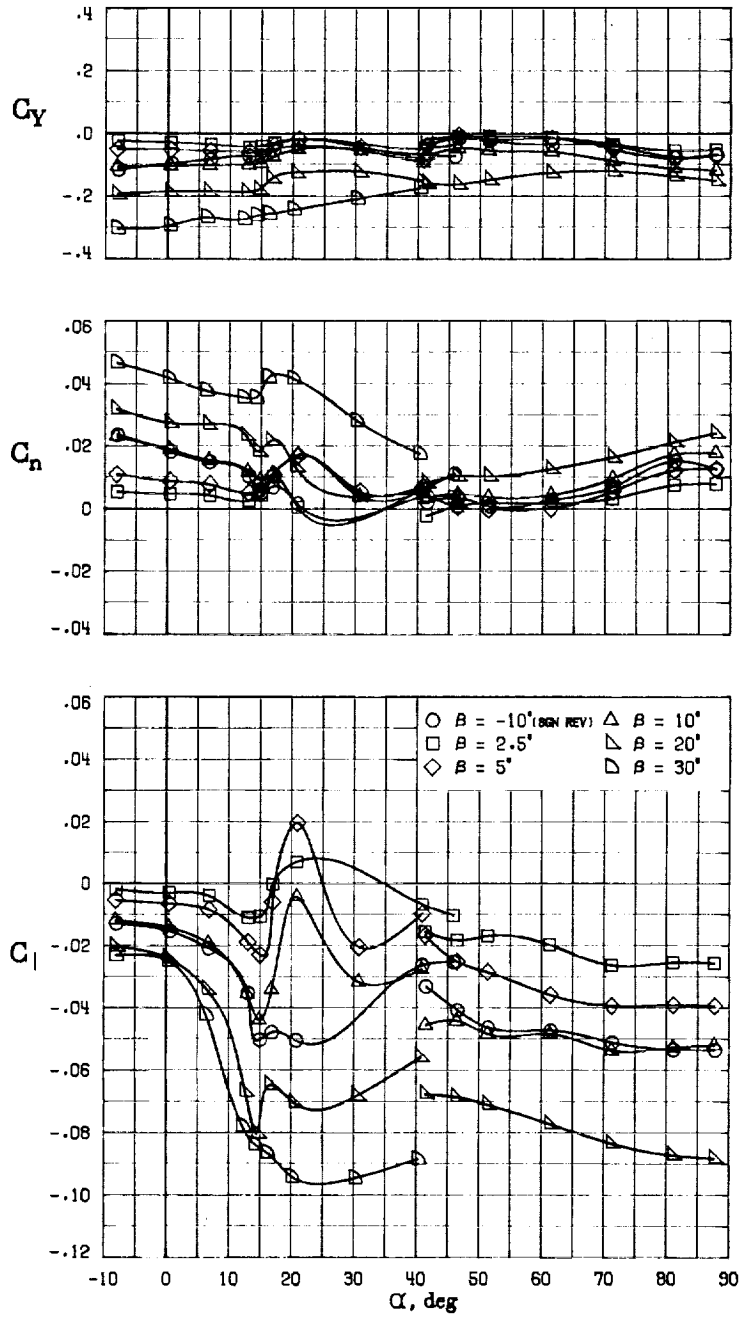

(D) LATERAL - DIRECTIONAL FORCE AND MOMENT COEFFICIENTS ABOUT BODY AXES.

FIGURE 23. - CONTINUED.

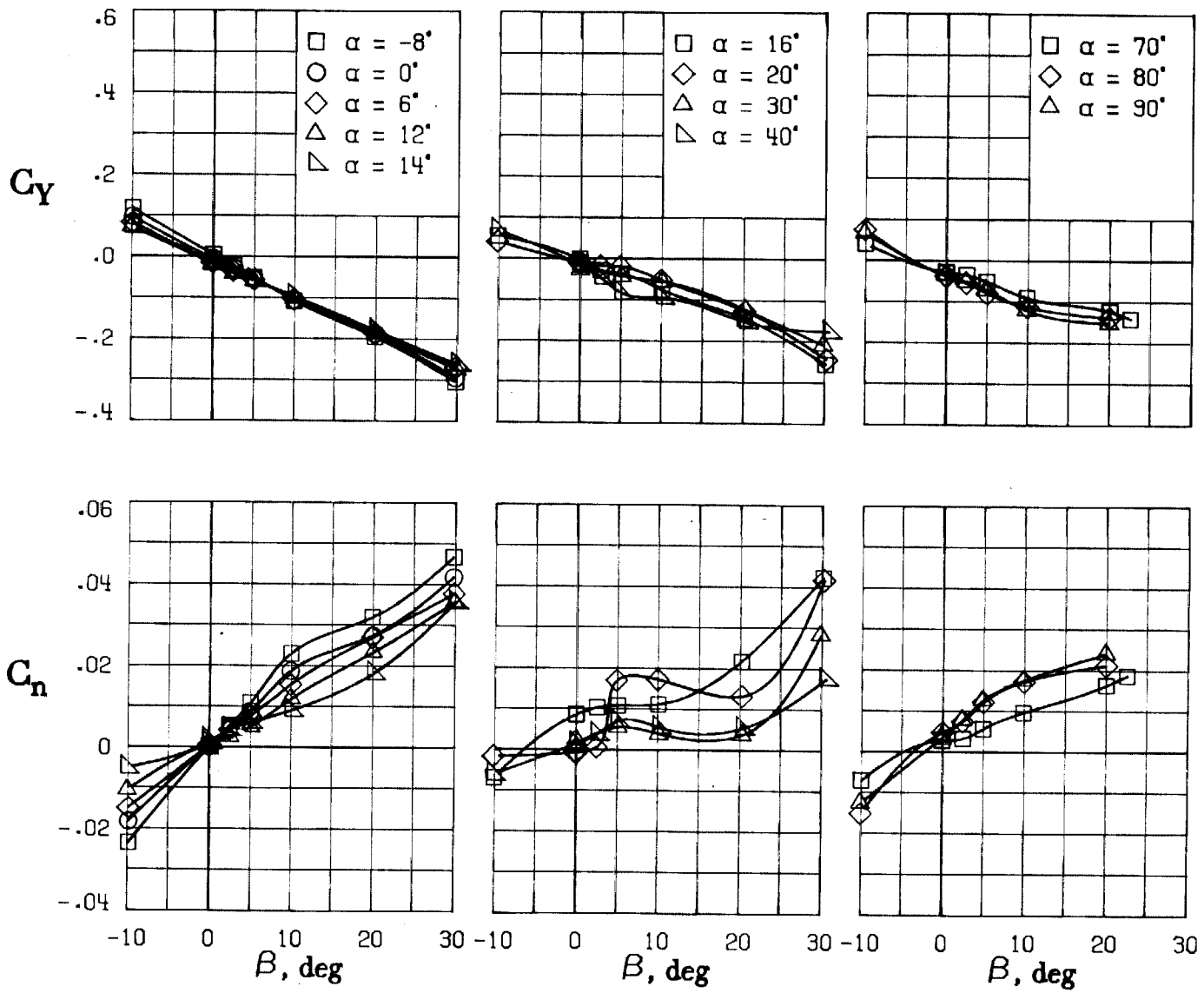

(E) DIRECTIONAL - STABILITY CHARACTERISTICS ABOUT BODY AXES AT VARIOUS ANGLES OF ATTACK.

FIGURE 23. - CONTINUED.

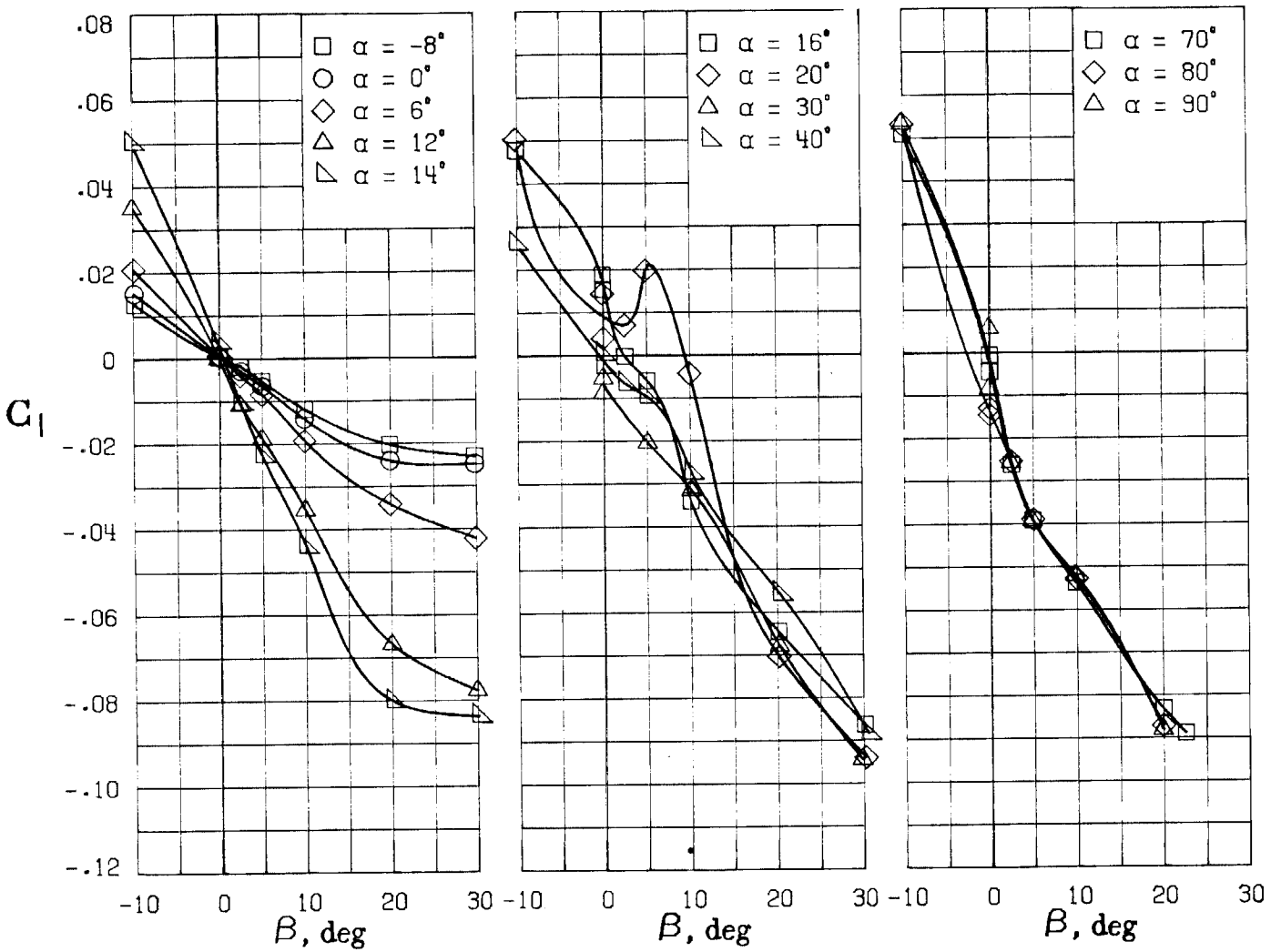

(F) LATERAL - STABILITY CHARACTERISTICS ABOUT BODY AXES AT VARIOUS ANGLES OF ATTACK.

FIGURE 23. - CONCLUDED.

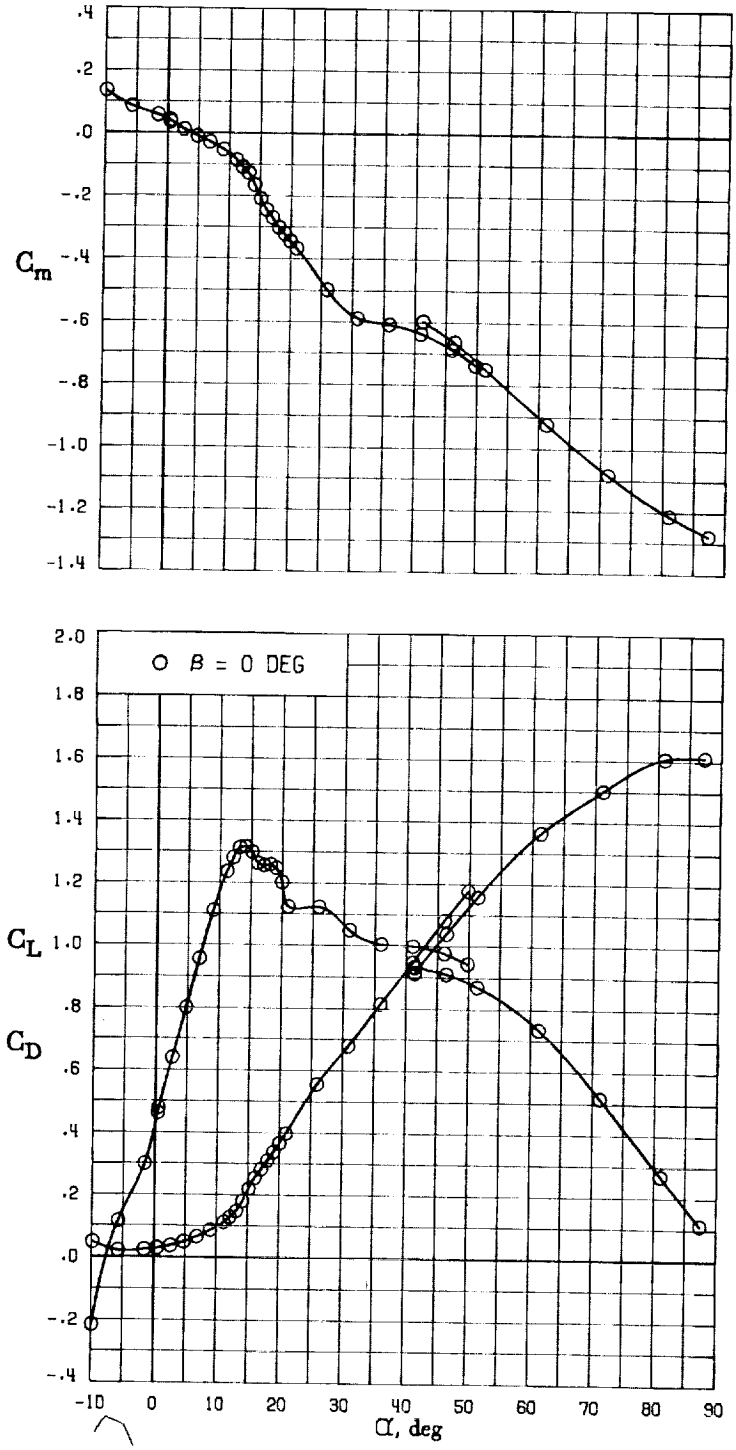

(A) LONGITUDINAL FORCE AND MOMENT COEFFICIENTS ABOUT STABILITY AXES.

FIGURE 24. - EFFECT OF ANGLE OF ATTACK AND SIDESLIP ANGLE ON AERODYNAMIC CHARACTERISTICS AT RE = 3.45 E+06 FOR CONFIGURATION B W1 H4 V SV. $\delta_E = 0°$, $\delta_A = 0°$, $\delta_R = 0°$.

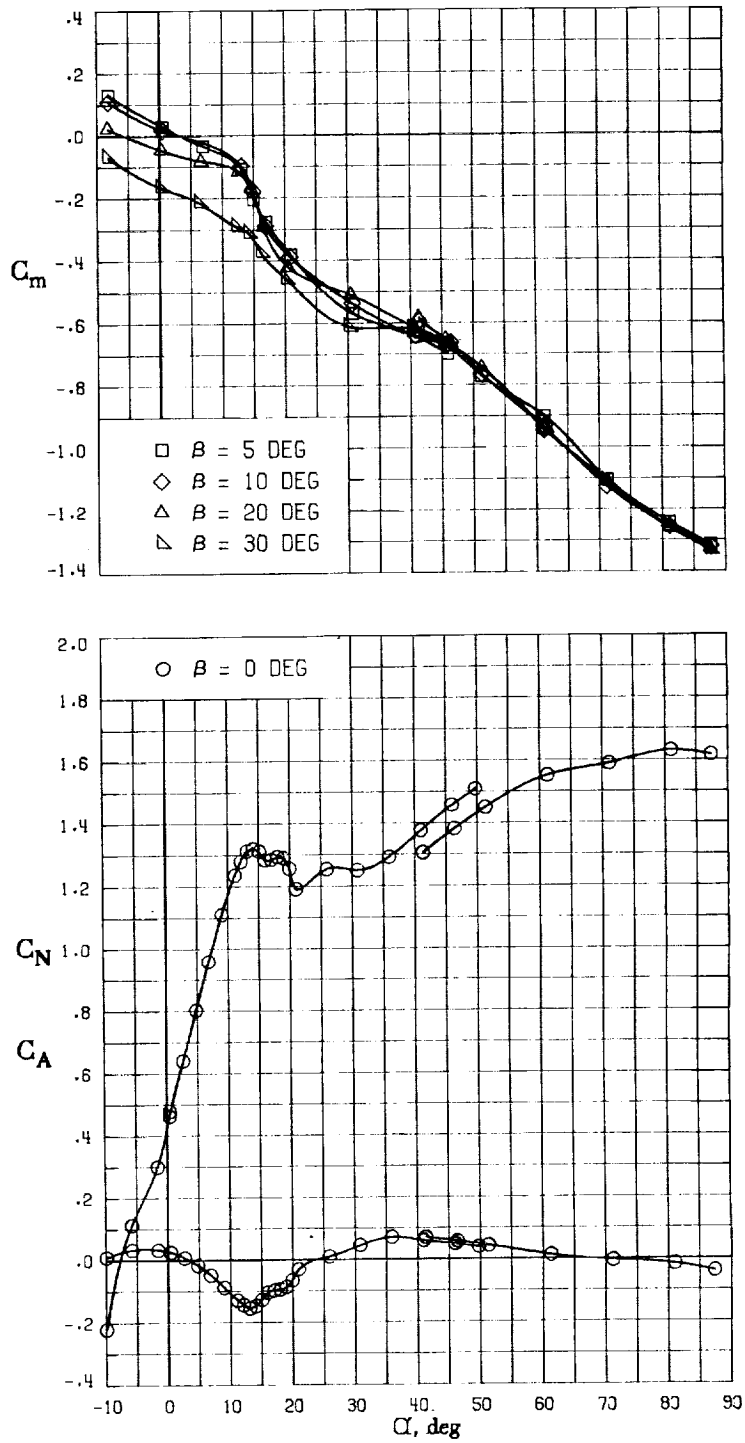

(B) LONGITUDINAL FORCE AND MOMENT COEFFICIENTS ABOUT BODY AXES.

FIGURE 24. - CONTINUED.

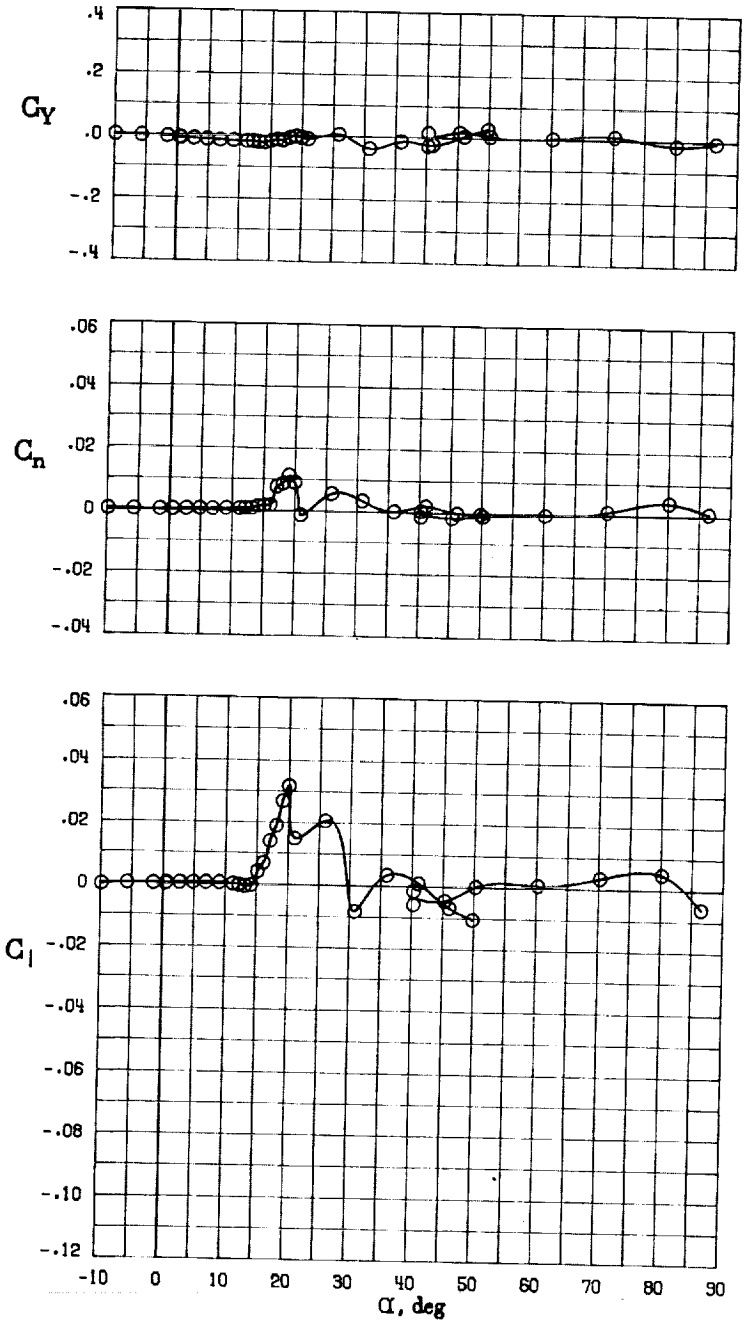

(C) LATERAL - DIRECTIONAL FORCE AND MOMENT COEFFICIENTS ABOUT BODY AXES AT ZERO SIDESLIP.

FIGURE 24. - CONTINUED.

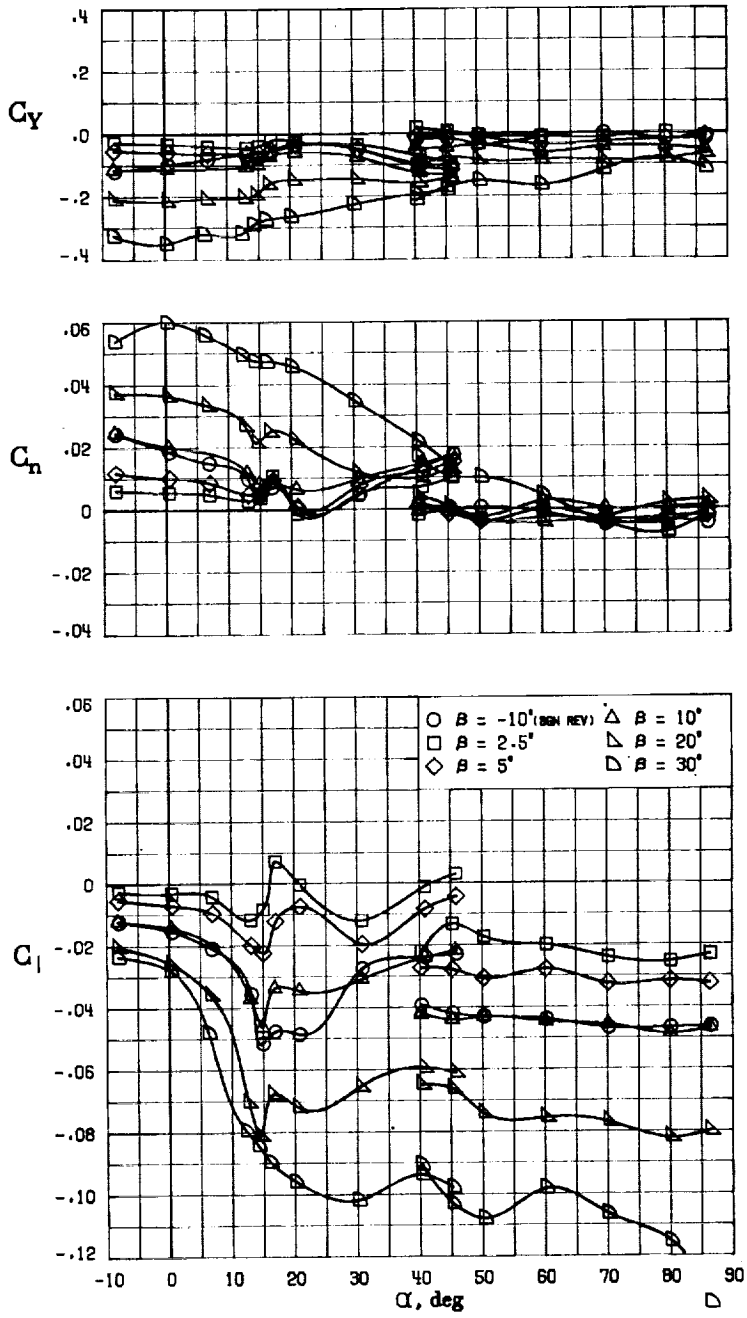

(D) LATERAL - DIRECTIONAL FORCE AND MOMENT COEFFICIENTS ABOUT BODY AXES.

FIGURE 24. - CONTINUED.

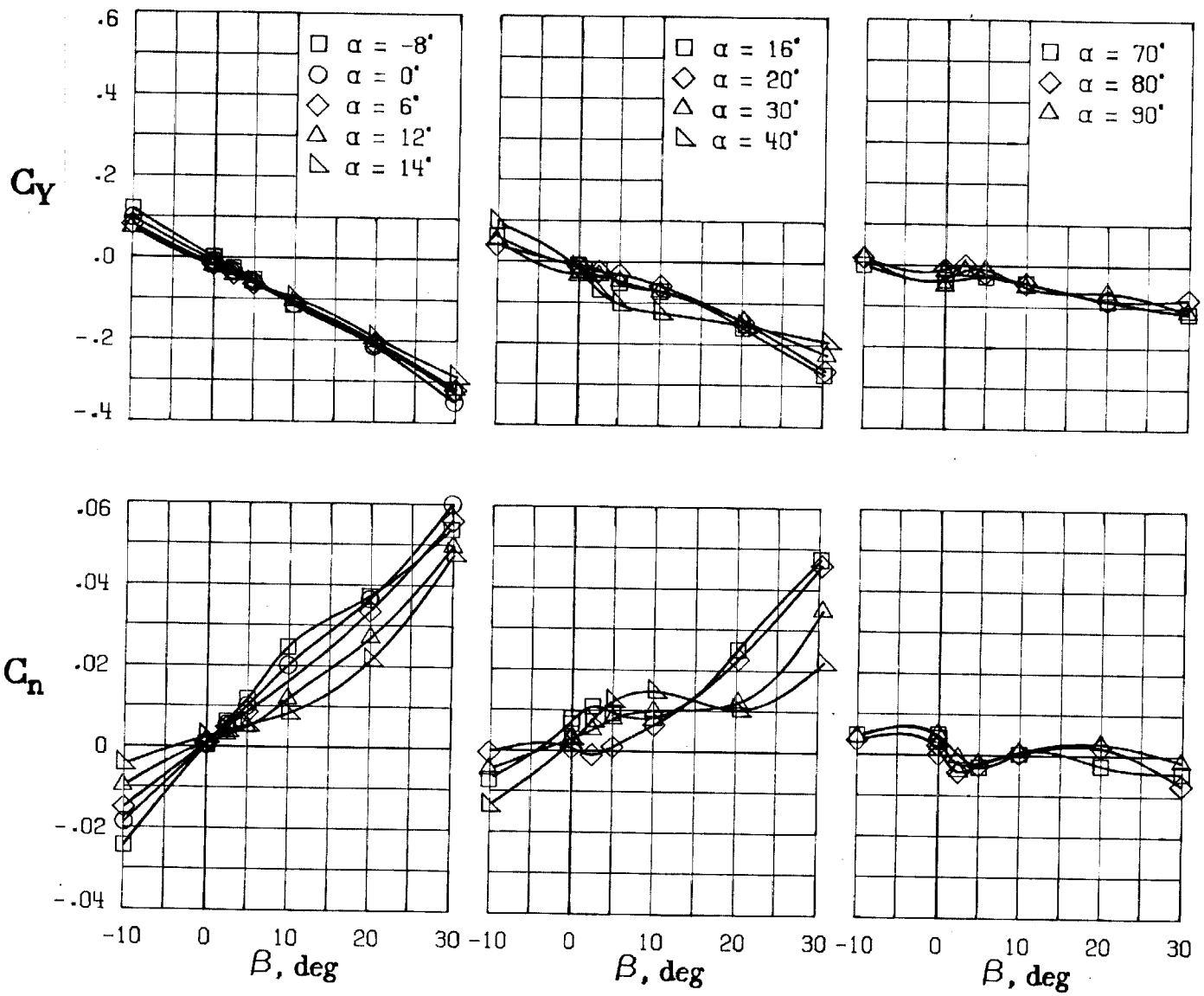

(E) DIRECTIONAL - STABILITY CHARACTERISTICS ABOUT BODY AXES AT VARIOUS ANGLES OF ATTACK.

FIGURE 24. - CONTINUED.

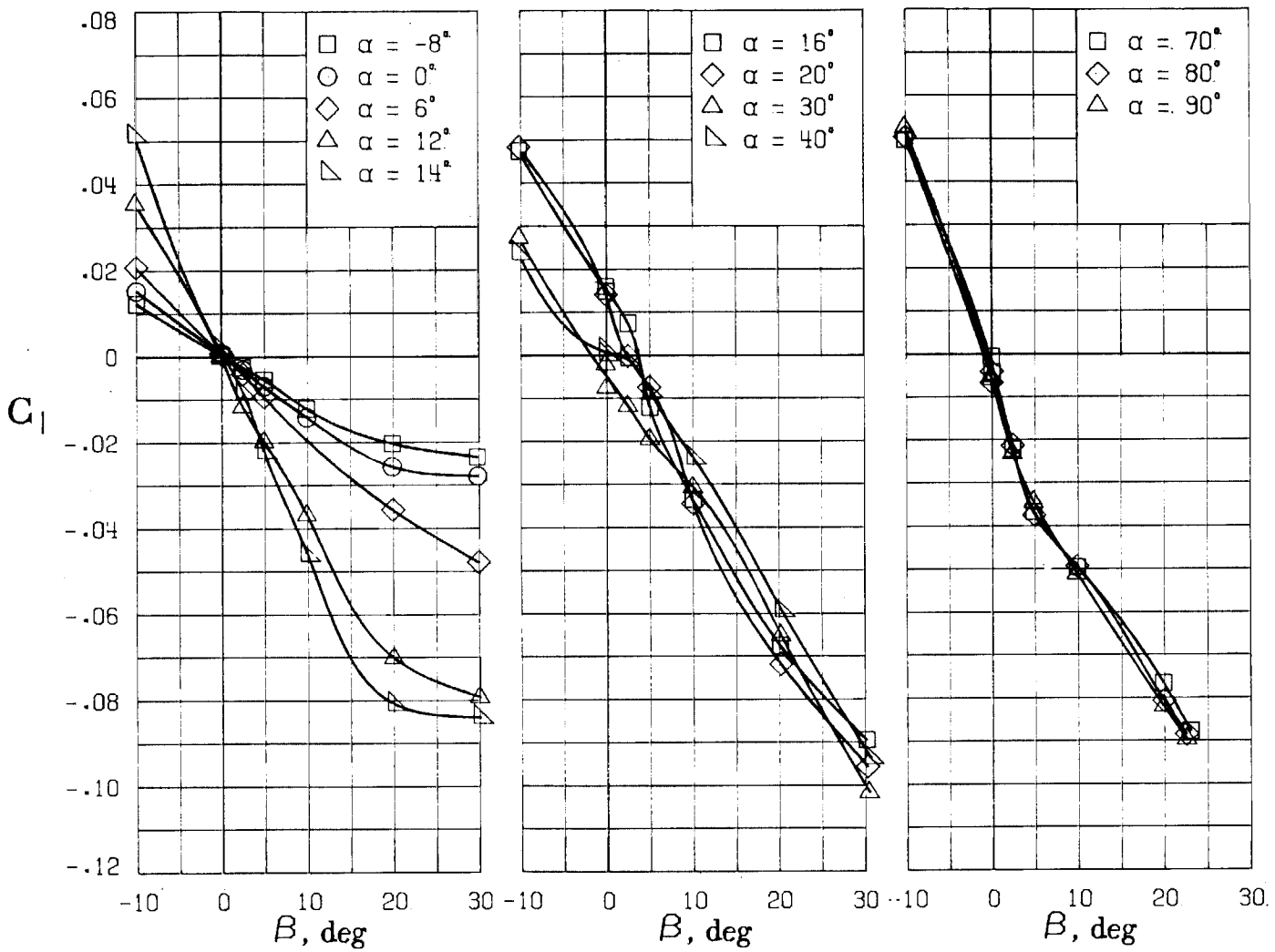

(F) LATERAL - STABILITY CHARACTERISTICS ABOUT BODY AXES AT VARIOUS ANGLES OF ATTACK.

FIGURE 24. - CONCLUDED.

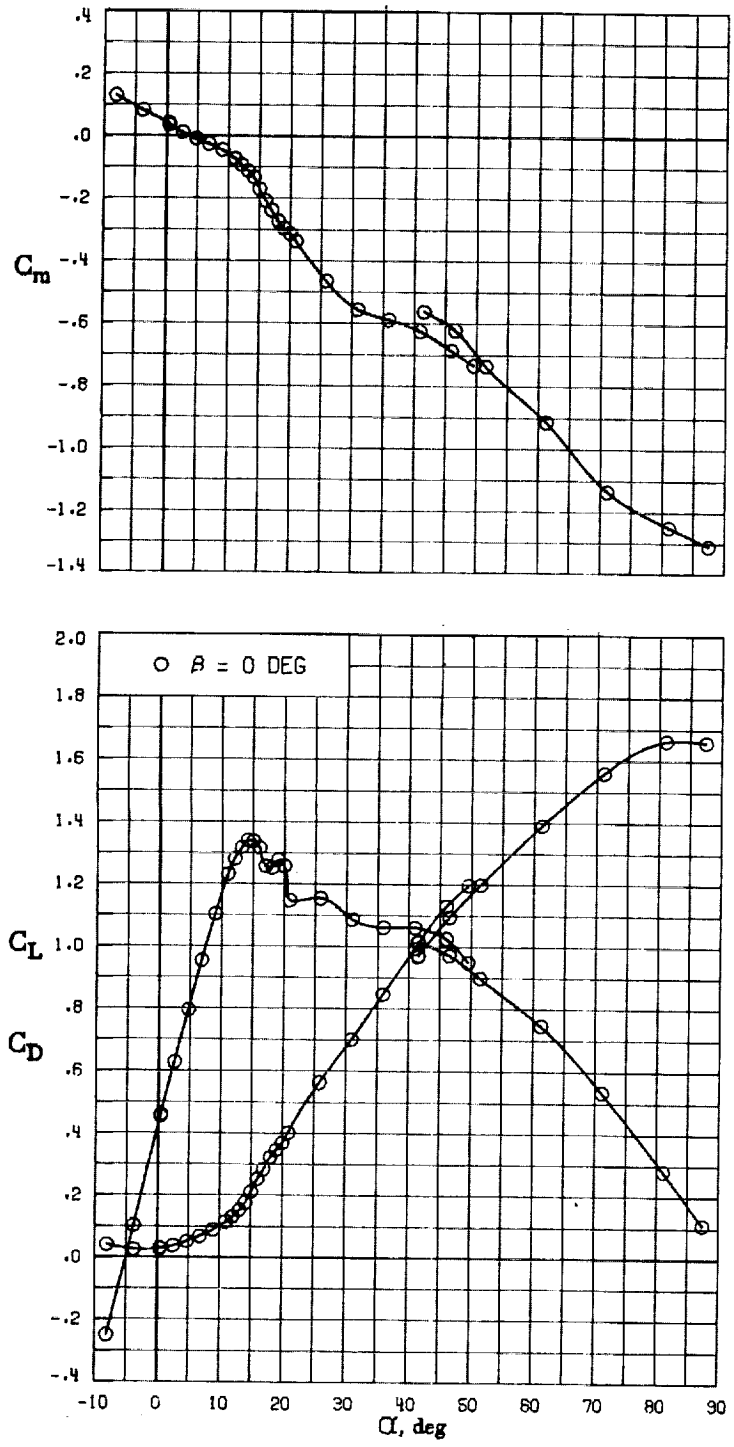

(A) LONGITUDINAL FORCE AND MOMENT COEFFICIENTS ABOUT STABILITY AXES.

FIGURE 25. - EFFECT OF ANGLE OF ATTACK AND SIDESLIP ANGLE ON AERODYNAMIC CHARACTERISTICS AT RE = 3.45 E+06 FOR CONFIGURATION B W1 H4 V SC. $\delta_E = 0°$, $\delta_A = 0°$, $\delta_R = 0°$.

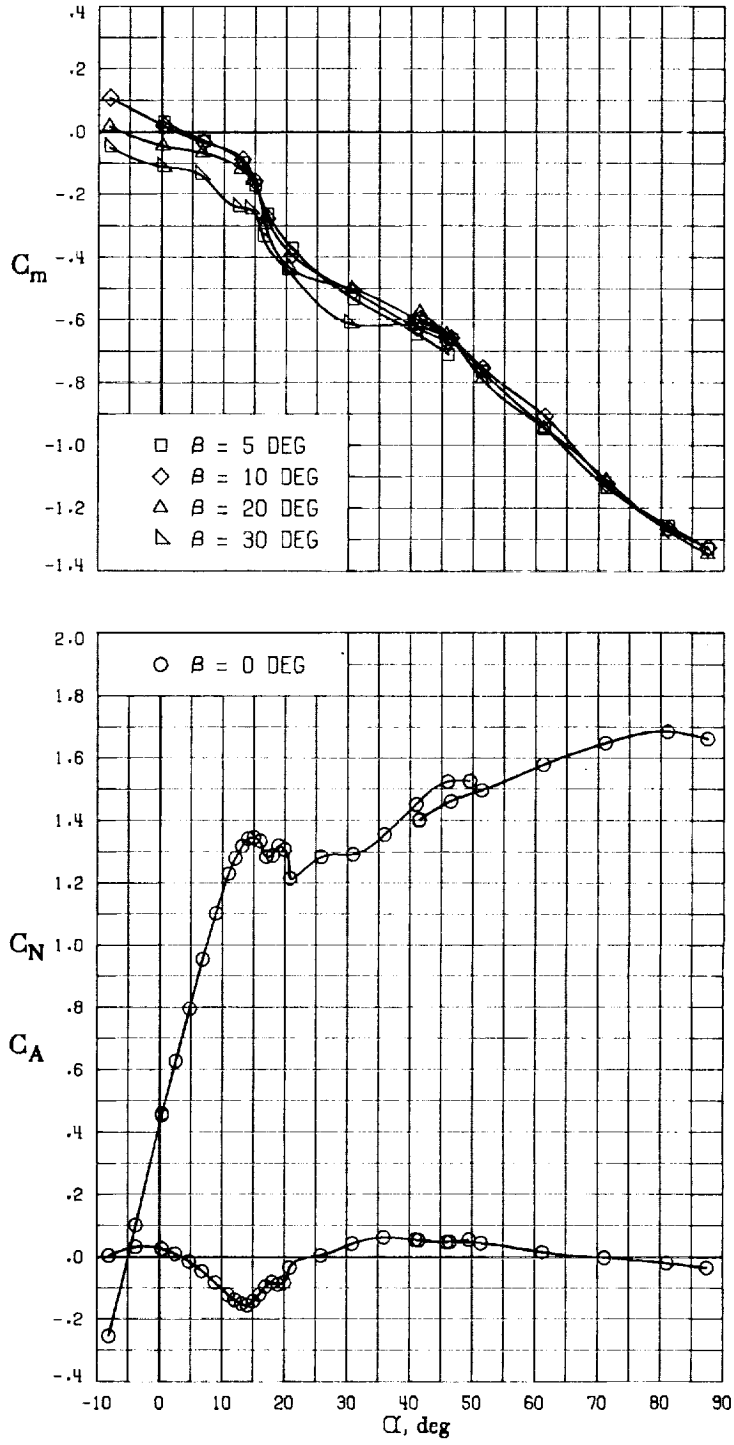

(B) LONGITUDINAL FORCE AND MOMENT COEFFICIENTS ABOUT BODY AXES.

FIGURE 25. - CONTINUED.

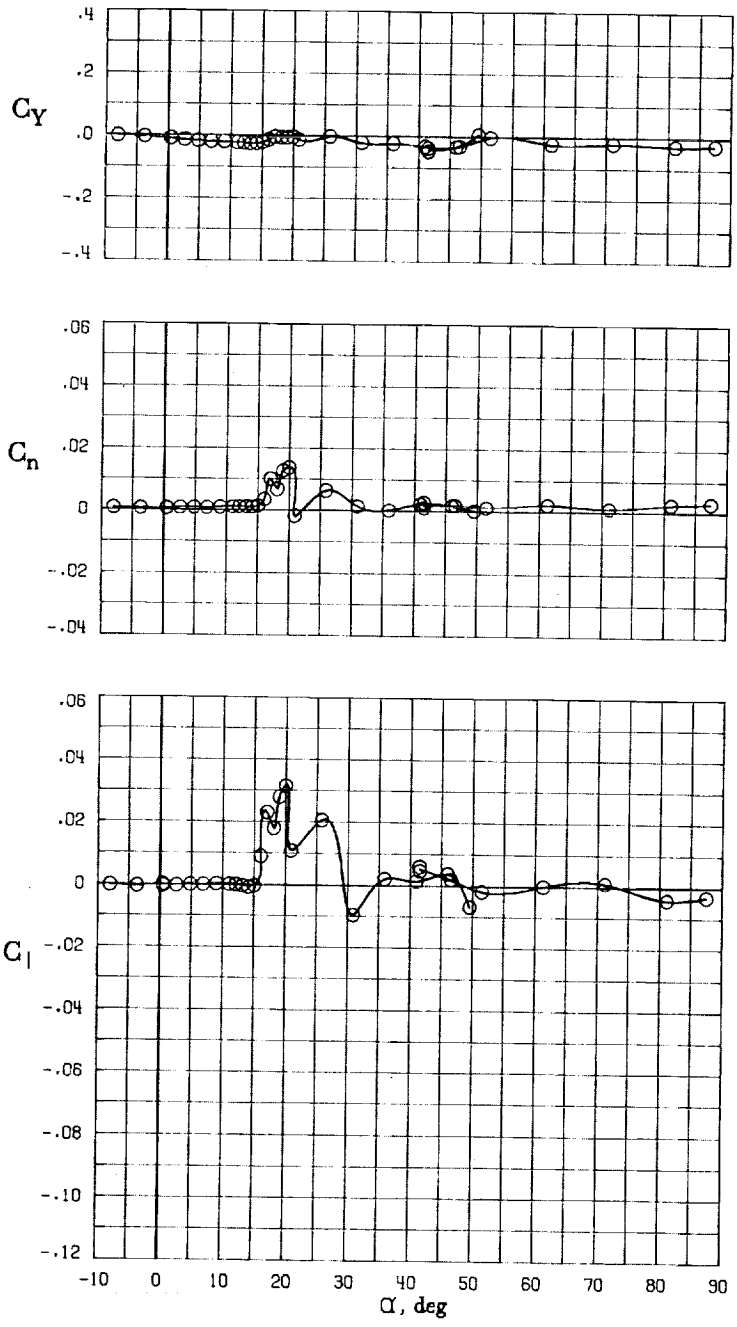

(C) LATERAL - DIRECTIONAL FORCE AND MOMENT COEFFICIENTS ABOUT BODY AXES AT ZERO SIDESLIP.

FIGURE 25. - CONTINUED.

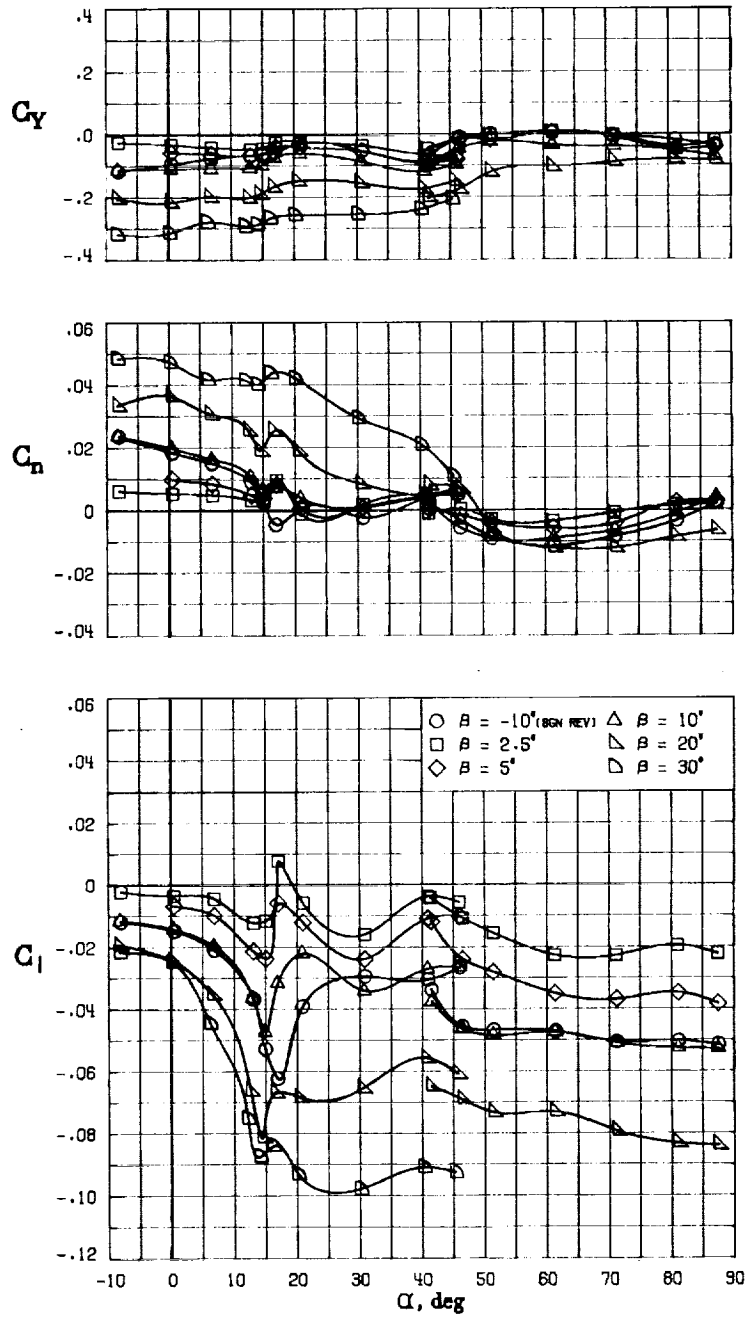

(D) LATERAL - DIRECTIONAL FORCE AND MOMENT COEFFICIENTS ABOUT BODY AXES.

FIGURE 25. - CONTINUED.

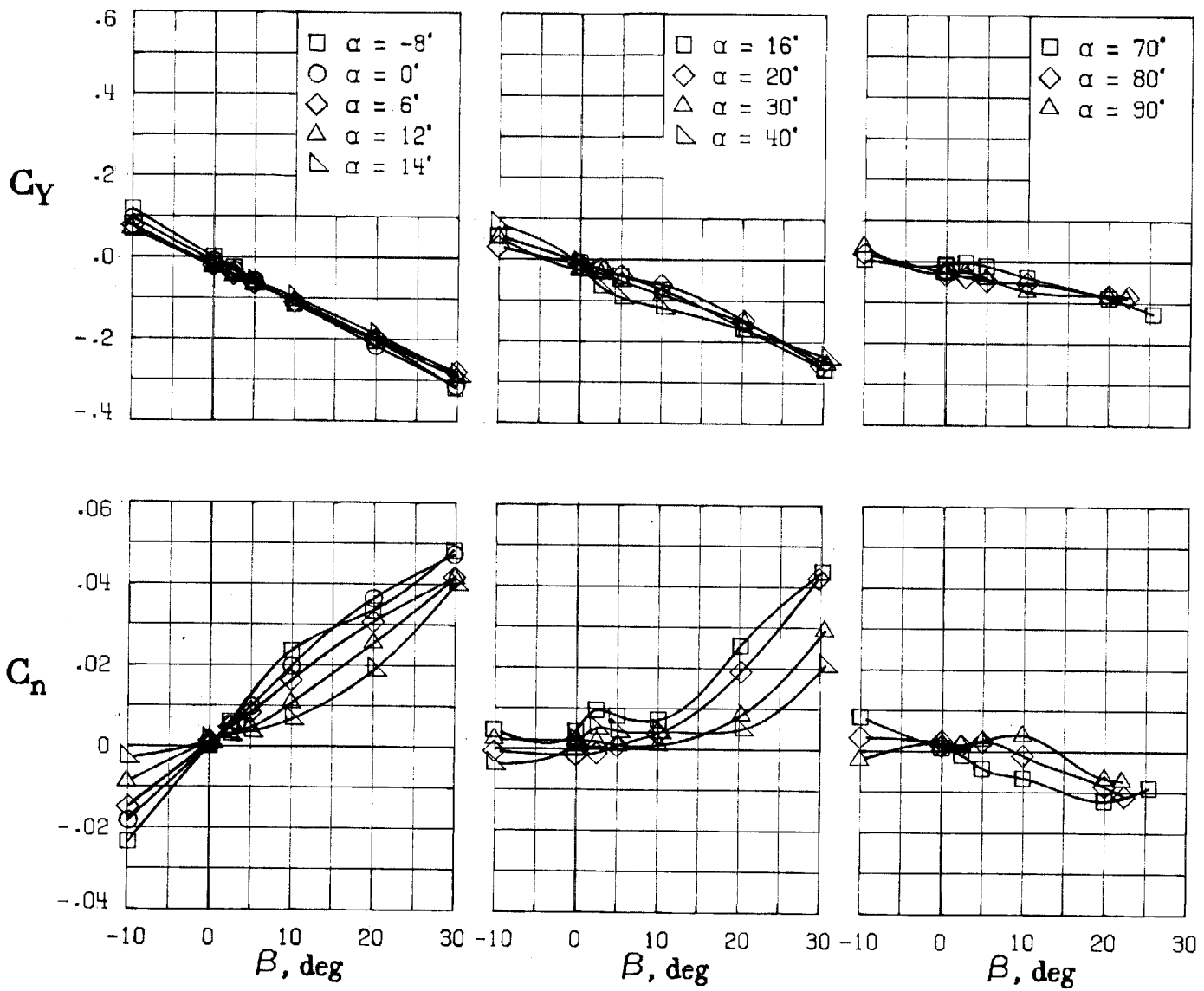

(E) DIRECTIONAL - STABILITY CHARACTERISTICS ABOUT BODY AXES AT VARIOUS ANGLES OF ATTACK.

FIGURE 25. - CONTINUED.

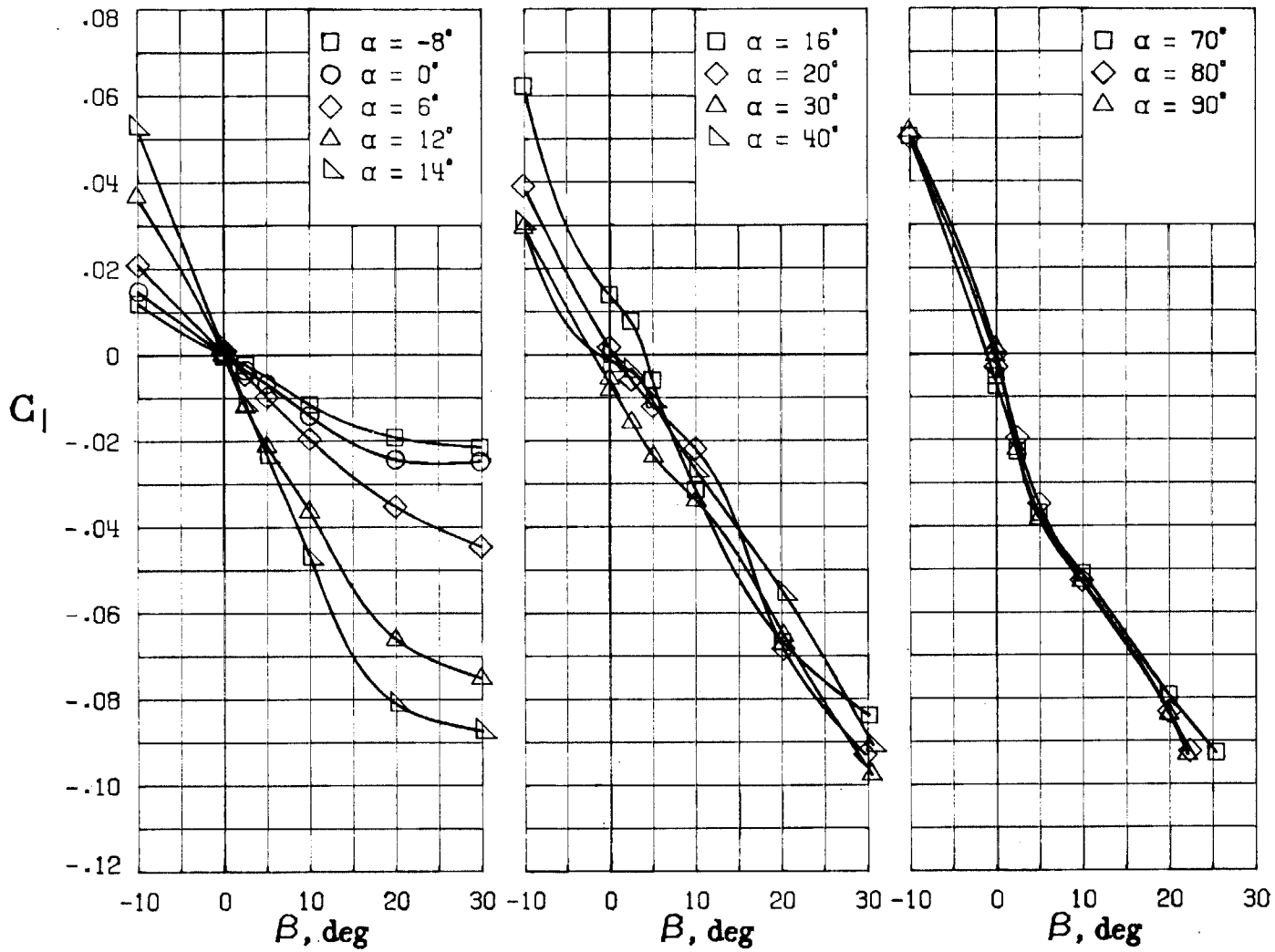

(F) LATERAL - STABILITY CHARACTERISTICS ABOUT BODY AXES AT VARIOUS ANGLES OF ATTACK.

FIGURE 25. - CONCLUDED.

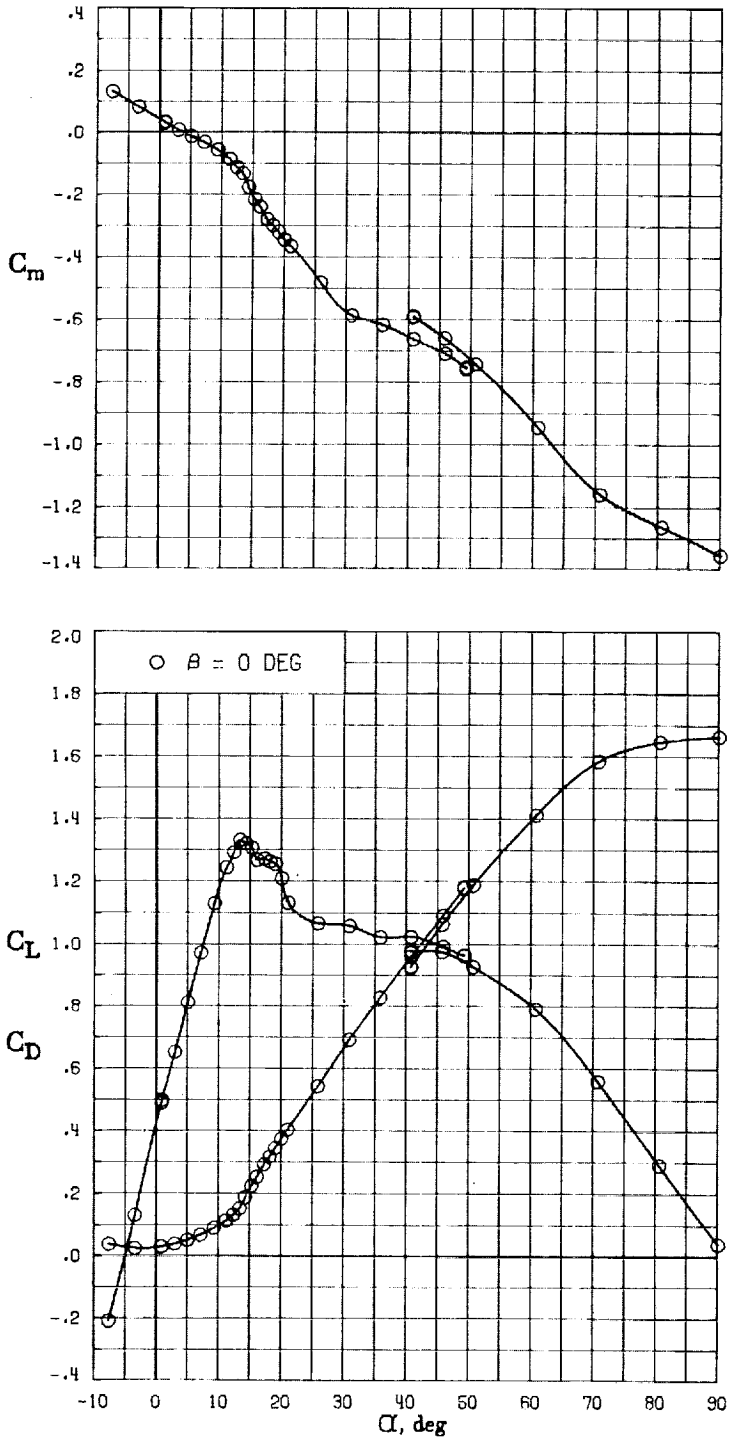

(A) LONGITUDINAL FORCE AND MOMENT COEFFICIENTS ABOUT STABILITY AXES.

FIGURE 26. – EFFECT OF ANGLE OF ATTACK AND SIDESLIP ANGLE ON AERODYNAMIC CHARACTERISTICS AT RE = 3.45 E+06 FOR CONFIGURATION B W1 H4 V U. $\delta_E = 0°$, $\delta_A = 0°$, $\delta_R = 0°$.

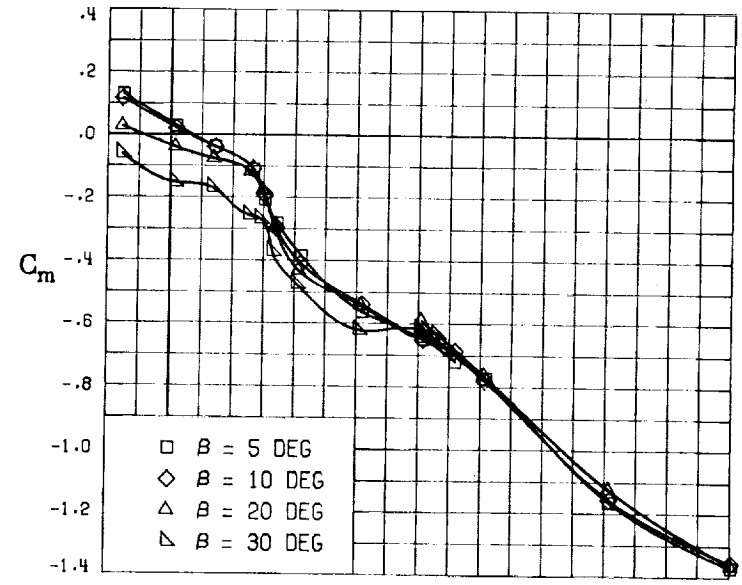

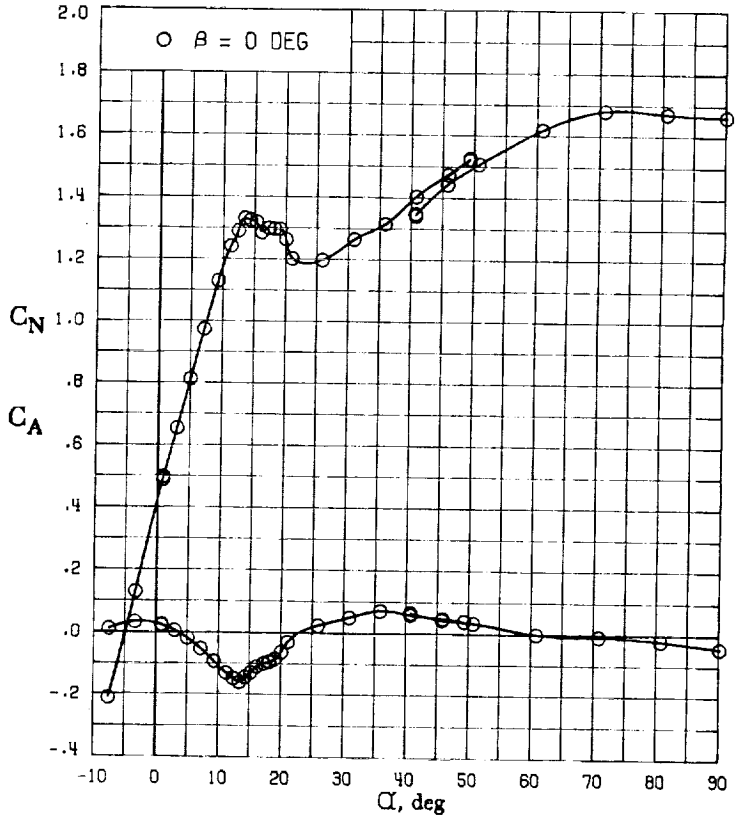

(B) LONGITUDINAL FORCE AND MOMENT COEFFICIENTS ABOUT BODY AXES.

FIGURE 26. - CONTINUED.

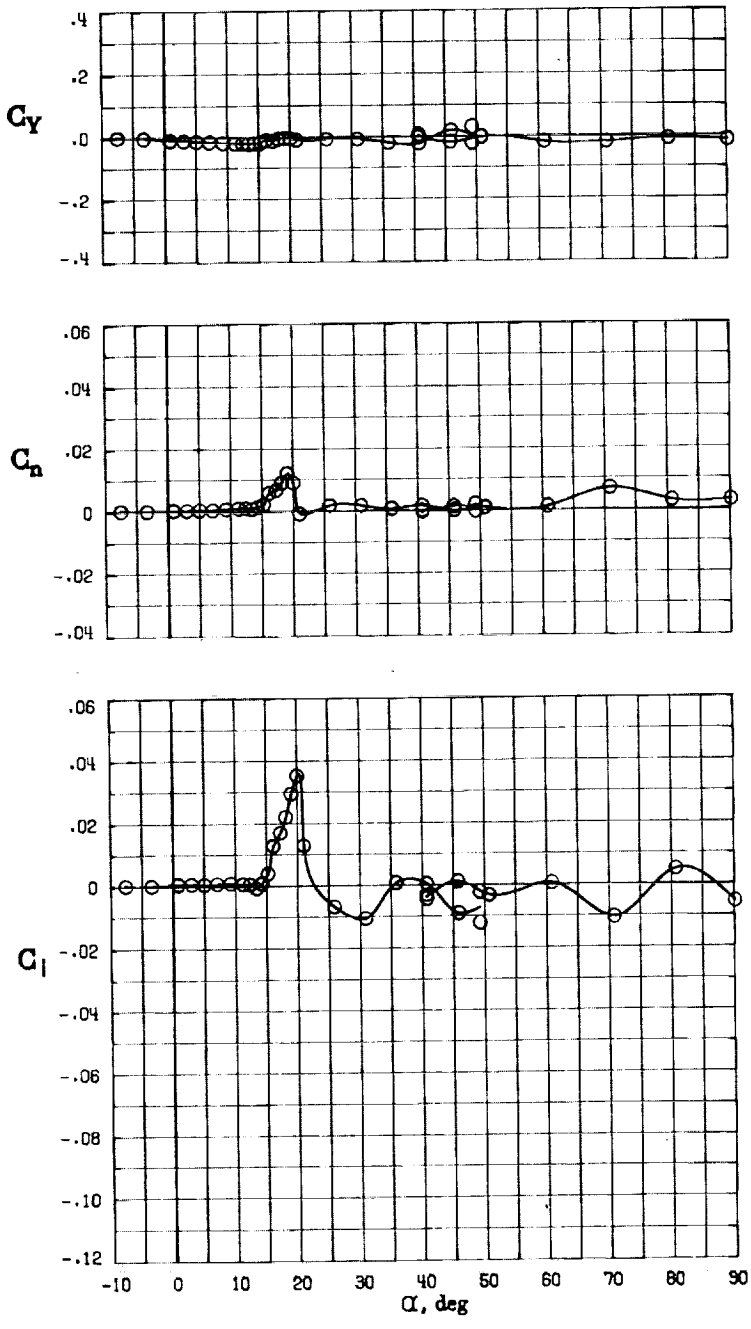

(C) LATERAL - DIRECTIONAL FORCE AND MOMENT COEFFICIENTS ABOUT BODY AXES AT ZERO SIDESLIP.

FIGURE 26. - CONTINUED.

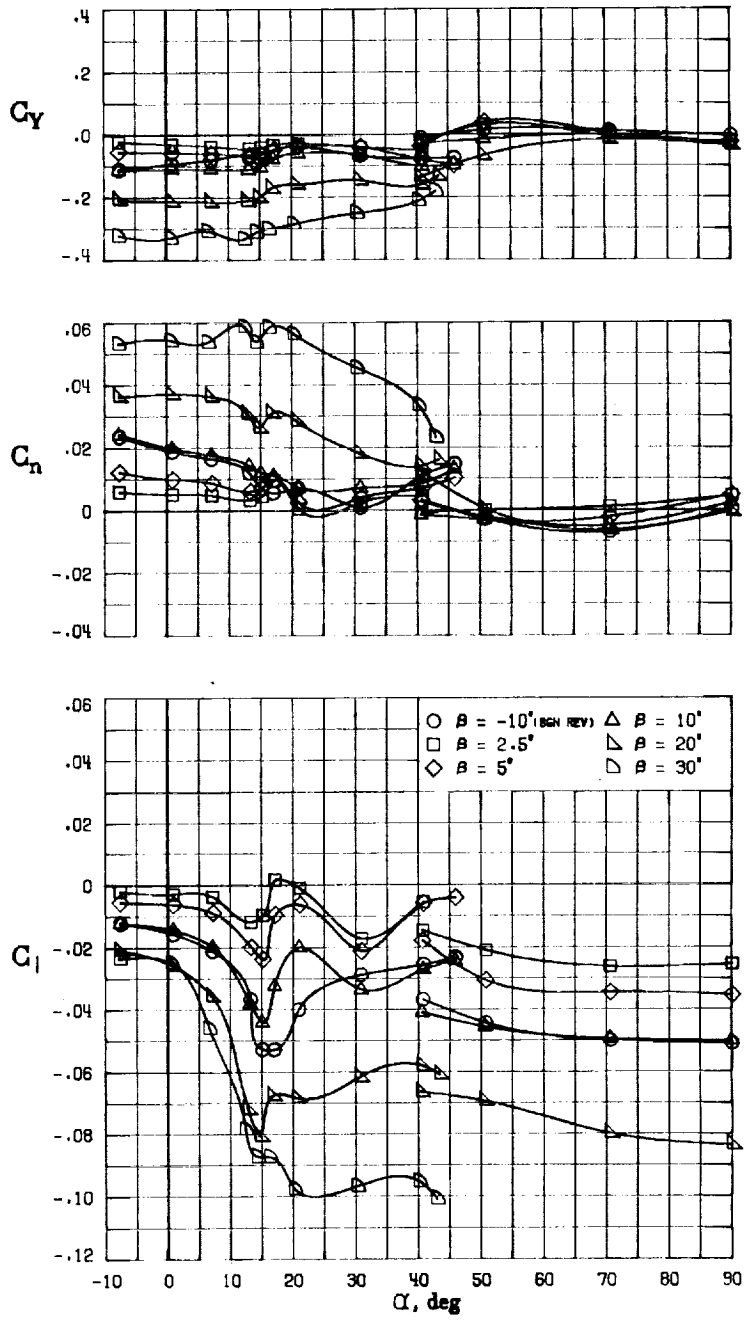

(D) LATERAL - DIRECTIONAL FORCE AND MOMENT COEFFICIENTS ABOUT BODY AXES.

FIGURE 26. - CONTINUED.

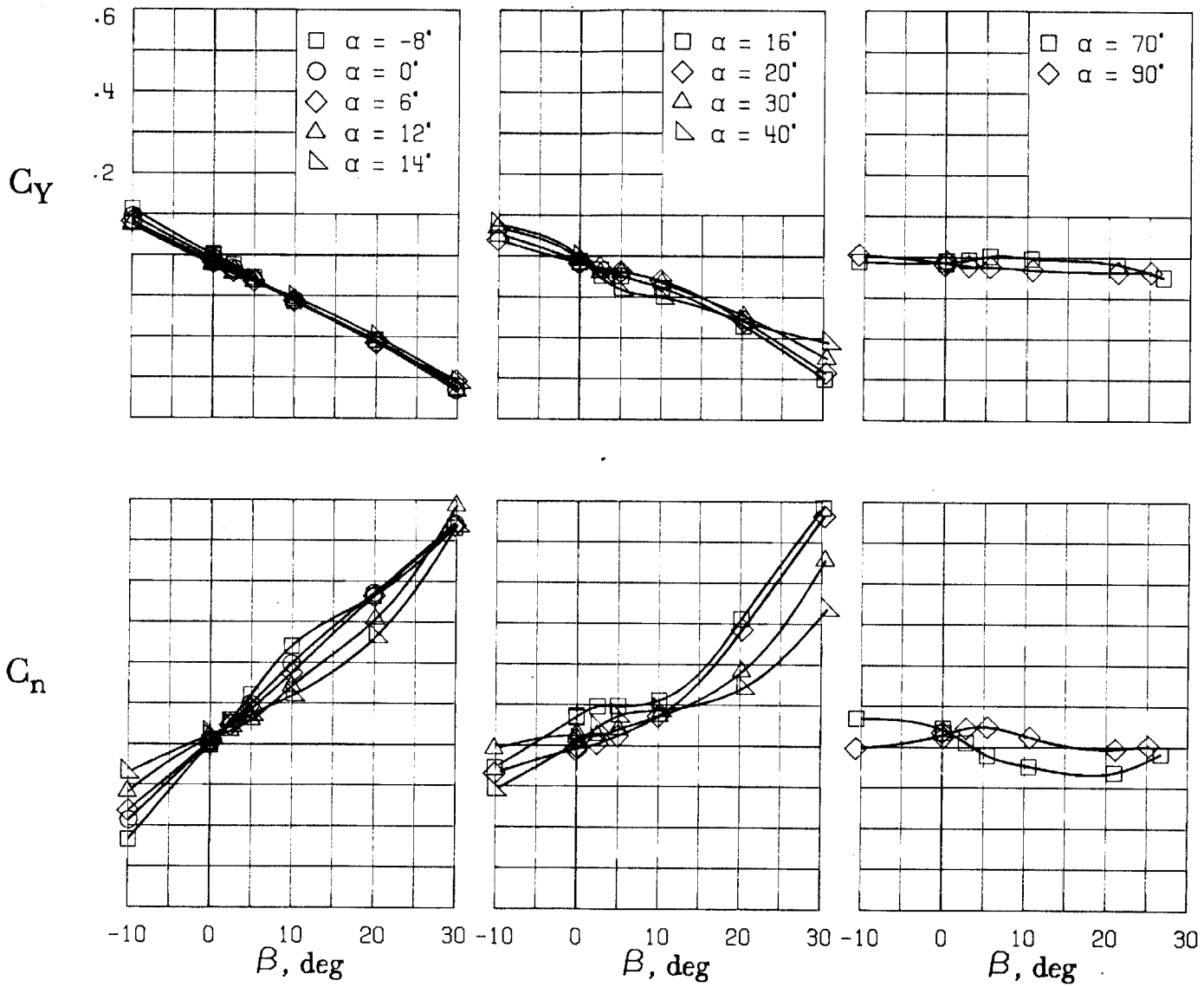

(E) DIRECTIONAL - STABILITY CHARACTERISTICS ABOUT BODY AXES AT VARIOUS ANGLES OF ATTACK.

FIGURE 26. - CONTINUED.

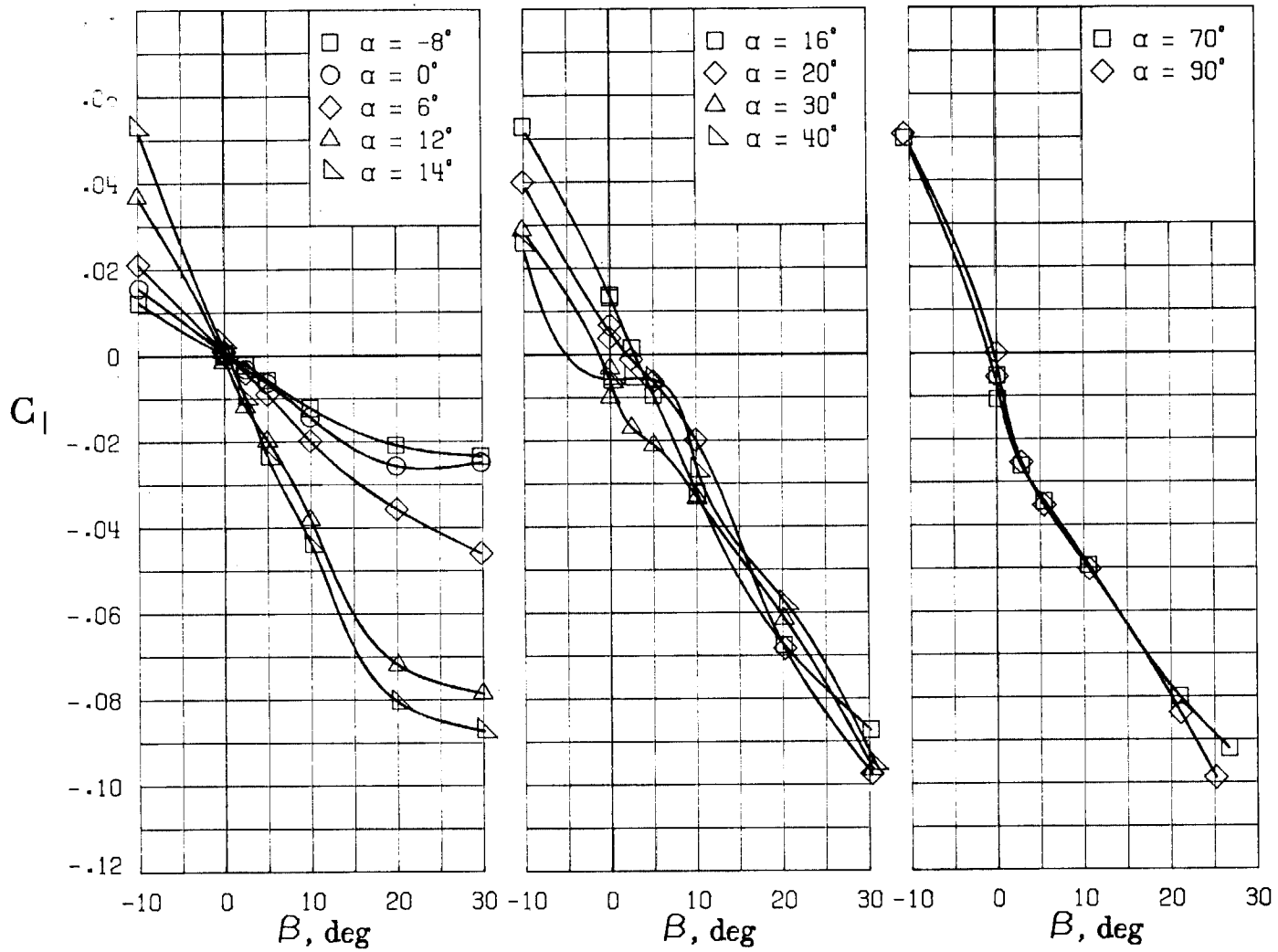

(F) LATERAL - STABILITY CHARACTERISTICS ABOUT BODY AXES AT VARIOUS ANGLES OF ATTACK.

FIGURE 26. - CONCLUDED.

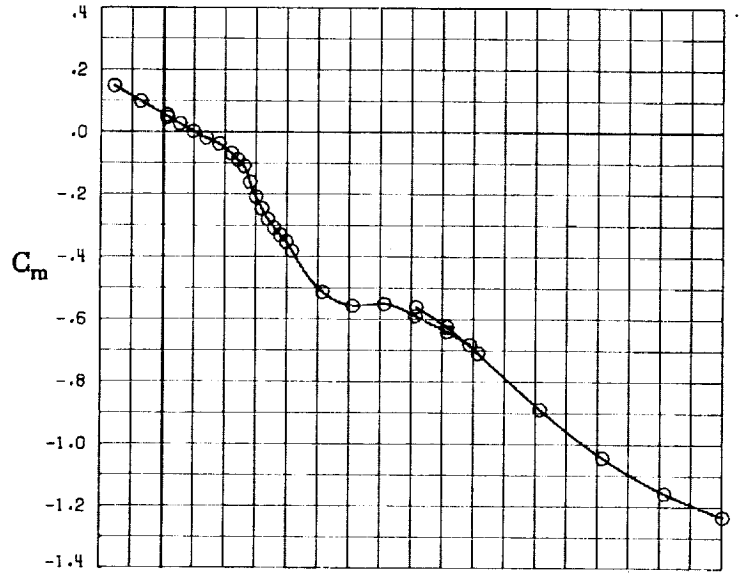

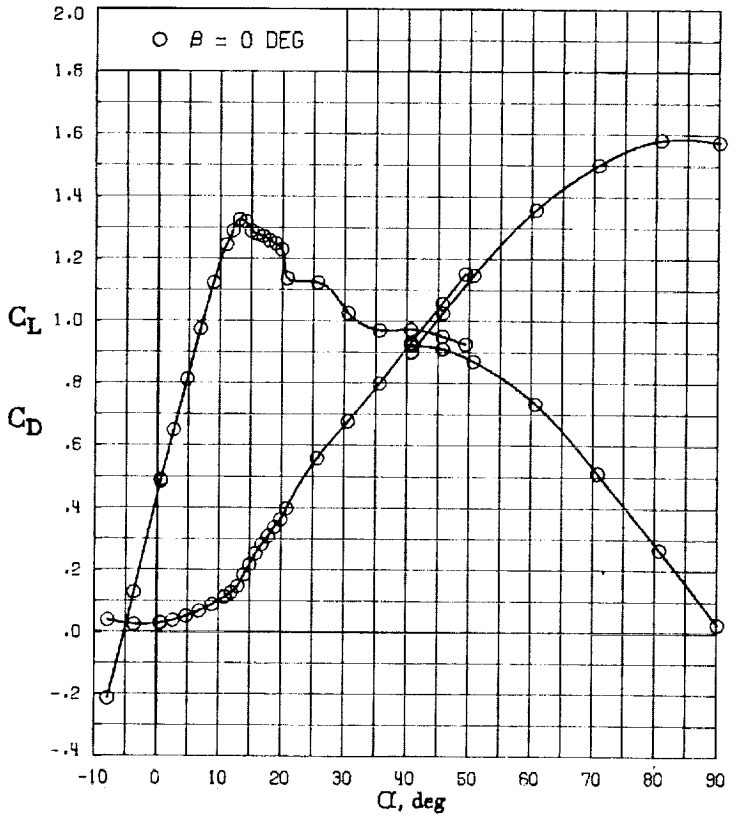

(A) LONGITUDINAL FORCE AND MOMENT COEFFICIENTS ABOUT STABILITY AXES.

FIGURE 27. - EFFECT OF ANGLE OF ATTACK AND SIDESLIP ANGLE ON AERODYNAMIC CHARACTERISTICS AT RE = 3.45 E+06 FOR CONFIGURATION B W1 H4 V D. $\delta_E = 0°$, $\delta_A = 0°$, $\delta_R = 0°$.

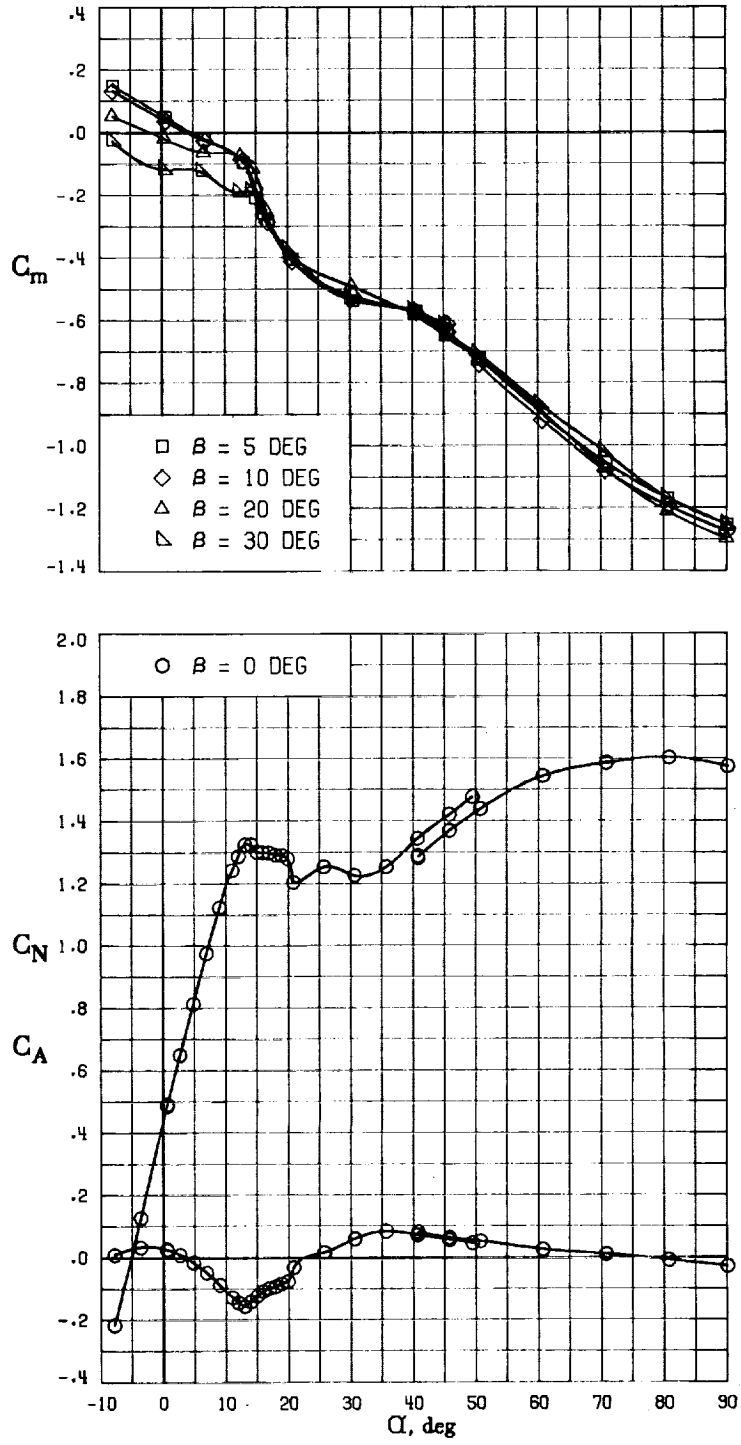

(B) LONGITUDINAL FORCE AND MOMENT COEFFICIENTS ABOUT BODY AXES.

FIGURE 27. - CONTINUED.

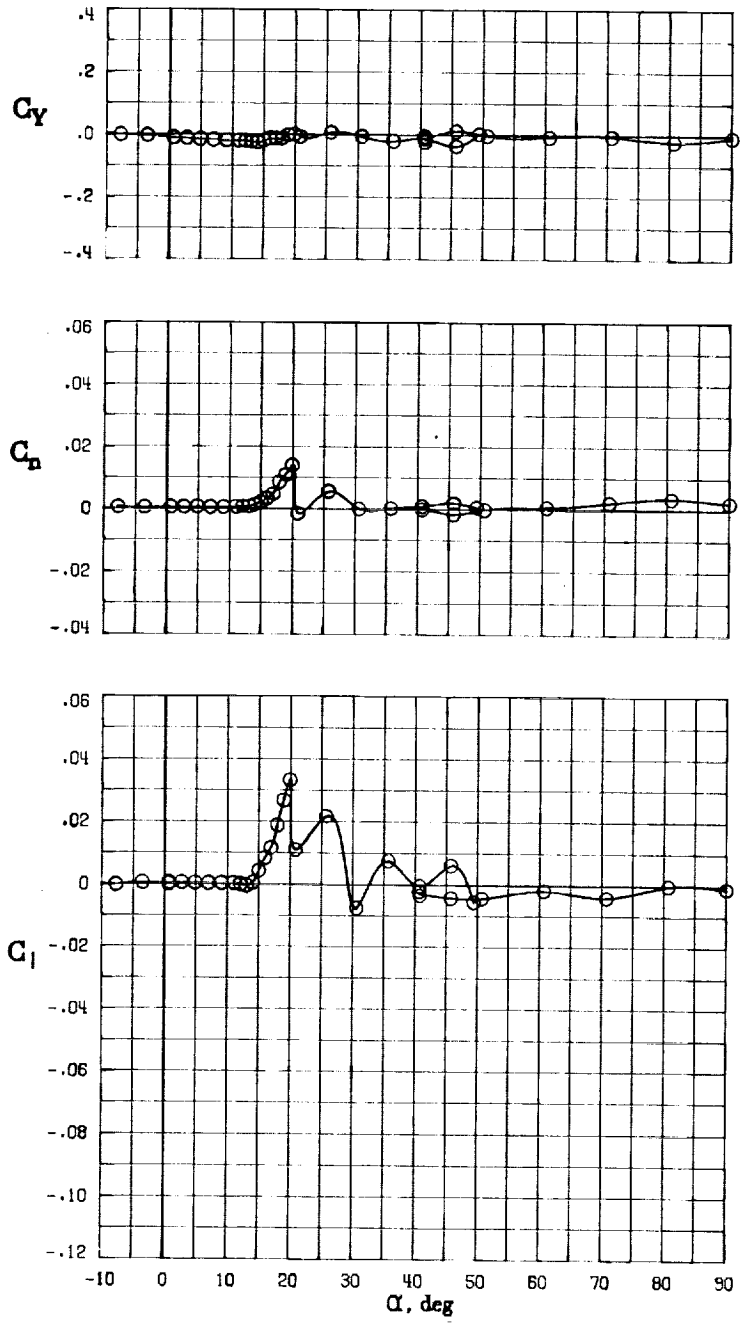

(C) LATERAL - DIRECTIONAL FORCE AND MOMENT COEFFICIENTS ABOUT BODY AXES AT ZERO SIDESLIP.

FIGURE 27. - CONTINUED.

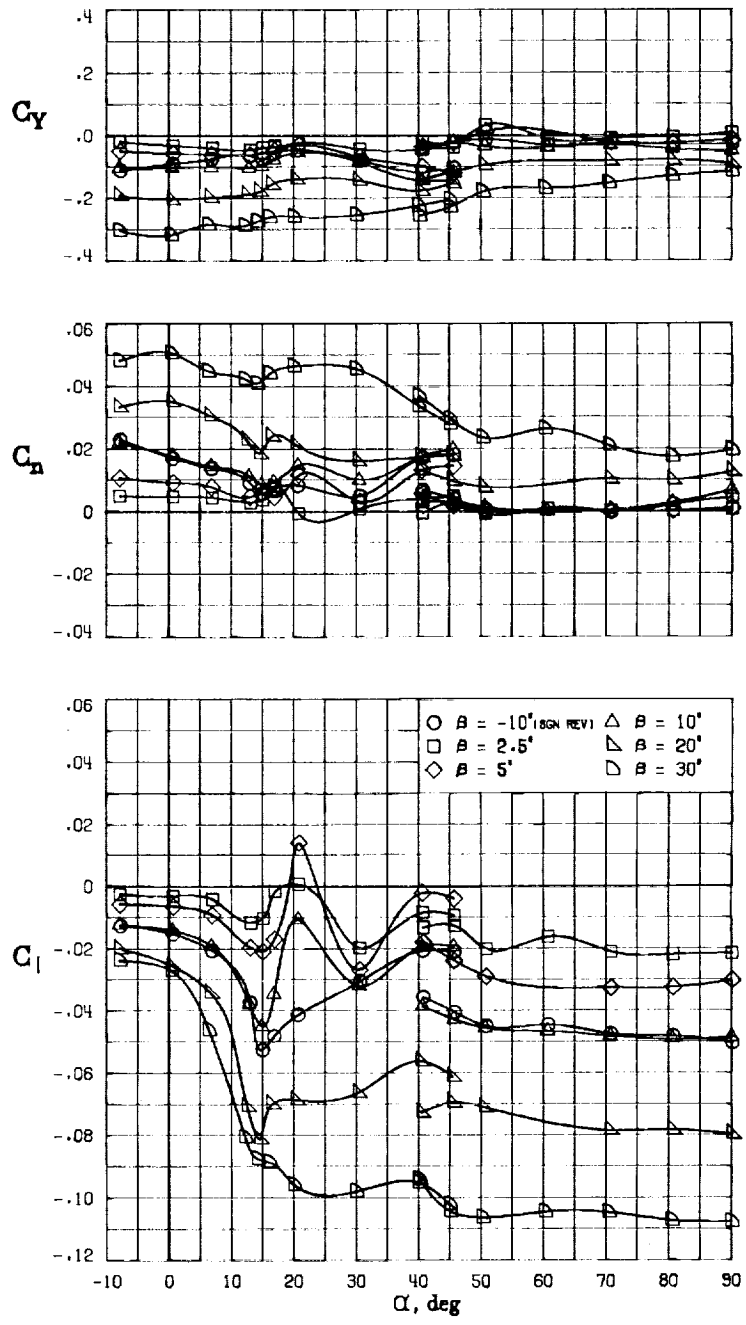

(D) LATERAL - DIRECTIONAL FORCE AND MOMENT COEFFICIENTS ABOUT BODY AXES.

FIGURE 27. - CONTINUED.

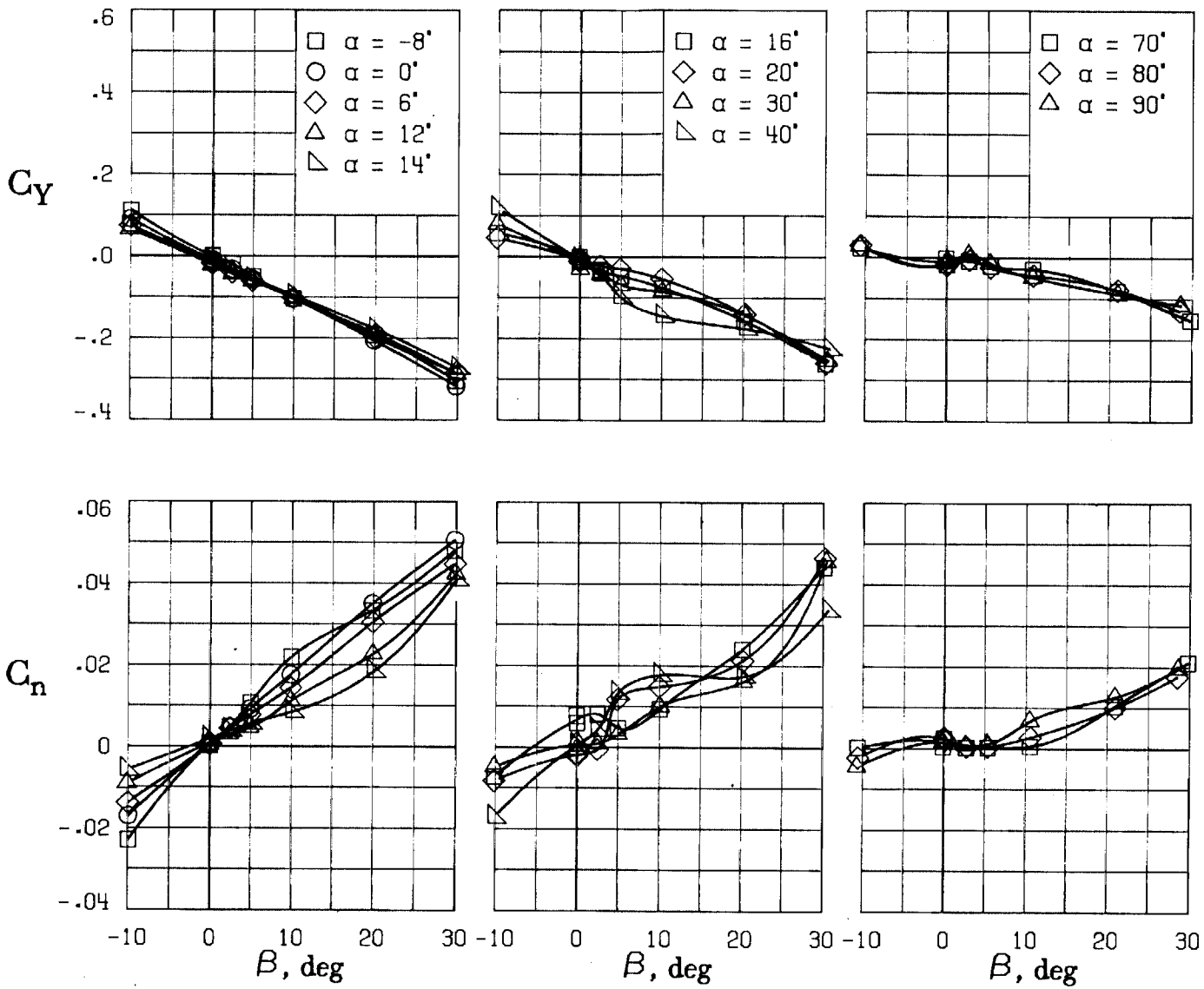

(E) DIRECTIONAL - STABILITY CHARACTERISTICS ABOUT BODY AXES AT VARIOUS ANGLES OF ATTACK.

FIGURE 27. - CONTINUED.

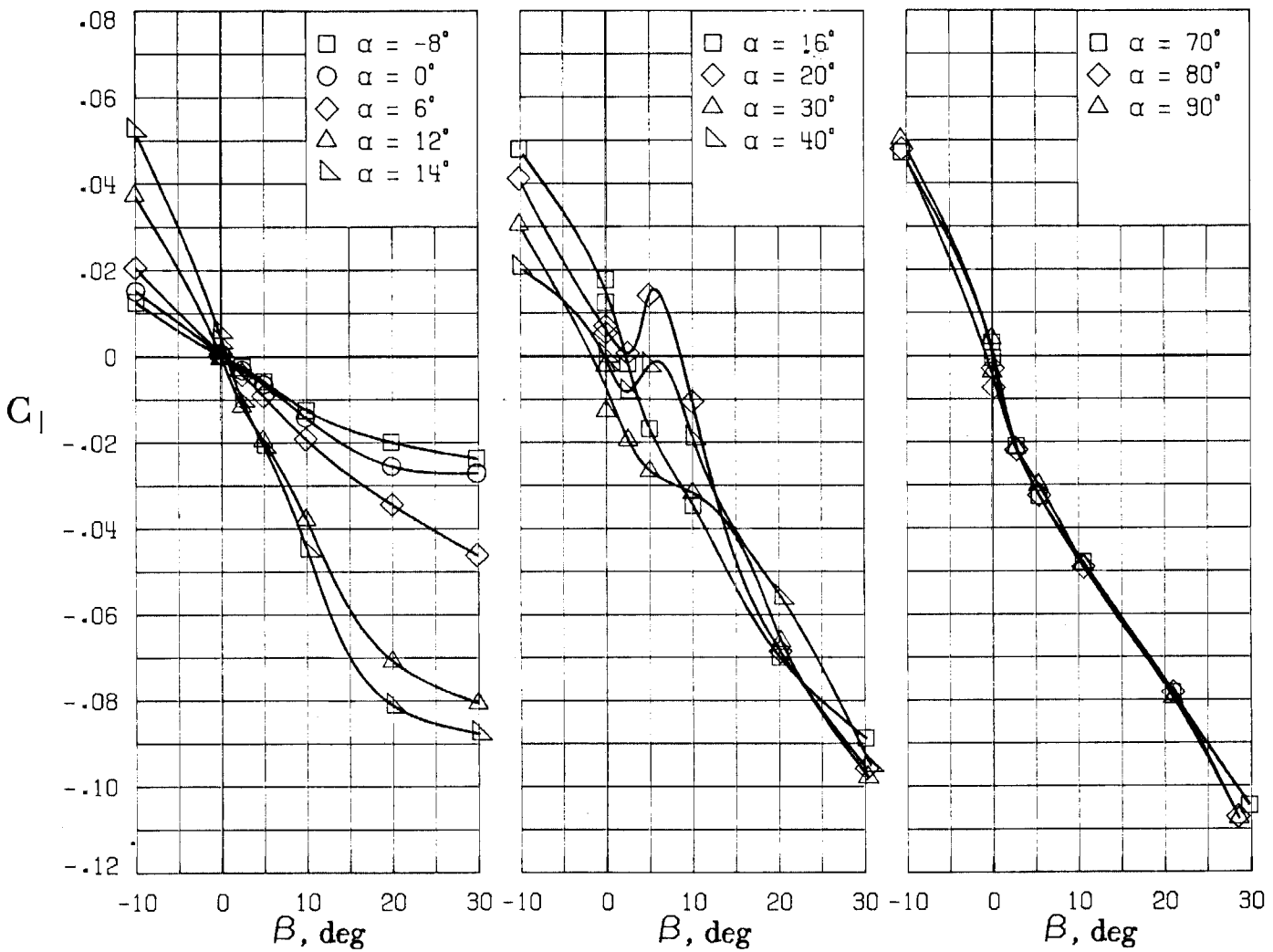

(F) LATERAL - STABILITY CHARACTERISTICS ABOUT BODY AXES AT VARIOUS ANGLES OF ATTACK.

FIGURE 27. - CONCLUDED.

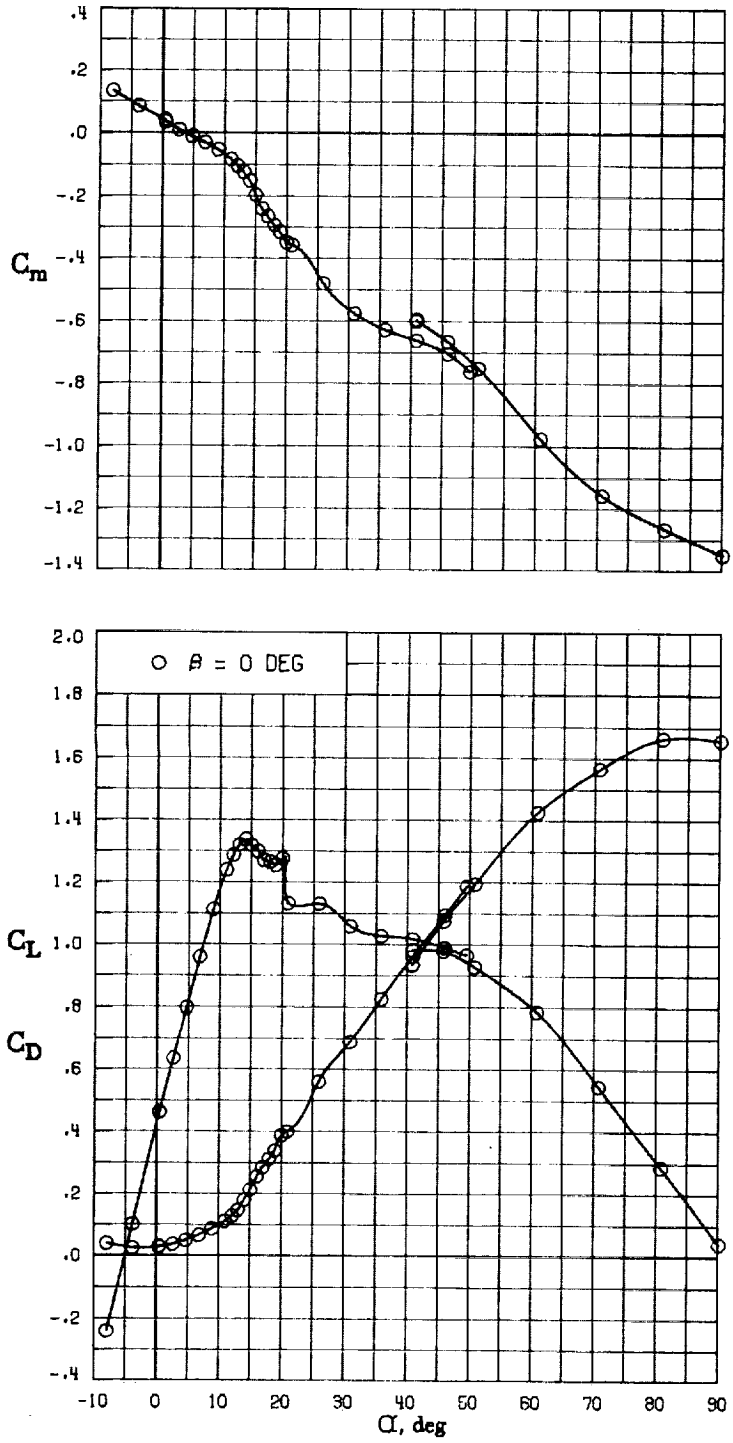

(A) LONGITUDINAL FORCE AND MOMENT COEFFICIENTS ABOUT STABILITY AXES.

FIGURE 28. - EFFECT OF ANGLE OF ATTACK AND SIDESLIP ANGLE ON AERODYNAMIC CHARACTERISTICS AT RE = 3.45 E+06 FOR CONFIGURATION B W1 H4 V FM. $\delta_E = 0°$, $\delta_A = 0°$, $\delta_R = 0°$.

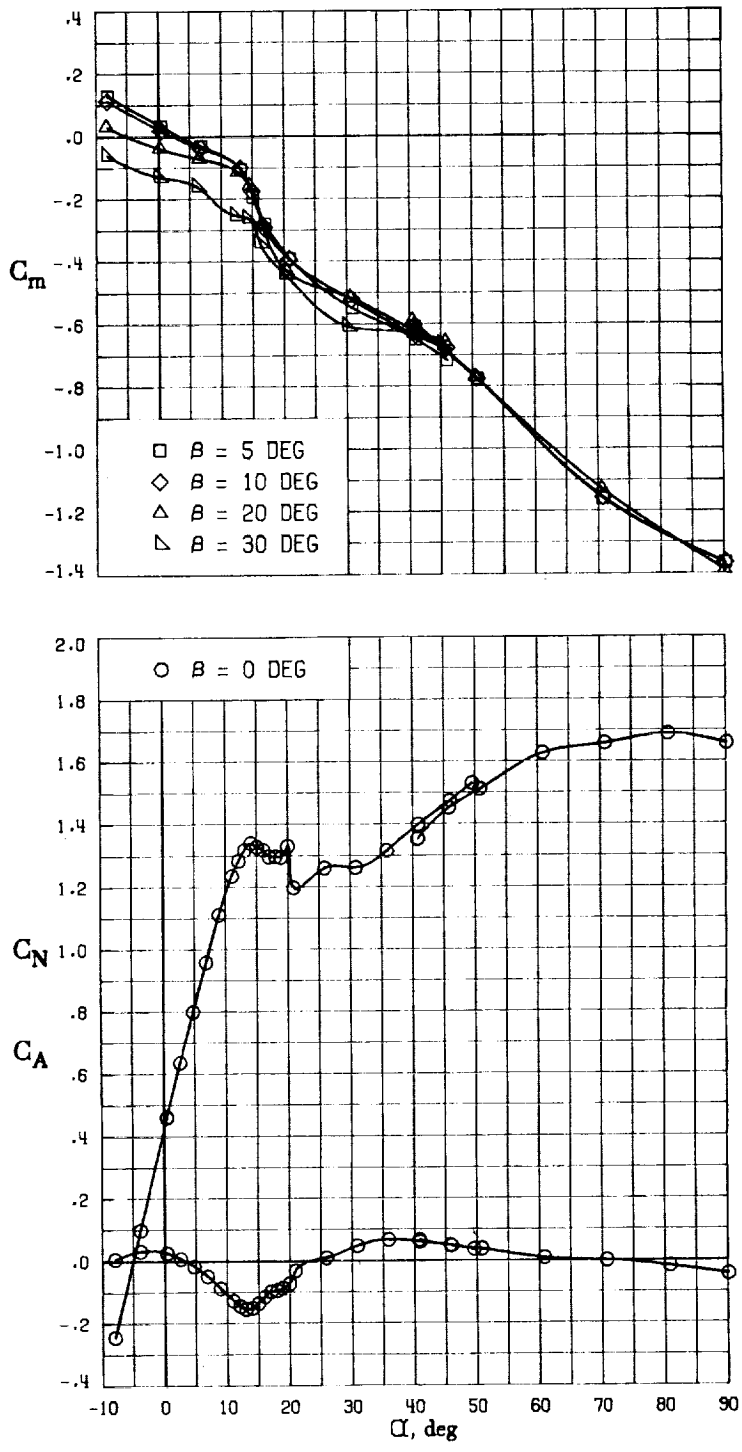

(B) LONGITUDINAL FORCE AND MOMENT COEFFICIENTS ABOUT BODY AXES.

FIGURE 28. - CONTINUED.

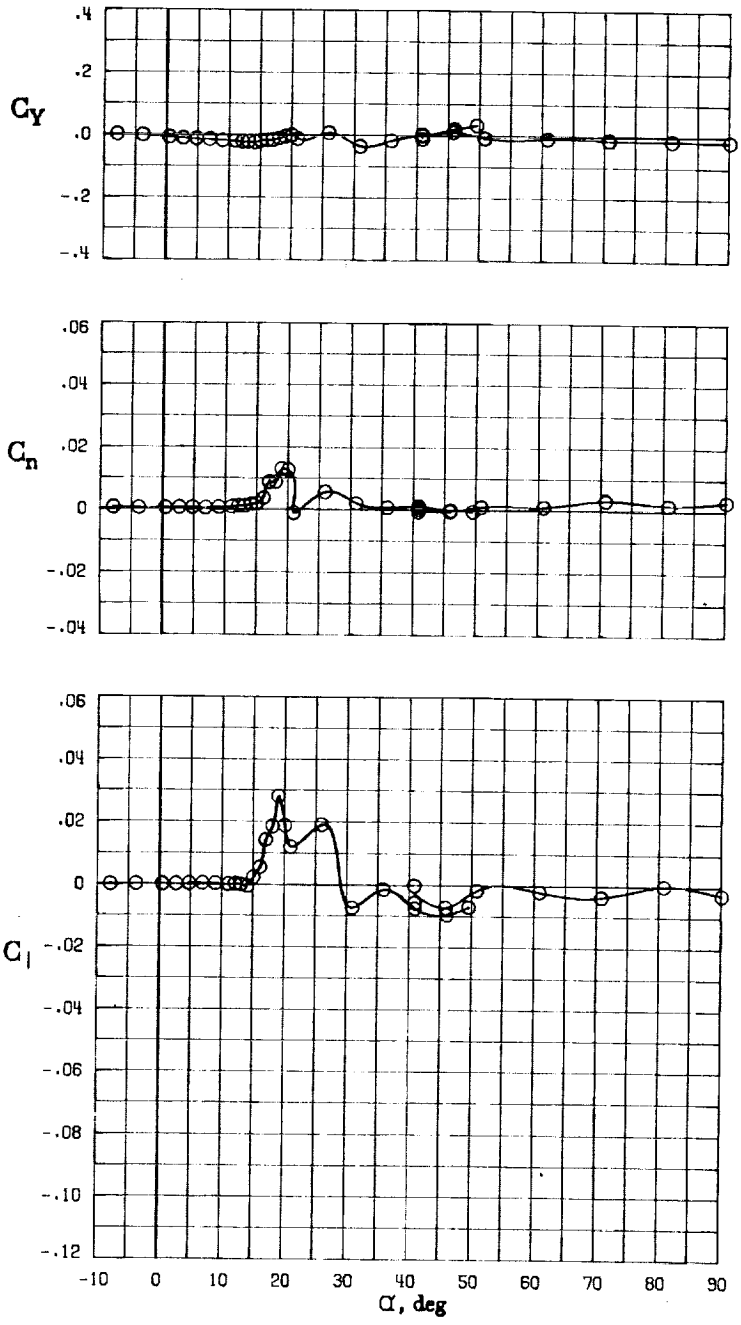

(C) LATERAL - DIRECTIONAL FORCE AND MOMENT COEFFICIENTS ABOUT BODY AXES AT ZERO SIDESLIP.

FIGURE 28. - CONTINUED.

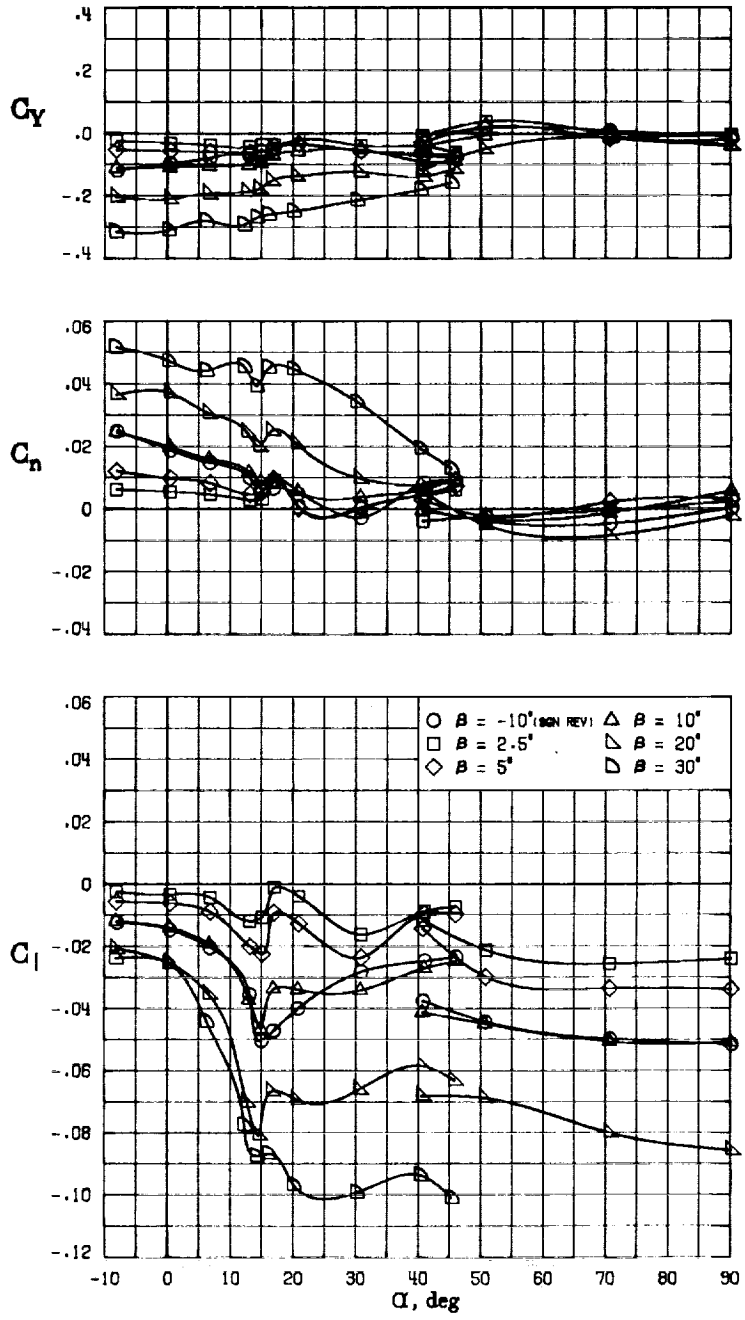

(D) LATERAL - DIRECTIONAL FORCE AND MOMENT COEFFICIENTS ABOUT BODY AXES.

FIGURE 28. - CONTINUED.

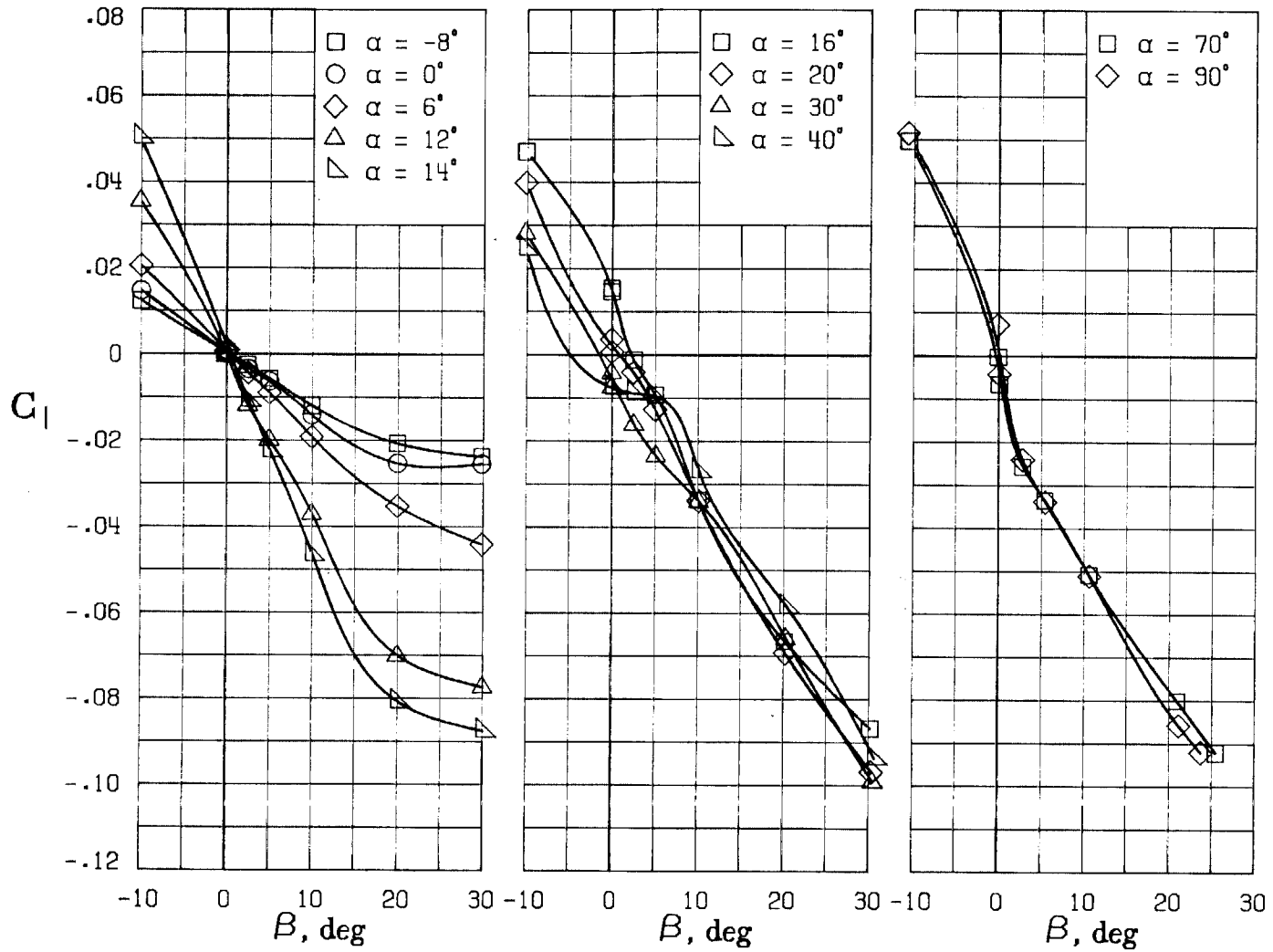

(F) LATERAL - STABILITY CHARACTERISTICS ABOUT BODY AXES AT VARIOUS ANGLES OF ATTACK.

FIGURE 28. - CONCLUDED.

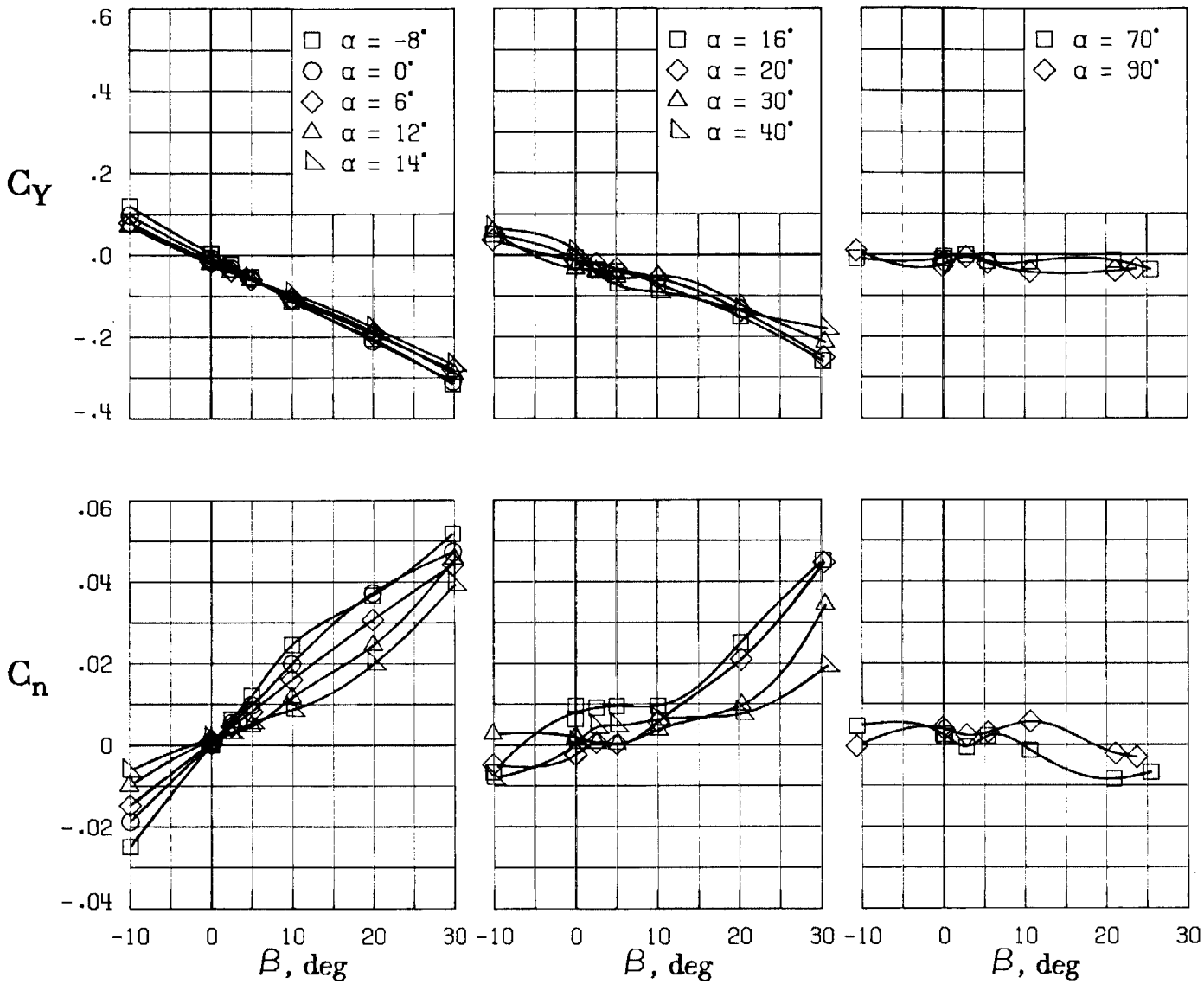

(E) DIRECTIONAL - STABILITY CHARACTERISTICS ABOUT BODY AXES AT VARIOUS ANGLES OF ATTACK.

FIGURE 28. - CONTINUED.

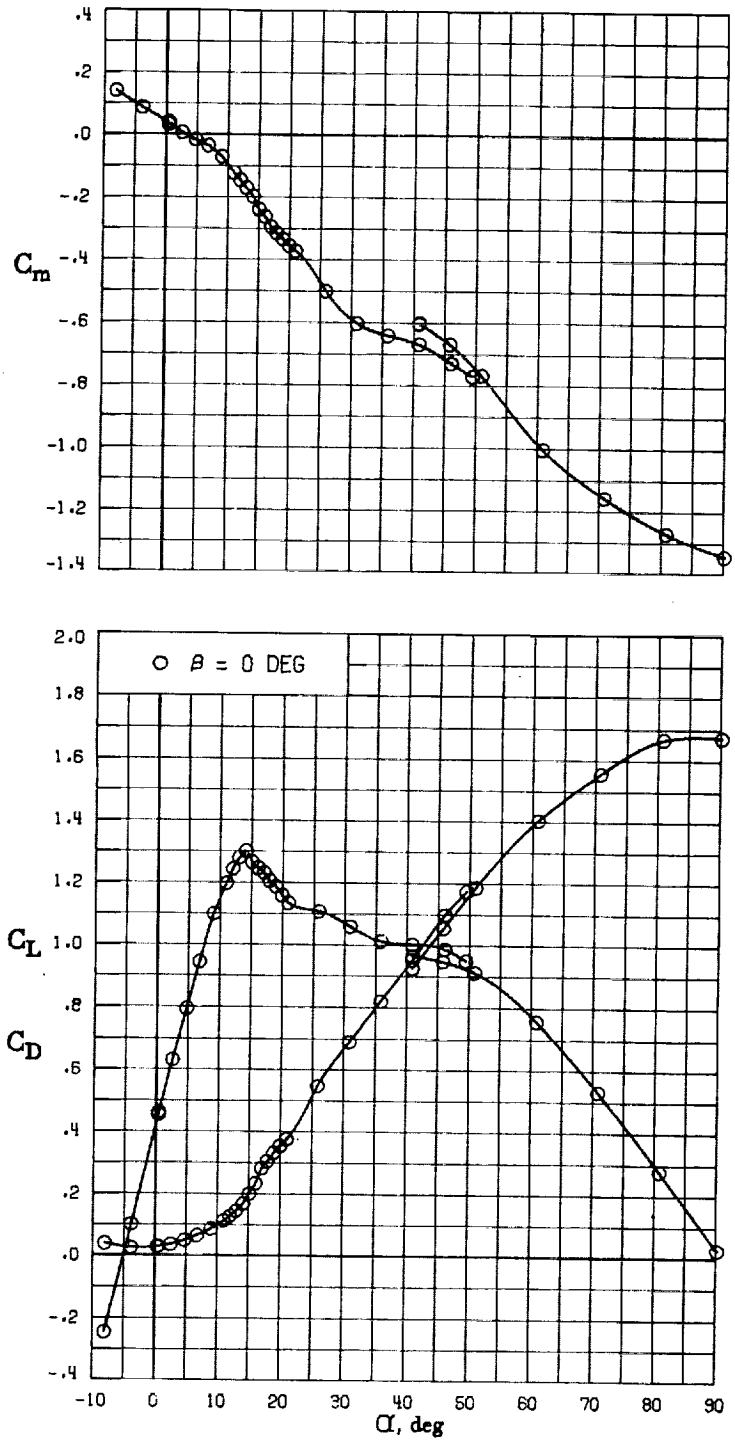

(A) LONGITUDINAL FORCE AND MOMENT COEFFICIENTS ABOUT STABILITY AXES.

FIGURE 29. - EFFECT OF ANGLE OF ATTACK AND SIDESLIP ANGLE ON AERODYNAMIC CHARACTERISTICS AT RE = 3.45 E+06 FOR CONFIGURATION B W1 H4 V -F. $\delta_E = 0°$, $\delta_A = 0°$, $\delta_R = 0°$.

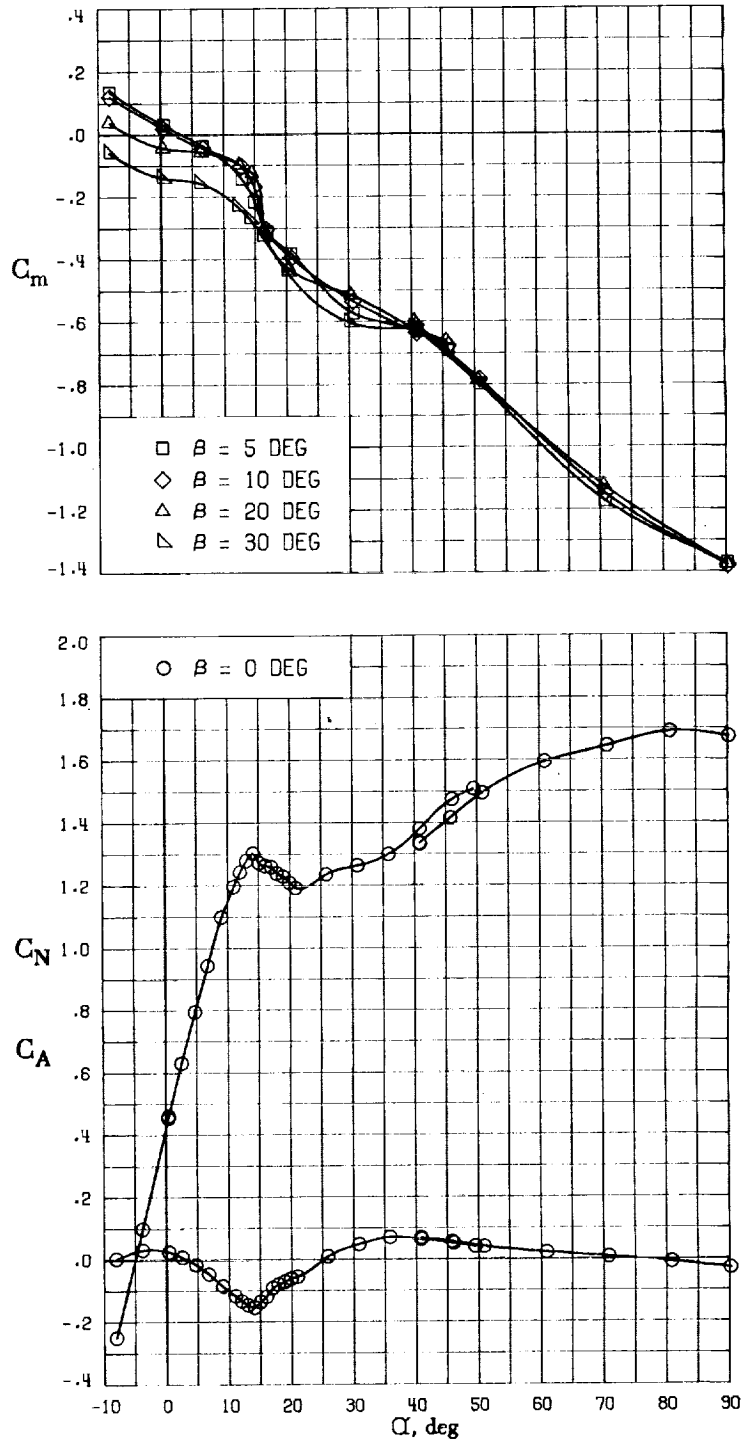

(B) LONGITUDINAL FORCE AND MOMENT COEFFICIENTS ABOUT BODY AXES.

FIGURE 29. - CONTINUED.

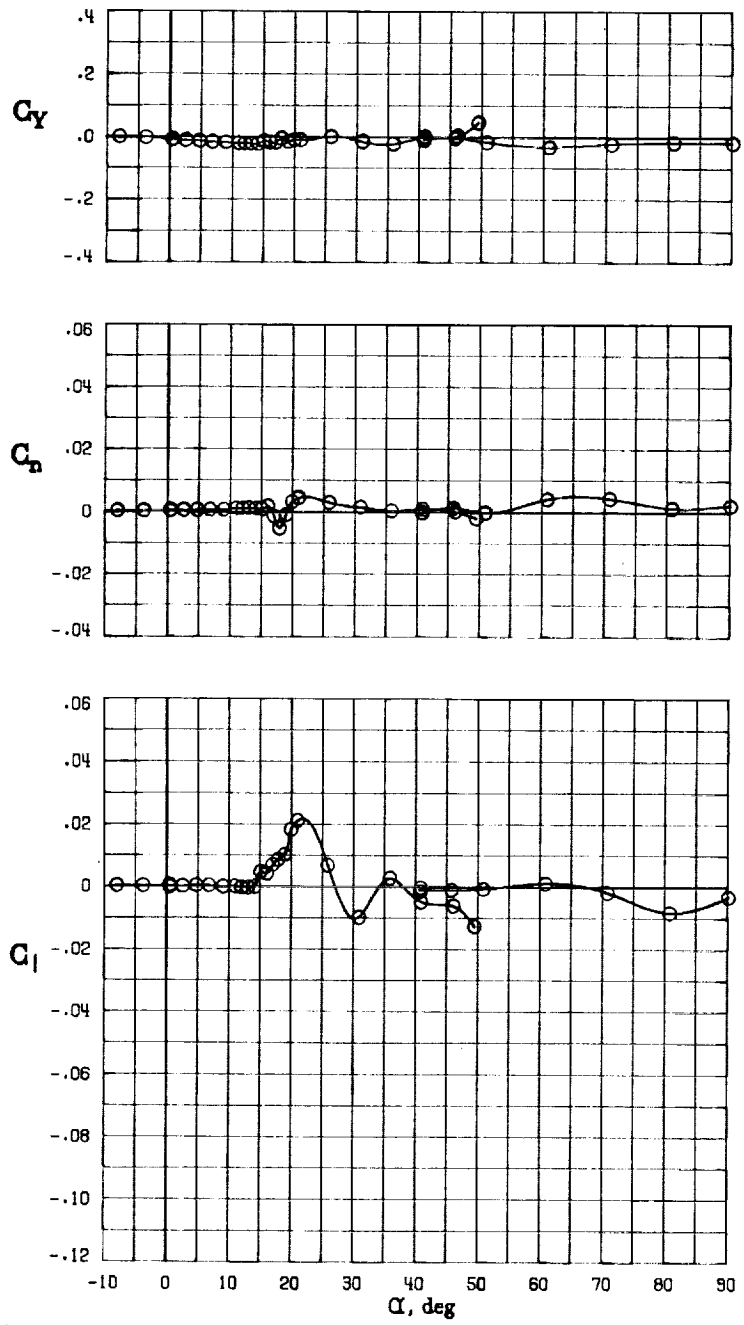

(C) LATERAL - DIRECTIONAL FORCE AND MOMENT COEFFICIENTS ABOUT BODY AXES AT ZERO SIDESLIP.

FIGURE 29. - CONTINUED.

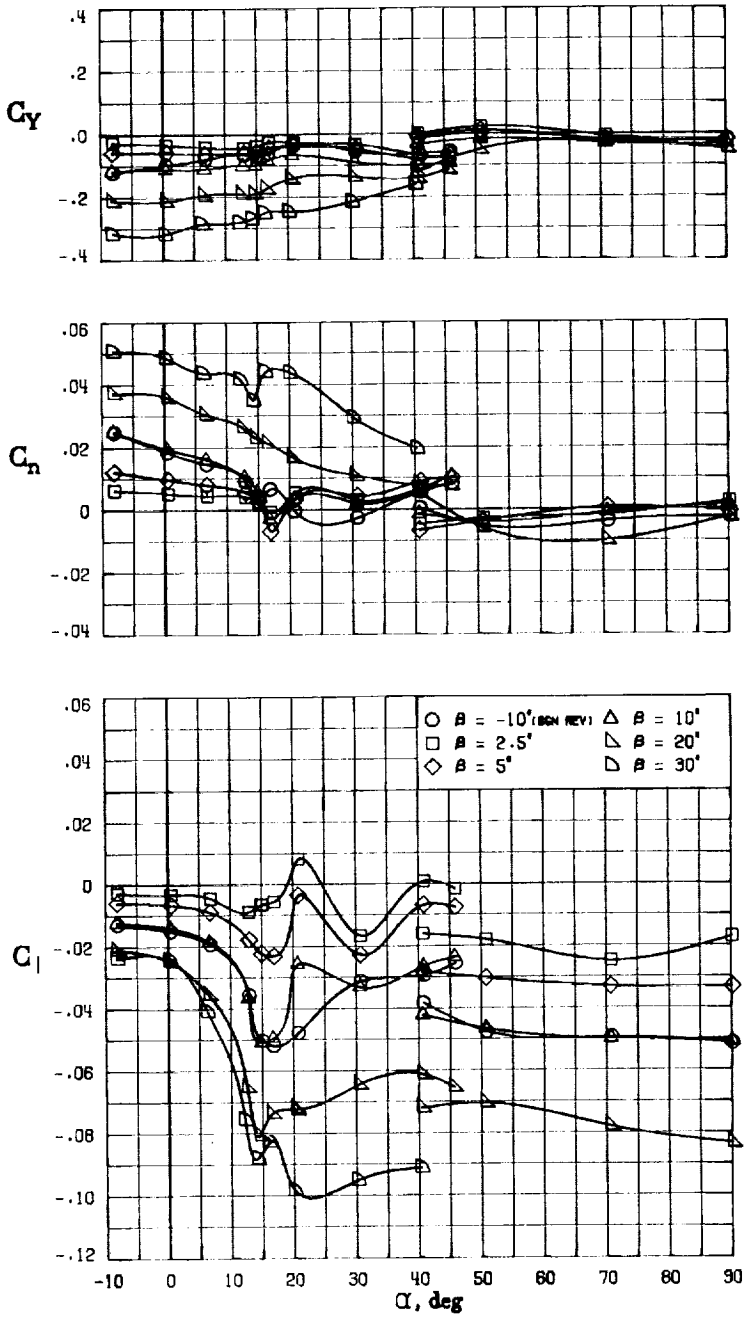

(D) LATERAL - DIRECTIONAL FORCE AND MOMENT COEFFICIENTS ABOUT BODY AXES.

FIGURE 29. - CONTINUED.

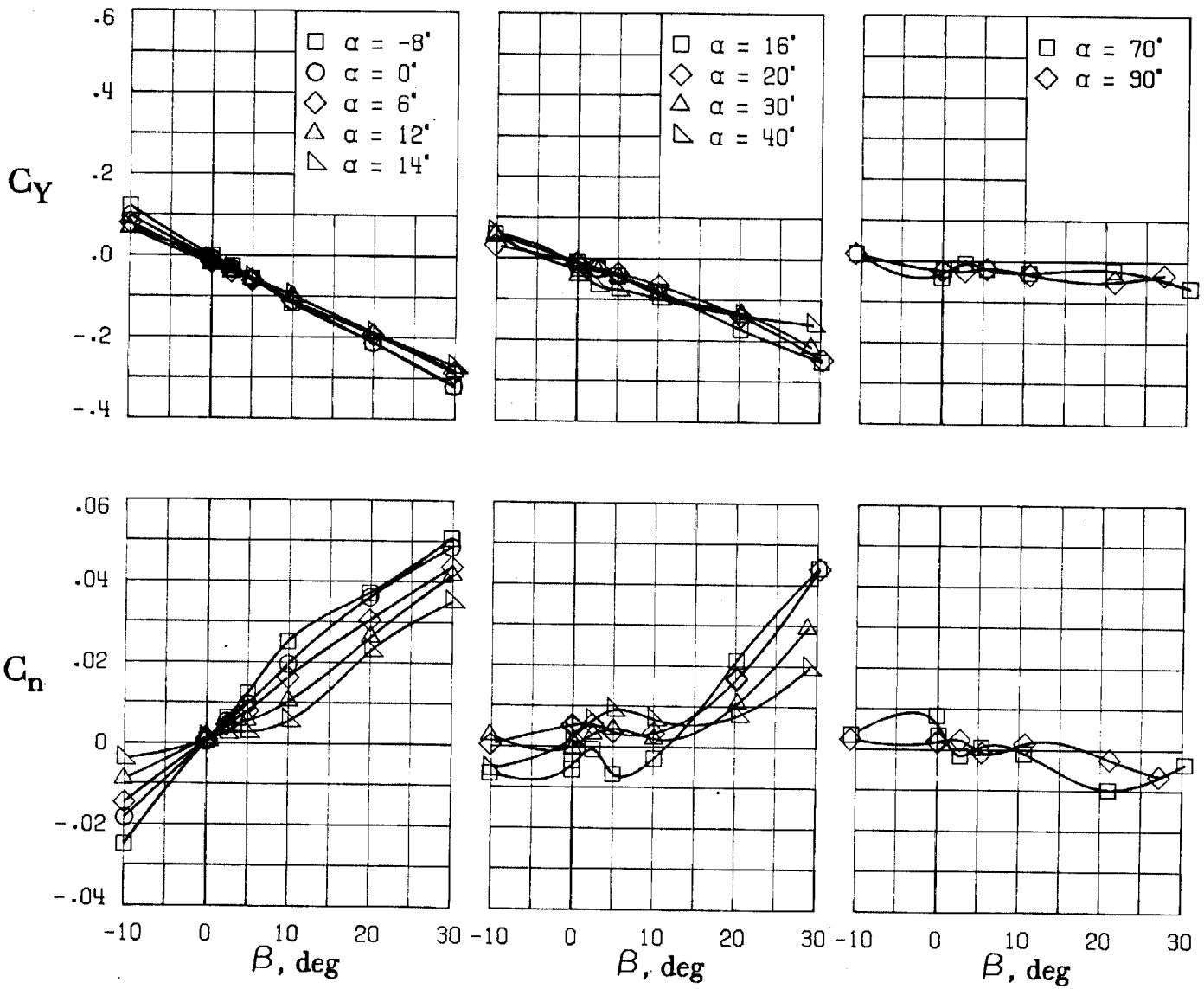

(E) DIRECTIONAL - STABILITY CHARACTERISTICS ABOUT BODY AXES AT VARIOUS ANGLES OF ATTACK.

FIGURE 29. - CONTINUED.

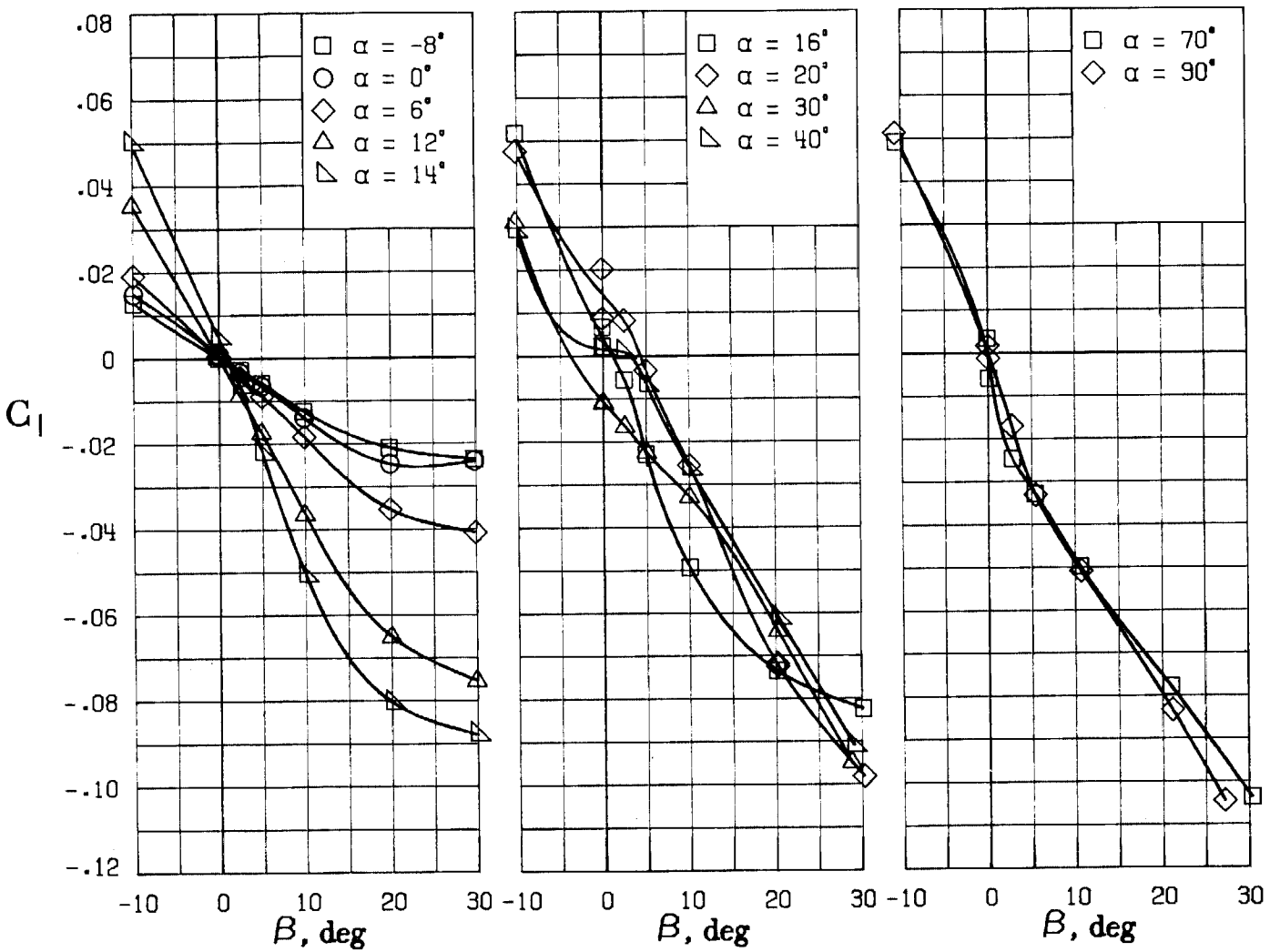

(F) LATERAL - STABILITY CHARACTERISTICS ABOUT BODY AXES AT VARIOUS ANGLES OF ATTACK.

FIGURE 29. - CONCLUDED.

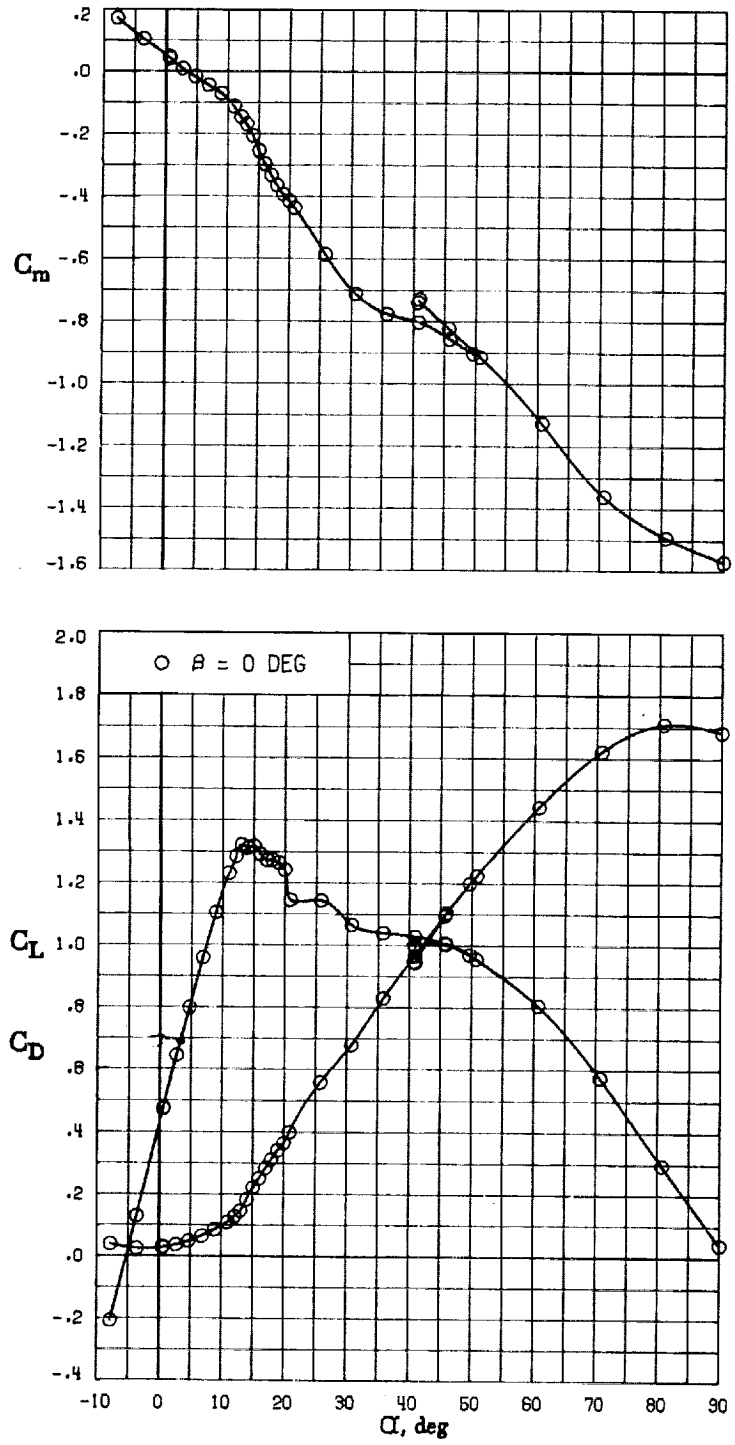

(A) LONGITUDINAL FORCE AND MOMENT COEFFICIENTS ABOUT STABILITY AXES.

FIGURE 30. - EFFECT OF ANGLE OF ATTACK AND SIDESLIP ANGLE ON AERODYNAMIC CHARACTERISTICS AT RE = 3.45 E+06 FOR CONFIGURATION B W1 H4 V E. $\delta_E = 0°$, $\delta_A = 0°$, $\delta_R = 0°$.

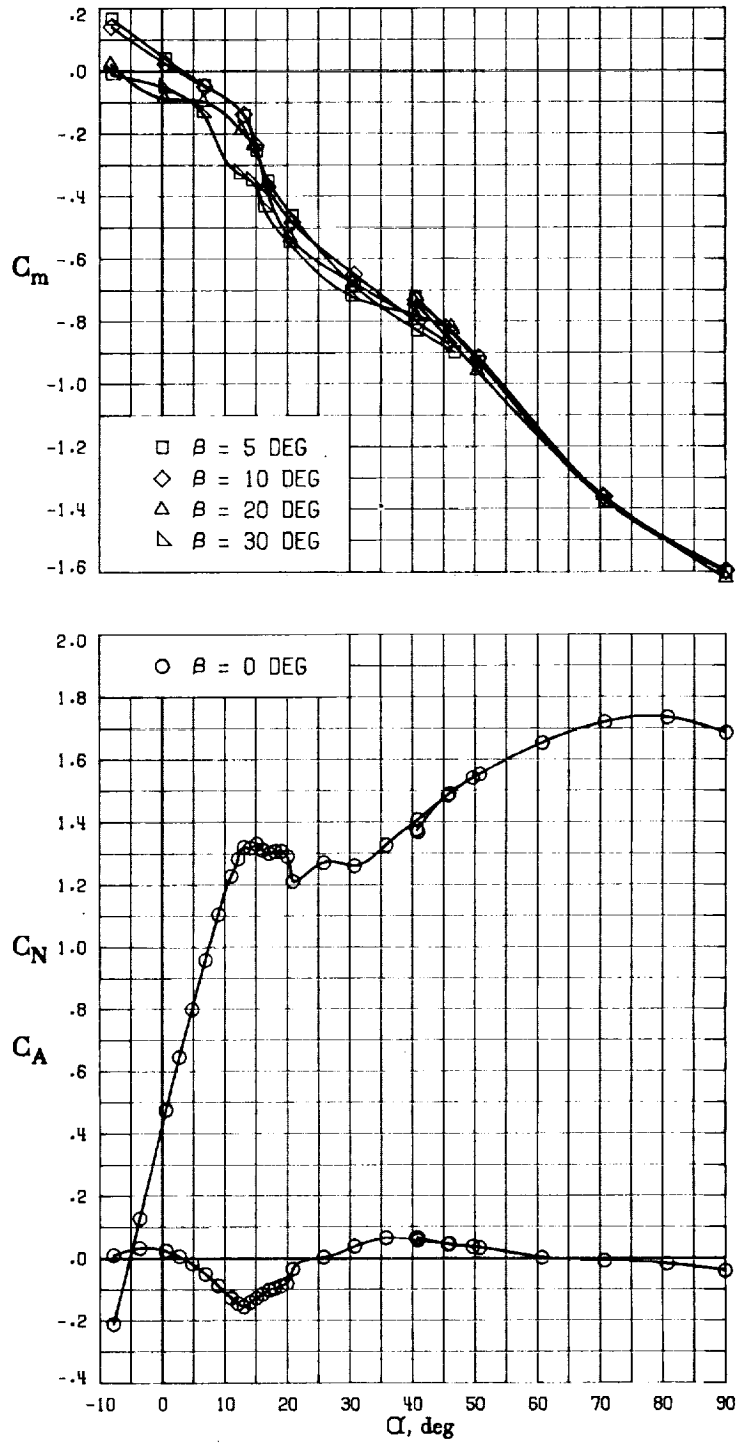

(B) LONGITUDINAL FORCE AND MOMENT COEFFICIENTS ABOUT BODY AXES.

FIGURE 30. - CONTINUED.

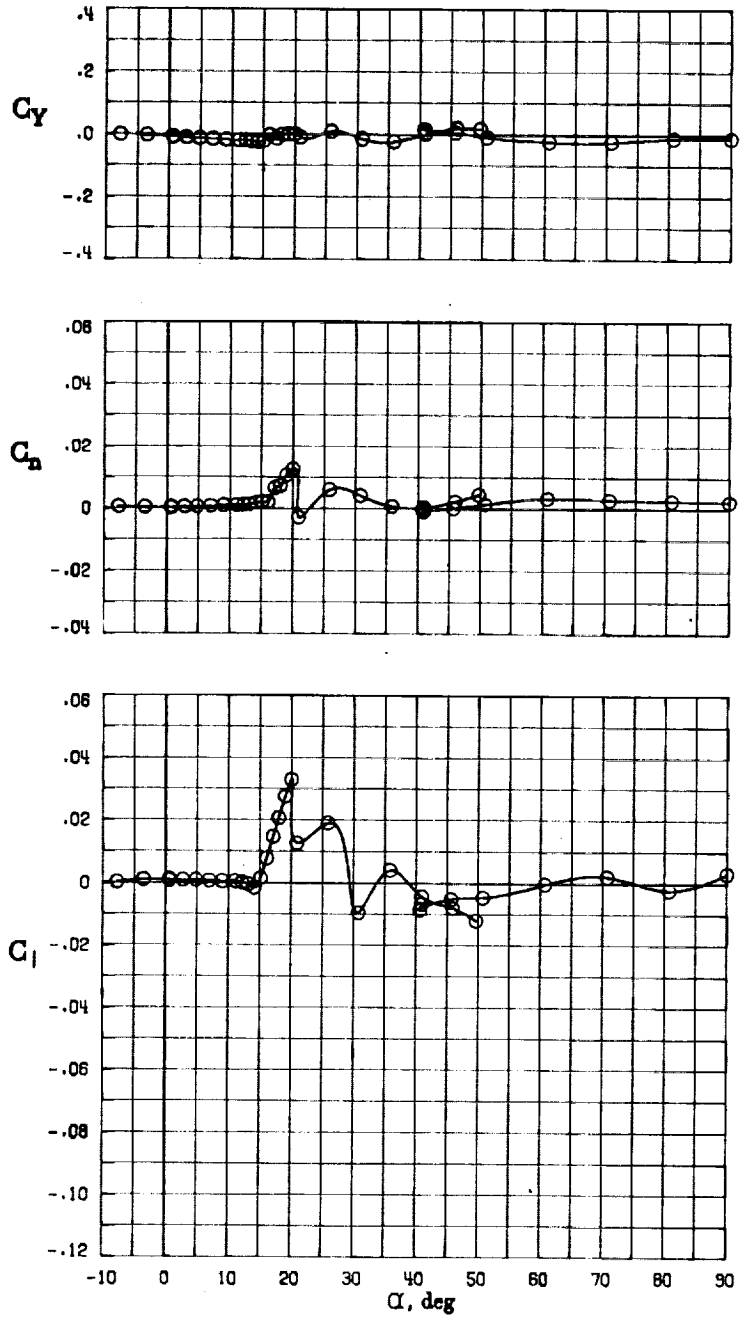

(C) LATERAL - DIRECTIONAL FORCE AND MOMENT COEFFICIENTS ABOUT BODY AXES AT ZERO SIDESLIP.

FIGURE 30. - CONTINUED.

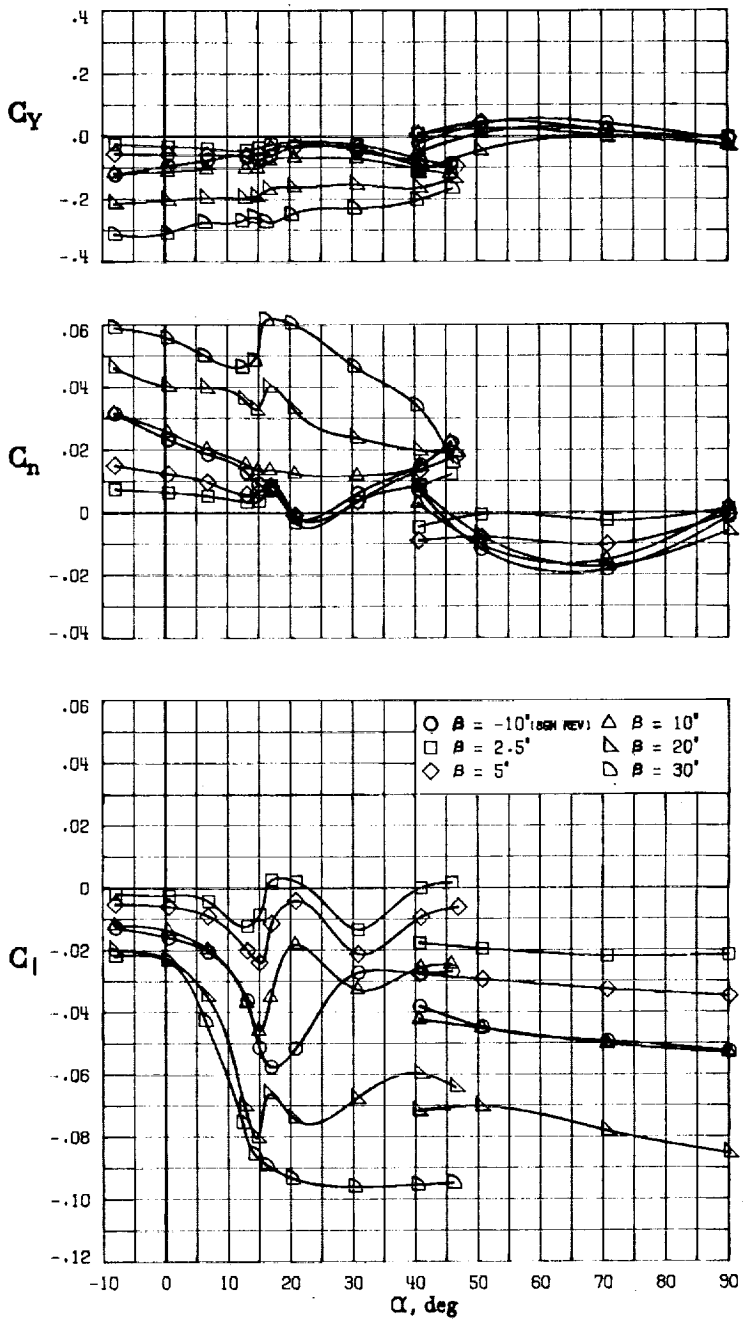

(D) LATERAL - DIRECTIONAL FORCE AND MOMENT COEFFICIENTS ABOUT BODY AXES.

FIGURE 30. - CONTINUED.

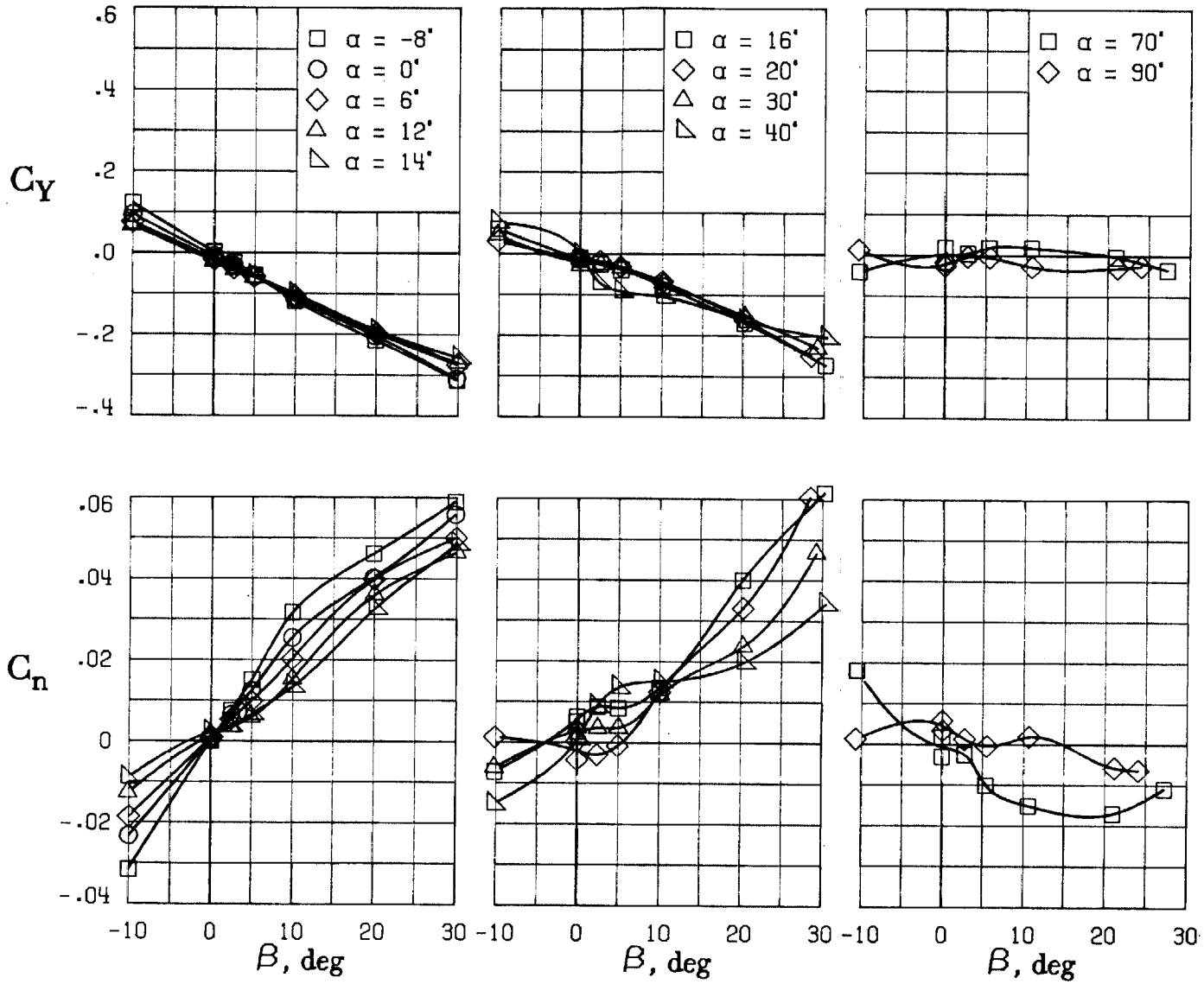

(E) DIRECTIONAL - STABILITY CHARACTERISTICS ABOUT BODY AXES AT VARIOUS ANGLES OF ATTACK.

FIGURE 30. - CONTINUED.

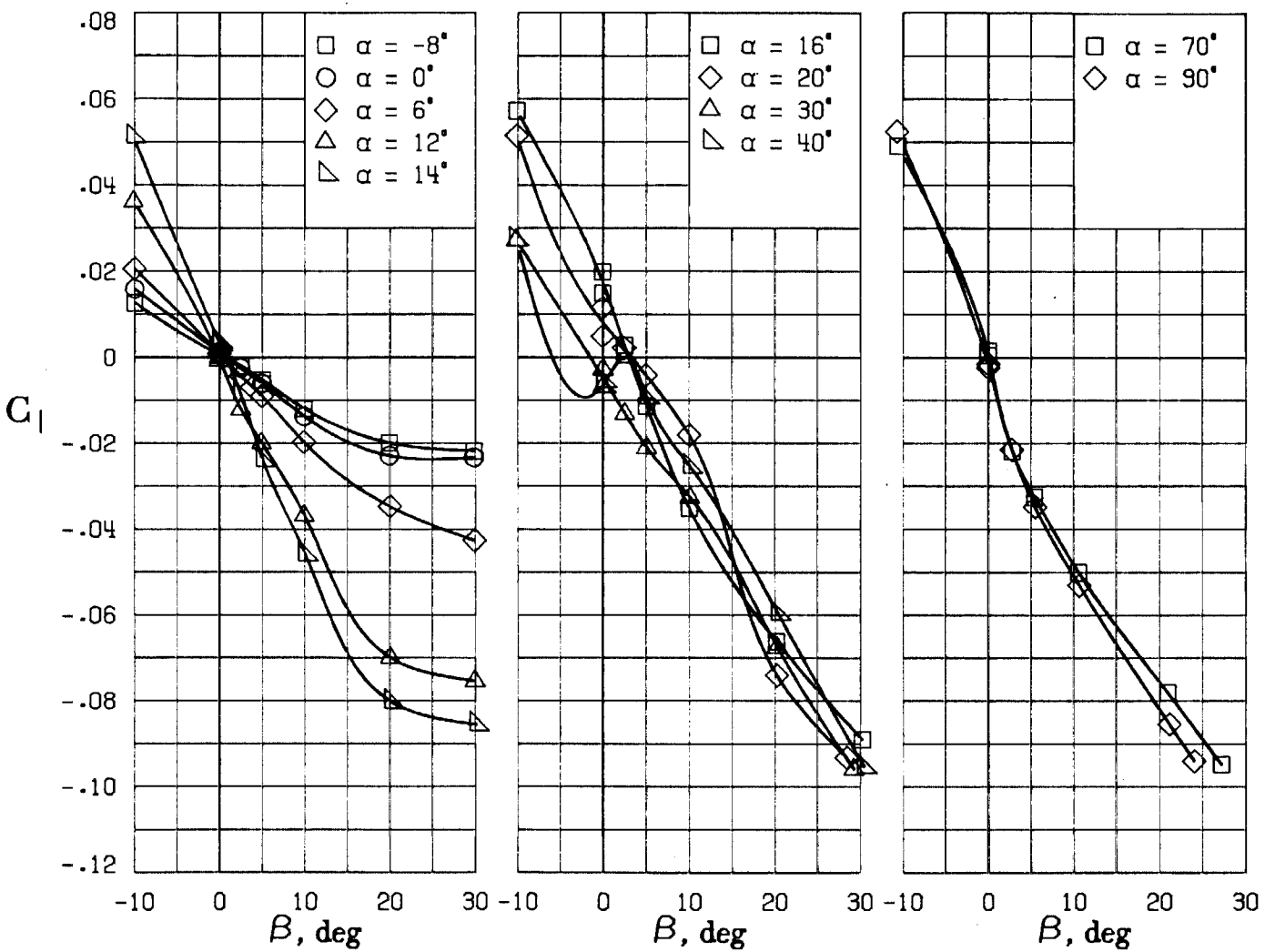

(F) LATERAL - STABILITY CHARACTERISTICS ABOUT BODY AXES AT VARIOUS ANGLES OF ATTACK.

FIGURE 30. - CONCLUDED.

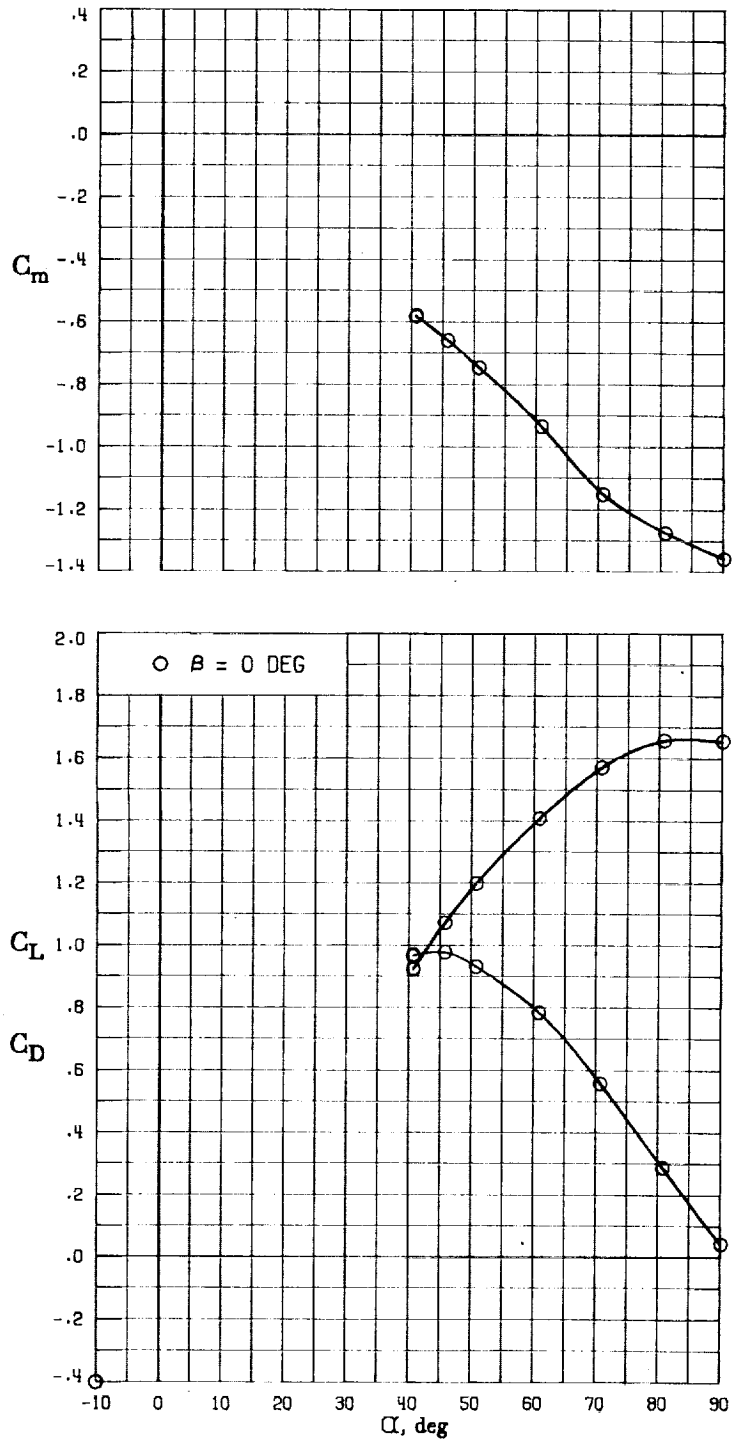

(A) LONGITUDINAL FORCE AND MOMENT COEFFICIENTS ABOUT STABILITY AXES.

FIGURE 31. - EFFECT OF ANGLE OF ATTACK AND SIDESLIP ANGLE ON AERODYNAMIC CHARACTERISTICS AT RE = 3.45 E+06 FOR CONFIGURATION B W1 H4 V. δ_E = 0°, δ_A = 0°, δ_R = -25°.

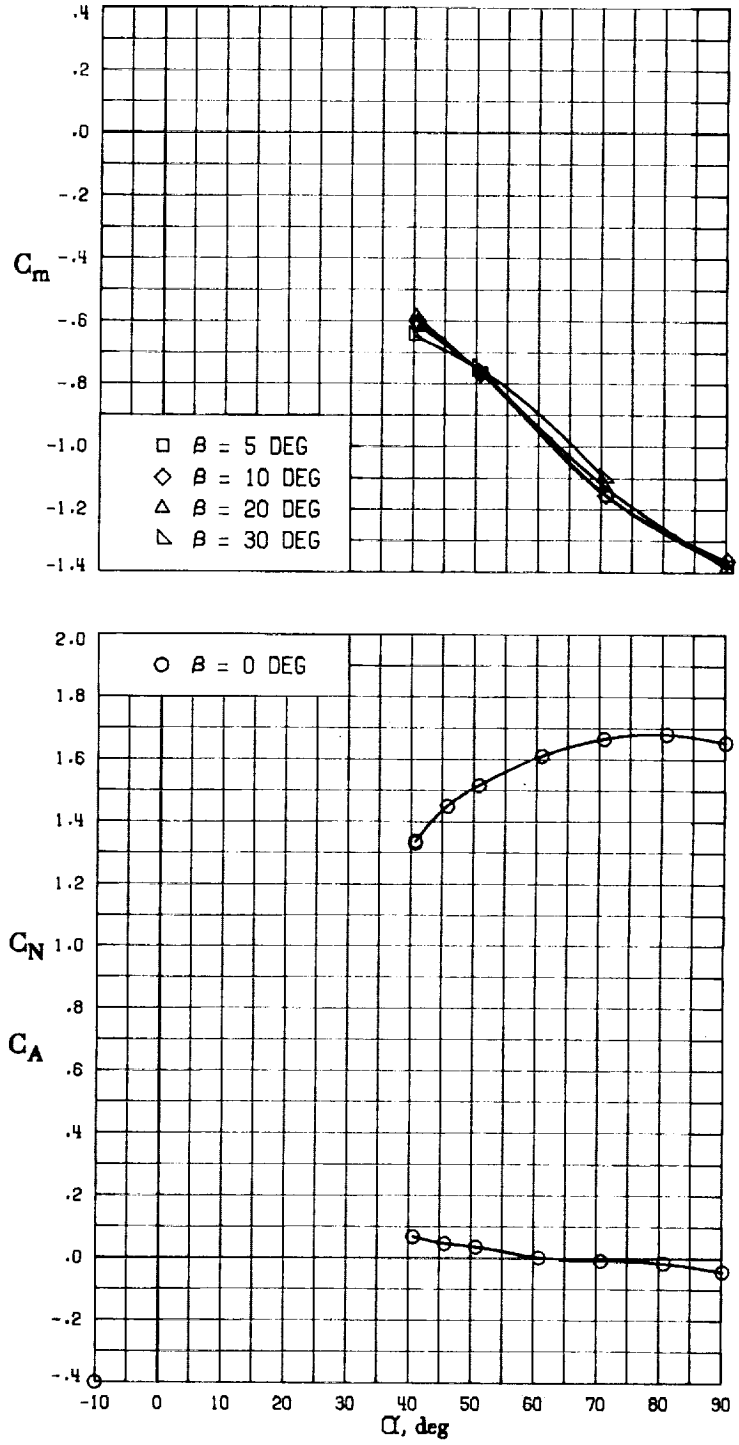

(B) LONGITUDINAL FORCE AND MOMENT COEFFICIENTS ABOUT BODY AXES.

FIGURE 31. - CONTINUED.

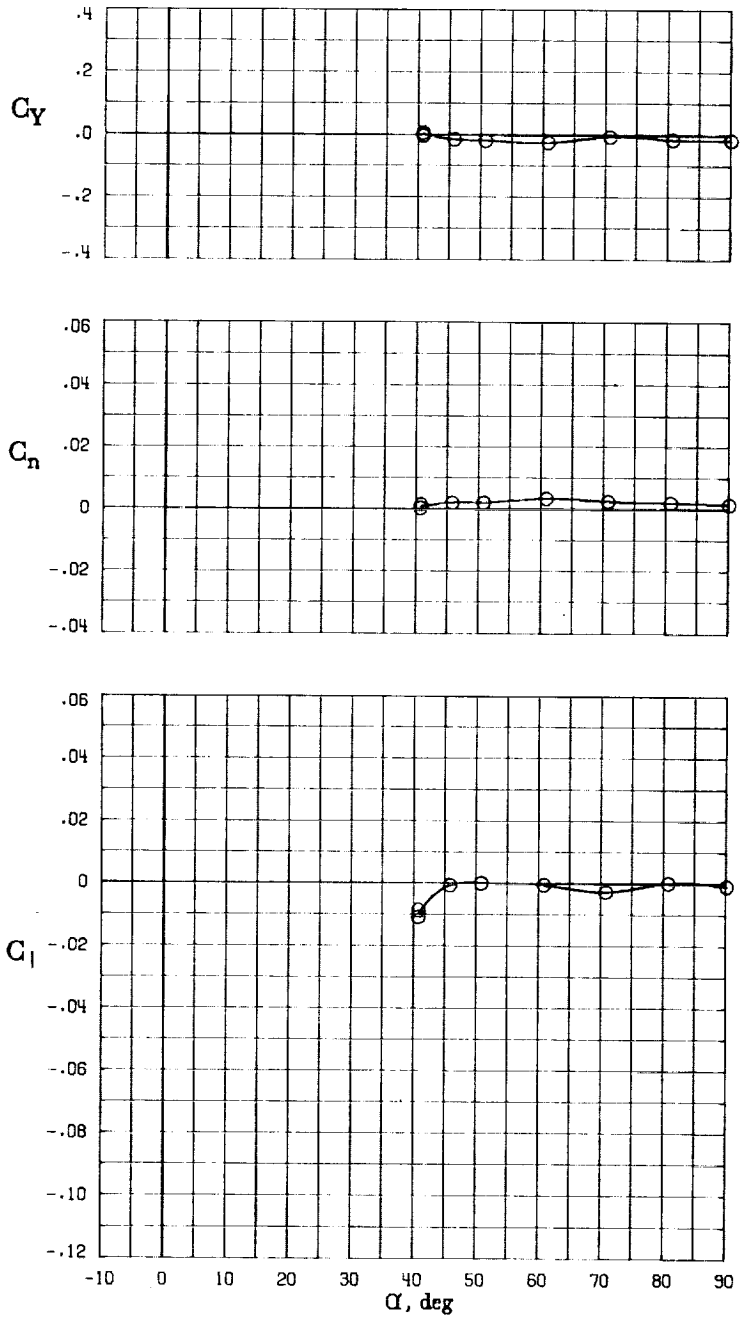

(C) LATERAL - DIRECTIONAL FORCE AND MOMENT COEFFICIENTS ABOUT BODY AXES AT ZERO SIDESLIP.

FIGURE 31. - CONTINUED.

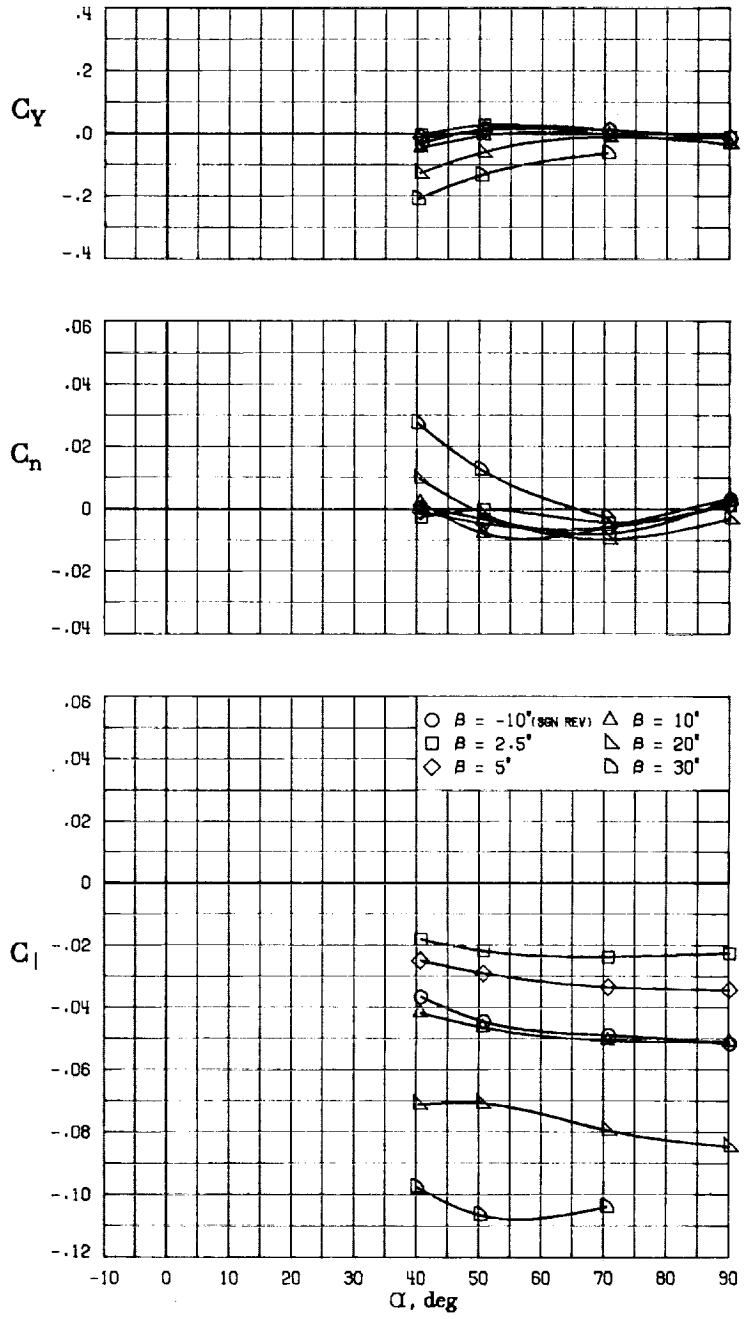

(D) LATERAL - DIRECTIONAL FORCE AND MOMENT COEFFICIENTS ABOUT BODY AXES.

FIGURE 31. - CONTINUED.

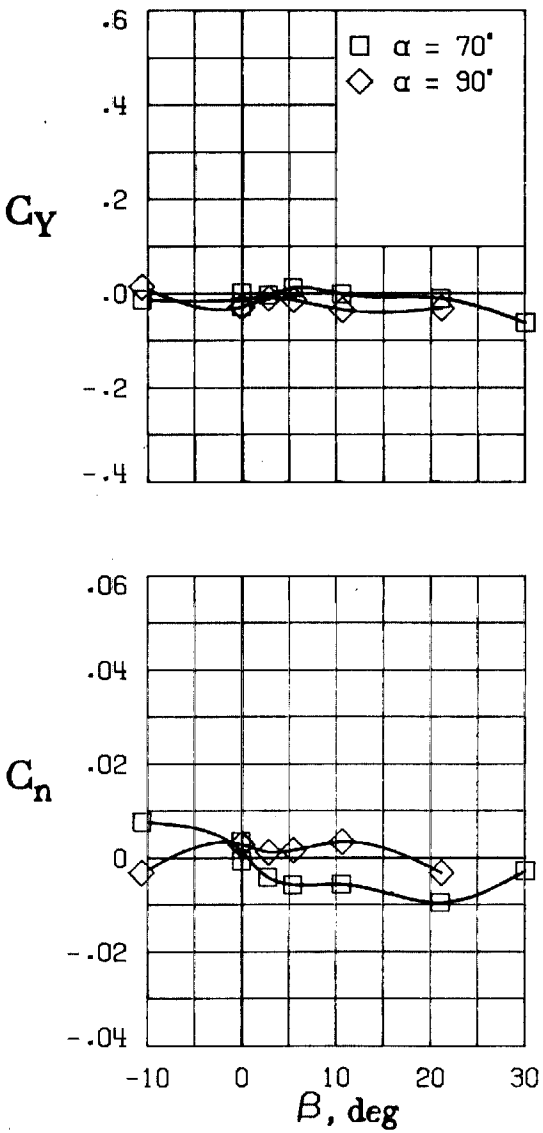

(E) DIRECTIONAL - STABILITY CHARACTERISTICS ABOUT BODY AXES AT VARIOUS ANGLES OF ATTACK.

FIGURE 31. - CONTINUED.

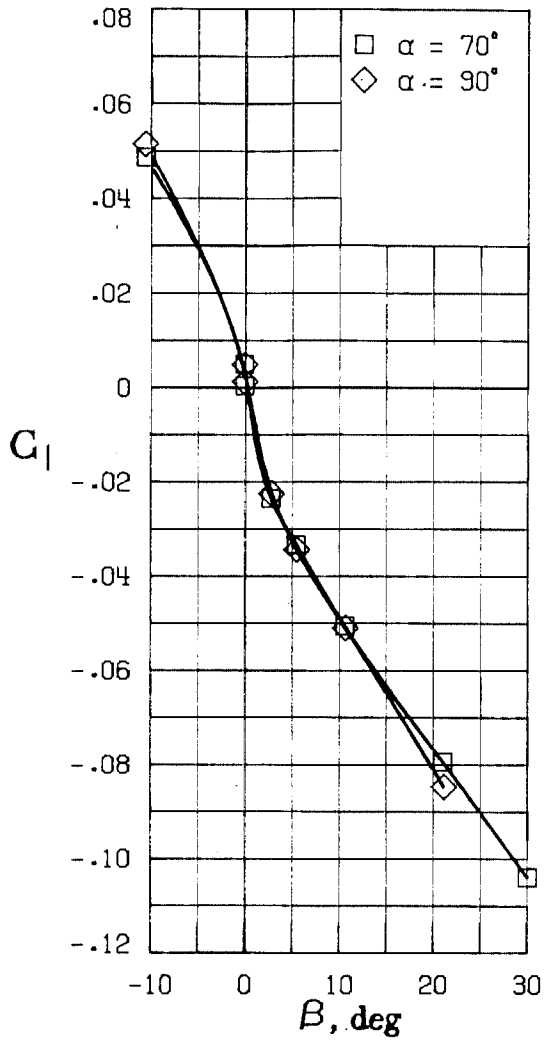

(F) LATERAL - STABILITY CHARACTERISTICS ABOUT BODY AXES AT VARIOUS ANGLES OF ATTACK.

FIGURE. 31. - CONCLUDED.

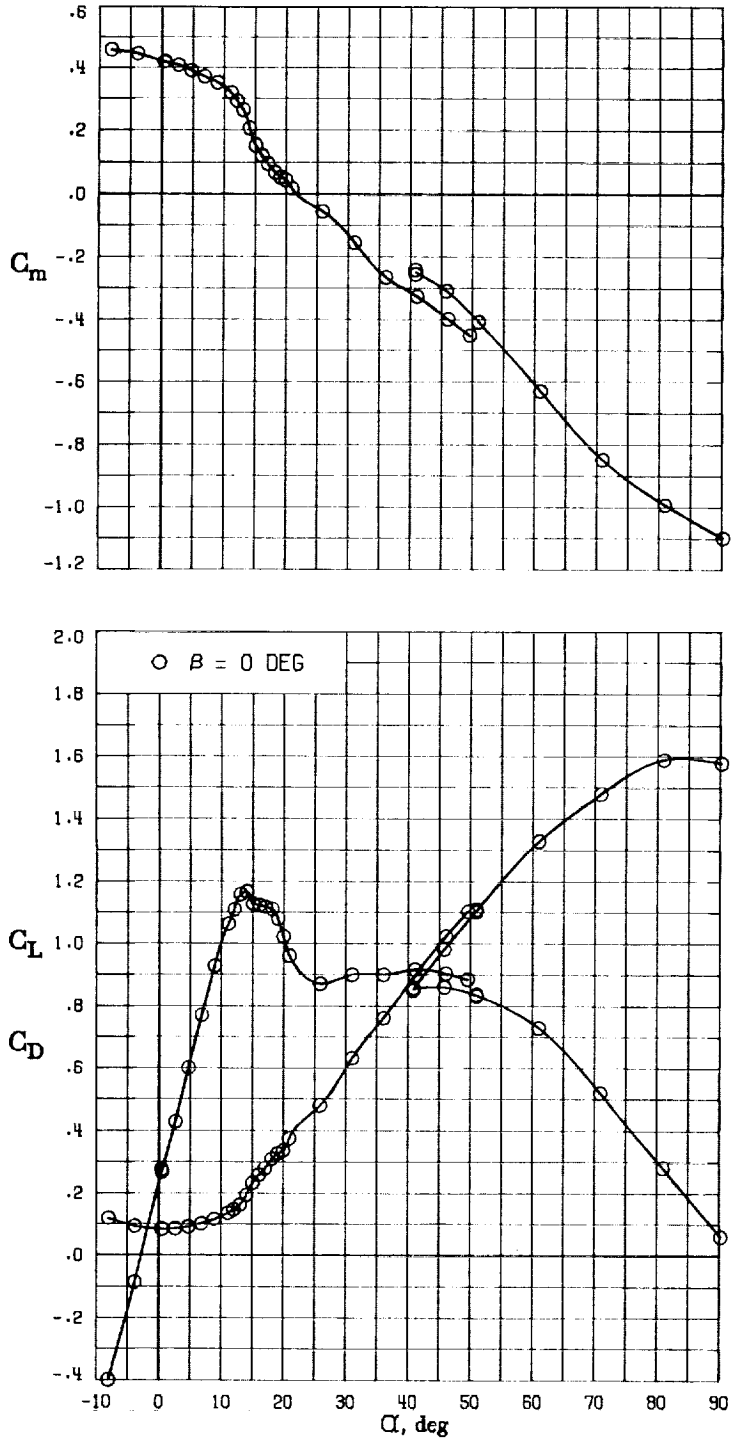

(A) LONGITUDINAL FORCE AND MOMENT COEFFICIENTS ABOUT STABILITY AXES.

FIGURE 32. - EFFECT OF ANGLE OF ATTACK AND SIDESLIP ANGLE ON AERODYNAMIC CHARACTERISTICS AT RE = 3.45 E+06 FOR CONFIGURATION B W1 H3 V. δ_E = -25°, δ_A = 22°, δ_R = -25°.

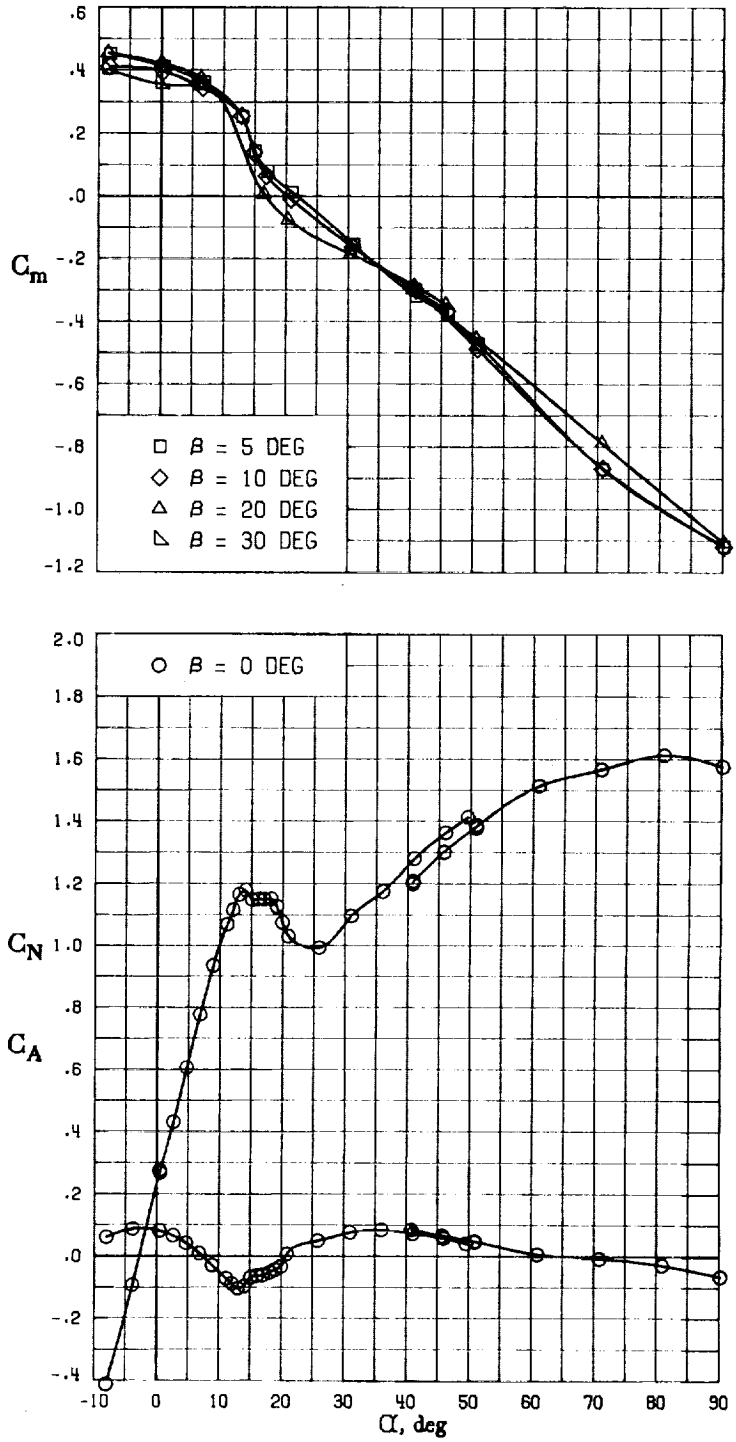

(B) LONGITUDINAL FORCE AND MOMENT COEFFICIENTS ABOUT BODY AXES.

FIGURE 32. - CONTINUED.

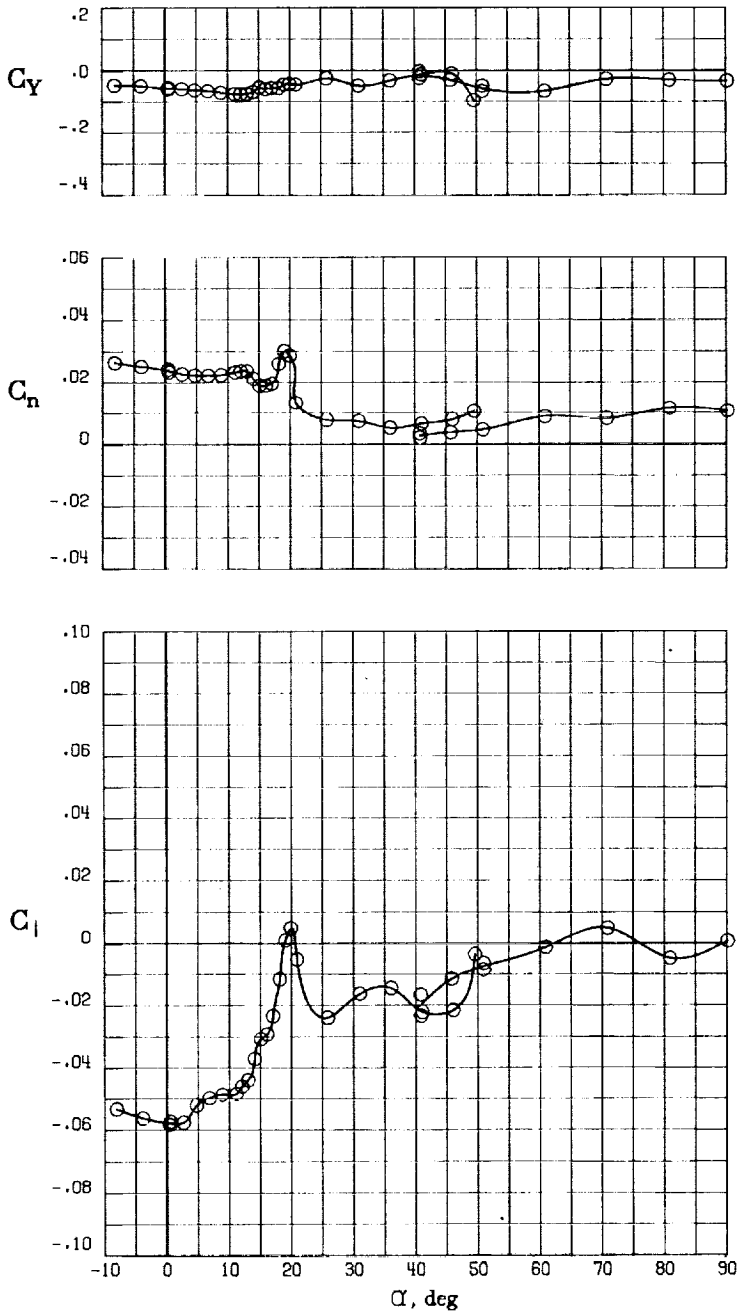

(C) LATERAL - DIRECTIONAL FORCE AND MOMENT COEFFICIENTS ABOUT BODY AXES AT ZERO SIDESLIP.

FIGURE 32. - CONTINUED.

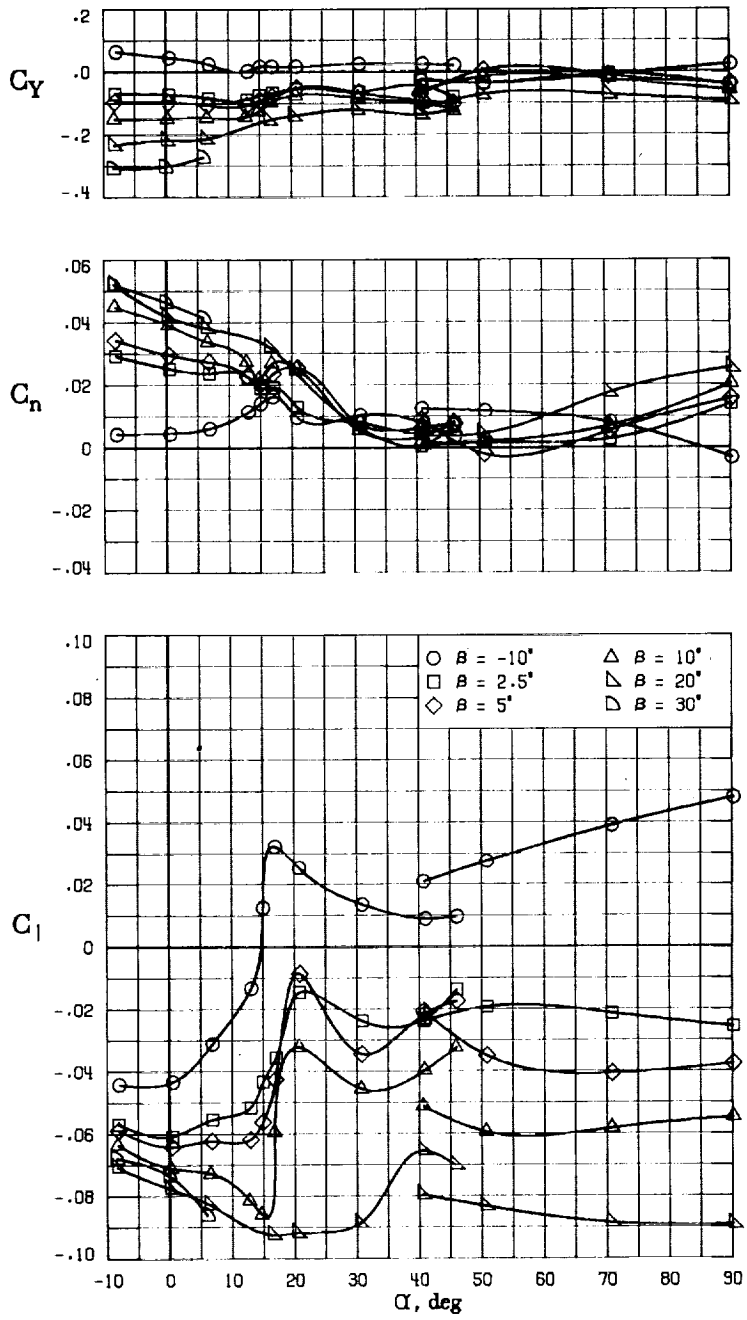

'D) LATERAL - DIRECTIONAL FORCE AND MOMENT COEFFICIENTS ABOUT BODY AXES.

FIGURE 32. - CONTINUED.

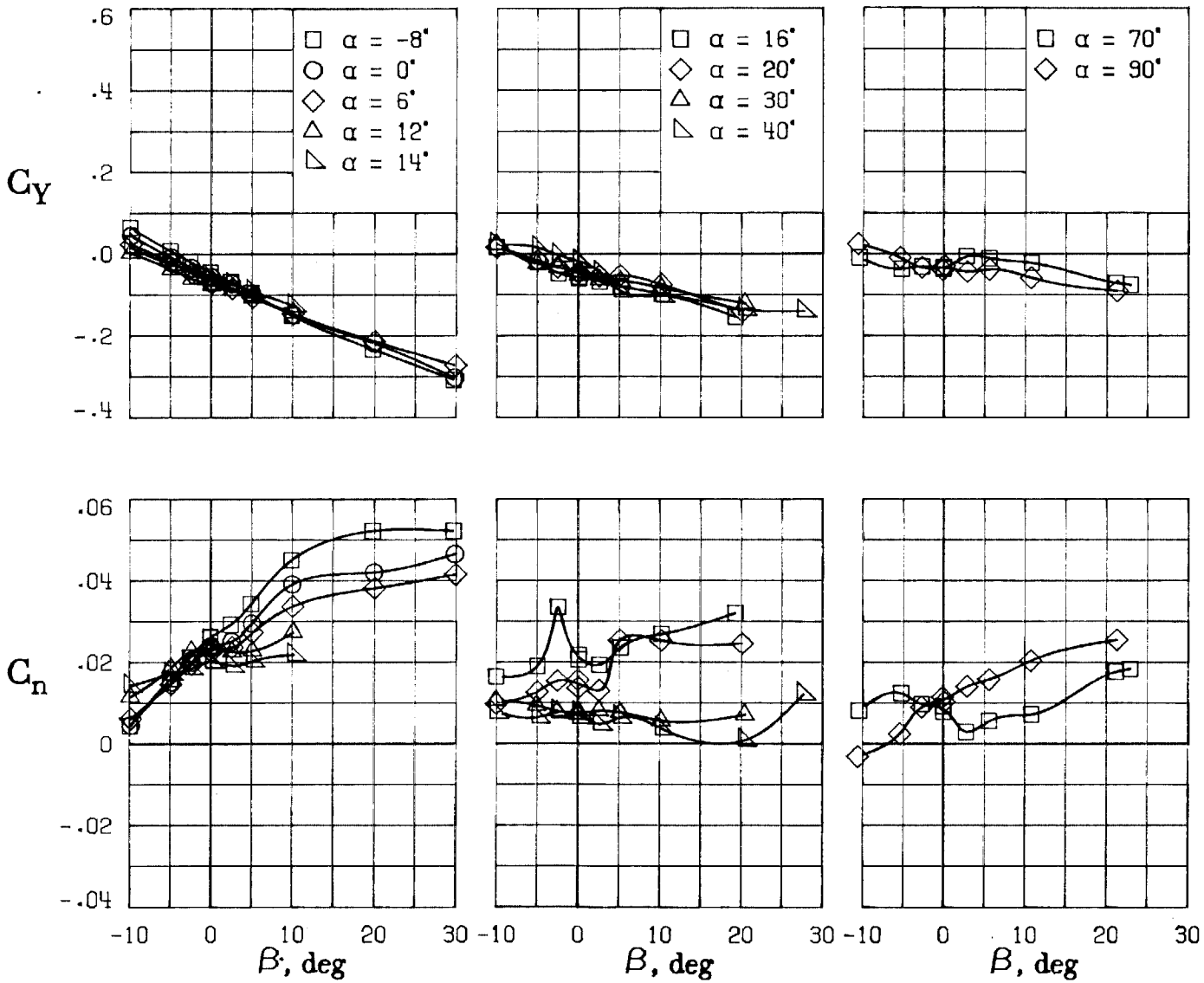

(E) DIRECTIONAL - STABILITY CHARACTERISTICS ABOUT BODY AXES AT VARIOUS ANGLES OF ATTACK.

FIGURE 32. - CONTINUED.

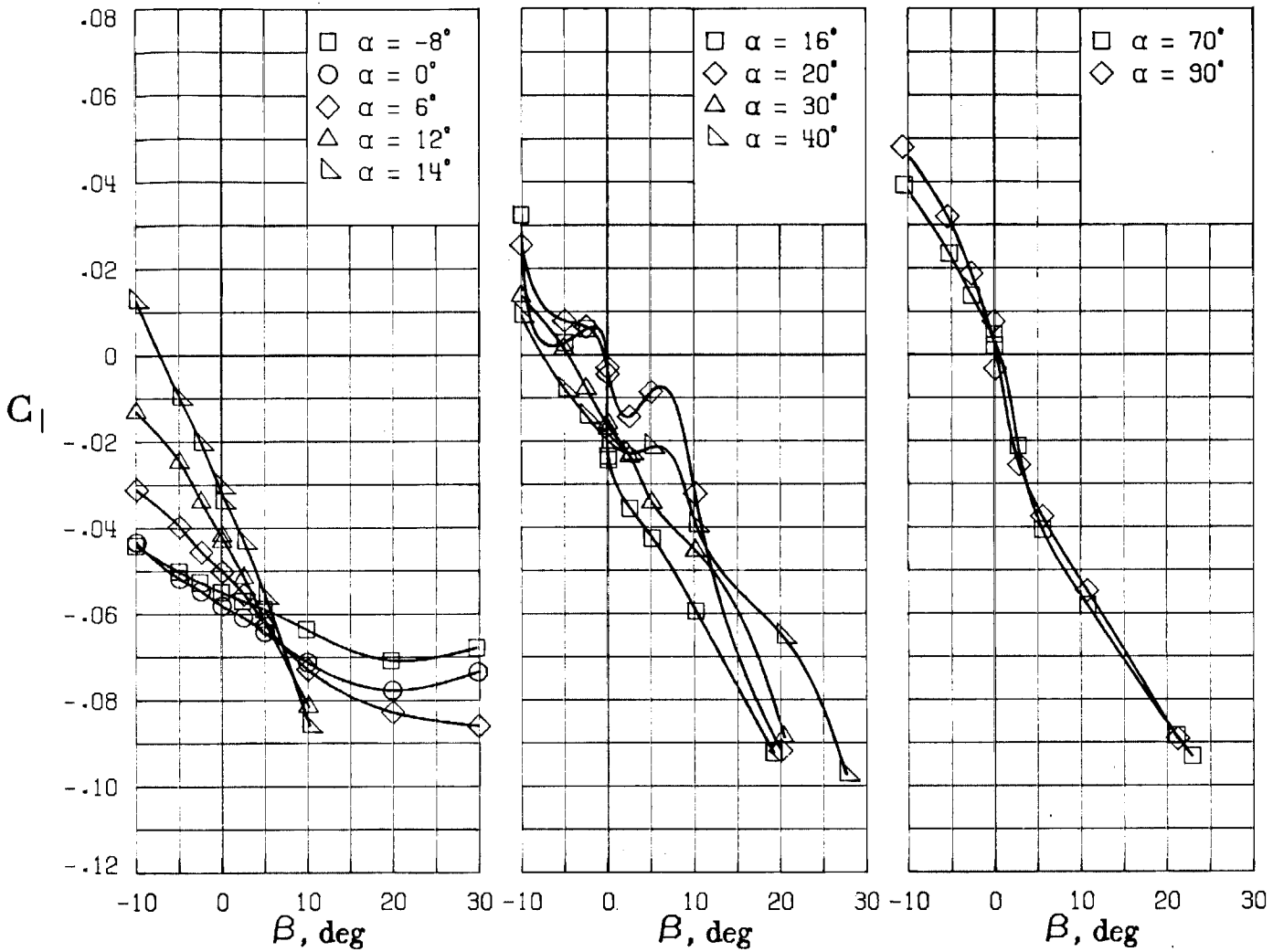

(F) LATERAL - STABILITY CHARACTERISTICS ABOUT BODY AXES AT VARIOUS ANGLES OF ATTACK.

FIGURE 32. - CONCLUDED.

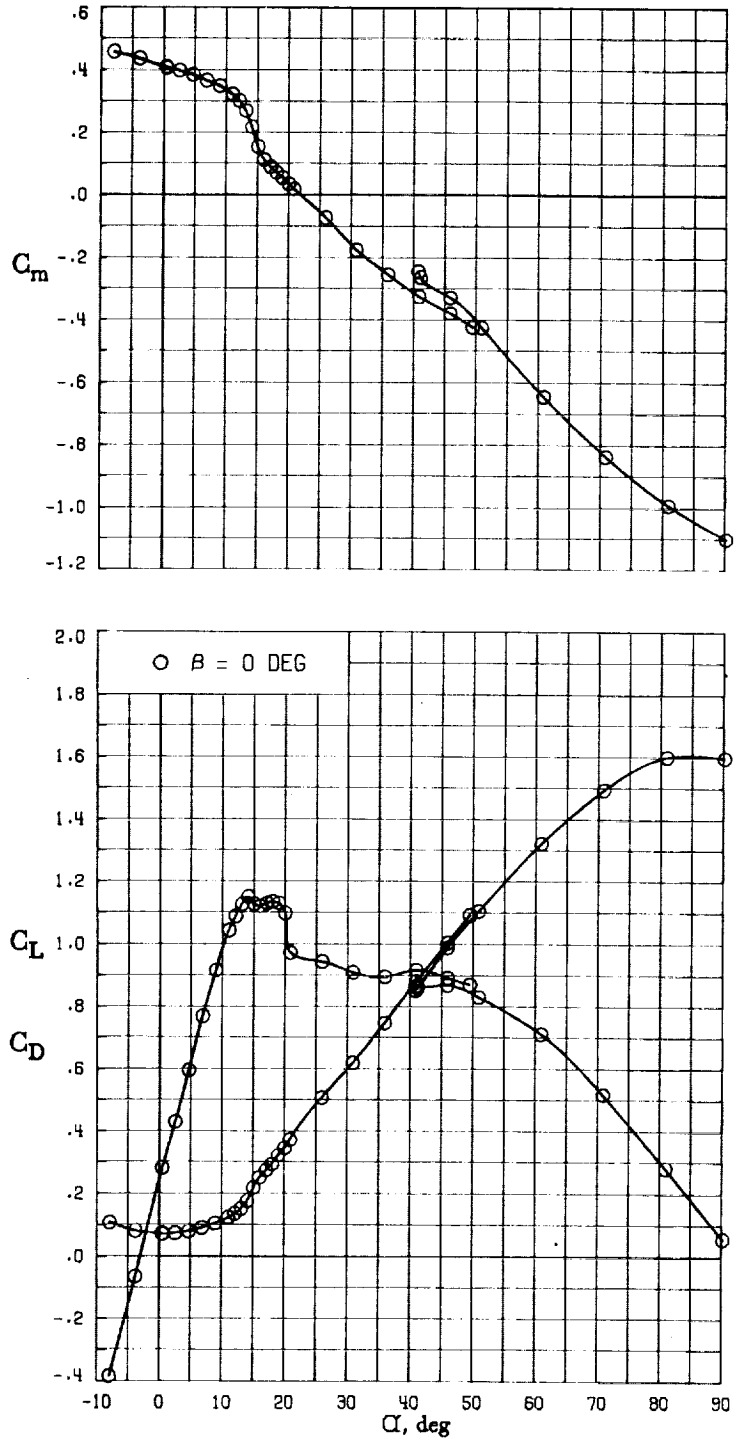

(A) LONGITUDINAL FORCE AND MOMENT COEFFICIENTS ABOUT STABILITY AXES.

FIGURE 33. - EFFECT OF ANGLE OF ATTACK AND SIDESLIP ANGLE ON AERODYNAMIC CHARACTERISTICS AT RE = 3.45 E+06 FOR CONFIGURATION B W1 H3 V. δ_E = -25°, δ_A = -22°, δ_R = -25°.

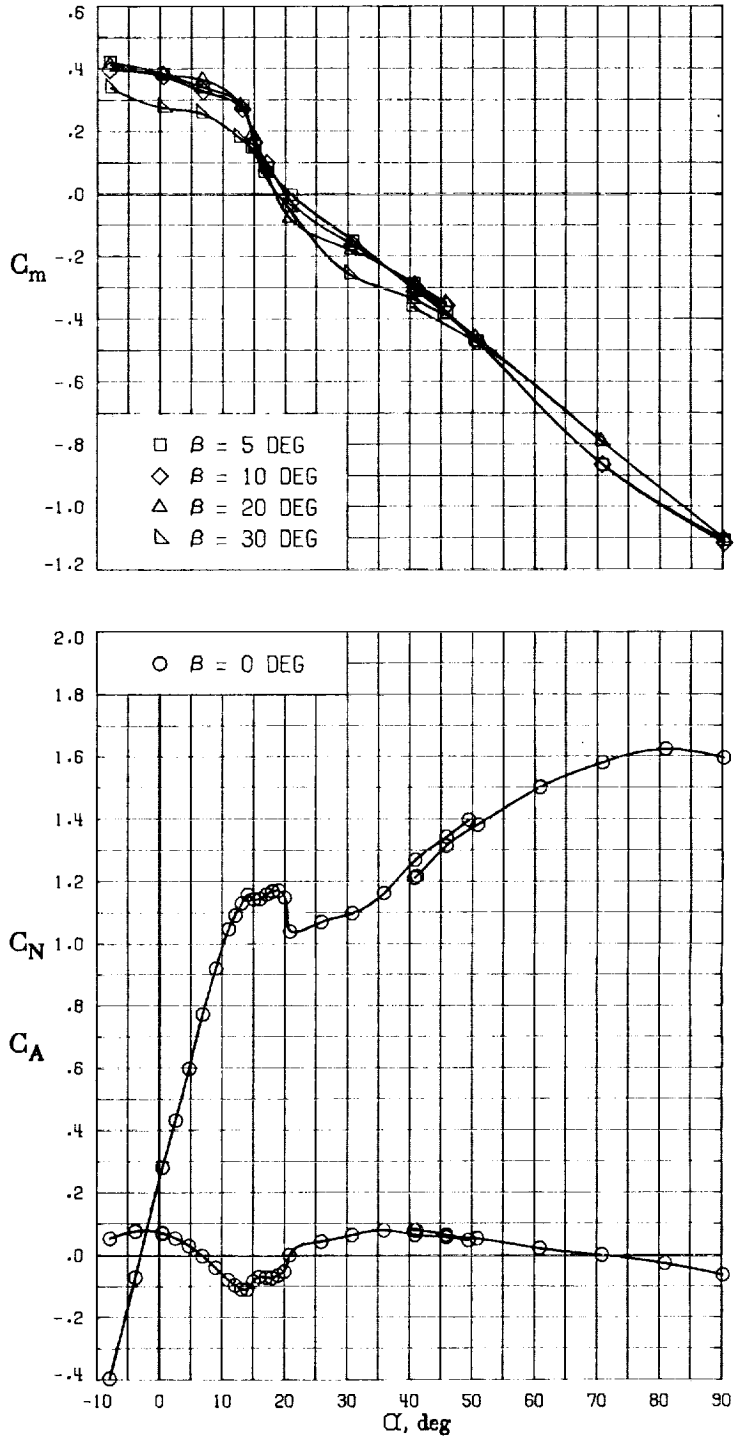

(B) LONGITUDINAL FORCE AND MOMENT COEFFICIENTS ABOUT BODY AXES.

FIGURE 33. - CONTINUED.

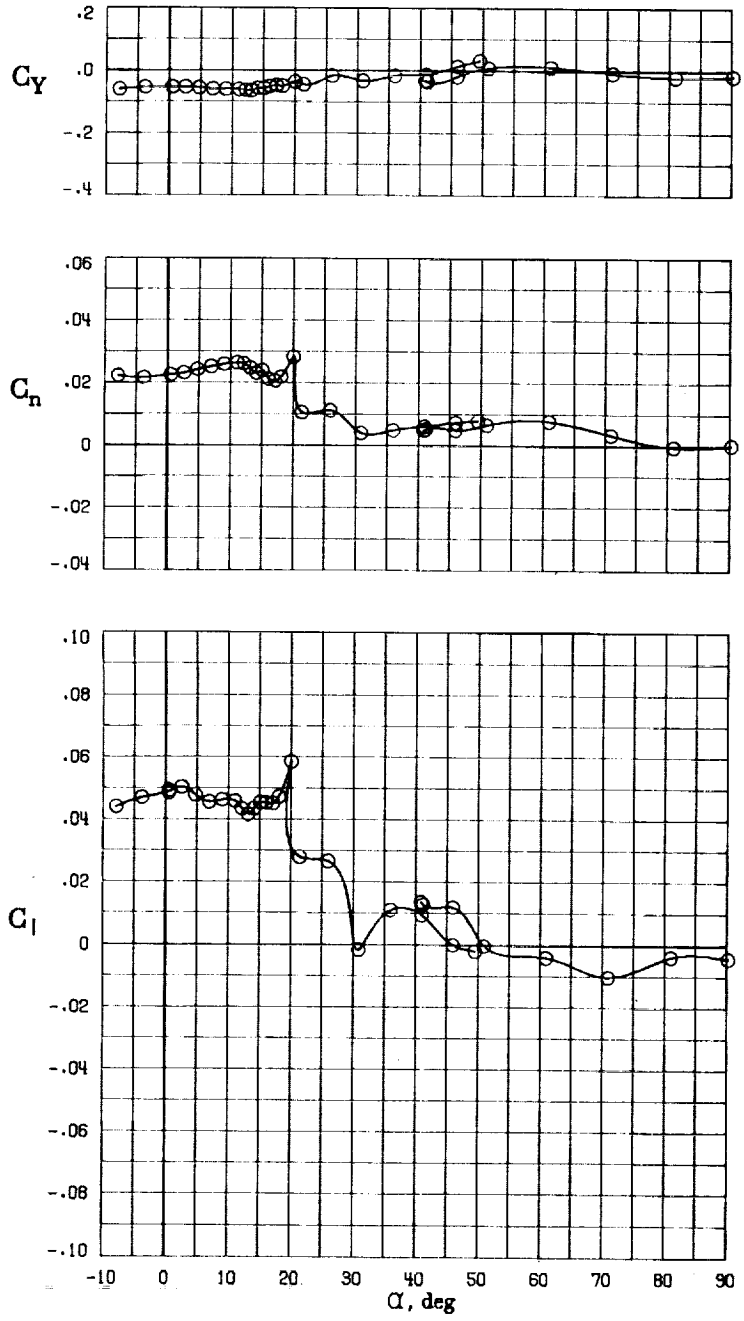

(C) LATERAL - DIRECTIONAL FORCE AND MOMENT COEFFICIENTS ABOUT BODY AXES AT ZERO SIDESLIP.

FIGURE 33. - CONTINUED.

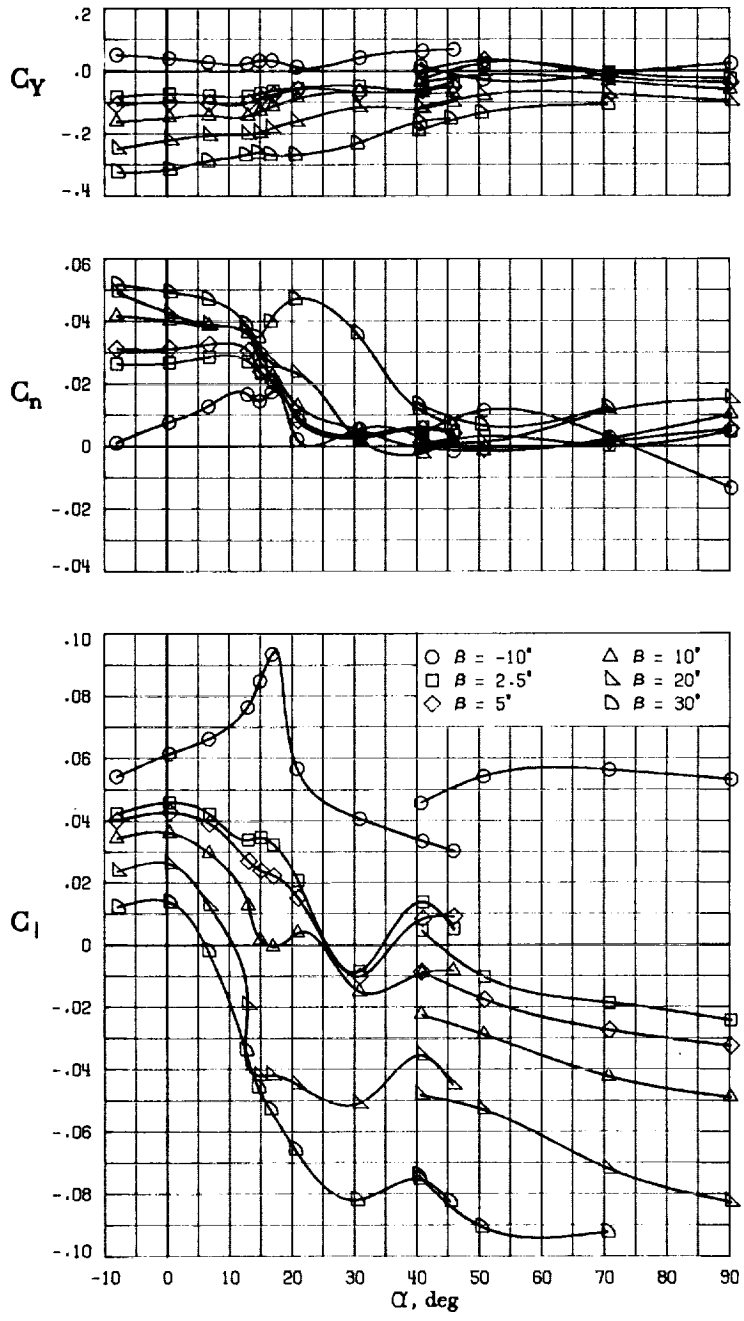

(D) LATERAL - DIRECTIONAL FORCE AND MOMENT COEFFICIENTS ABOUT BODY AXES.

FIGURE 33. - CONTINUED.

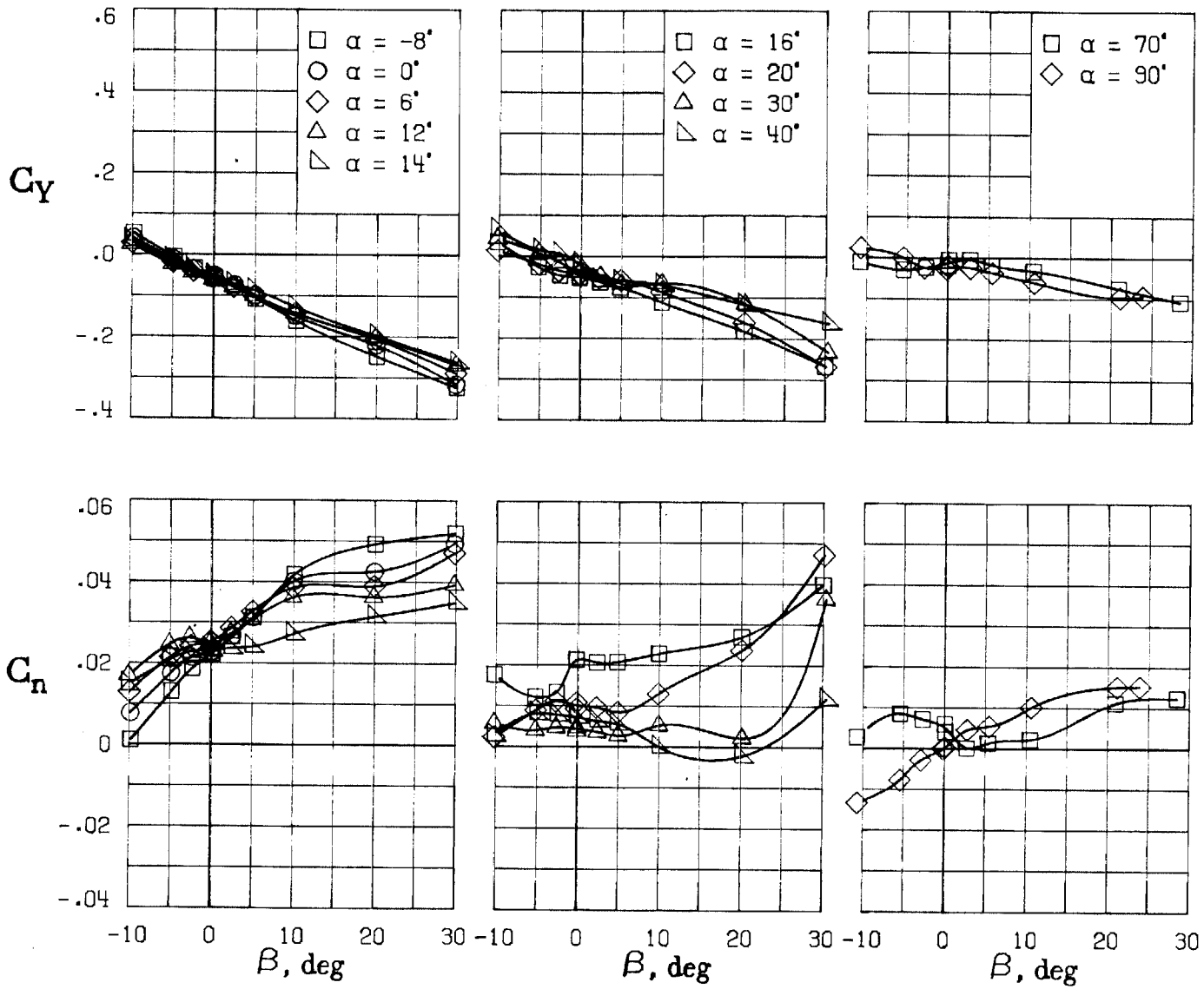

(E) DIRECTIONAL - STABILITY CHARACTERISTICS ABOUT BODY AXES AT VARIOUS ANGLES OF ATTACK.

FIGURE 33. - CONTINUED.

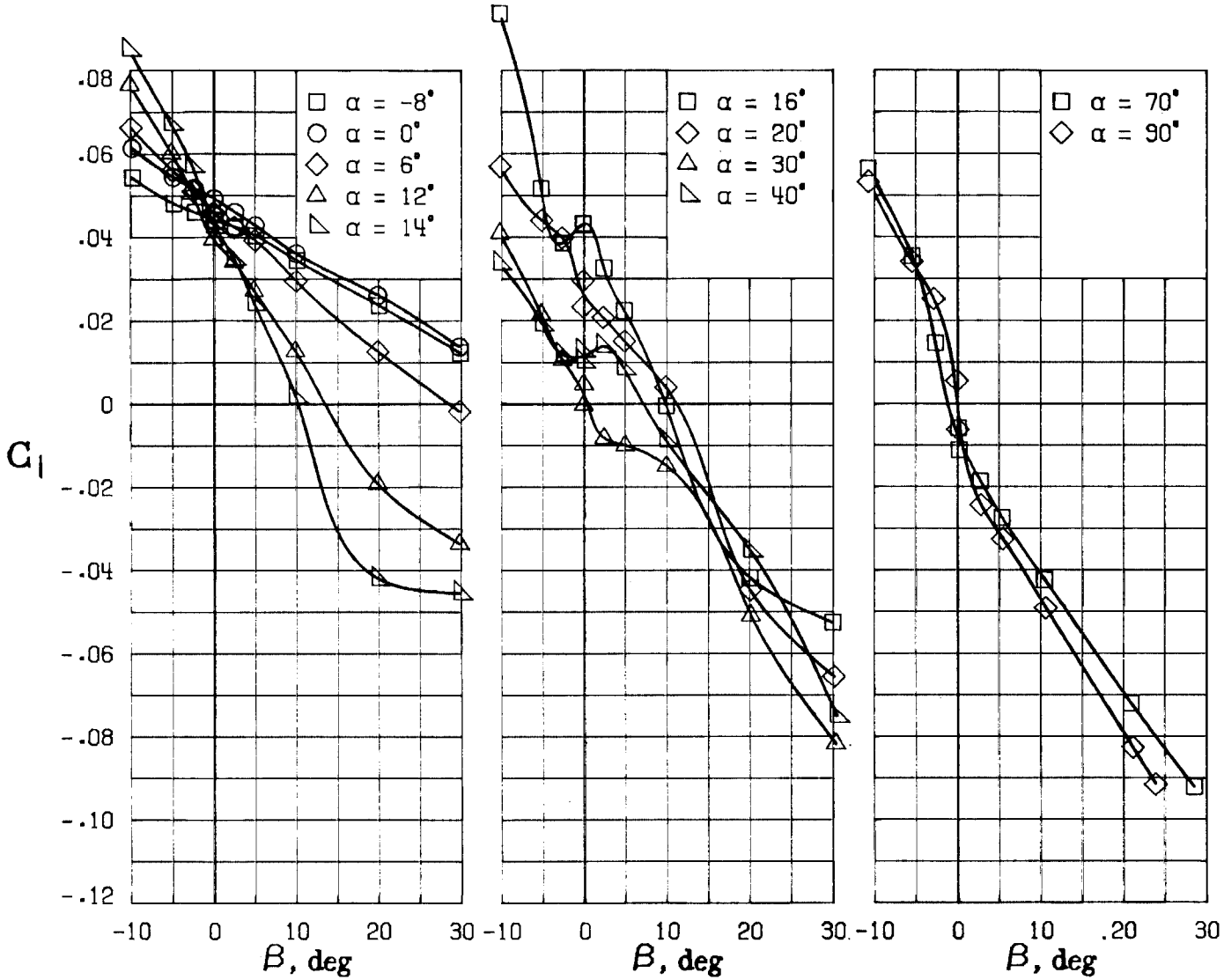

(F) LATERAL - STABILITY CHARACTERISTICS ABOUT BODY AXES AT VARIOUS ANGLES OF ATTACK.

FIGURE 33. - CONCLUDED.

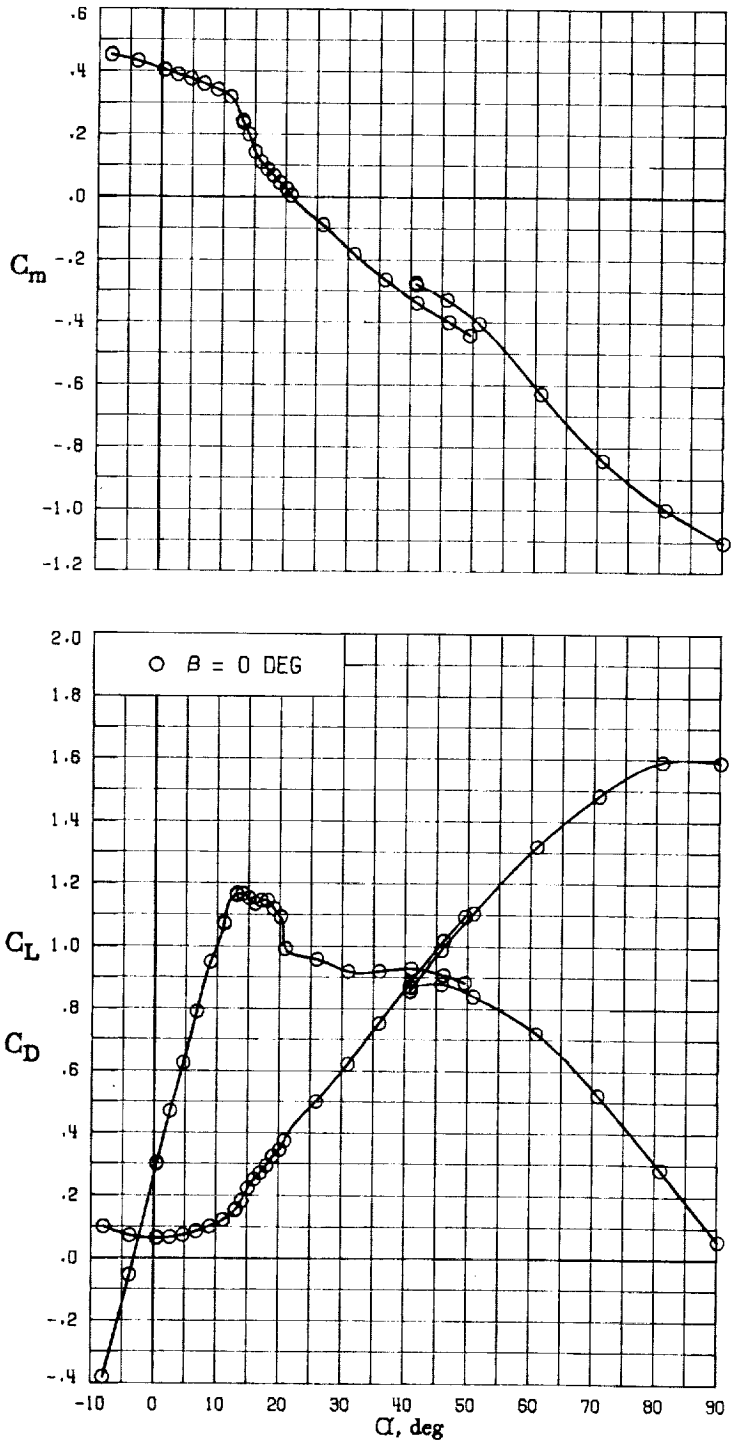

(A) LONGITUDINAL FORCE AND MOMENT COEFFICIENTS ABOUT STABILITY AXES.

FIGURE 34. - EFFECT OF ANGLE OF ATTACK AND SIDESLIP ANGLE ON AERODYNAMIC CHARACTERISTICS AT RE = 3.45 E+06 FOR CONFIGURATION B W1 H3 V. $\delta_E = -25°$, $\delta_A = 0°$, $\delta_R = -25°$.

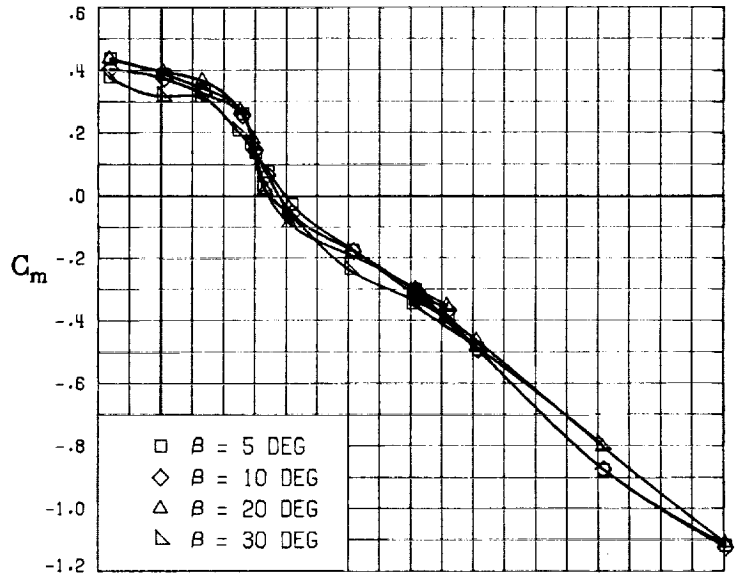

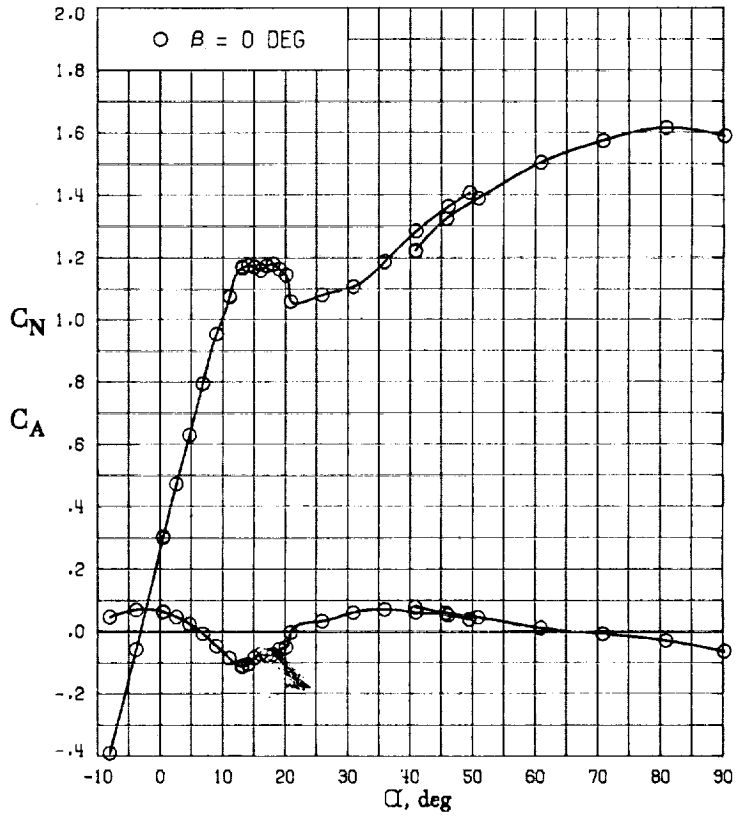

(B) LONGITUDINAL FORCE AND MOMENT COEFFICIENTS ABOUT BODY AXES.

FIGURE 34. - CONTINUED.

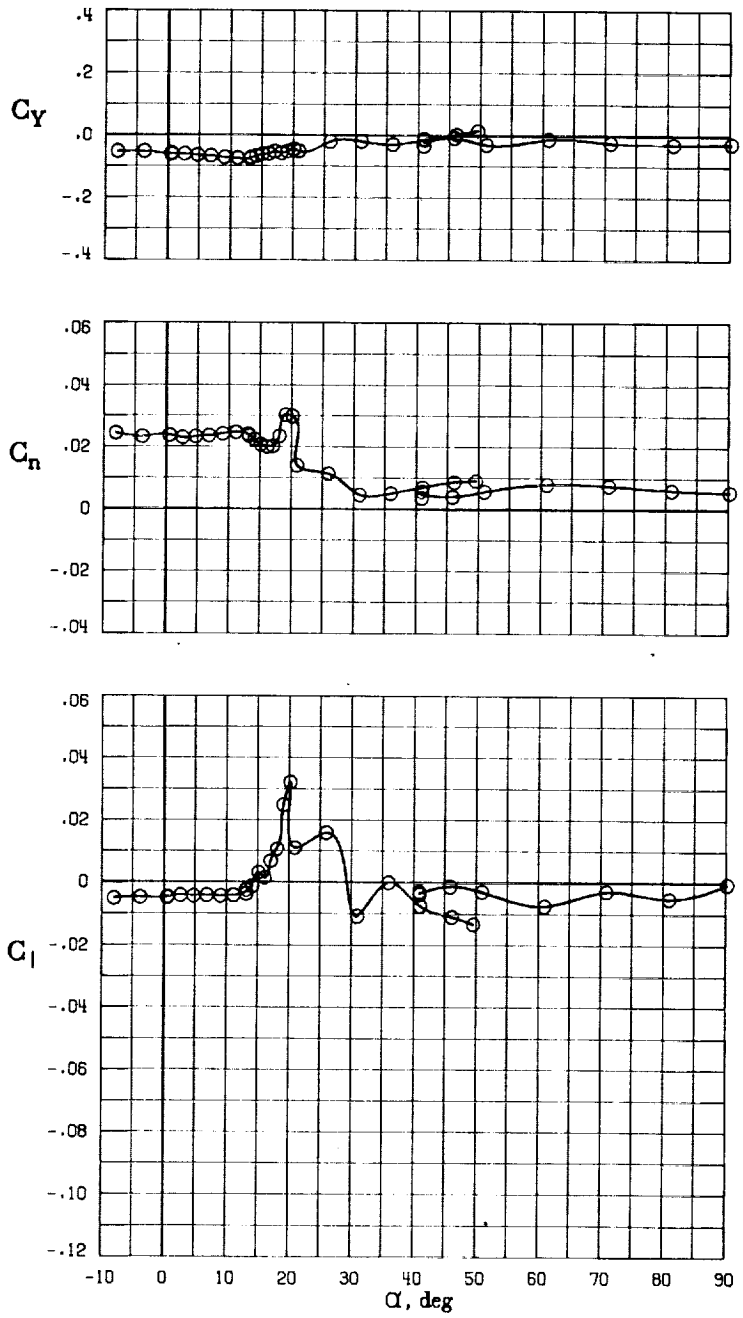

(C) LATERAL - DIRECTIONAL FORCE AND MOMENT COEFFICIENTS ABOUT BODY AXES AT ZERO SIDESLIP.

FIGURE 34. - CONTINUED.

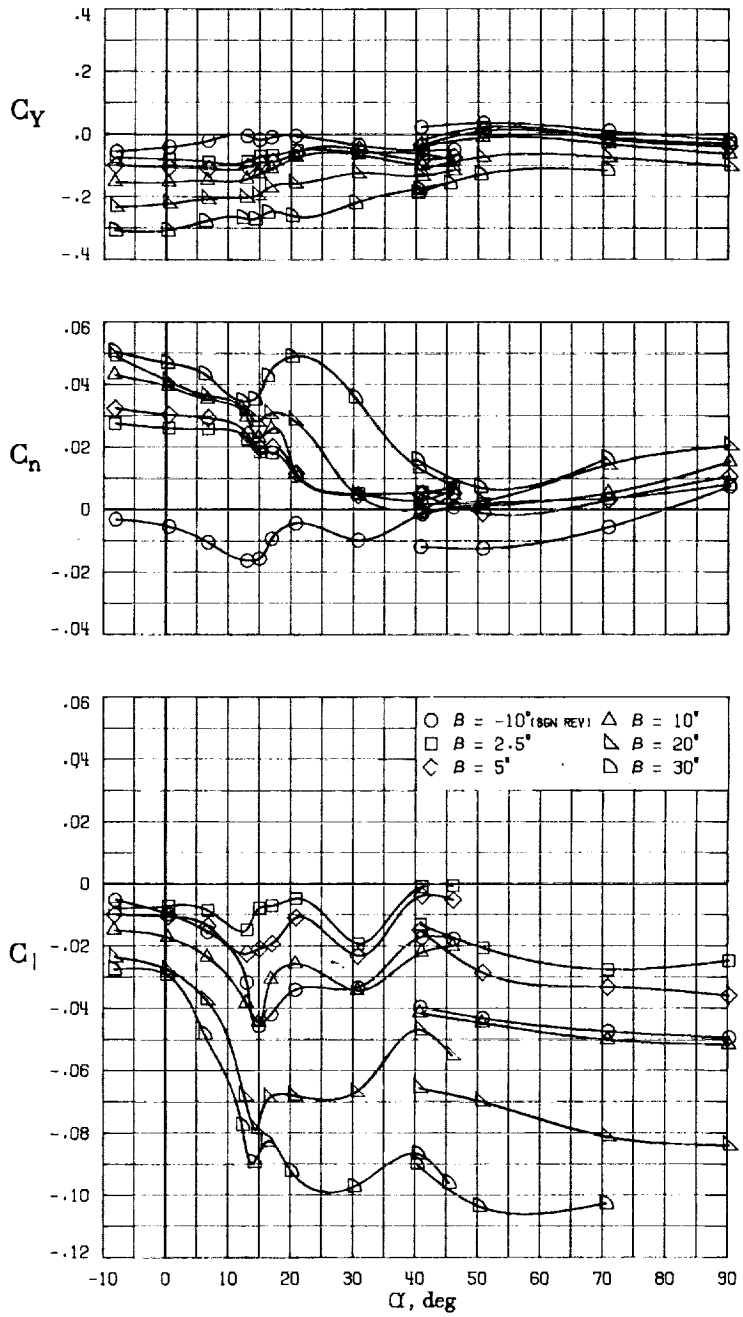

(D) LATERAL - DIRECTIONAL FORCE AND MOMENT COEFFICIENTS ABOUT BODY AXES.

FIGURE 34. - CONTINUED.

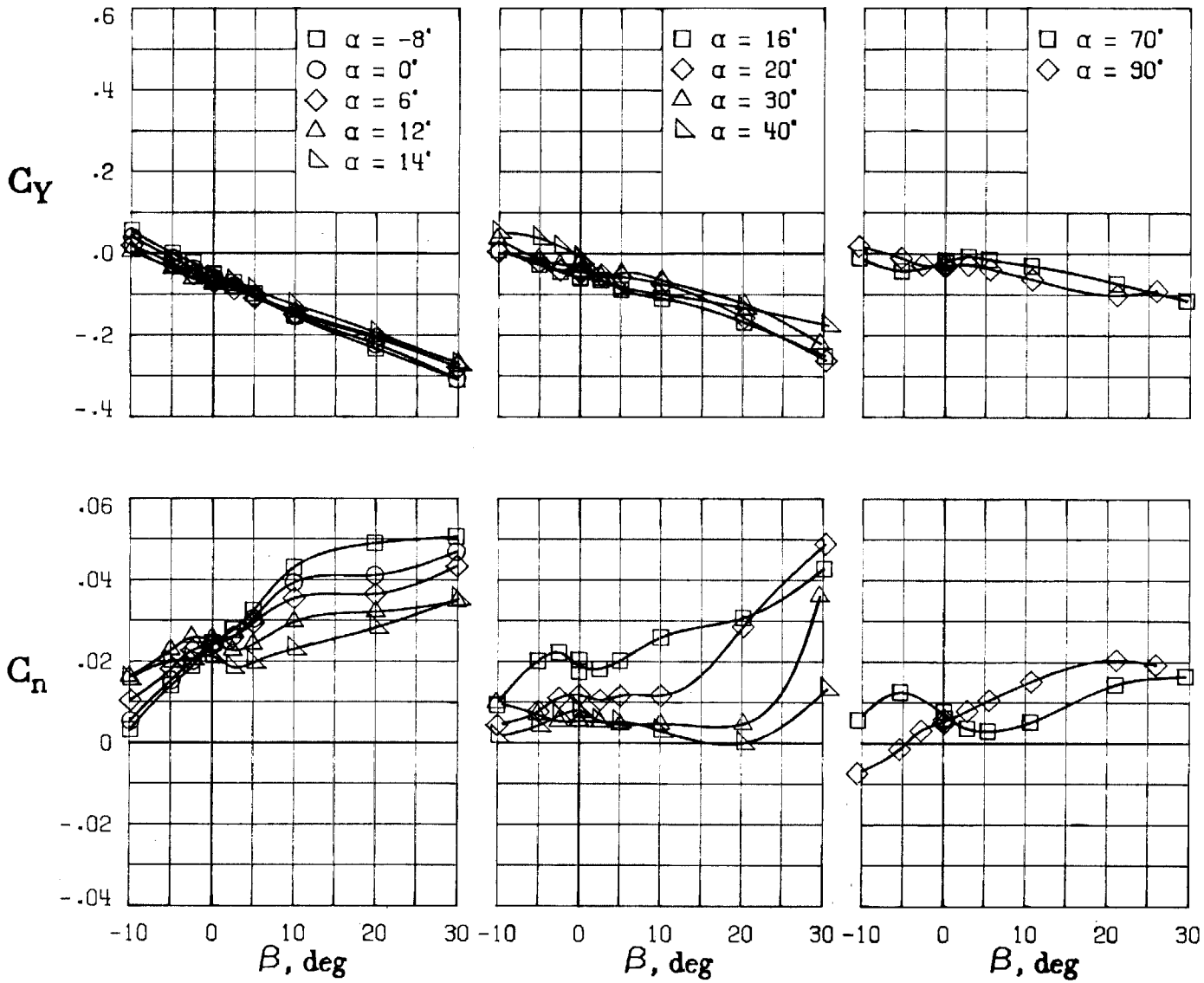

(E) DIRECTIONAL - STABILITY CHARACTERISTICS ABOUT BODY AXES AT VARIOUS ANGLES OF ATTACK.

FIGURE 34. - CONTINUED.

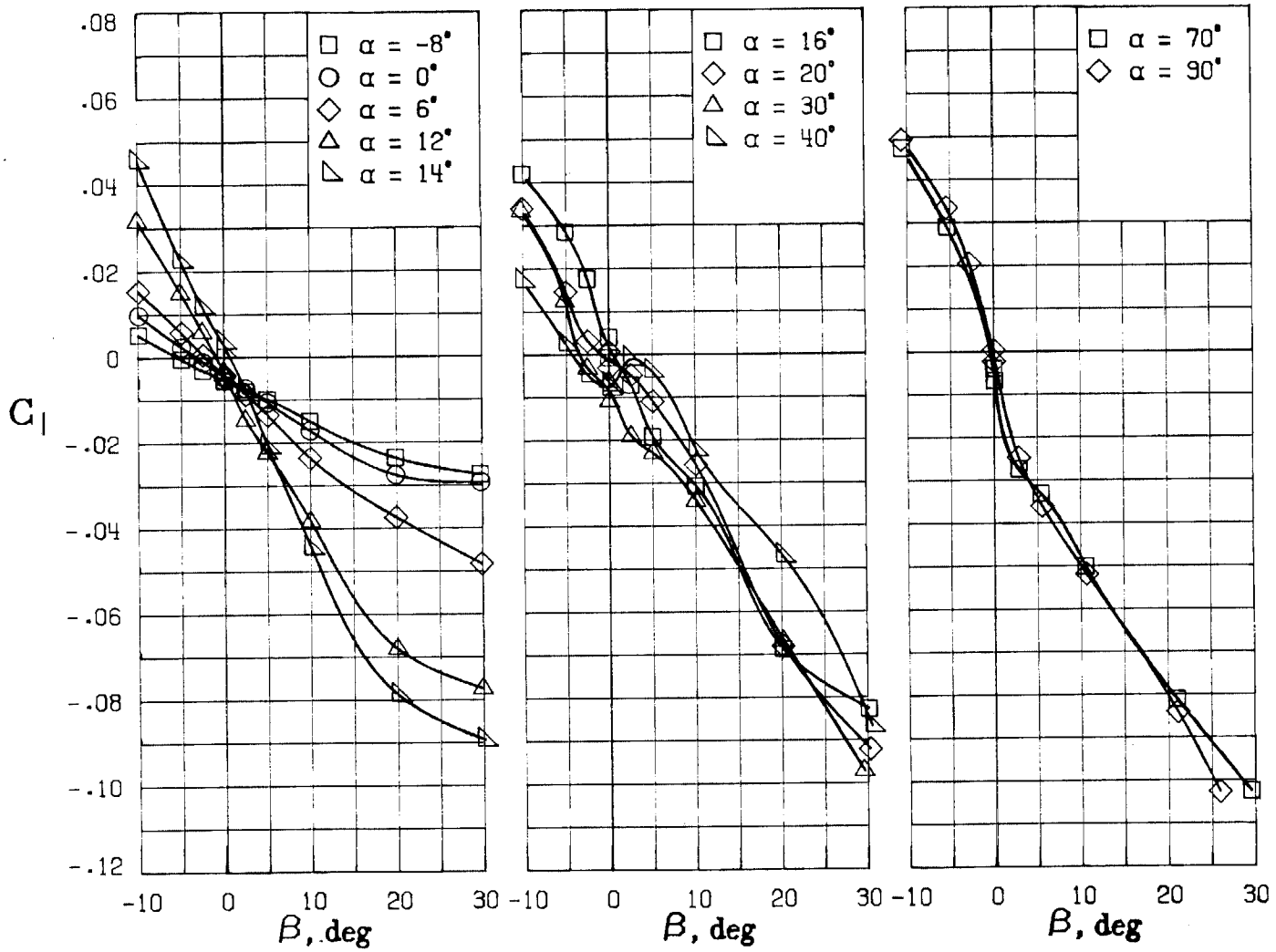

(F) LATERAL - STABILITY CHARACTERISTICS ABOUT BODY AXES AT VARIOUS ANGLES OF ATTACK.

FIGURE 34. - CONCLUDED.

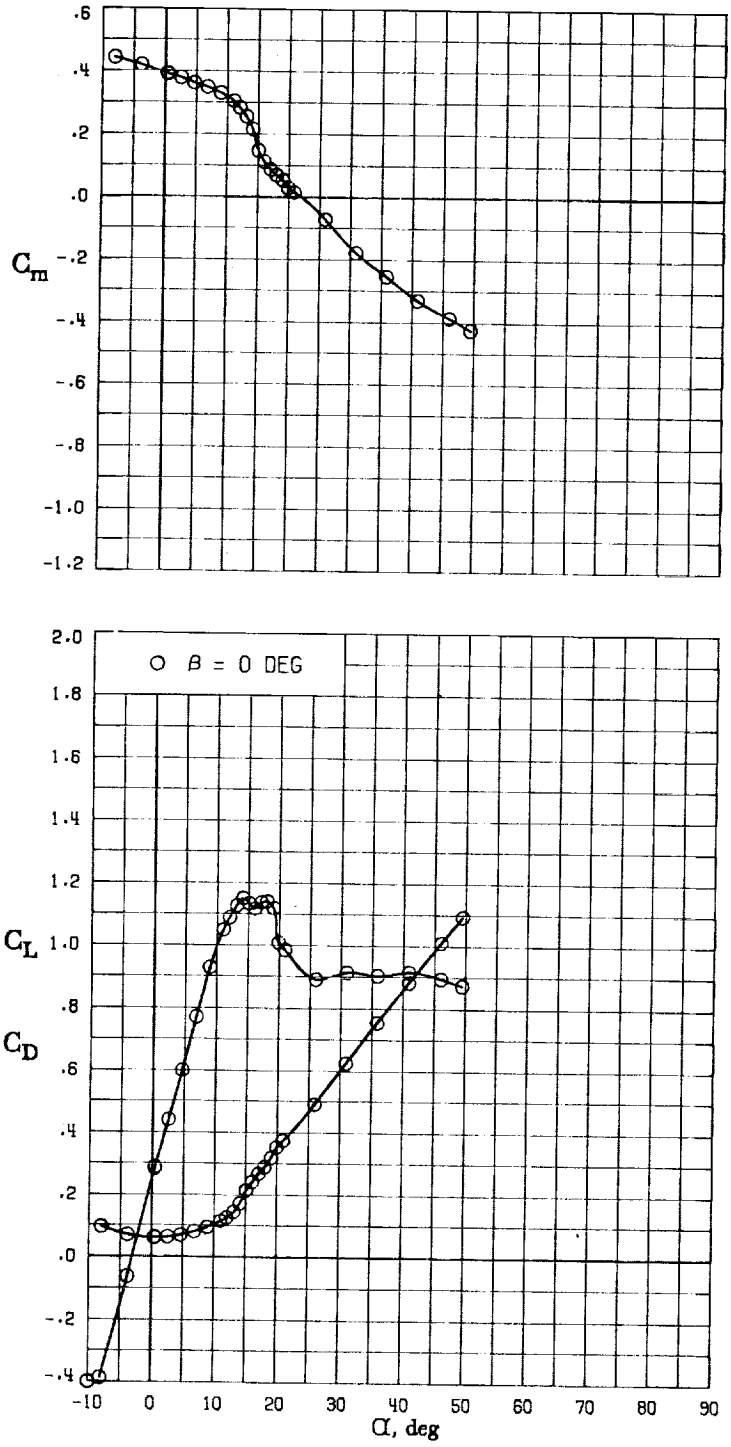

(A) LONGITUDINAL FORCE AND MOMENT COEFFICIENTS ABOUT STABILITY AXES.

FIGURE 35. - EFFECT OF ANGLE OF ATTACK AND SIDESLIP ANGLE ON AERODYNAMIC CHARACTERISTICS AT RE = 3.45 E+06 FOR CONFIGURATION B W1 H3 V. $\delta_E = -25°$, $\delta_A = -22°$, $\delta_R = 0°$.

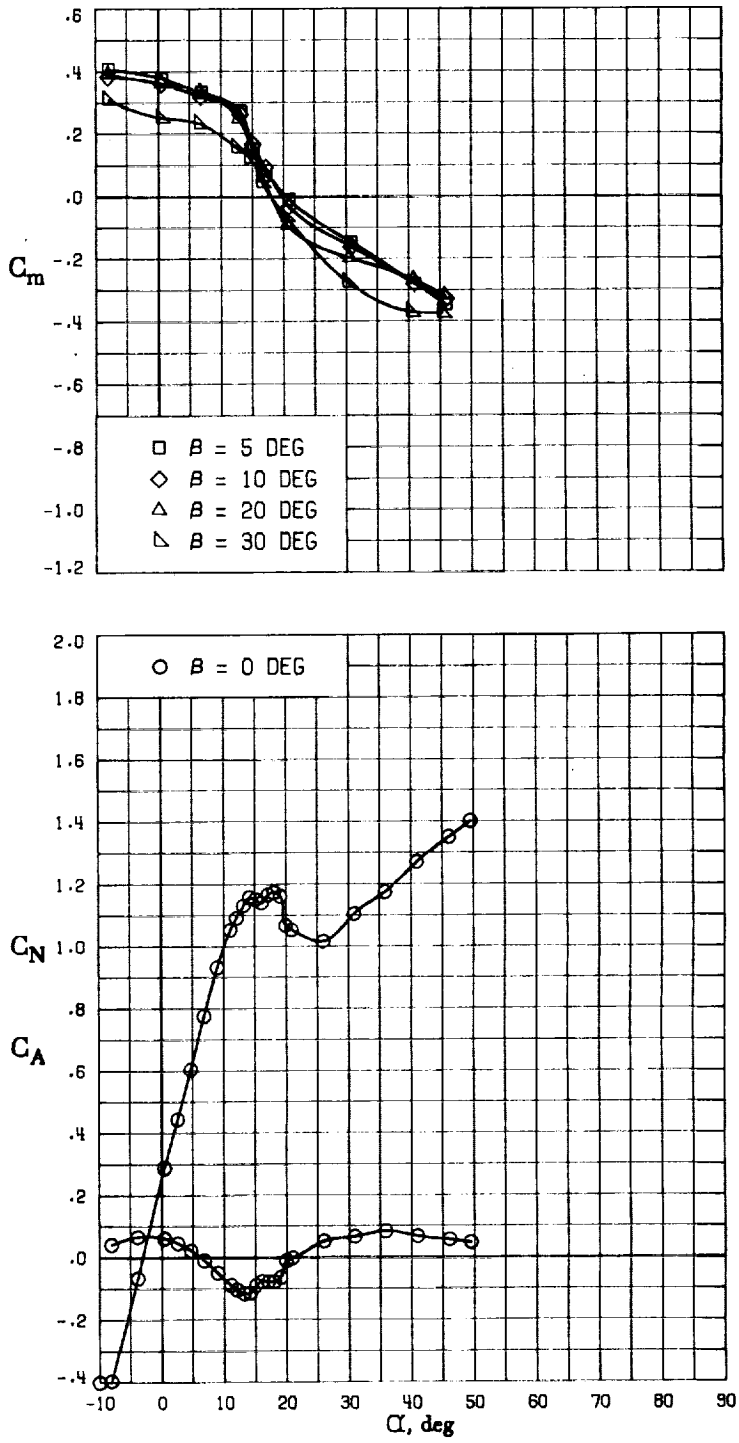

(B) LONGITUDINAL FORCE AND MOMENT COEFFICIENTS ABOUT BODY AXES.

FIGURE 35. - CONTINUED.

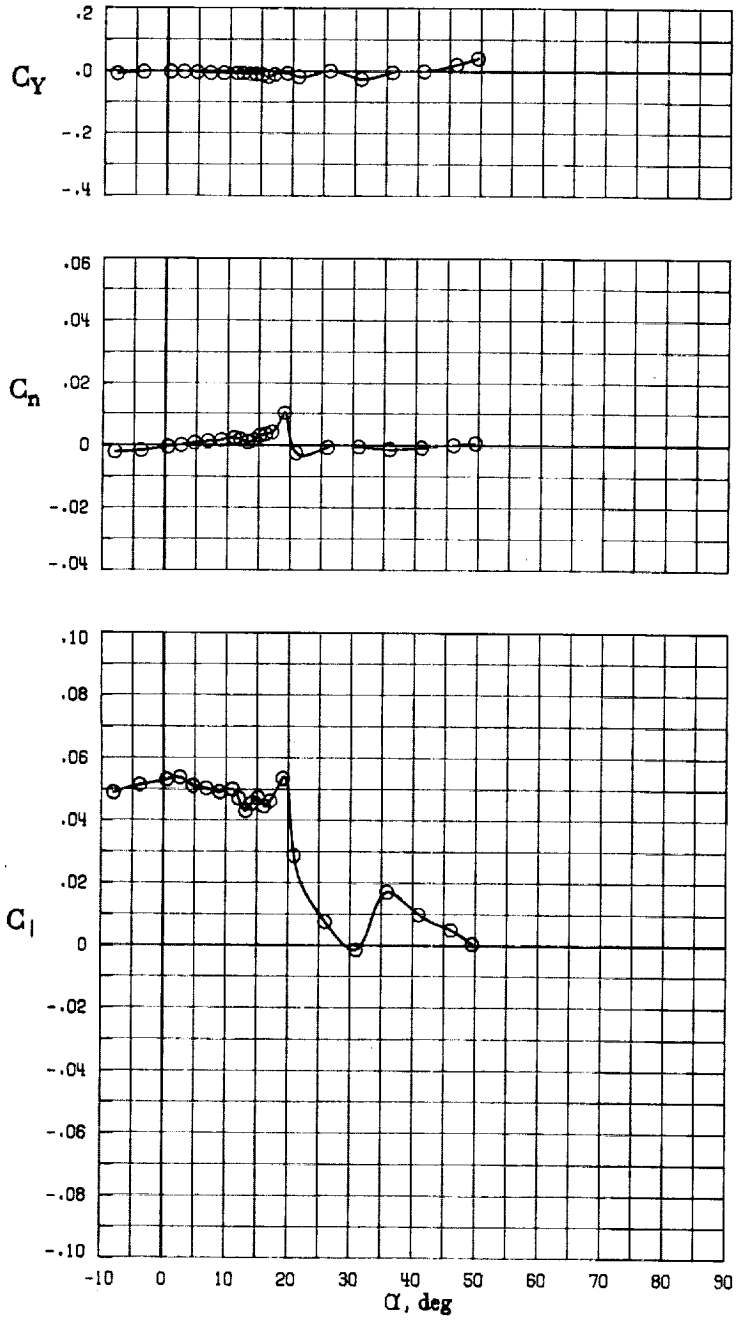

(C) LATERAL - DIRECTIONAL FORCE AND MOMENT COEFFICIENTS ABOUT BODY AXES AT ZERO SIDESLIP.

FIGURE 35. - CONTINUED.

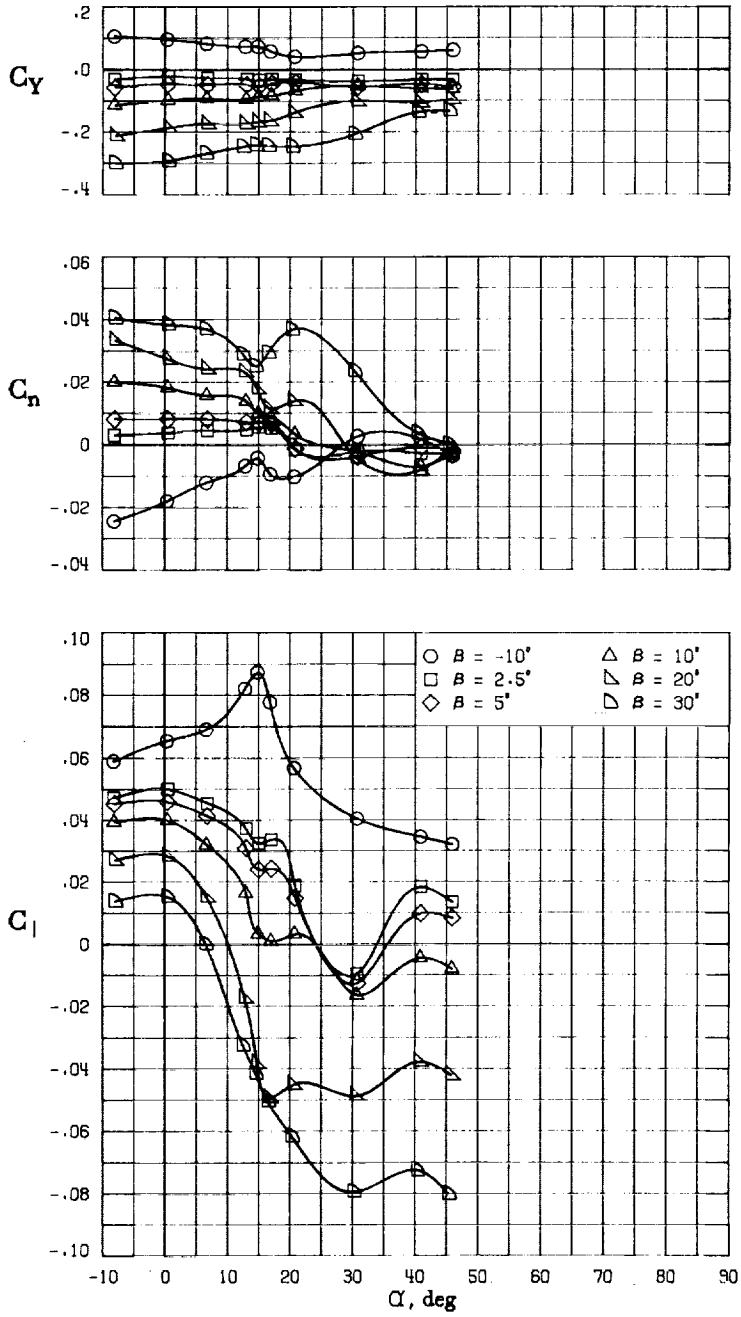

(D) LATERAL - DIRECTIONAL FORCE AND MOMENT COEFFICIENTS ABOUT BODY AXES.

FIGURE 35. - CONTINUED.

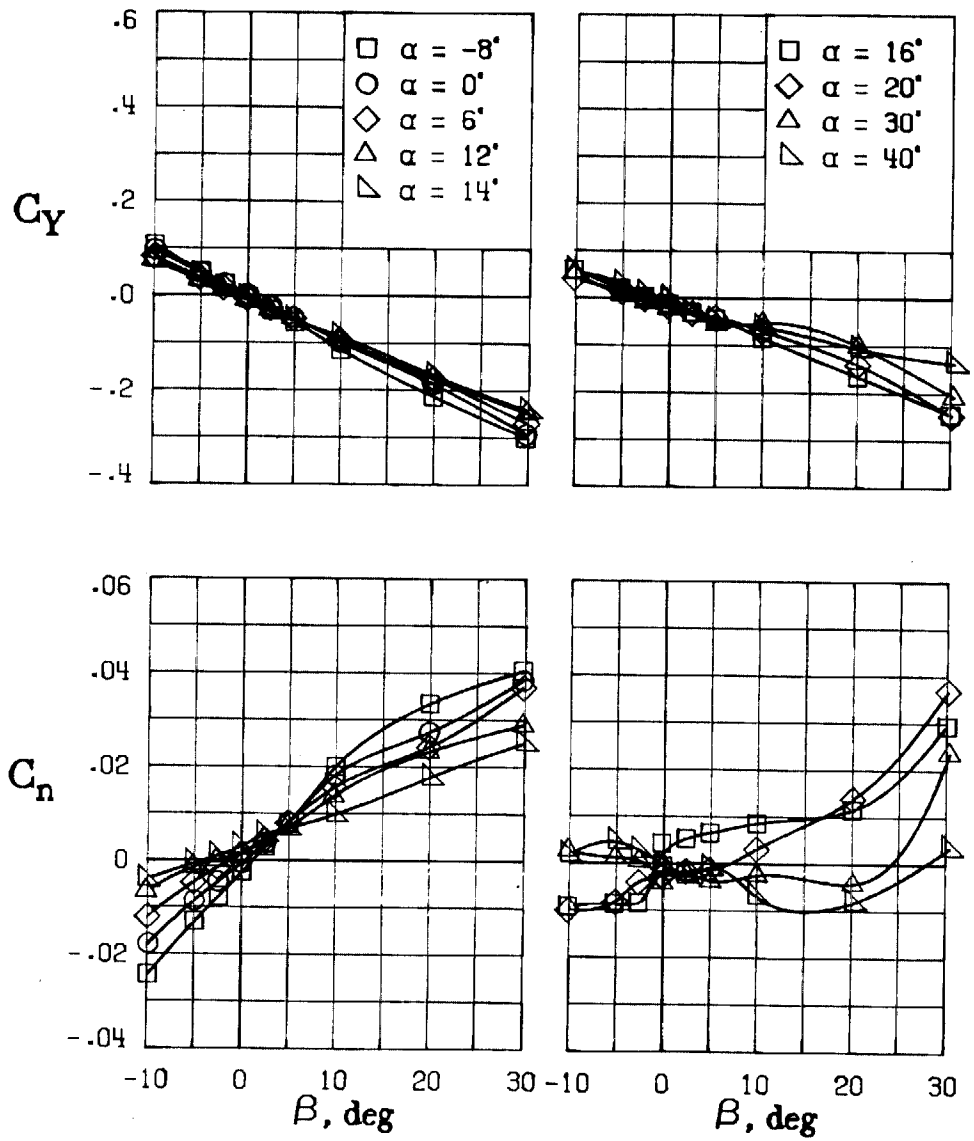

(E) DIRECTIONAL - STABILITY CHARACTERISTICS ABOUT BODY AXES AT VARIOUS ANGLES OF ATTACK.

FIGURE 35. - CONTINUED.

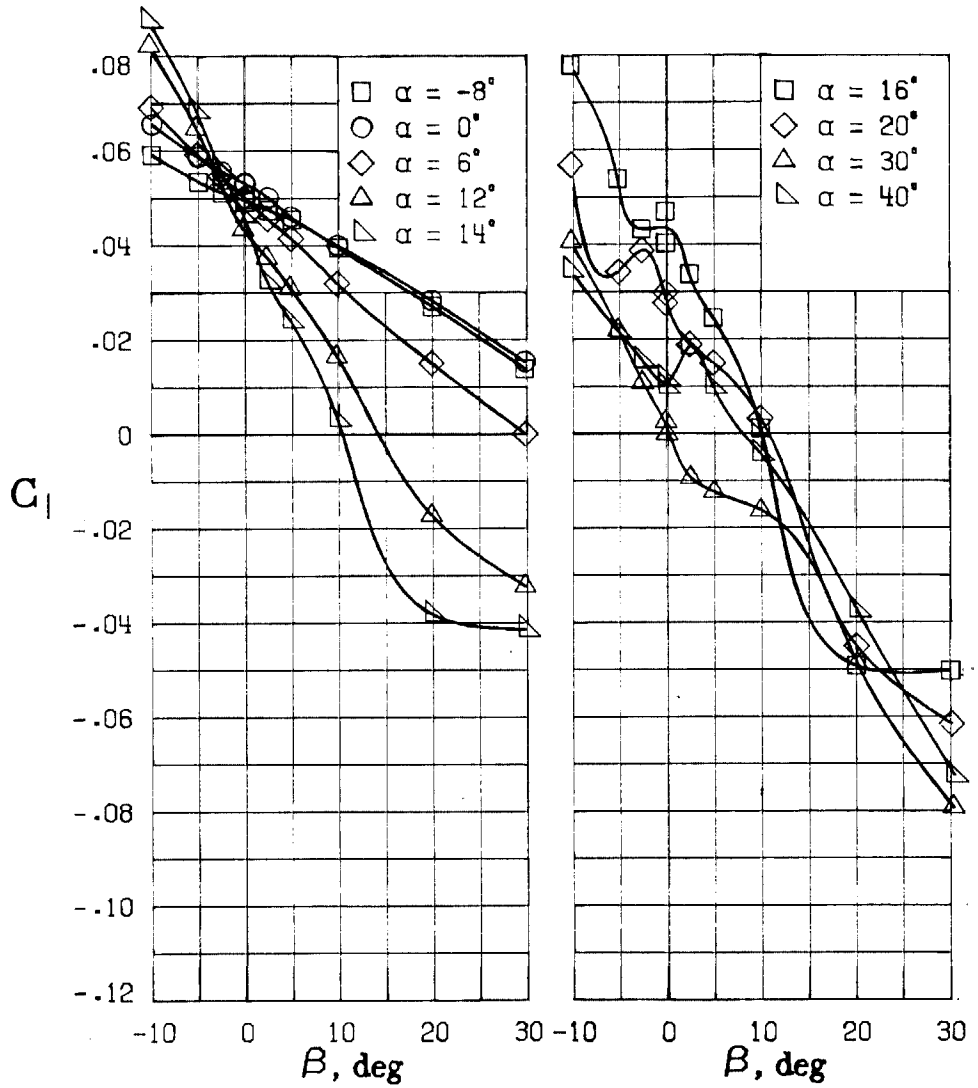

(F) LATERAL - STABILITY CHARACTERISTICS ABOUT BODY AXES AT VARIOUS ANGLES OF ATTACK.

FIGURE 35. - CONCLUDED.

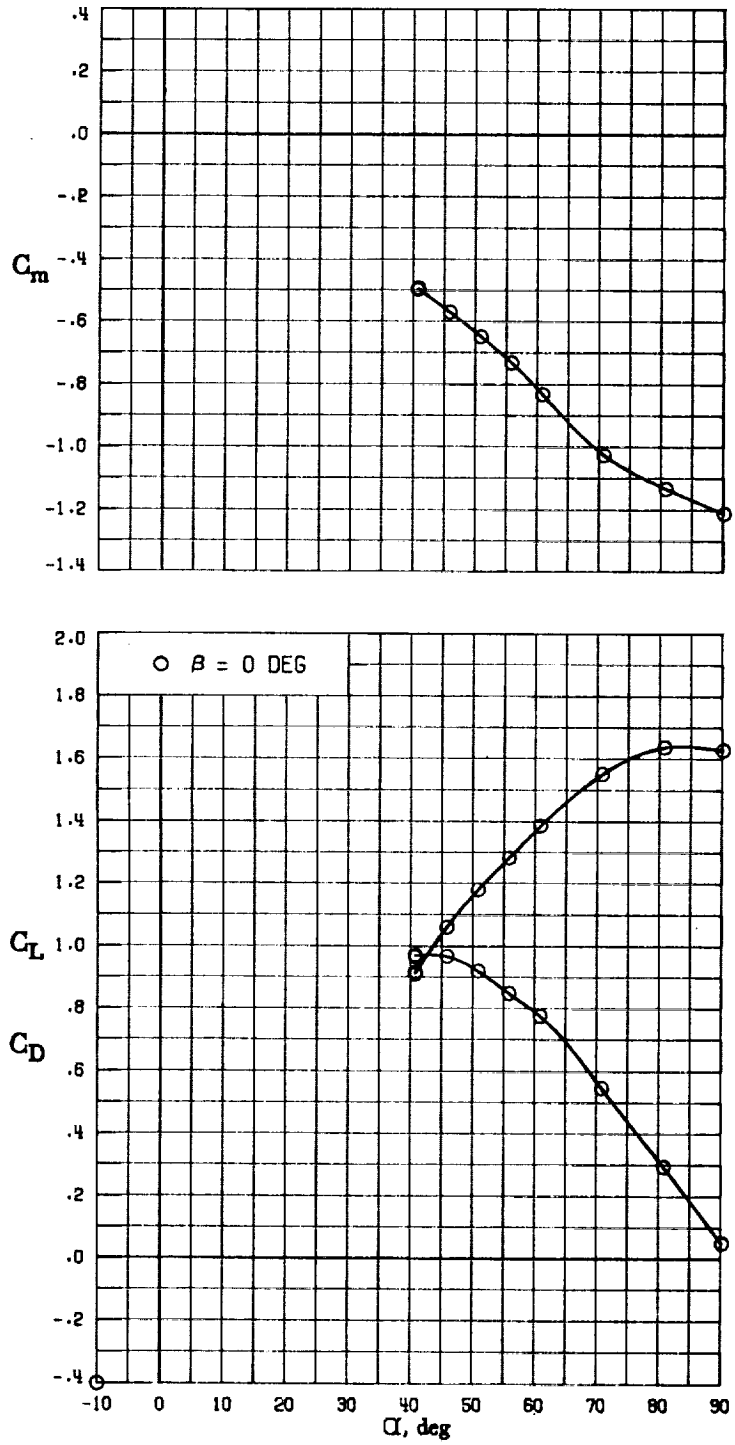

(A) LONGITUDINAL FORCE AND MOMENT COEFFICIENTS ABOUT STABILITY AXES.

FIGURE 36. - EFFECT OF ANGLE OF ATTACK AND SIDESLIP ANGLE ON AERODYNAMIC CHARACTERISTICS AT RE = 3.45 E+06 FOR CONFIGURATION B W1 H3 V. δ_E = 0°, δ_A = 0°, δ_R = -25°.

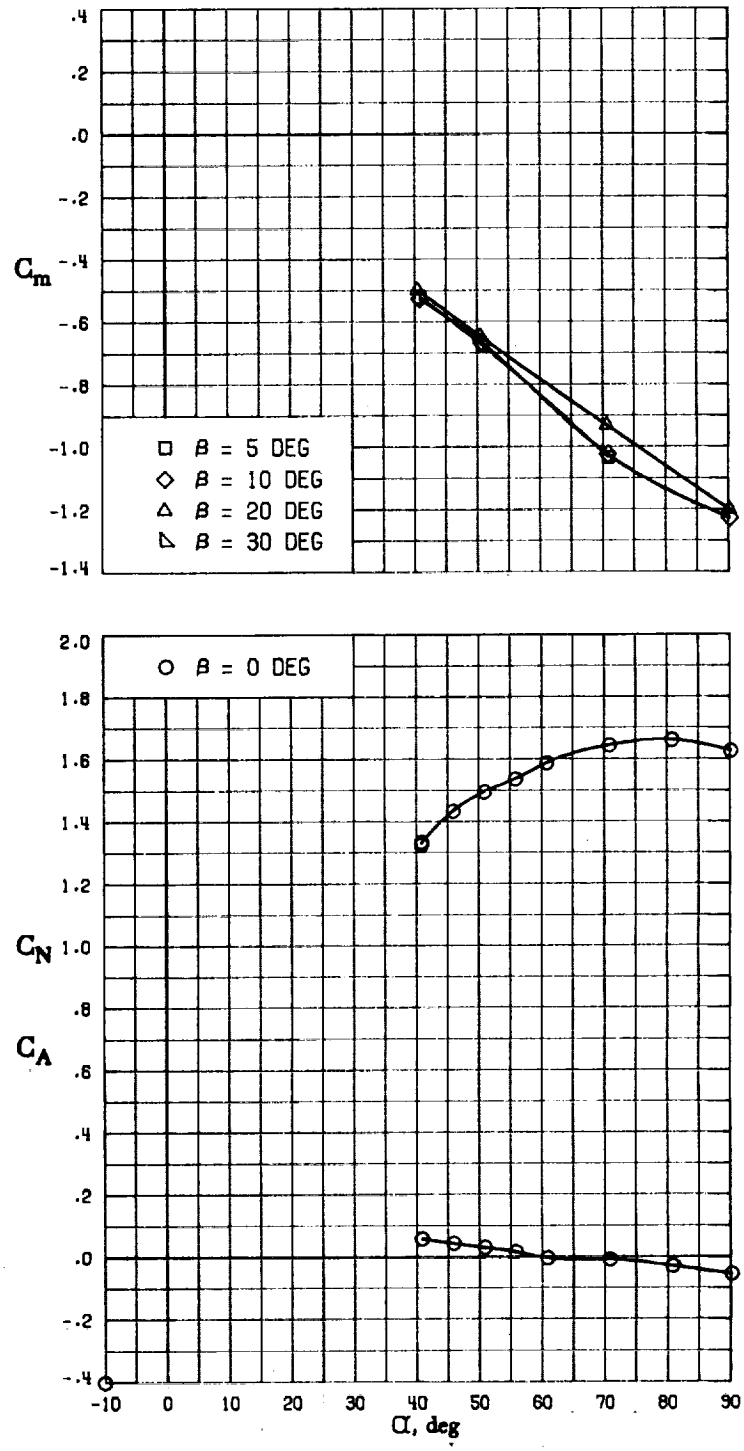

(B) LONGITUDINAL FORCE AND MOMENT COEFFICIENTS ABOUT BODY AXES.

FIGURE 36. - CONTINUED.

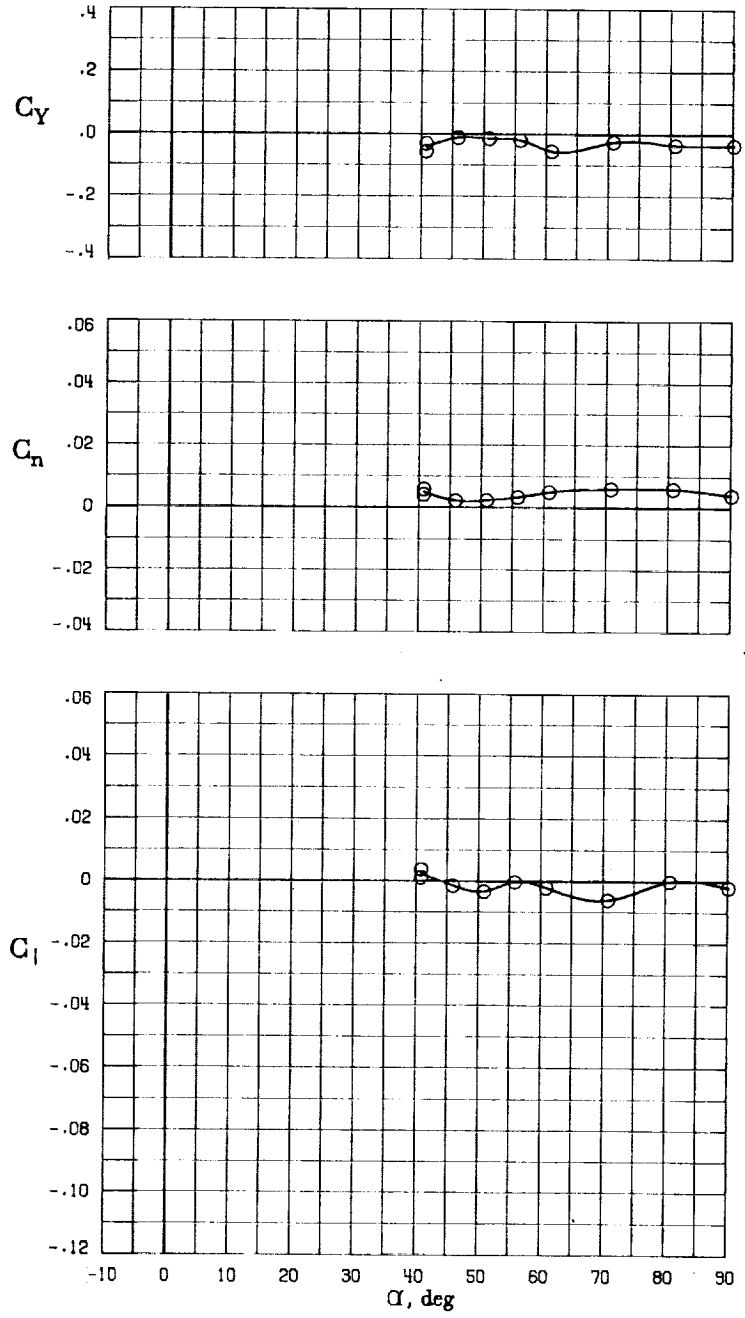

(C) LATERAL - DIRECTIONAL FORCE AND MOMENT COEFFICIENTS ABOUT BODY AXES AT ZERO SIDESLIP.

FIGURE 36. - CONTINUED.

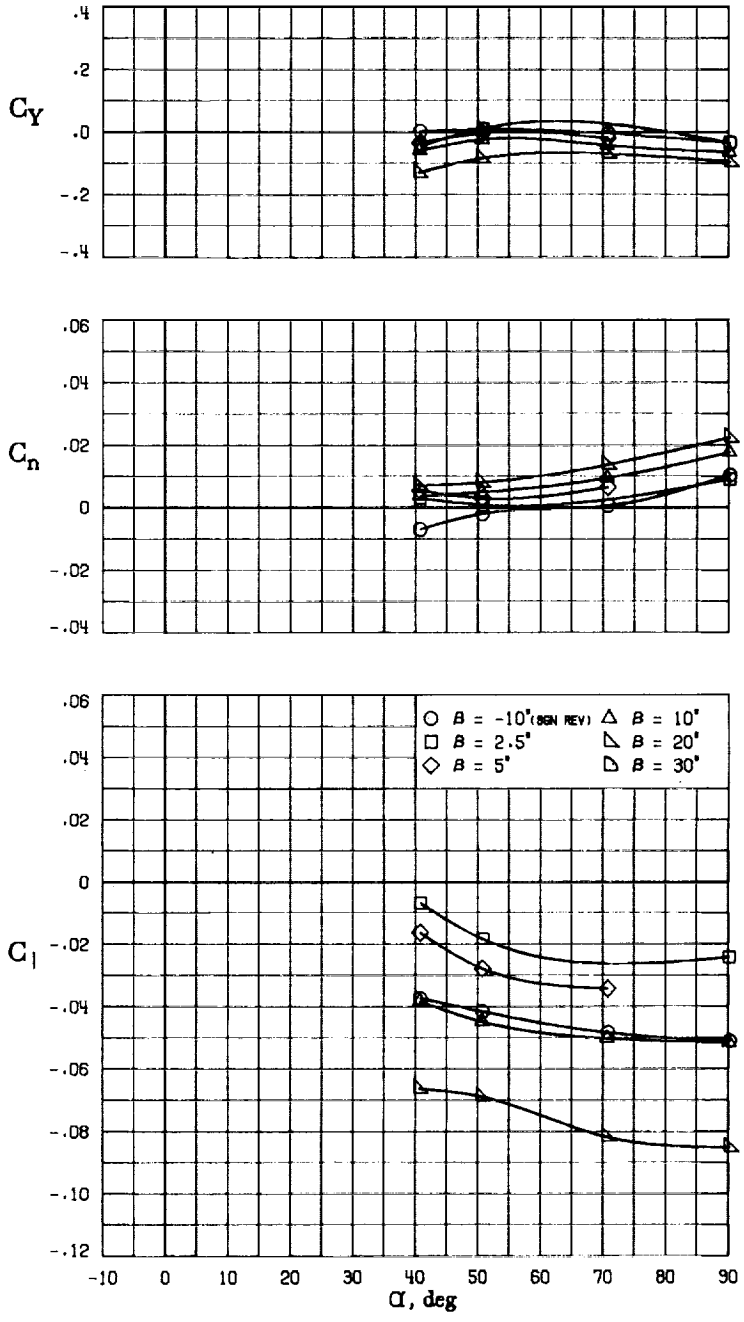

(D) LATERAL - DIRECTIONAL FORCE AND MOMENT COEFFICIENTS ABOUT BODY AXES.

FIGURE 36. - CONTINUED.

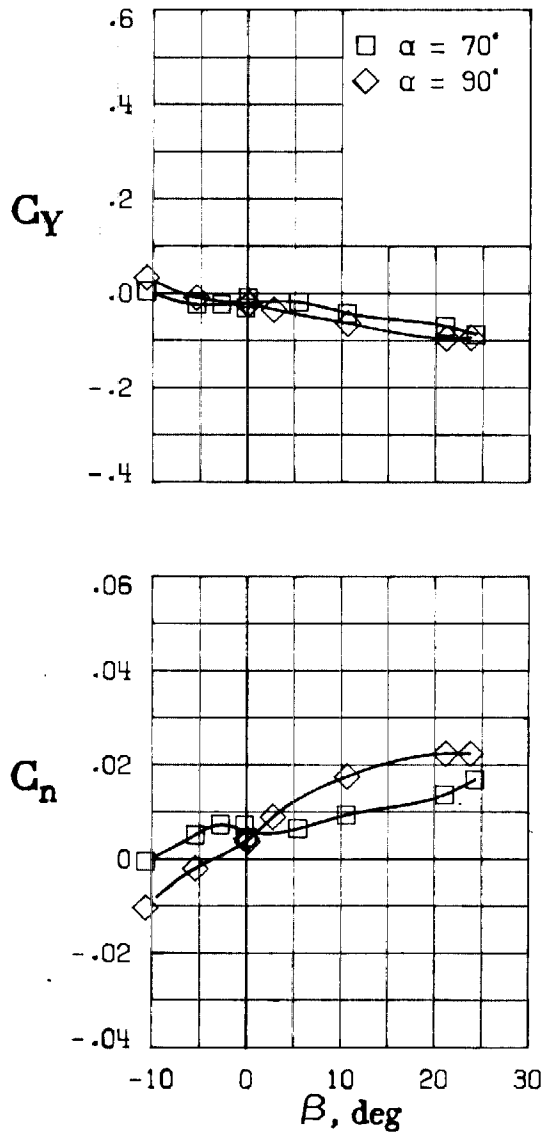

(E) DIRECTIONAL - STABILITY CHARACTERISTICS ABOUT BODY AXES AT VARIOUS ANGLES OF ATTACK.

FIGURE 36. - CONTINUED.

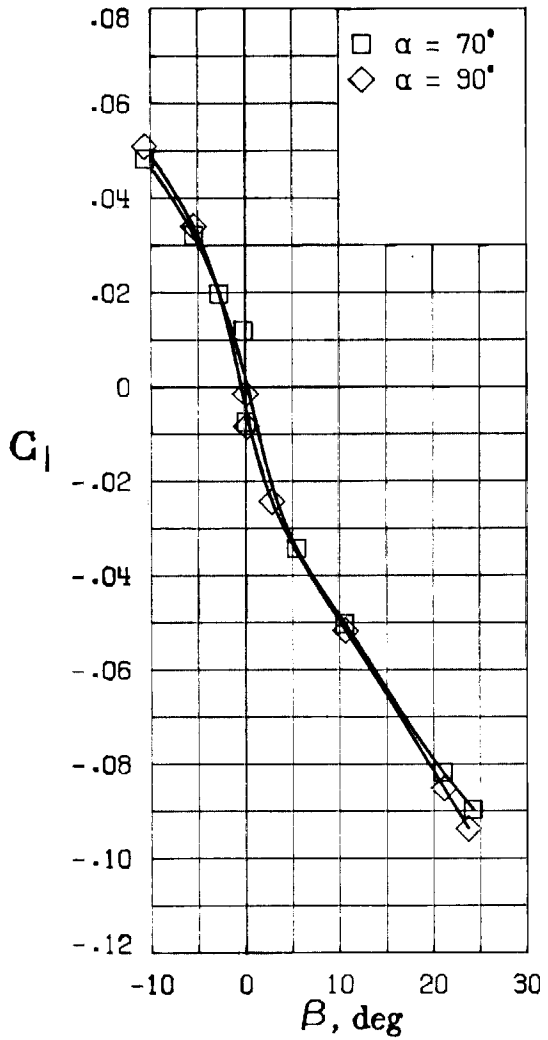

(F) LATERAL - STABILITY CHARACTERISTICS ABOUT BODY AXES AT VARIOUS ANGLES OF ATTACK.

FIGURE 36. - CONCLUDED.

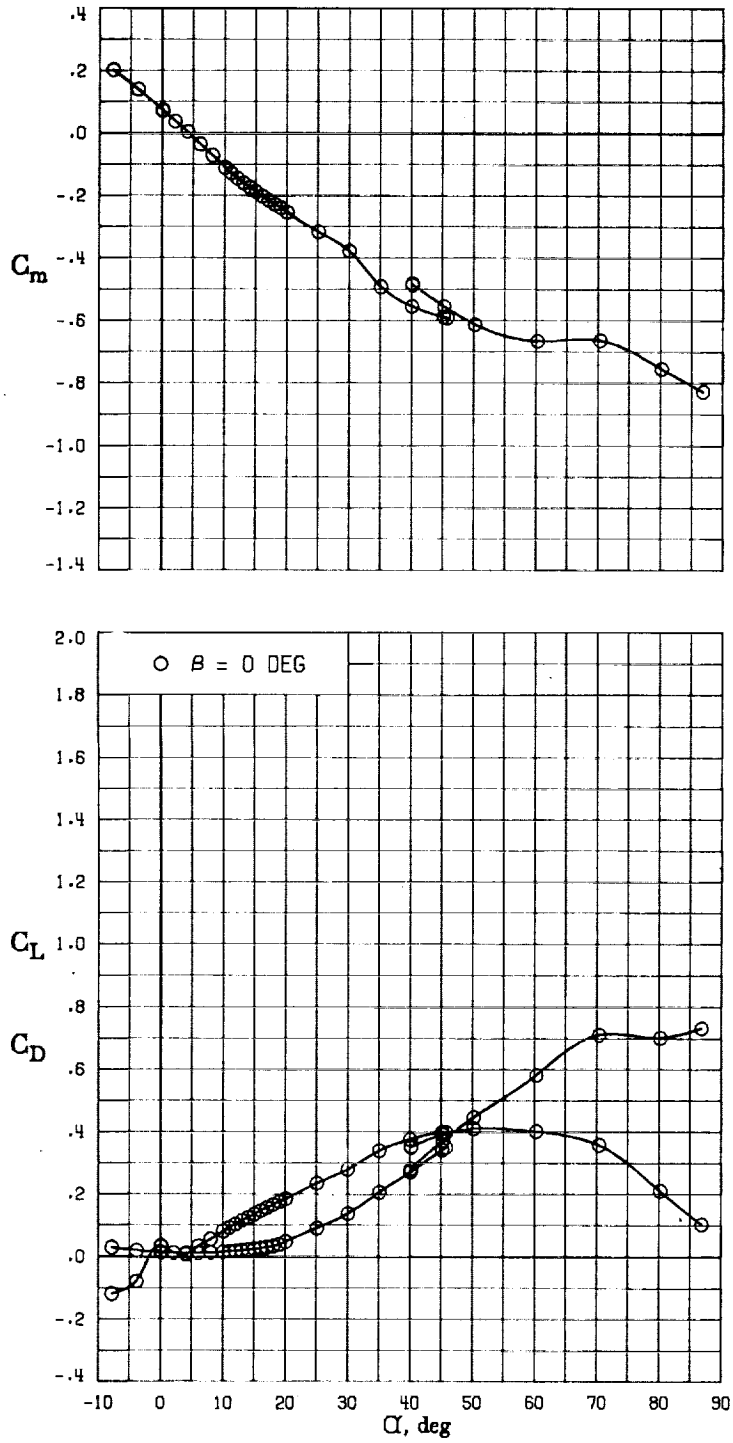

(a) LONGITUDINAL FORCE AND MOMENT COEFFICIENTS ABOUT STABILITY AXES.

FIGURE 37. - EFFECT OF ANGLE OF ATTACK AND SIDESLIP ANGLE ON AERODYNAMIC CHARACTERISTICS AT RE = 3.45 E+06 FOR CONFIGURATION B H3 V. δ_E = 0°, δ_A = 0°, δ_R = 0°.

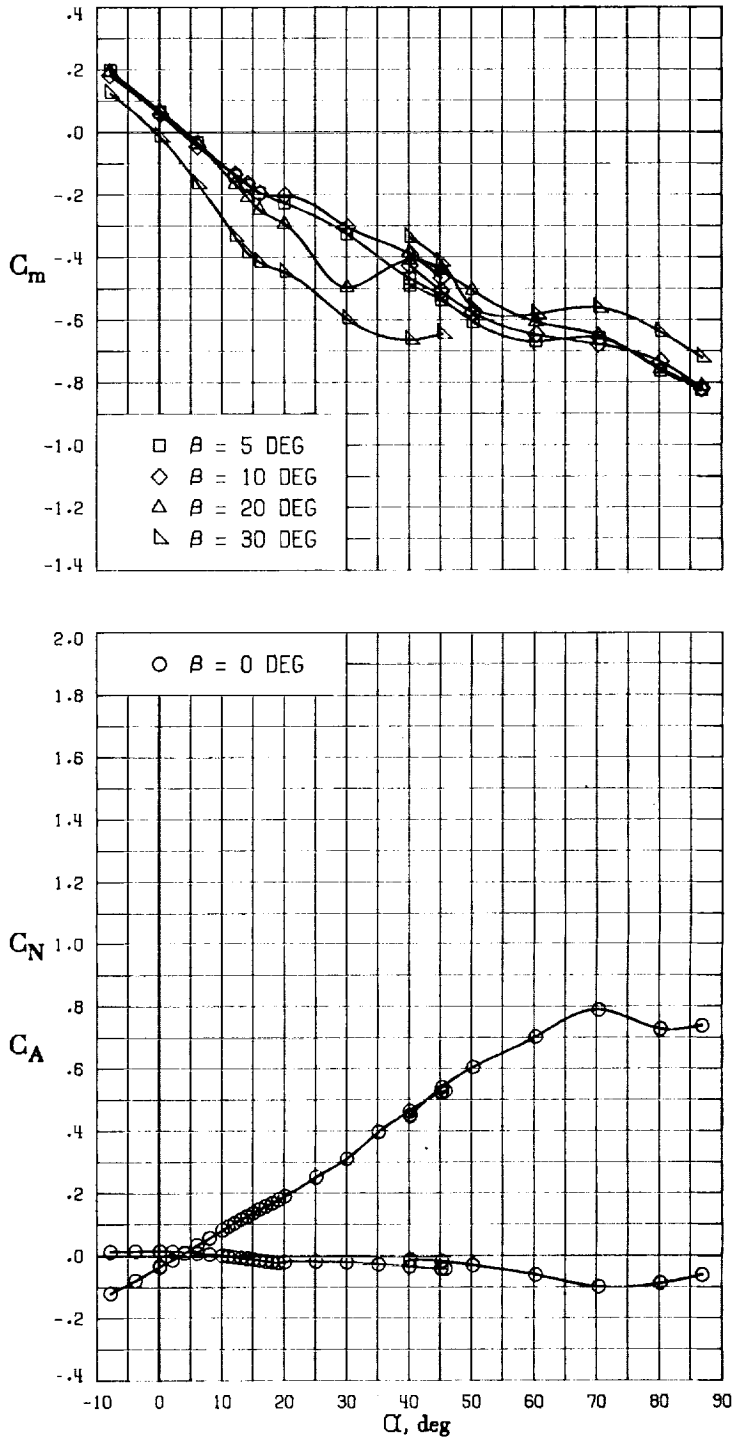

(B) LONGITUDINAL FORCE AND MOMENT COEFFICIENTS ABOUT BODY AXES.

FIGURE 37. - CONTINUED.

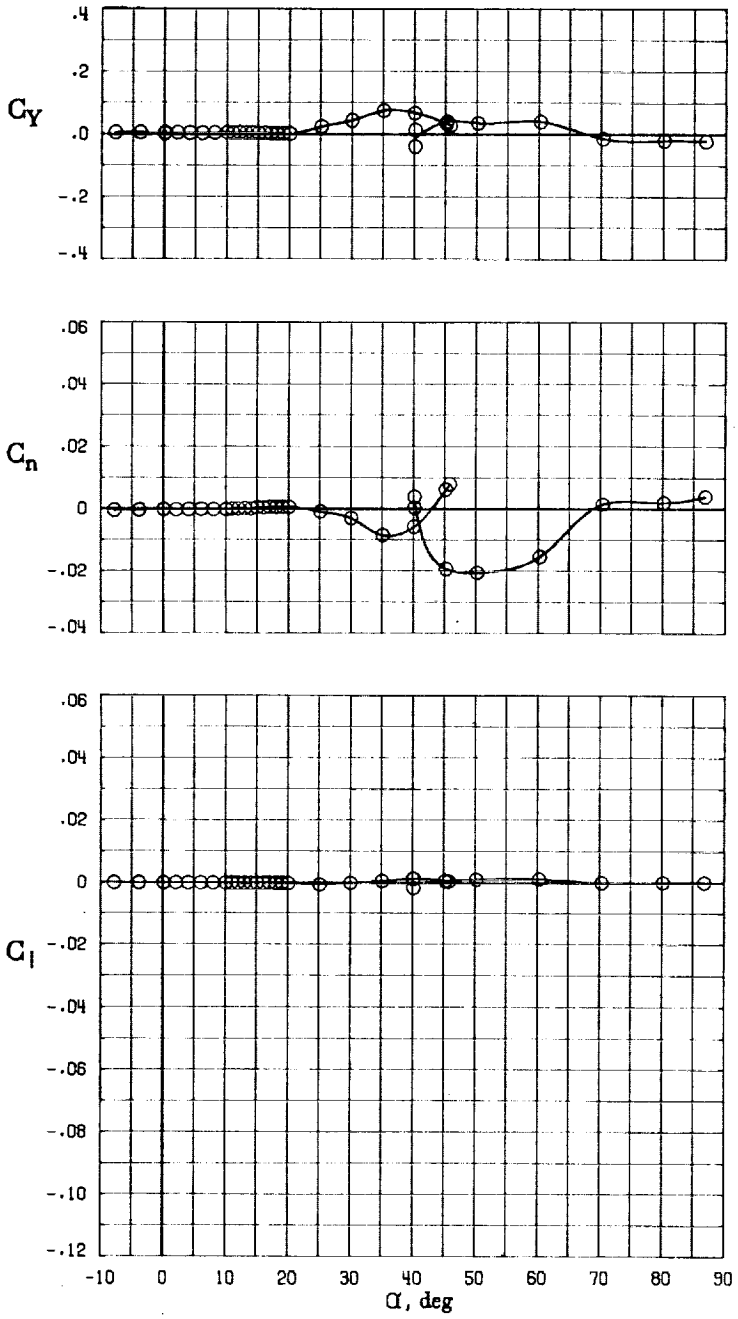

(C) LATERAL - DIRECTIONAL FORCE AND MOMENT COEFFICIENTS ABOUT BODY AXES AT ZERO SIDESLIP.

FIGURE 37. - CONTINUED.

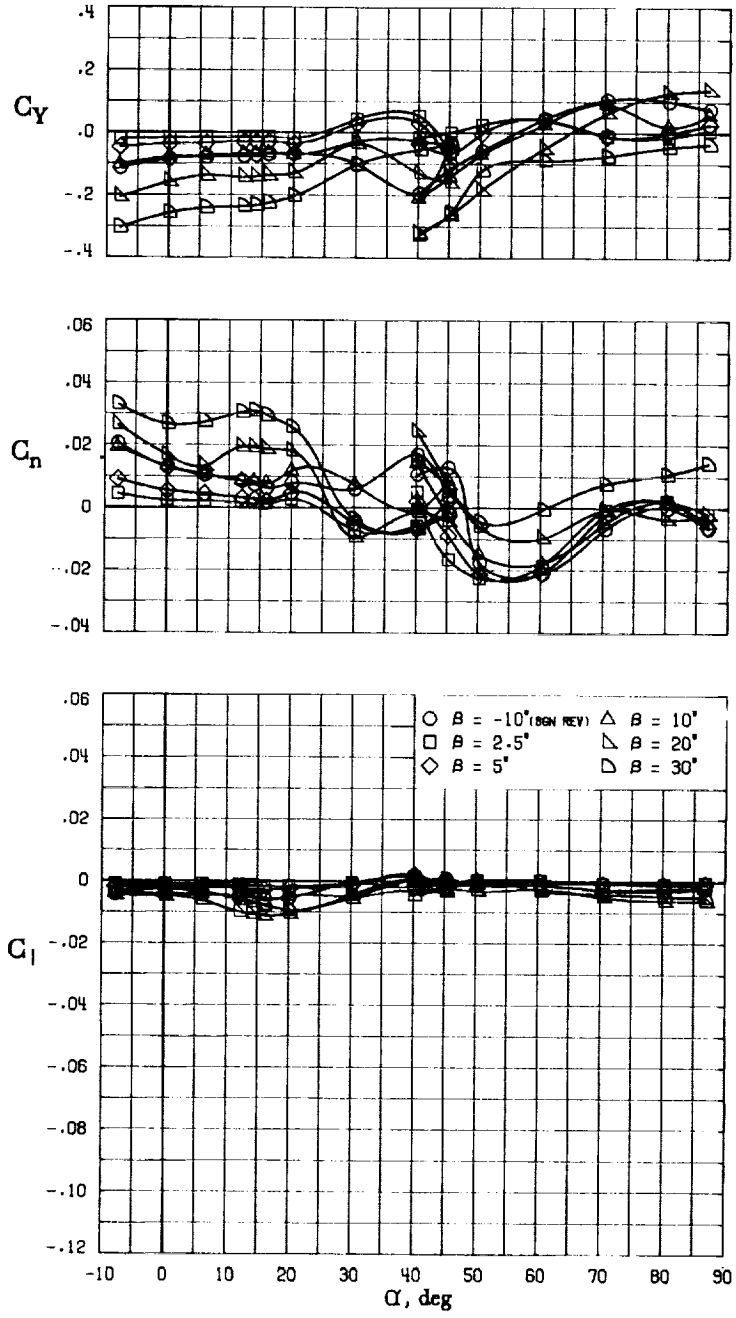

(D) LATERAL - DIRECTIONAL FORCE AND MOMENT COEFFICIENTS ABOUT BODY AXES.

FIGURE 37. - CONTINUED.

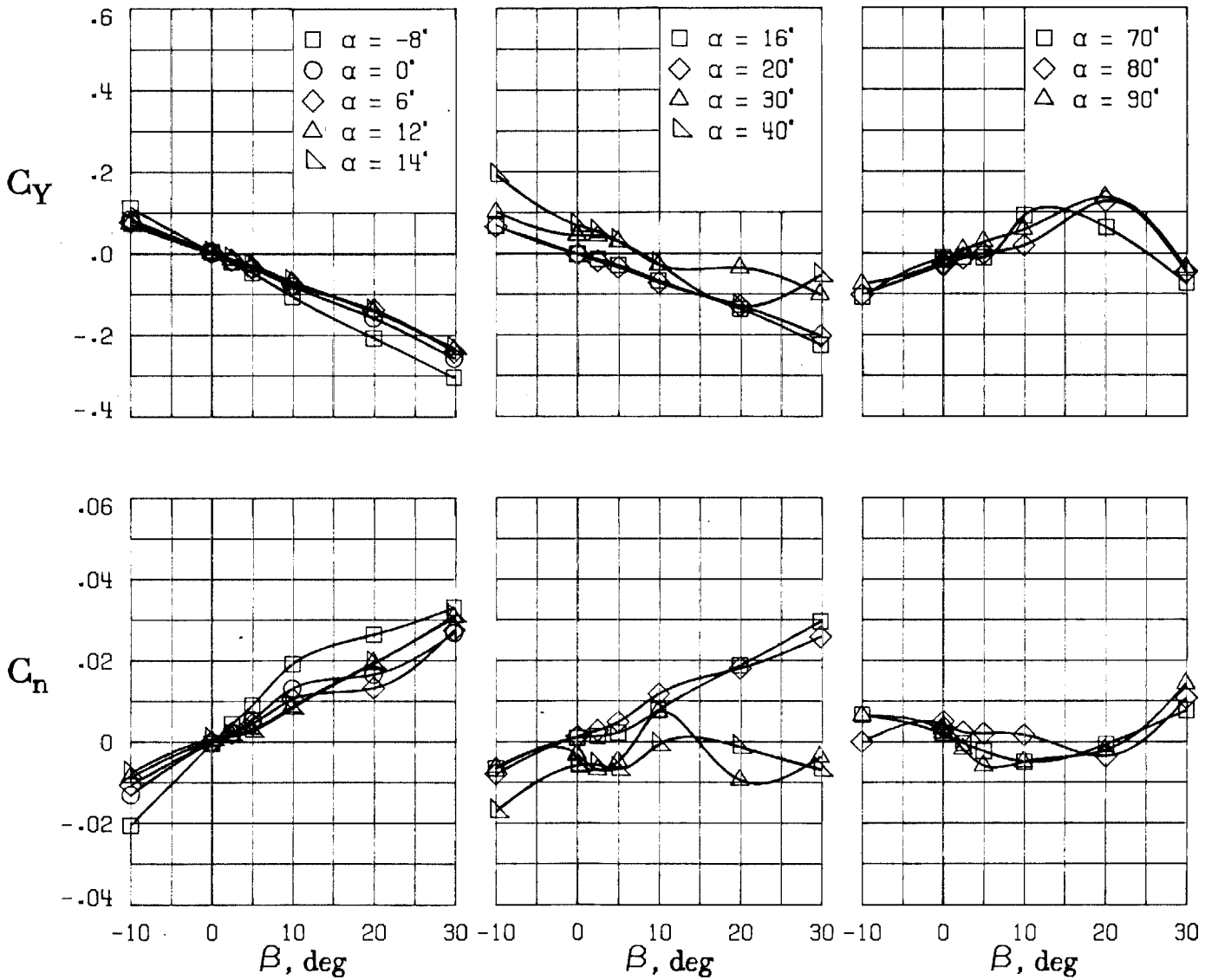

(E) DIRECTIONAL - STABILITY CHARACTERISTICS ABOUT BODY AXES AT VARIOUS ANGLES OF ATTACK.

FIGURE 37. - CONTINUED.

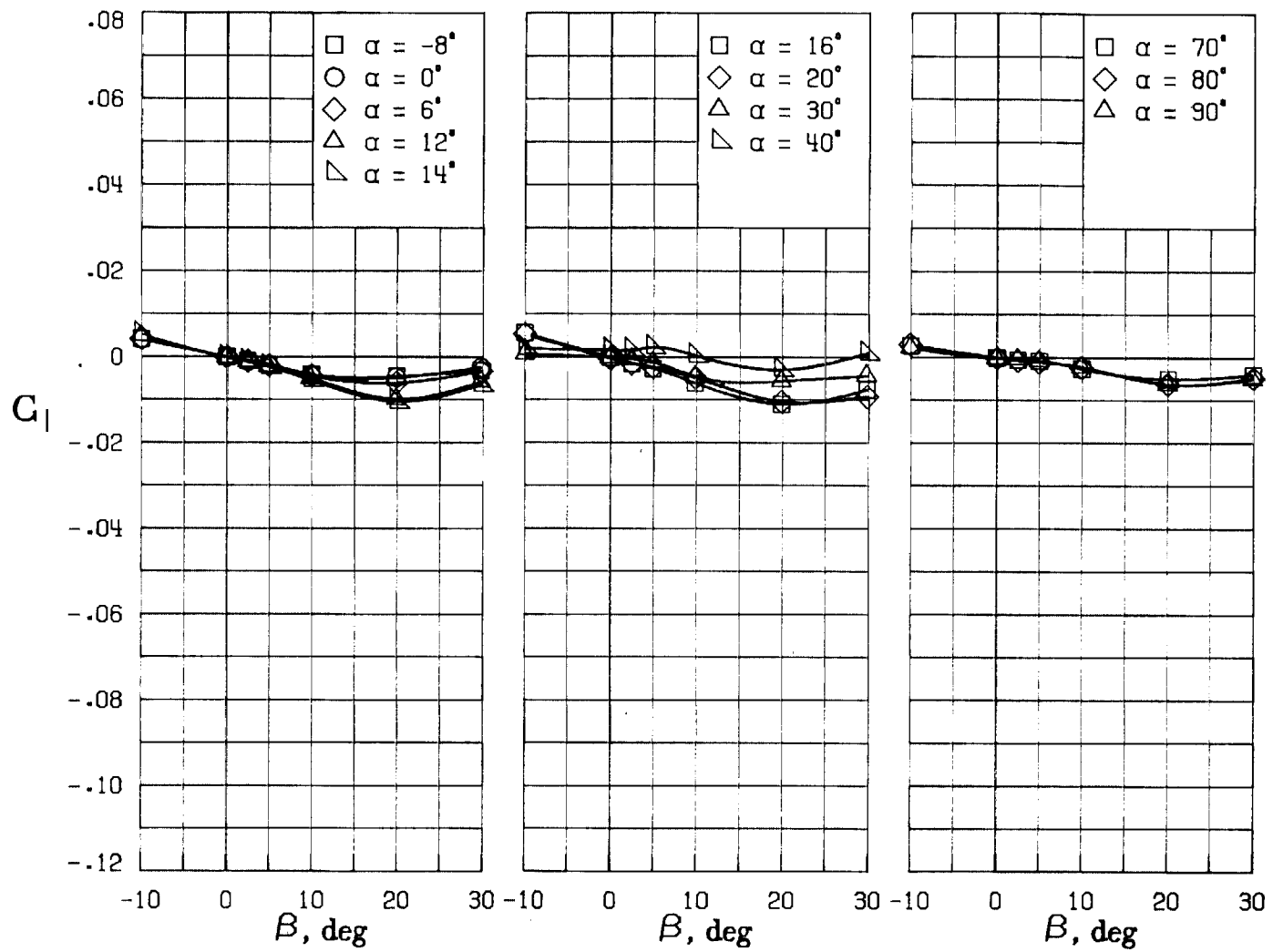

(F) LATERAL - STABILITY CHARACTERISTICS ABOUT BODY AXES AT VARIOUS ANGLES OF ATTACK.

FIGURE 37. - CONCLUDED.

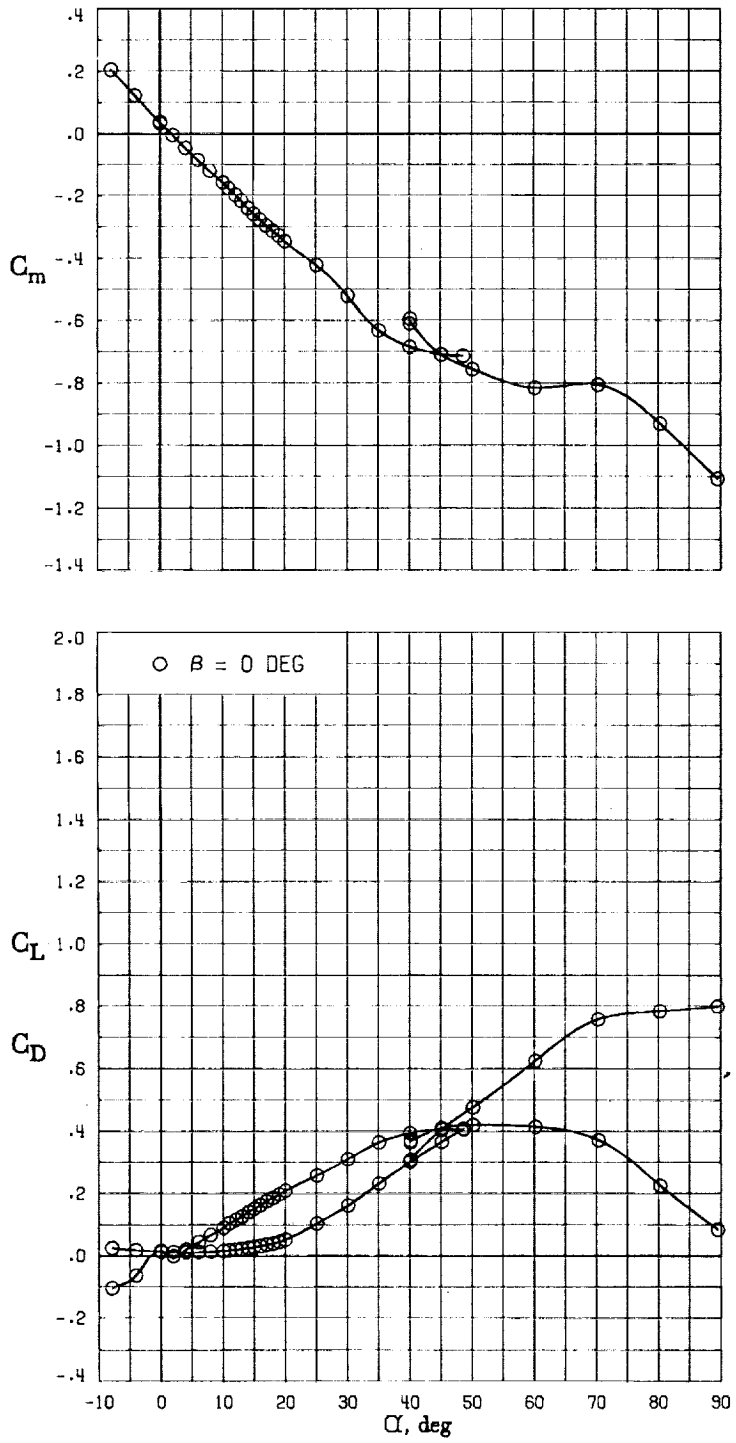

(A) LONGITUDINAL FORCE AND MOMENT COEFFICIENTS ABOUT STABILITY AXES.

FIGURE 38. - EFFECT OF ANGLE OF ATTACK AND SIDESLIP ANGLE ON AERODYNAMIC CHARACTERISTICS AT RE = 3.45 E+06 FOR CONFIGURATION B H4 V. $\delta_E = 0°$, $\delta_A = 0°$, $\delta_R = 0°$.

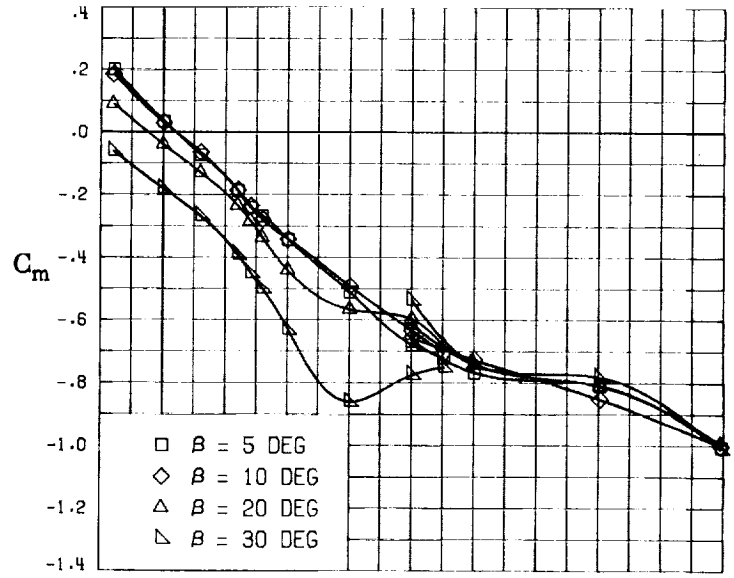

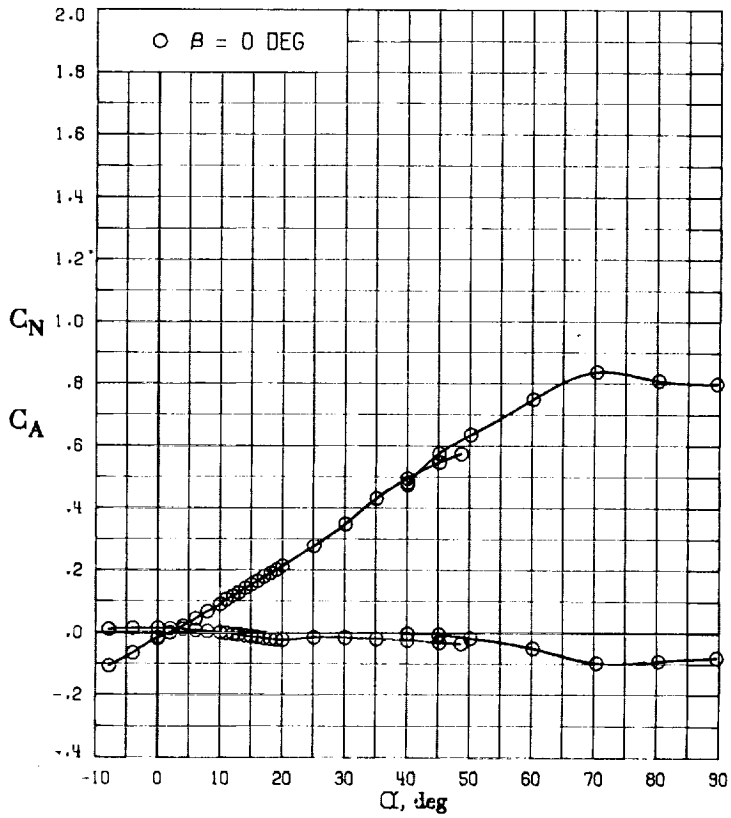

(B) LONGITUDINAL FORCE AND MOMENT COEFFICIENTS ABOUT BODY AXES.

FIGURE 38. - CONTINUED.

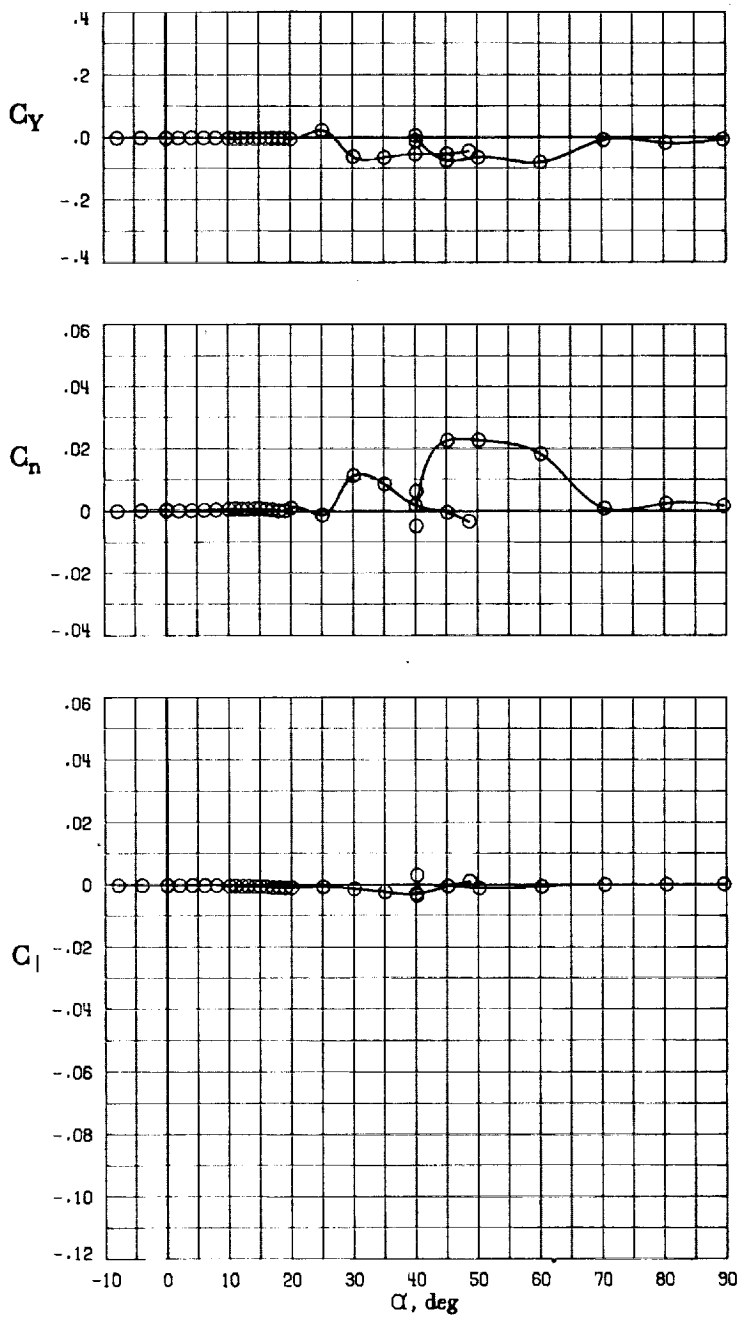

(C) LATERAL - DIRECTIONAL FORCE AND MOMENT COEFFICIENTS ABOUT BODY AXES AT ZERO SIDESLIP.

FIGURE 38. - CONTINUED.

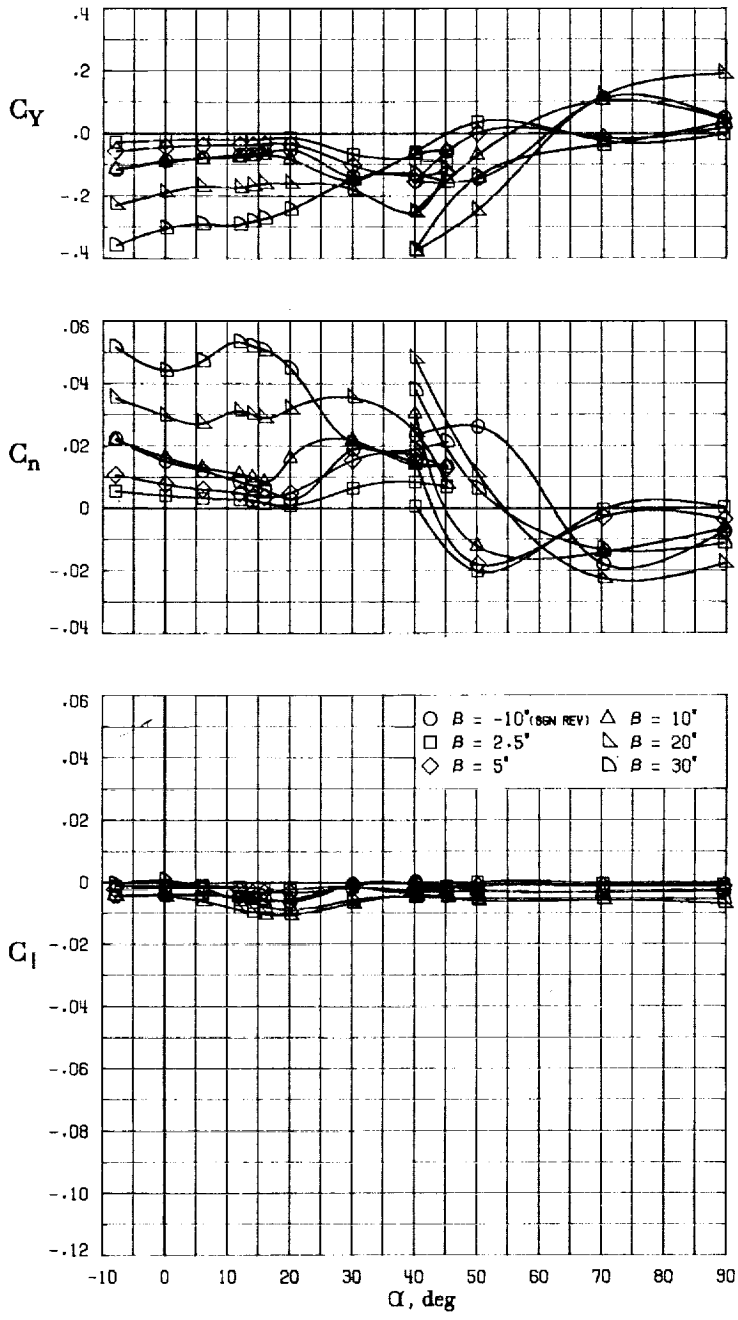

(D) LATERAL - DIRECTIONAL FORCE AND MOMENT COEFFICIENTS ABOUT BODY AXES.

FIGURE 38. - CONTINUED.

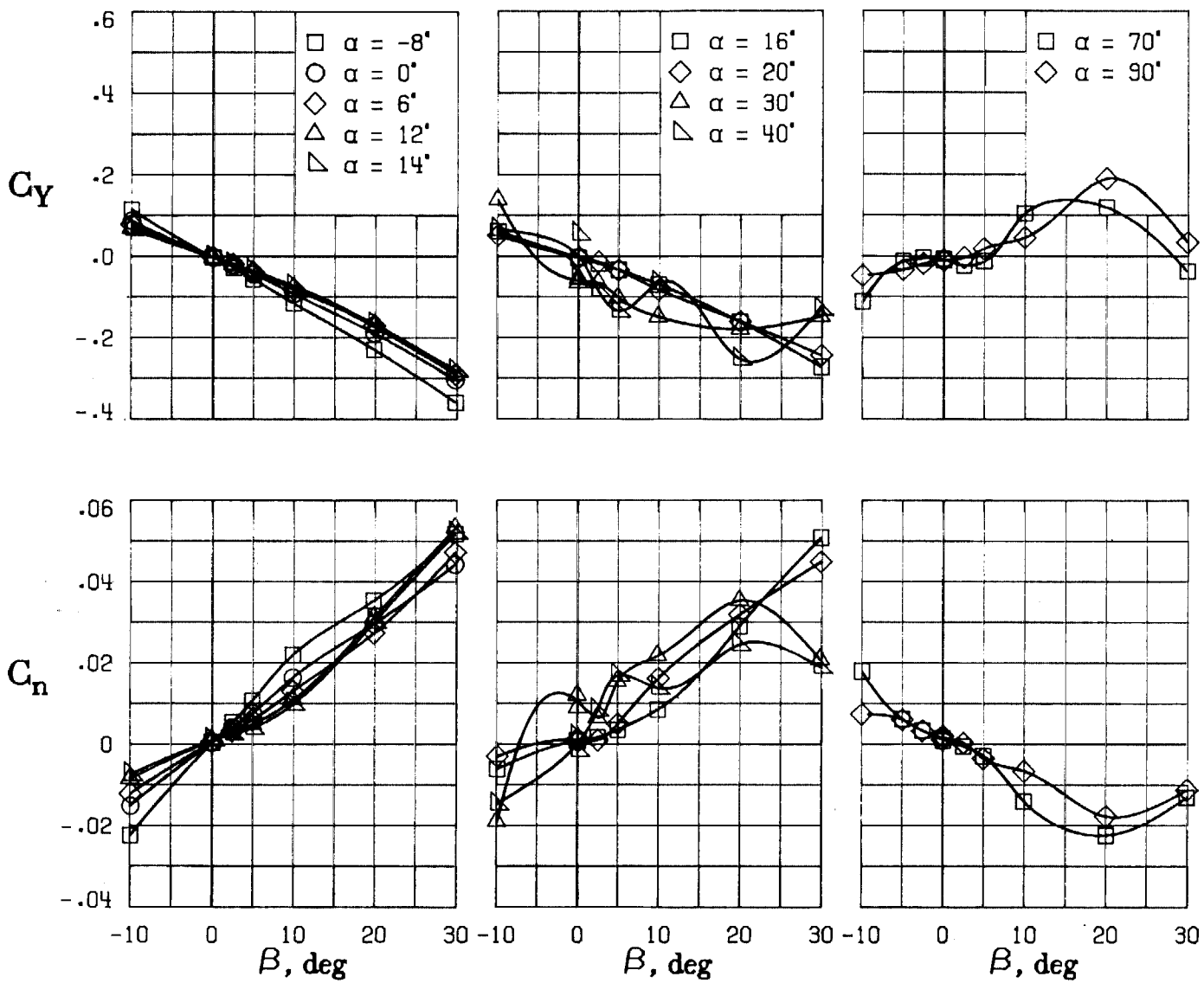

(E) DIRECTIONAL - STABILITY CHARACTERISTICS ABOUT BODY AXES AT VARIOUS ANGLES OF ATTACK.

FIGURE 38. - CONTINUED.

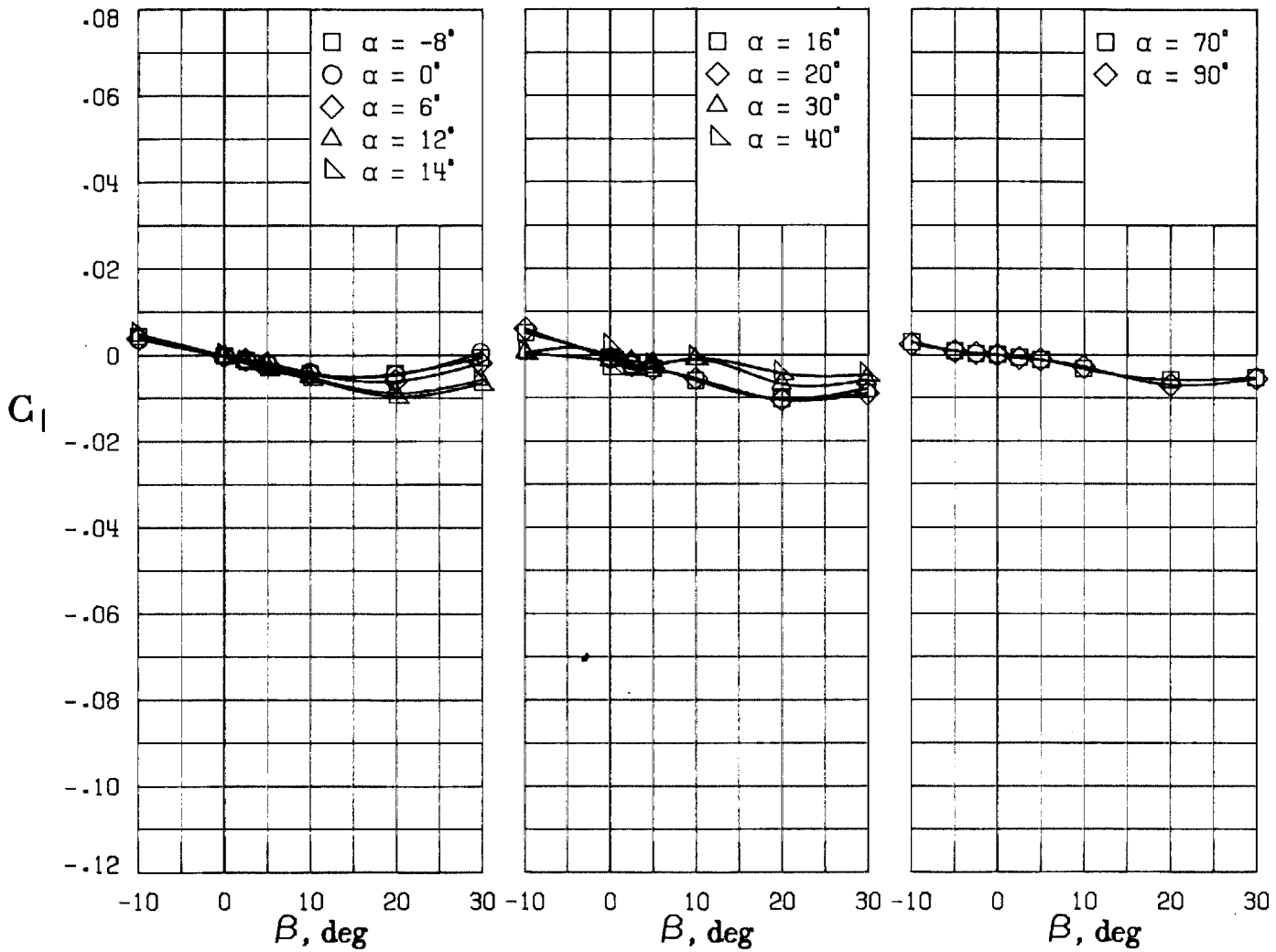

(F) LATERAL - STABILITY CHARACTERISTICS ABOUT BODY AXES AT VARIOUS ANGLES OF ATTACK.

FIGURE 38. - CONCLUDED.

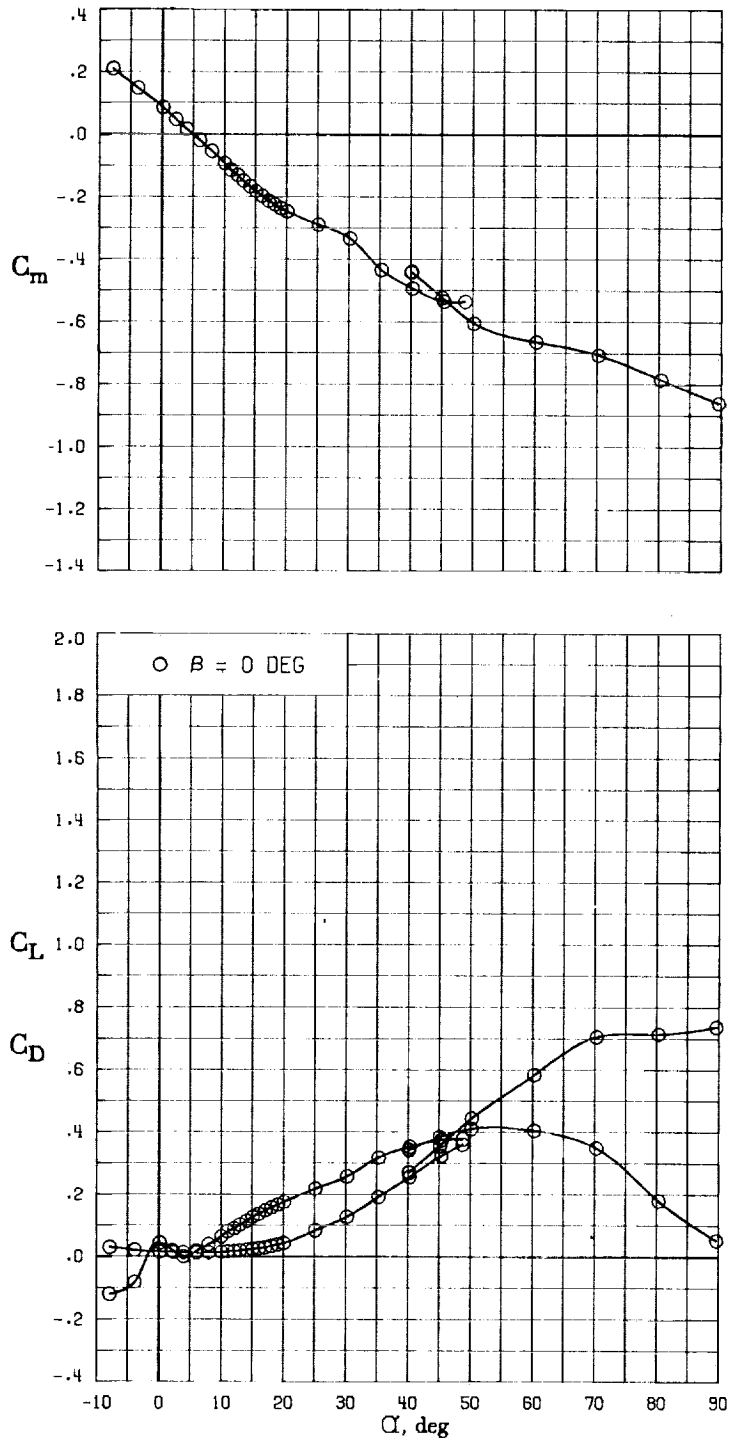

(A) LONGITUDINAL FORCE AND MOMENT COEFFICIENTS ABOUT STABILITY AXES.

FIGURE 39. - EFFECT OF ANGLE OF ATTACK AND SIDESLIP ANGLE ON AERODYNAMIC CHARACTERISTICS AT RE = 3.45 E+06 FOR CONFIGURATION B H6 V. $\delta_E = 0°$, $\delta_A = 0°$, $\delta_R = 0°$.

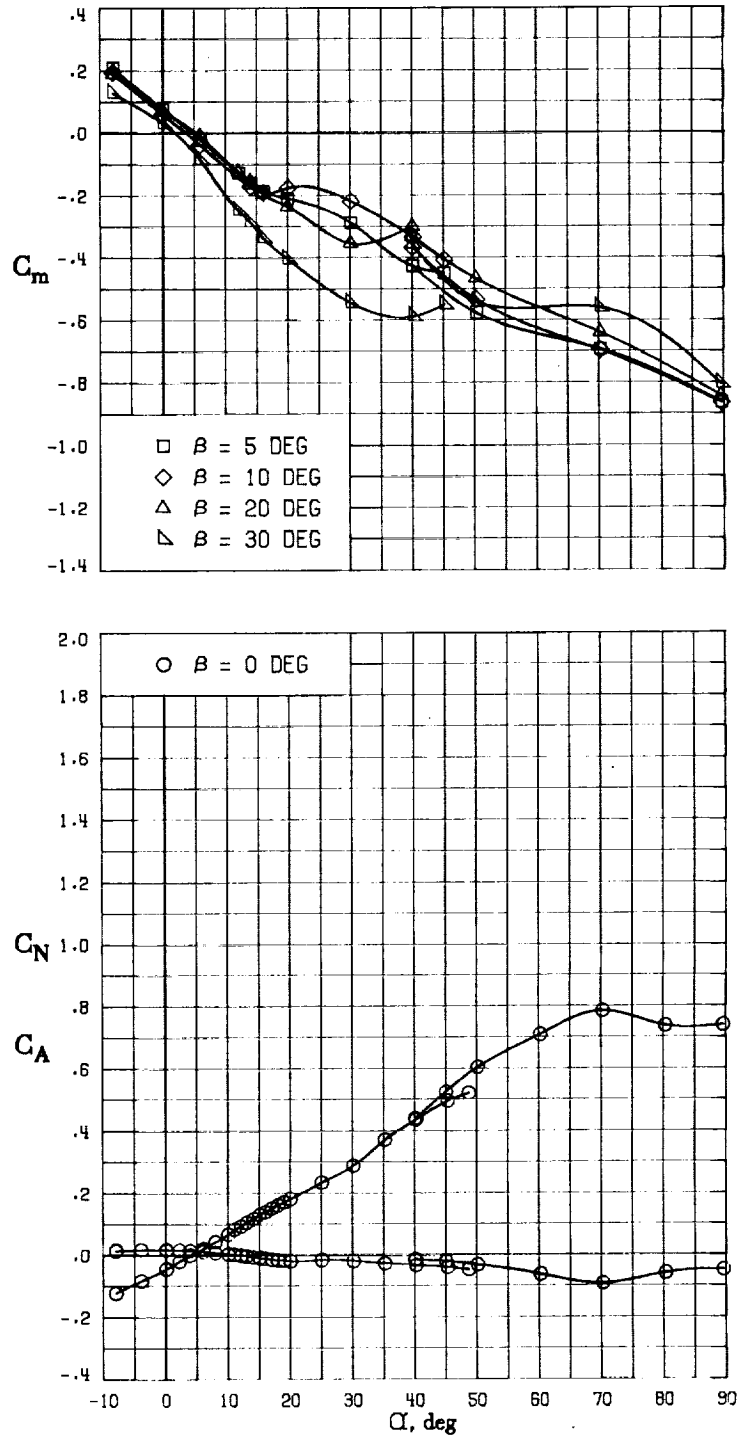

(B) LONGITUDINAL FORCE AND MOMENT COEFFICIENTS ABOUT BODY AXES.

FIGURE 39. - CONTINUED.

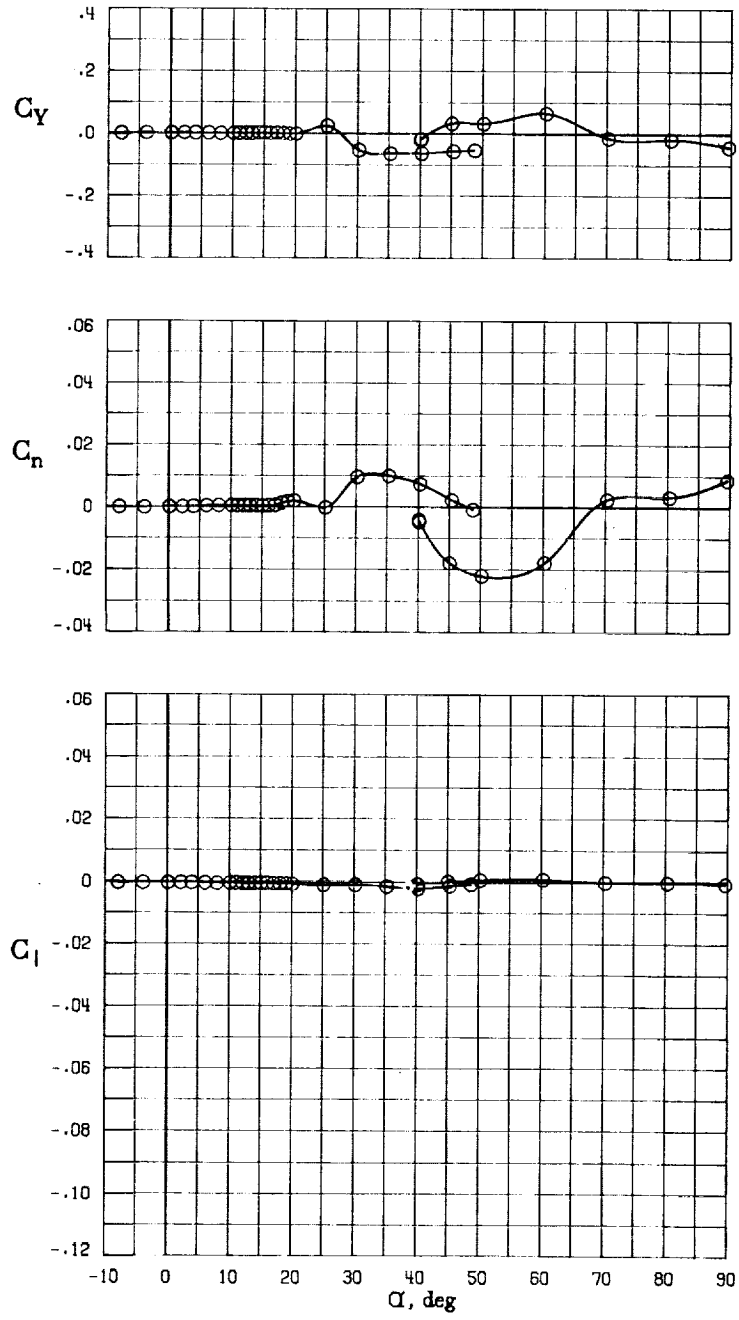

C) LATERAL - DIRECTIONAL FORCE AND MOMENT COEFFICIENTS ABOUT BODY AXES AT ZERO SIDESLIP.

FIGURE 39. - CONTINUED.

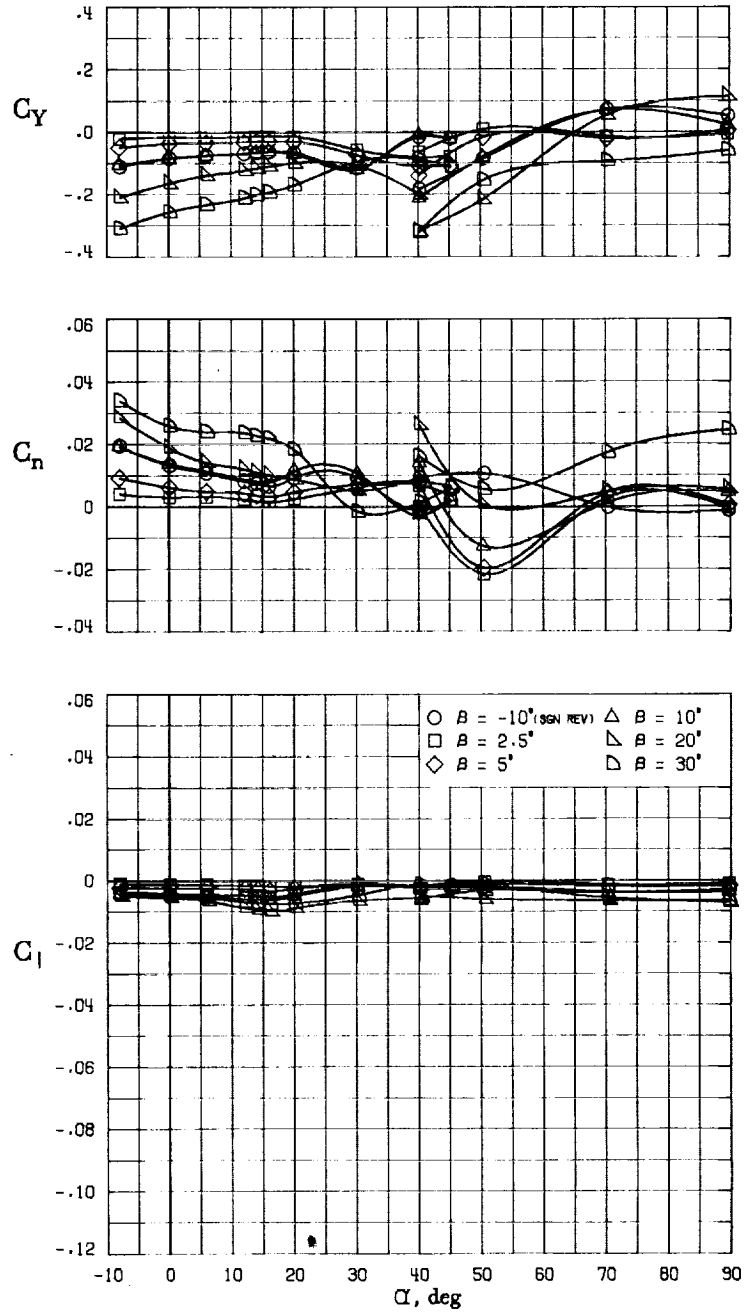

(D) LATERAL - DIRECTIONAL FORCE AND MOMENT COEFFICIENTS ABOUT BODY AXES.

FIGURE 39. - CONTINUED.

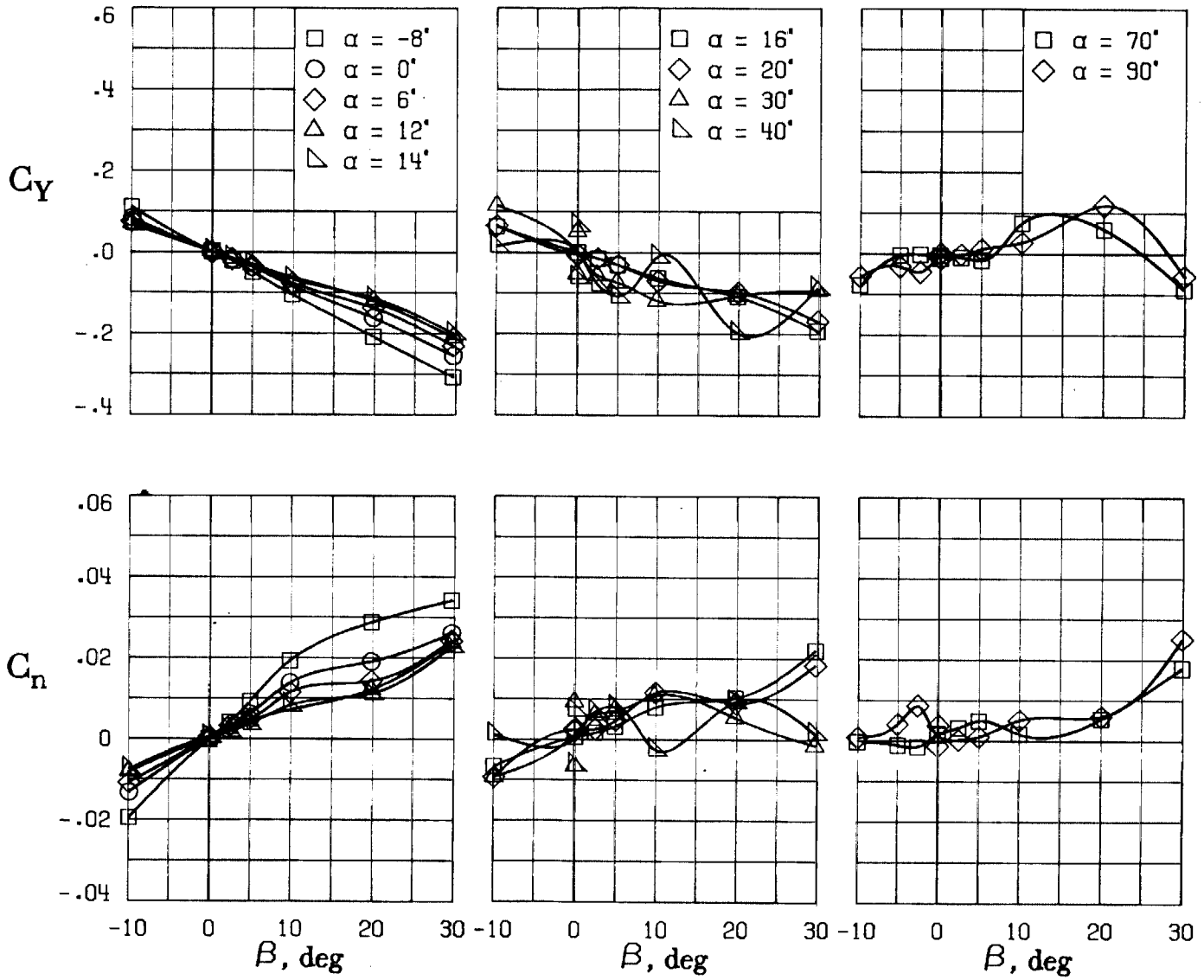

(E) DIRECTIONAL - STABILITY CHARACTERISTICS ABOUT BODY AXES AT VARIOUS ANGLES OF ATTACK.

FIGURE 39. - CONTINUED.

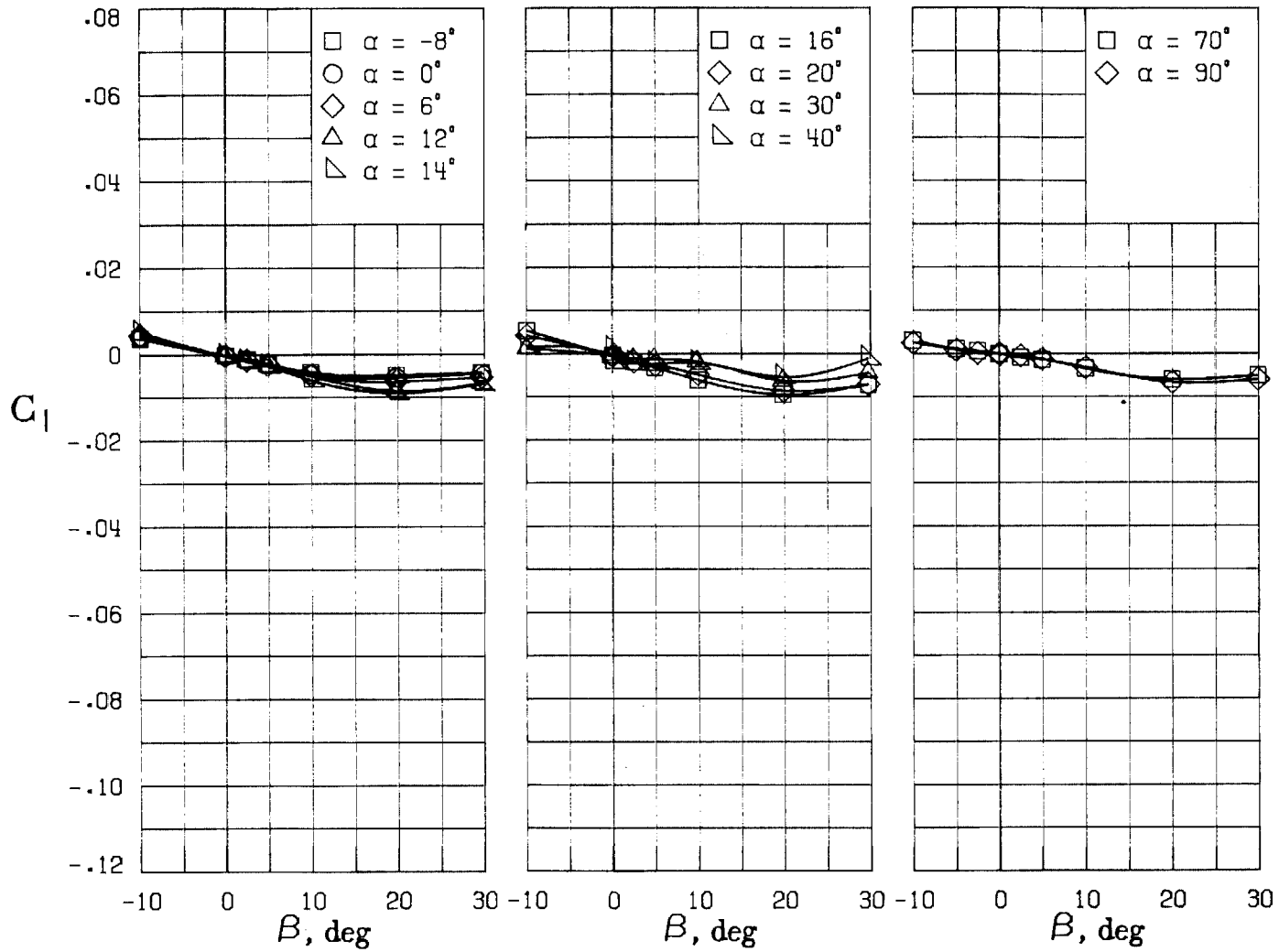

(F) LATERAL - STABILITY CHARACTERISTICS ABOUT BODY AXES AT VARIOUS ANGLES OF ATTACK.

FIGURE 39. - CONCLUDED.

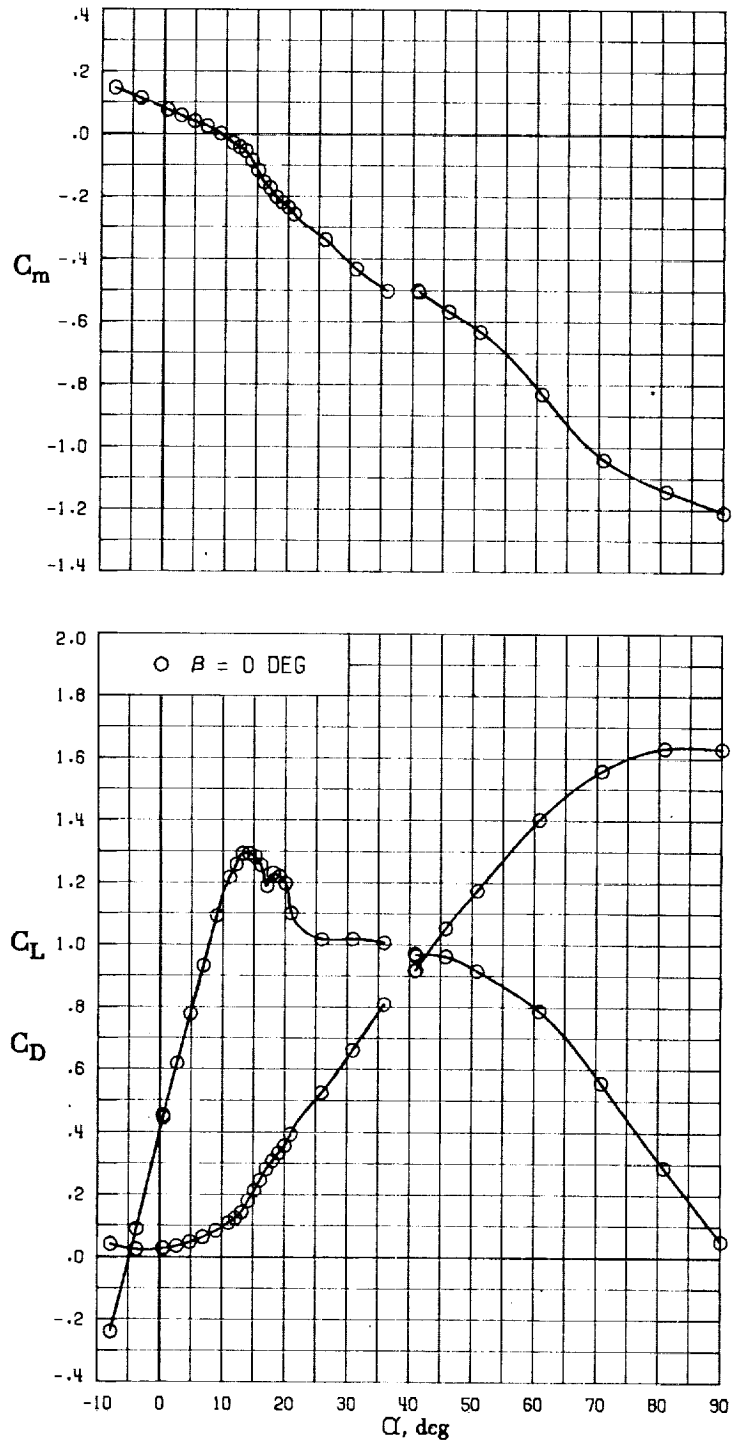

(A) LONGITUDINAL FORCE AND MOMENT COEFFICIENTS ABOUT STABILITY AXES.

FIGURE 40. - EFFECT OF ANGLE OF ATTACK AND SIDESLIP ANGLE ON AERODYNAMIC CHARACTERISTICS AT RE = 3.45 E+06 FOR CONFIGURATION B W1 H3. δ_E = 0°, δ_A = 0°, δ_R = 0°.

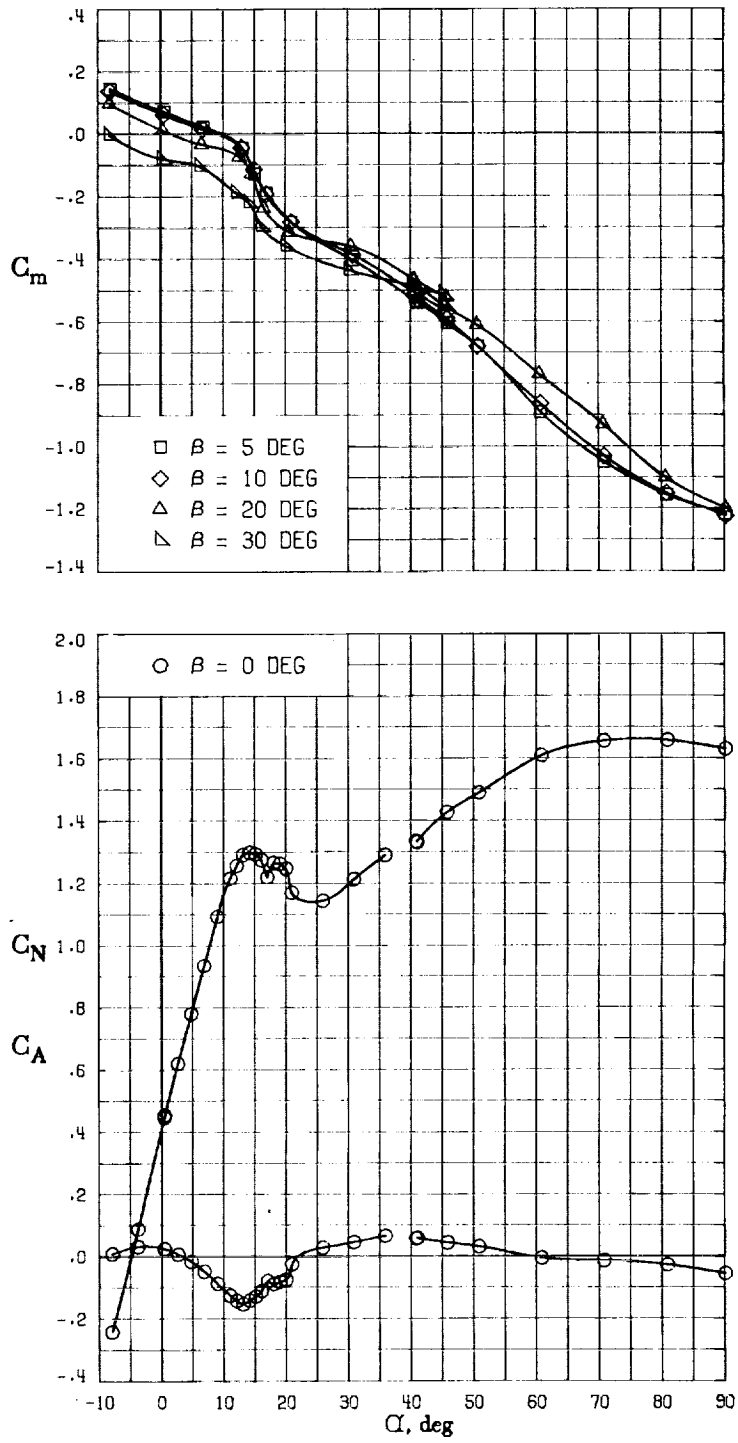

(B) LONGITUDINAL FORCE AND MOMENT COEFFICIENTS ABOUT BODY AXES.

FIGURE 40. - CONTINUED.

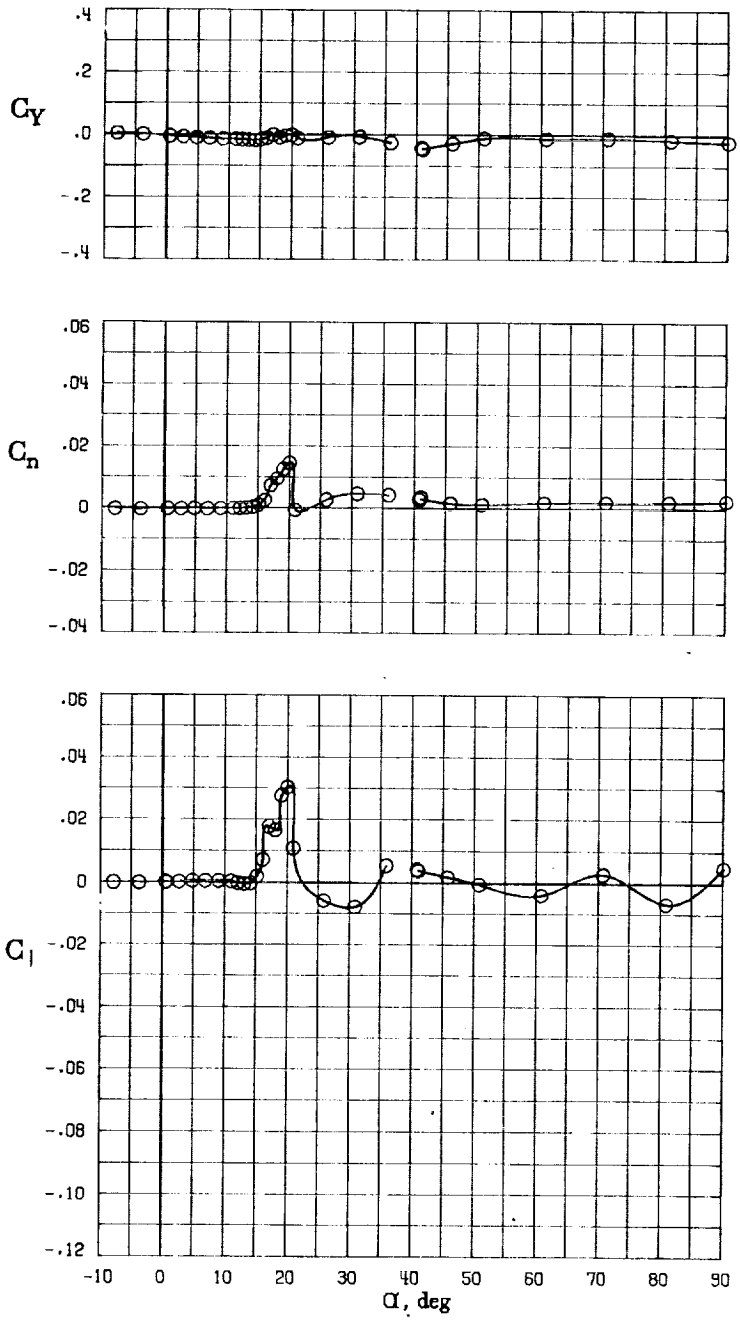

(C) LATERAL - DIRECTIONAL FORCE AND MOMENT COEFFICIENTS ABOUT BODY AXES AT ZERO SIDESLIP.

FIGURE 40. - CONTINUED.

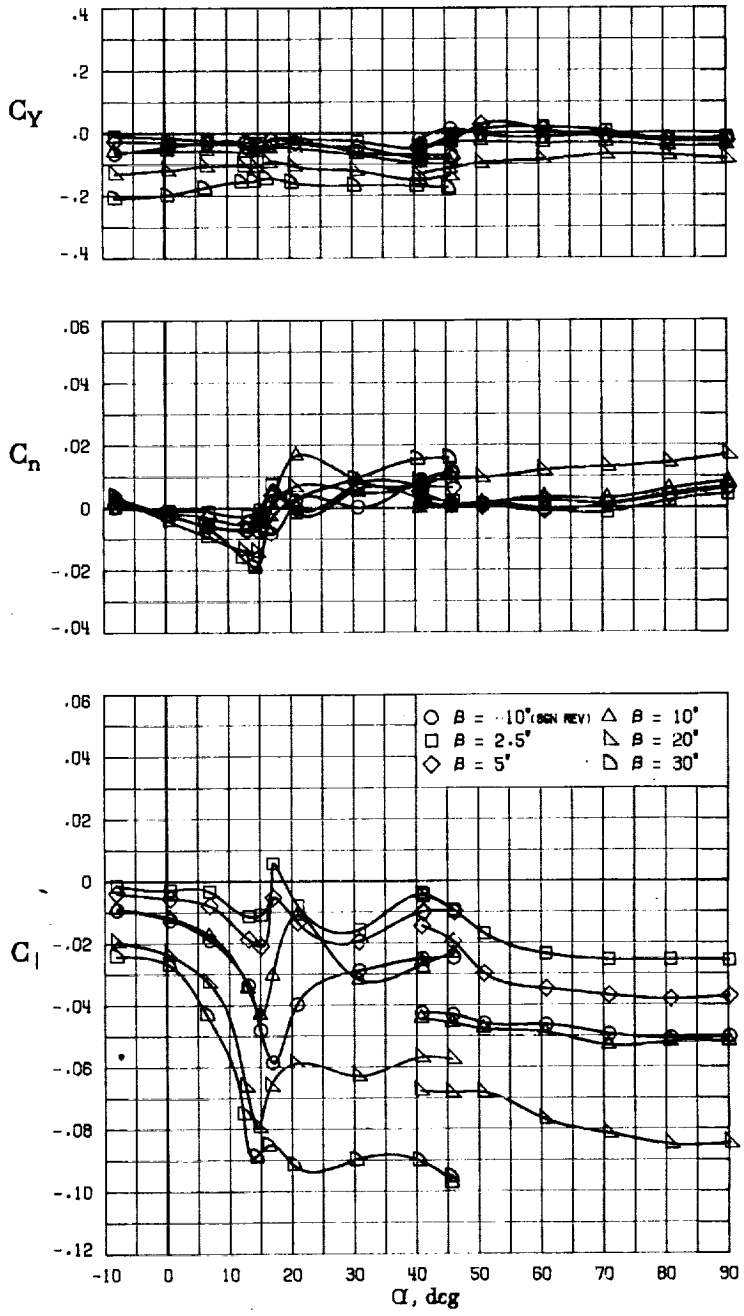

(D) LATERAL - DIRECTIONAL FORCE AND MOMENT COEFFICIENTS ABOUT BODY AXES.

FIGURE 40. - CONTINUED.

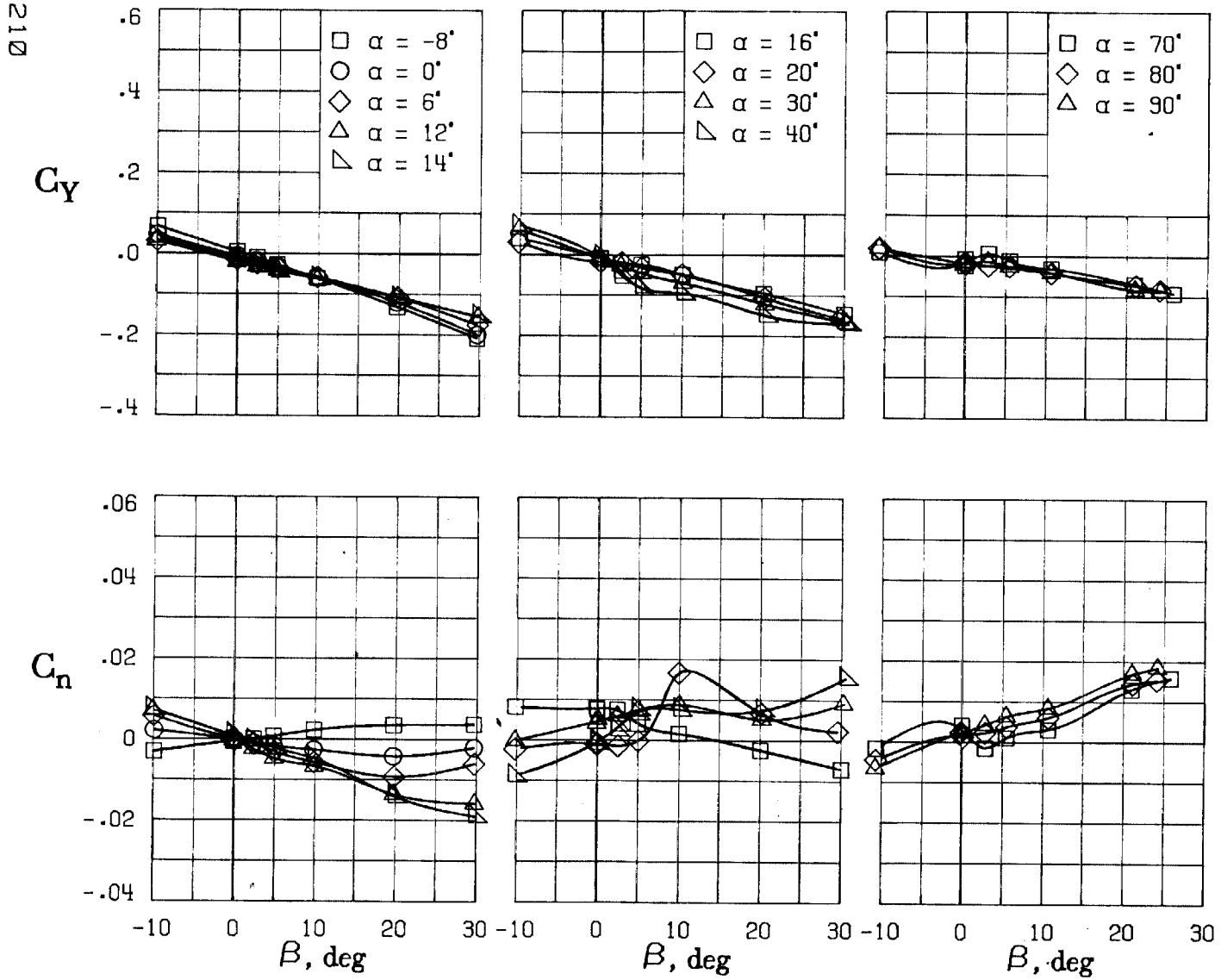

(E) DIRECTIONAL - STABILITY CHARACTERISTICS ABOUT BODY AXES AT VARIOUS ANGLES OF ATTACK.

FIGURE 40. - CONTINUED.

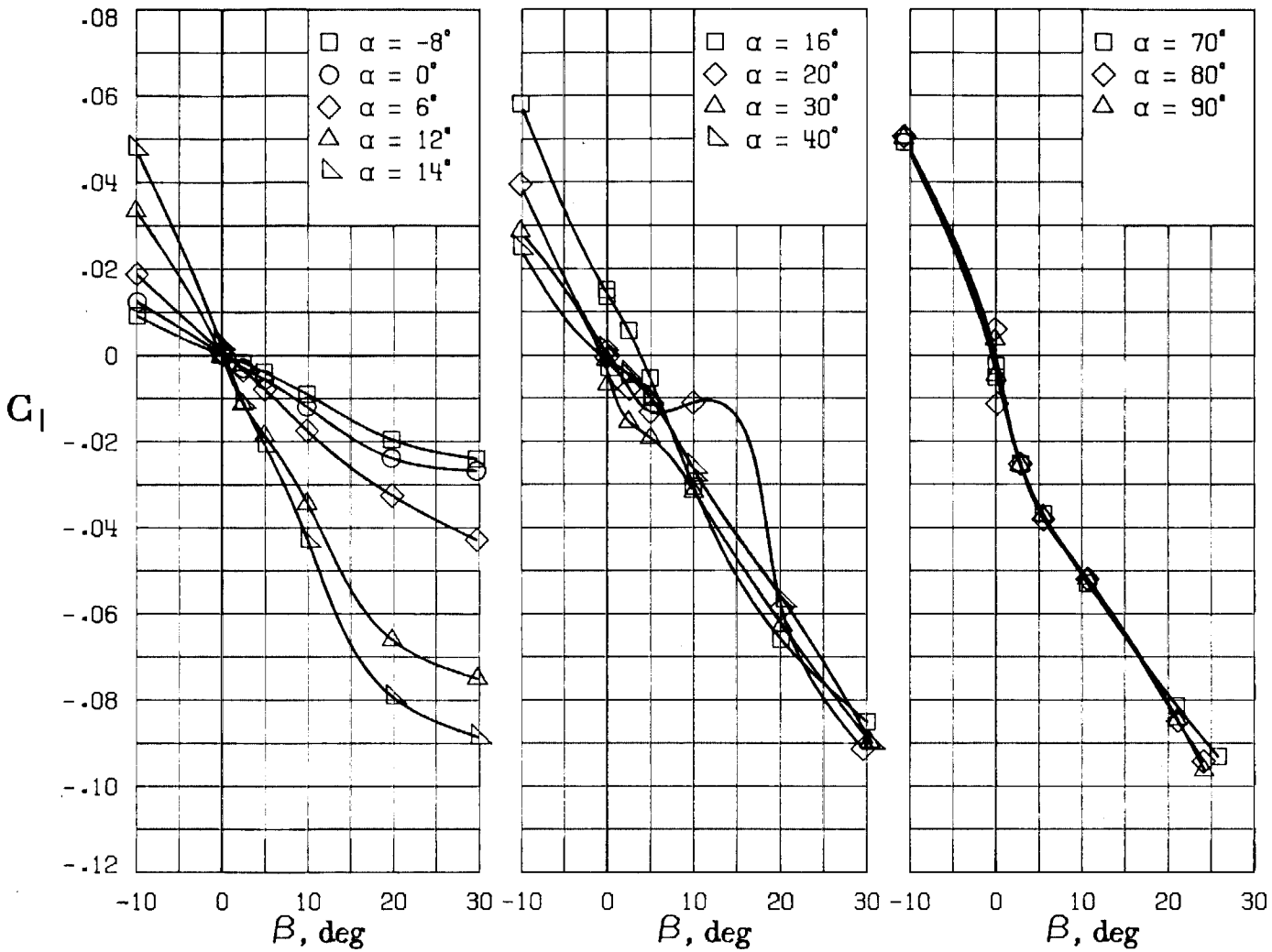

(F) LATERAL - STABILITY CHARACTERISTICS ABOUT BODY AXES AT VARIOUS ANGLES OF ATTACK.

FIGURE 40. - CONCLUDED.

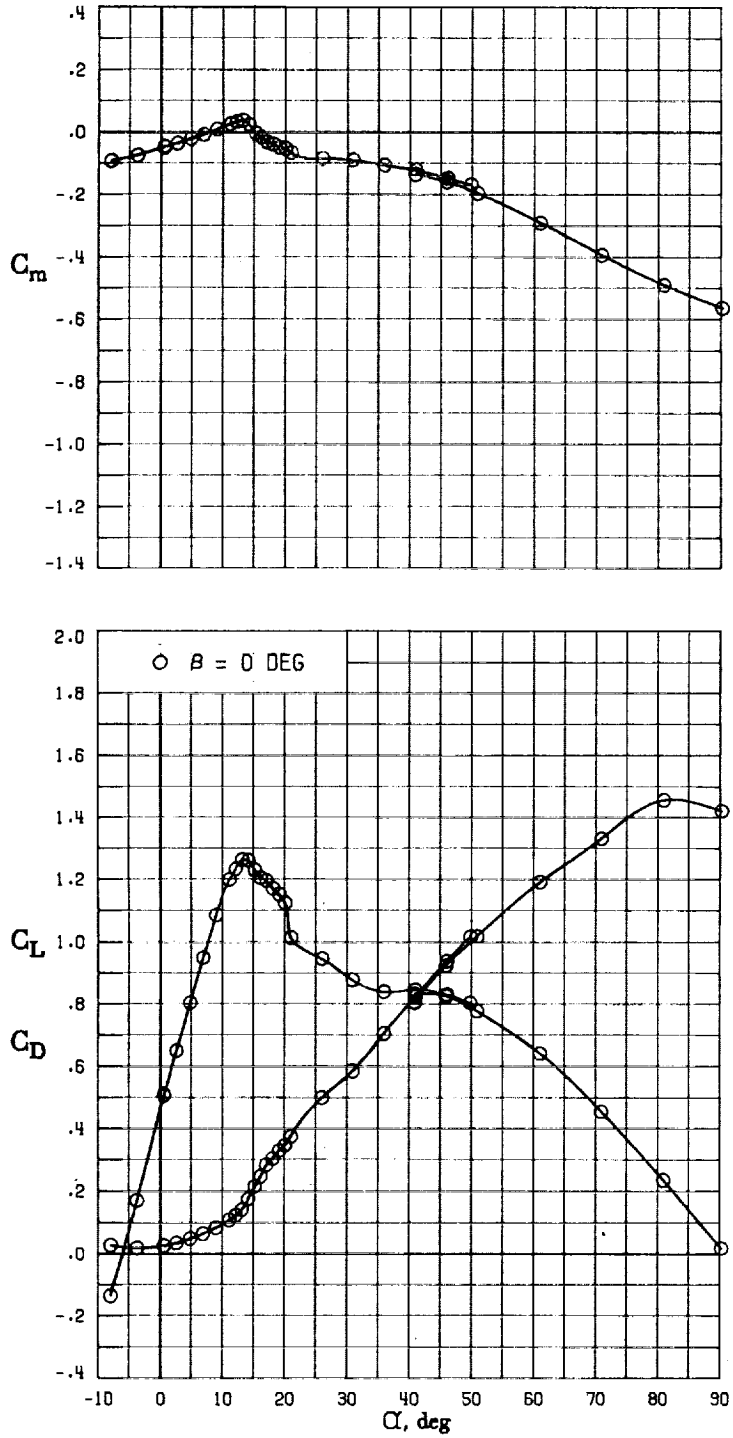

(A) LONGITUDINAL FORCE AND MOMENT COEFFICIENTS ABOUT STABILITY AXES.

FIGURE 41. - EFFECT OF ANGLE OF ATTACK AND SIDESLIP ANGLE ON AERODYNAMIC CHARACTERISTICS AT RE = 3.45 E+06 FOR CONFIGURATION B W1 V. δ_E = 0°, δ_A = 0°, δ_R = 0°.

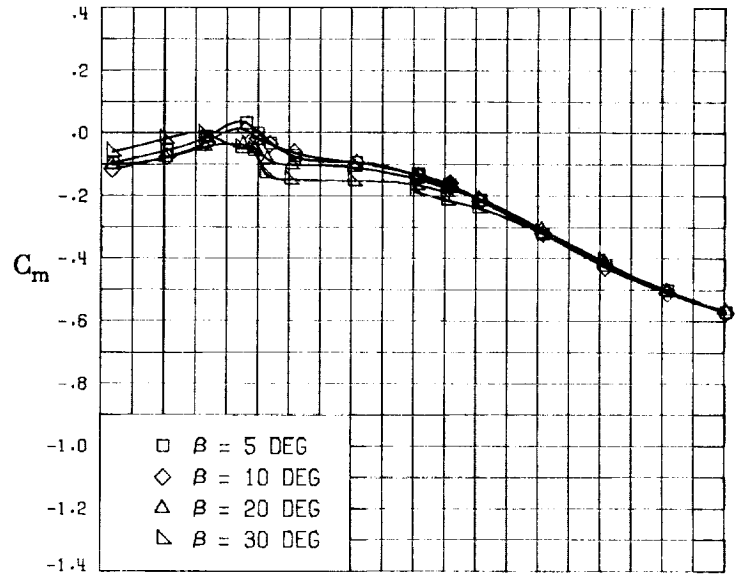

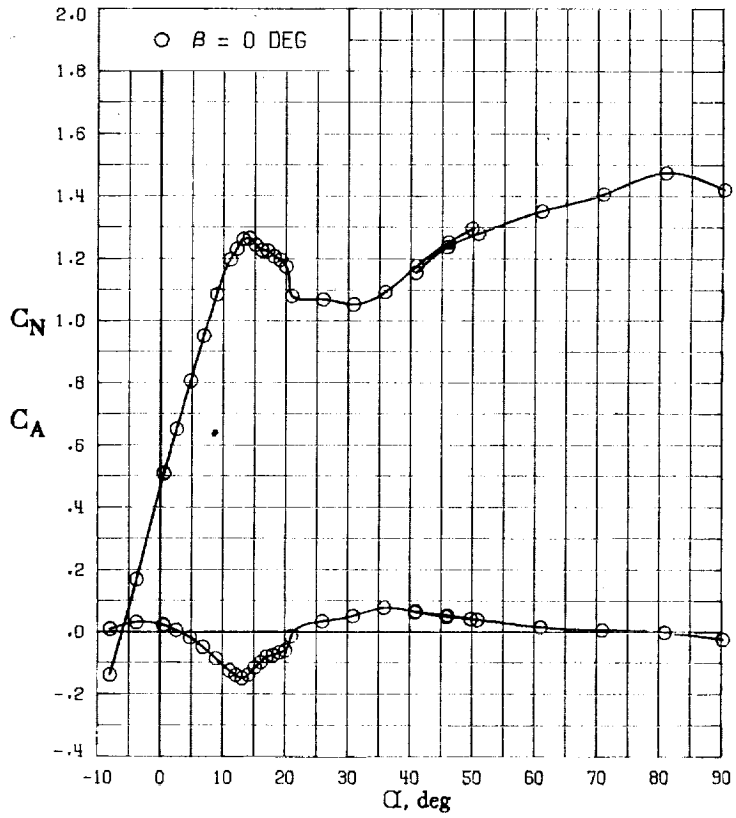

(B) LONGITUDINAL FORCE AND MOMENT COEFFICIENTS ABOUT BODY AXES.

FIGURE 41. - CONTINUED.

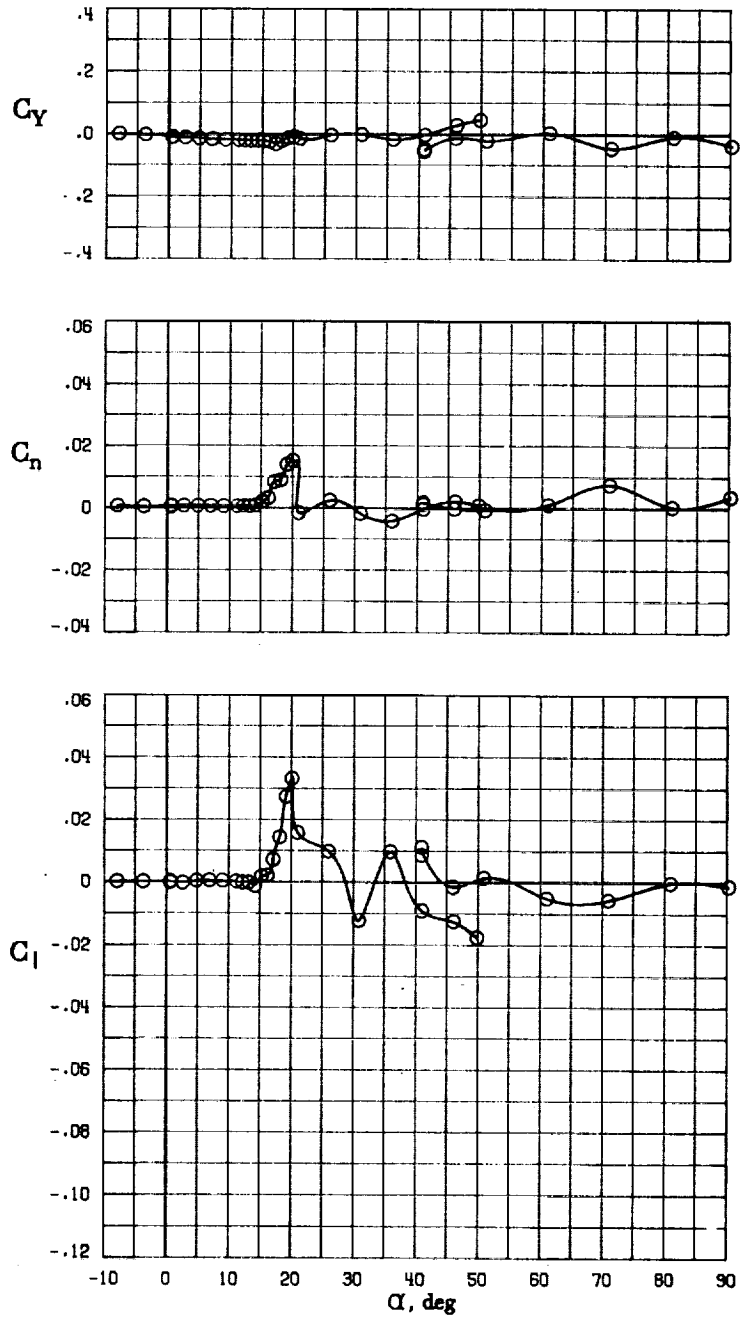

(C) LATERAL - DIRECTIONAL FORCE AND MOMENT COEFFICIENTS ABOUT BODY AXES AT ZERO SIDESLIP.

FIGURE 41. - CONTINUED.

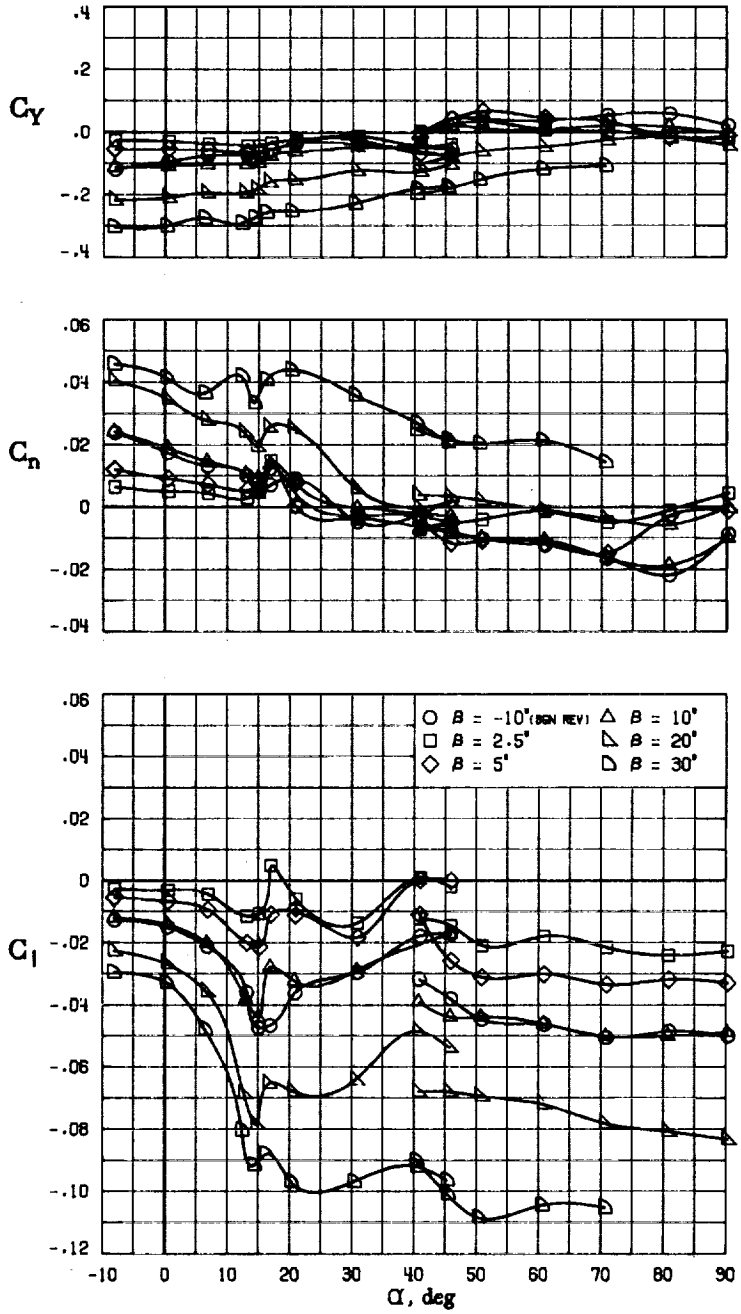

(D) LATERAL - DIRECTIONAL FORCE AND MOMENT COEFFICIENTS ABOUT BODY AXES.

FIGURE 41. - CONTINUED.

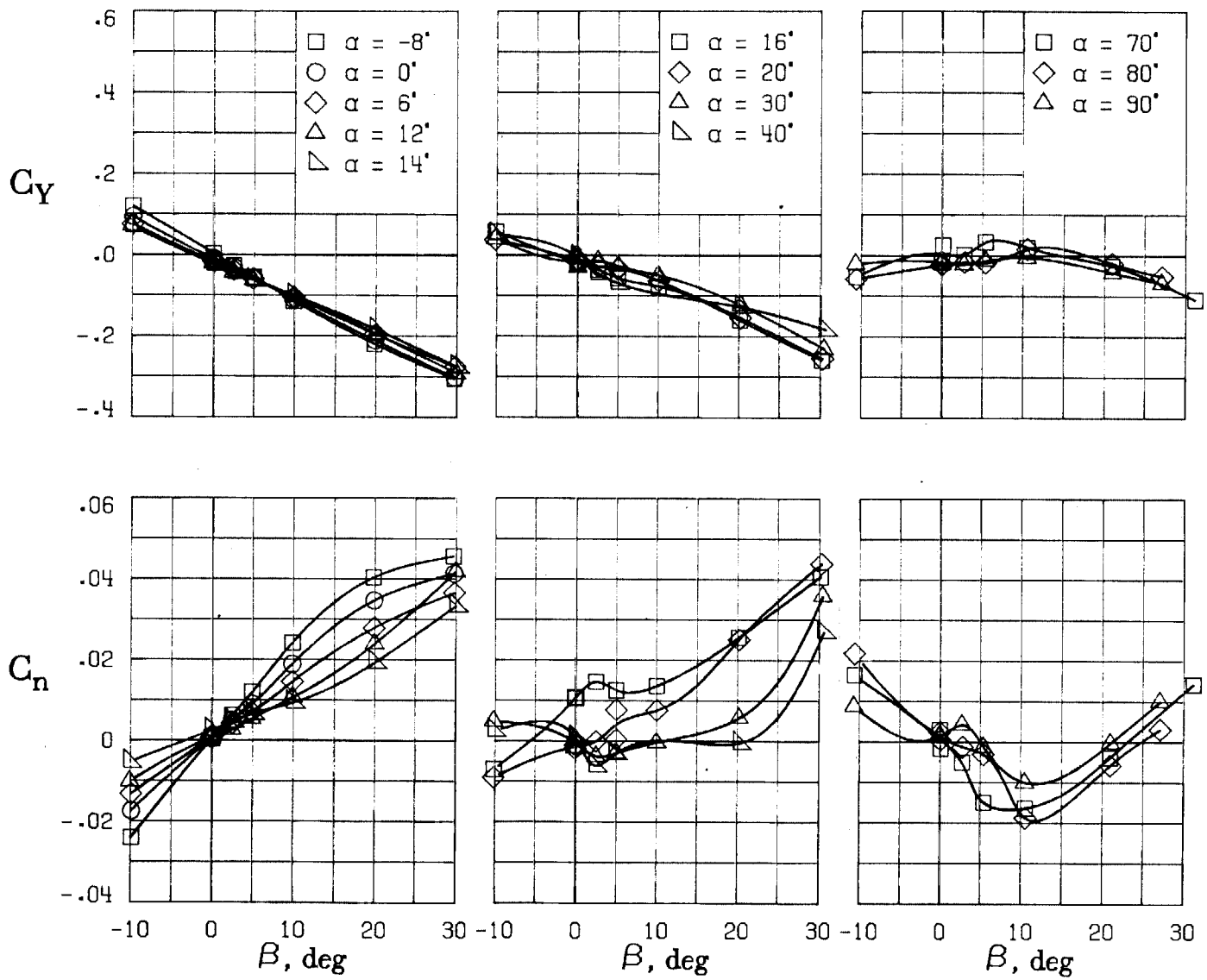

(E) DIRECTIONAL - STABILITY CHARACTERISTICS ABOUT BODY AXES AT VARIOUS ANGLES OF ATTACK.

FIGURE 41. - CONTINUED.

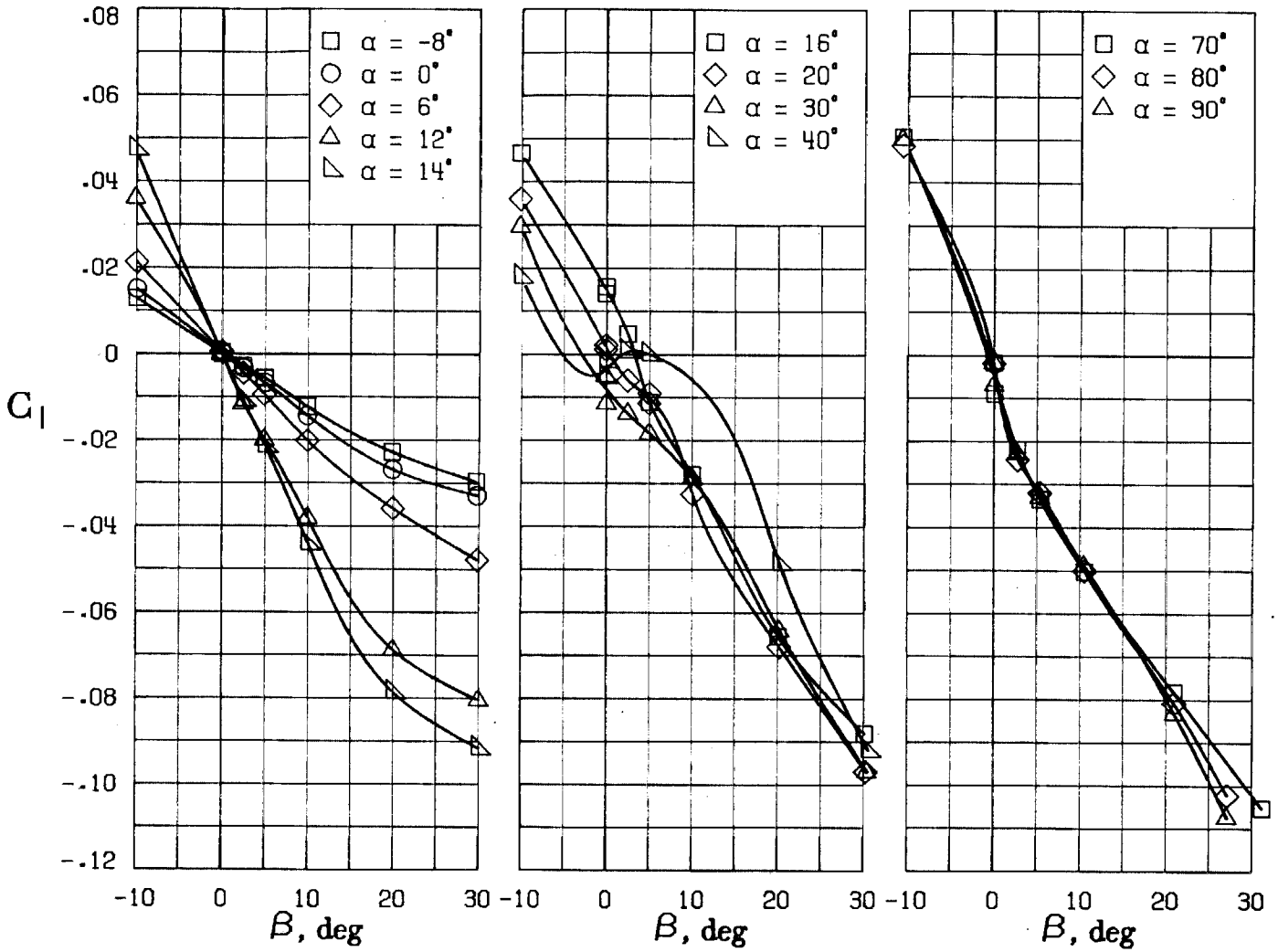

(F) LATERAL - STABILITY CHARACTERISTICS ABOUT BODY AXES AT VARIOUS ANGLES OF ATTACK.

FIGURE 41. - CONCLUDED.

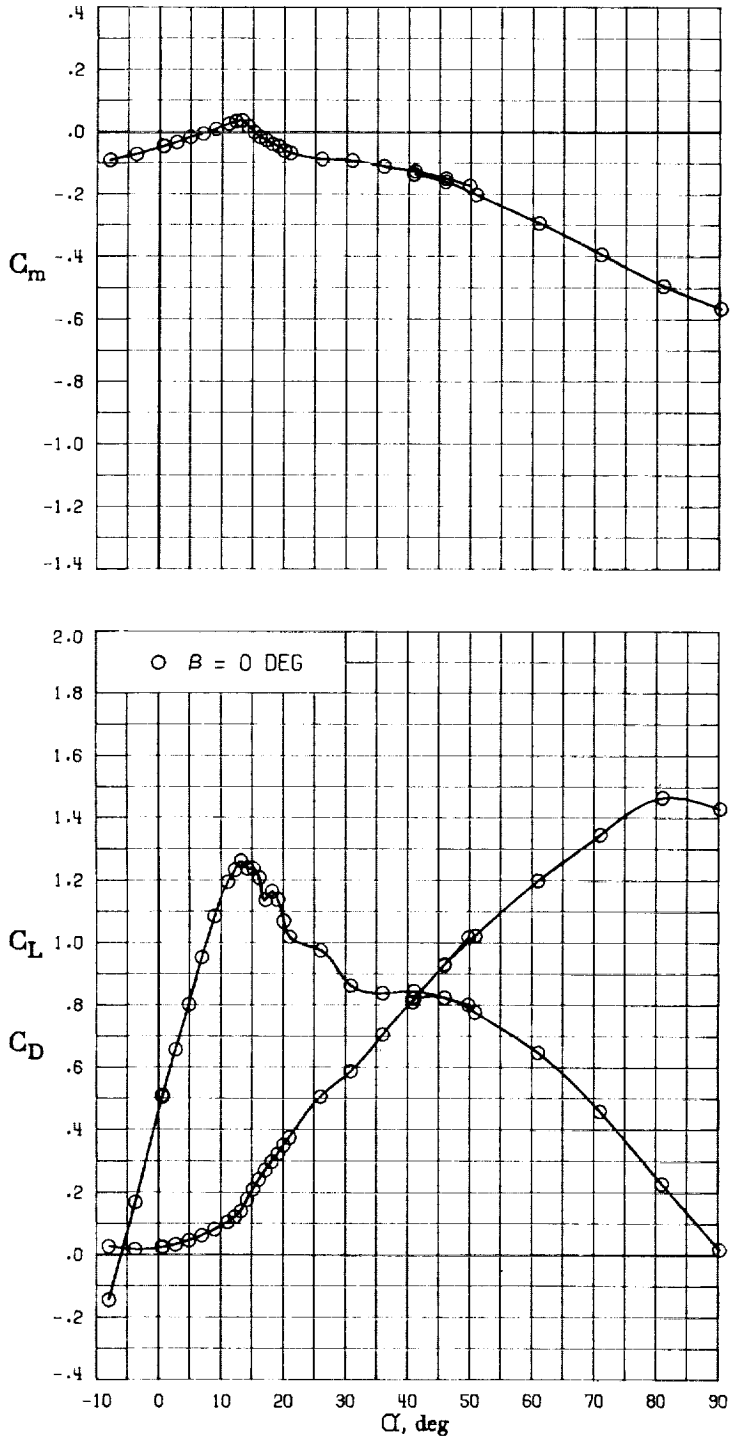

(A) LONGITUDINAL FORCE AND MOMENT COEFFICIENTS ABOUT STABILITY AXES.

FIGURE 42. - EFFECT OF ANGLE OF ATTACK AND SIDESLIP ANGLE ON AERODYNAMIC CHARACTERISTICS AT RE = 3.45 E+06 FOR CONFIGURATION B W1. $\delta_E = 0°$, $\delta_A = 0°$, $\delta_R = 0°$.

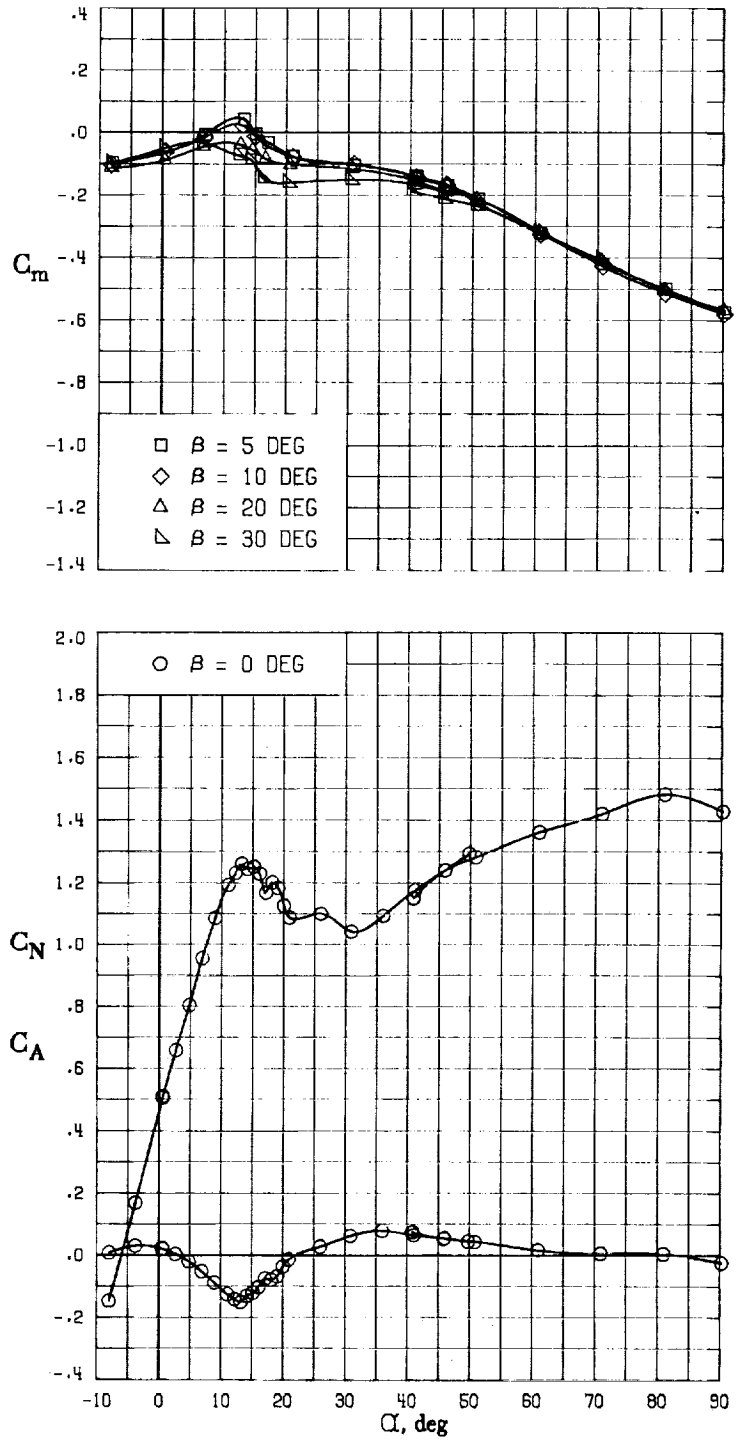

(B) LONGITUDINAL FORCE AND MOMENT COEFFICIENTS ABOUT BODY AXES.

FIGURE 42. - CONTINUED.

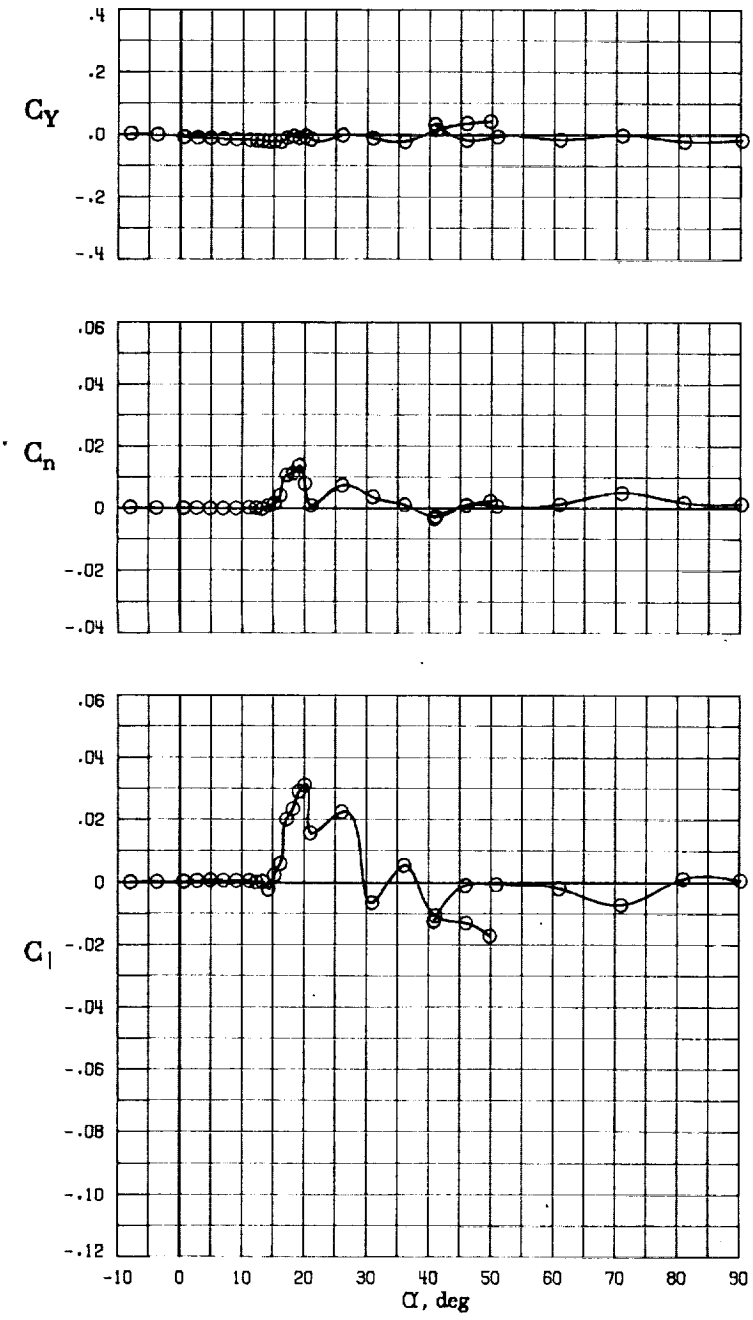

(C) LATERAL - DIRECTIONAL FORCE AND MOMENT COEFFICIENTS ABOUT BODY AXES AT ZERO SIDESLIP.

FIGURE 42. - CONTINUED.

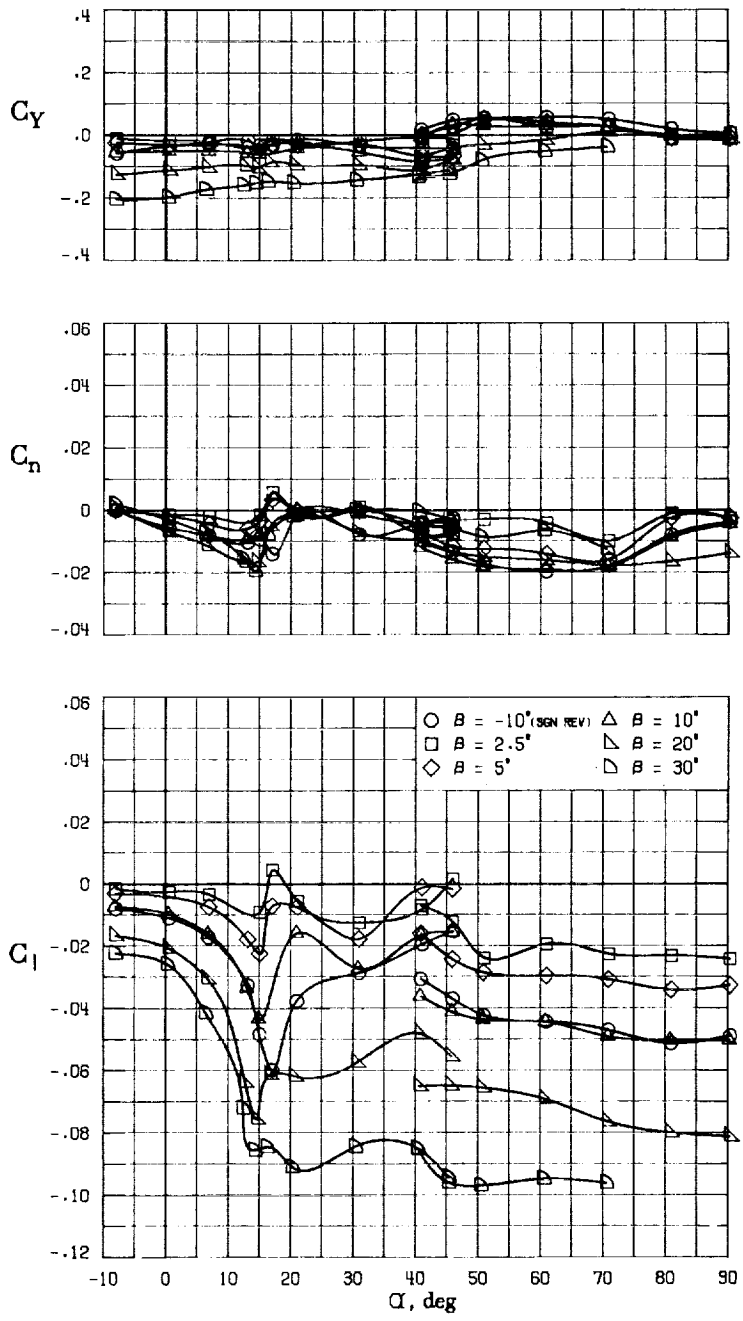

) LATERAL - DIRECTIONAL FORCE AND MOMENT COEFFICIENTS ABOUT BODY AXES.

FIGURE 42. - CONTINUED.

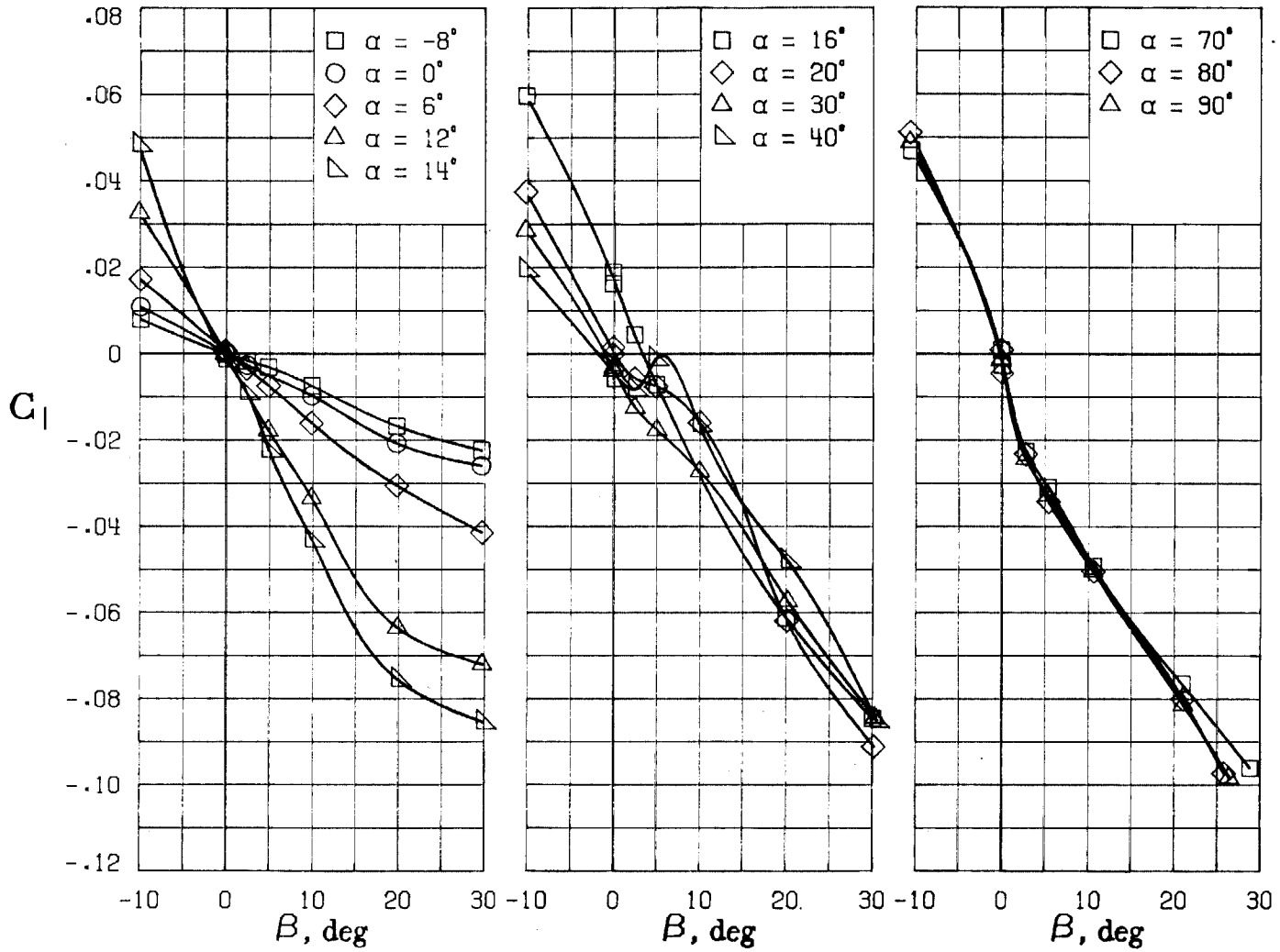

(F) LATERAL - STABILITY CHARACTERISTICS ABOUT BODY AXES AT VARIOUS ANGLES OF ATTACK.

FIGURE 42. - CONCLUDED.

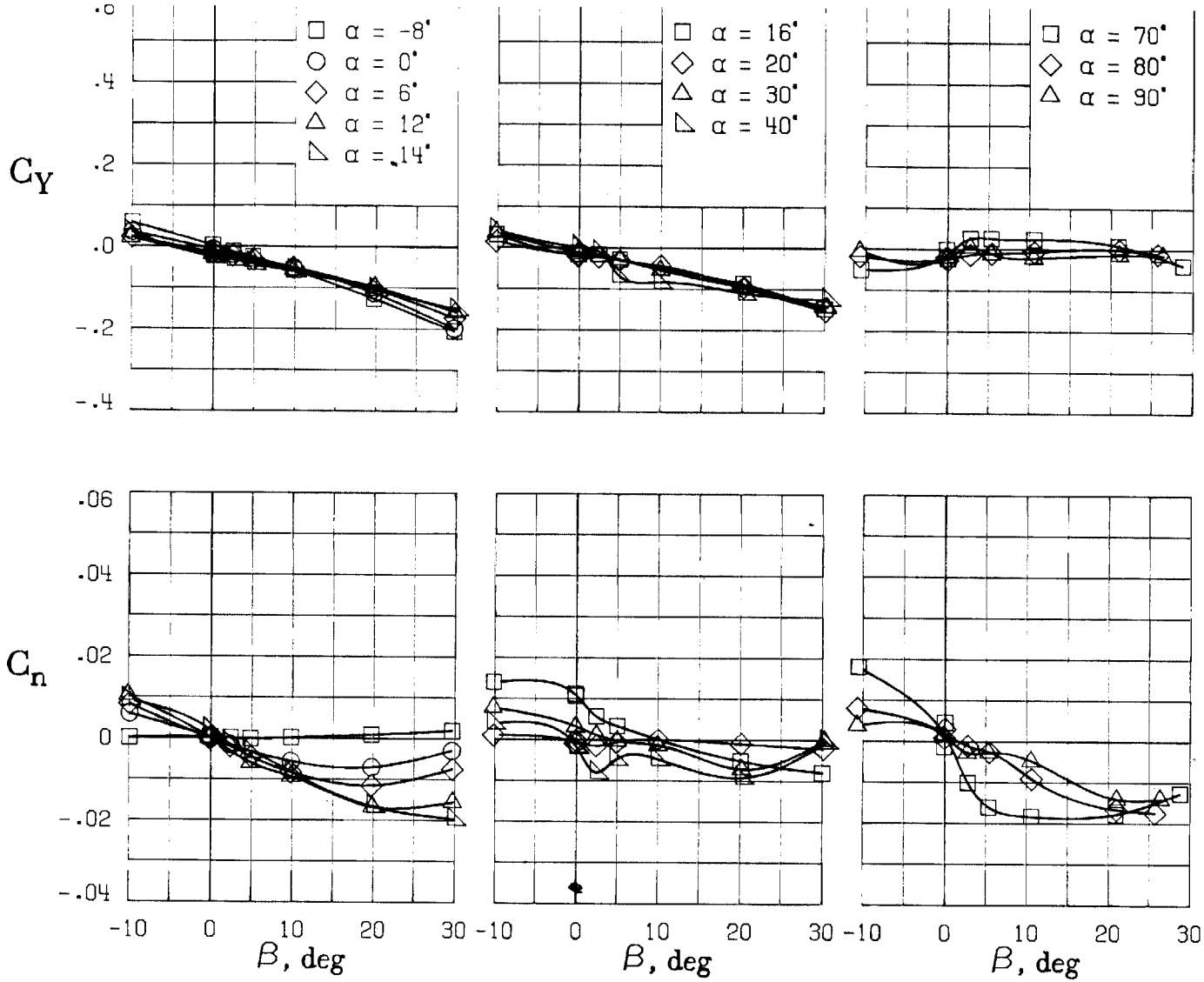

(E) DIRECTIONAL - STABILITY CHARACTERISTICS ABOUT BODY AXES AT VARIOUS ANGLES OF ATTACK.

FIGURE 42. - CONTINUED.

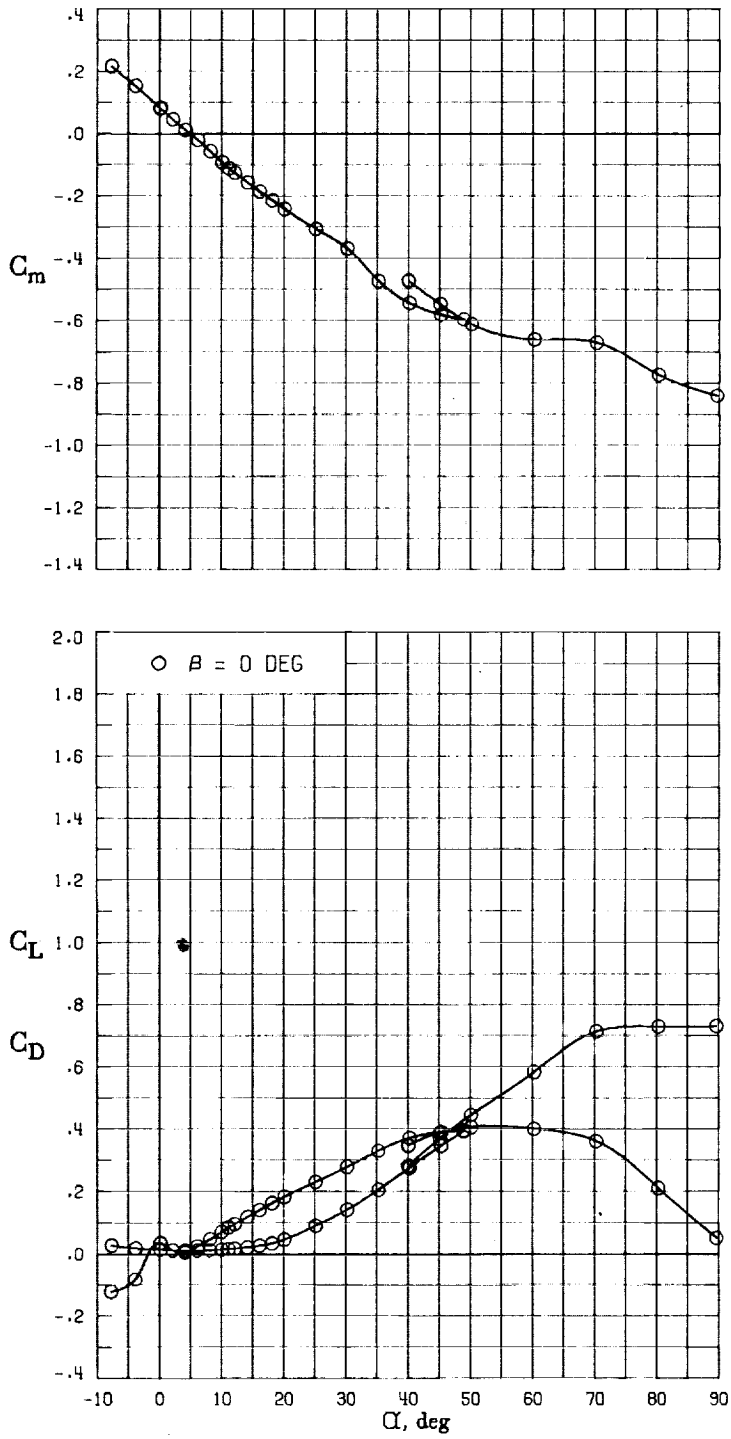

(A) LONGITUDINAL FORCE AND MOMENT COEFFICIENTS ABOUT STABILITY AXES.

FIGURE 43. - EFFECT OF ANGLE OF ATTACK AND SIDESLIP ANGLE ON AERODYNAMIC CHARACTERISTICS AT RE = 3.45 E+06 FOR CONFIGURATION B H3. $\delta_E = 0°$, $\delta_A = 0°$, $\delta_R = 0°$.

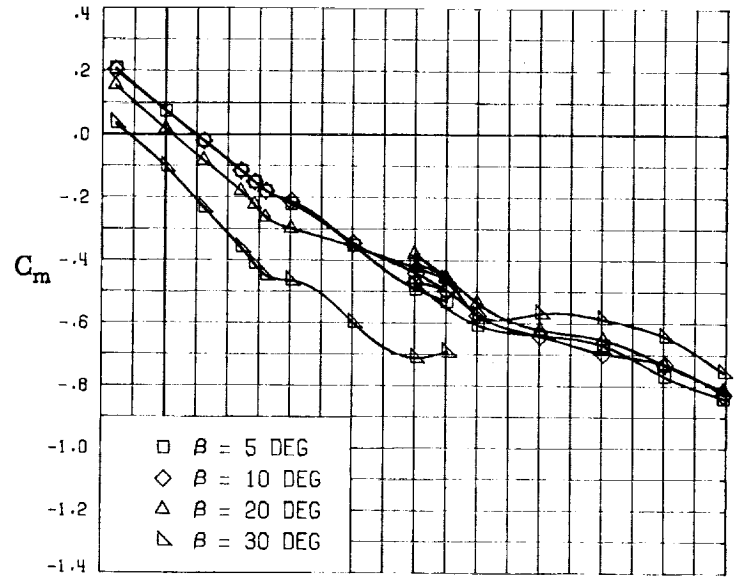

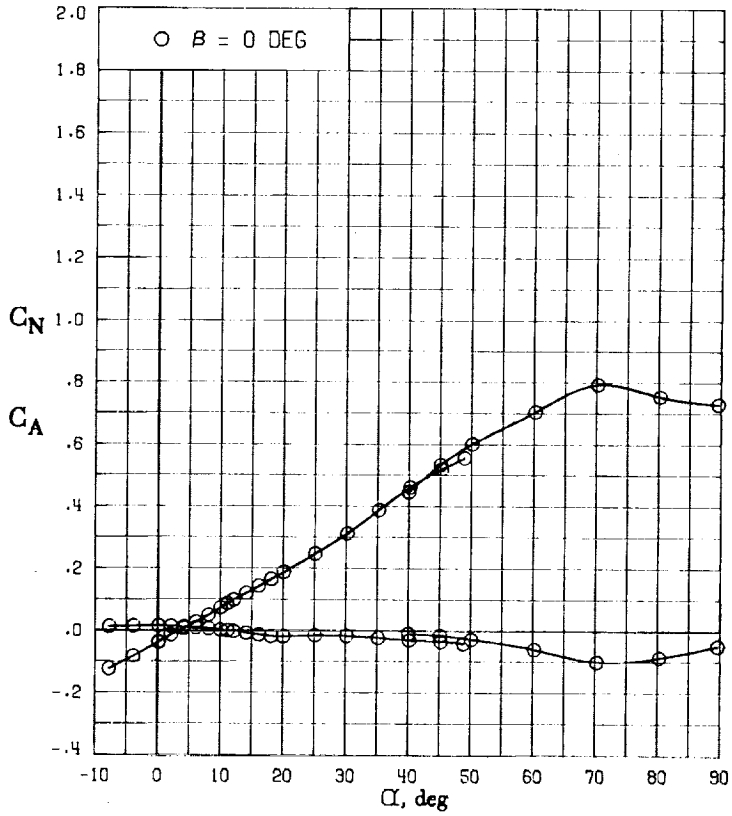

(B) LONGITUDINAL FORCE AND MOMENT COEFFICIENTS ABOUT BODY AXES.

FIGURE 43. - CONTINUED.

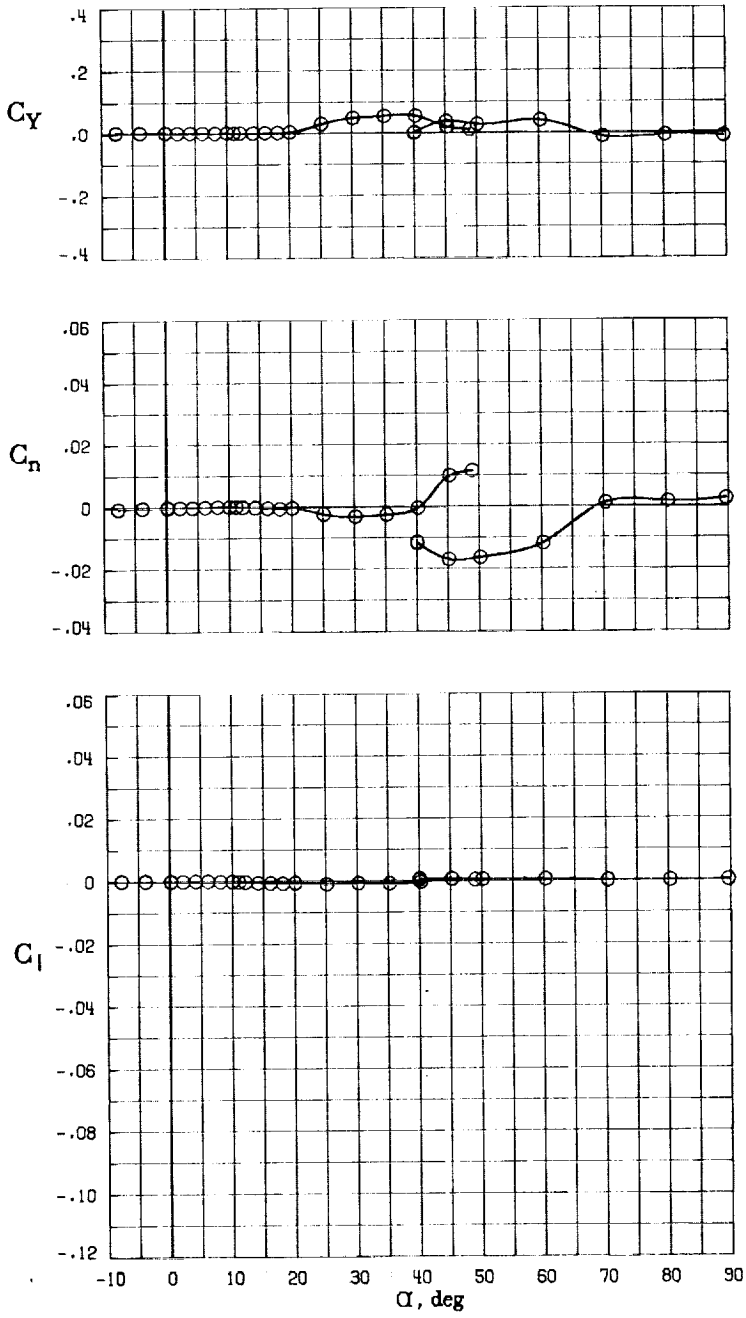

(C) LATERAL - DIRECTIONAL FORCE AND MOMENT COEFFICIENTS ABOUT BODY AXES AT ZERO SIDESLIP.

FIGURE 43. - CONTINUED.

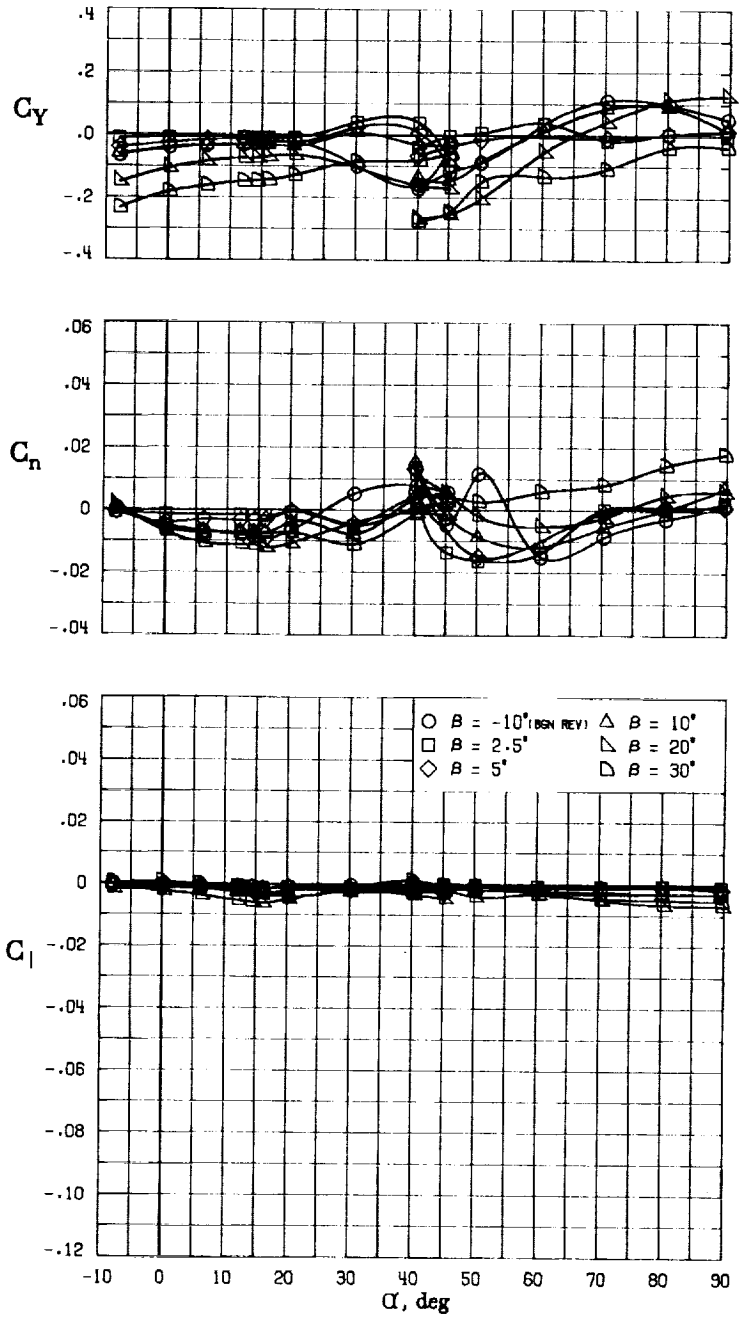

(D) LATERAL - DIRECTIONAL FORCE AND MOMENT COEFFICIENTS ABOUT BODY AXES.

FIGURE 43. - CONTINUED.

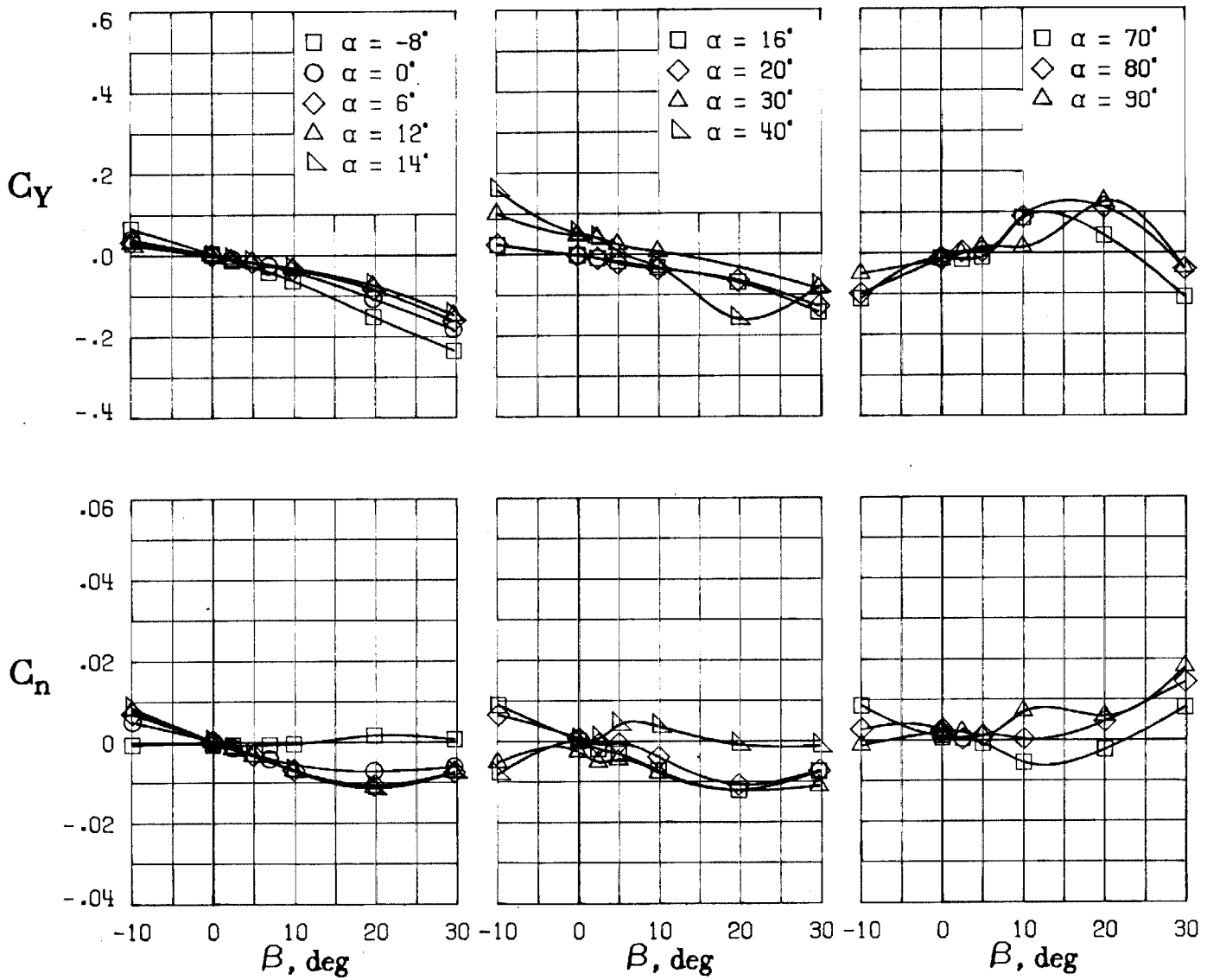

(E) DIRECTIONAL - STABILITY CHARACTERISTICS ABOUT BODY AXES AT VARIOUS ANGLES OF ATTACK.

FIGURE 43. - CONTINUED.

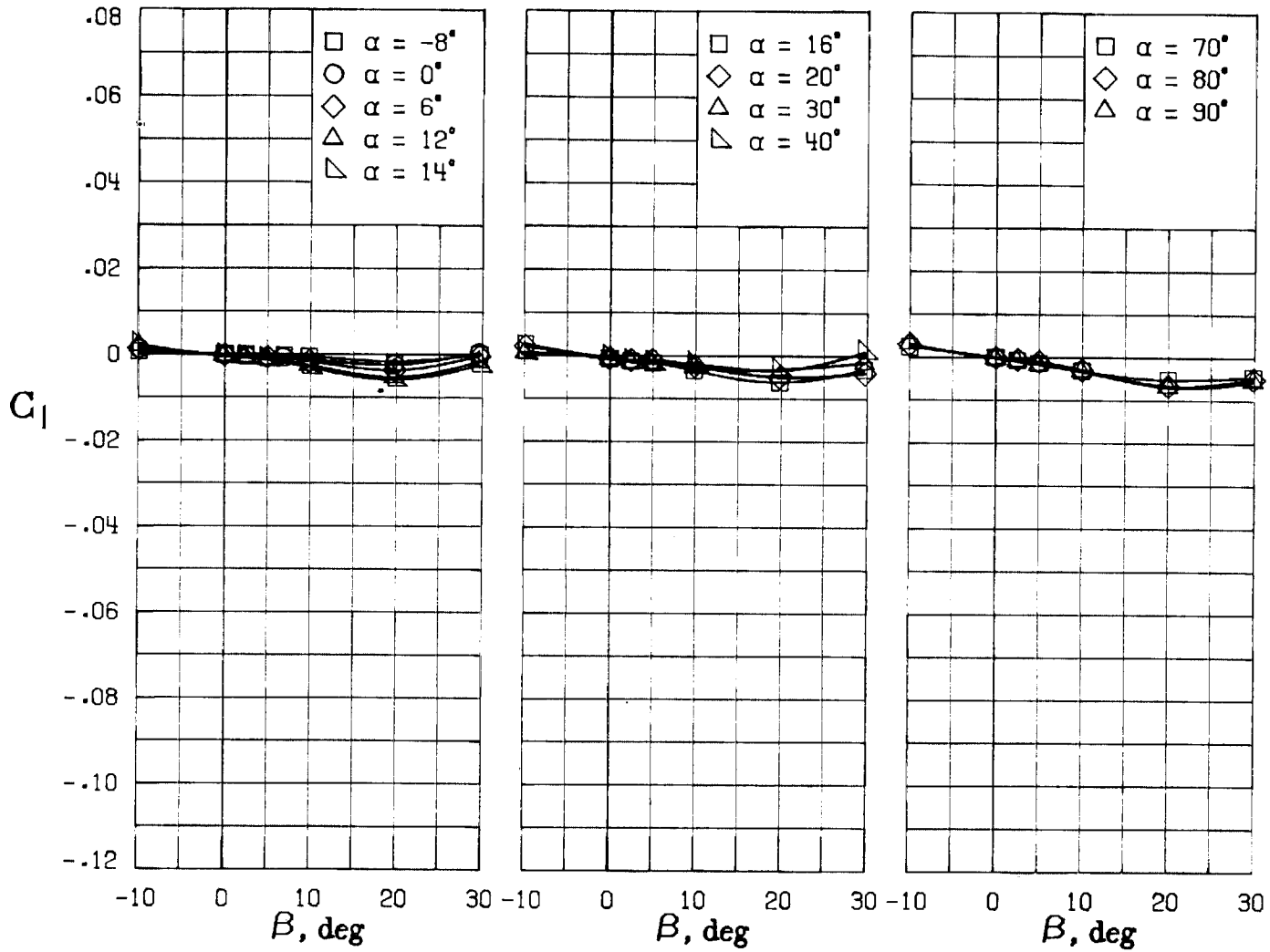

(F) LATERAL - STABILITY CHARACTERISTICS ABOUT BODY AXES AT VARIOUS ANGLES OF ATTACK.

FIGURE 43. - CONCLUDED.

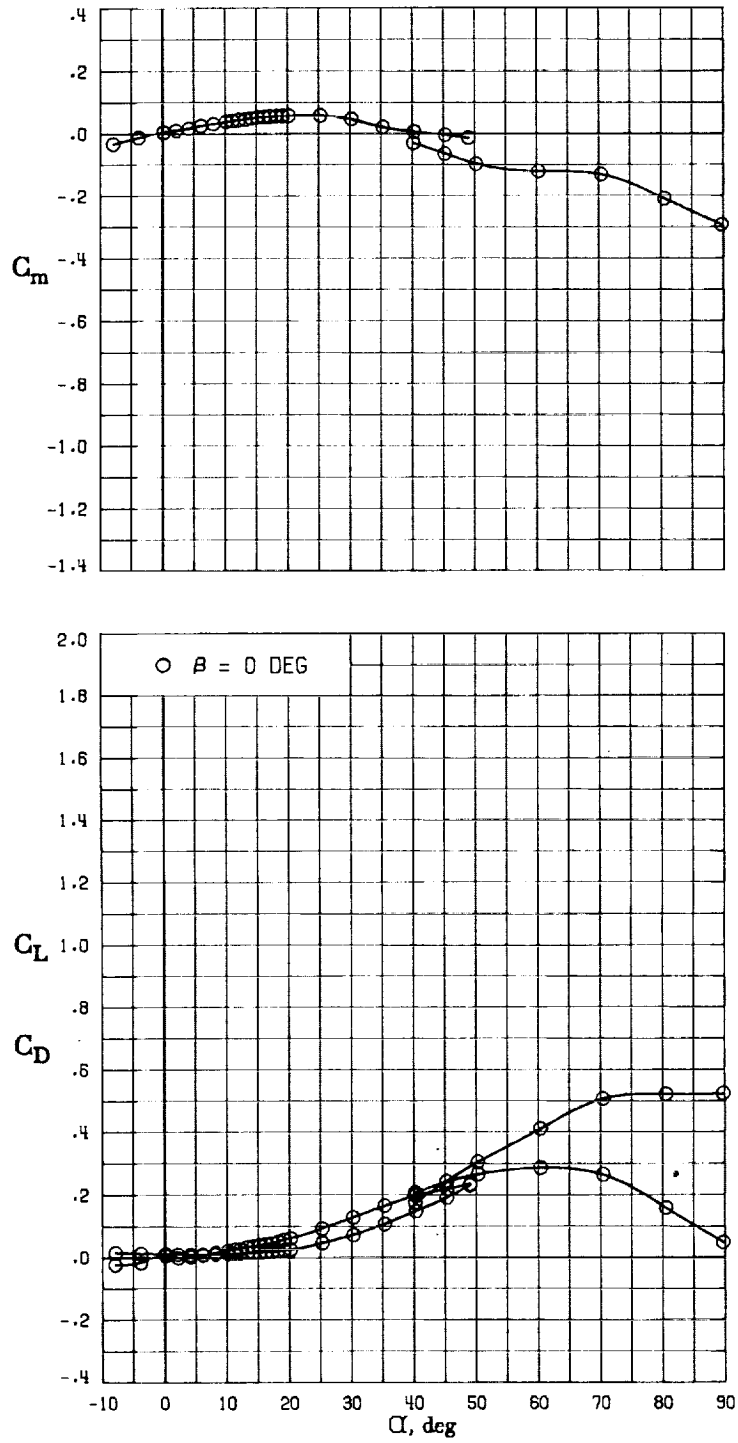

(A) LONGITUDINAL FORCE AND MOMENT COEFFICIENTS ABOUT STABILITY AXES.

FIGURE 44. - EFFECT OF ANGLE OF ATTACK AND SIDESLIP ANGLE ON AERODYNAMIC CHARACTERISTICS AT RE = 3.45 E+06 FOR CONFIGURATION B V. $\delta_E = 0°$, $\delta_A = 0°$, $\delta_R = 0°$.

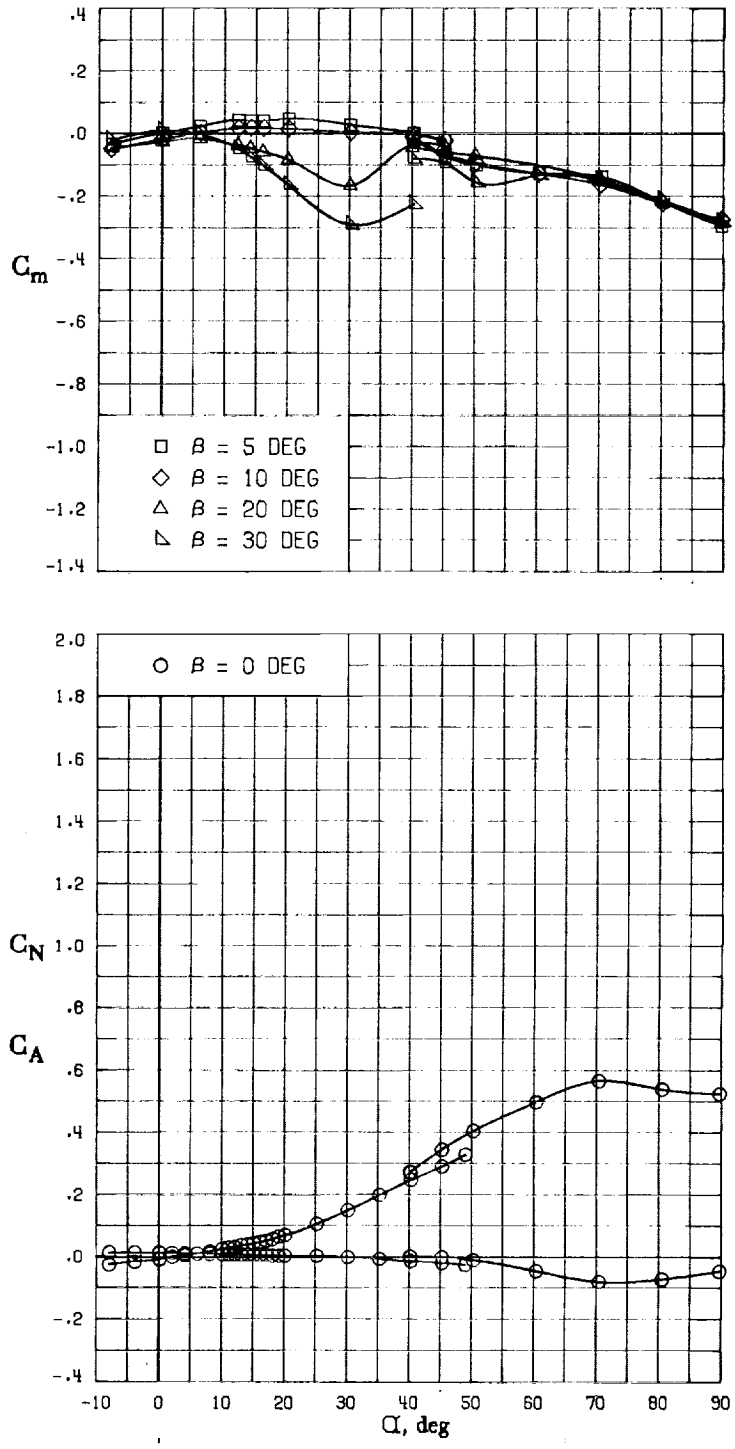

(3) LONGITUDINAL FORCE AND MOMENT COEFFICIENTS ABOUT BODY AXES.

FIGURE 44. - CONTINUED.

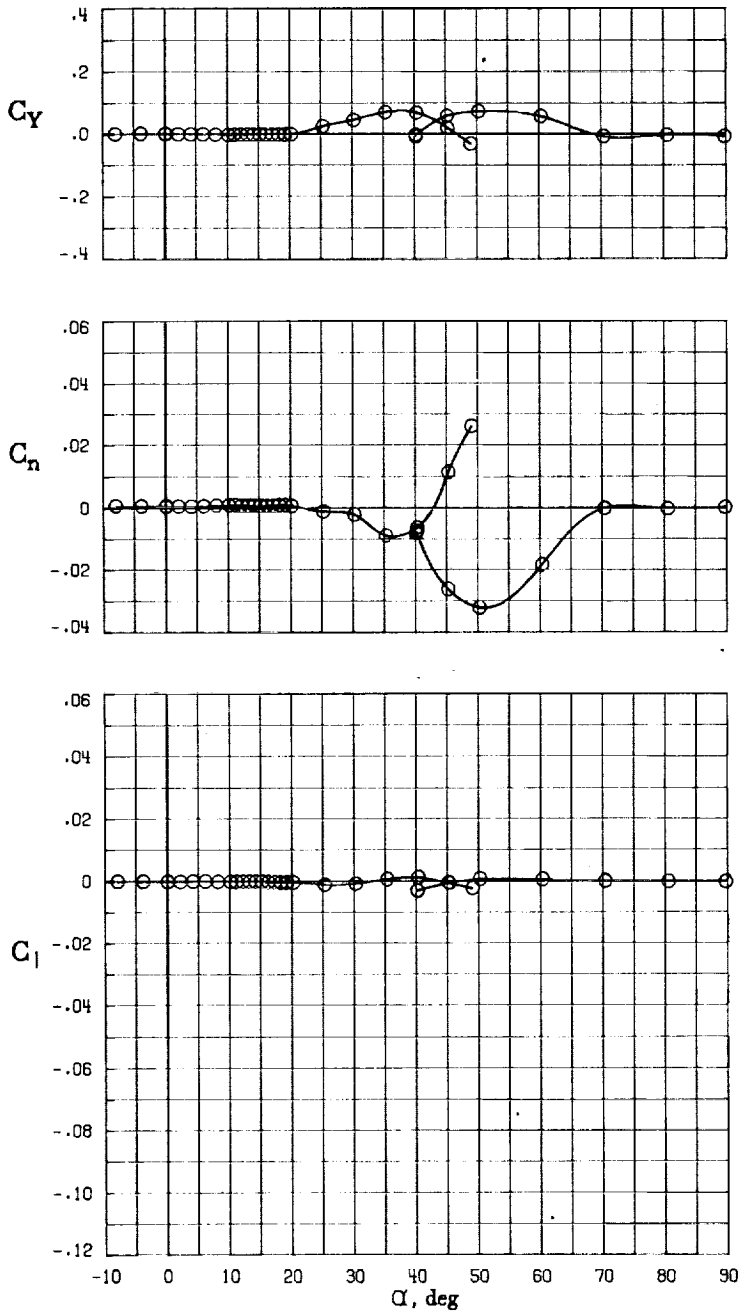

(C) LATERAL - DIRECTIONAL FORCE AND MOMENT COEFFICIENTS ABOUT BODY AXES AT ZERO SIDESLIP.

FIGURE 44. - CONTINUED.

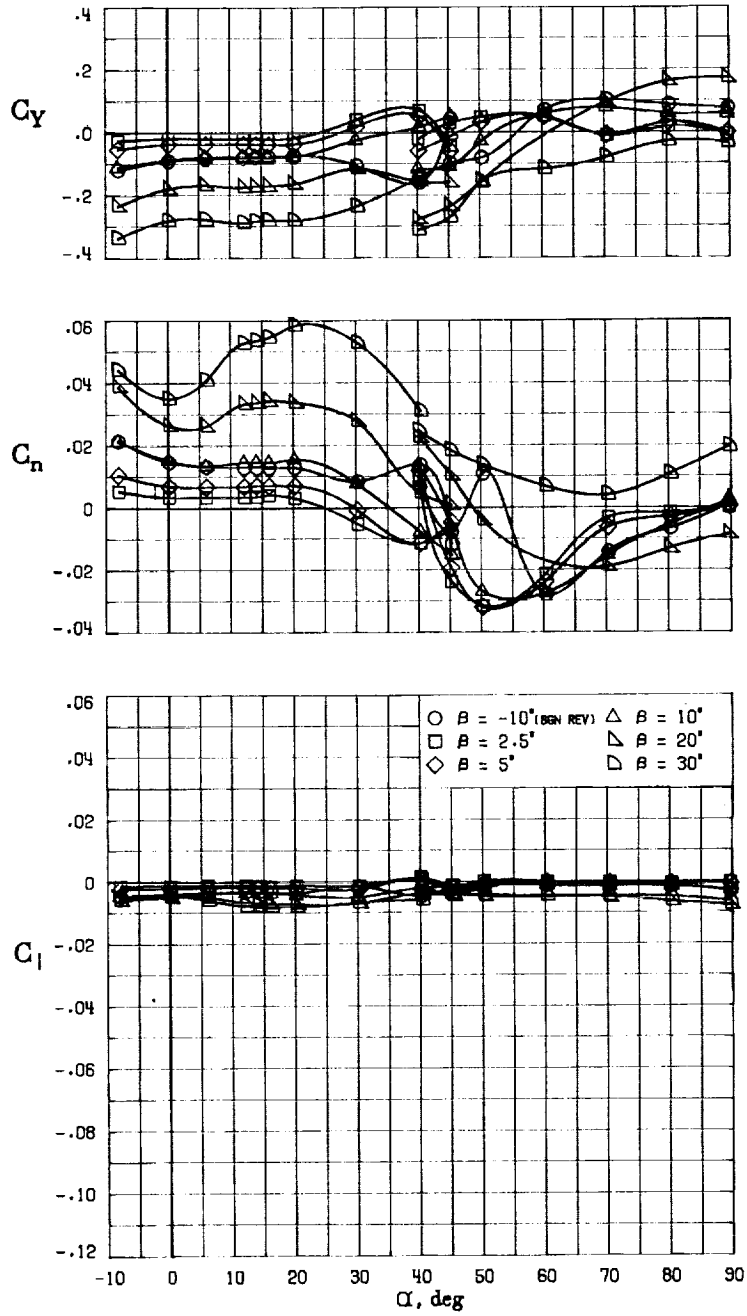

(D) LATERAL - DIRECTIONAL FORCE AND MOMENT COEFFICIENTS ABOUT BODY AXES.

FIGURE 44. - CONTINUED.

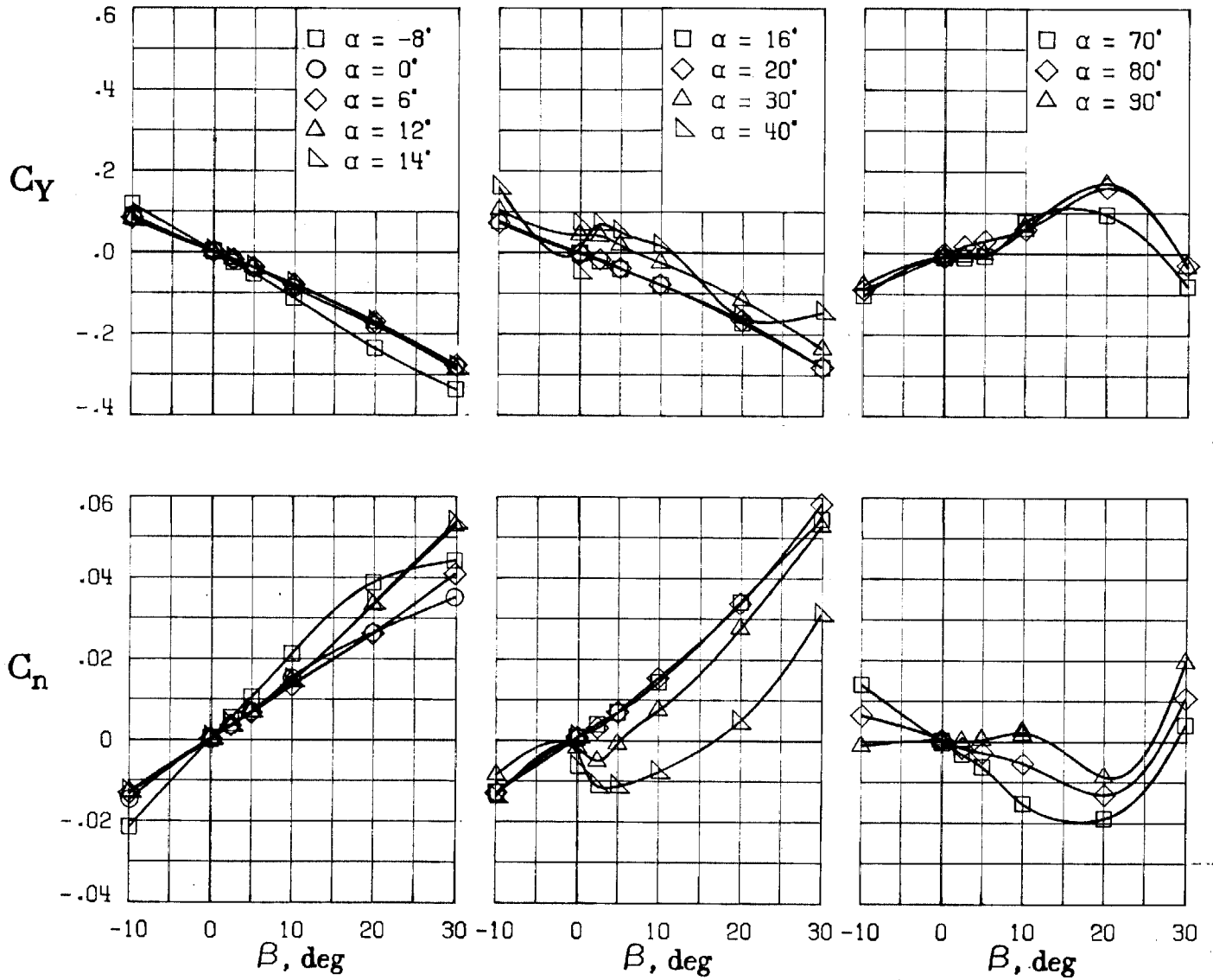

(E) DIRECTIONAL - STABILITY CHARACTERISTICS ABOUT BODY AXES AT VARIOUS ANGLES OF ATTACK.

FIGURE 44. - CONTINUED.

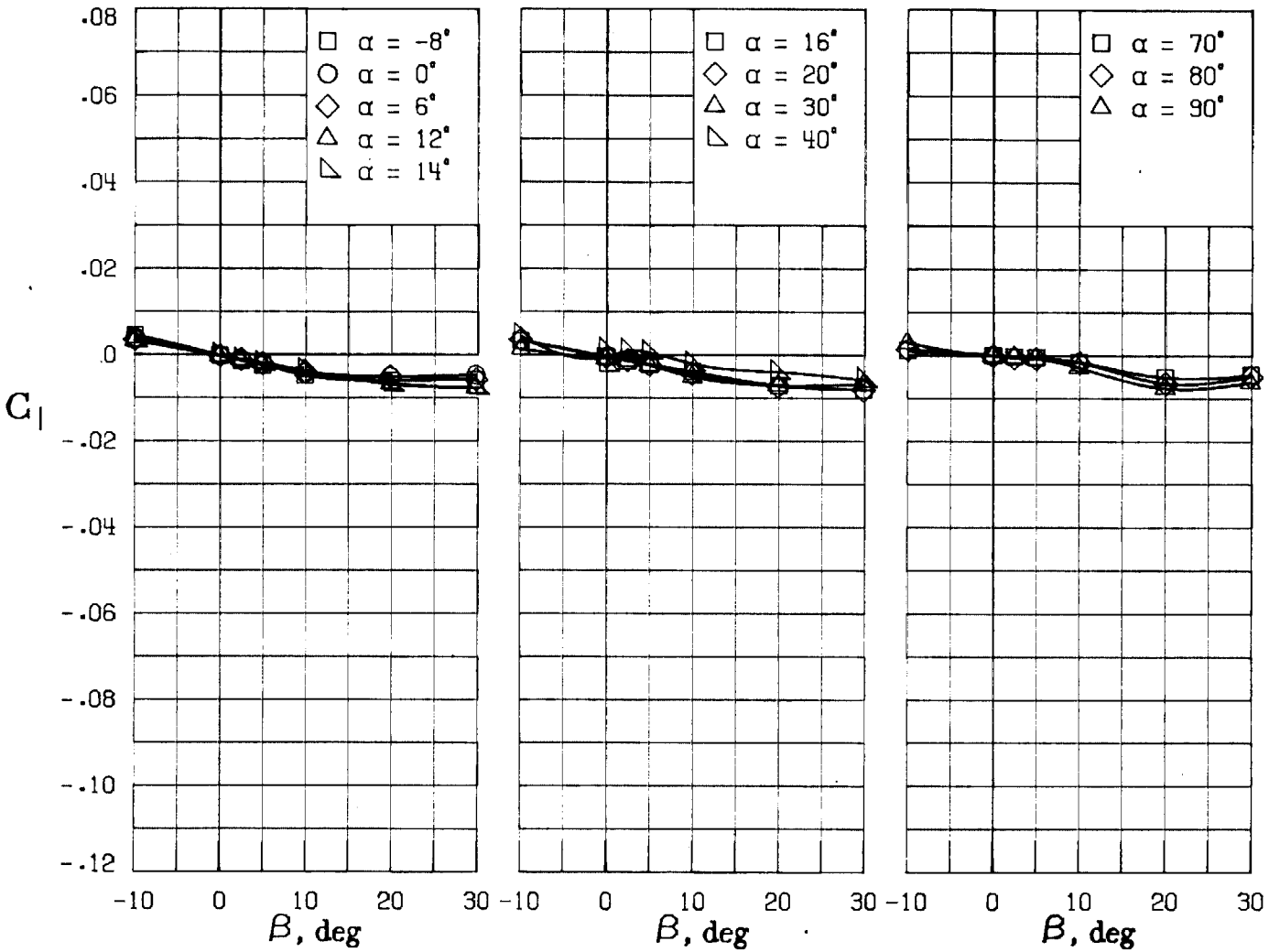

(F) LATERAL - STABILITY CHARACTERISTICS ABOUT BODY AXES AT VARIOUS ANGLES OF ATTACK.

FIGURE 44. - CONCLUDED.

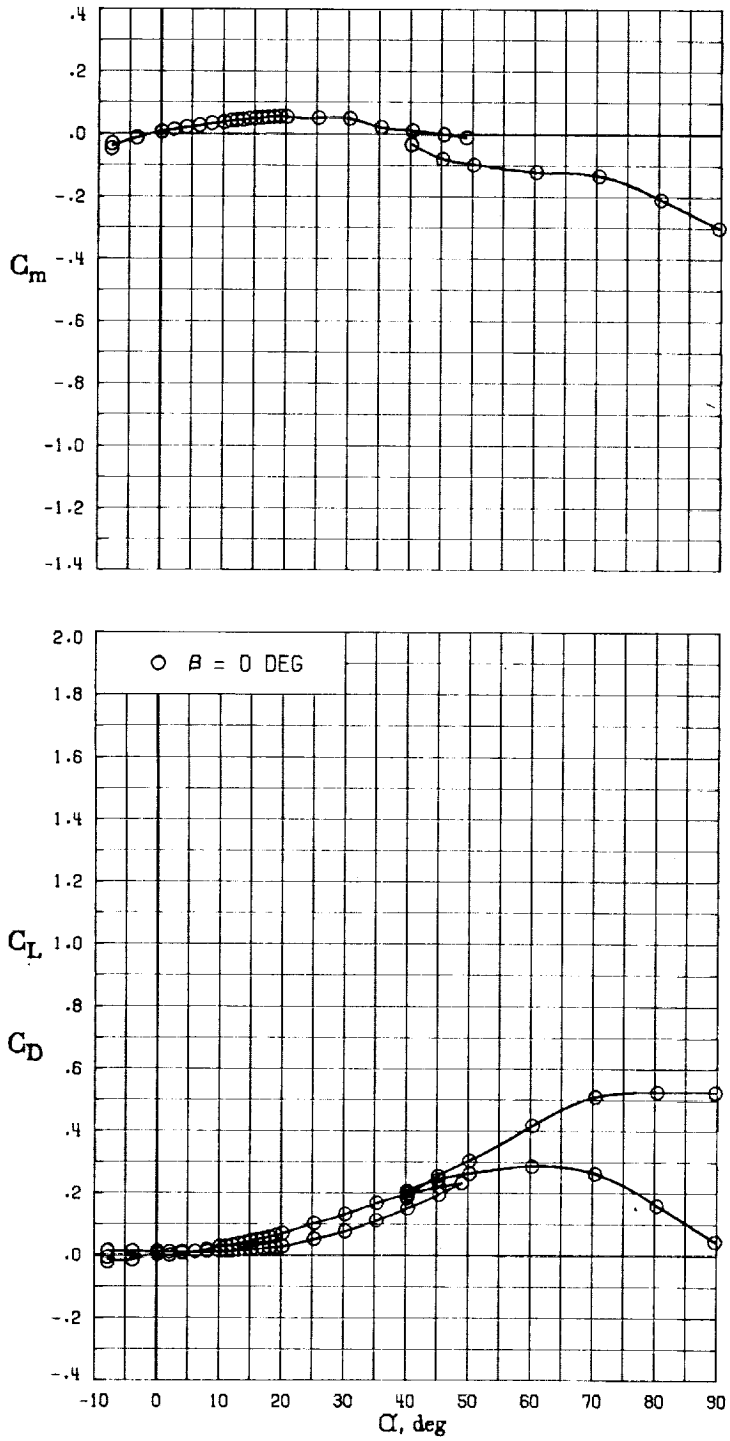

(A) LONGITUDINAL FORCE AND MOMENT COEFFICIENTS ABOUT STABILITY AXES.

FIGURE 45. - EFFECT OF ANGLE OF ATTACK AND SIDESLIP ANGLE ON AERODYNAMIC CHARACTERISTICS AT RE = 3.45 E+06 FOR CONFIGURATION B.
$\delta_E = 0°$, $\delta_A = 0°$, $\delta_R = 0°$.

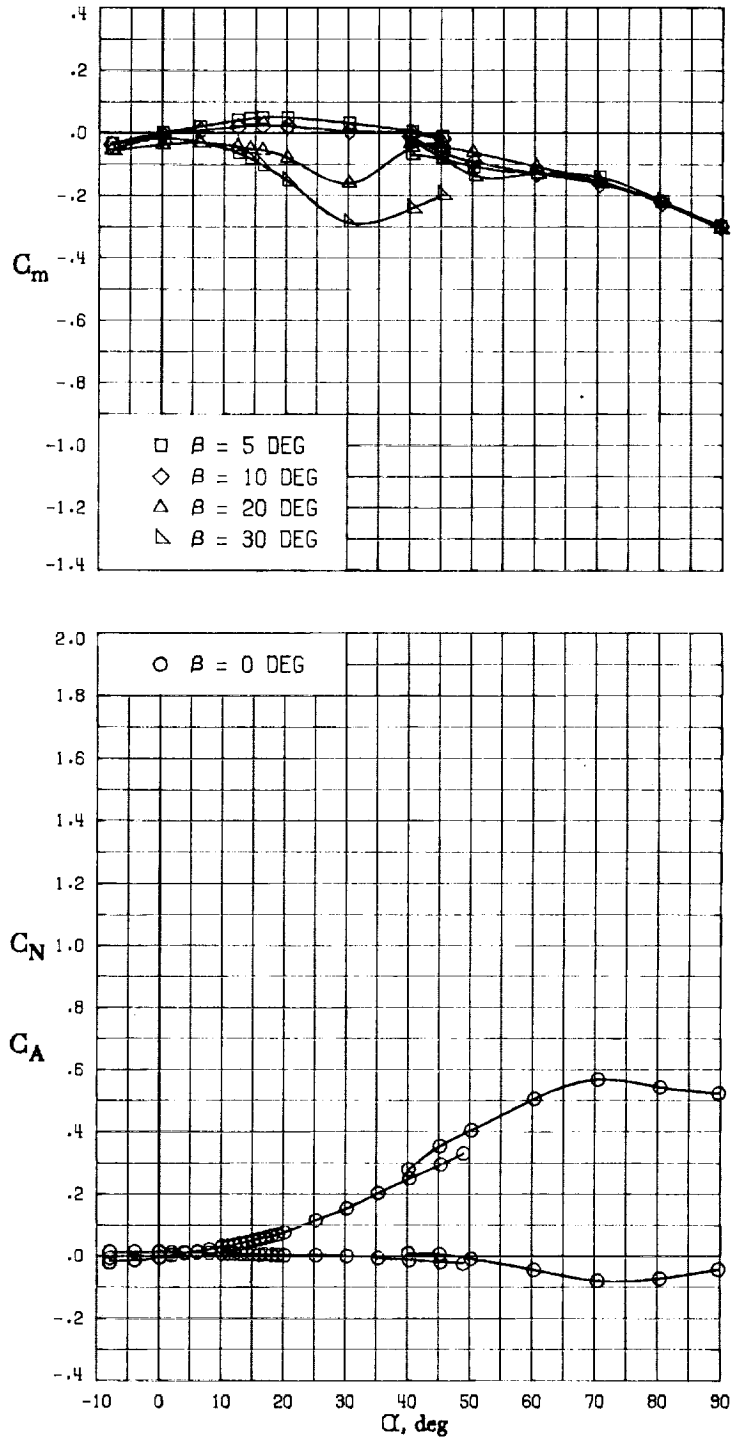

(B) LONGITUDINAL FORCE AND MOMENT COEFFICIENTS ABOUT BODY AXES.

FIGURE 45. - CONTINUED.

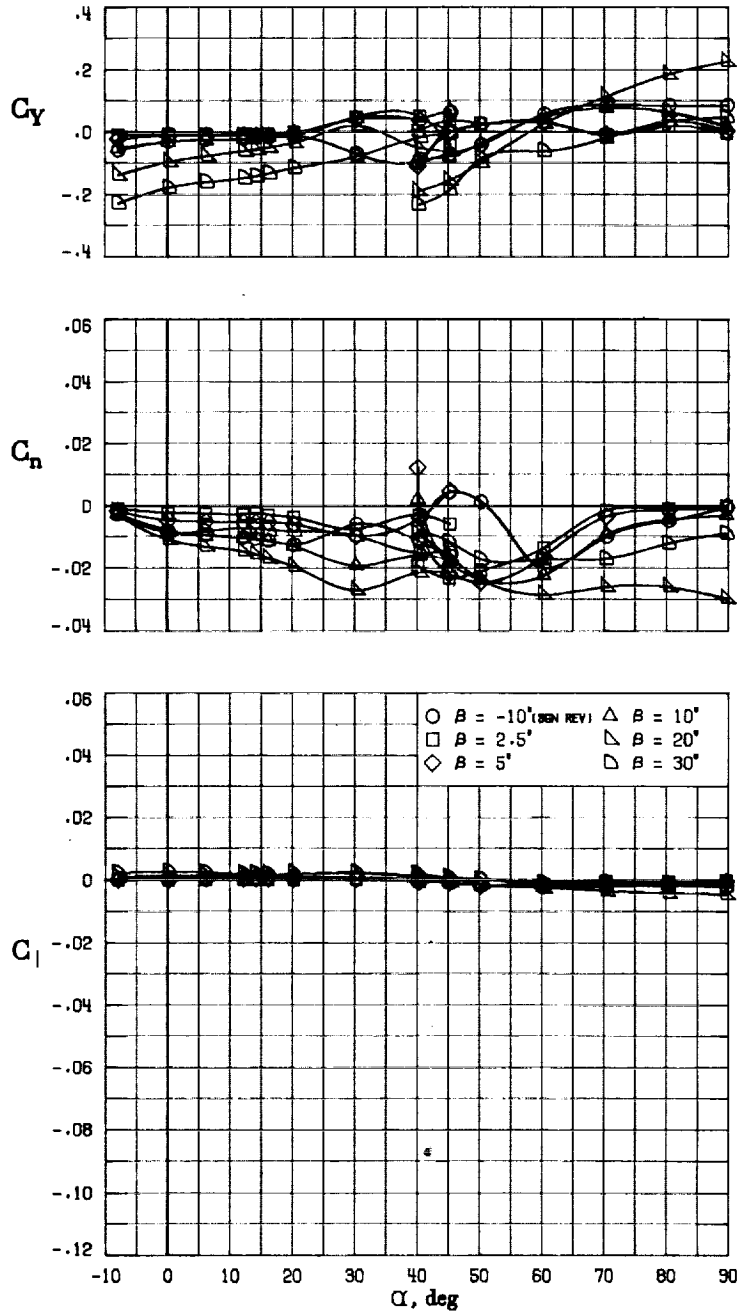

(D) LATERAL - DIRECTIONAL FORCE AND MOMENT COEFFICIENTS ABOUT BODY AXES.

FIGURE 45. - CONTINUED.

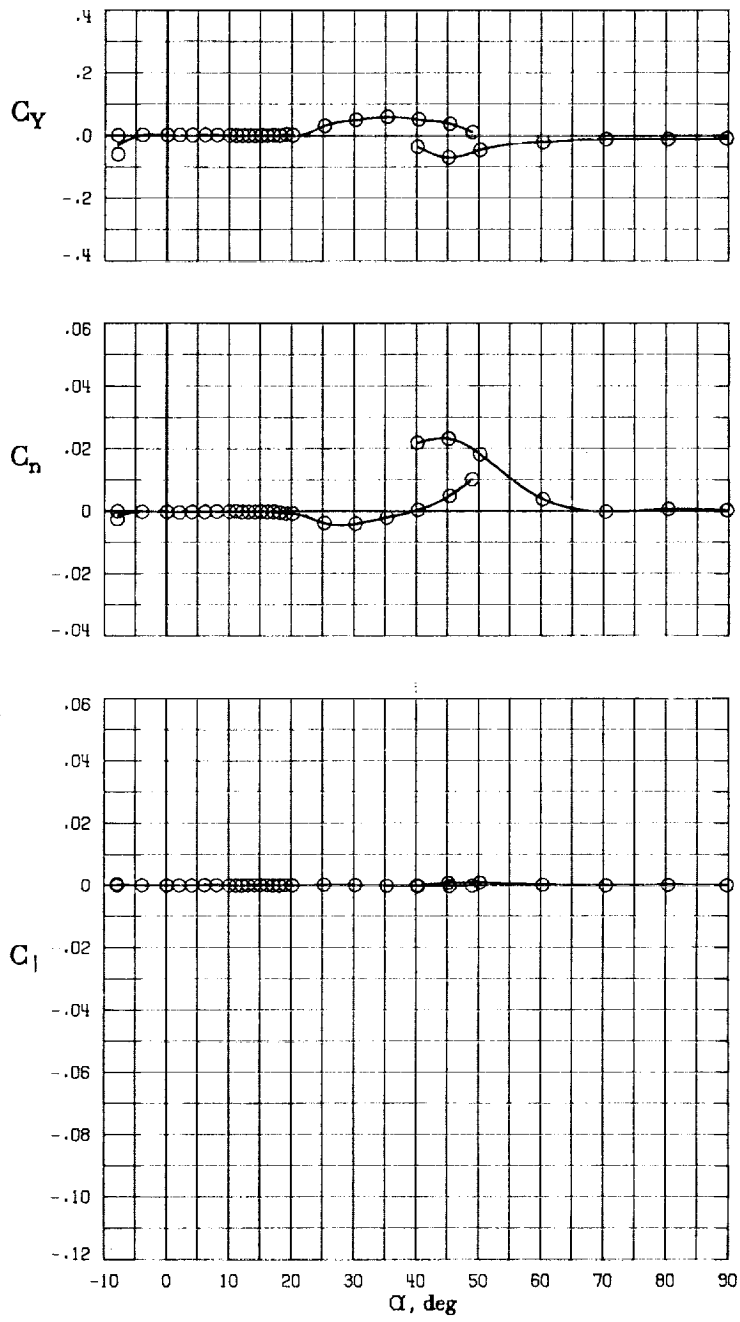

(C) LATERAL - DIRECTIONAL FORCE AND MOMENT COEFFICIENTS ABOUT BODY AXES AT ZERO SIDESLIP.

FIGURE 45. - CONTINUED.

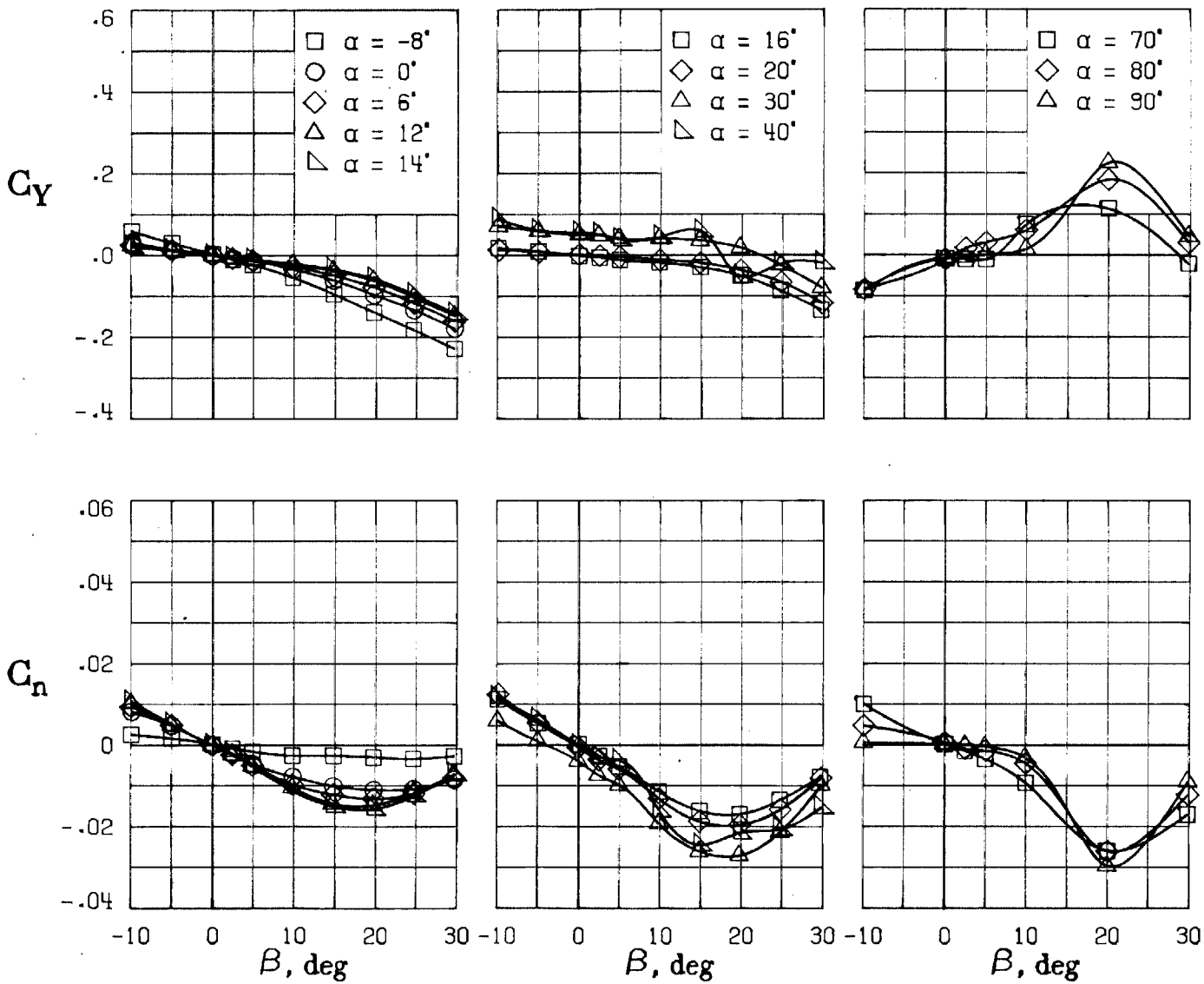

(E) DIRECTIONAL - STABILITY CHARACTERISTICS ABOUT BODY AXES AT VARIOUS ANGLES OF ATTACK.

FIGURE 45. - CONTINUED.

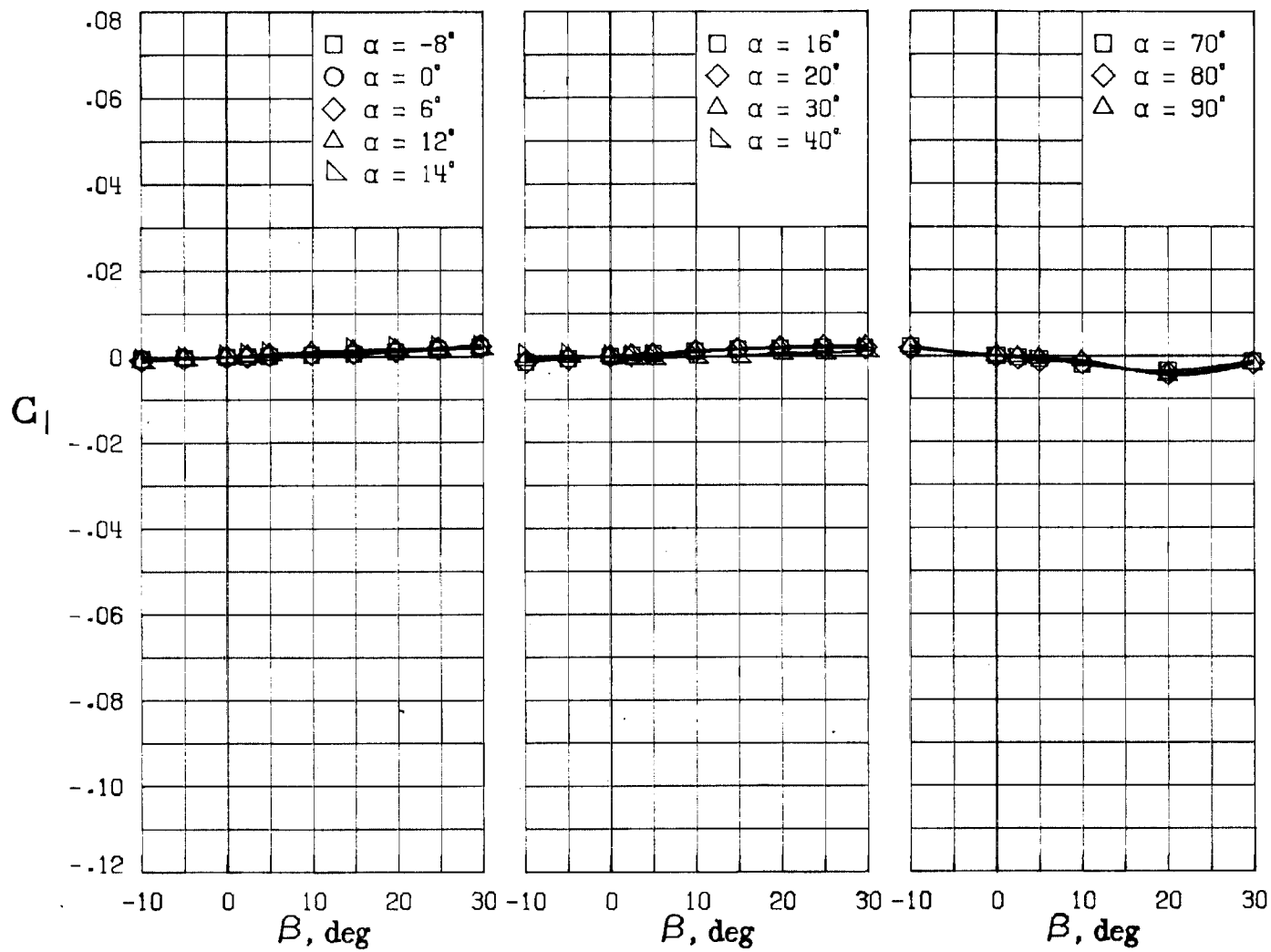

(F) LATERAL - STABILITY CHARACTERISTICS ABOUT BODY AXES AT VARIOUS ANGLES OF ATTACK.

FIGURE 45. - CONCLUDED.

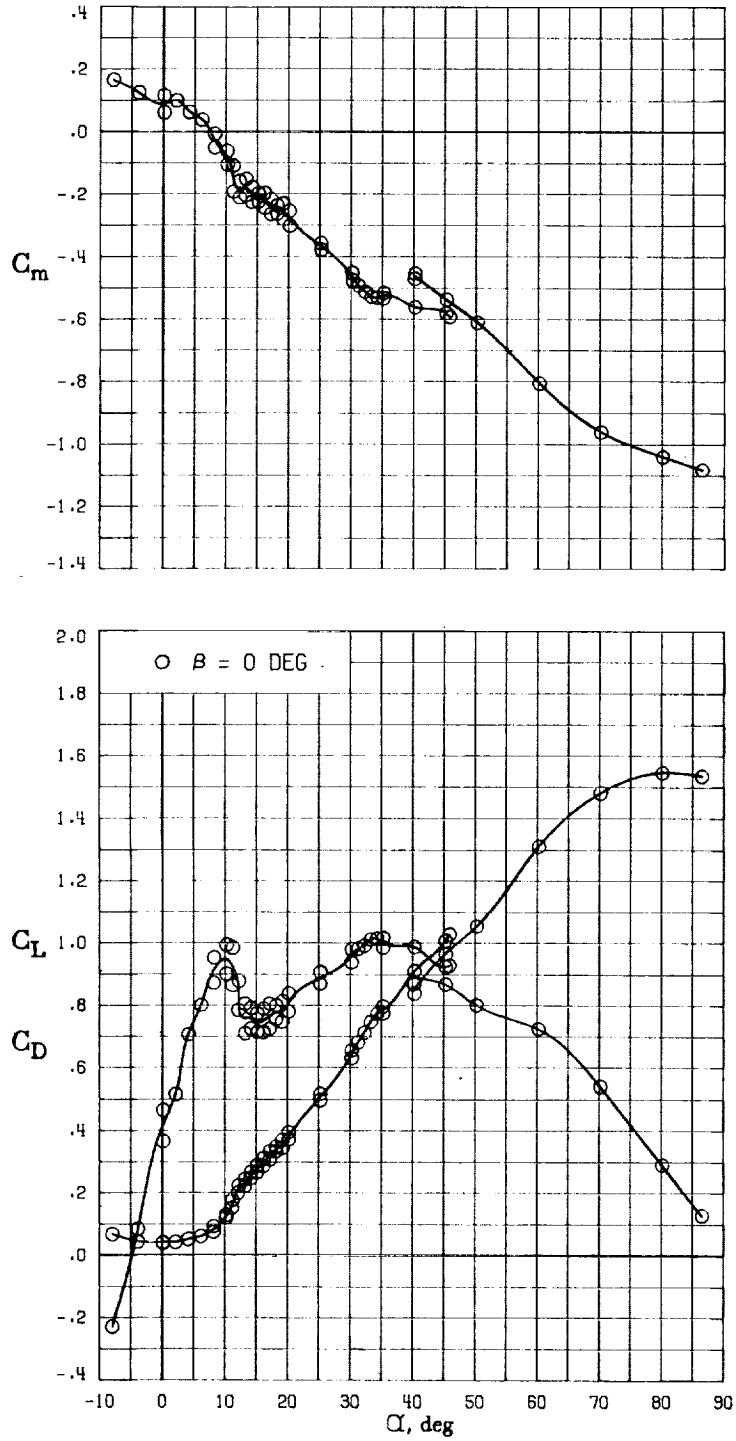

(A) LONGITUDINAL FORCE AND MOMENT COEFFICIENTS ABOUT STABILITY AXES.

FIGURE 46. - EFFECT OF ANGLE OF ATTACK AND SIDESLIP ANGLE ON AERODYNAMIC CHARACTERISTICS AT RE = .288 E+06 FOR CONFIGURATION B W1 H6 V. $\delta_E = 0°$, $\delta_A = 0°$, $\delta_R = 0°$.

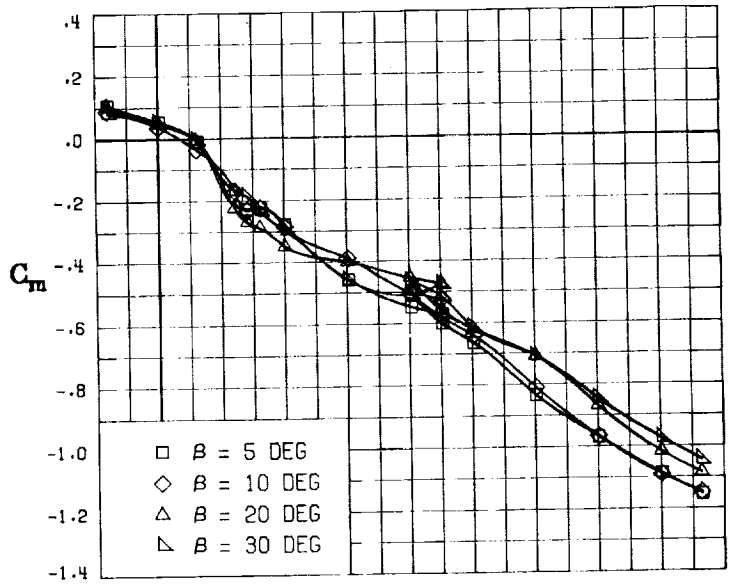

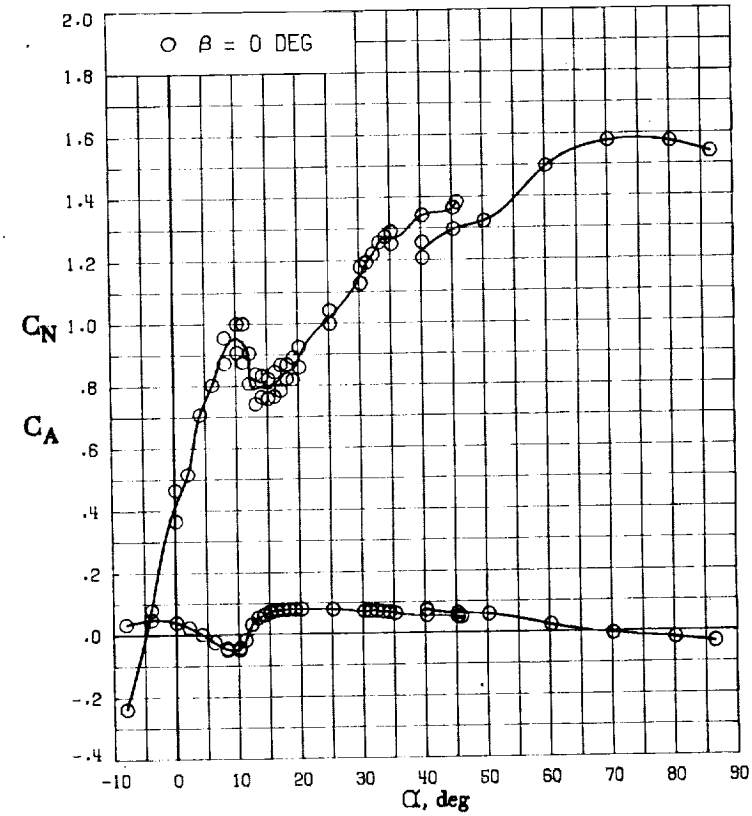

B.) LONGITUDINAL FORCE AND MOMENT COEFFICIENTS ABOUT BODY AXES.

FIGURE 46. - CONTINUED.

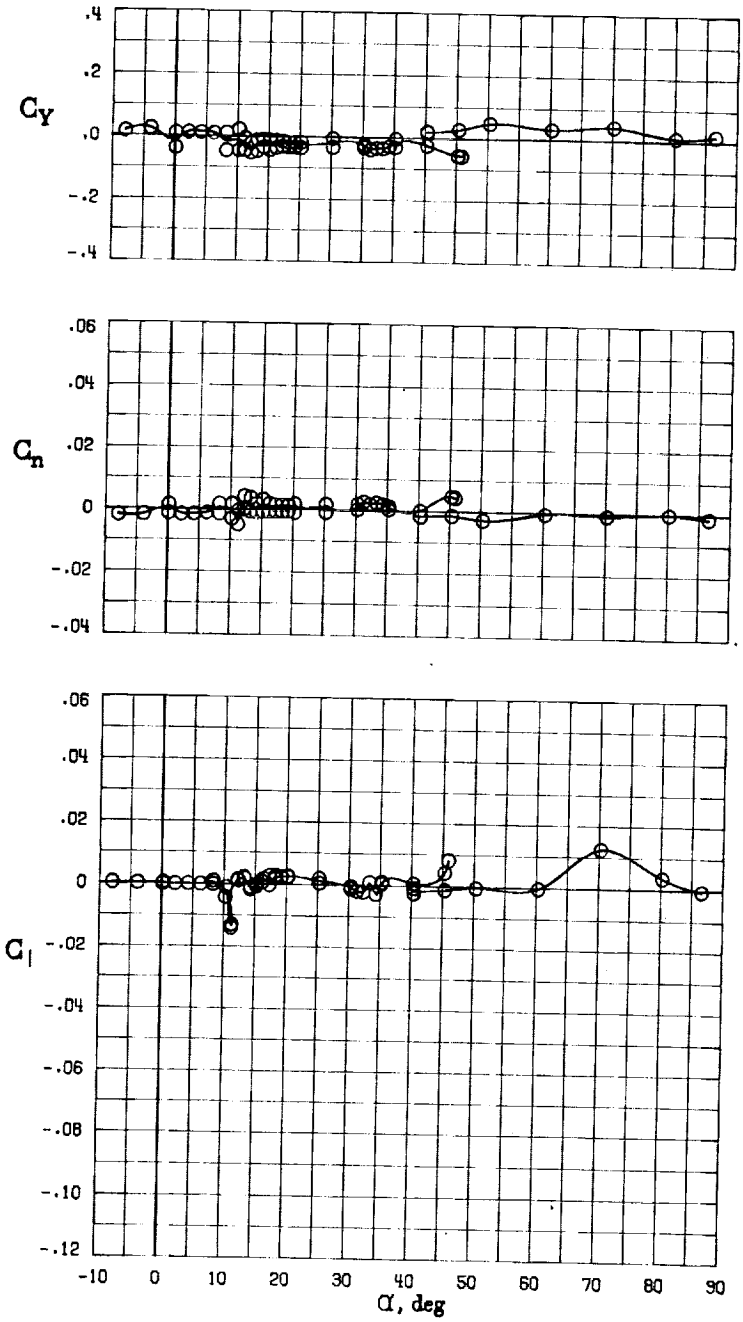

(C) LATERAL - DIRECTIONAL FORCE AND MOMENT COEFFICIENTS ABOUT BODY AXES AT ZERO SIDESLIP.

FIGURE 46. - CONTINUED.

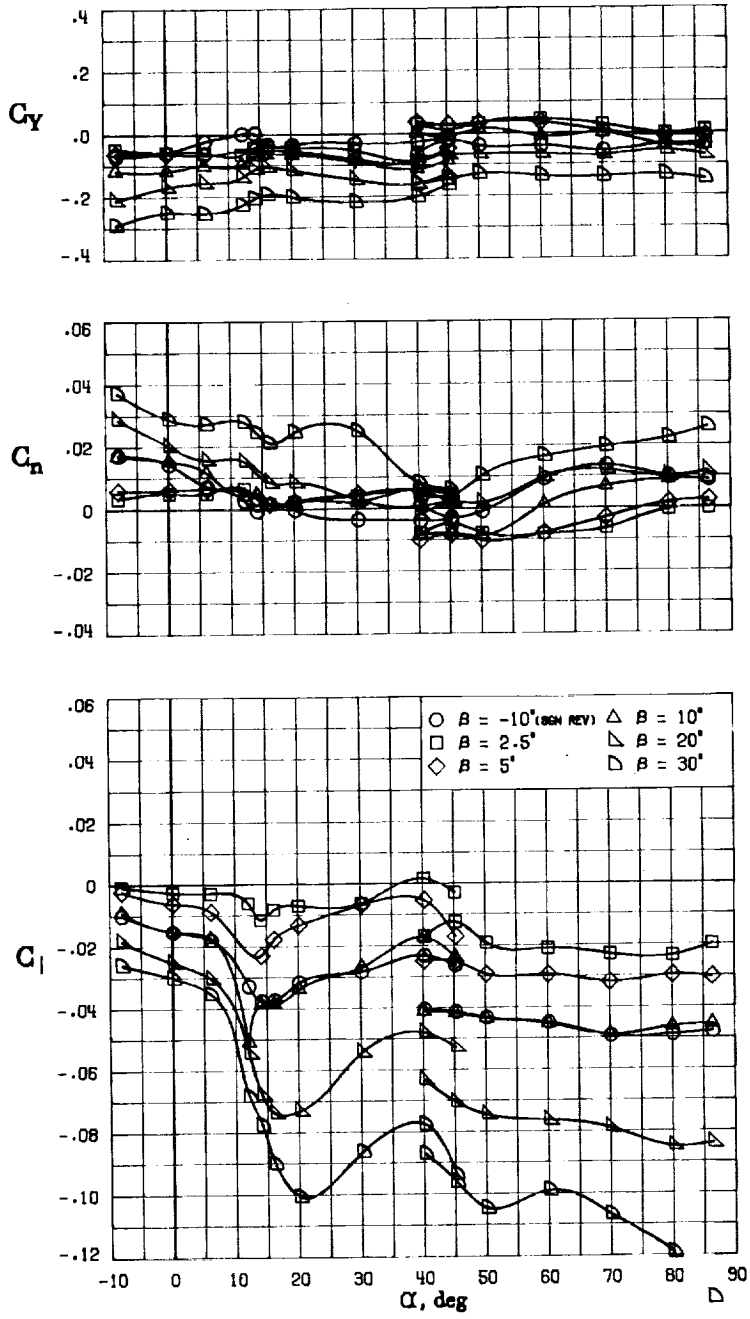

(D) LATERAL - DIRECTIONAL FORCE AND MOMENT COEFFICIENTS ABOUT BODY AXES.

FIGURE 46. - CONTINUED.

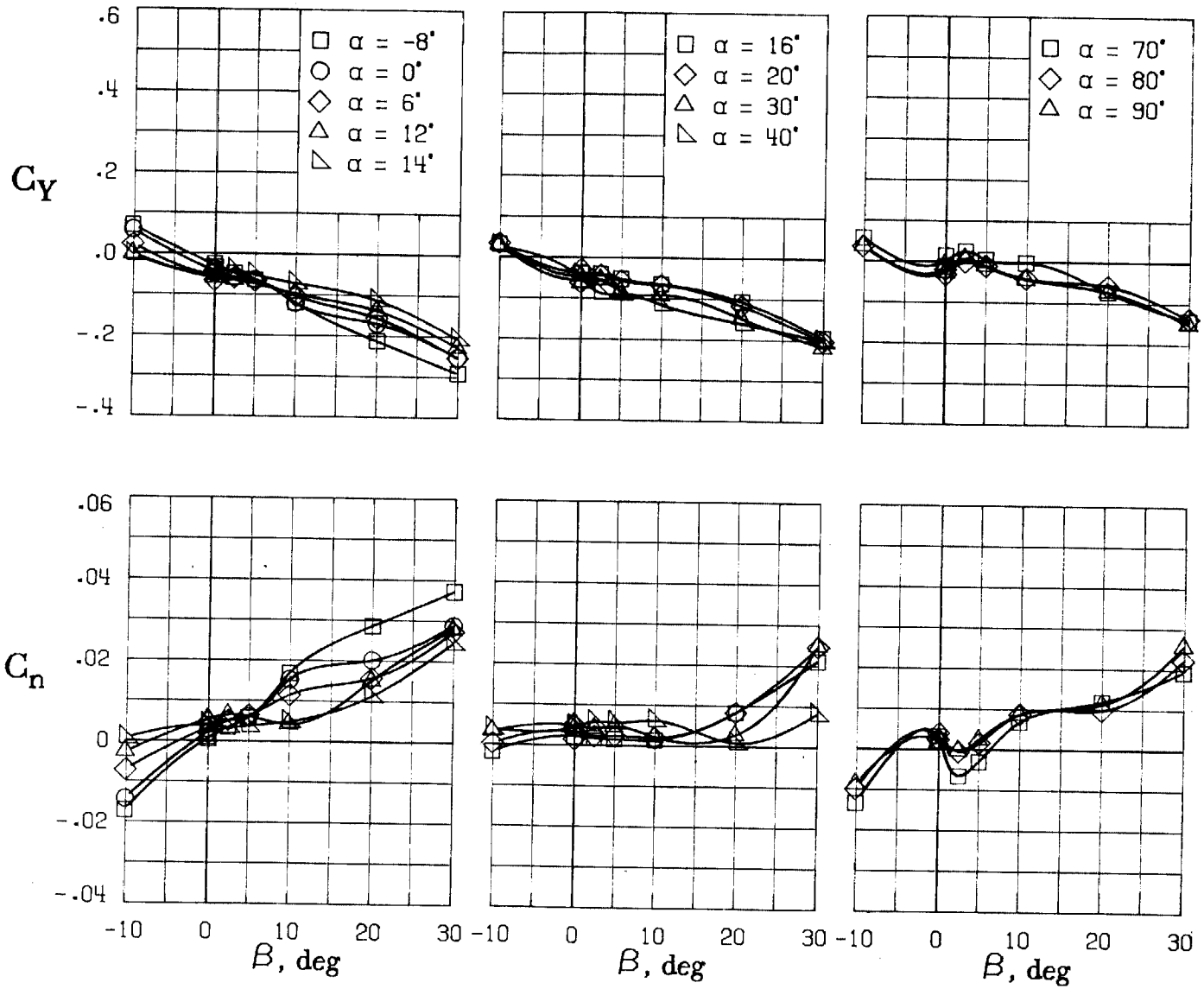

(E) DIRECTIONAL - STABILITY CHARACTERISTICS ABOUT BODY AXES AT VARIOUS ANGLES OF ATTACK .

FIGURE 46. - CONTINUED.

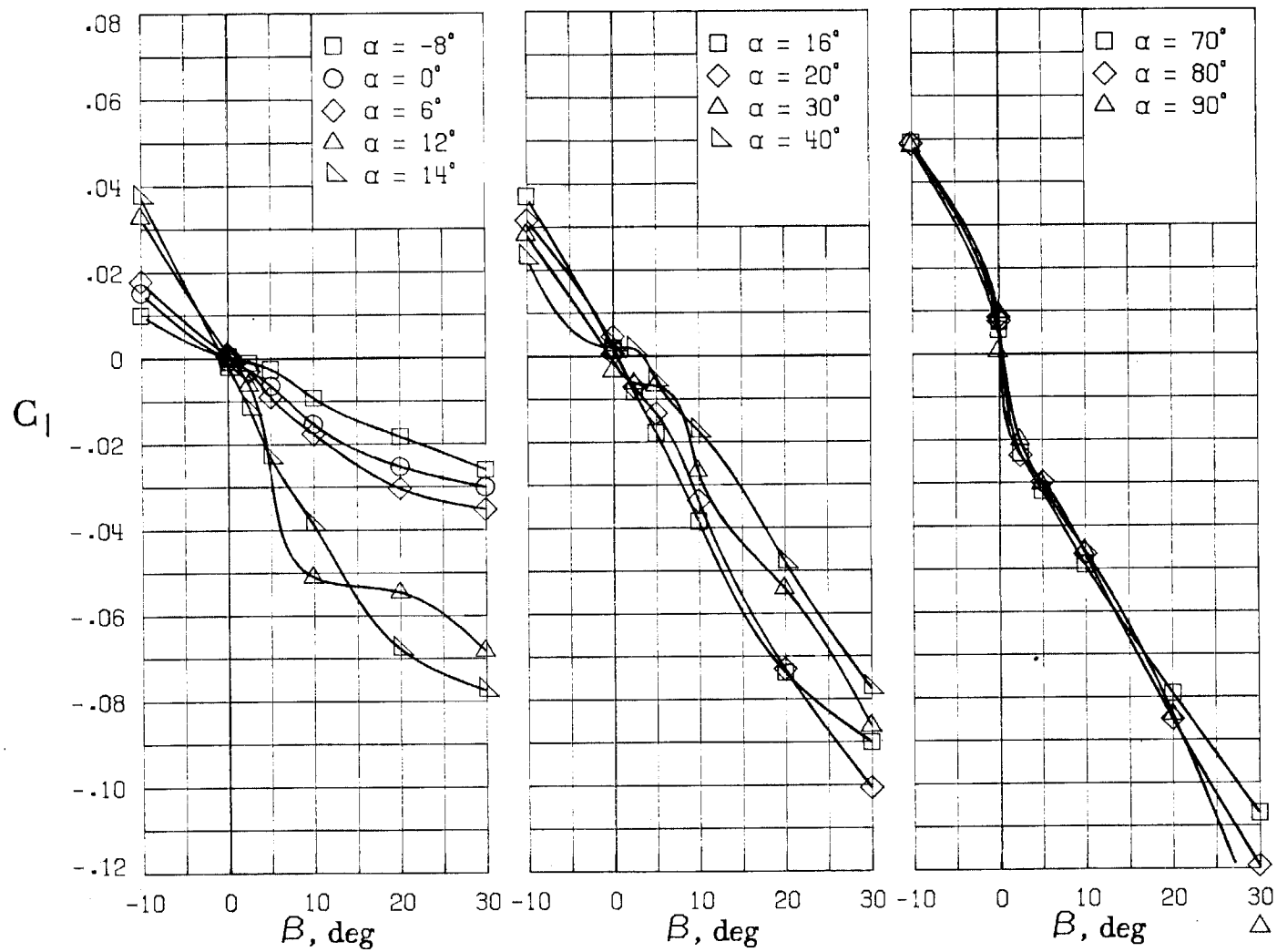

(F) LATERAL - STABILITY CHARACTERISTICS ABOUT BODY AXIS AT VARIOUS ANGLES OF ATTACK

FIGURE 46. - CONCLUDED.

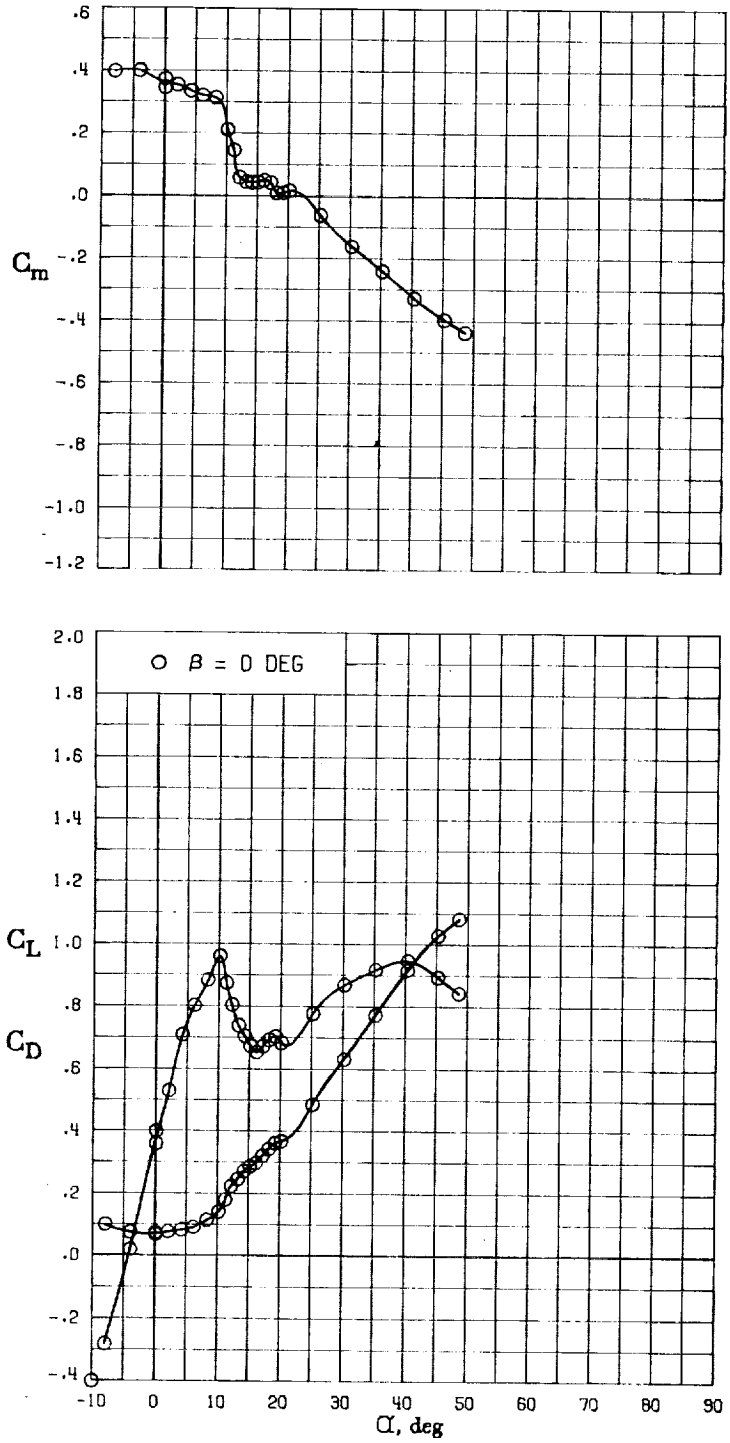

(A) LONGITUDINAL FORCE AND MOMENT COEFFICIENTS ABOUT STABILITY AXES.

FIGURE 47. - EFFECT OF ANGLE OF ATTACK AND SIDESLIP ANGLE ON AERODYNAMIC CHARACTERISTICS AT RE = .288 E+06 FOR CONFIGURATION B W1 H6 V. δ_E = -25°, δ_A = 0°, δ_R = 0°.

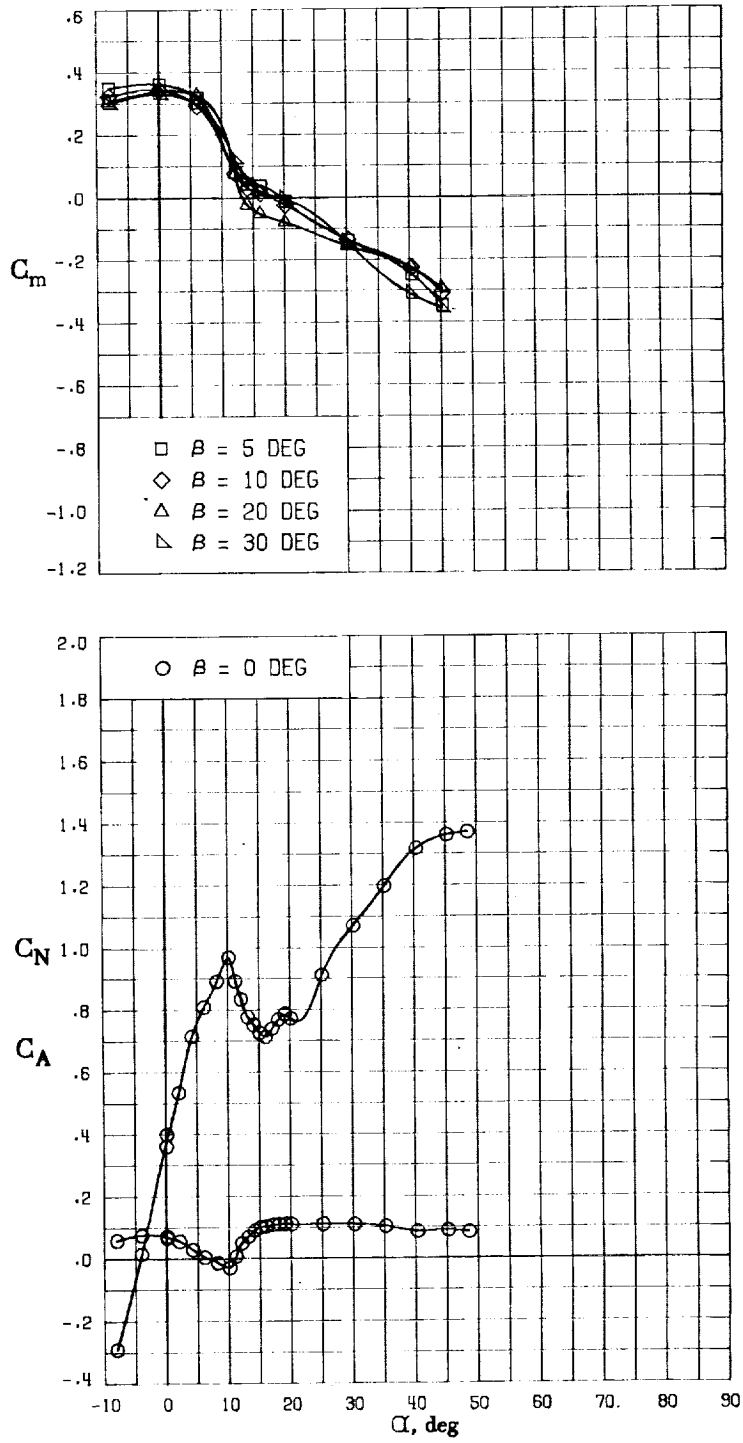

(B) LONGITUDINAL FORCE AND MOMENT COEFFICIENTS ABOUT BODY AXES.

FIGURE 47. - CONTINUED.

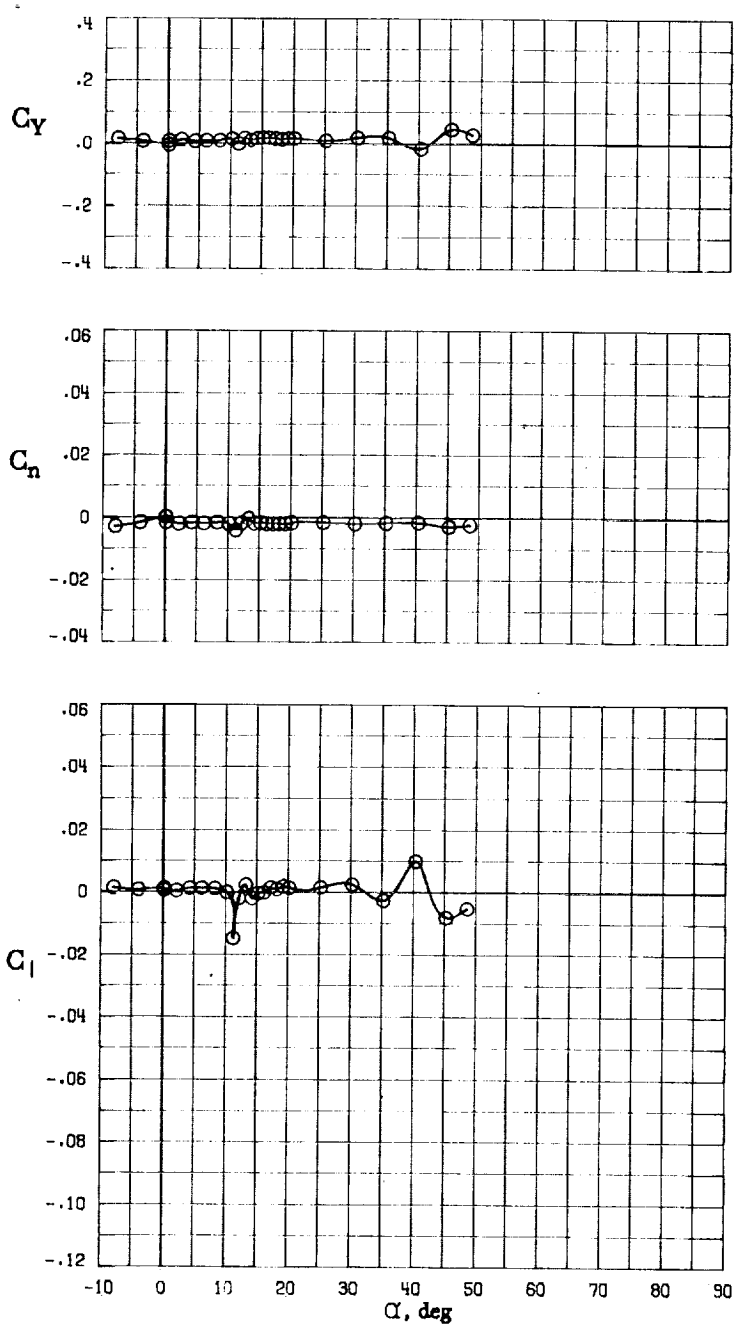

(C) LATERAL - DIRECTIONAL FORCE AND MOMENT COEFFICIENTS ABOUT BODY AXES AT ZERO SIDESLIP.

FIGURE 47. - CONTINUED.

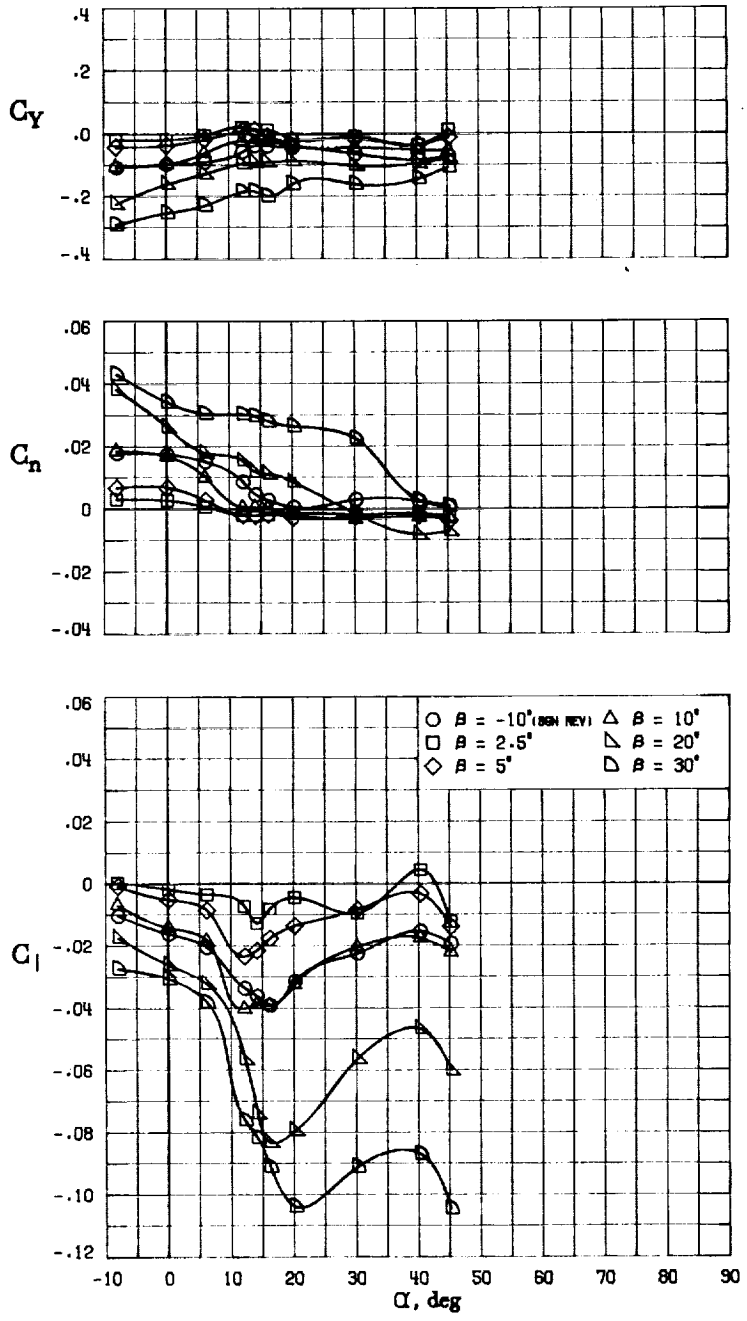

(D) LATERAL - DIRECTIONAL FORCE AND MOMENT COEFFICIENTS ABOUT BODY AXES.

FIGURE 47. - CONTINUED.

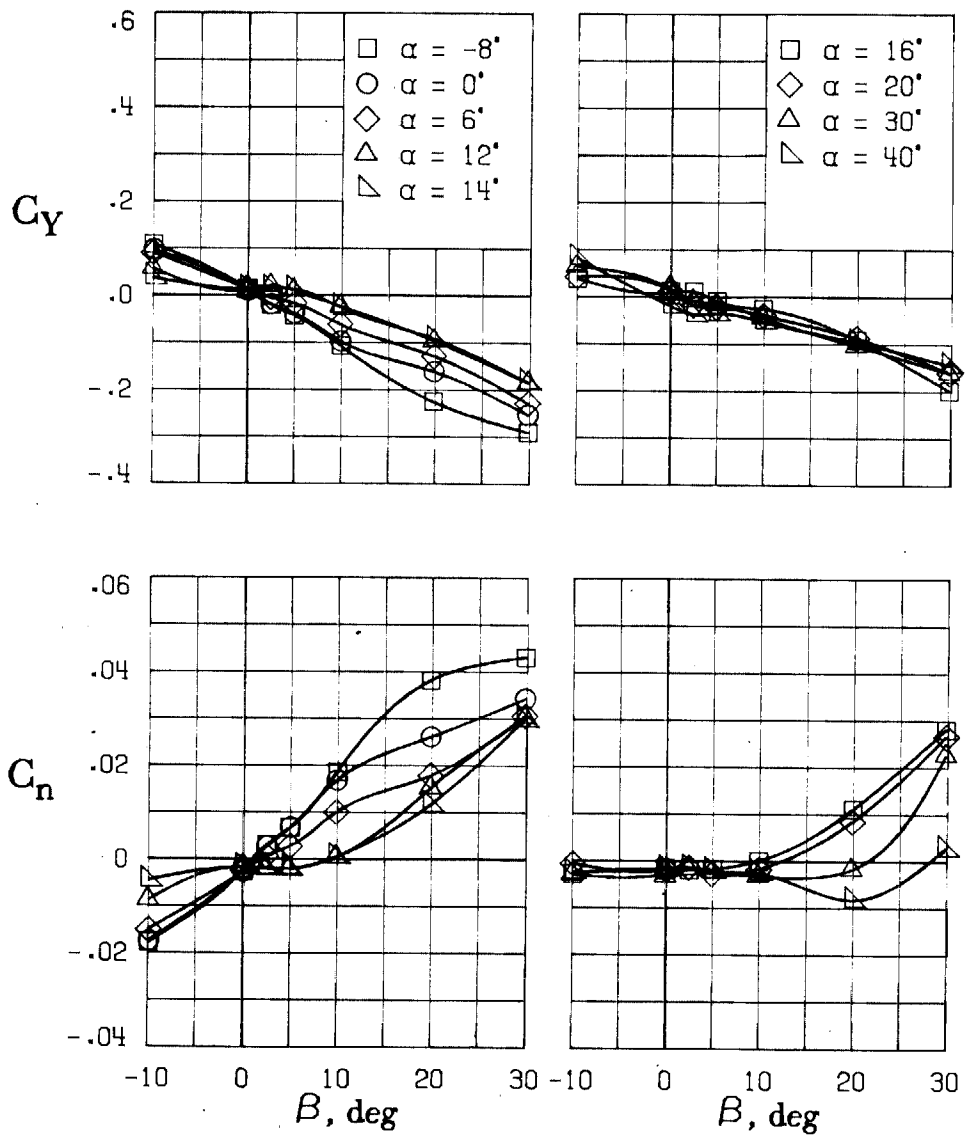

(E) DIRECTIONAL - STABILITY CHARACTERISTICS ABOUT BODY AXES AT VARIOUS ANGLES OF ATTACK.

FIGURE 47. - CONTINUED.

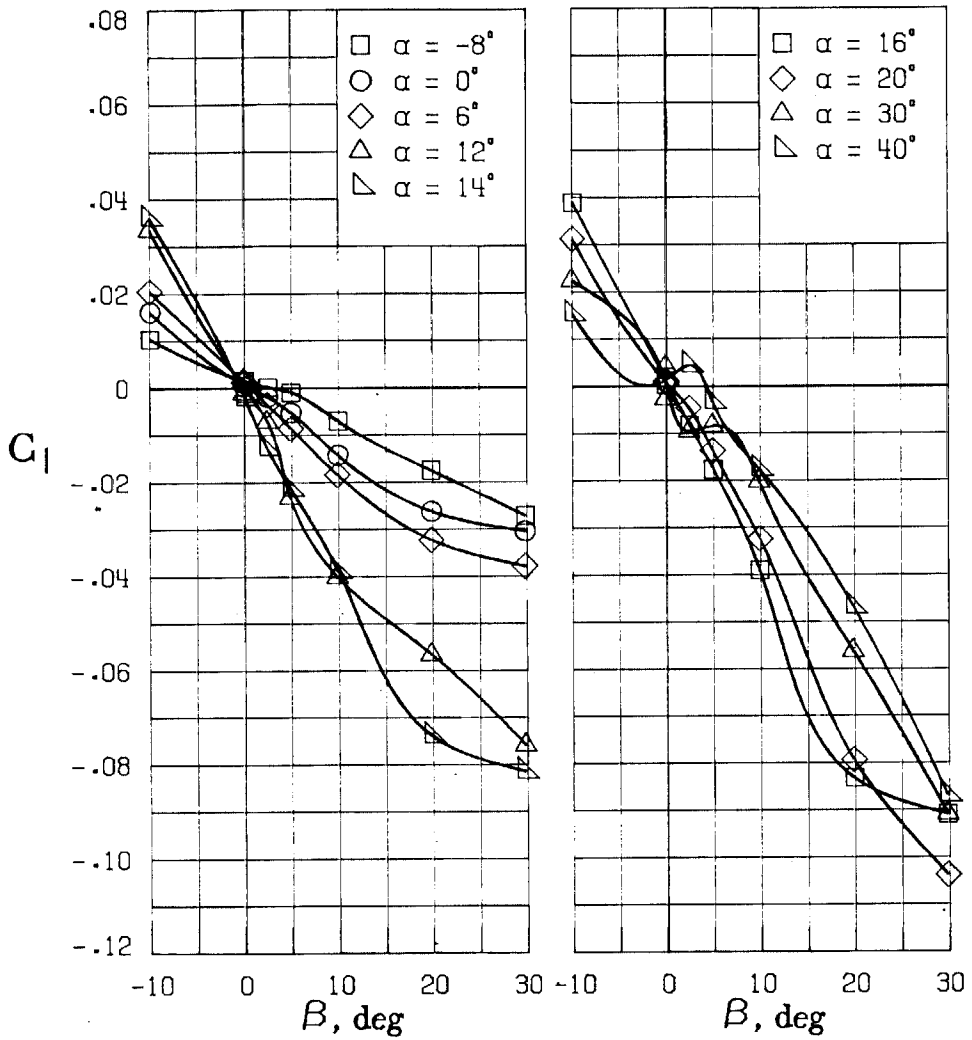

(F) LATERAL - STABILITY CHARACTERISTICS ABOUT BODY AXES AT VARIOUS ANGLES OF ATTACK.

FIGURE 47. - CONCLUDED.

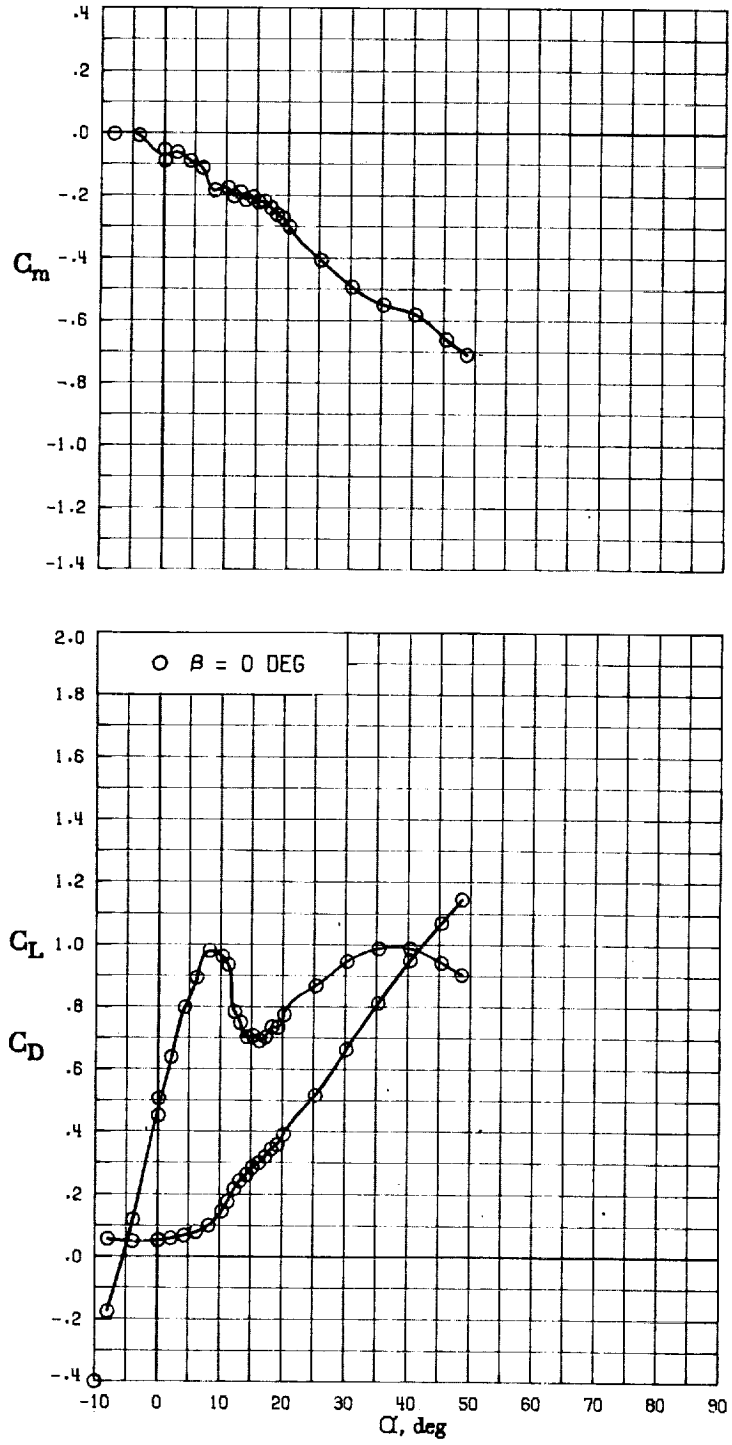

(A) LONGITUDINAL FORCE AND MOMENT COEFFICIENTS ABOUT STABILITY AXES.

FIGURE 48. - EFFECT OF ANGLE OF ATTACK AND SIDESLIP ANGLE ON AERODYNAMIC CHARACTERISTICS AT RE = .288 E+06 FOR CONFIGURATION B W1 H6 V. δ_E = 15°, δ_A = 0°, δ_R = 0°.

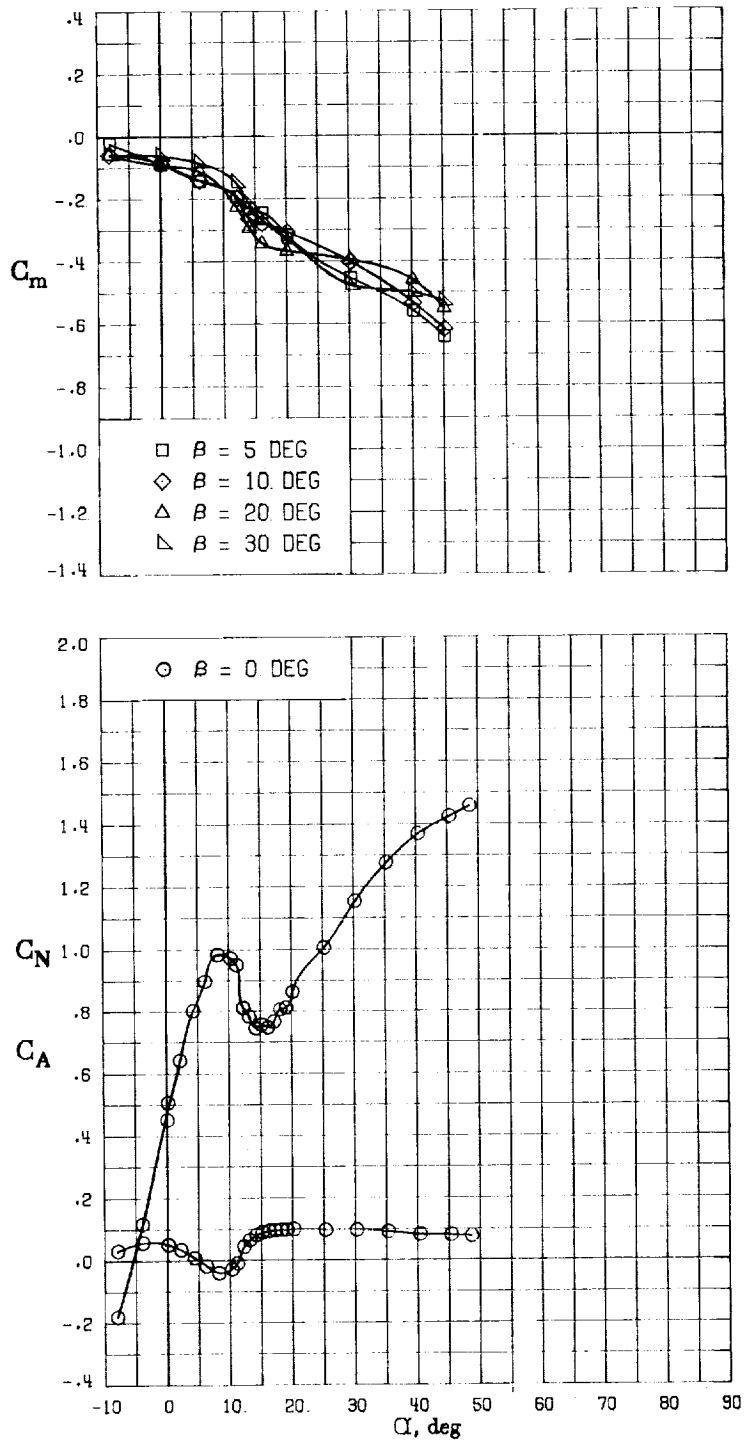

(B) LONGITUDINAL FORCE AND MOMENT COEFFICIENTS ABOUT BODY AXES.

FIGURE 48. - CONTINUED.

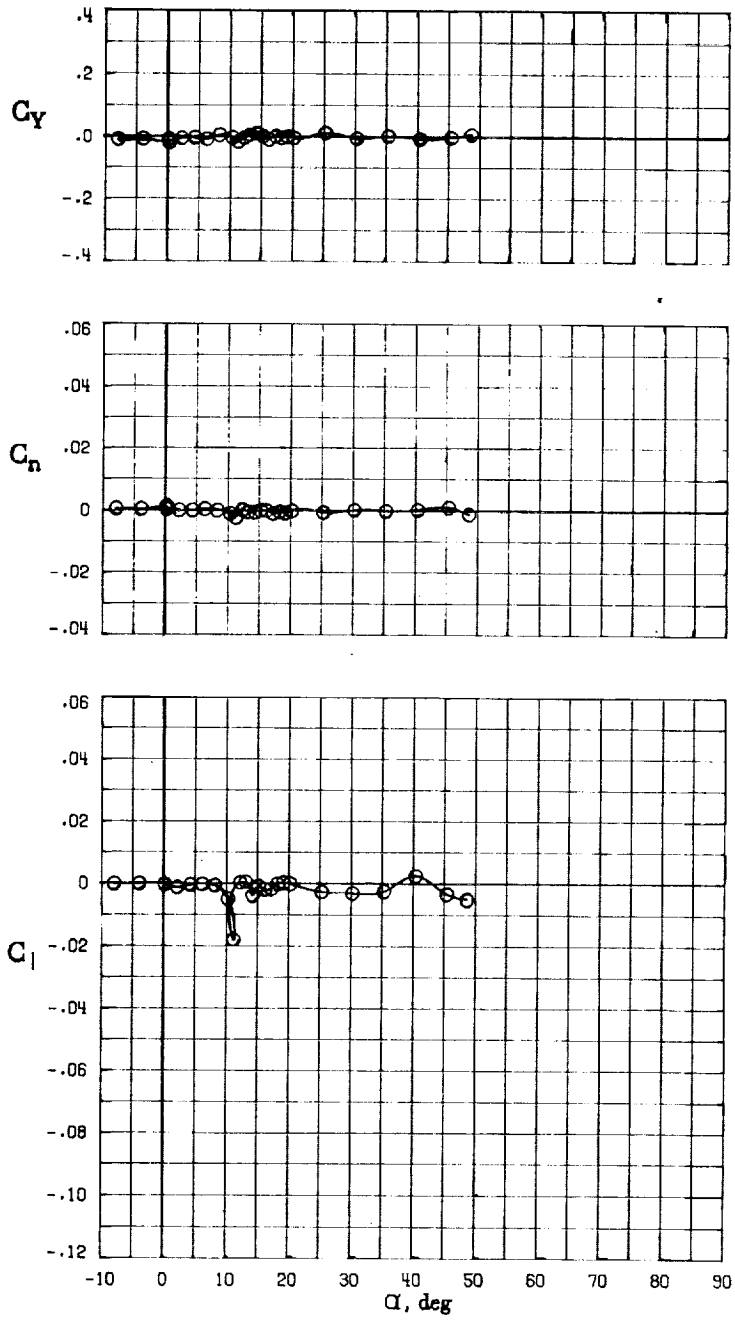

(C) LATERAL - DIRECTIONAL FORCE AND MOMENT COEFFICIENTS ABOUT BODY AXES AT ZERO SIDESLIP.

FIGURE 48. - CONTINUED.

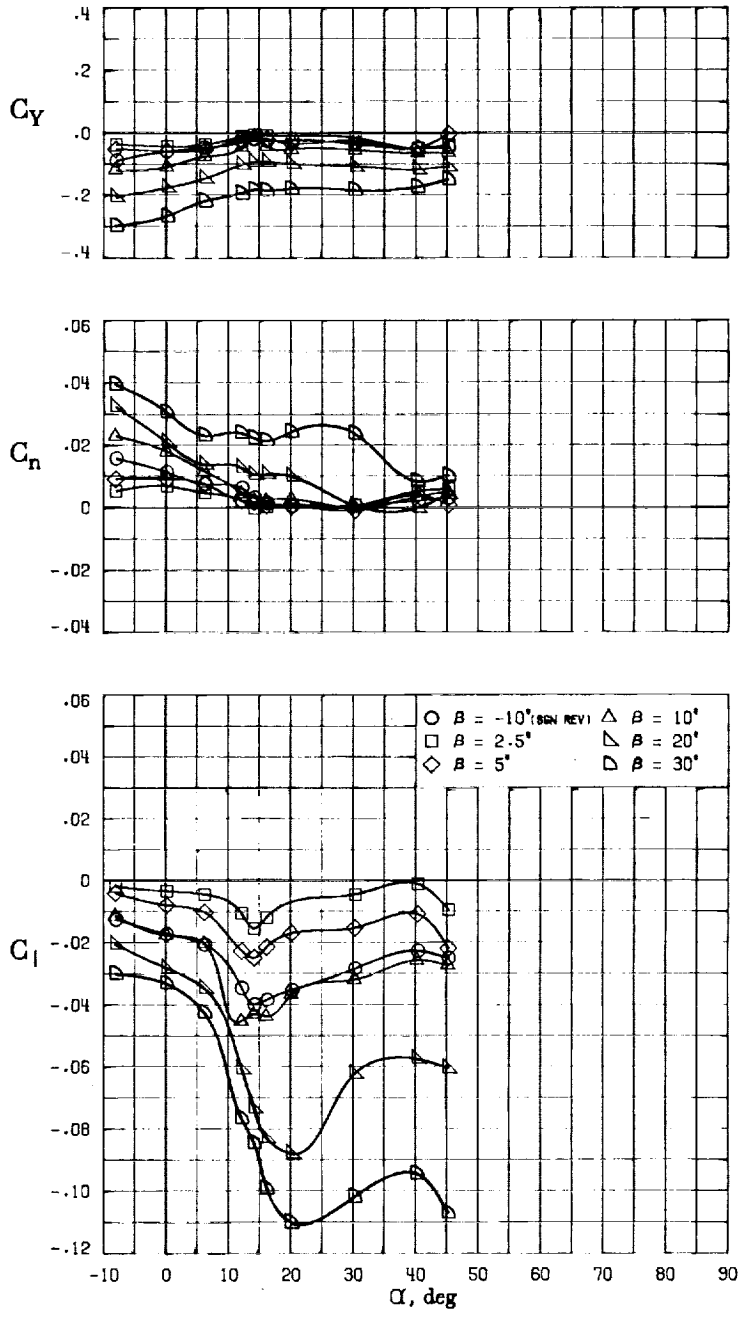

(D) LATERAL - DIRECTIONAL FORCE AND MOMENT COEFFICIENTS ABOUT BODY AXES.

FIGURE 48. - CONTINUED.

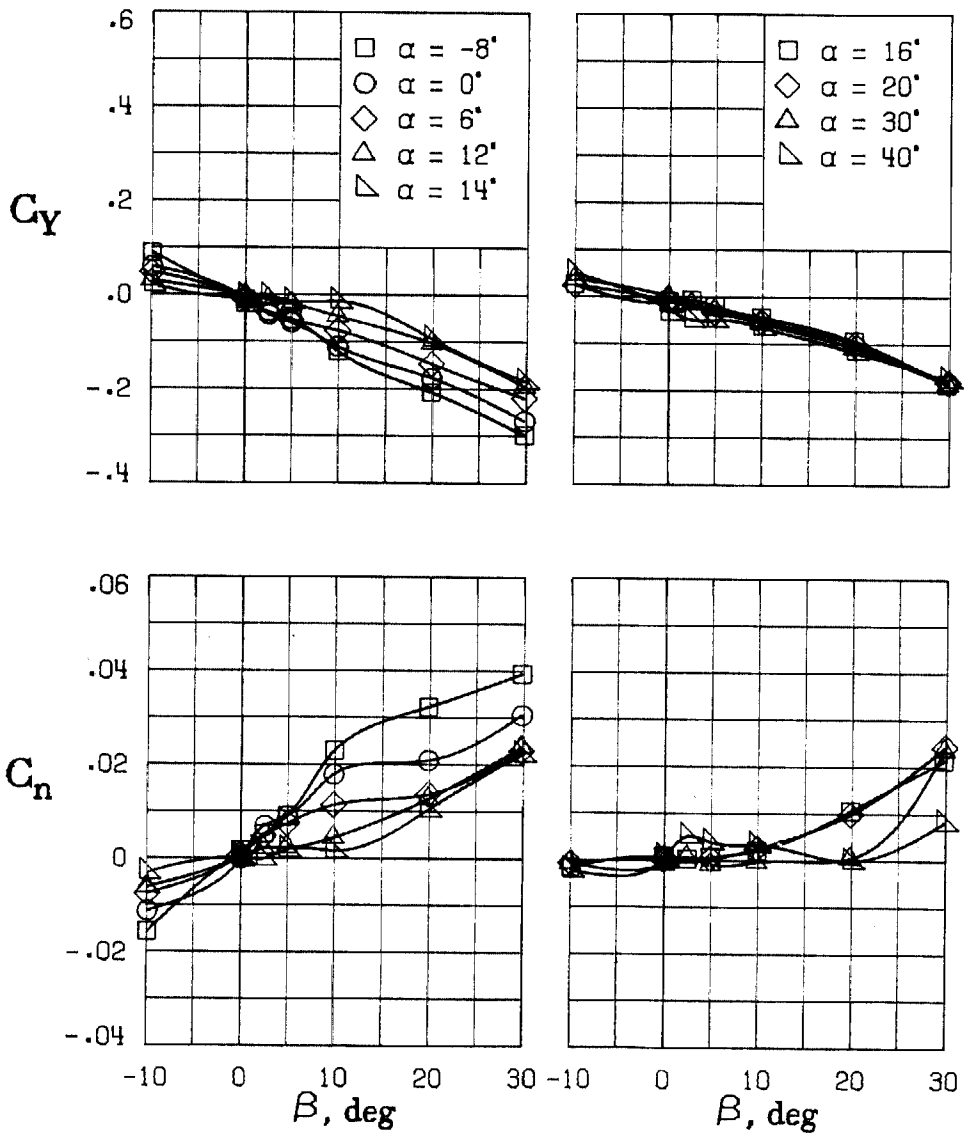

(E) DIRECTIONAL - STABILITY CHARACTERISTICS ABOUT BODY AXES AT VARIOUS ANGLES OF ATTACK.

FIGURE 48. - CONTINUED.

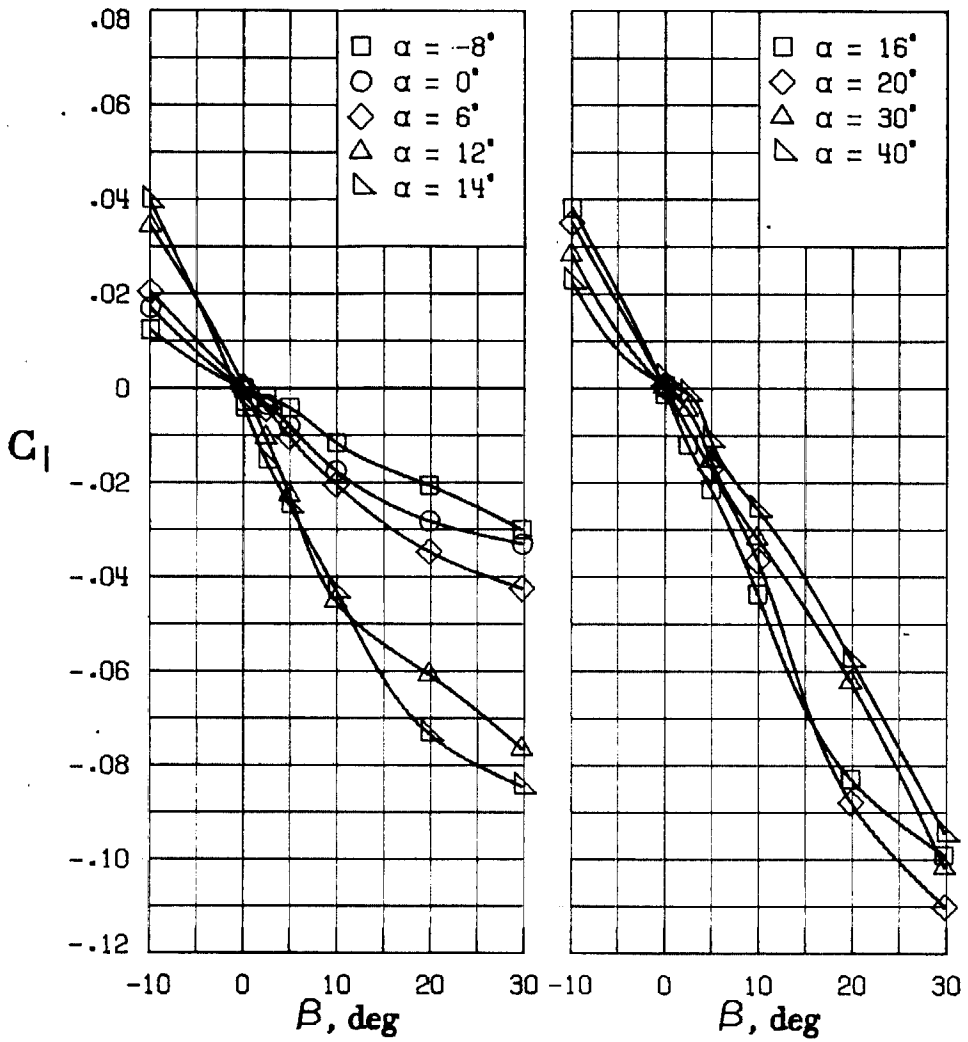

(F) LATERAL - STABILITY CHARACTERISTICS ABOUT BODY AXES AT VARIOUS ANGLES OF ATTACK.

FIGURE 48. - CONCLUDED.

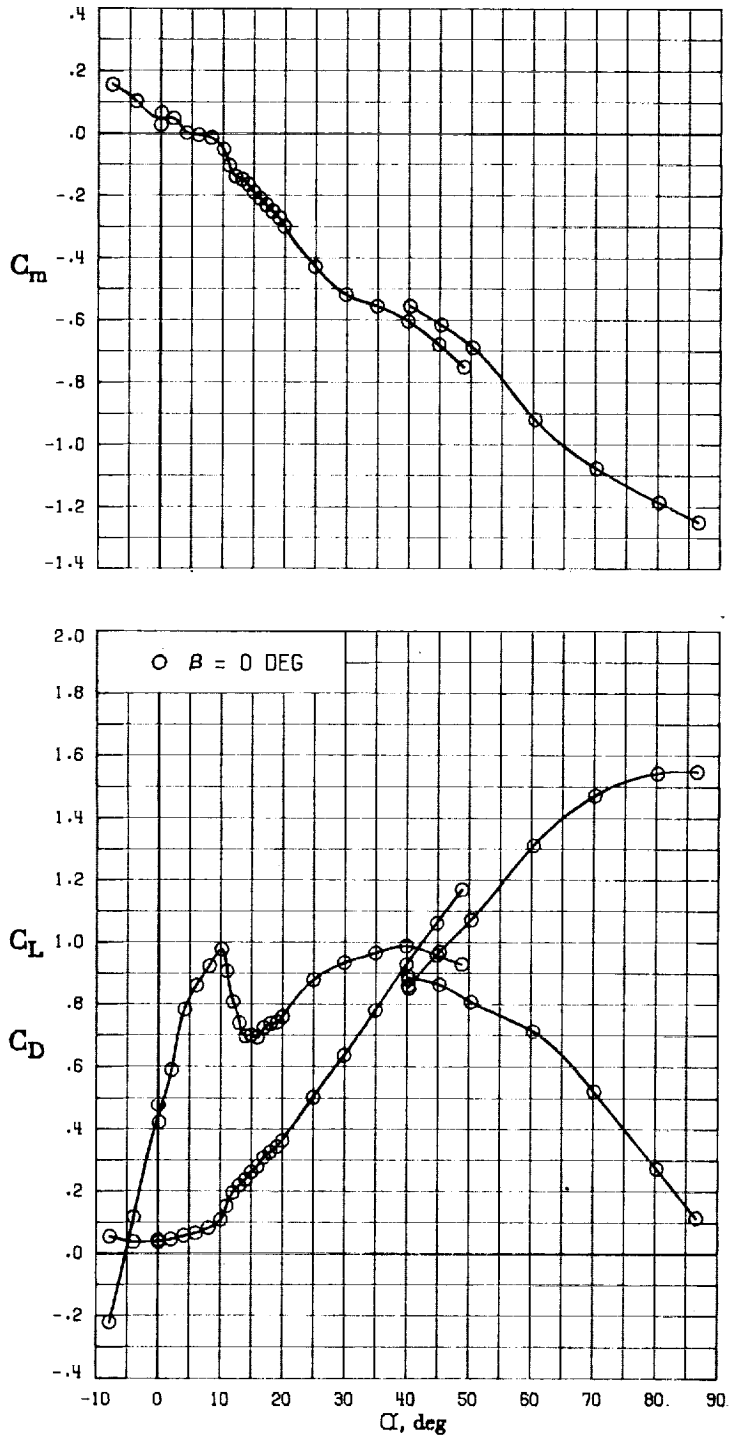

(A) LONGITUDINAL FORCE AND MOMENT COEFFICIENTS ABOUT STABILITY AXES.

FIGURE 49. - EFFECT OF ANGLE OF ATTACK AND SIDESLIP ANGLE ON AERODYNAMIC CHARACTERISTICS AT RE = .288 E+06 FOR CONFIGURATION B W1 H4 V. $\delta_E = 0°$, $\delta_A = 0°$, $\delta_R = 0°$.

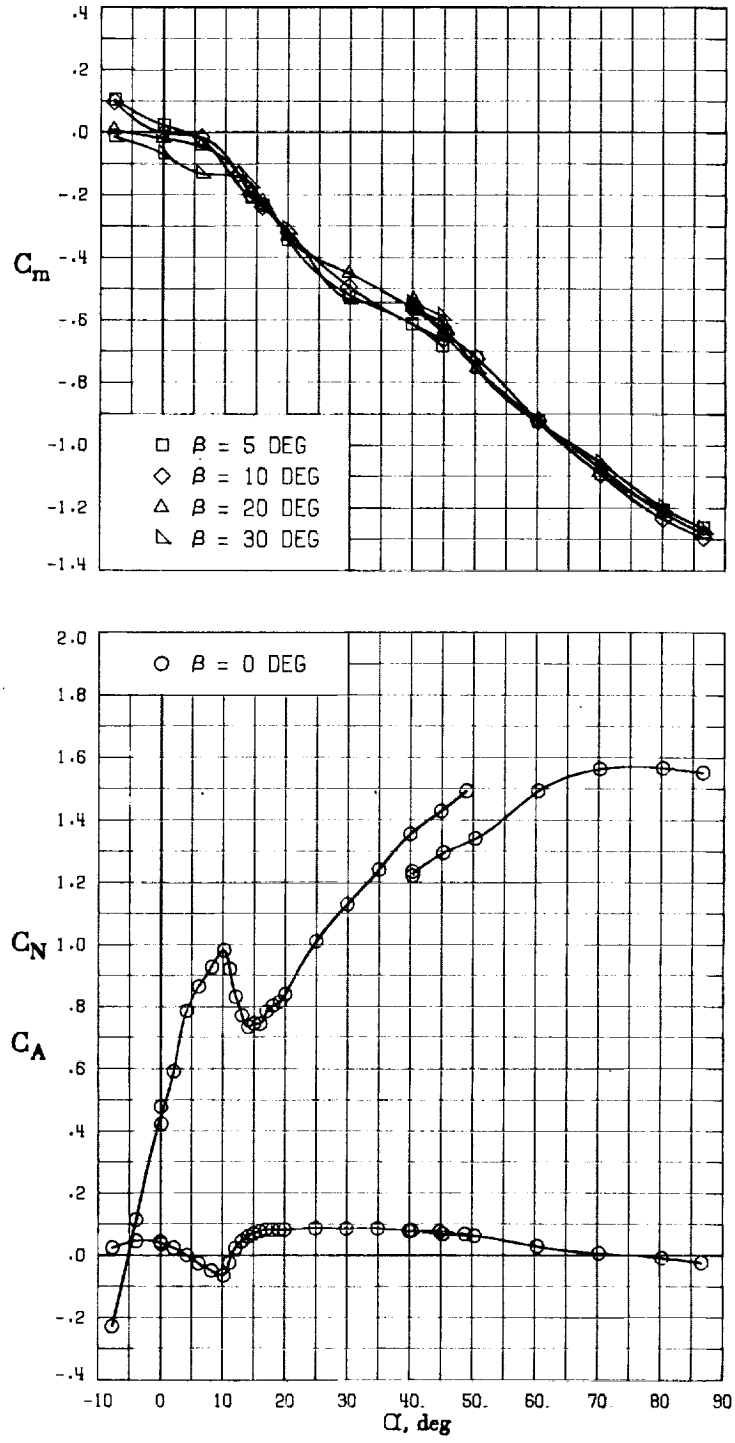

(B) LONGITUDINAL FORCE AND MOMENT COEFFICIENTS ABOUT BODY AXES.

FIGURE 49. - CONTINUED.

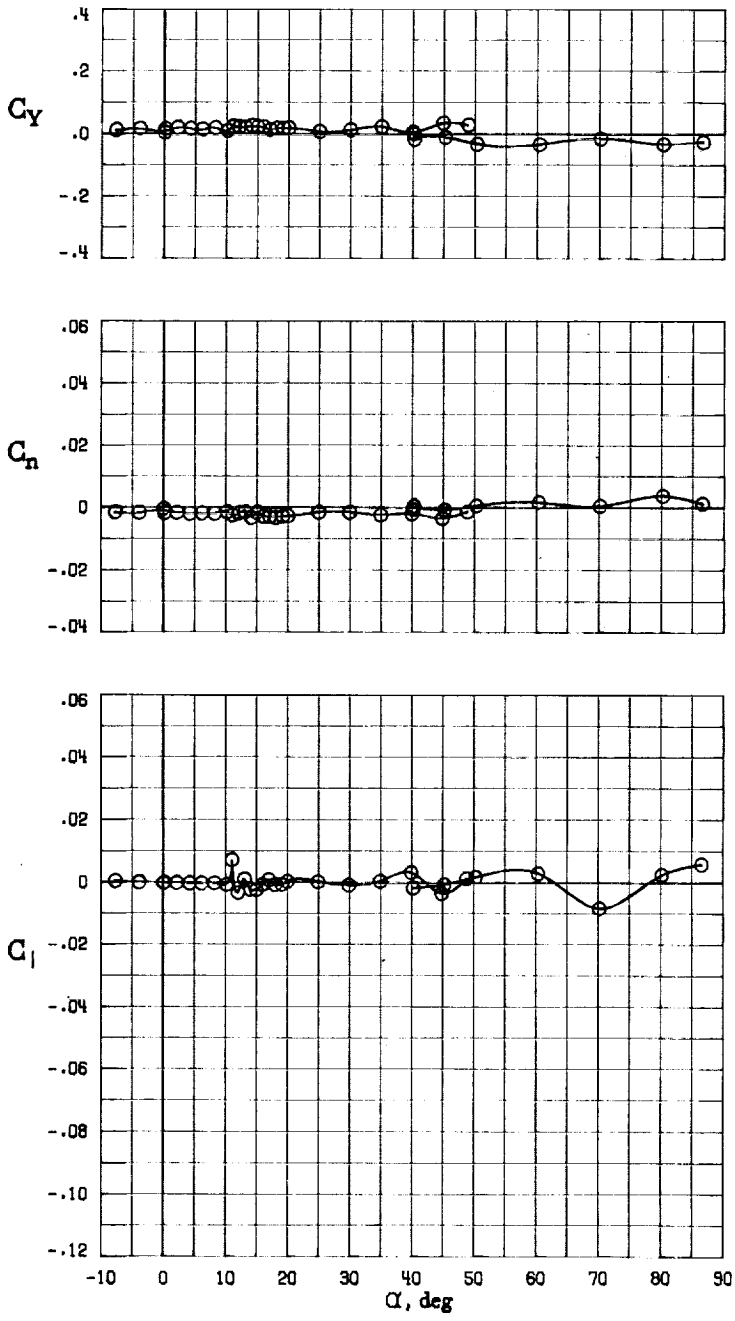

(C) LATERAL - DIRECTIONAL FORCE AND MOMENT COEFEICIENTS ABOUT BODY AXES AT ZERO SIDESLIP.

FIGURE 49. - CONTINUED.

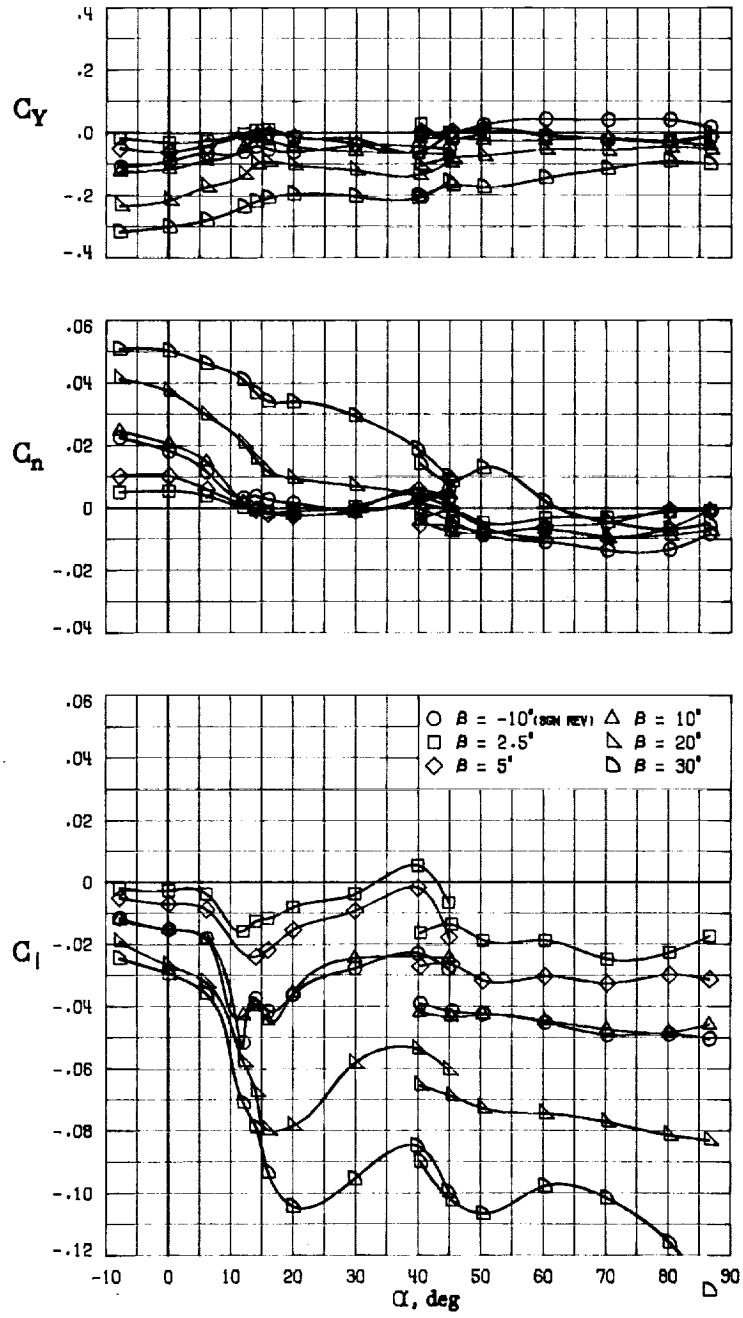

(D) LATERAL - DIRECTIONAL FORCE AND MOMENT COEFFICIENTS ABOUT BODY AXES.

FIGURE 49. - CONTINUED.

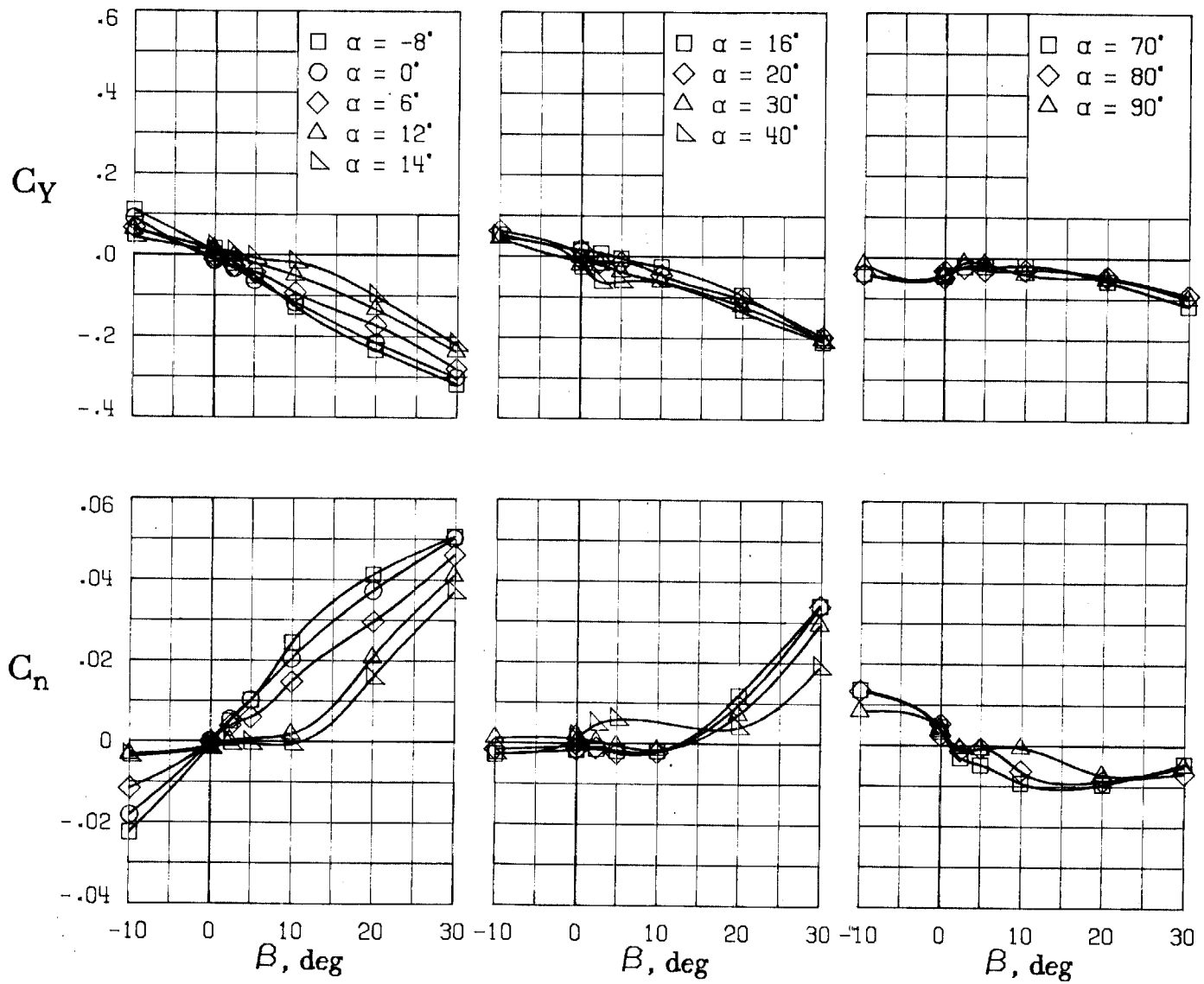

(E) DIRECTIONAL - STABILITY CHARACTERISTICS ABOUT BODY AXES AT VARIOUS ANGLES OF ATTACK.

FIGURE 49. - CONTINUED

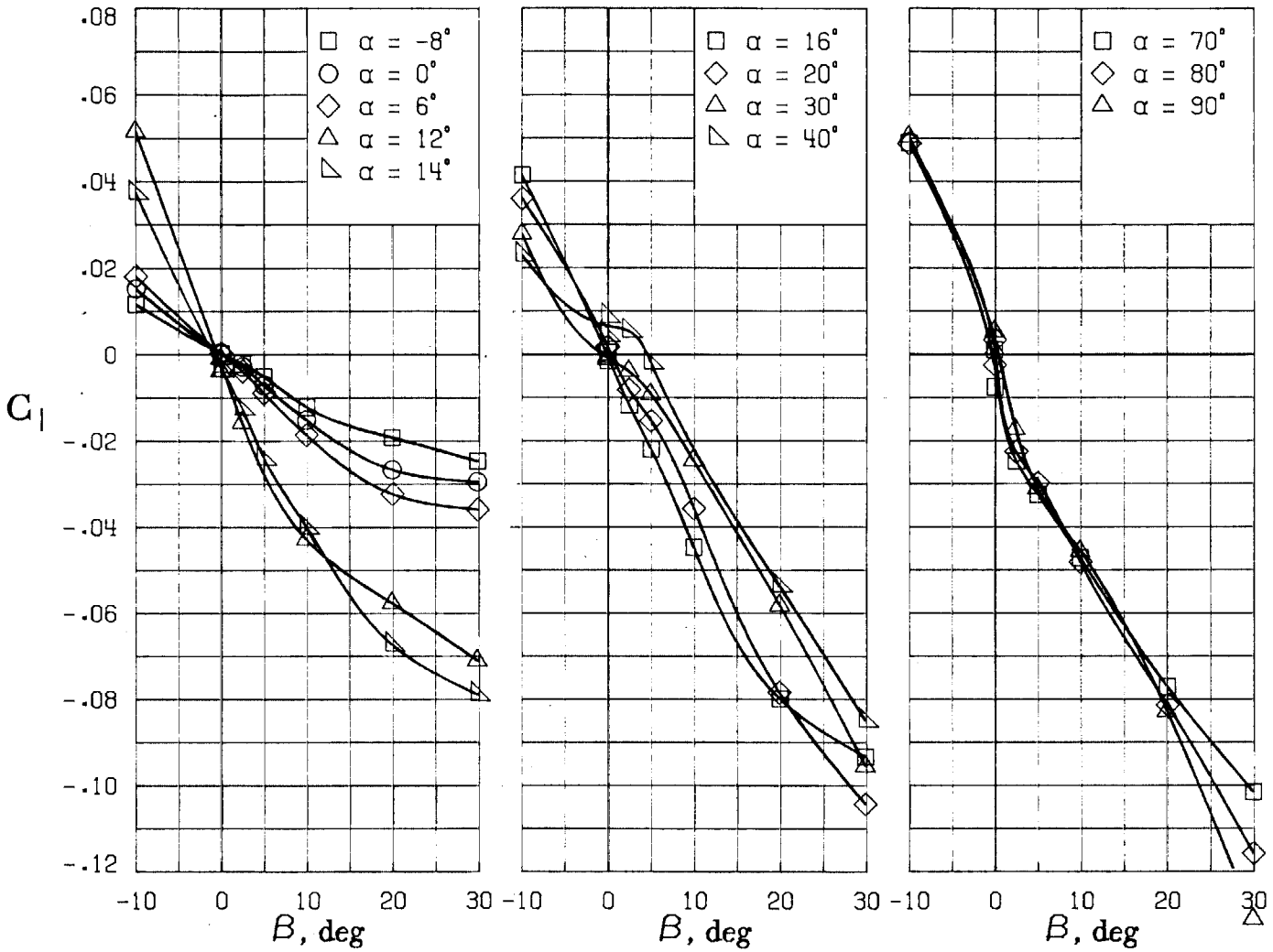

(F) LATERAL - STABILITY CHARACTERISTICS ABOUT BODY AXES AT VARIOUS ANGLES OF ATTACK.

FIGURE 49. - CONCLUDED.

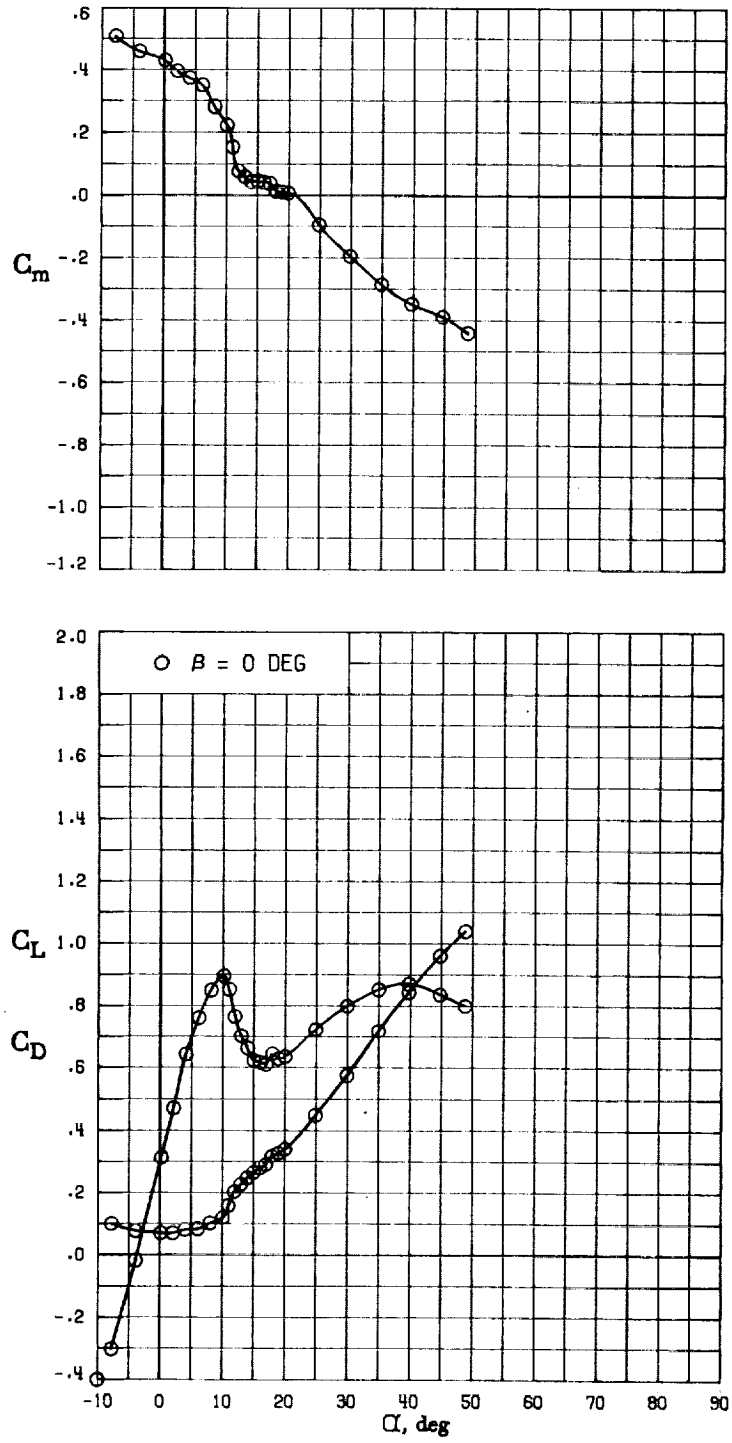

(A) LONGITUDINAL FORCE AND MOMENT COEFFICIENTS ABOUT STABILITY AXES.

FIGURE 50. - EFFECT OF ANGLE OF ATTACK AND SIDESLIP ANGLE ON AERODYNAMIC CHARACTERISTICS AT RE = .288 E+06 FOR CONFIGURATION B W1 H4 V. δ_E = -25°, δ_A = 0°, δ_R = 0°.

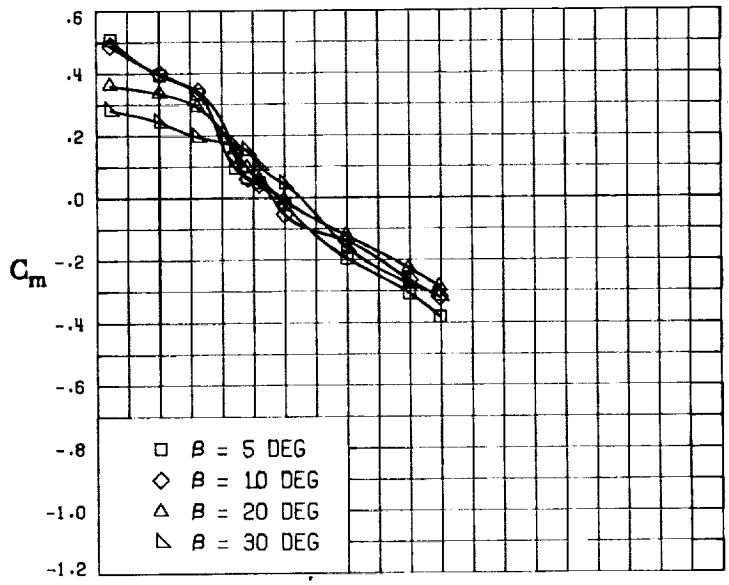

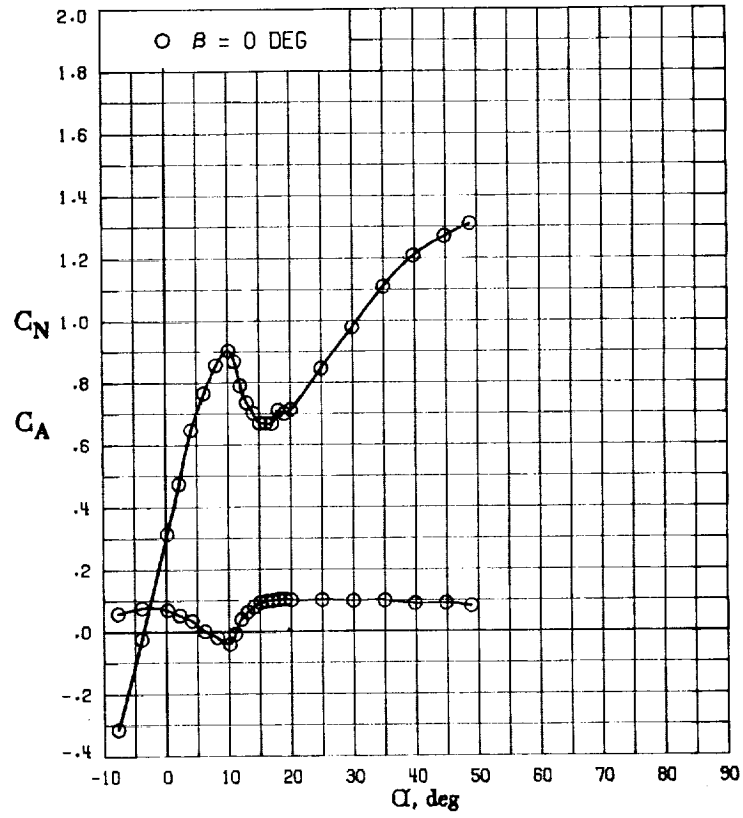

(B) LONGITUDINAL FORCE AND MOMENT COEFFICIENTS ABOUT BODY AXES.

FIGURE 50. - CONTINUED.

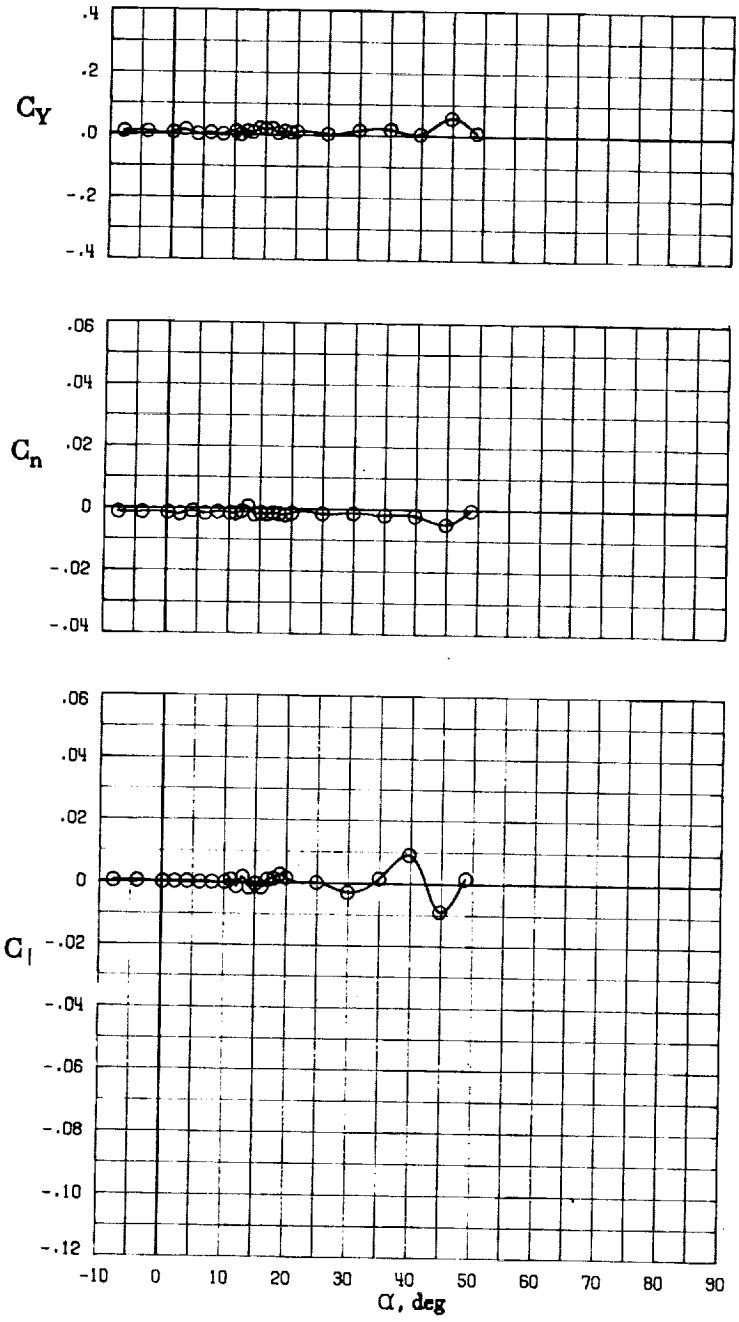

(C) LATERAL - DIRECTIONAL FORCE AND MOMENT COEFFICIENTS ABOUT BODY AXES AT ZERO SIDESLIP.

FIGURE 50. - CONTINUED.

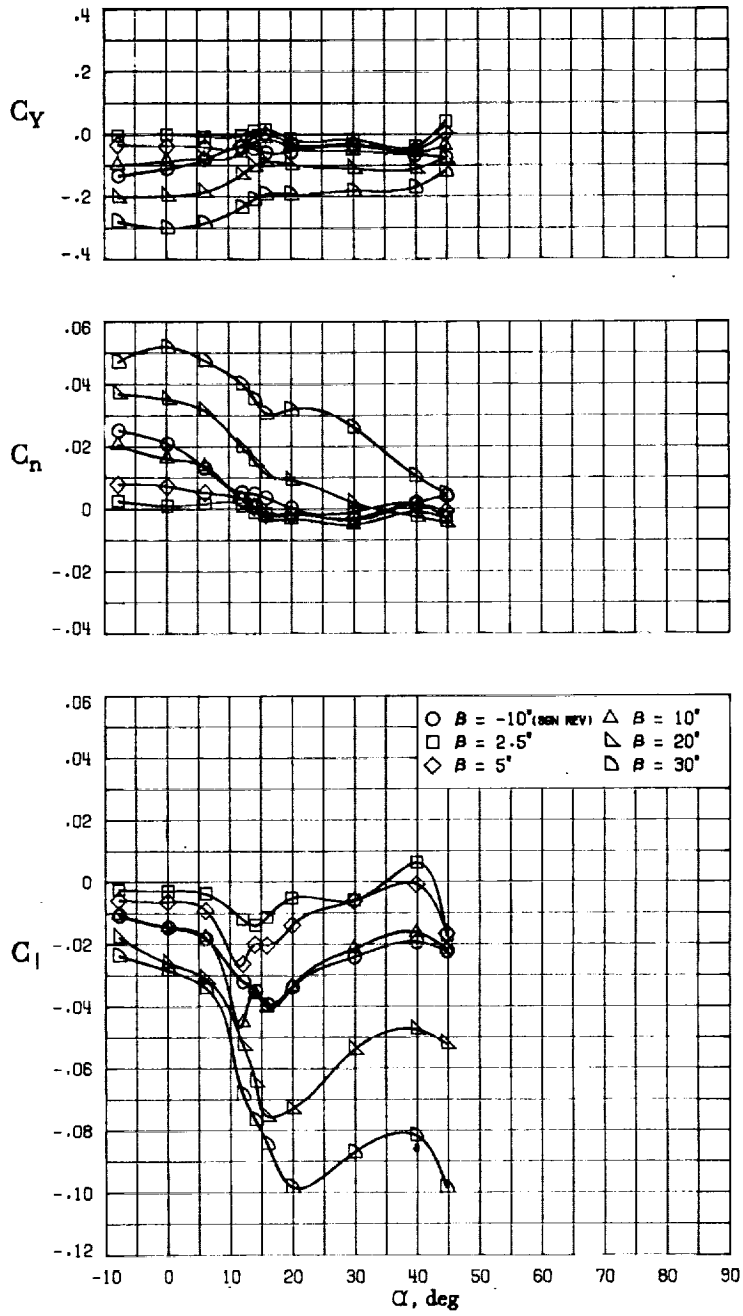

(D) LATERAL - DIRECTIONAL FORCE AND MOMENT COEFFICIENTS ABOUT BODY AXES.

FIGURE 50. - CONTINUED.

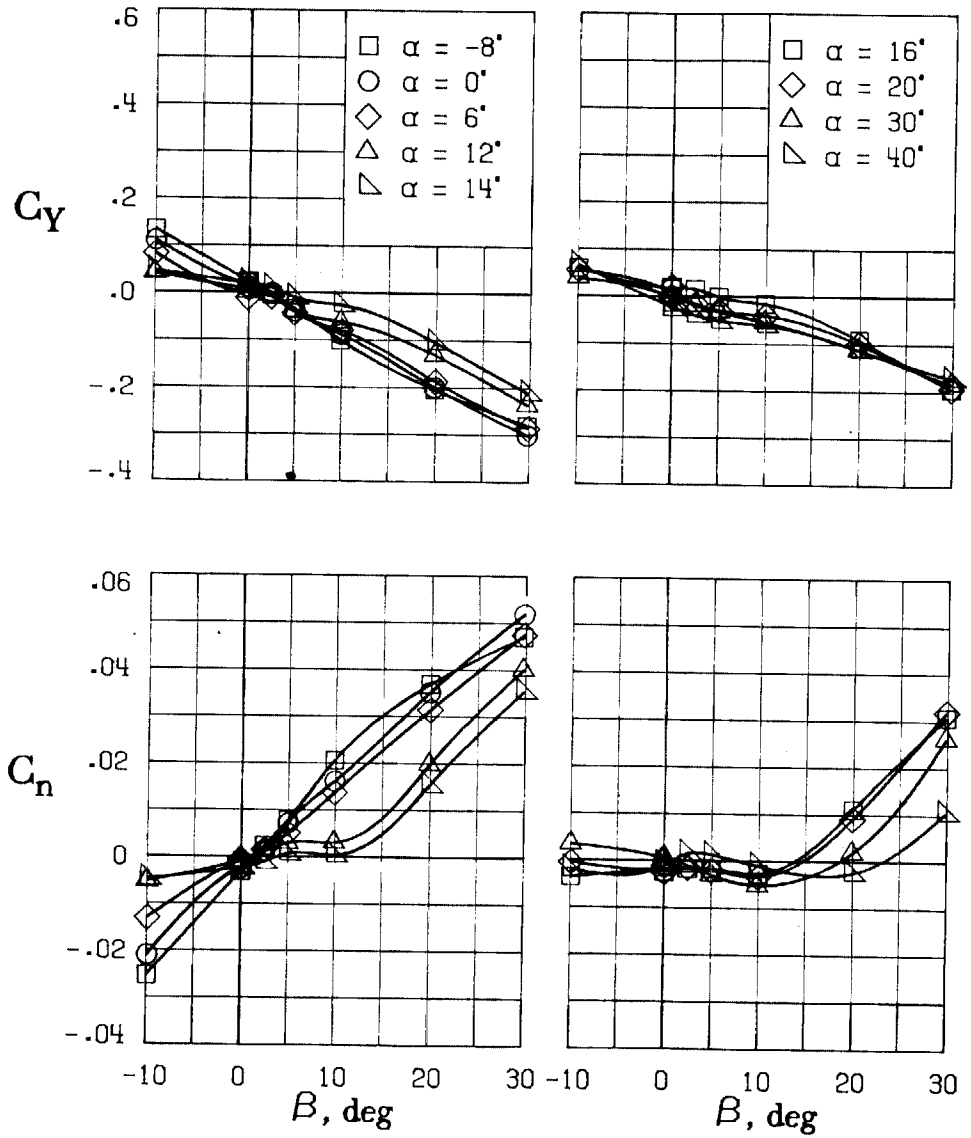

(E) DIRECTIONAL - STABILITY CHARACTERISTICS ABOUT BODY AXES AT VARIOUS ANGLES OF ATTACK.

FIGURE 50. - CONTINUED.

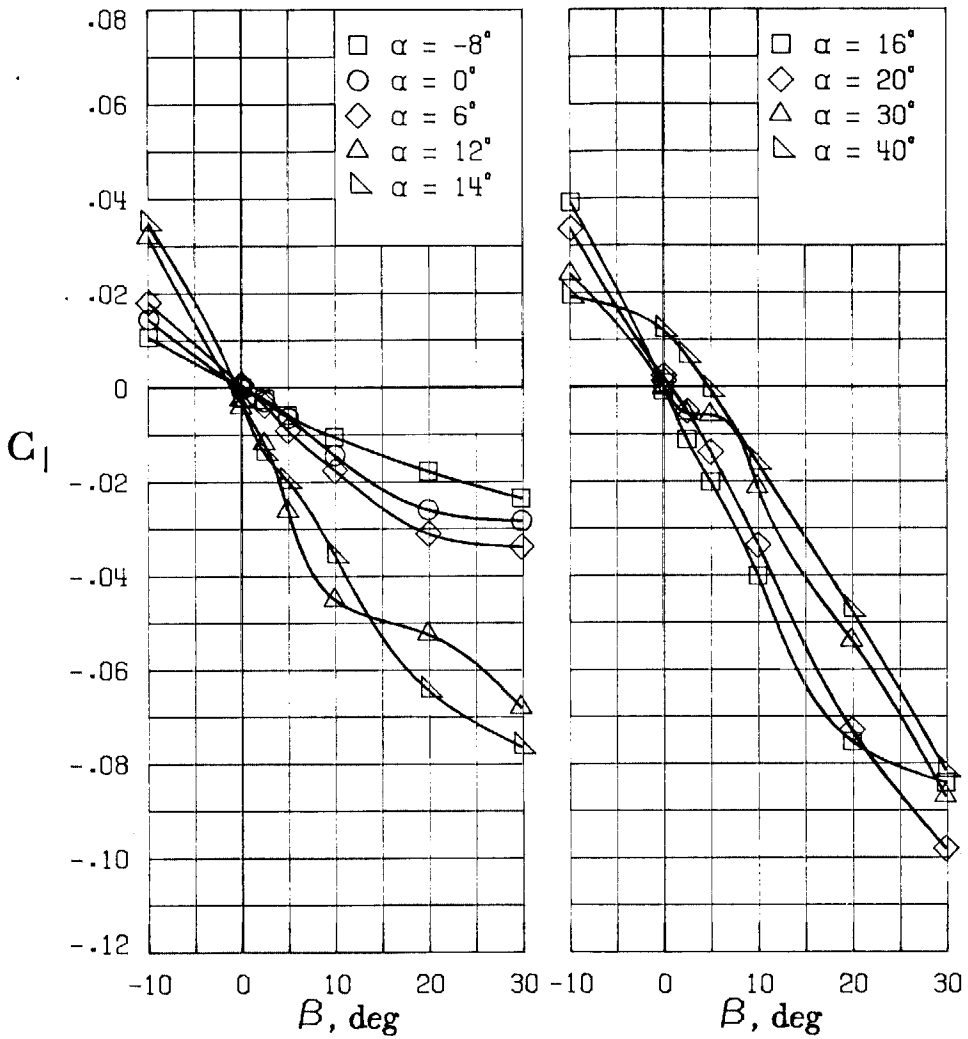

(F) LATERAL - STABILITY CHARACTERISTICS ABOUT BODY AXES AT VARIOUS ANGLES OF ATTACK.

FIGURE 50. - CONCLUDED.

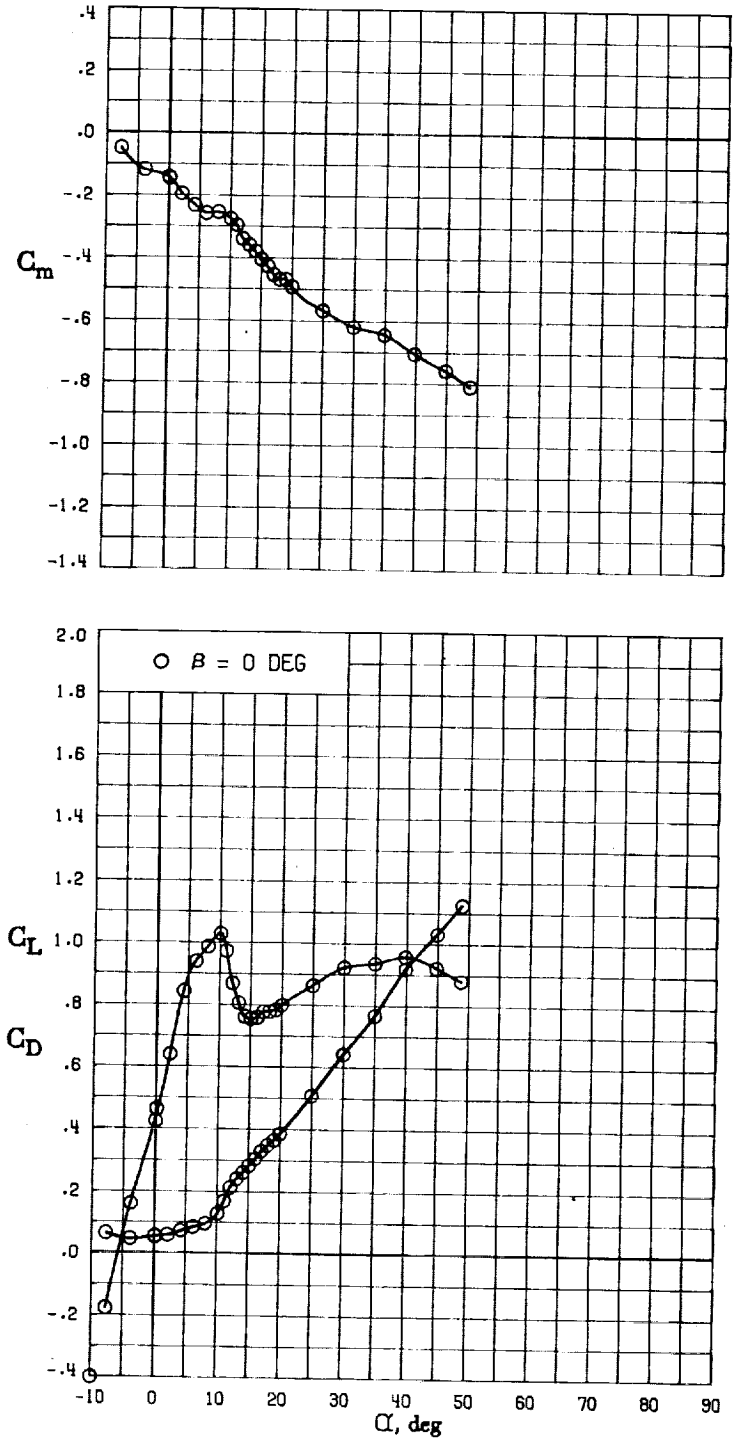

(A) LONGITUDINAL FORCE AND MOMENT COEFFICIENTS ABOUT STABILITY AXES.

FIGURE 51. - EFFECT OF ANGLE OF ATTACK AND SIDESLIP ANGLE ON AERODYNAMIC CHARACTERISTICS AT RE = .288 E+06 FOR CONFIGURATION B W1 H4 V. $\delta_E = 15°$, $\delta_A = 0°$, $\delta_R = 0°$.

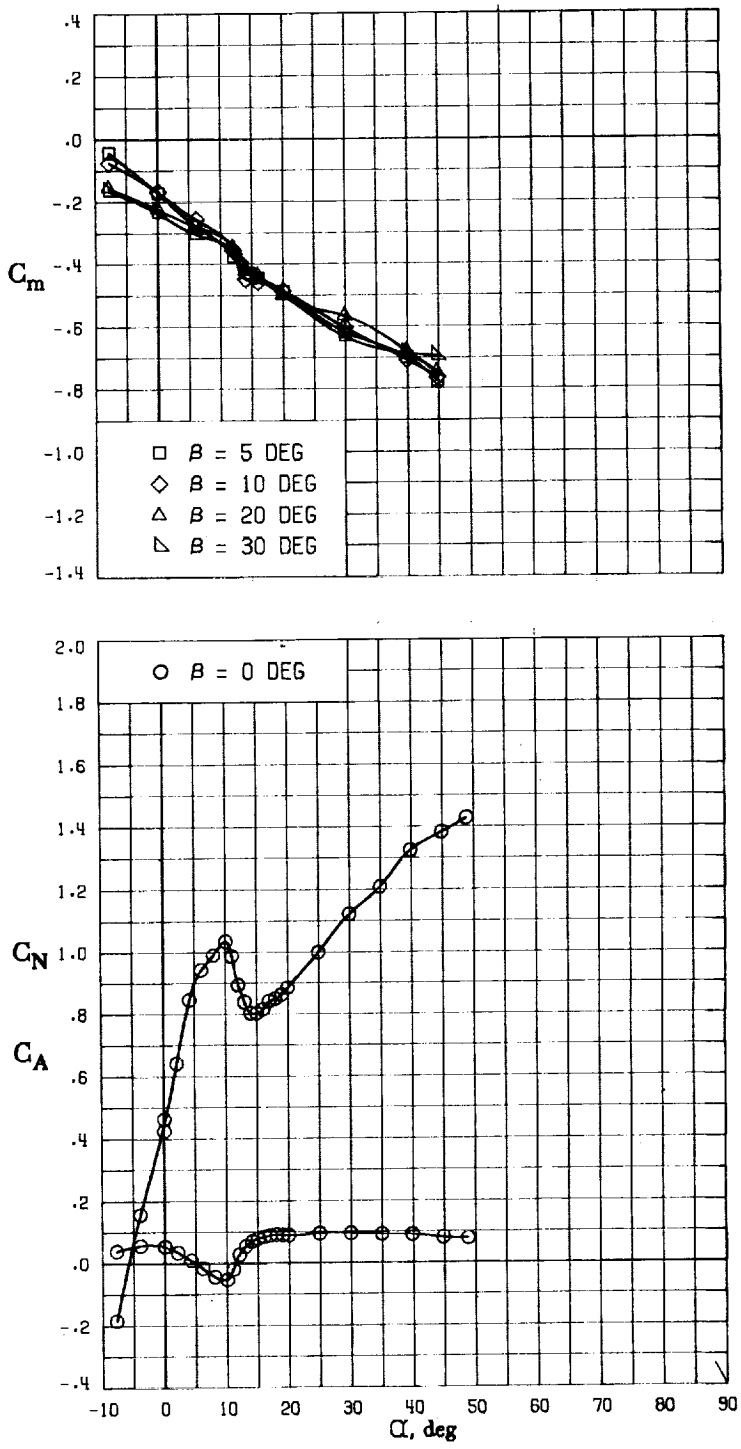

(B) LONGITUDINAL FORCE AND MOMENT COEFFICIENTS ABOUT BODY AXES.

FIGURE 51. - CONTINUED.

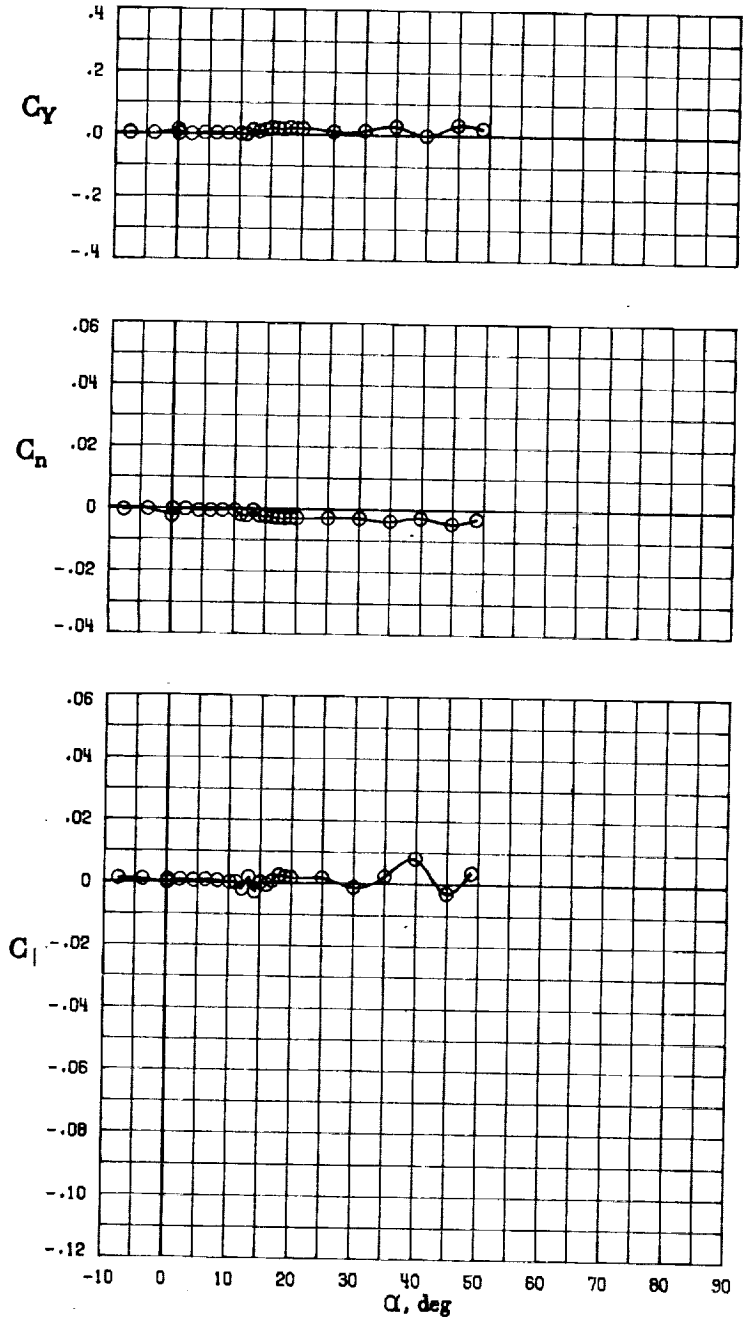

(C) LATERAL - DIRECTIONAL FORCE AND MOMENT COEFFICIENTS ABOUT BODY AXES AT ZERO SIDESLIP.

FIGURE 51. - CONTINUED.

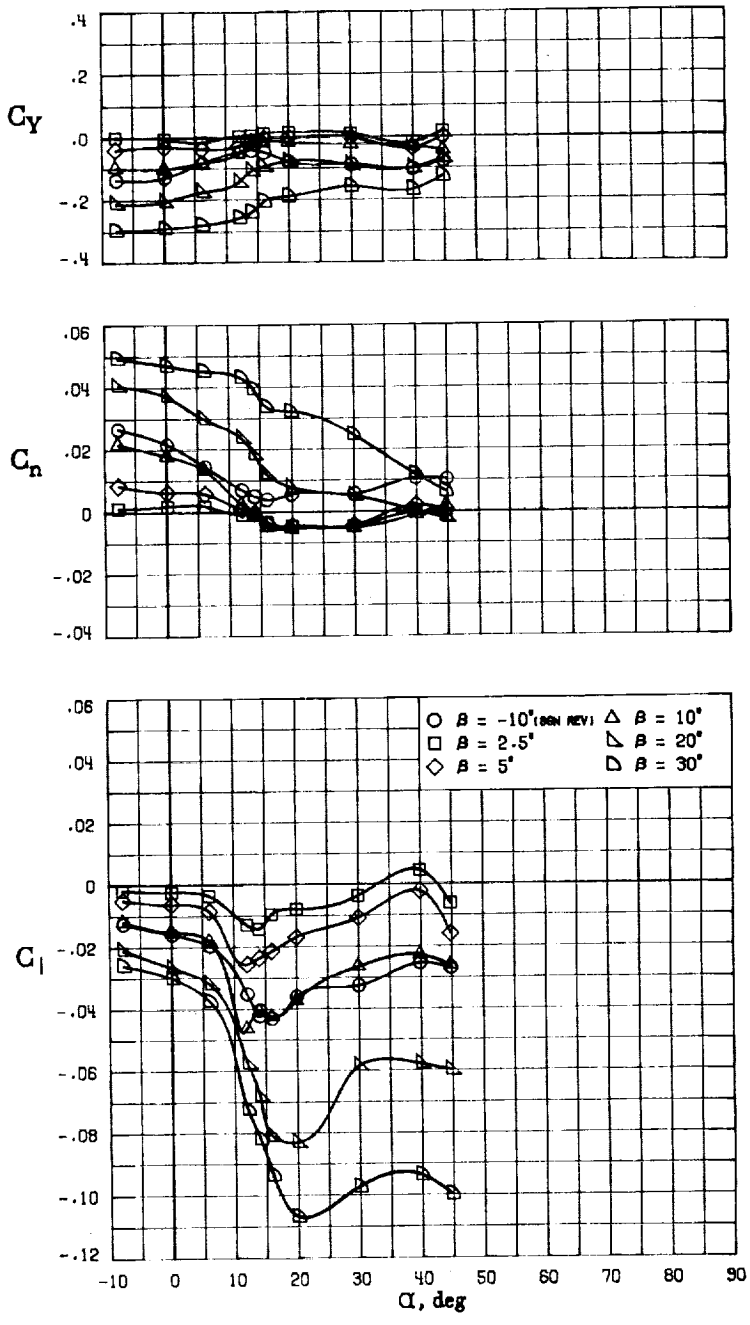

(D) LATERAL - DIRECTIONAL FORCE AND MOMENT COEFFICIENTS ABOUT BODY AXES.

FIGURE 51. - CONTINUED.

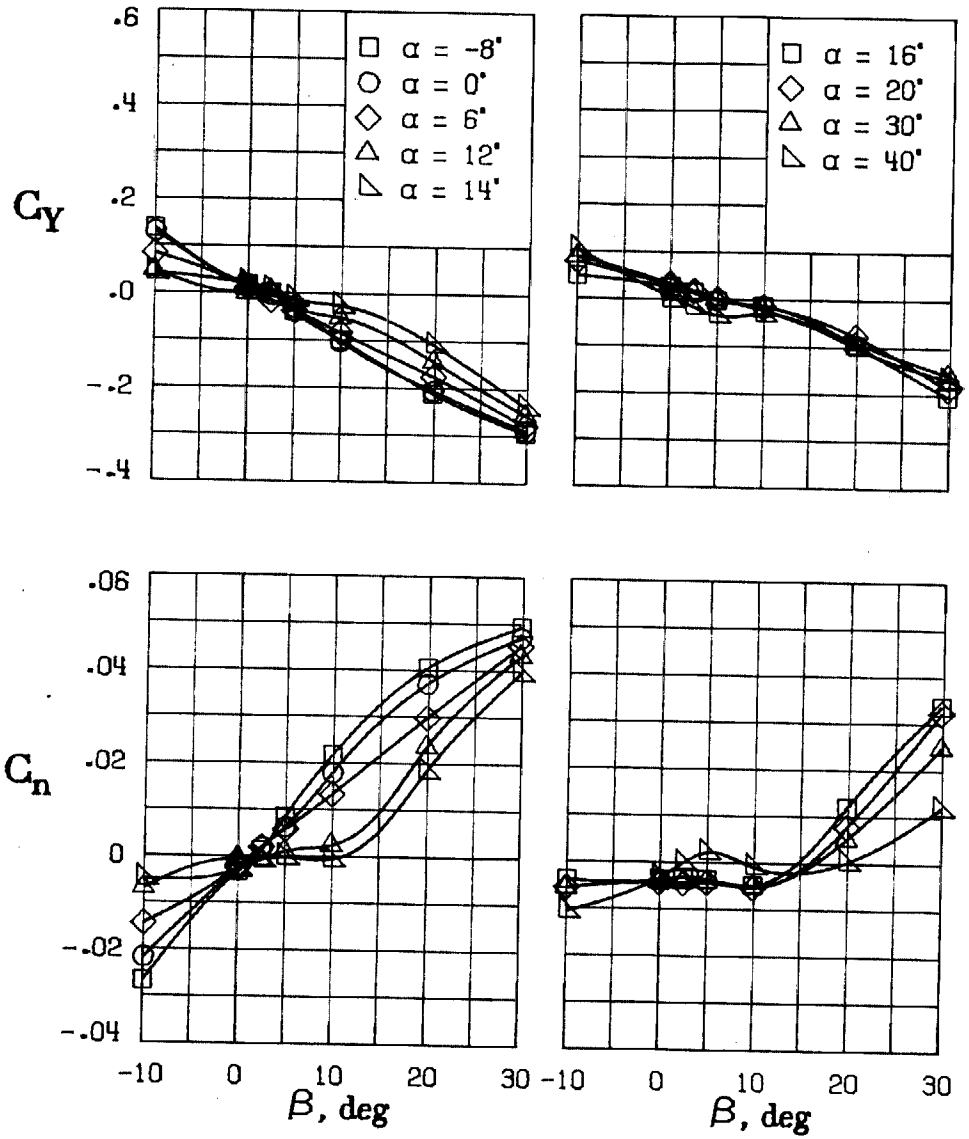

(E) DIRECTIONAL - STABILITY CHARACTERISTICS ABOUT BODY AXES AT VARIOUS ANGLES OF ATTACK.

FIGURE 51. - CONTINUED.

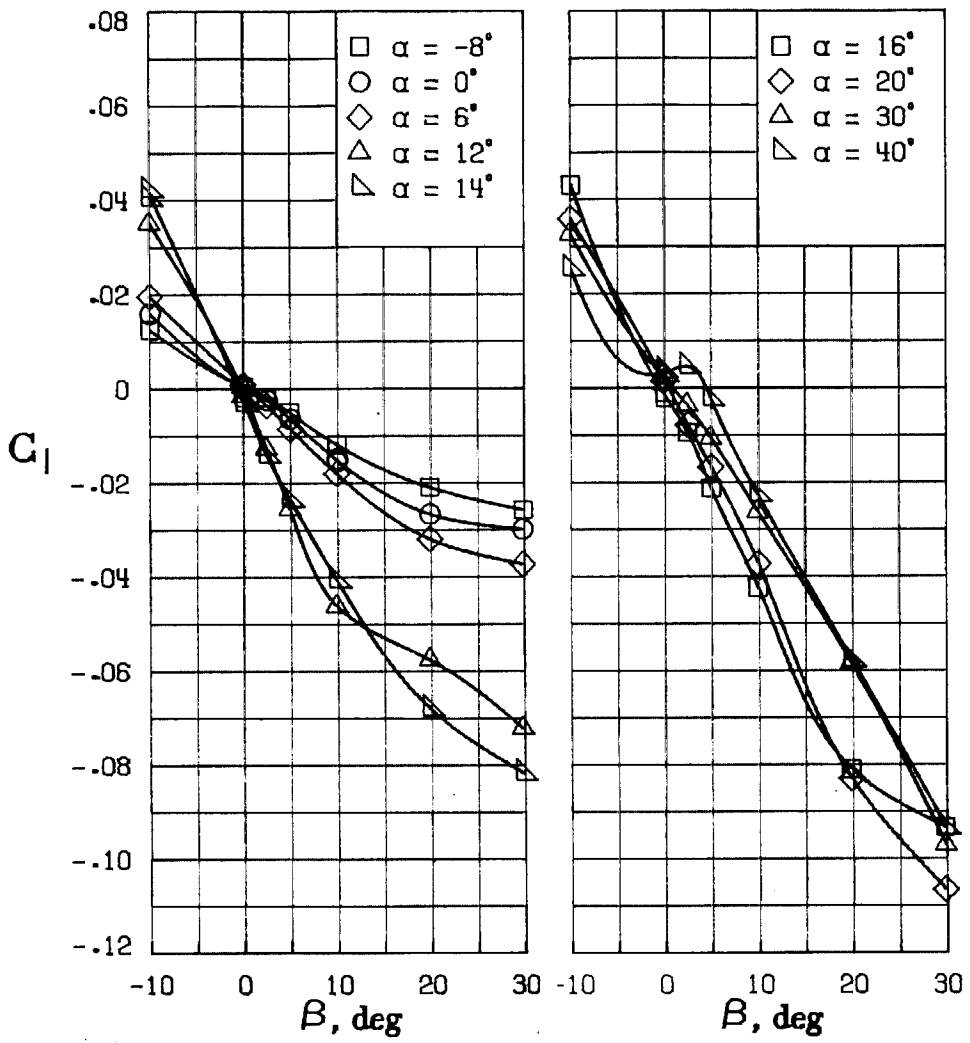

(F) LATERAL - STABILITY CHARACTERISTICS ABOUT BODY AXES AT VARIOUS ANGLES OF ATTACK.

FIGURE 51. - CONCLUDED.

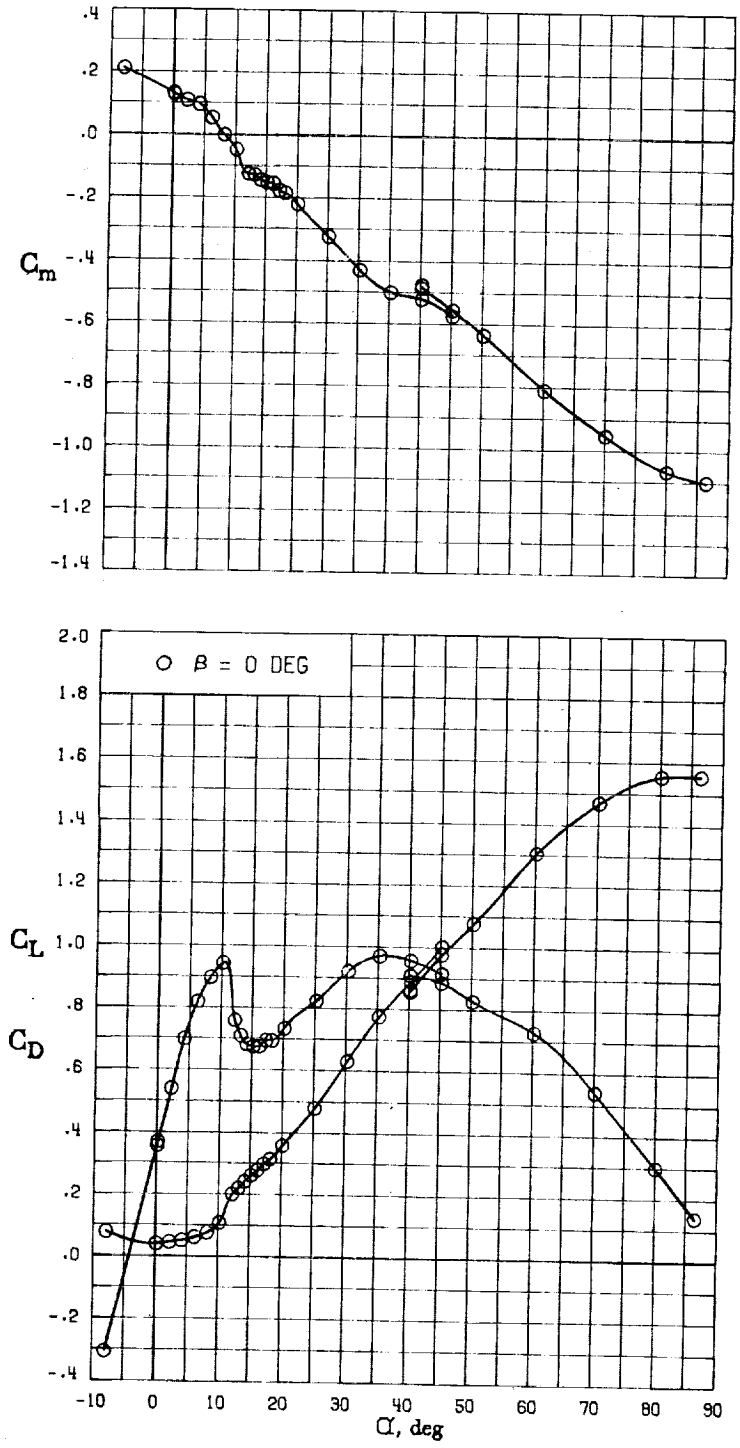

(A) LONGITUDINAL FORCE AND MOMENT COEFFICIENTS ABOUT STABILITY AXES.

FIGURE 52. - EFFECT OF ANGLE OF ATTACK AND SIDESLIP ANGLE ON AERODYNAMIC CHARACTERISTICS AT RE = .288 E+06 FOR CONFIGURATION B W1 H3 V. $\delta_E = 0°$, $\delta_A = 0°$, $\delta_R = 0°$.

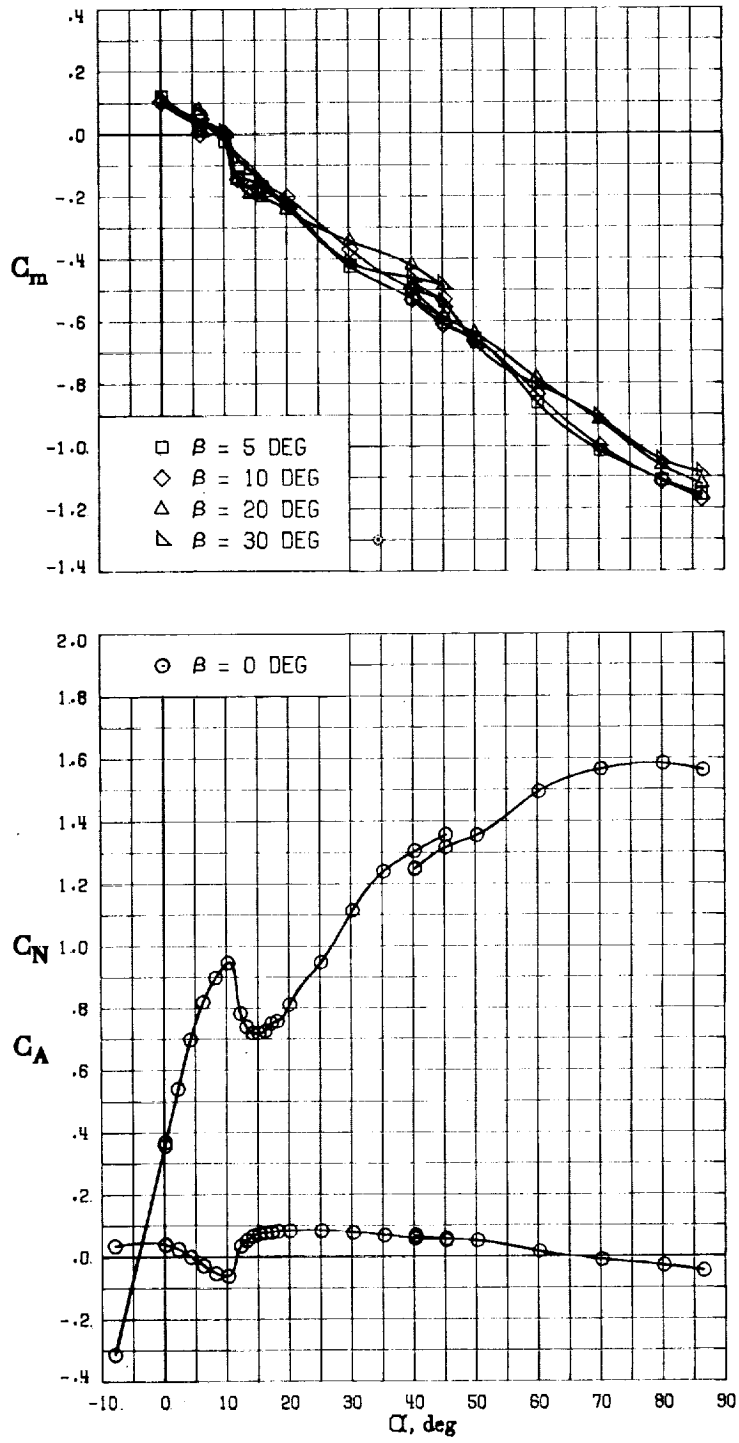

(B) LONGITUDINAL FORCE AND MOMENT COEFFICIENTS ABOUT BODY AXES.

FIGURE 52. - CONTINUED.

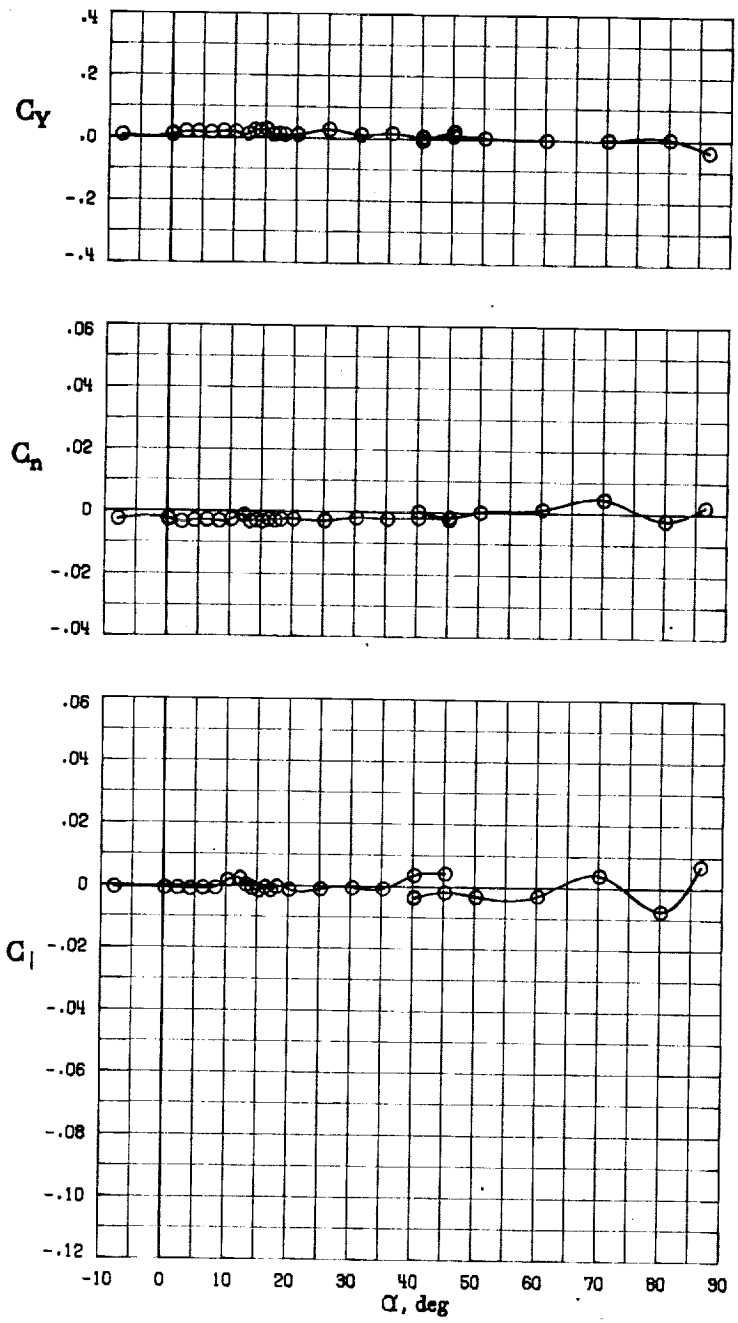

(C) LATERAL - DIRECTIONAL FORCE AND MOMENT COEFFICIENTS ABOUT BODY AXES AT ZERO SIDESLIP.

FIGURE 52. - CONTINUED.

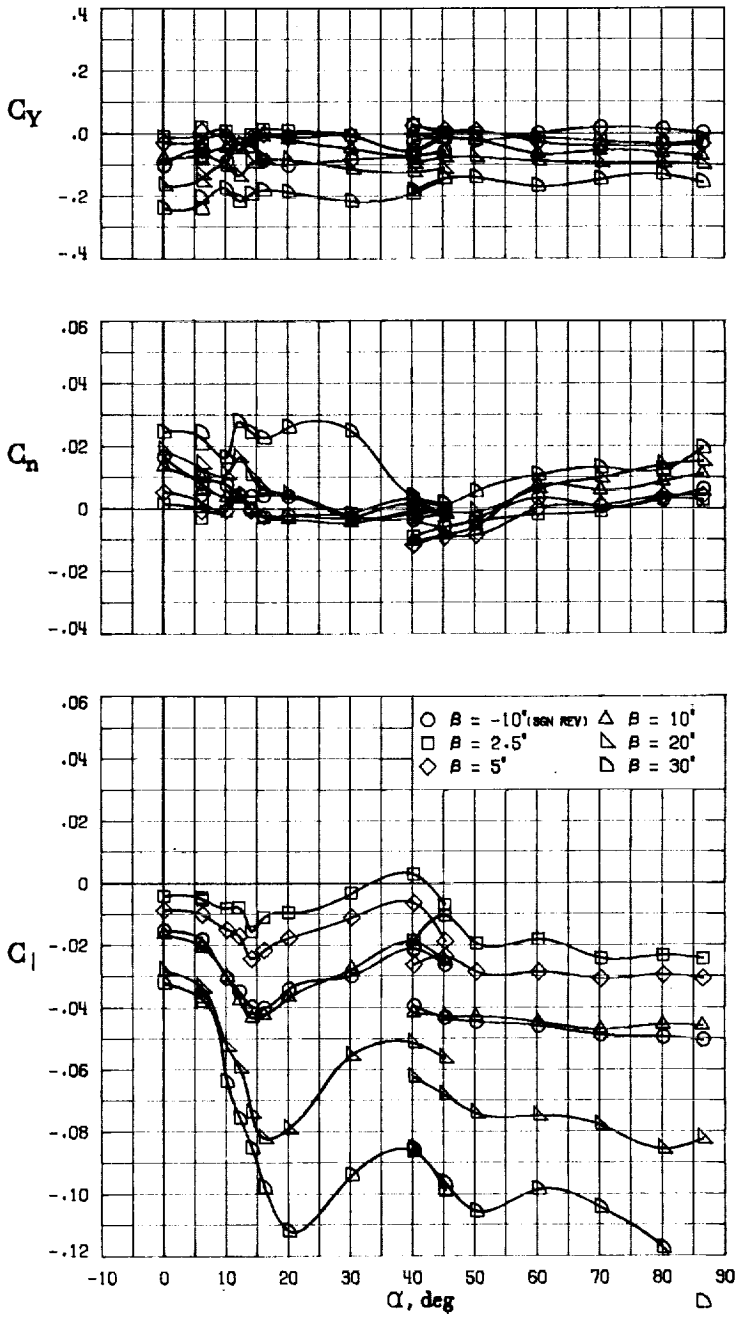

(D) LATERAL - DIRECTIONAL FORCE AND MOMENT COEFFICIENTS ABOUT BODY AXES.

FIGURE 52. - CONTINUED.

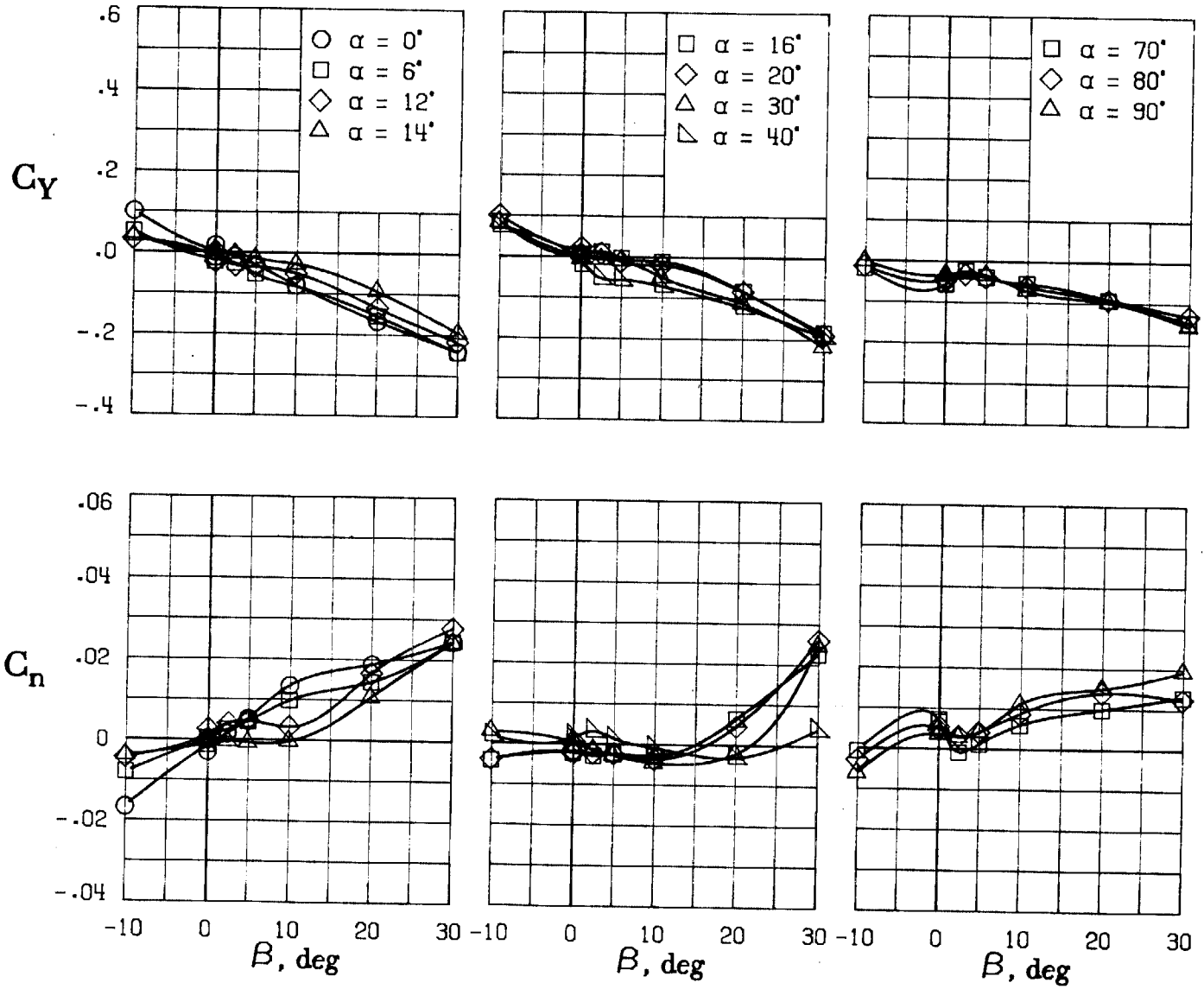

(E) DIRECTIONAL - STABILITY CHARACTERISTICS ABOUT BODY AXES AT VARIOUS ANGLES OF ATTACK.

FIGURE 52. - CONTINUED.

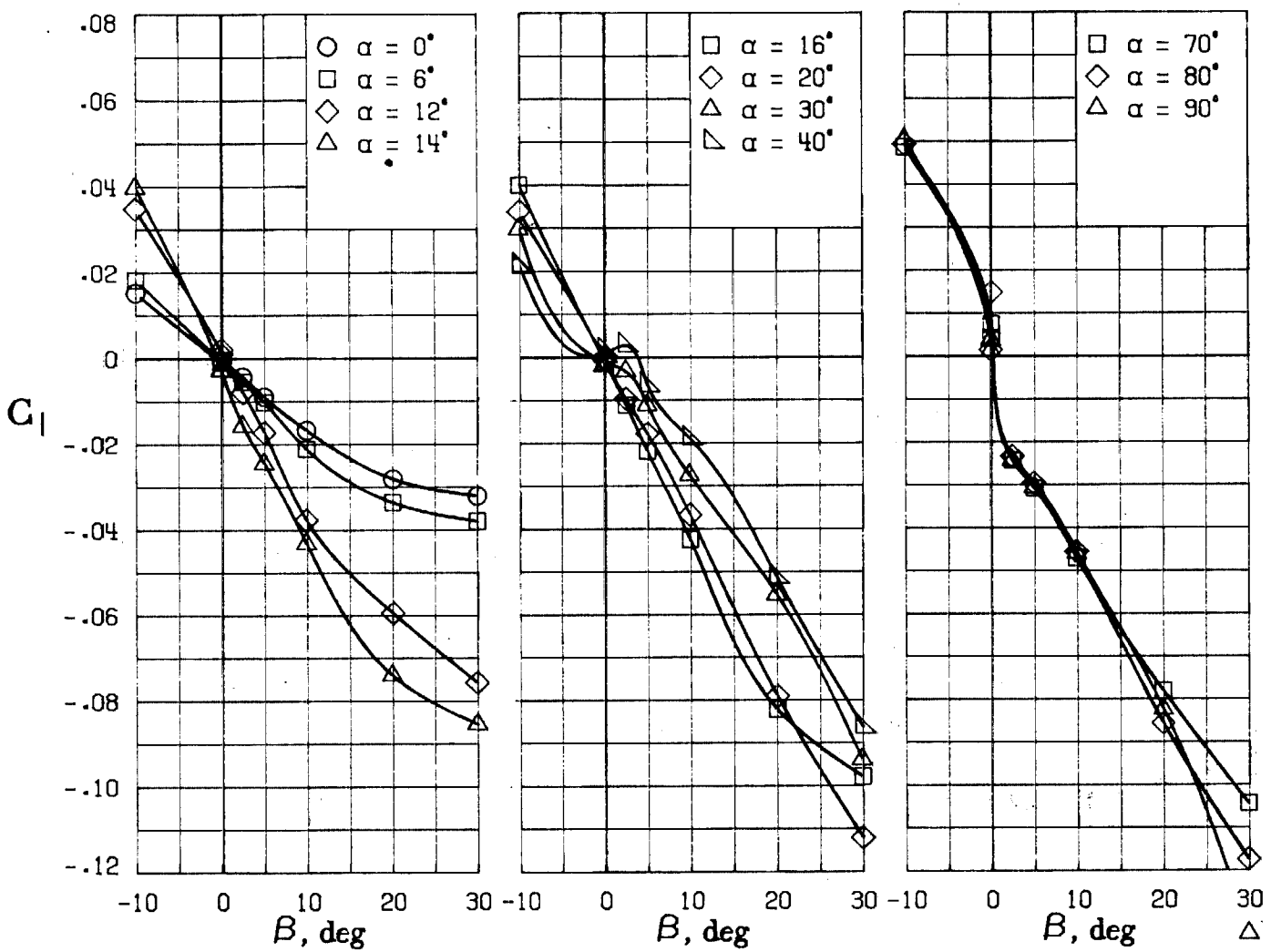

(F) LATERAL - STABILITY CHARACTERISTICS ABOUT BODY AXES AT VARIOUS ANGLES OF ATTACK.

FIGURE 52. - CONCLUDED.

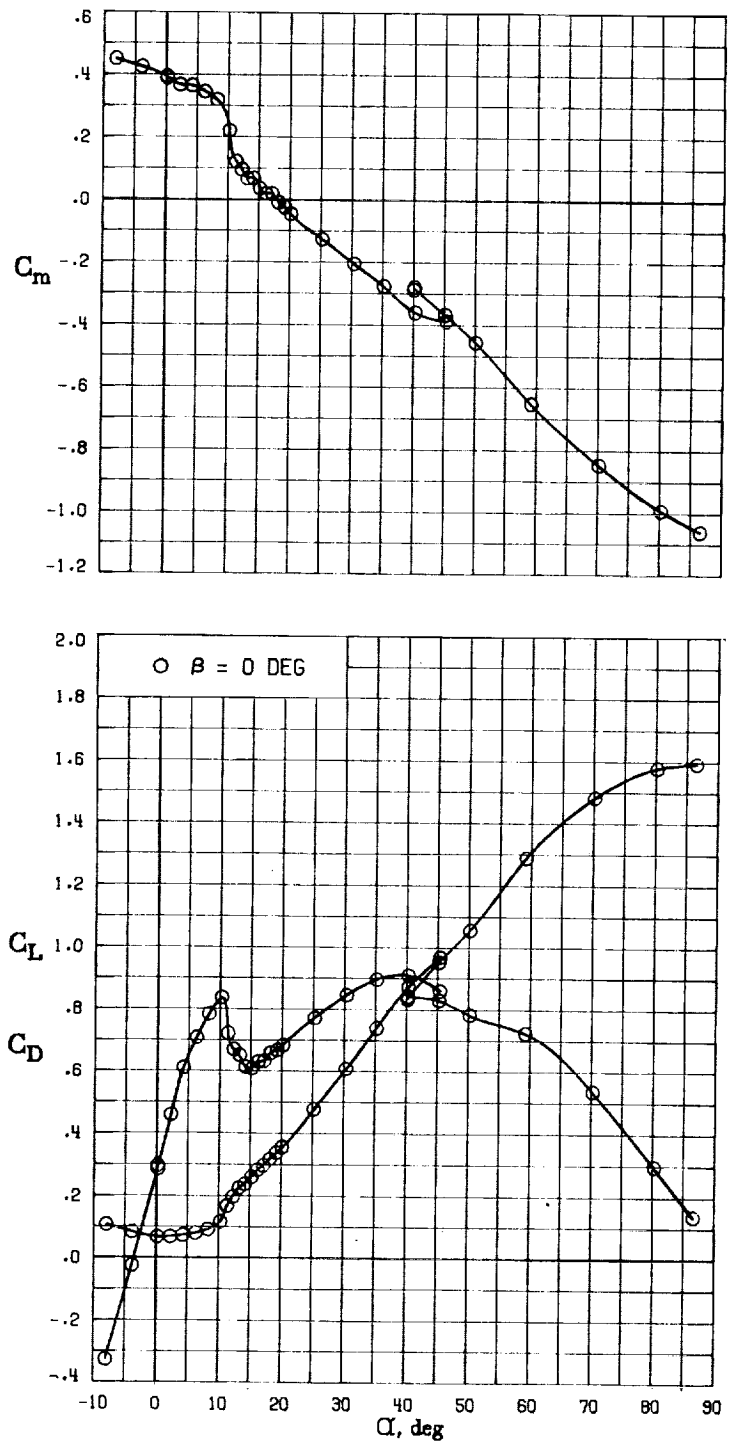

(A) LONGITUDINAL FORCE AND MOMENT COEFFICIENTS ABOUT STABILITY AXES.

FIGURE 53. - EFFECT OF ANGLE OF ATTACK AND SIDESLIP ANGLE ON AERODYNAMIC CHARACTERISTICS AT RE = .288 E+06 FOR CONFIGURATION B W1 H3 V. $\delta_E = -25°$, $\delta_A = 0°$, $\delta_R = 0°$.

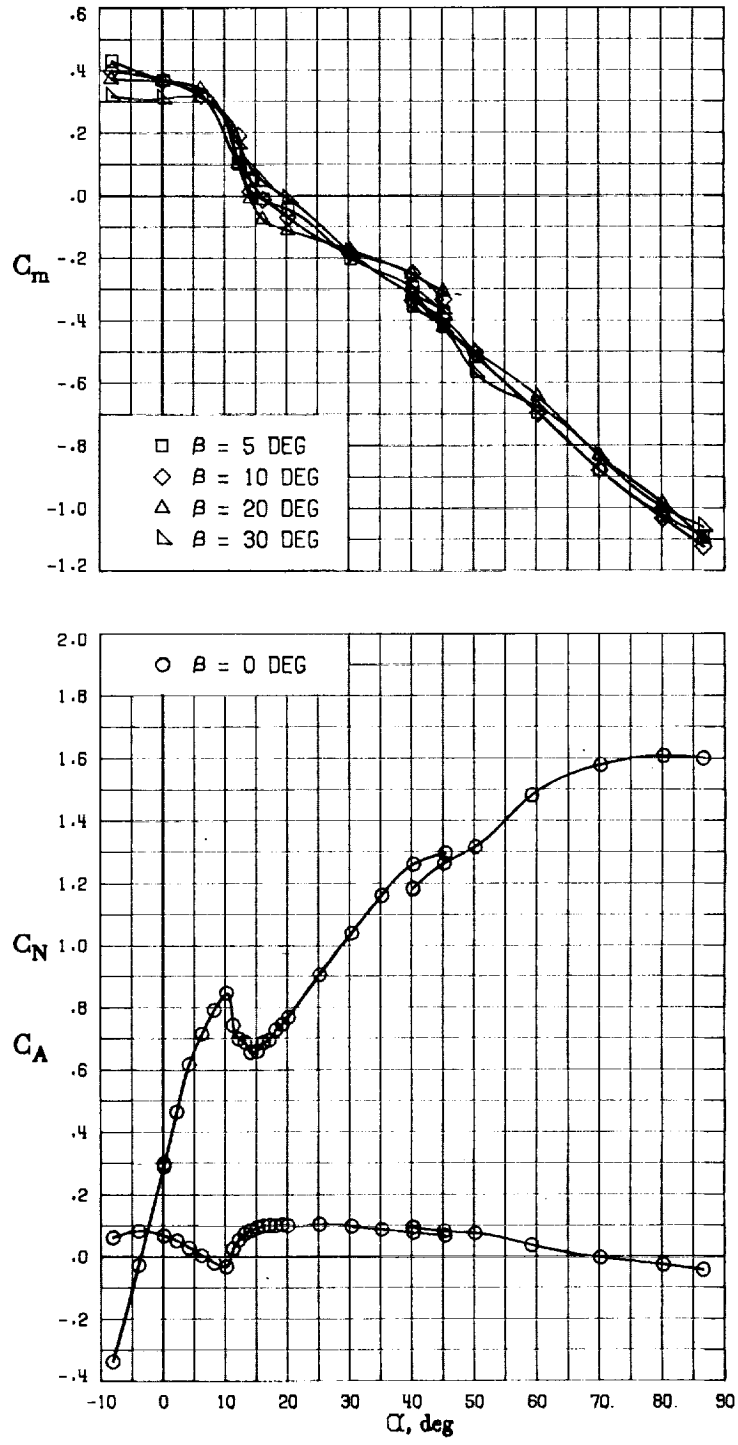

(B) LONGITUDINAL FORCE AND MOMENT COEFFICIENTS ABOUT BODY AXES.

FIGURE 53. - CONTINUED.

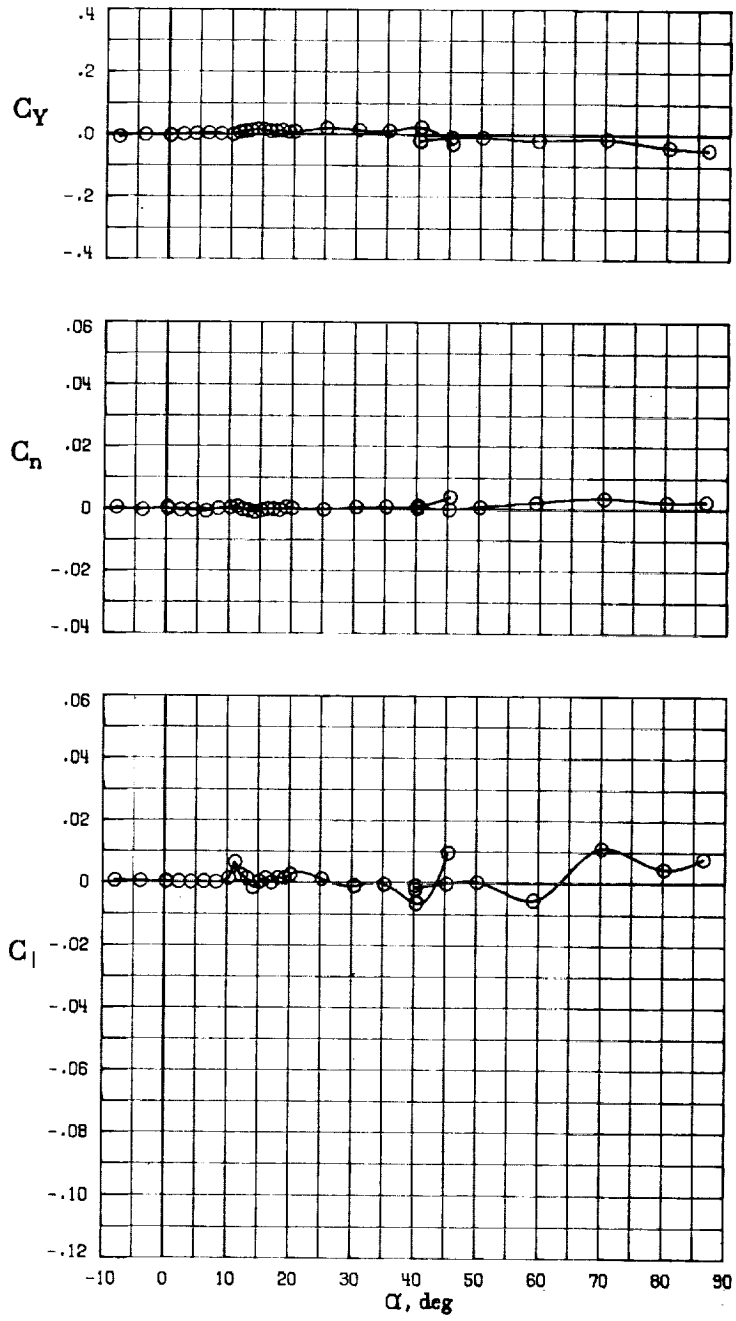

(C) LATERAL - DIRECTIONAL FORCE AND MOMENT COEFFICIENTS ABOUT BODY AXES AT ZERO SIDESLIP.

FIGURE 53. - CONTINUED.

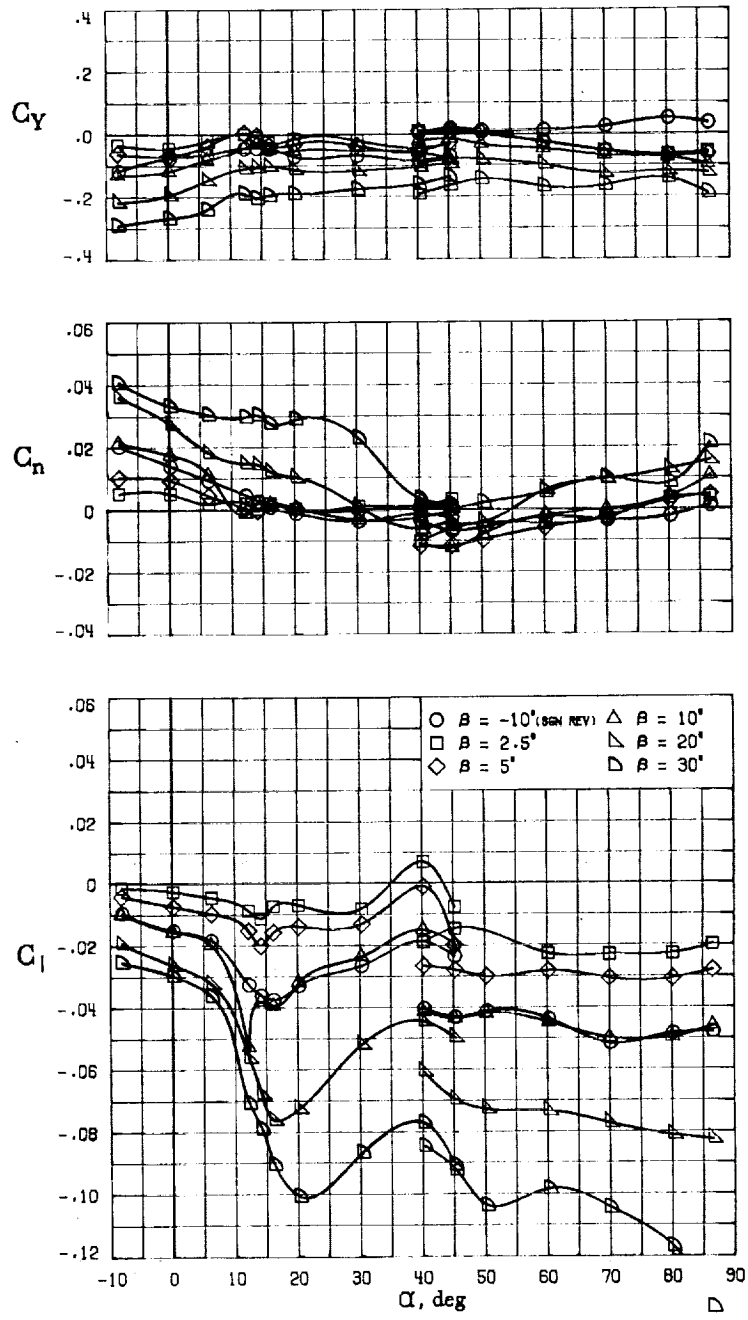

(D) LATERAL - DIRECTIONAL FORCE AND MOMENT COEFFICIENTS ABOUT BODY AXES.

FIGURE 53. - CONTINUED.

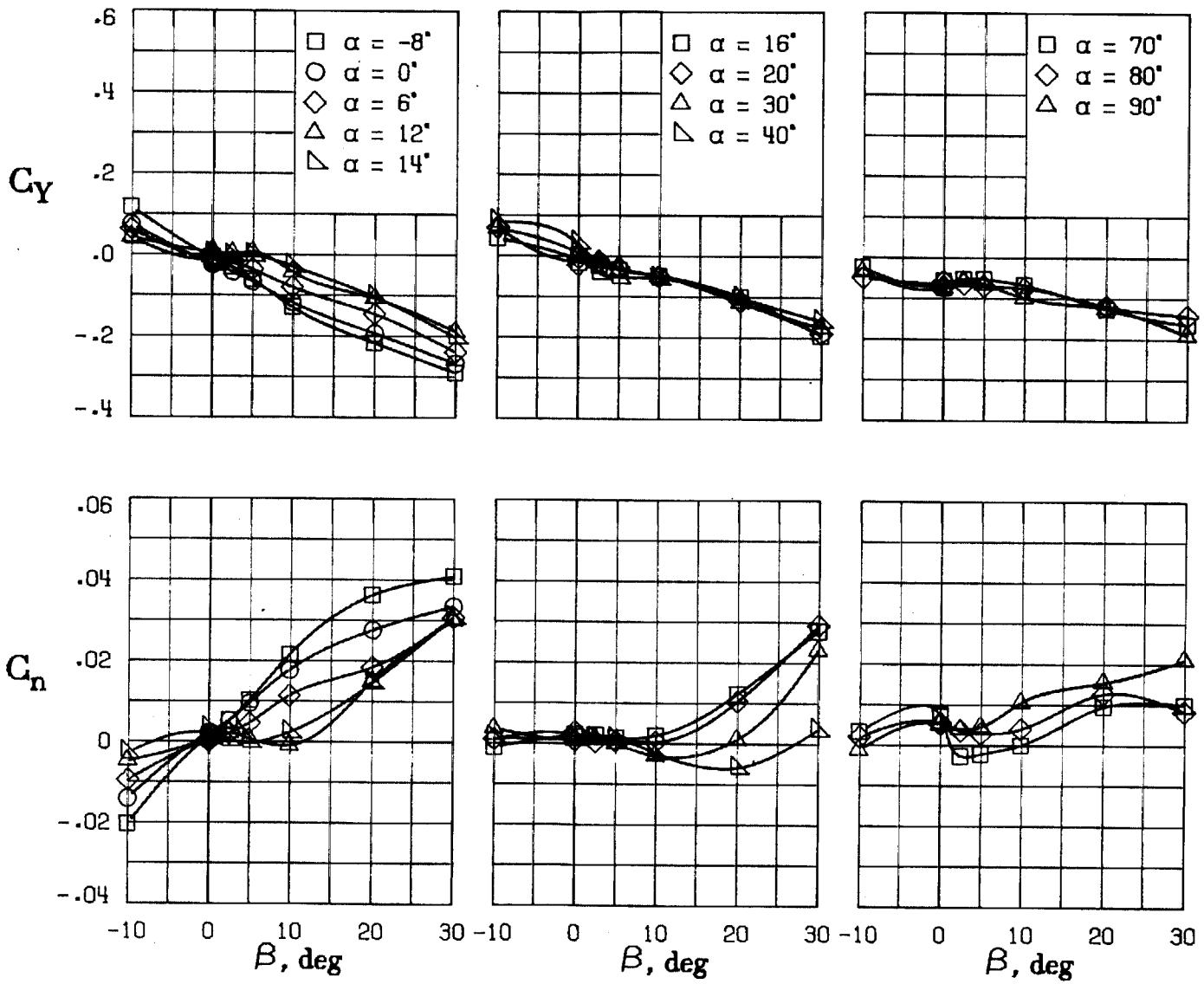

(E) DIRECTIONAL - STABILITY CHARACTERISTICS ABOUT BODY AXES AT VARIOUS ANGLES OF ATTACK.

FIGURE 53. - CONTINUED.

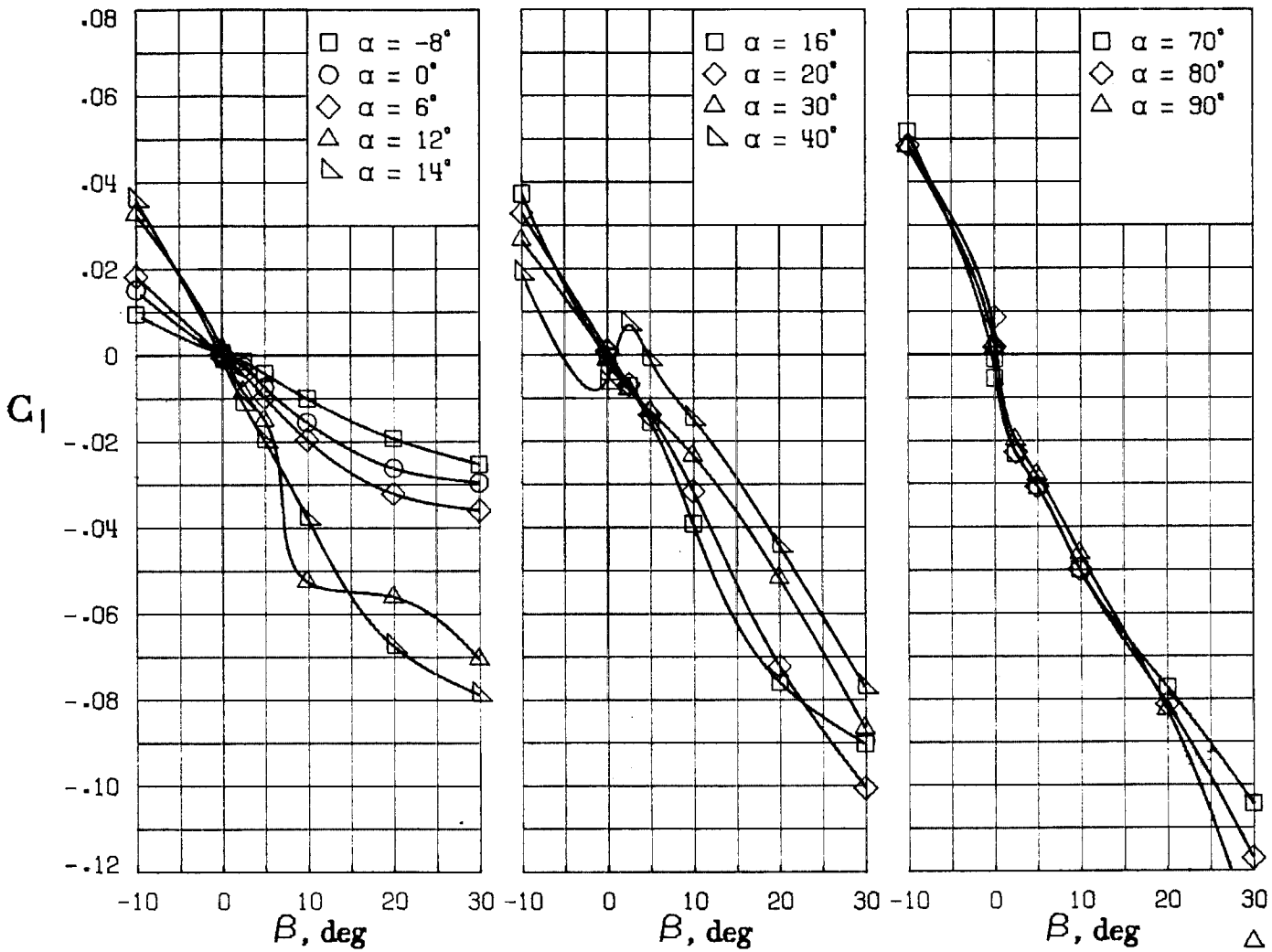

(F) LATERAL - STABILITY CHARACTERISTICS ABOUT BODY AXES AT VARIOUS ANGLES OF ATTACK.

FIGURE 53. - CONCLUDED.

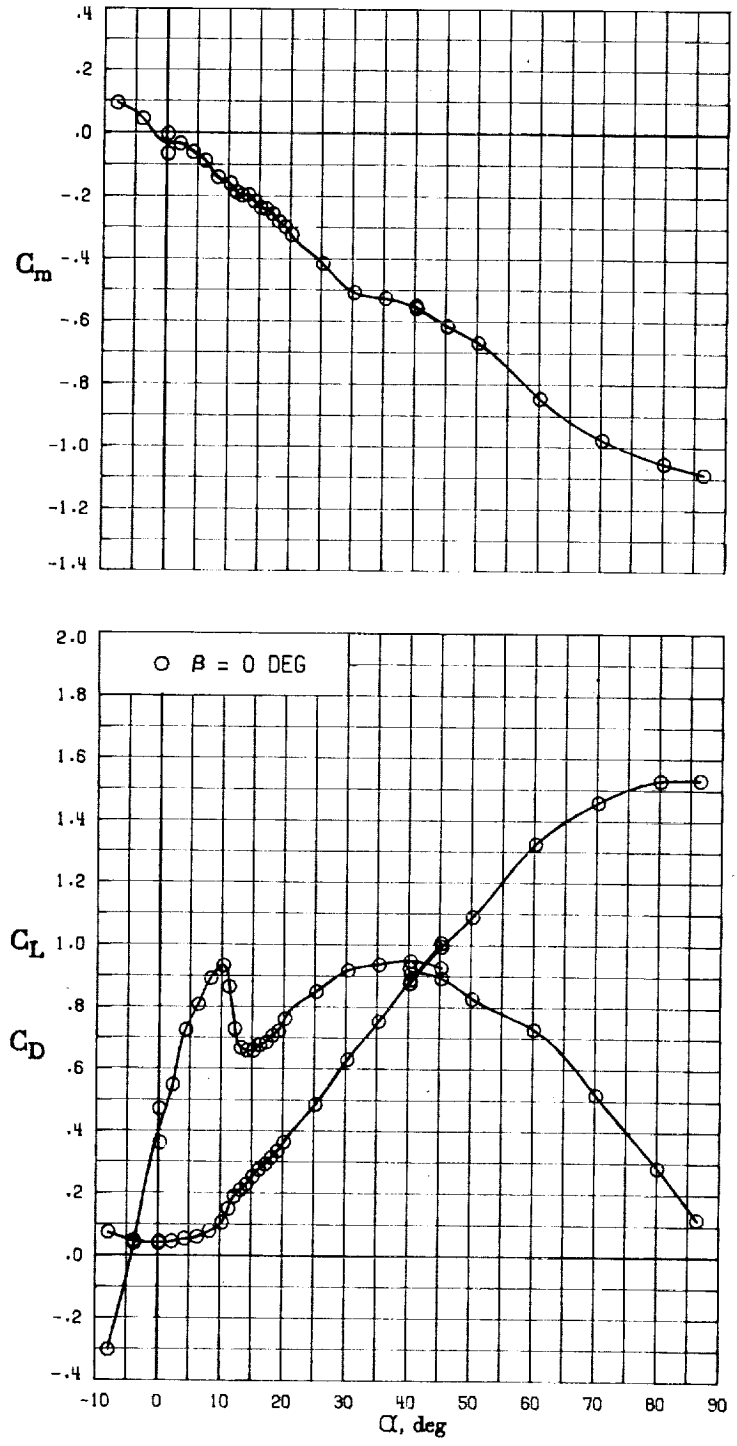

(A) LONGITUDINAL FORCE AND MOMENT COEFFICIENTS ABOUT STABILITY AXES.

FIGURE 54. - EFFECT OF ANGLE OF ATTACK AND SIDESLIP ANGLE ON AERODYNAMIC CHARACTERISTICS AT RE = .288 E+06 FOR CONFIGURATION B W1 H3 V. δ_E = 15°, δ_A = 0°, δ_R = 0°.

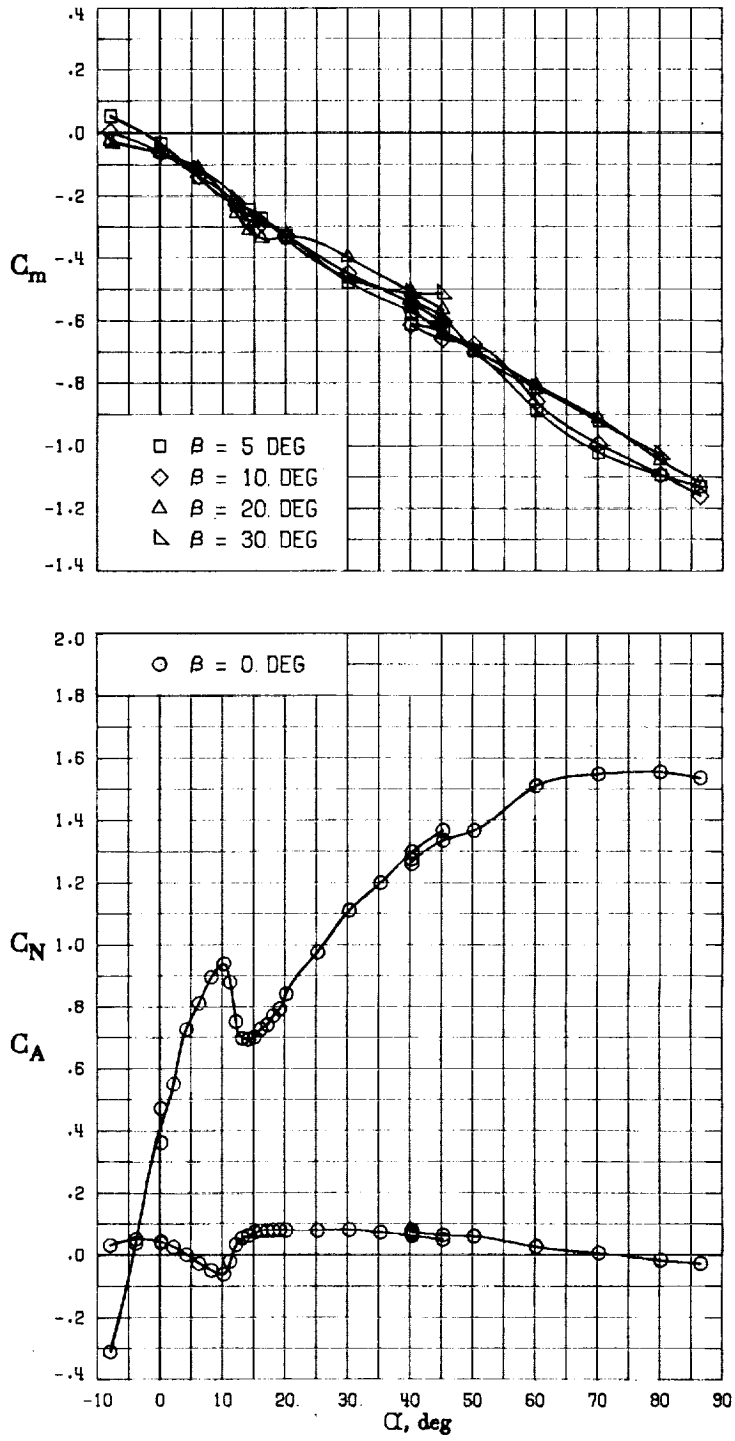

(B) LONGITUDINAL FORCE AND MOMENT COEFFICIENTS ABOUT BODY AXES.

FIGURE 54. - CONTINUED.

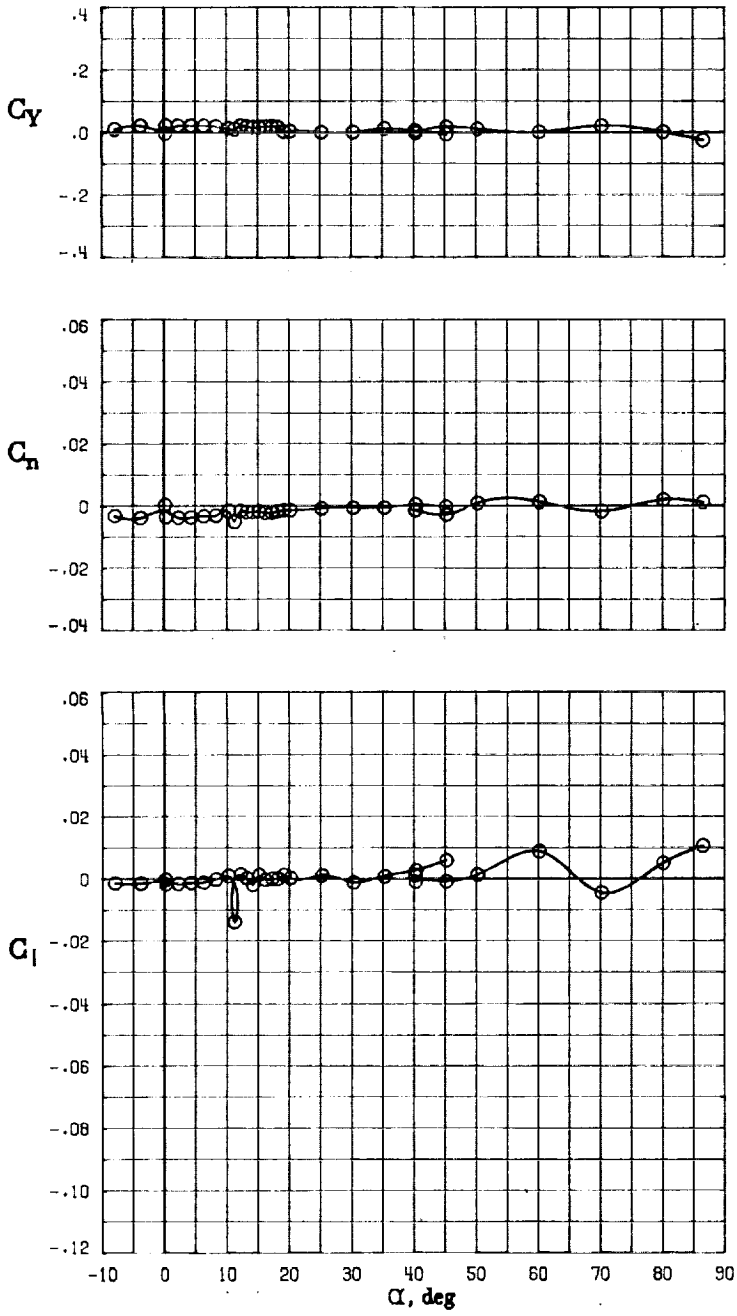

(C) LATERAL - DIRECTIONAL FORCE AND MOMENT COEFFICIENTS ABOUT BODY AXES AT ZERO SIDESLIP.

FIGURE 54. - CONTINUED.

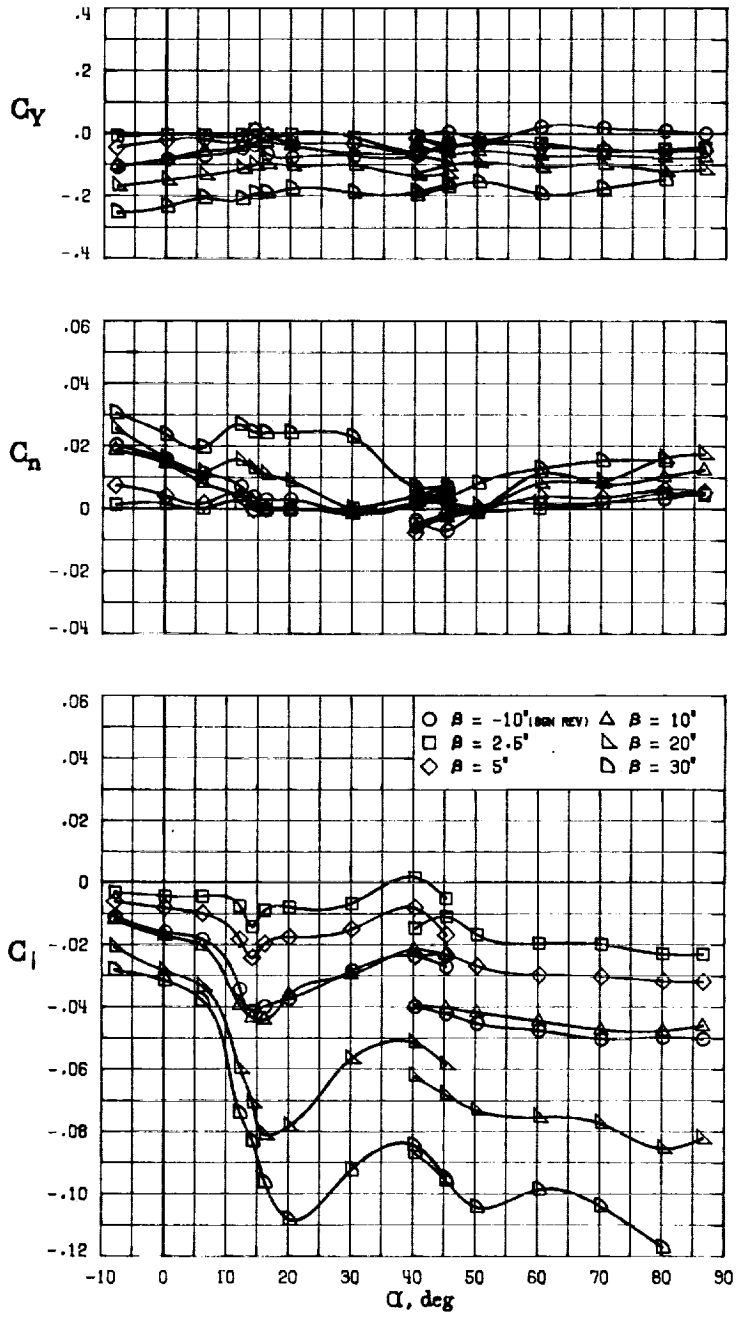

(D) LATERAL - DIRECTIONAL FORCE AND MOMENT COEFFICIENTS ABOUT BODY AXES.

FIGURE 54. - CONTINUED.

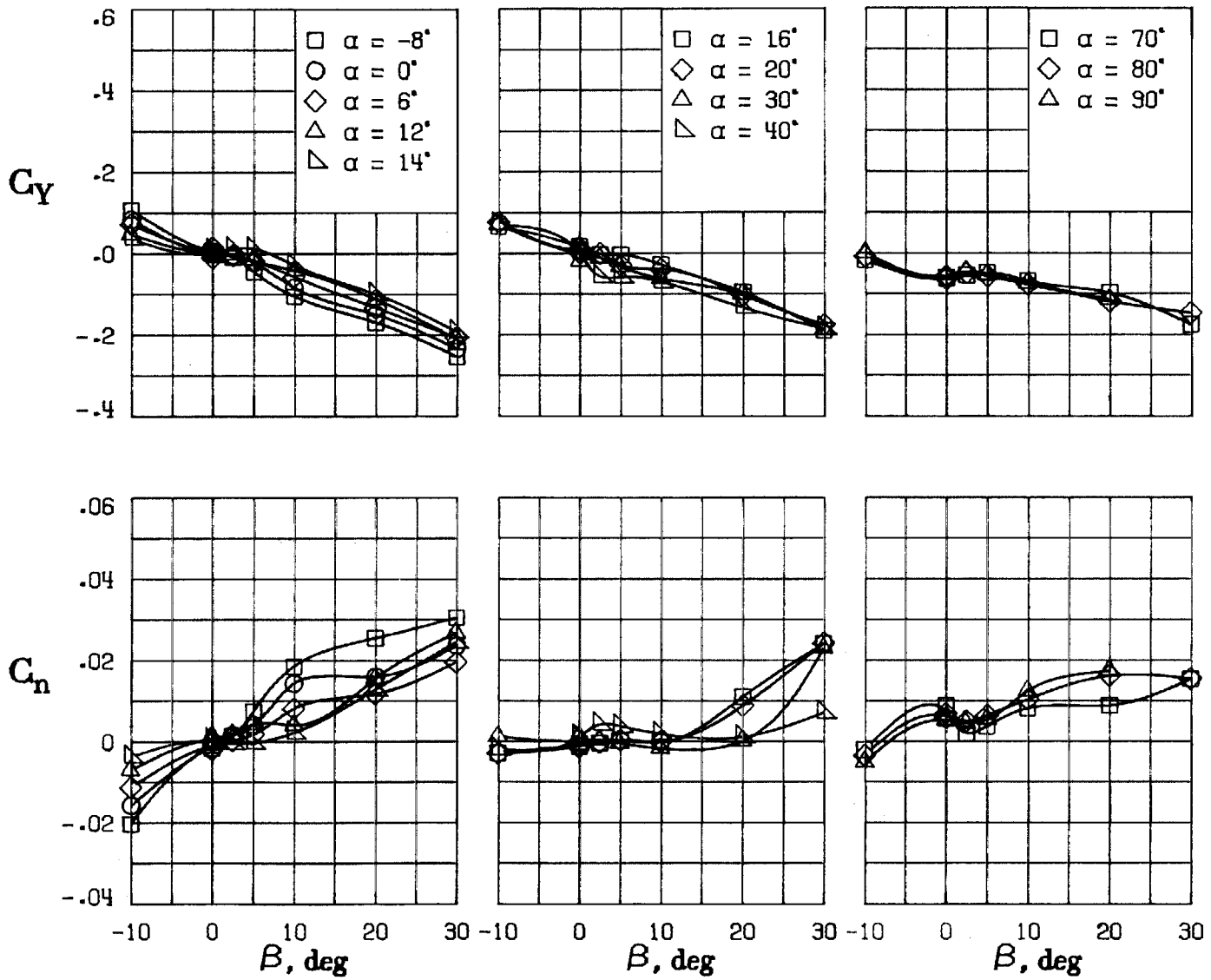

(E) DIRECTIONAL - STABILITY CHARACTERISTICS ABOUT BODY AXES AT VARIOUS ANGLES OF ATTACK.

FIGURE 54. - CONTINUED.

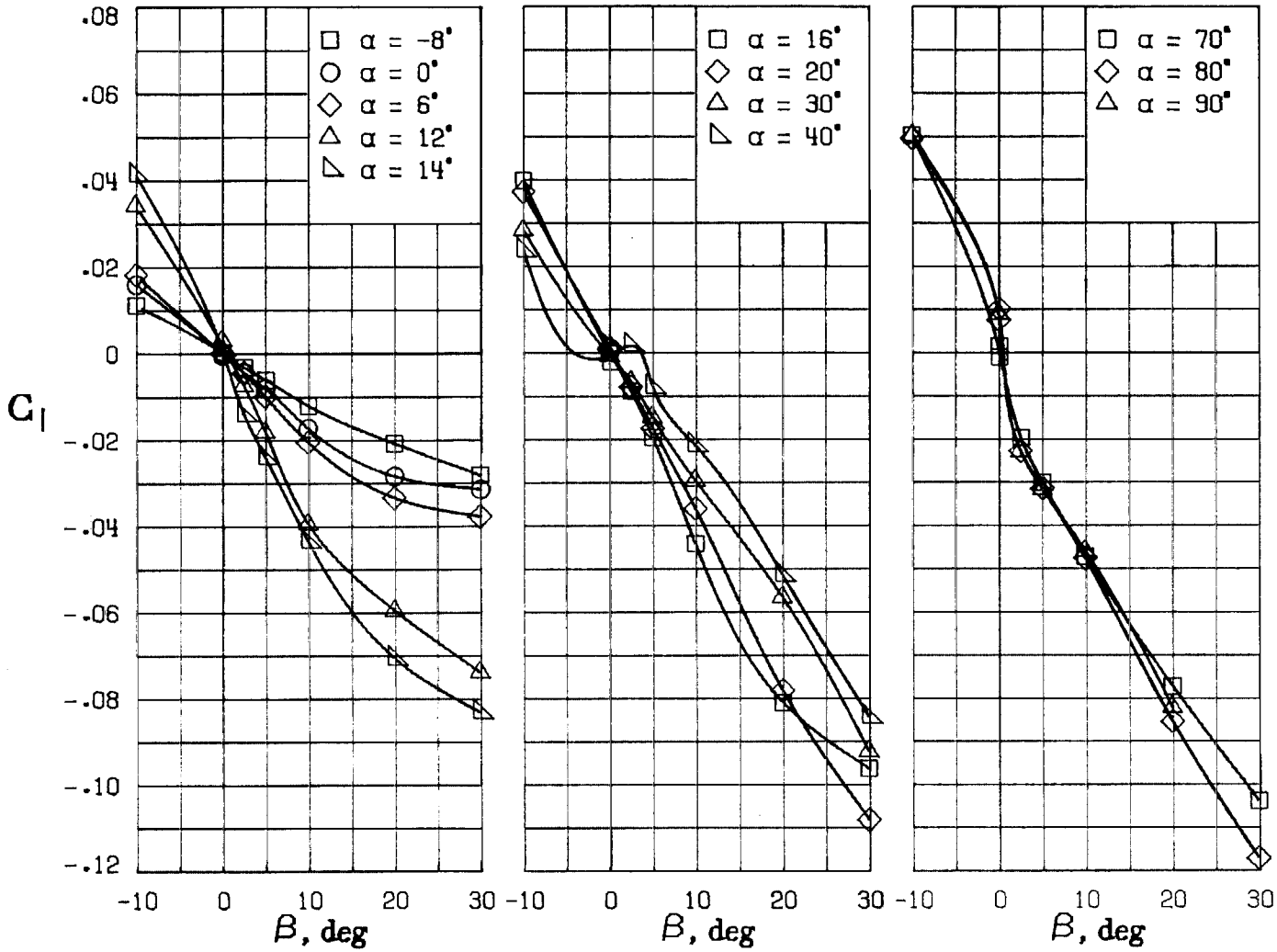

(F) LATERAL - STABILITY CHARACTERISTICS ABOUT BODY AXES AT VARIOUS ANGLES OF ATTACK.

FIGURE 54. - CONCLUDED.

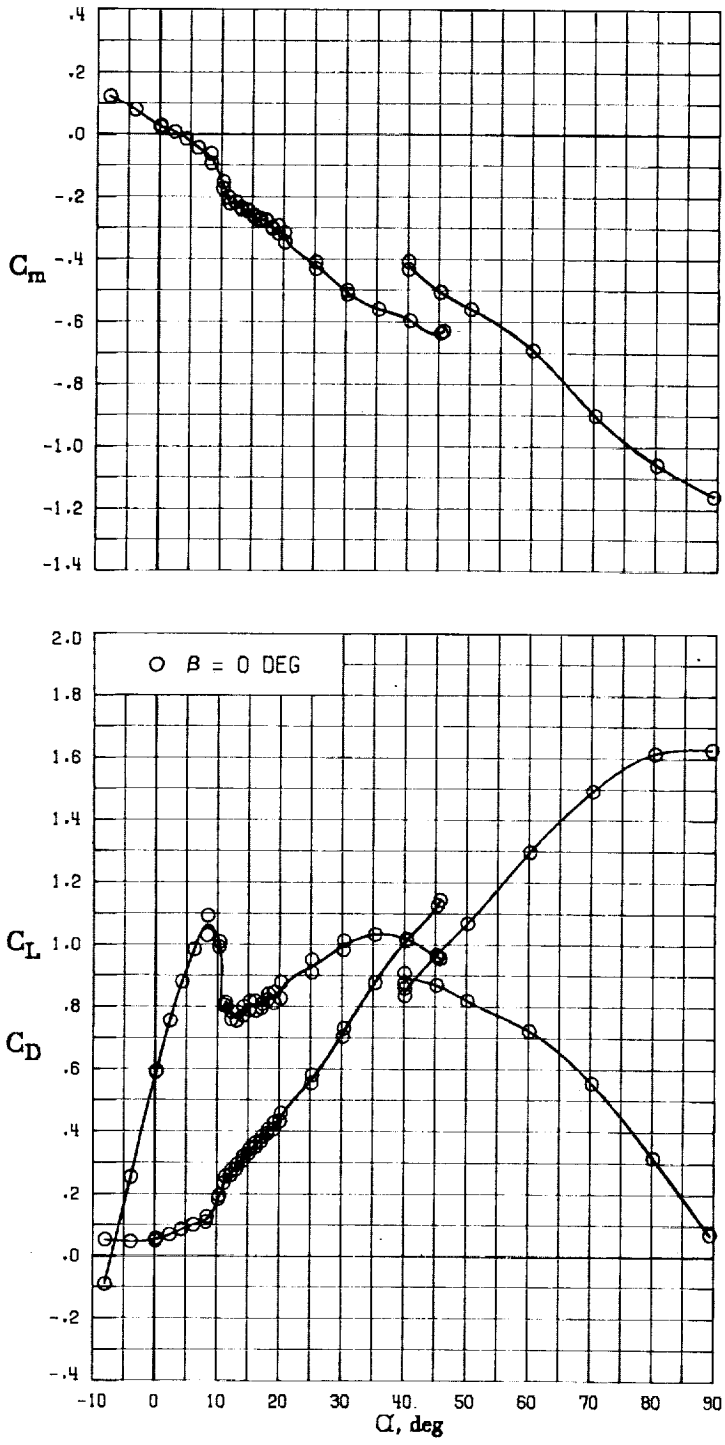

(A) LONGITUDINAL FORCE AND MOMENT COEFFICIENTS ABOUT STABILITY AXES.

FIGURE 55. - EFFECT OF ANGLE OF ATTACK AND SIDESLIP ANGLE ON AERODYNAMIC CHARACTERISTICS AT RE. = .288 E+06 FOR CONFIGURATION B W2 H3 V. $\delta_E = 0°$, $\delta_A = 0°$, $\delta_R = 0°$.

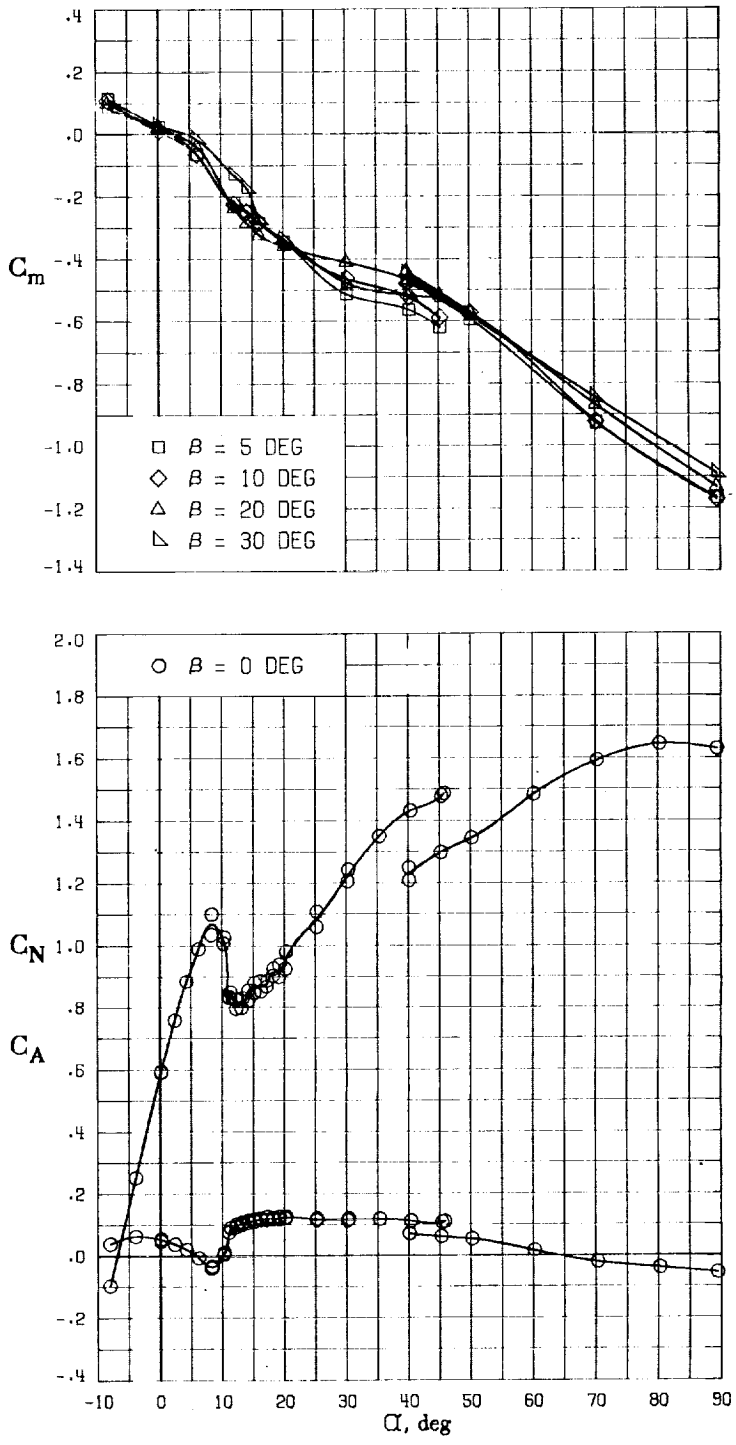

(B) LONGITUDINAL FORCE AND MOMENT COEFFICIENTS ABOUT BODY AXES.

FIGURE 55. - CONTINUED.

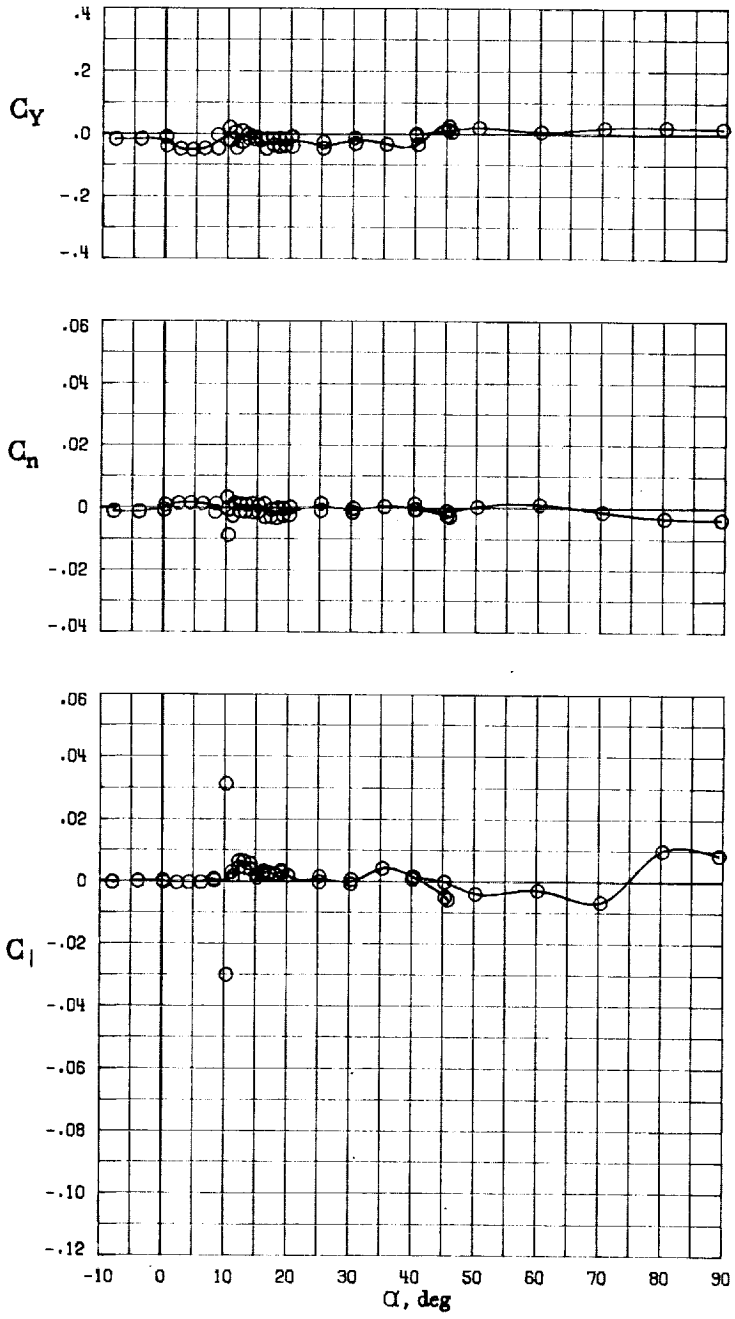

(C) LATERAL - DIRECTIONAL FORCE AND MOMENT COEFFICIENTS ABOUT BODY AXES AT ZERO SIDESLIP.

FIGURE 55. - CONTINUED.

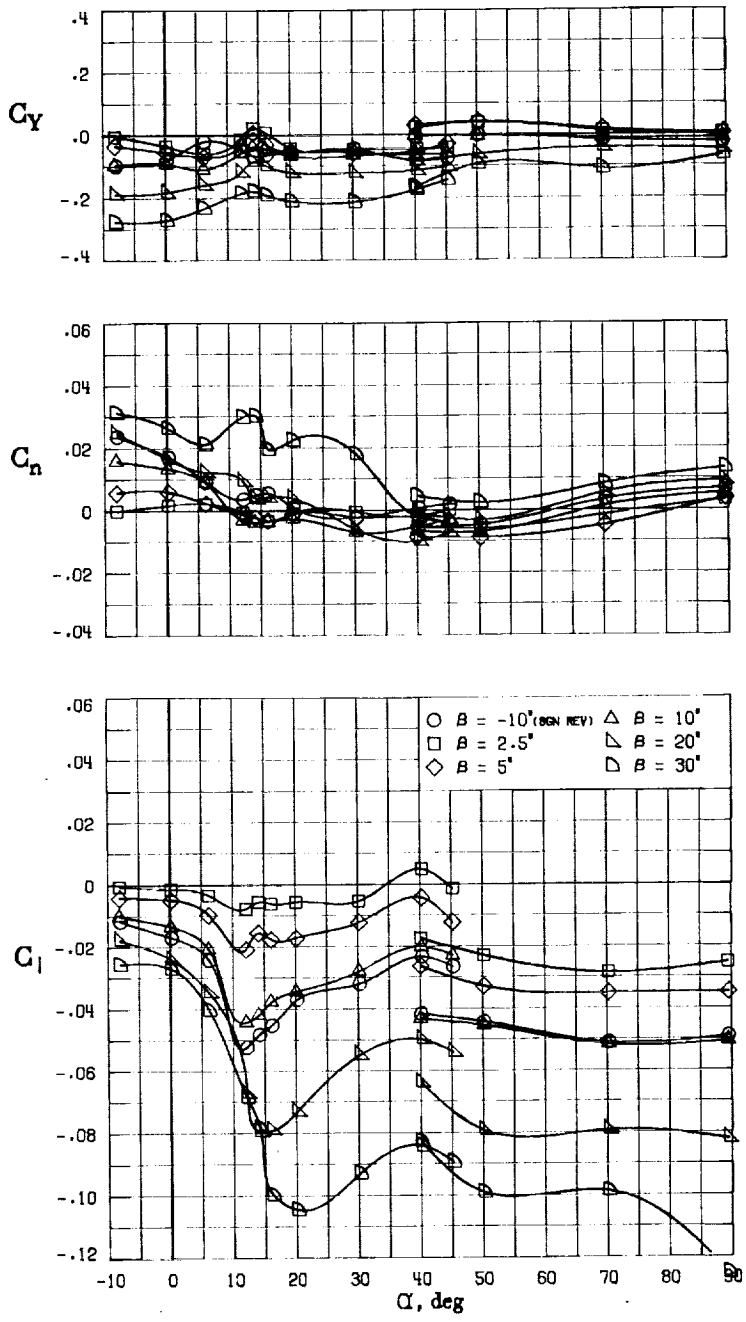

(D) LATERAL - DIRECTIONAL FORCE AND MOMENT COEFFICIENTS ABOUT BODY AXES.

FIGURE 55. - CONTINUED.

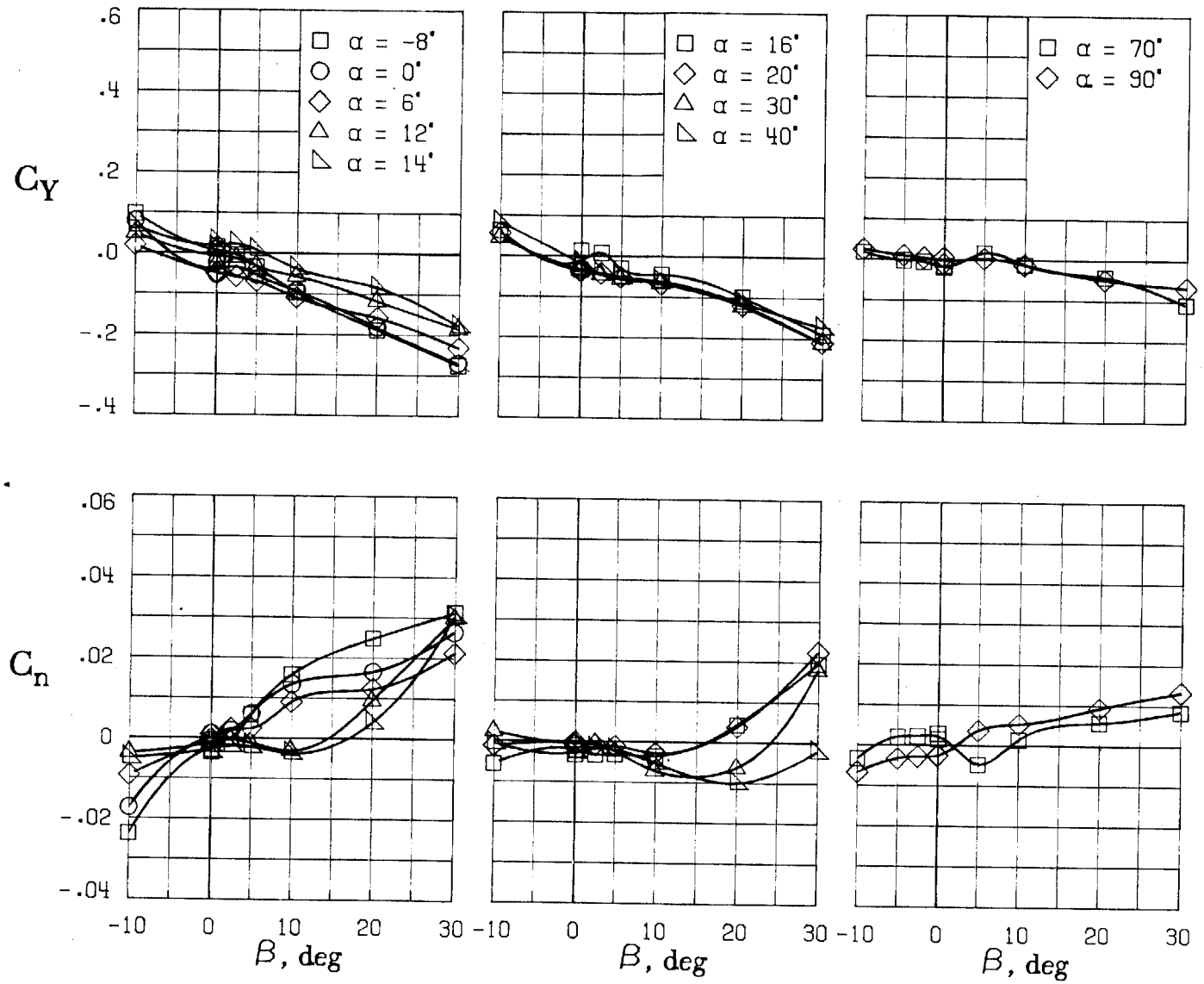

(E) DIRECTIONAL - STABILITY CHARACTERISTICS ABOUT BODY AXES AT VARIOUS ANGLES OF ATTACK.

FIGURE 55 - CONTINUED.

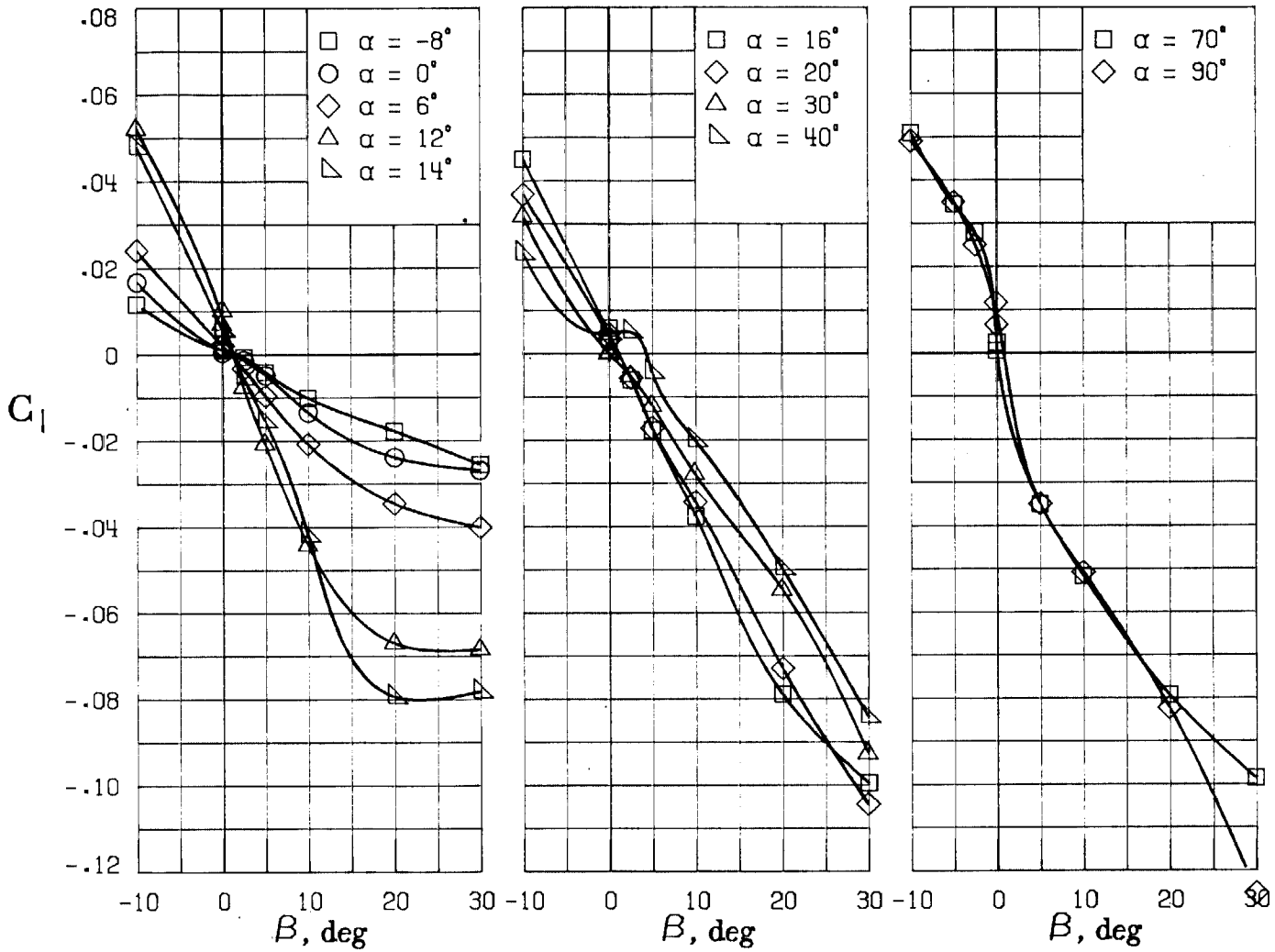

(F) LATERAL - STABILITY CHARACTERISTICS ABOUT BODY AXES AT VARIOUS ANGLES OF ATTACK.

FIGURE 55. - CONCLUDED.

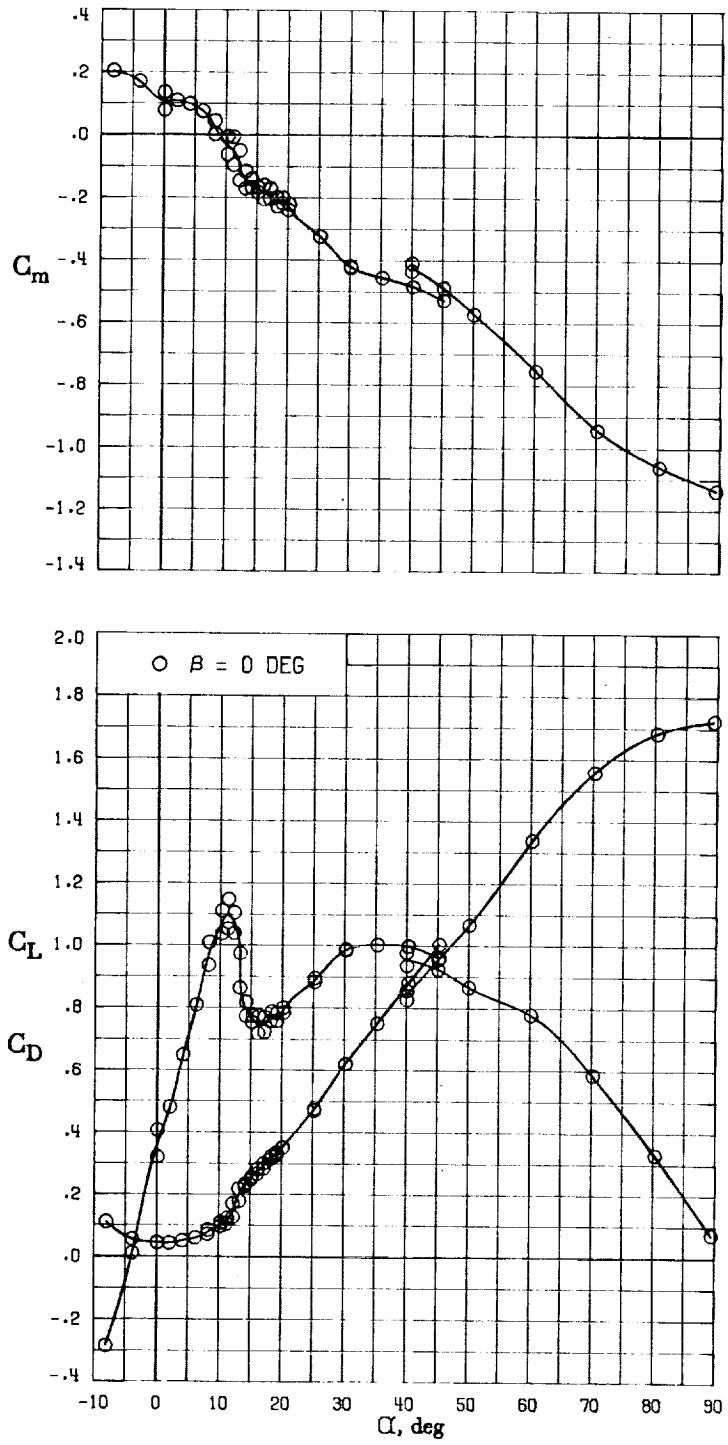

(A) LONGITUDINAL FORCE AND MOMENT COEFFICIENTS ABOUT STABILITY AXES.

FIGURE 56. - EFFECT OF ANGLE OF ATTACK AND SIDESLIP ANGLE ON AERODYNAMIC CHARACTERISTICS AT RE = .288 E+06 FOR CONFIGURATION B W3 H3 V. $\delta_E = 0°$, $\delta_A = 0°$, $\delta_R = 0°$.

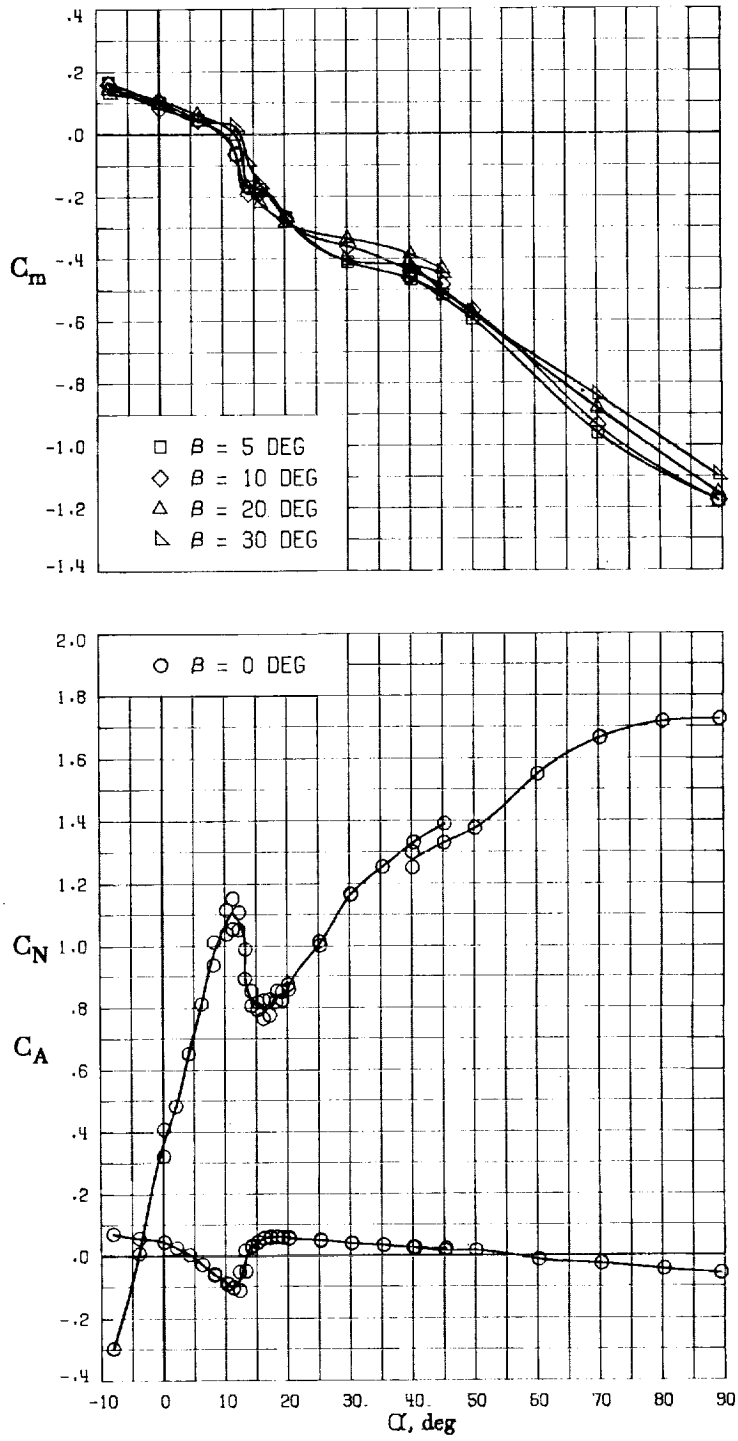

(B) LONGITUDINAL FORCE AND MOMENT COEFFICIENTS ABOUT BODY AXES.

FIGURE 56. - CONTINUED.

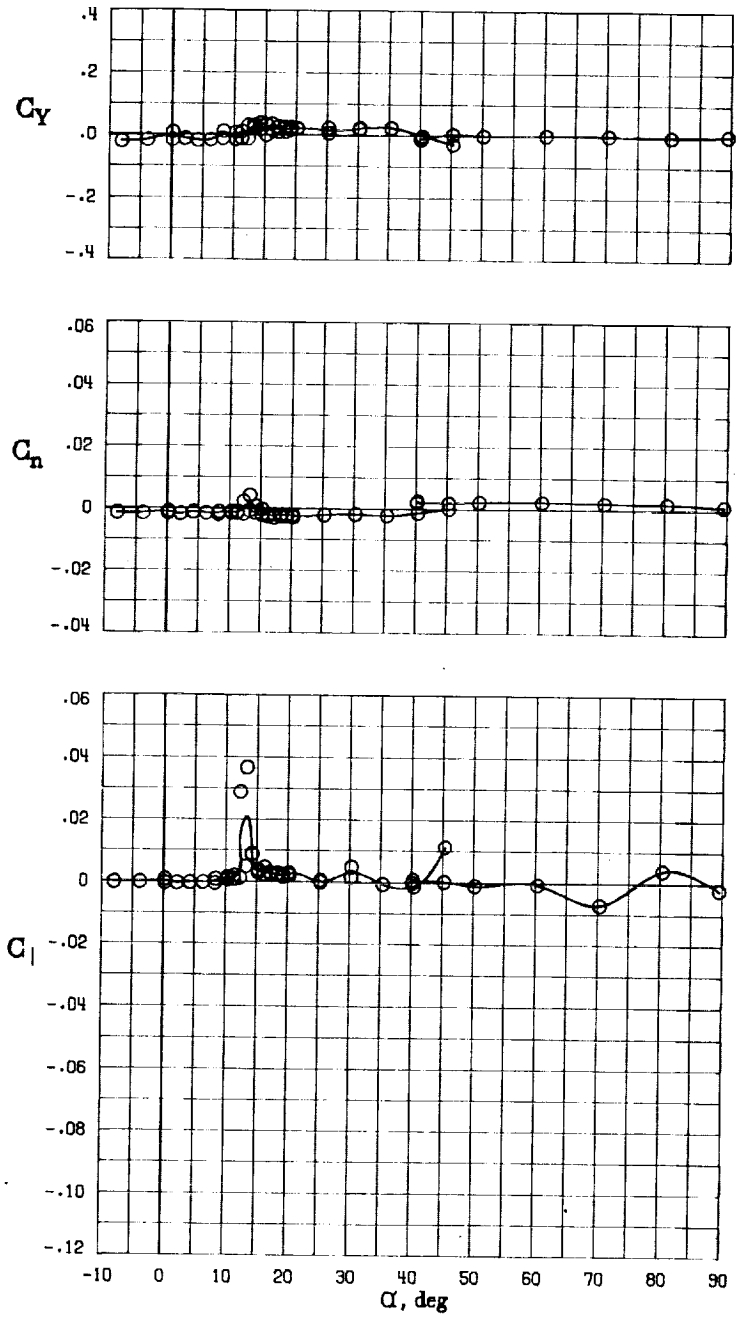

(C) LATERAL - DIRECTIONAL FORCE AND MOMENT COEFFICIENTS ABOUT BODY AXES AT ZERO SIDESLIP.

FIGURE 56. - CONTINUED.

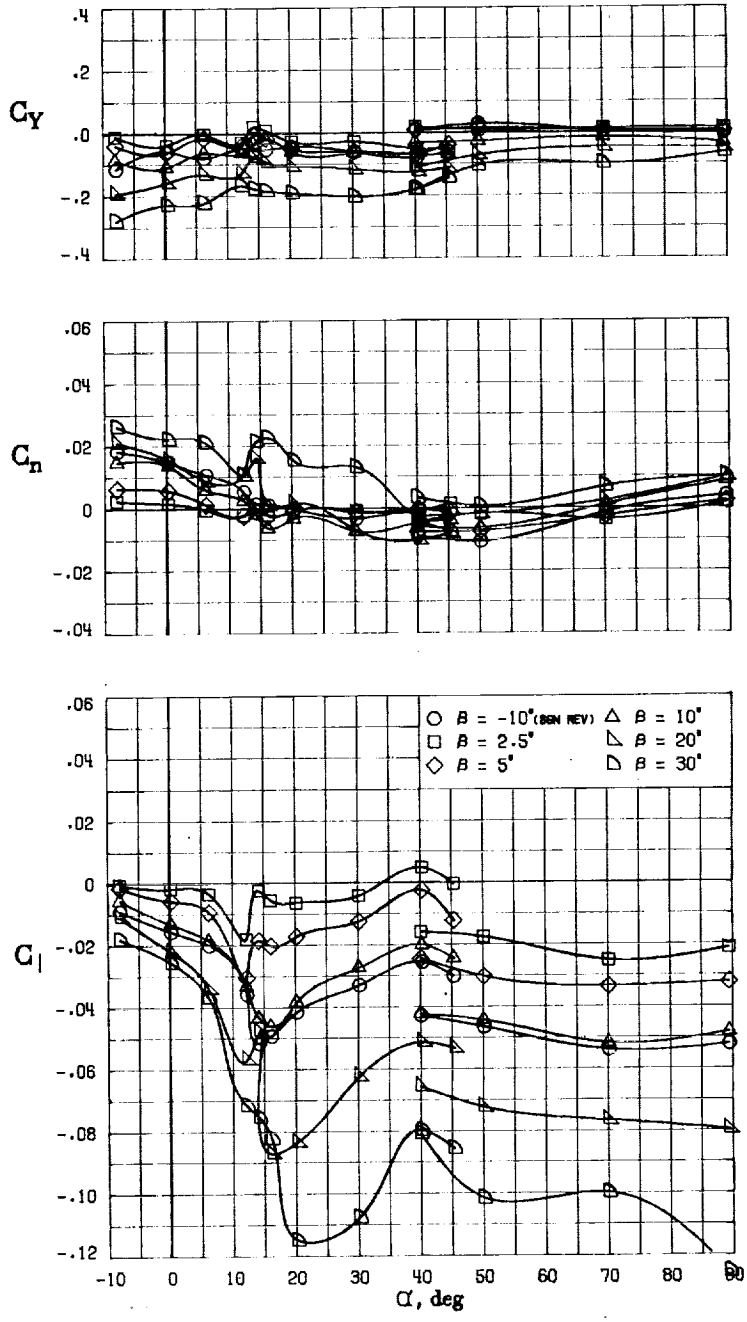

(D) LATERAL - DIRECTIONAL FORCE AND MOMENT COEFFICIENTS ABOUT BODY AXES.

FIGURE 56. - CONTINUED.

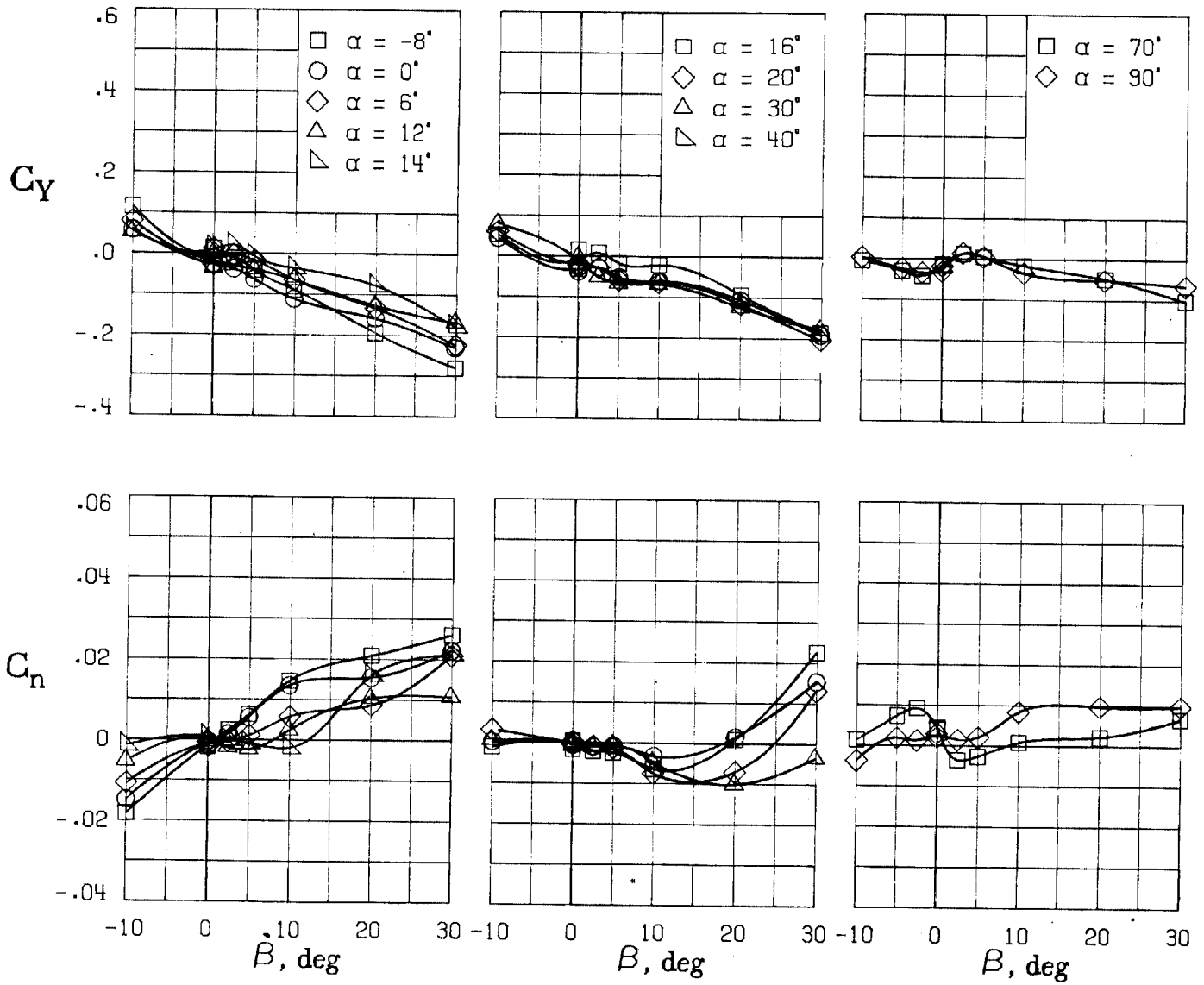

(E) DIRECTIONAL - STABILITY CHARACTERISTICS ABOUT BODY AXES AT VARIOUS ANGLES OF ATTACK.

FIGURE 56. - CONTINUED.

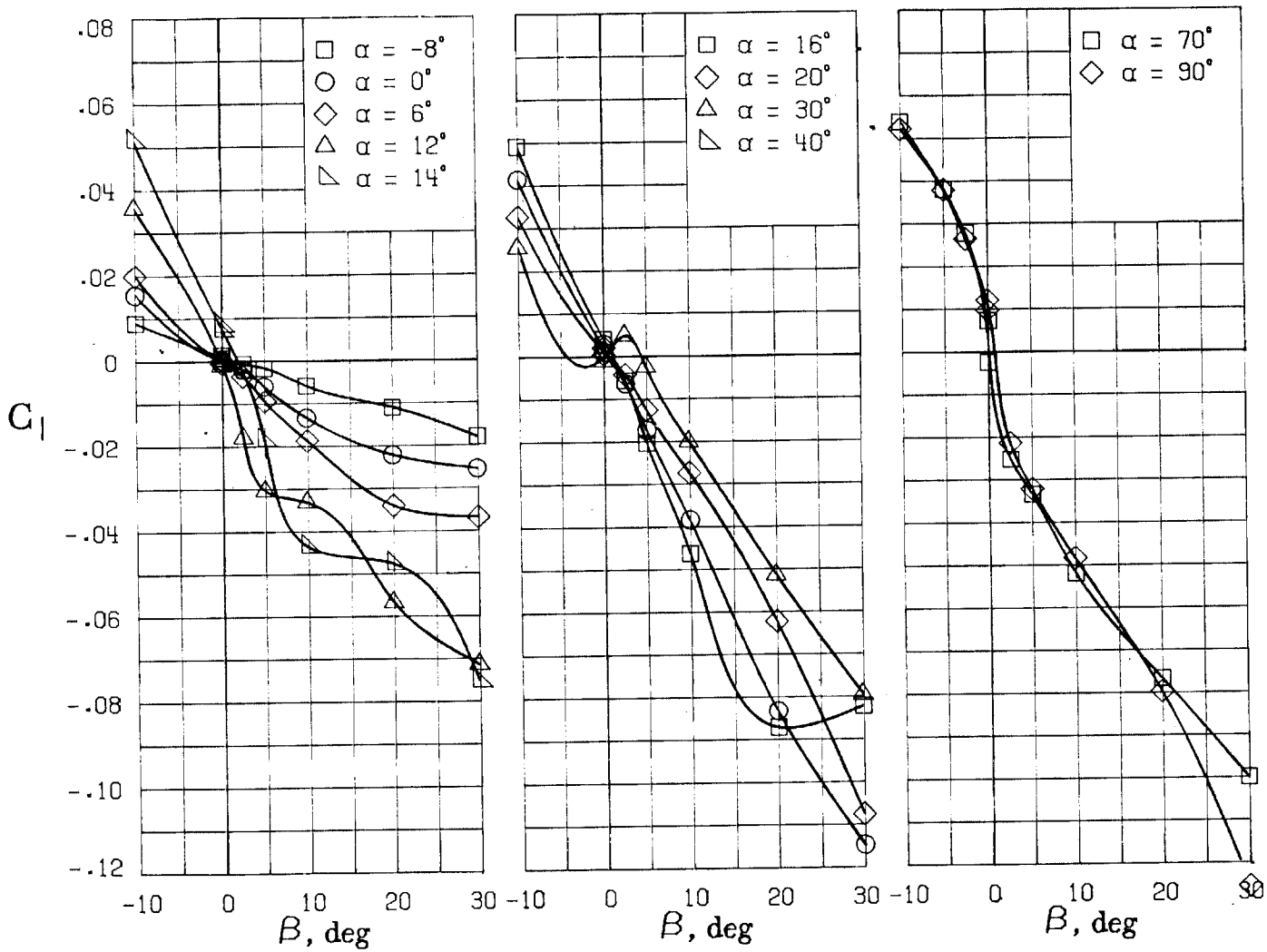

(F) LATERAL - STABILITY CHARACTERISTICS ABOUT BODY AXES AT VARIOUS ANGLES OF ATTACK.

FIGURE 56. - CONCLUDED.

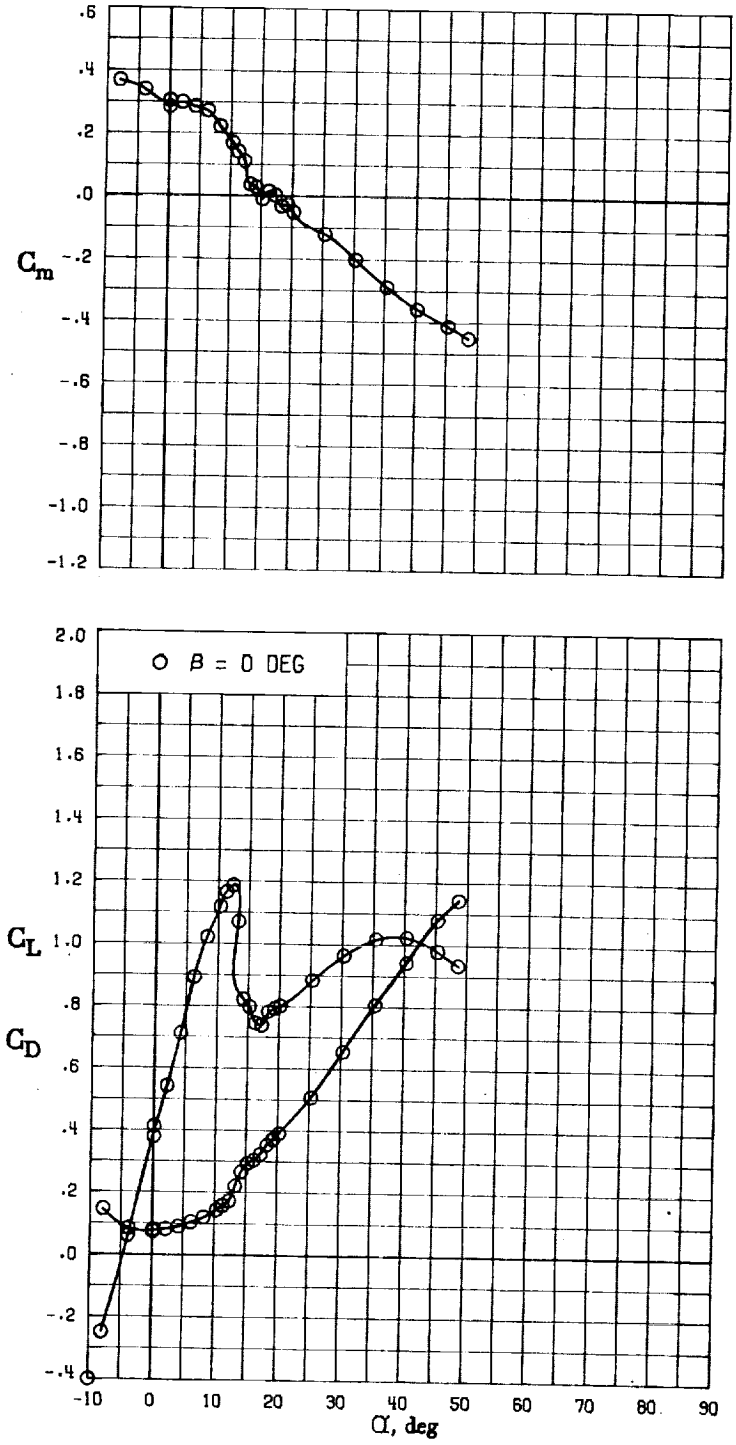

(A) LONGITUDINAL FORCE AND MOMENT COEFFICIENTS ABOUT STABILITY AXES.

FIGURE 57. - EFFECT OF ANGLE OF ATTACK AND SIDESLIP ANGLE ON AERODYNAMIC CHARACTERISTICS AT RE = .288 E+06 FOR CONFIGURATION B W3 H3 V. $\delta_E = -25°$, $\delta_A = 0°$, $\delta_R = 0°$.

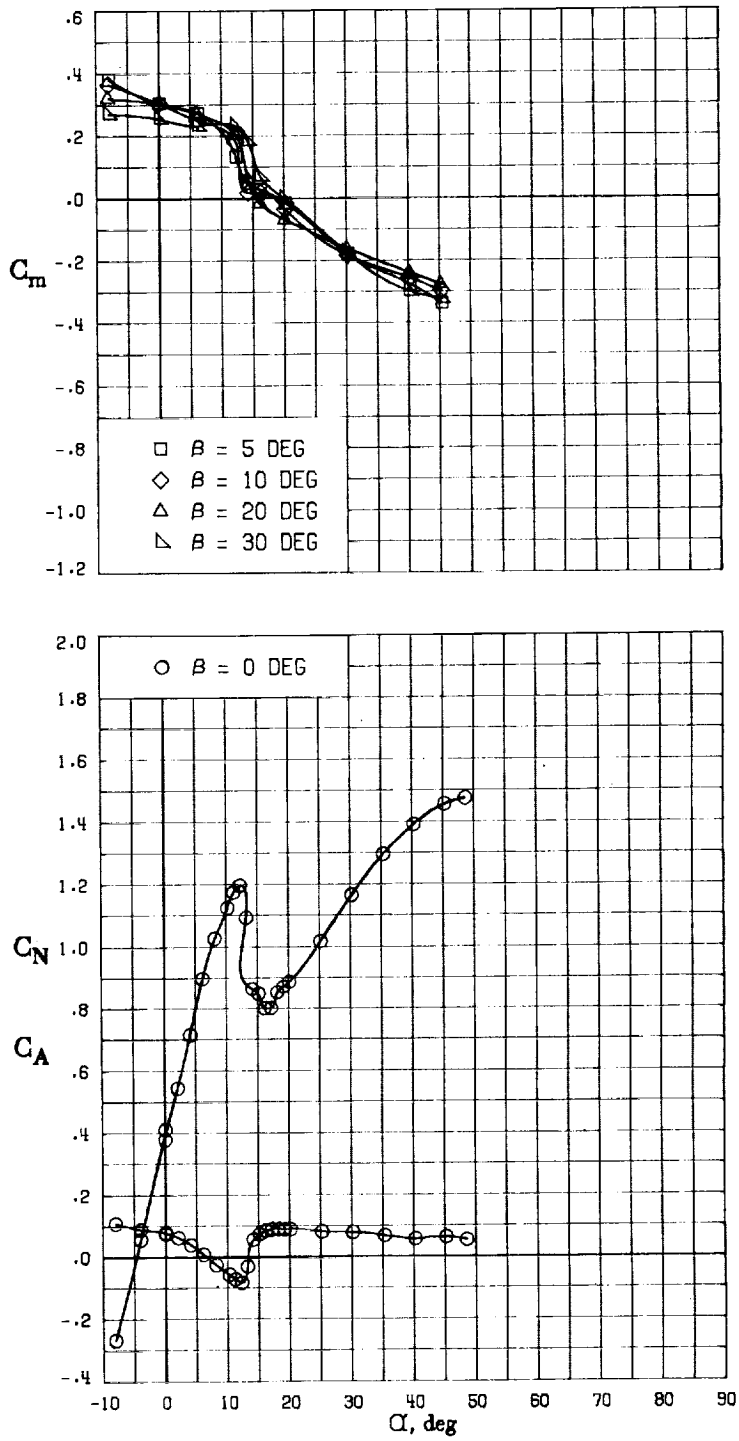

(B) LONGITUDINAL FORCE AND MOMENT COEFFICIENTS ABOUT BODY AXES.

FIGURE 57. - CONTINUED.

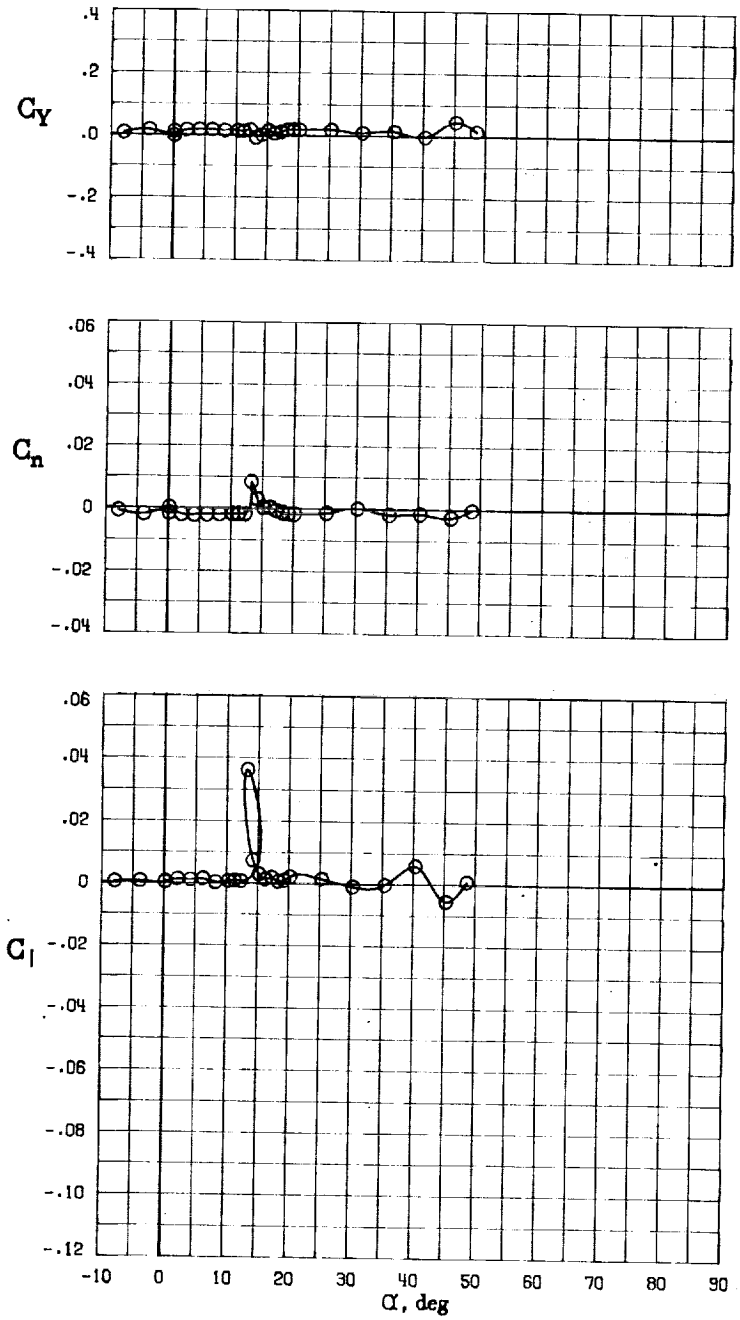

(C) LATERAL - DIRECTIONAL FORCE AND MOMENT COEFFICIENTS ABOUT BODY AXES AT ZERO SIDESLIP.

FIGURE 57. - CONTINUED.

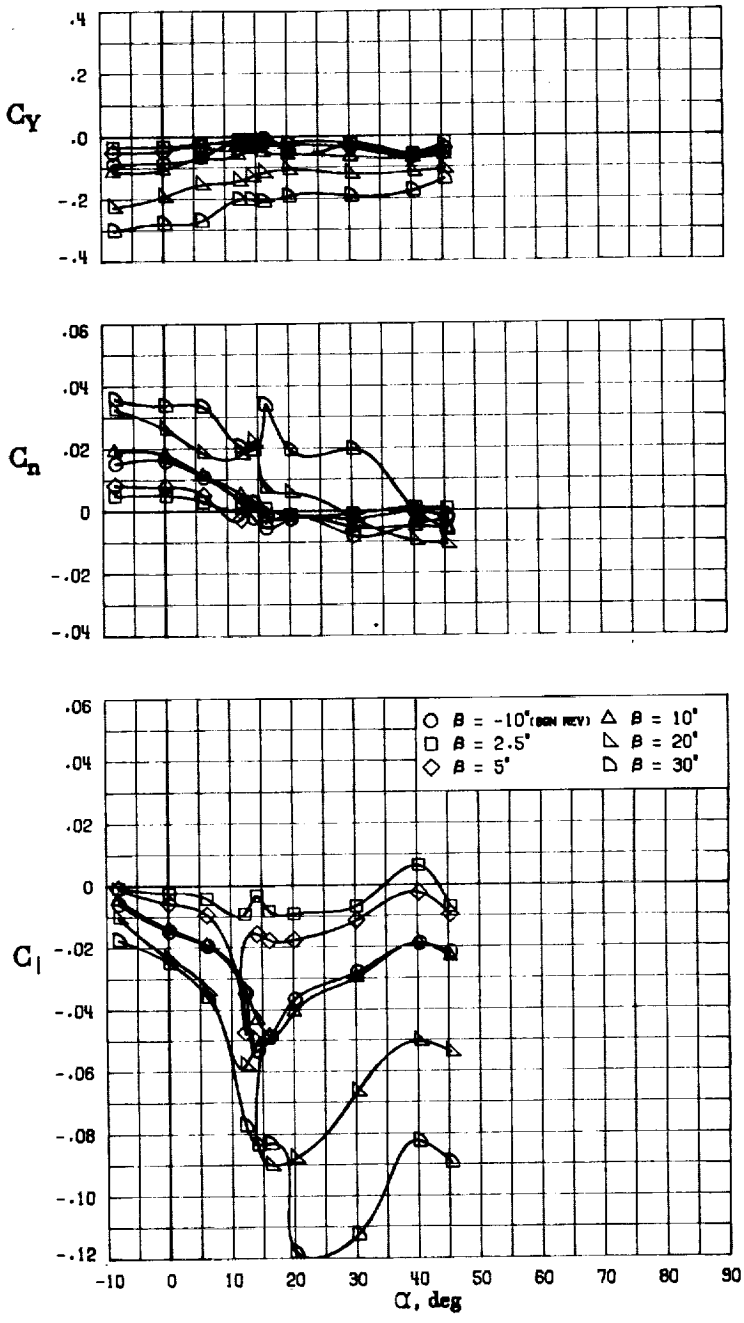

(D) LATERAL - DIRECTIONAL FORCE AND MOMENT COEFFICIENTS ABOUT BODY AXES.

FIGURE 57. - CONTINUED.

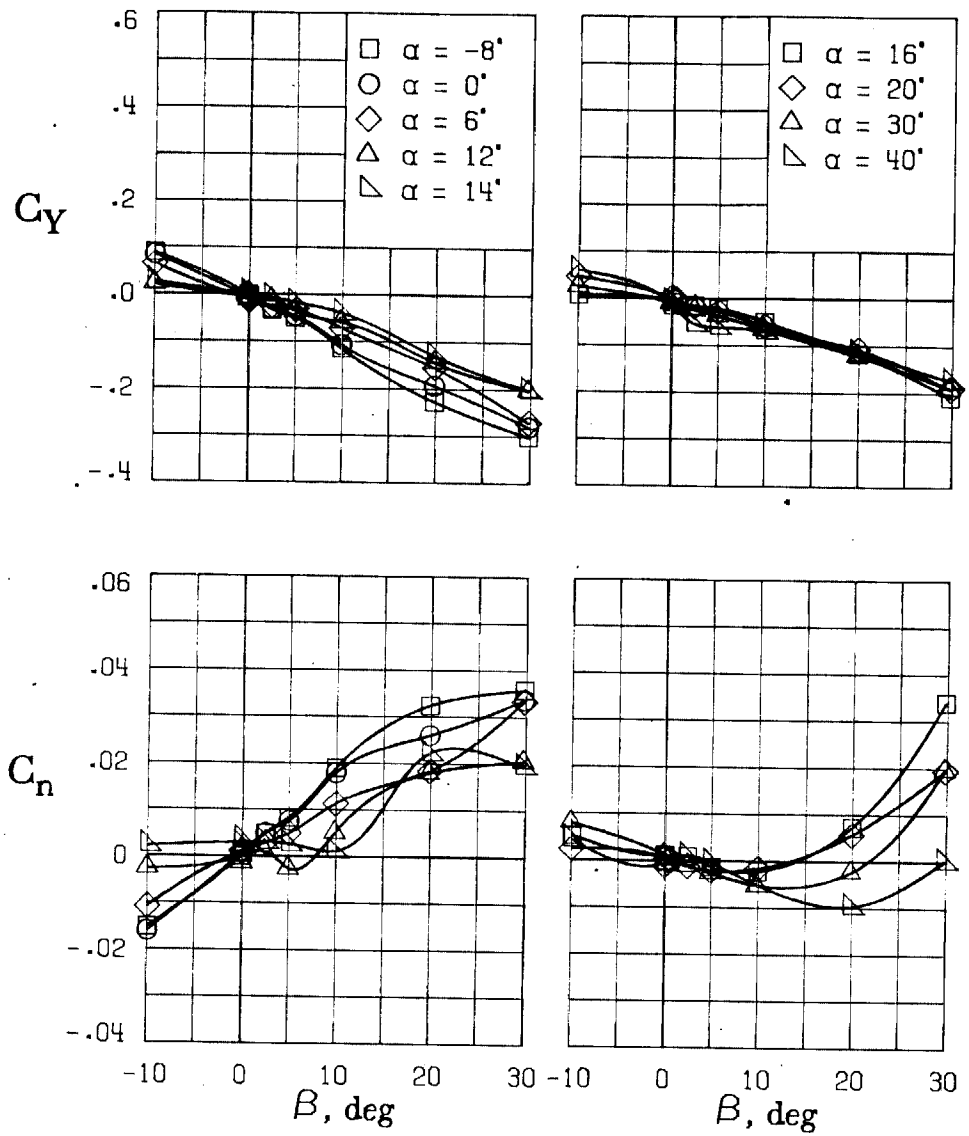

(E) DIRECTIONAL - STABILITY CHARACTERISTICS ABOUT BODY AXES AT VARIOUS ANGLES OF ATTACK.

FIGURE 57. - CONTINUED.

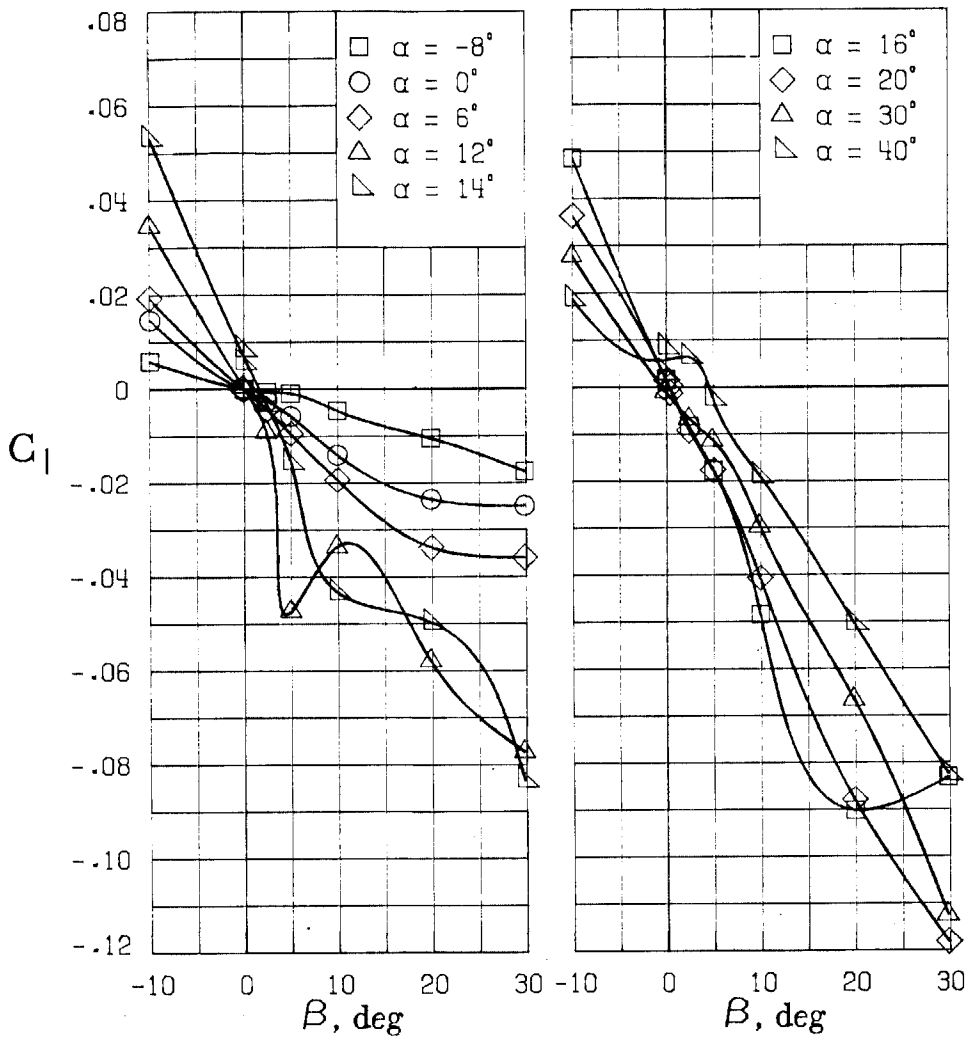

(F) LATERAL - STABILITY CHARACTERISTICS ABOUT BODY AXES AT VARIOUS ANGLES OF ATTACK.

FIGURE 57. - CONCLUDED.

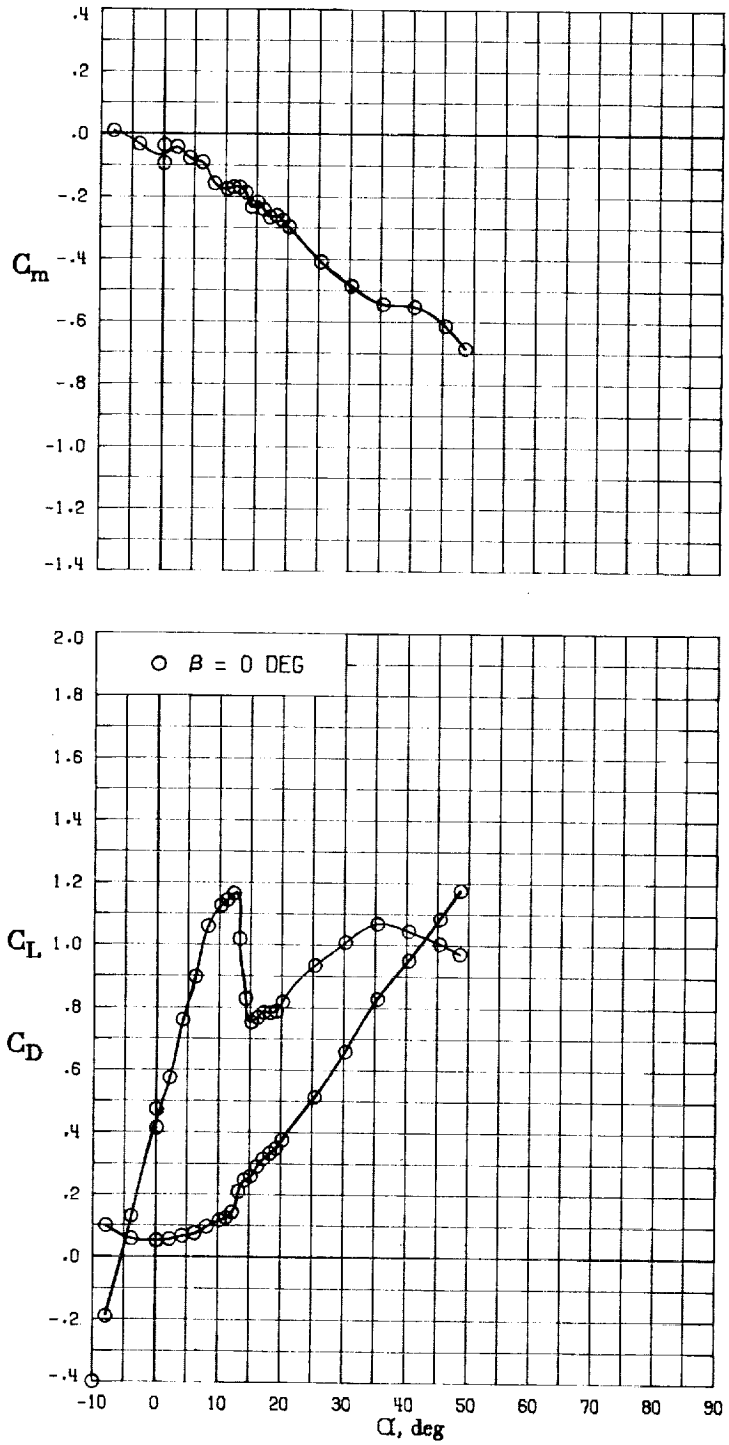

(A) LONGITUDINAL FORCE AND MOMENT COEFFICIENTS ABOUT STABILITY AXES.

FIGURE 58. - EFFECT OF ANGLE OF ATTACK AND SIDESLIP ANGLE ON AERODYNAMIC CHARACTERISTICS AT RE = .288 E+06 FOR CONFIGURATION B W3 H3 V. δ_E = 15°, δ_A = 0°, δ_R = 0°.

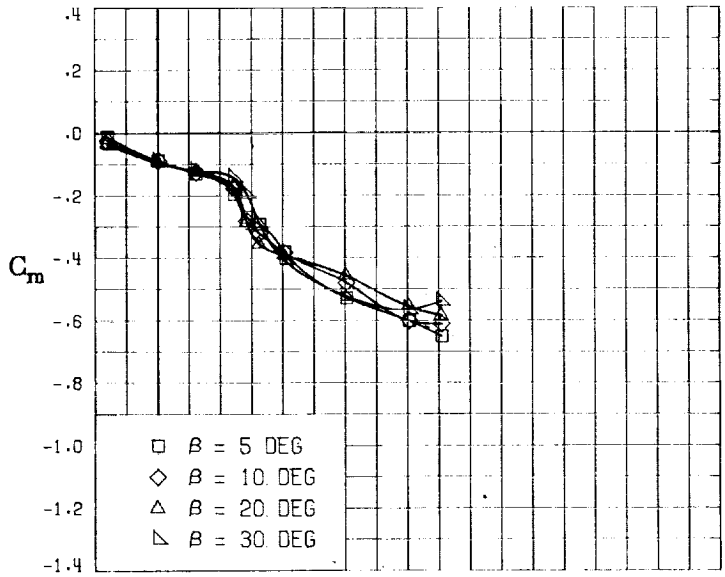

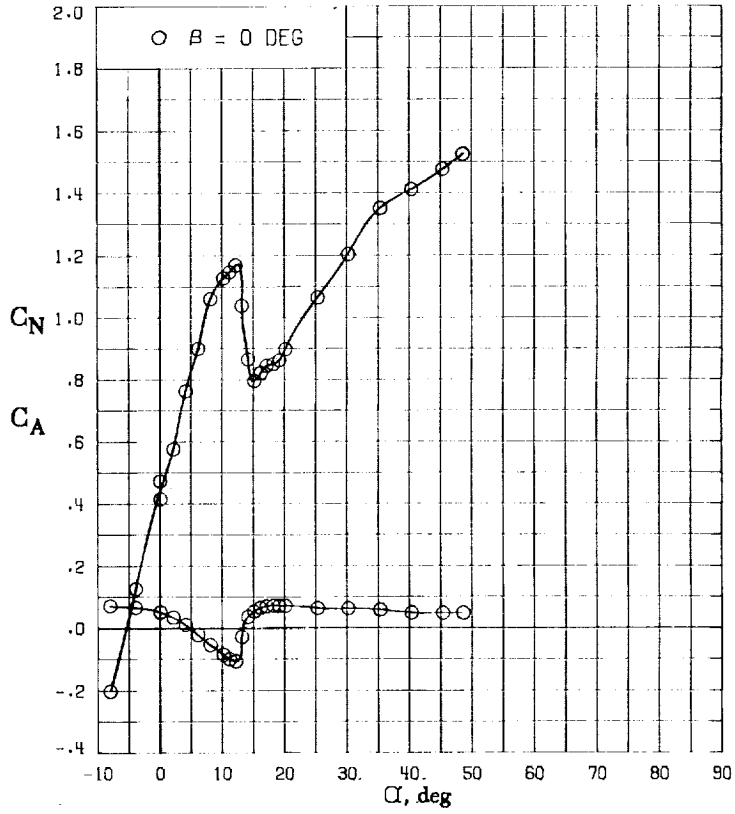

(B) LONGITUDINAL FORCE AND MOMENT COEFFICIENTS ABOUT BODY AXES.

FIGURE 58. - CONTINUED.

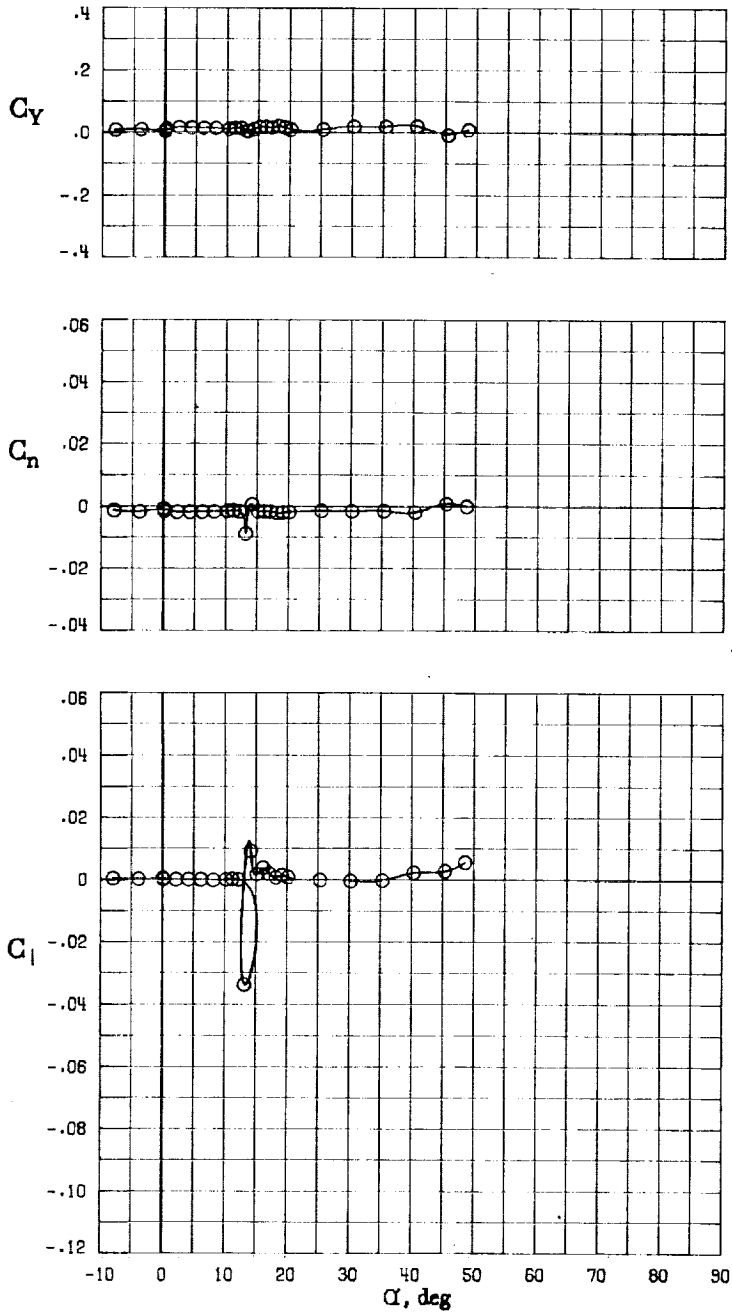

(C) LATERAL - DIRECTIONAL FORCE AND MOMENT COEFFICIENTS ABOUT BODY AXES AT ZERO SIDESLIP.

FIGURE 58. - CONTINUED.

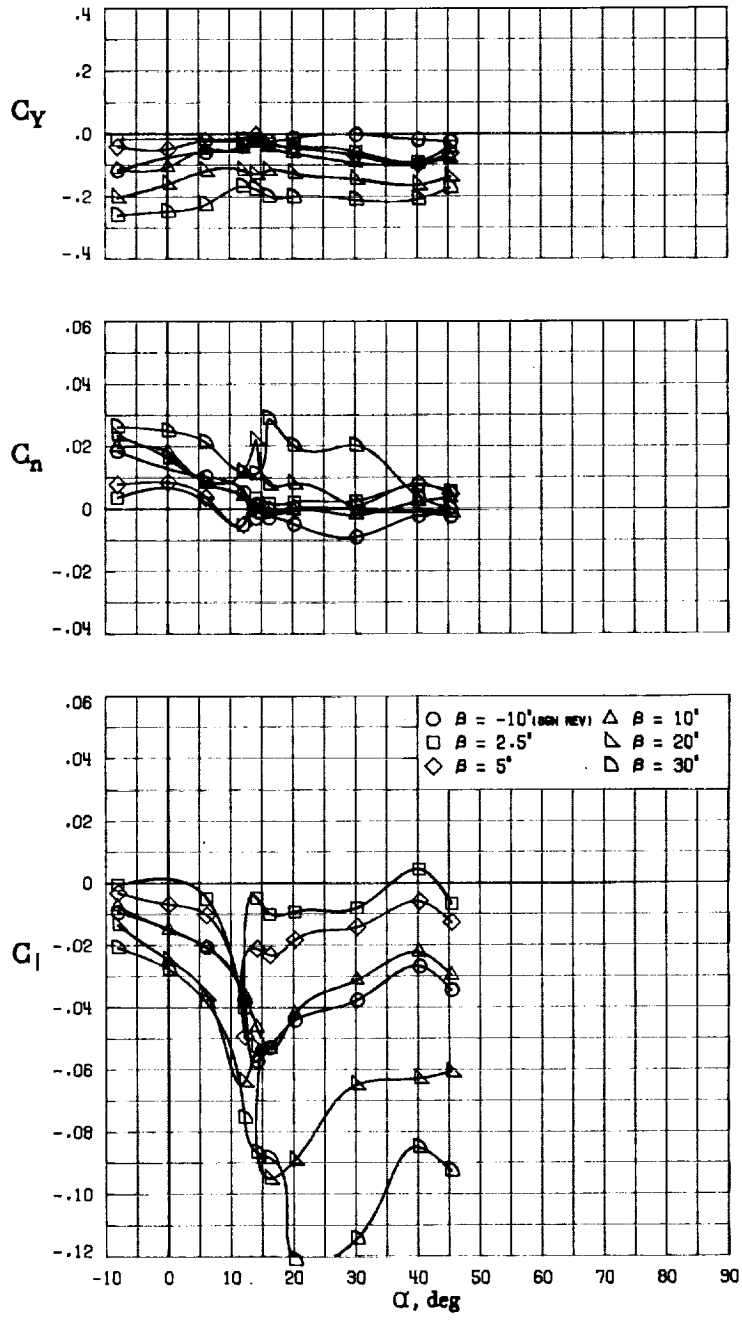

(D) LATERAL - DIRECTIONAL FORCE AND MOMENT COEFFICIENTS ABOUT BODY AXES.

FIGURE 58. - CONTINUED.

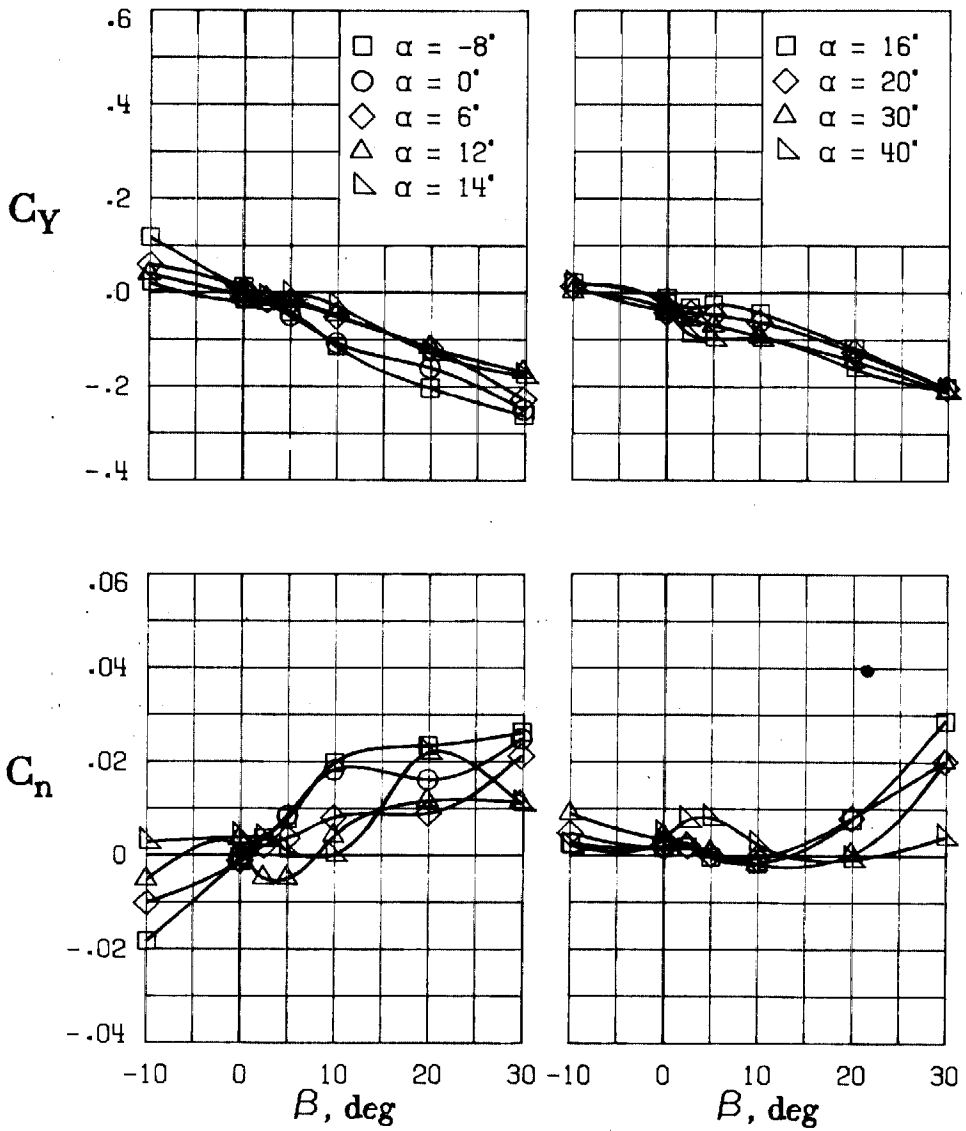

(E) DIRECTIONAL - STABILITY CHARACTERISTICS ABOUT BODY AXES AT VARIOUS ANGLES OF ATTACK.

FIGURE 58. - CONTINUED.

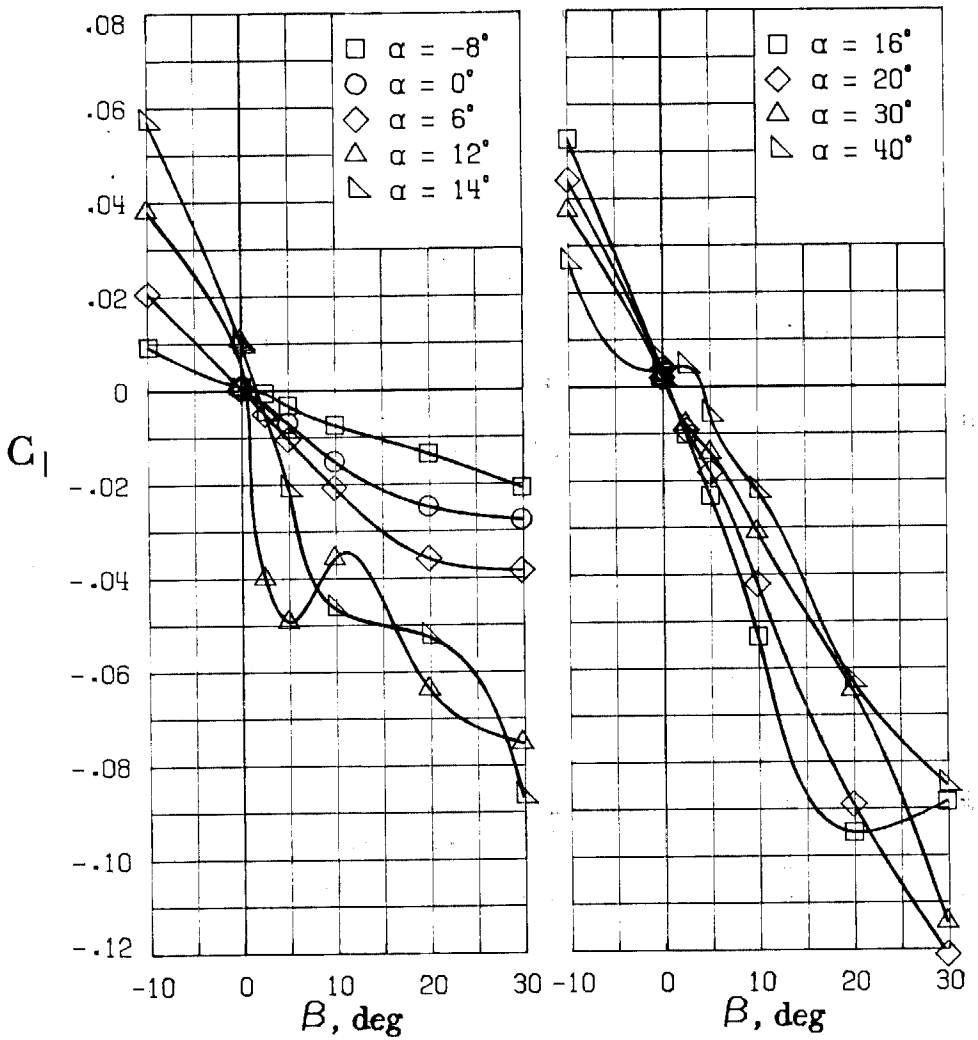

(F) LATERAL - STABILITY CHARACTERISTICS ABOUT BODY AXES AT VARIOUS ANGLES OF ATTACK.

FIGURE 58. - CONCLUDED.

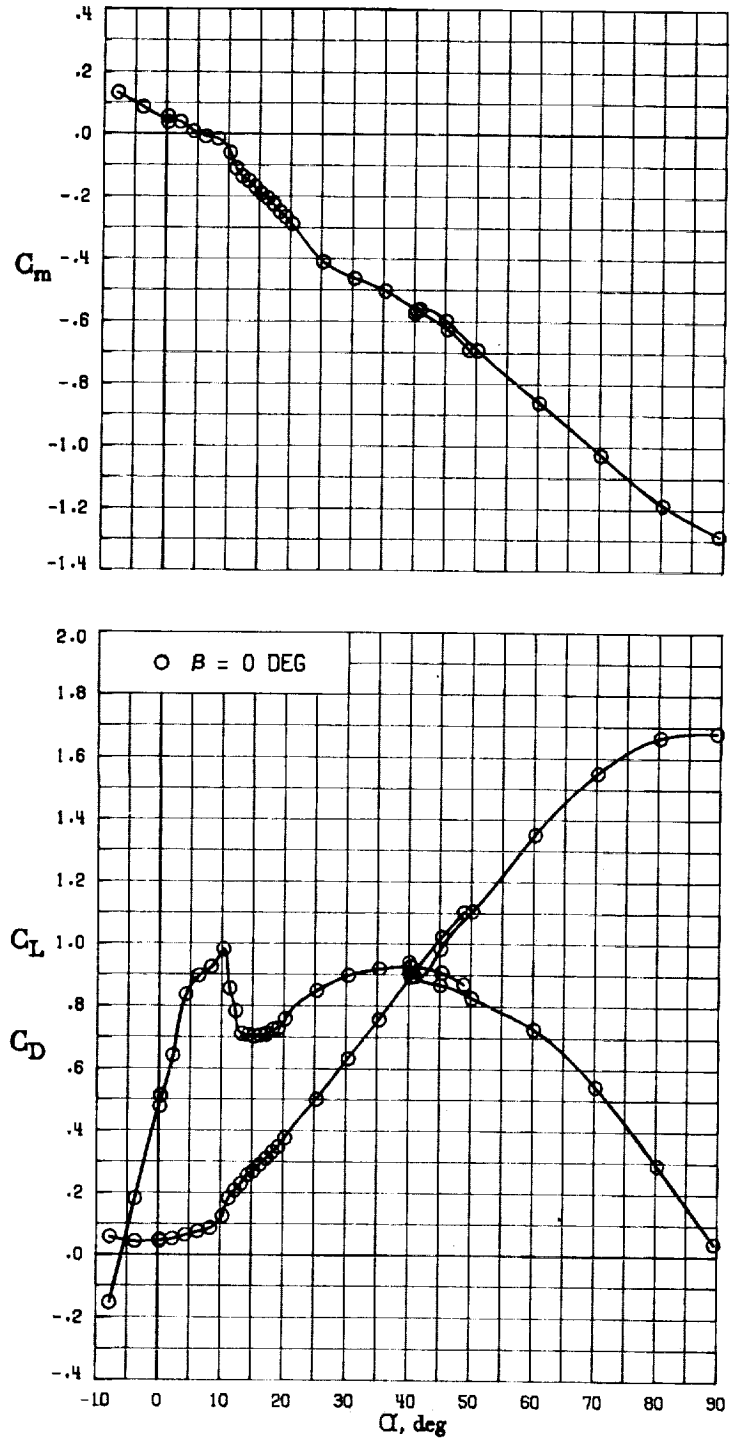

(A) LONGITUDINAL FORCE AND MOMENT COEFFICIENTS ABOUT STABILITY AXES.

FIGURE 59. - EFFECT OF ANGLE OF ATTACK AND SIDESLIP ANGLE ON AERODYNAMIC CHARACTERISTICS AT RE = .288 E+06 FOR CONFIGURATION B W1 H4 V C. $\delta_E = 0°$, $\delta_A = 0°$, $\delta_R = 0°$.

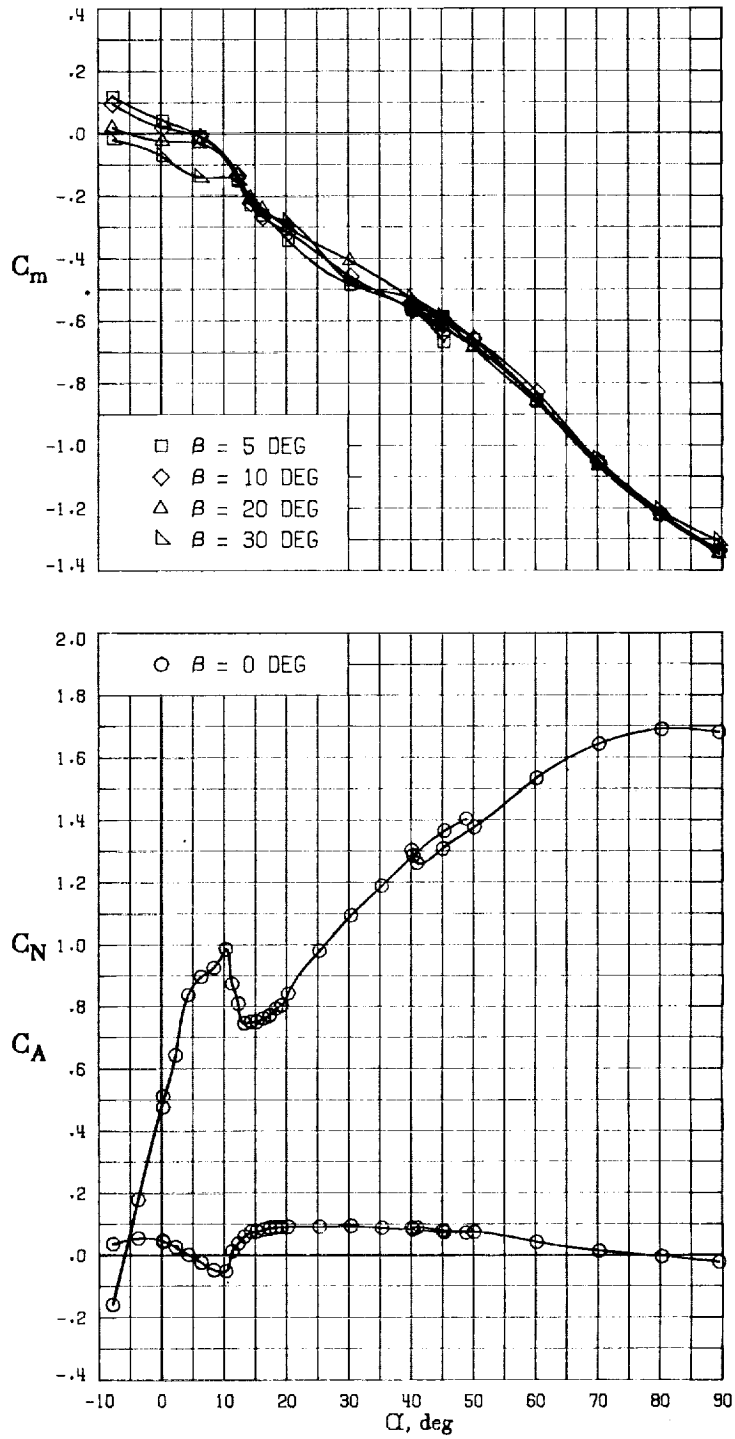

(B) LONGITUDINAL FORCE AND MOMENT COEFFICIENTS ABOUT BODY AXES.

FIGURE 59. - CONTINUED.

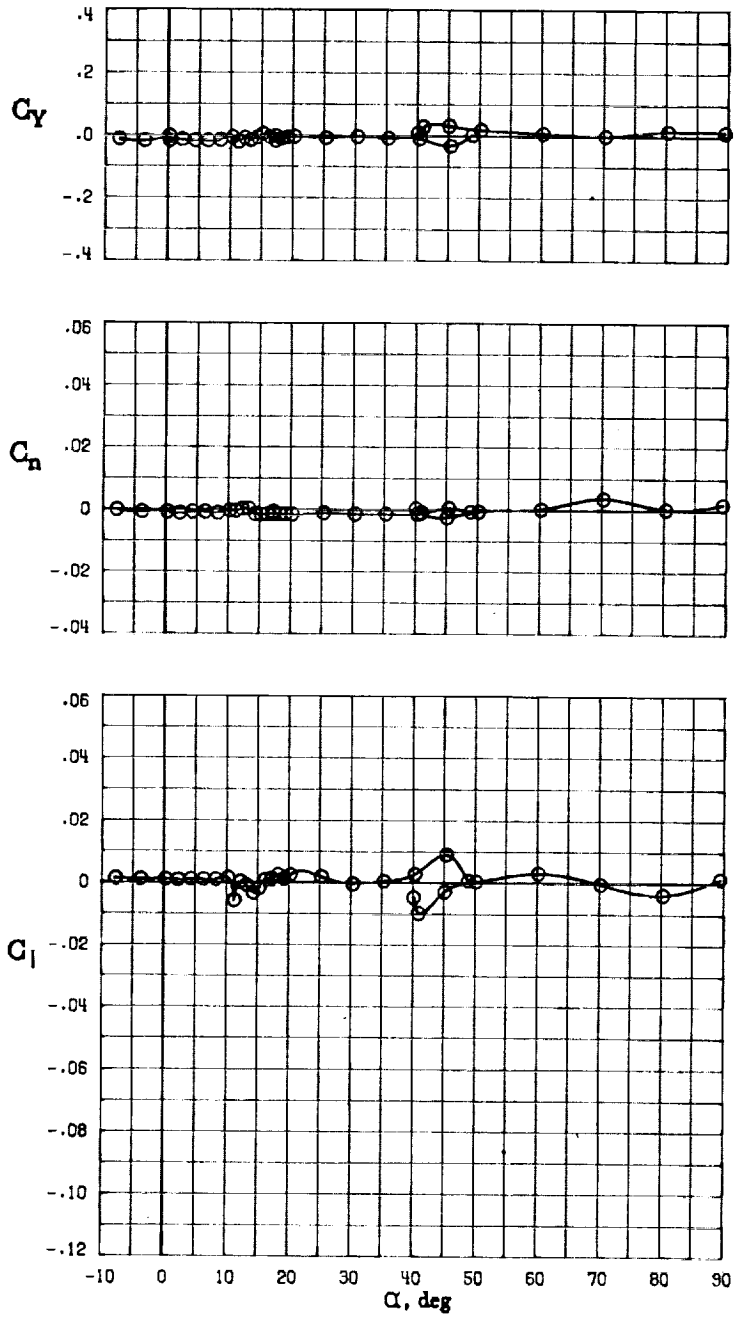

(C) LATERAL - DIRECTIONAL FORCE AND MOMENT COEFFICIENTS ABOUT BODY AXES AT ZERO SIDESLIP.

FIGURE 59. - CONTINUED.

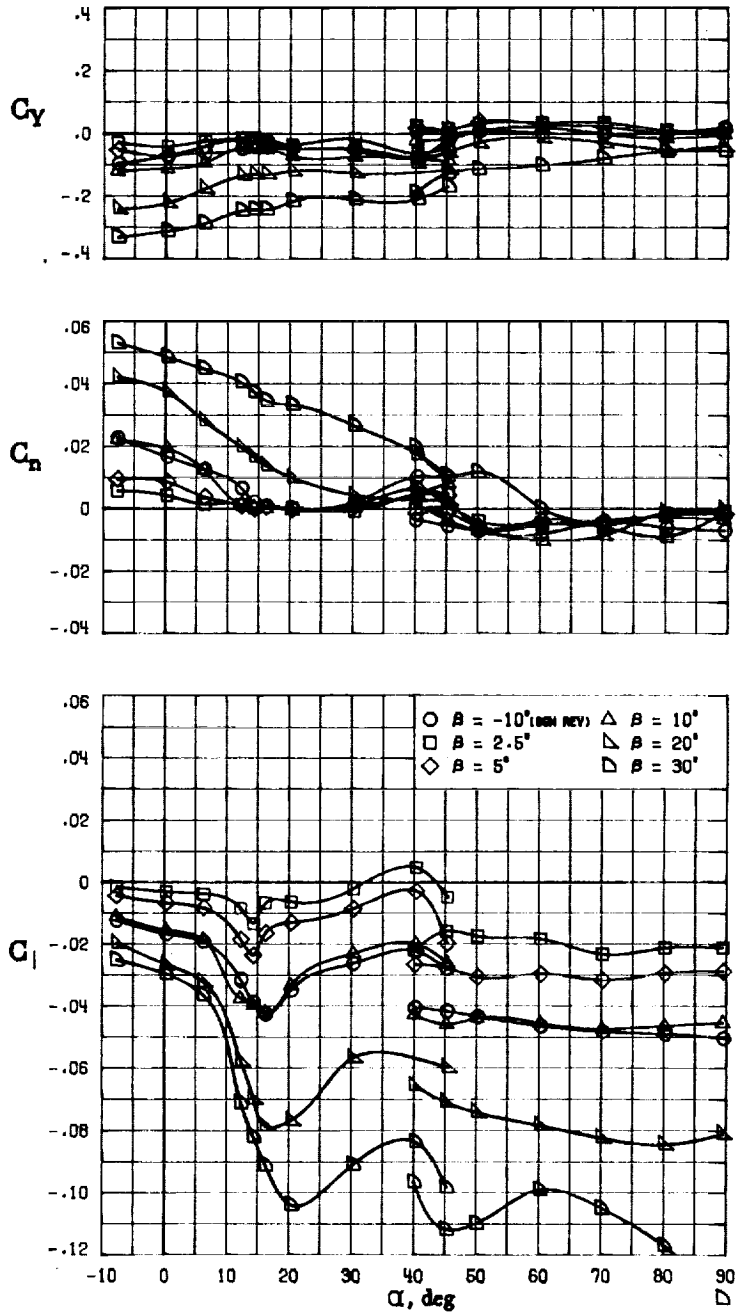

(D) LATERAL - DIRECTIONAL FORCE AND MOMENT COEFFICIENTS ABOUT BODY AXES.

FIGURE 59. - CONTINUED.

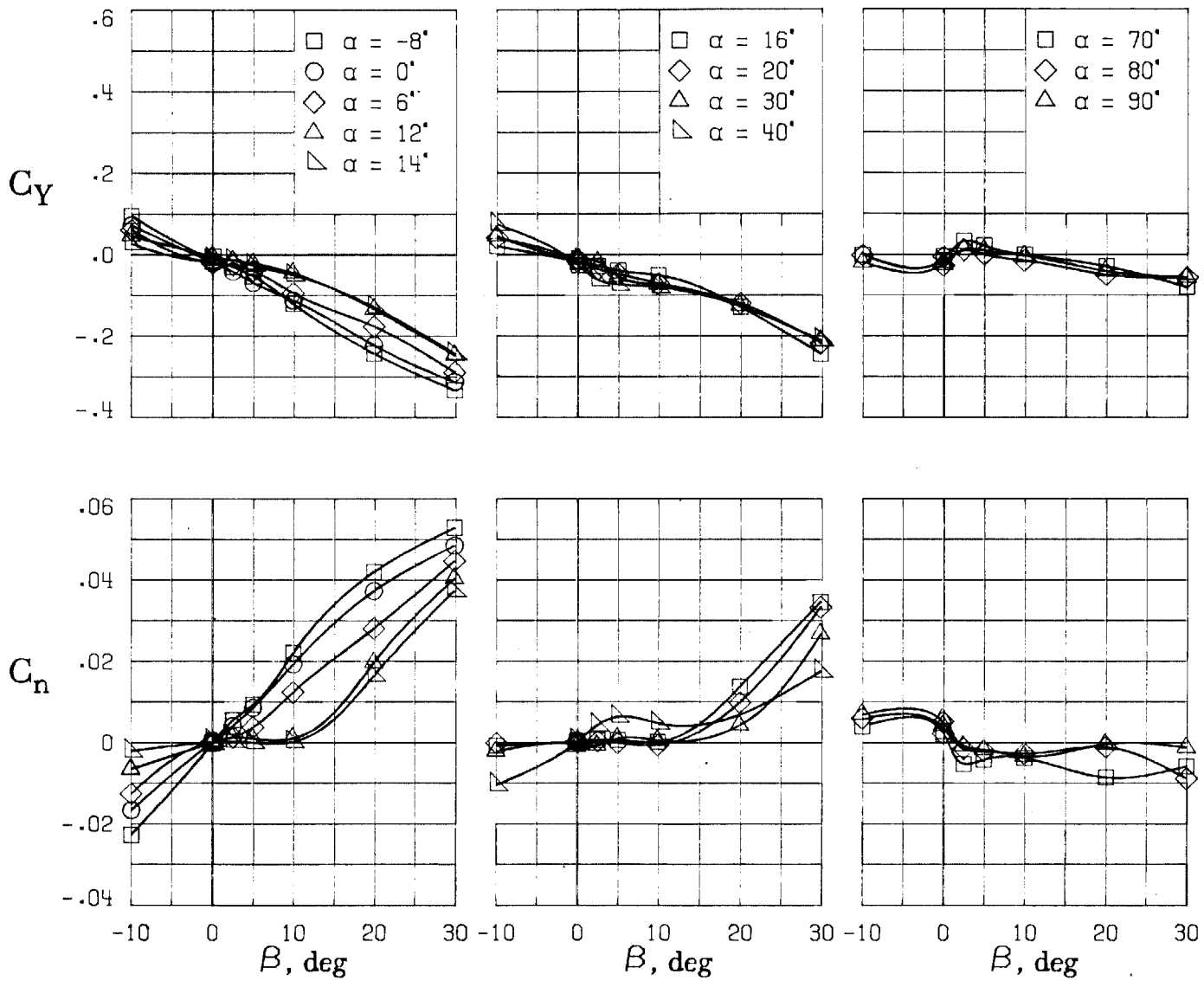

(E) DIRECTIONAL - STABILITY CHARACTERISTICS ABOUT BODY AXES AT VARIOUS ANGLES OF ATTACK.

FIGURE 59. - CONTINUED.

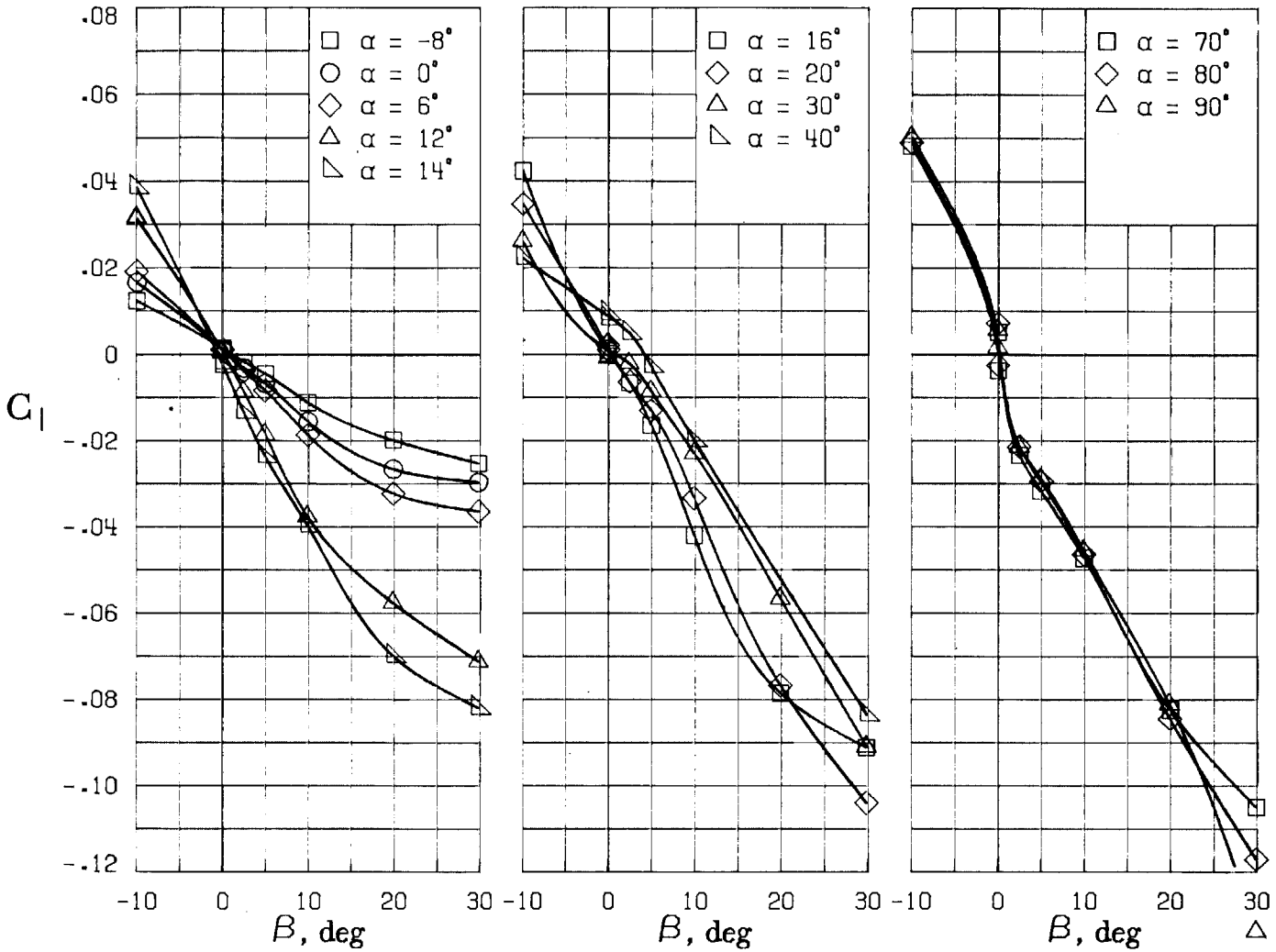

(F) LATERAL - STABILITY CHARACTERISTICS ABOUT BODY AXES AT VARIOUS ANGLES OF ATTACK.

FIGURE 59. - CONCLUDED.

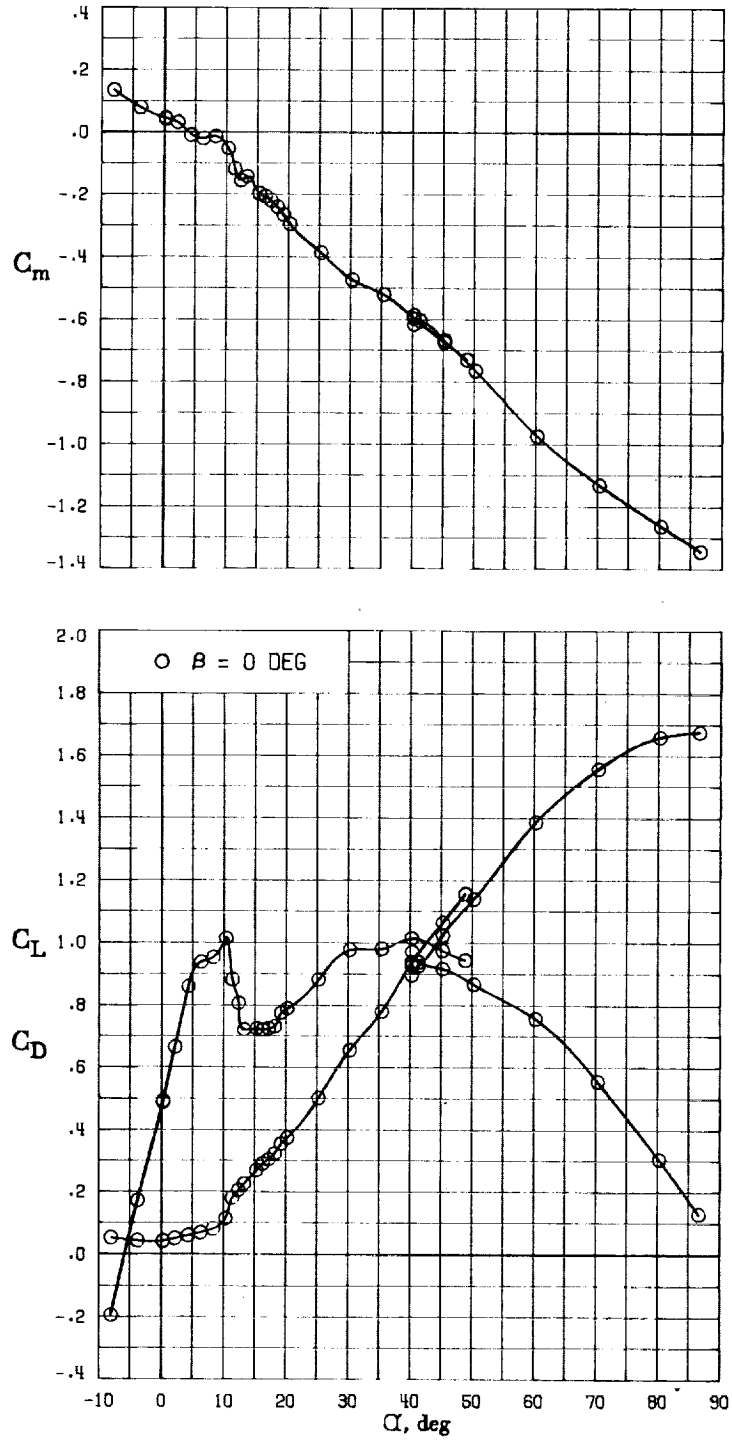

(A) LONGITUDINAL FORCE AND MOMENT COEFFICIENTS ABOUT STABILITY AXES.

FIGURE 60. - EFFECT OF ANGLE OF ATTACK AND SIDESLIP ANGLE ON AERODYNAMIC CHARACTERISTICS AT RE = .288 E+06 FOR CONFIGURATION B W1 H4 V SH. $\delta_E = 0°$, $\delta_A = 0°$, $\delta_R = 0°$.

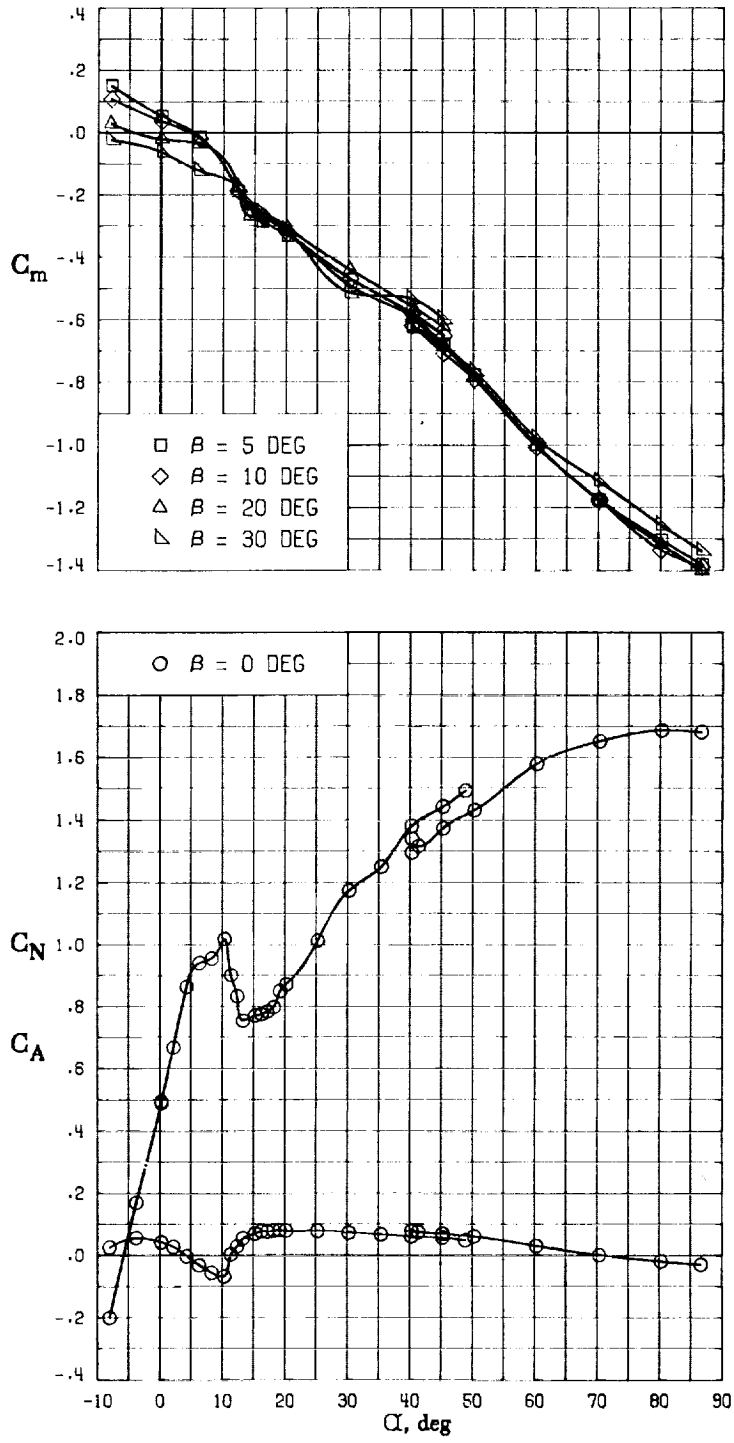

(B) LONGITUDINAL FORCE AND MOMENT COEFFICIENTS ABOUT BODY AXES.

FIGURE 60. - CONTINUED.

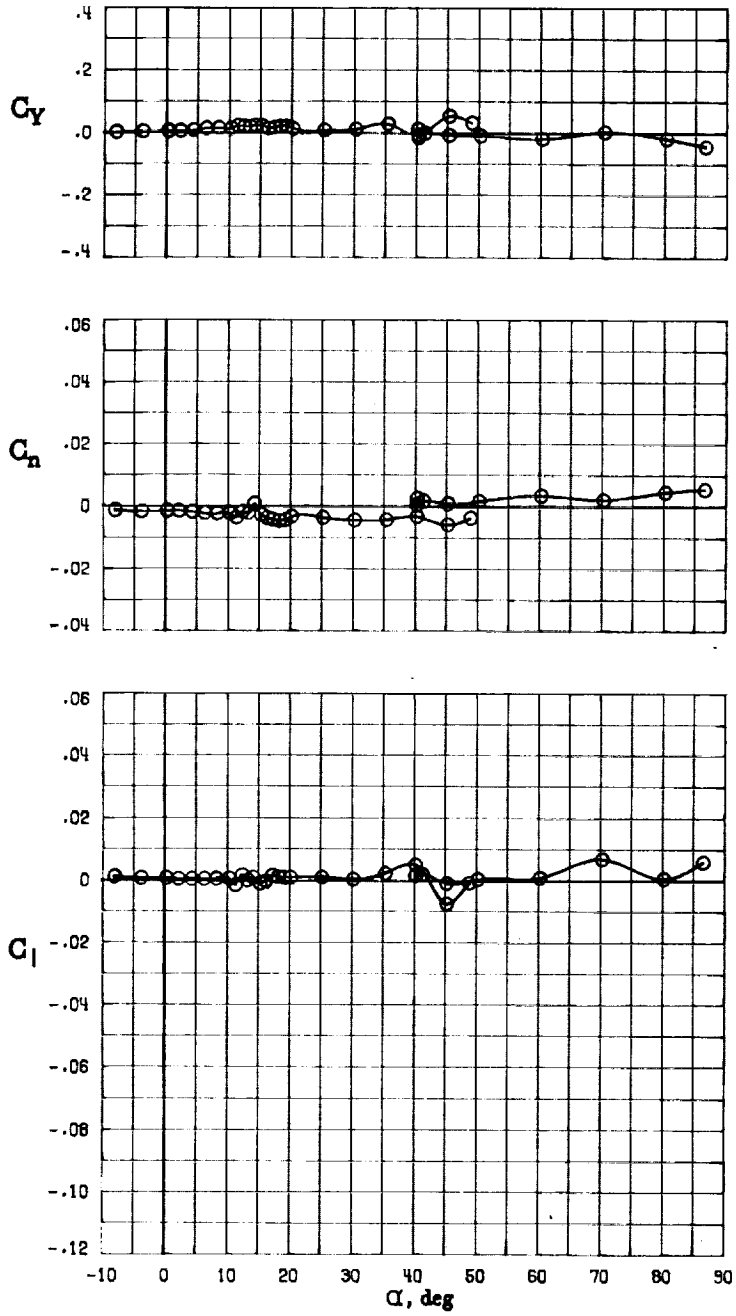

(C) LATERAL - DIRECTIONAL FORCE AND MOMENT COEFFICIENTS ABOUT BODY AXES AT ZERO SIDESLIP.

FIGURE 60. - CONTINUED.

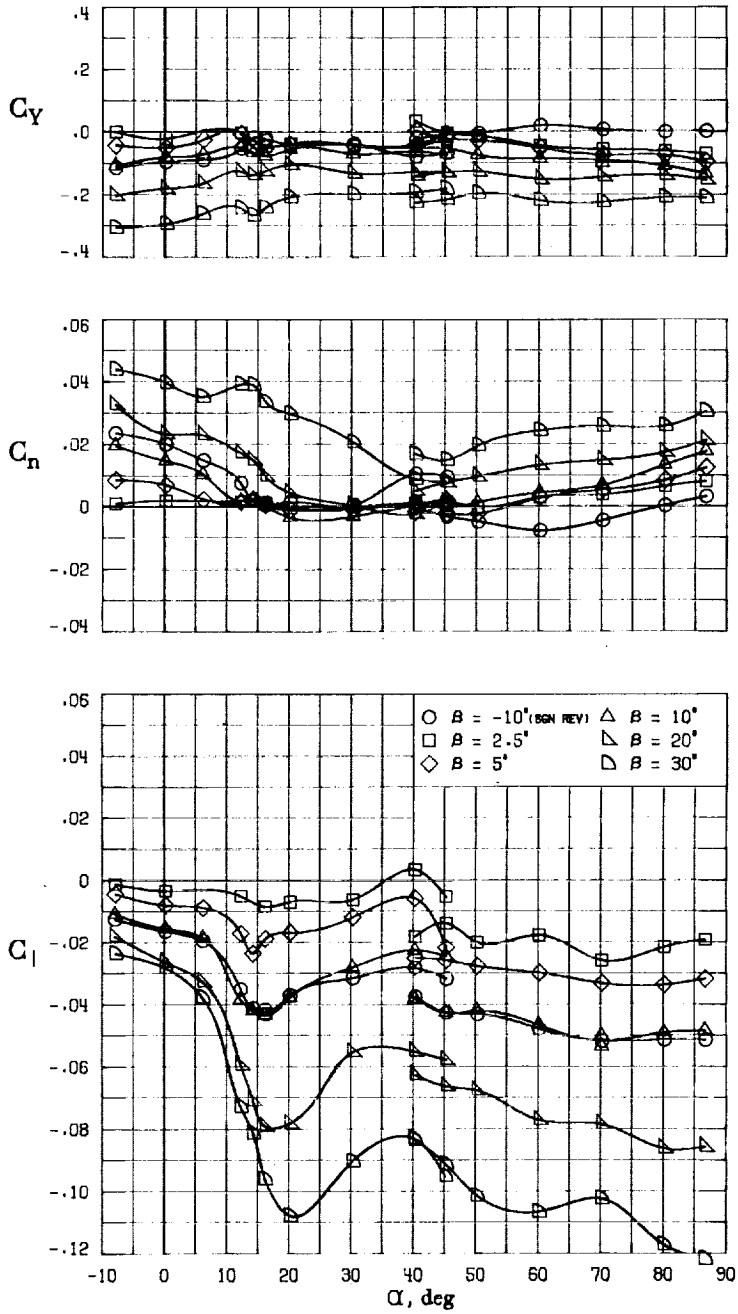

(D) LATERAL - DIRECTIONAL FORCE AND MOMENT COEFFICIENTS ABOUT BODY AXES.

FIGURE 60. - CONTINUED.

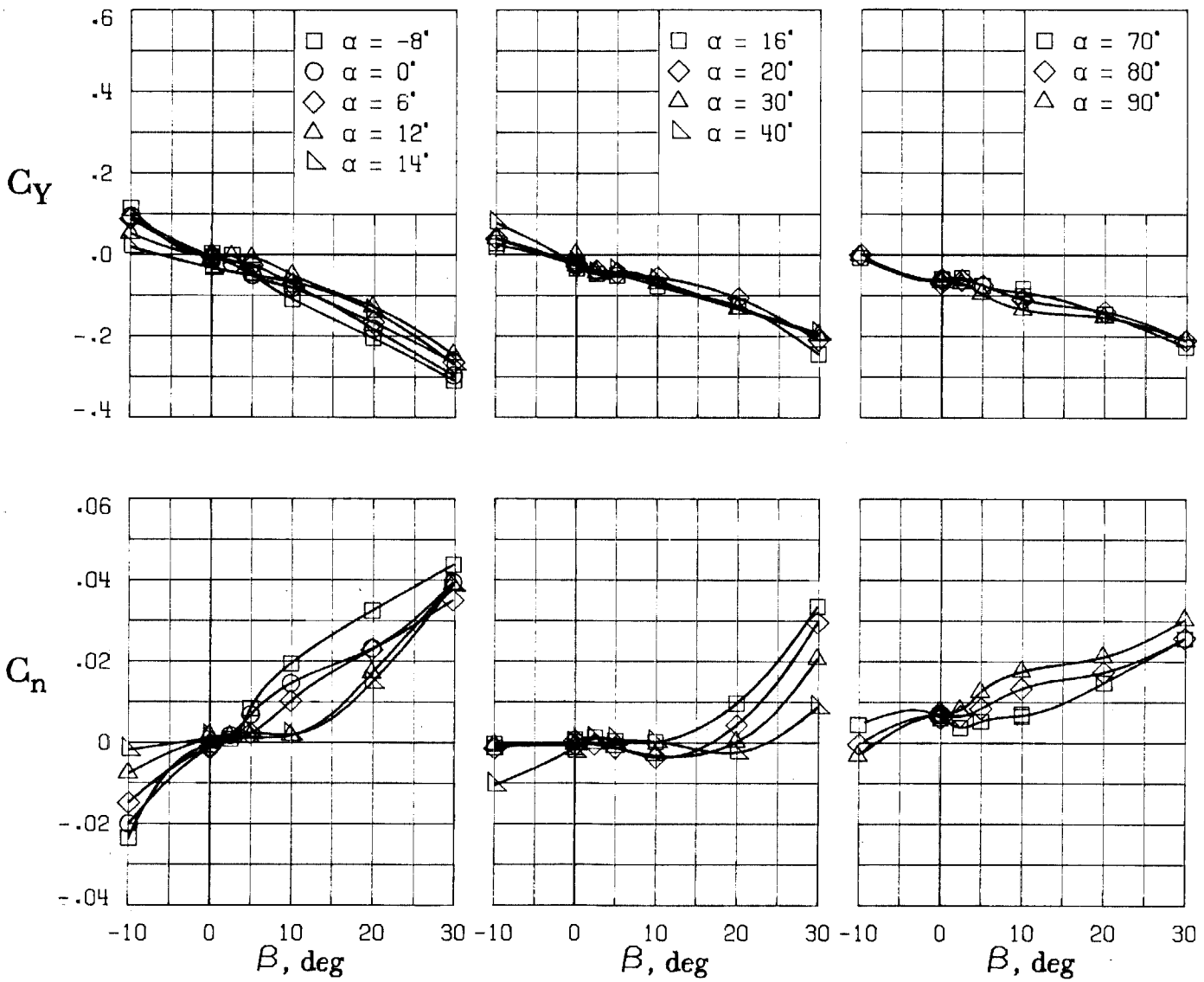

(E) DIRECTIONAL - STABILITY CHARACTERISTICS ABOUT BODY AXES AT VARIOUS ANGLES OF ATTACK.

FIGURE 60. - CONTINUED.

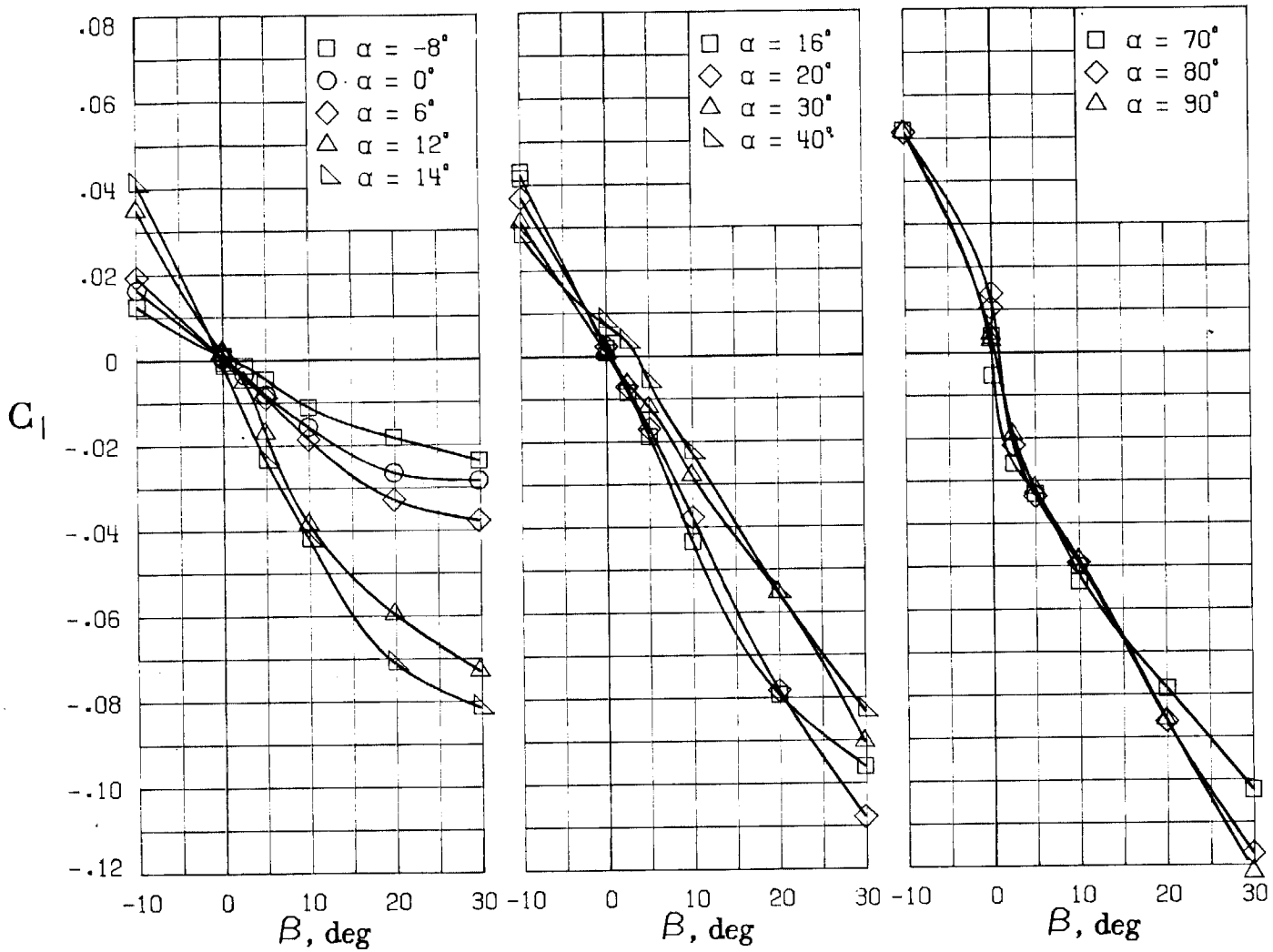

(F) LATERAL - STABILITY CHARACTERISTICS ABOUT BODY AXES AT VARIOUS ANGLES OF ATTACK.

FIGURE 60. - CONCLUDED.

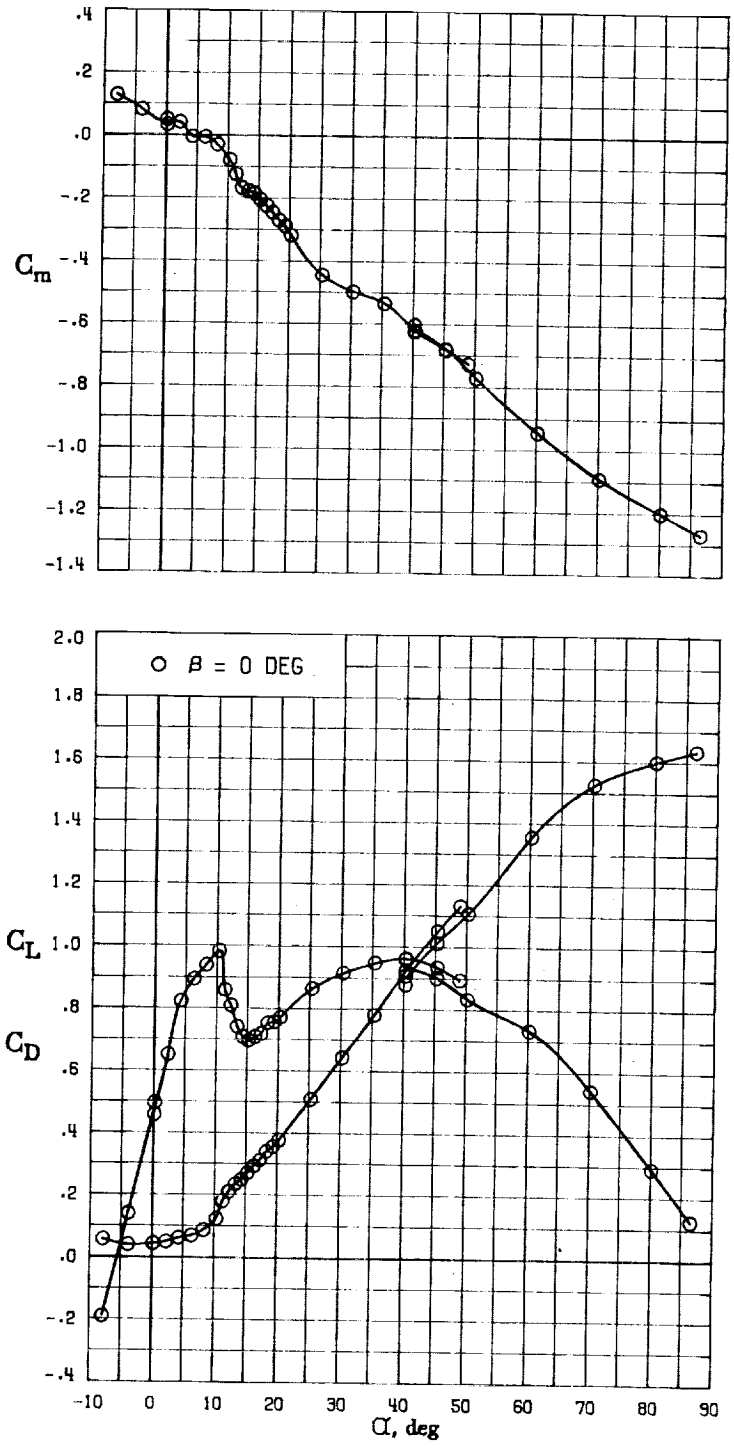

(A) LONGITUDINAL FORCE AND MOMENT COEFFICIENTS ABOUT STABILITY AXES.

FIGURE 61. - EFFECT OF ANGLE OF ATTACK AND SIDESLIP ANGLE ON AERODYNAMIC CHARACTERISTICS AT RE = .288 E+06 FOR CONFIGURATION B W1 H4 V SV. $\delta_E = 0°$, $\delta_A = 0°$, $\delta_R = 0°$.

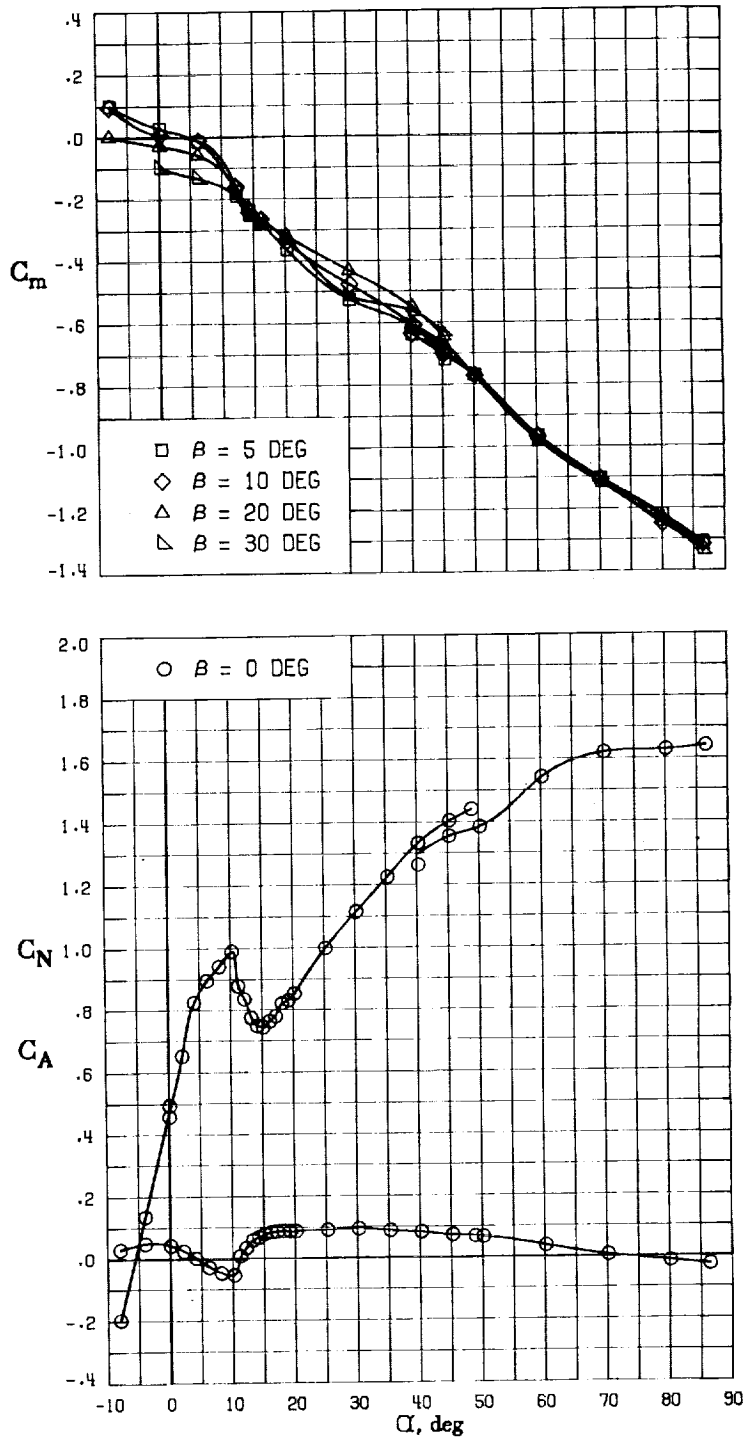

(B) LONGITUDINAL FORCE AND MOMENT COEFFICIENTS ABOUT BODY AXES.

FIGURE 61. - CONTINUED.

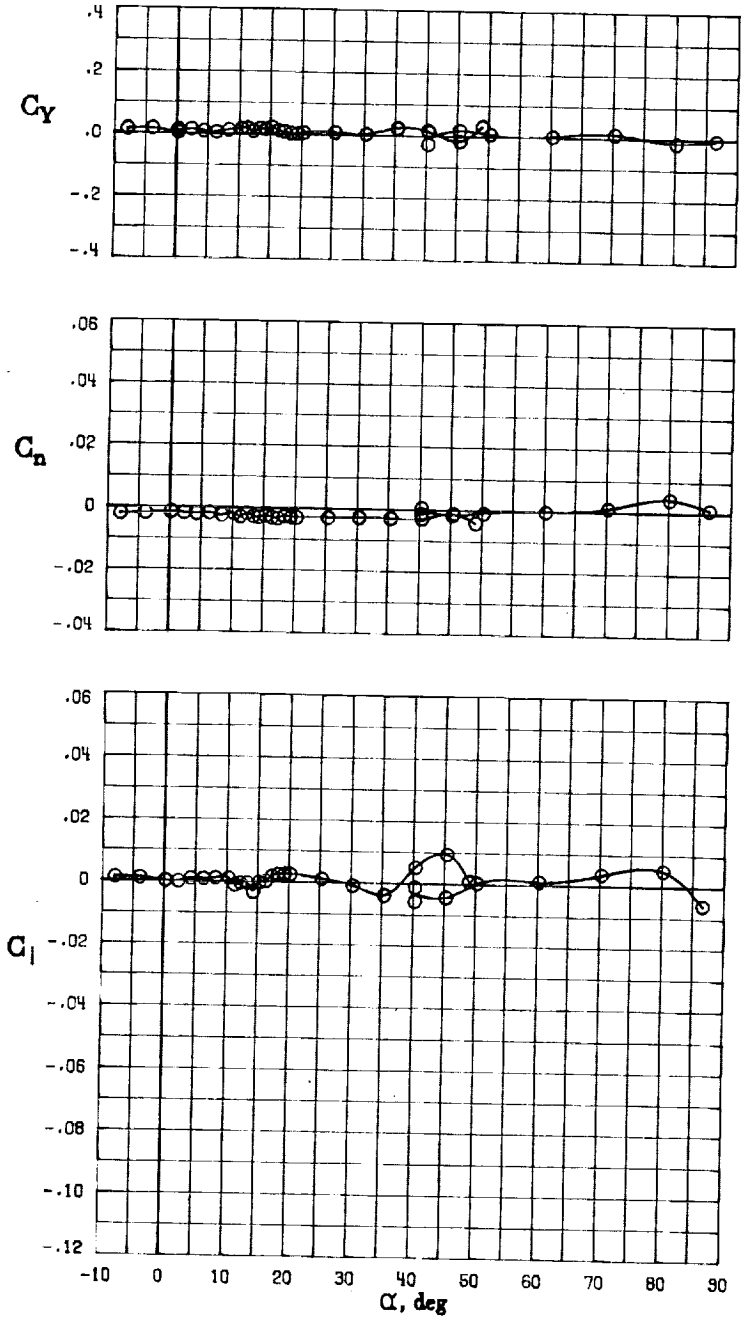

(C) LATERAL - DIRECTIONAL FORCE AND MOMENT COEFFICIENTS ABOUT BODY AXES AT ZERO SIDESLIP.

FIGURE 61. - CONTINUED.

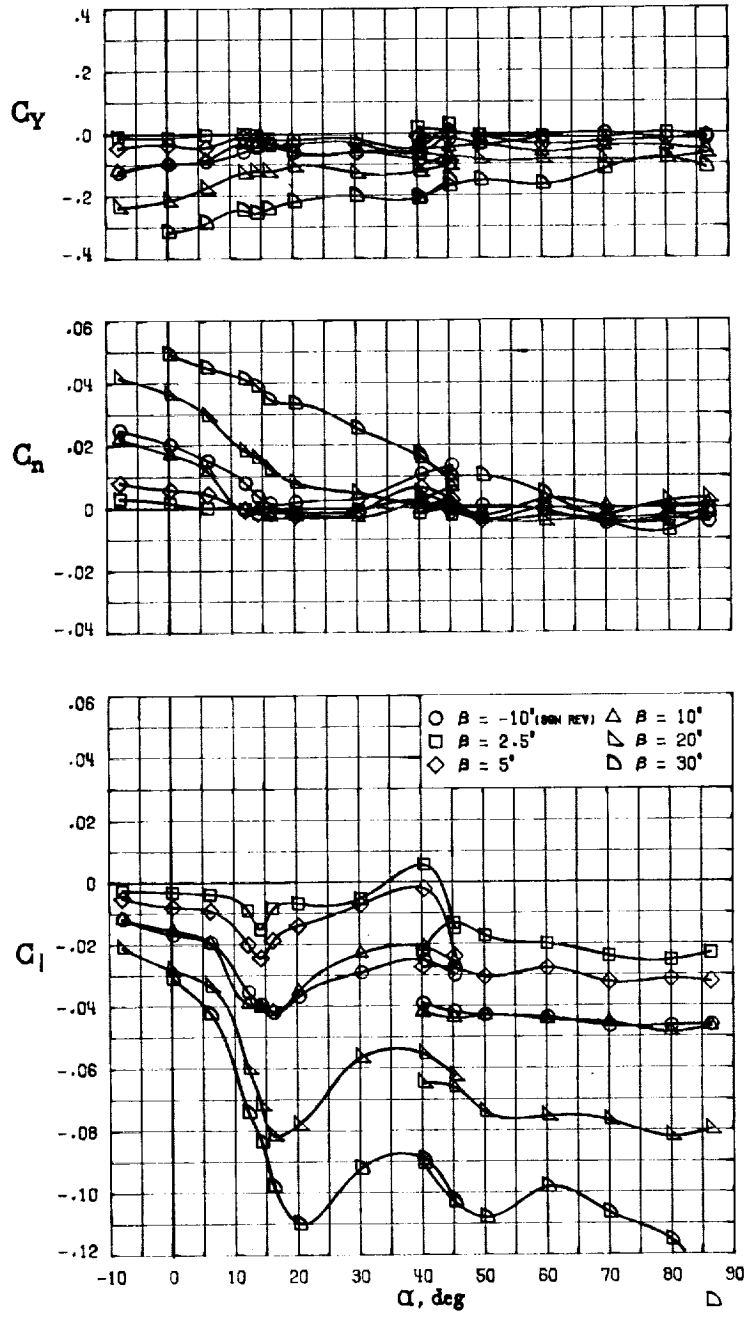

(D) LATERAL - DIRECTIONAL FORCE AND MOMENT COEFFICIENTS ABOUT BODY AXES.

FIGURE 61. - CONTINUED.

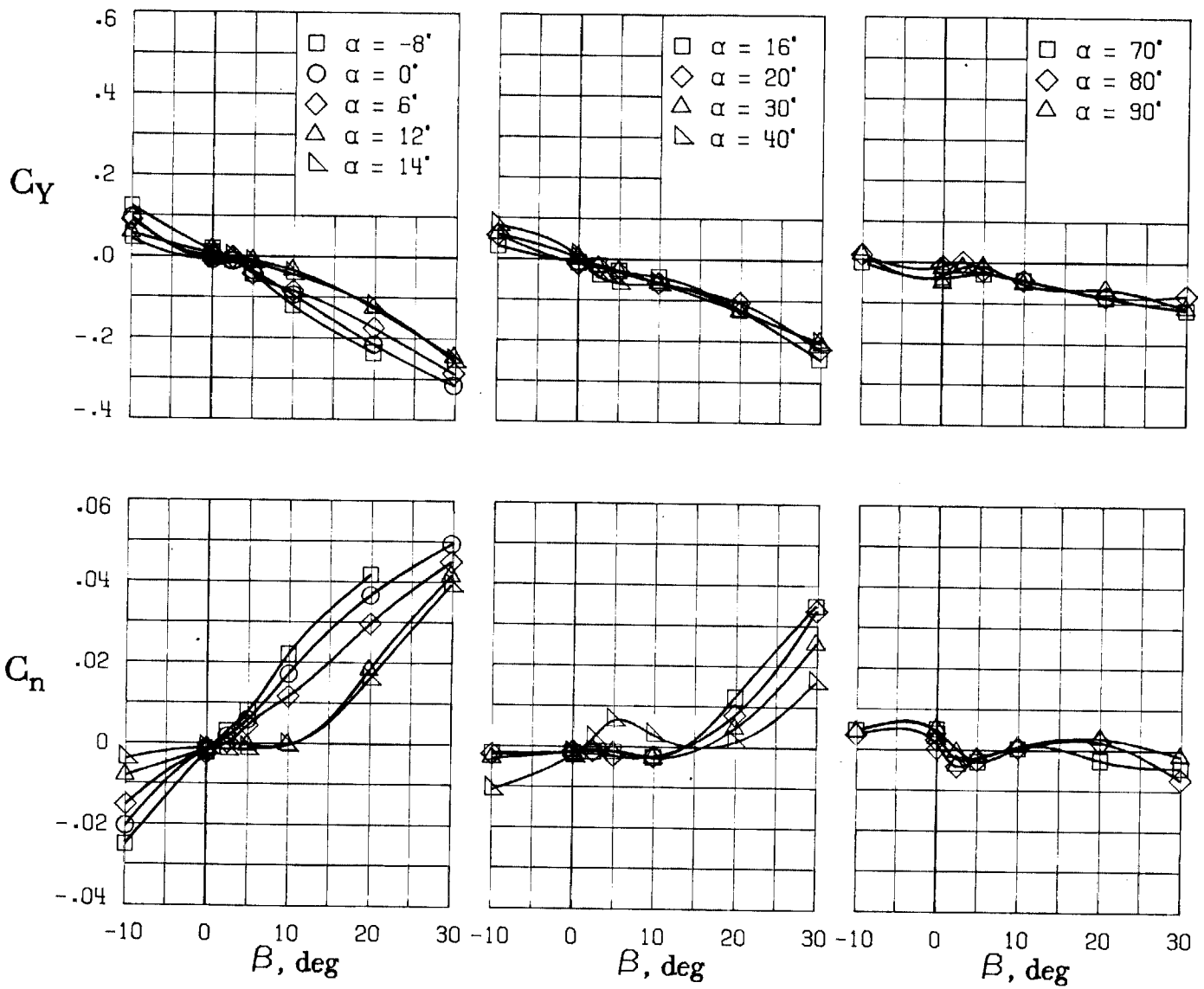

(E) DIRECTIONAL - STABILITY CHARACTERISTICS ABOUT BODY AXES AT VARIOUS ANGLES OF ATTACK.

FIGURE 61. - CONTINUED.

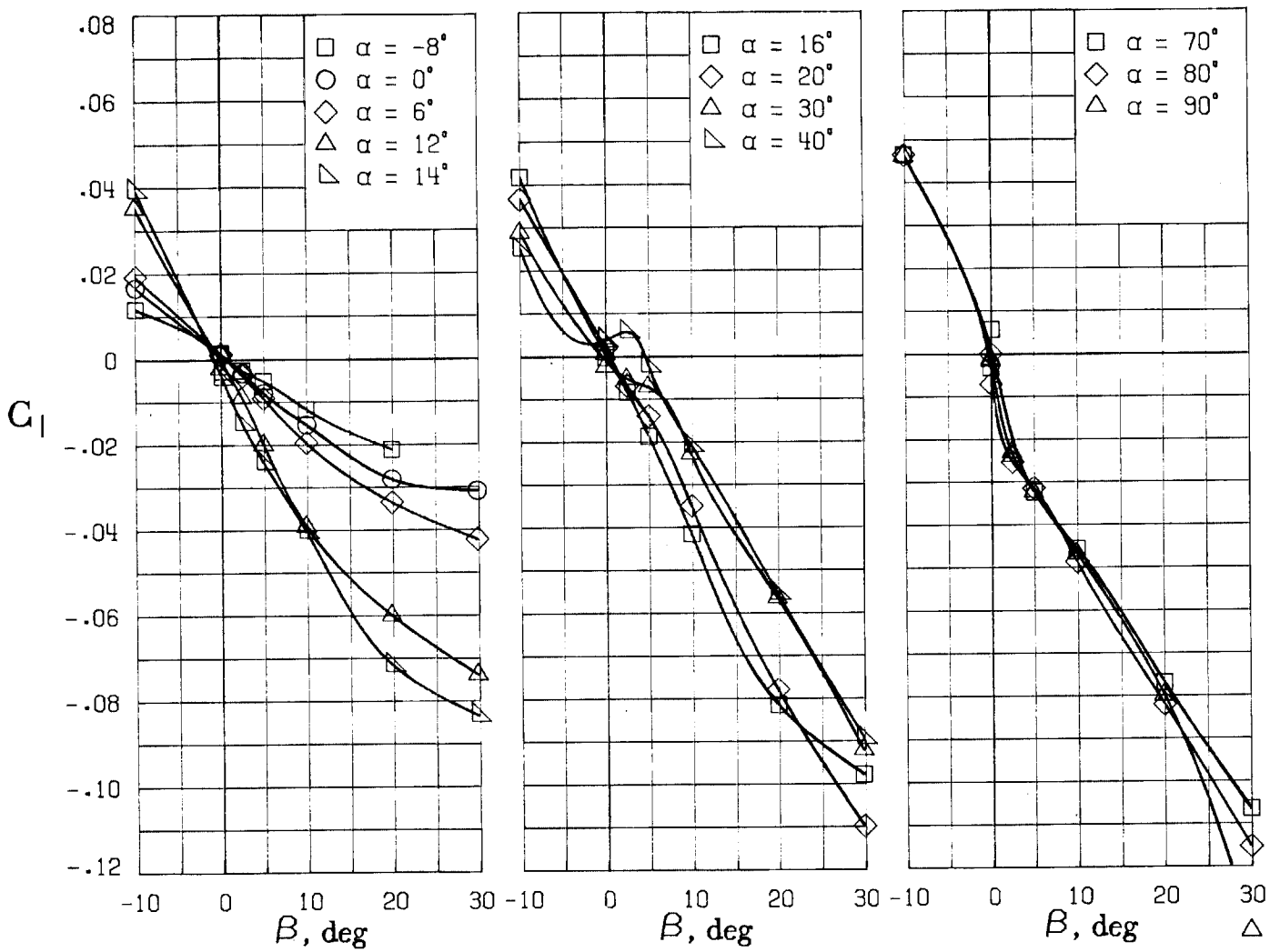

(F) LATERAL - STABILITY CHARACTERISTICS ABOUT BODY AXES AT VARIOUS ANGLES OF ATTACK.

FIGURE 61. - CONCLUDED.

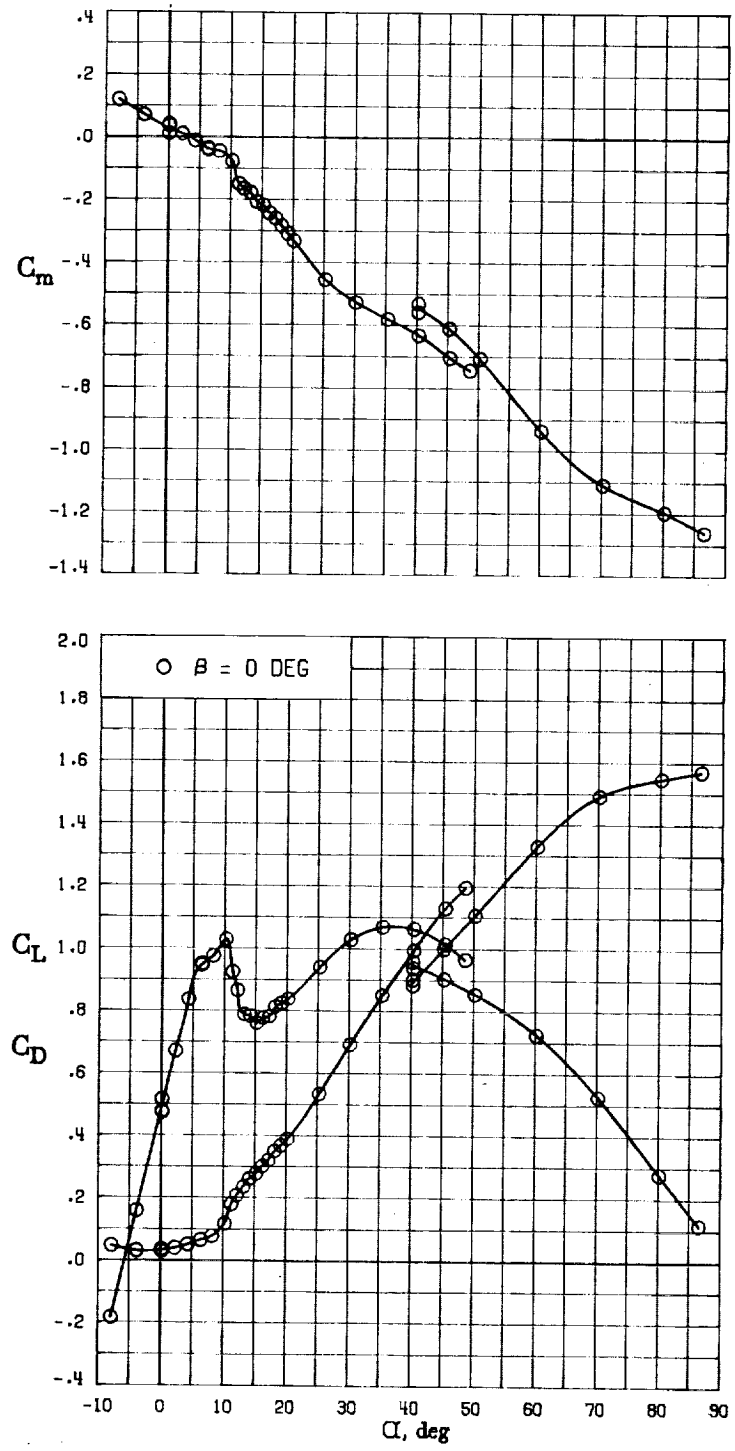

(A) LONGITUDINAL FORCE AND MOMENT COEFFICIENTS ABOUT STABILITY AXES.

FIGURE 62. - EFFECT OF ANGLE OF ATTACK AND SIDESLIP ANGLE ON AERODYNAMIC CHARACTERISTICS AT RE = .288 E+06 FOR CONFIGURATION B W1 H4 V SC. $\delta_E = 0°$, $\delta_A = 0°$, $\delta_R = 0°$.

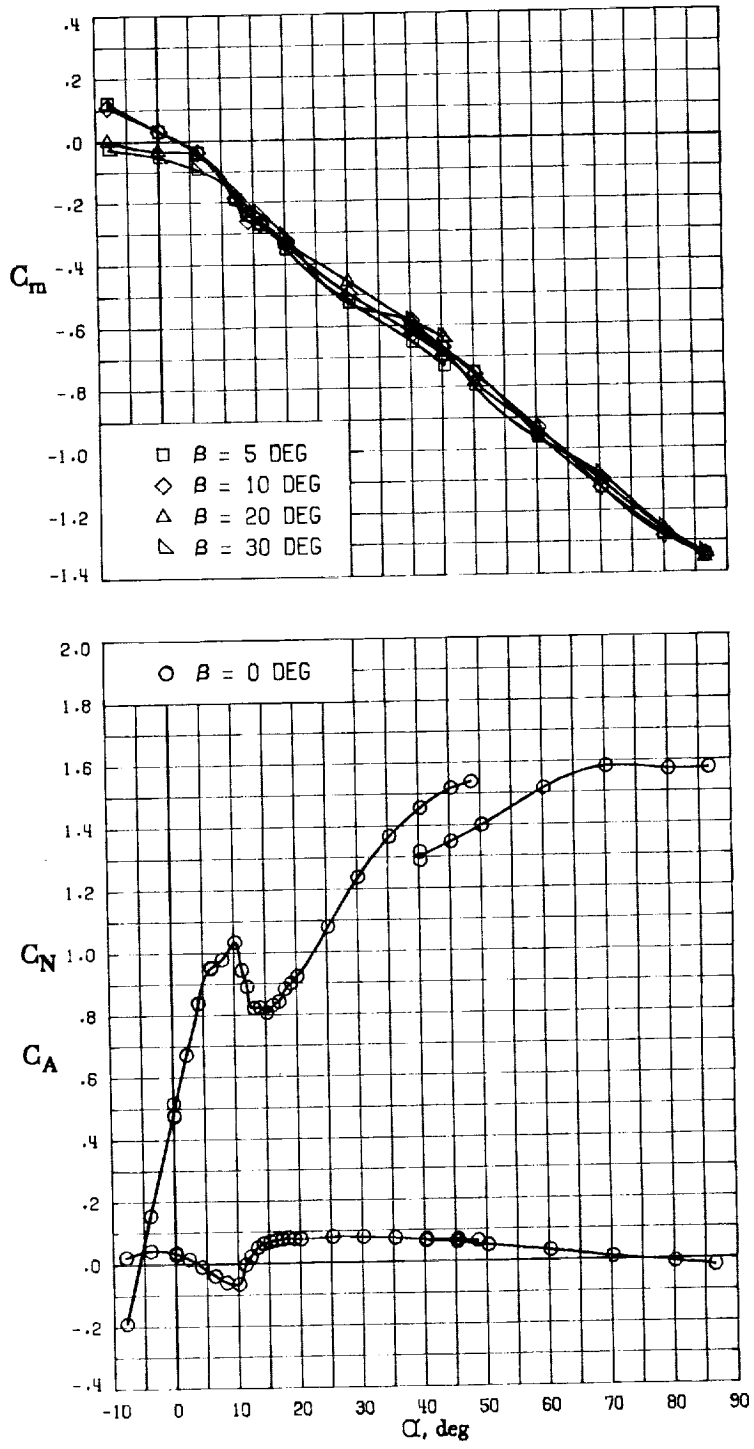

(B) LONGITUDINAL FORCE AND MOMENT COEFFICIENTS ABOUT BODY AXES.

FIGURE 62. - CONTINUED.

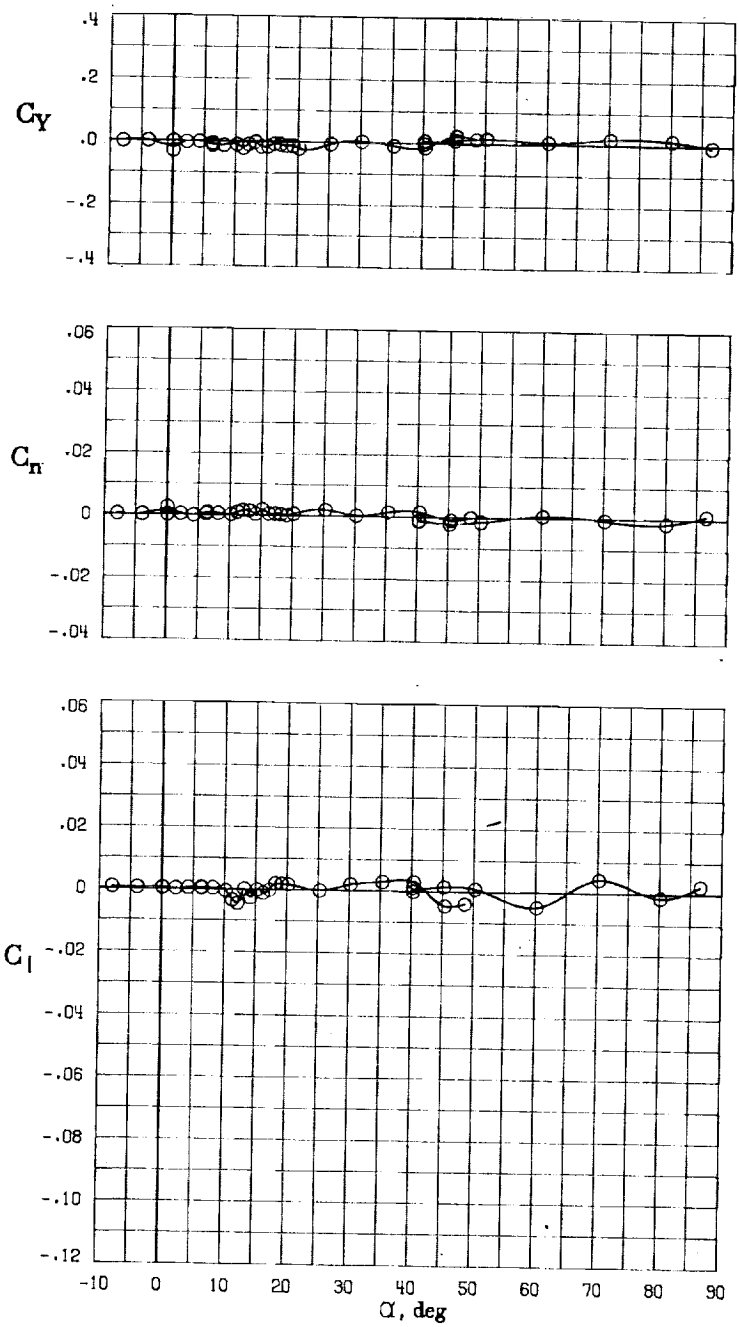

(C) LATERAL - DIRECTIONAL FORCE AND MOMENT COEFFICIENTS ABOUT BODY AXES AT ZERO SIDESLIP.

FIGURE 62. - CONTINUED.

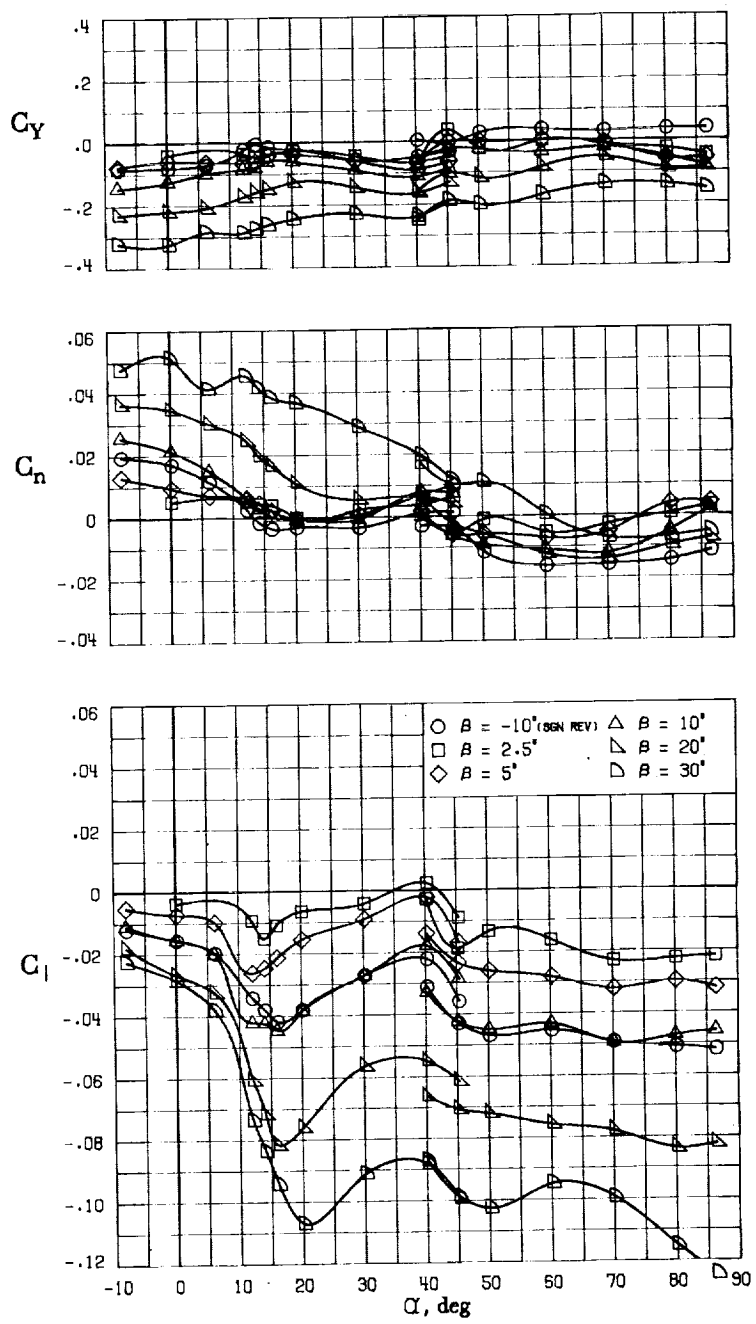

(D) LATERAL - DIRECTIONAL FORCE AND MOMENT COEFFICIENTS ABOUT BODY AXES.

FIGURE 62. - CONTINUED.

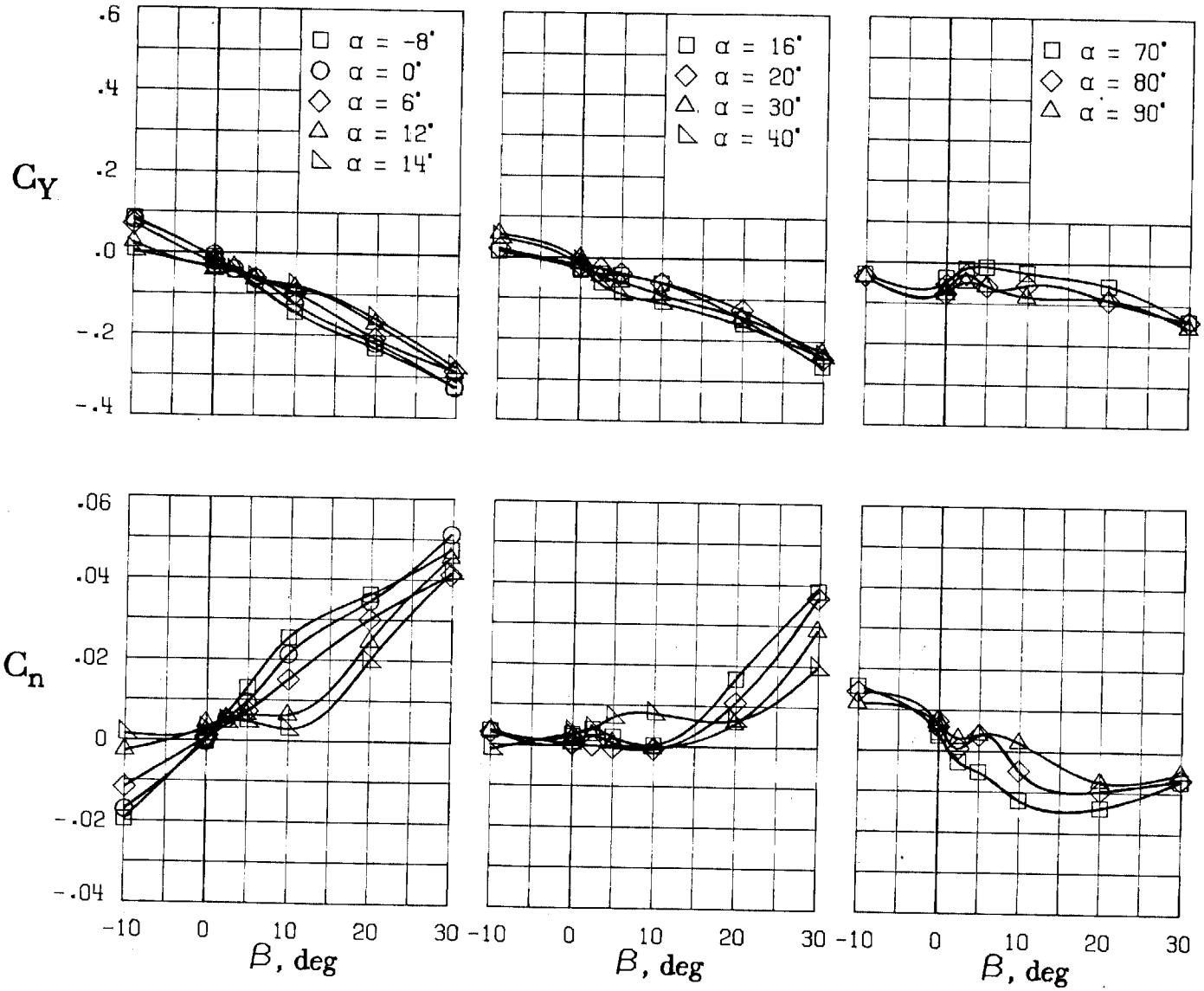

(E) DIRECTIONAL - STABILITY CHARACTERISTICS ABOUT BODY AXES AT VARIOUS ANGLES OF ATTACK.

FIGURE 62. - CONTINUED.

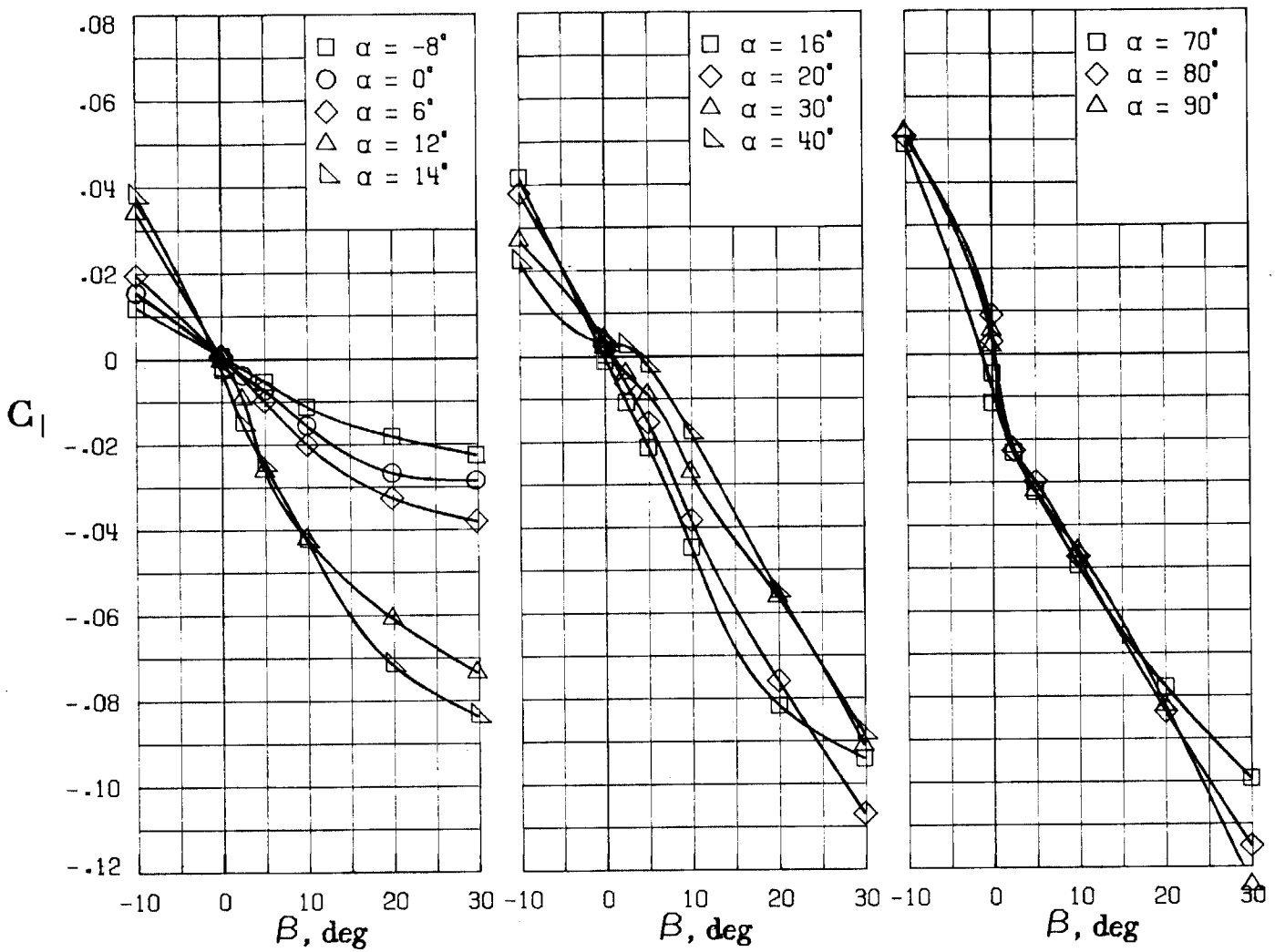

(F) LATERAL - STABILITY CHARACTERISTICS ABOUT BODY AXES AT VARIOUS ANGLES OF ATTACK.

FIGURE 62. - CONCLUDED.

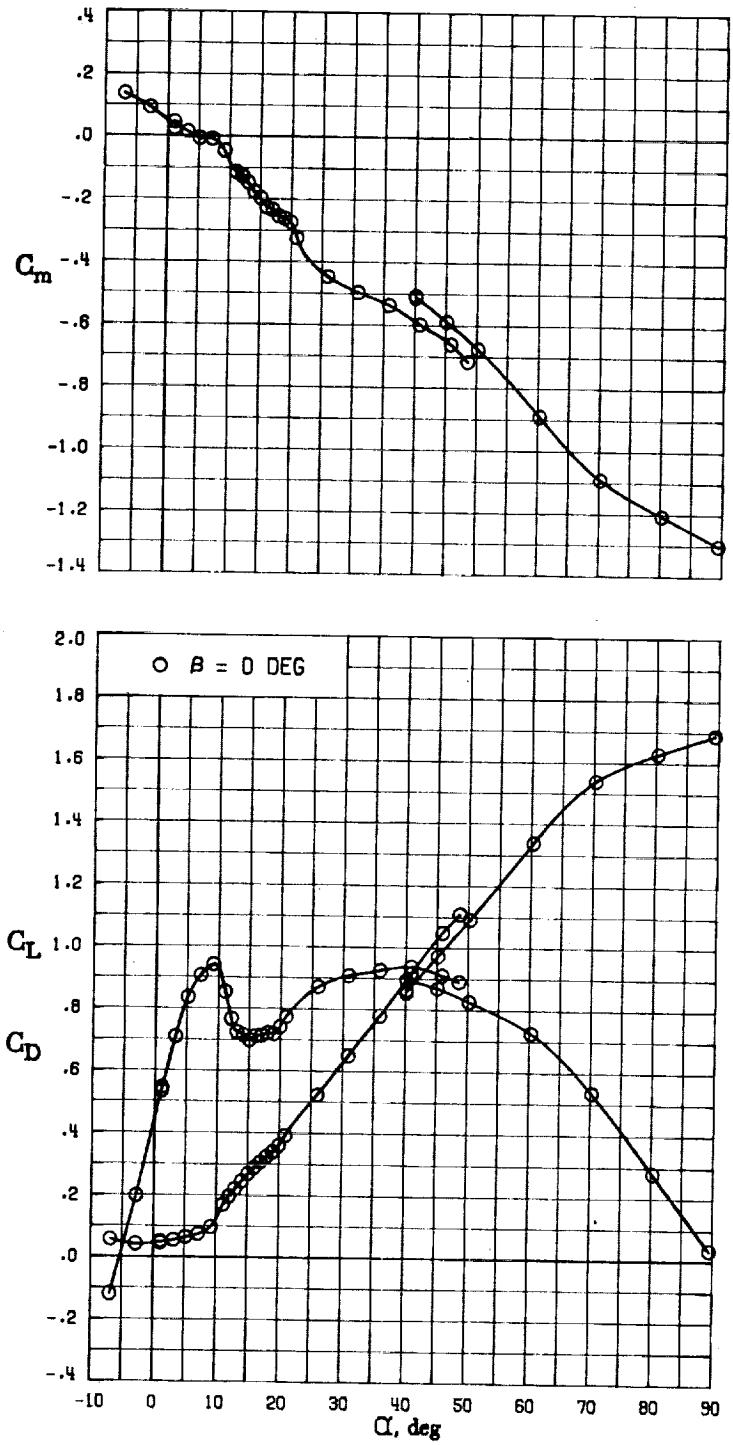

(A) LONGITUDINAL FORCE AND MOMENT COEFFICIENTS ABOUT STABILITY AXES.

FIGURE 63. - EFFECT OF ANGLE OF ATTACK AND SIDESLIP ANGLE ON AERODYNAMIC CHARACTERISTICS AT RE = .288 E+06 FOR CONFIGURATION B W1 H4 V U. $\delta_E = 0°$, $\delta_A = 0°$, $\delta_R = 0°$.

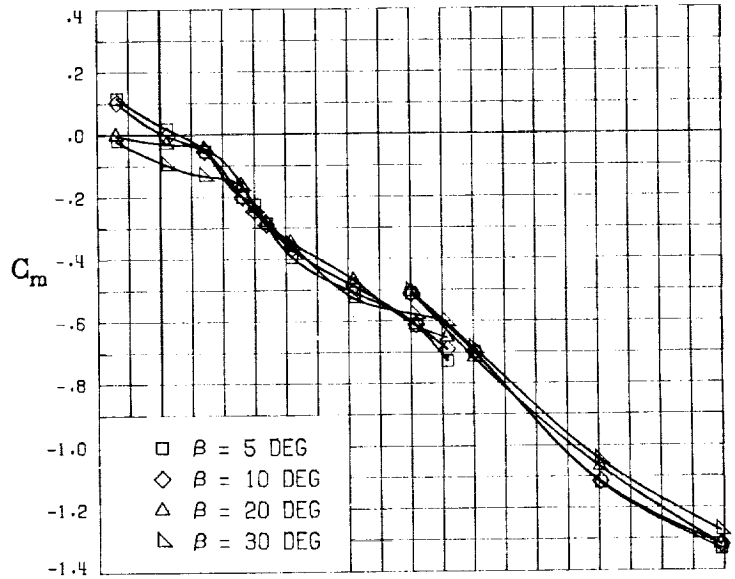

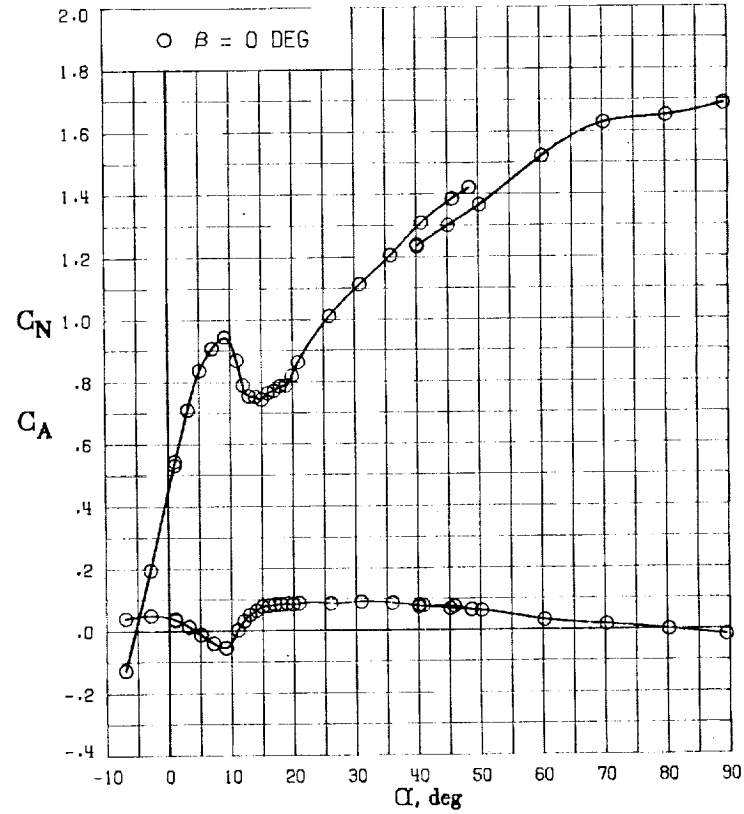

(B) LONGITUDINAL FORCE AND MOMENT COEFFICIENTS ABOUT BODY AXES.

FIGURE 63. - CONTINUED.

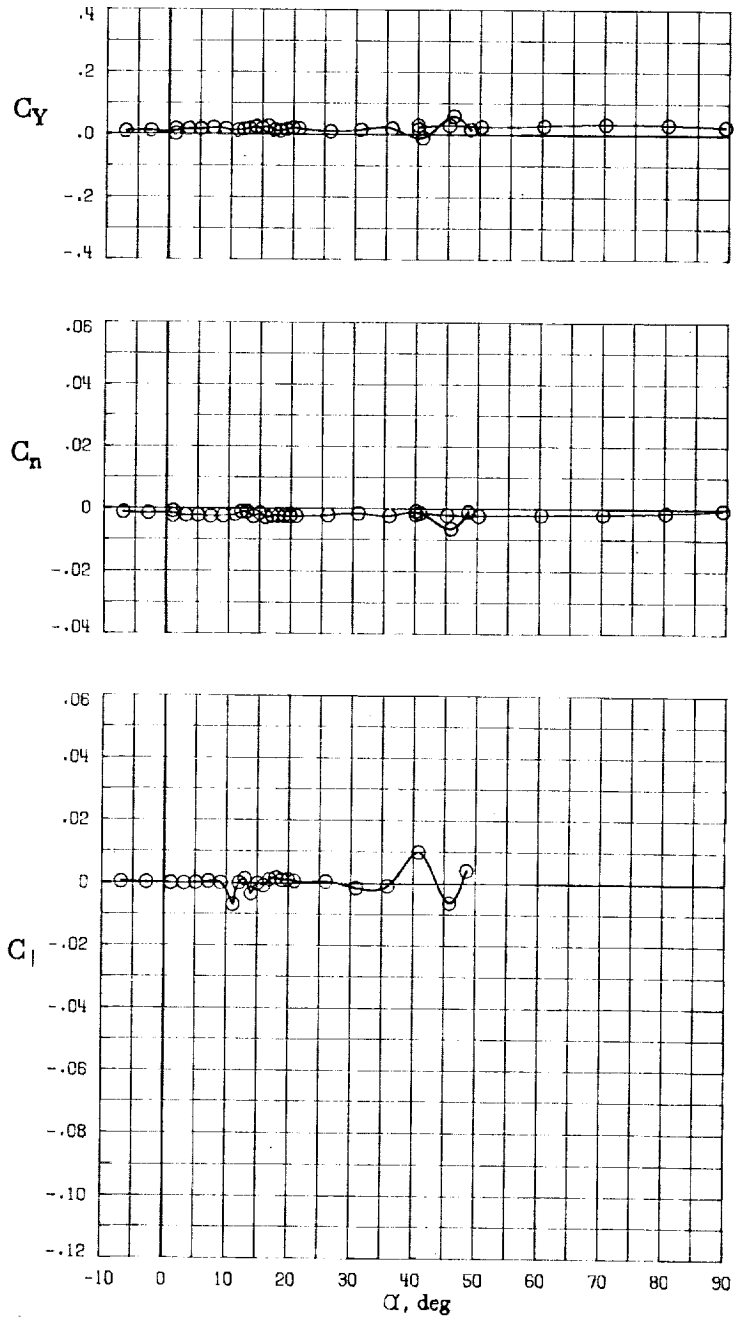

(C) LATERAL - DIRECTIONAL FORCE AND MOMENT COEFFICIENTS ABOUT BODY AXES AT ZERO SIDESLIP.

FIGURE 63. - CONTINUED.

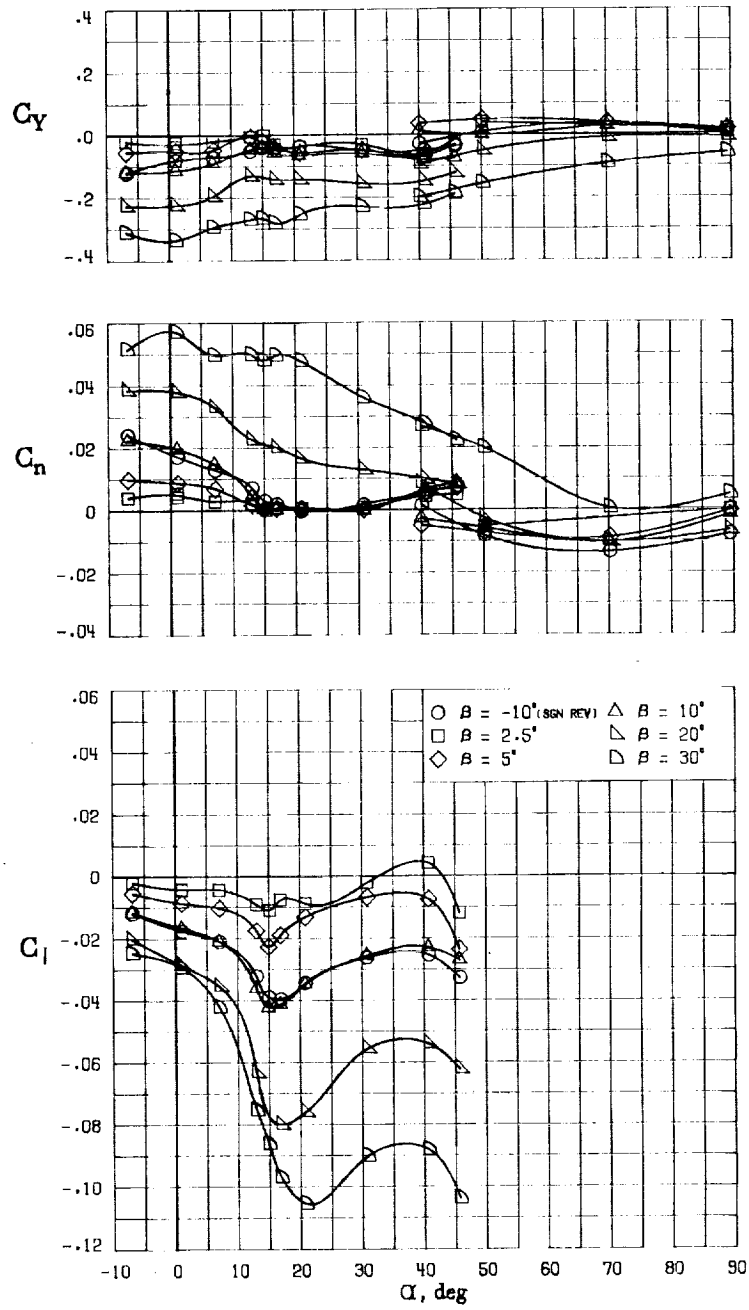

(D) LATERAL - DIRECTIONAL FORCE AND MOMENT COEFFICIENTS ABOUT BODY AXES.

FIGURE 63. - CONTINUED.

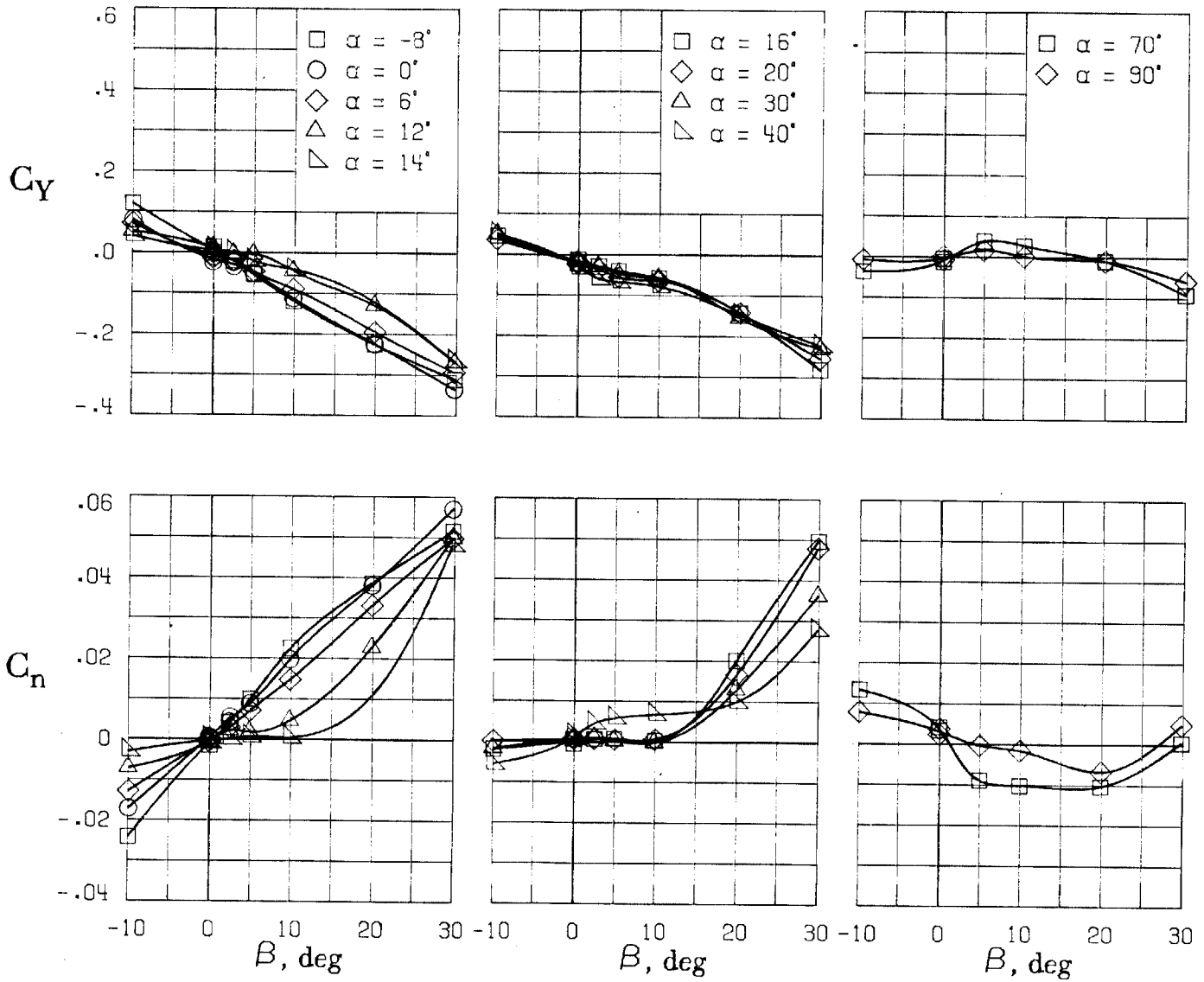

(E) DIRECTIONAL - STABILITY CHARACTERISTICS ABOUT BODY AXES AT VARIOUS ANGLES OF ATTACK.

FIGURE 63. - CONTINUED.

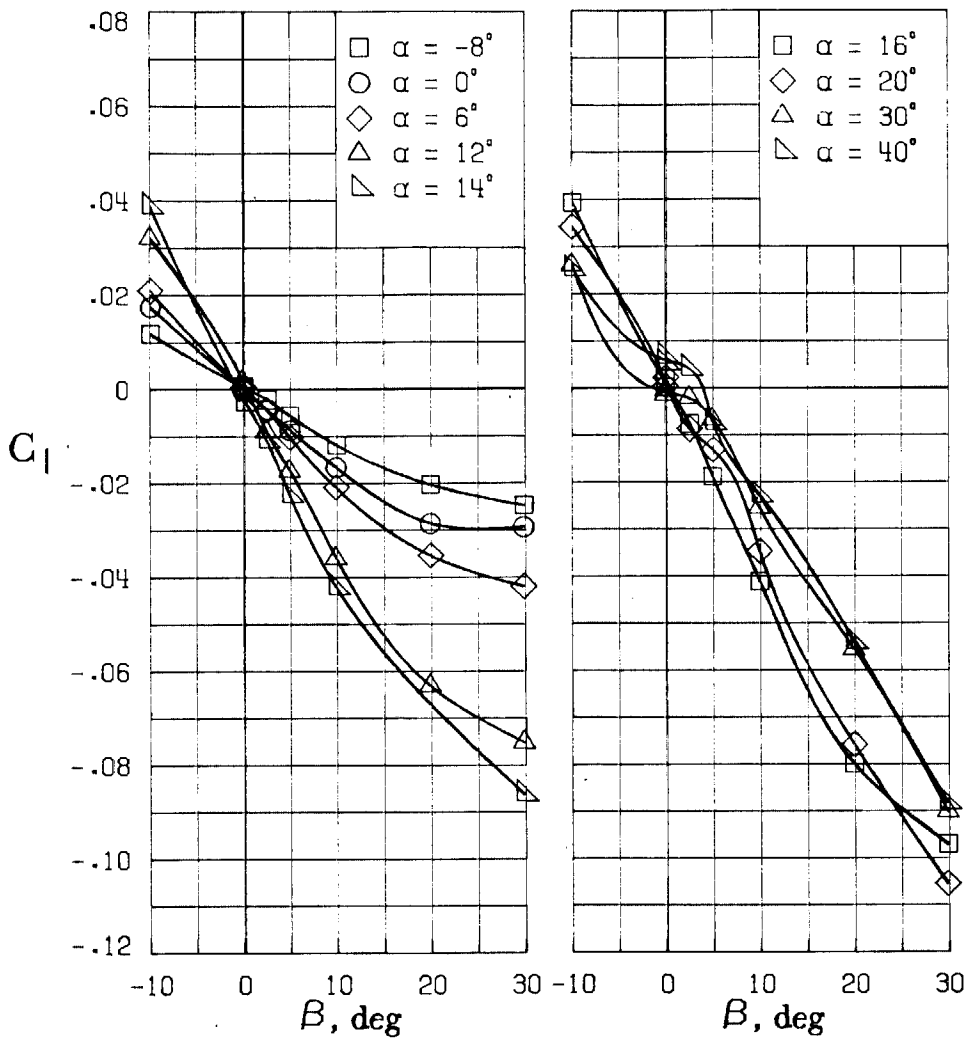

(F) LATERAL - STABILITY CHARACTERISTICS ABOUT BODY AXES AT VARIOUS ANGLES OF ATTACK.

FIGURE 63. - CONCLUDED.

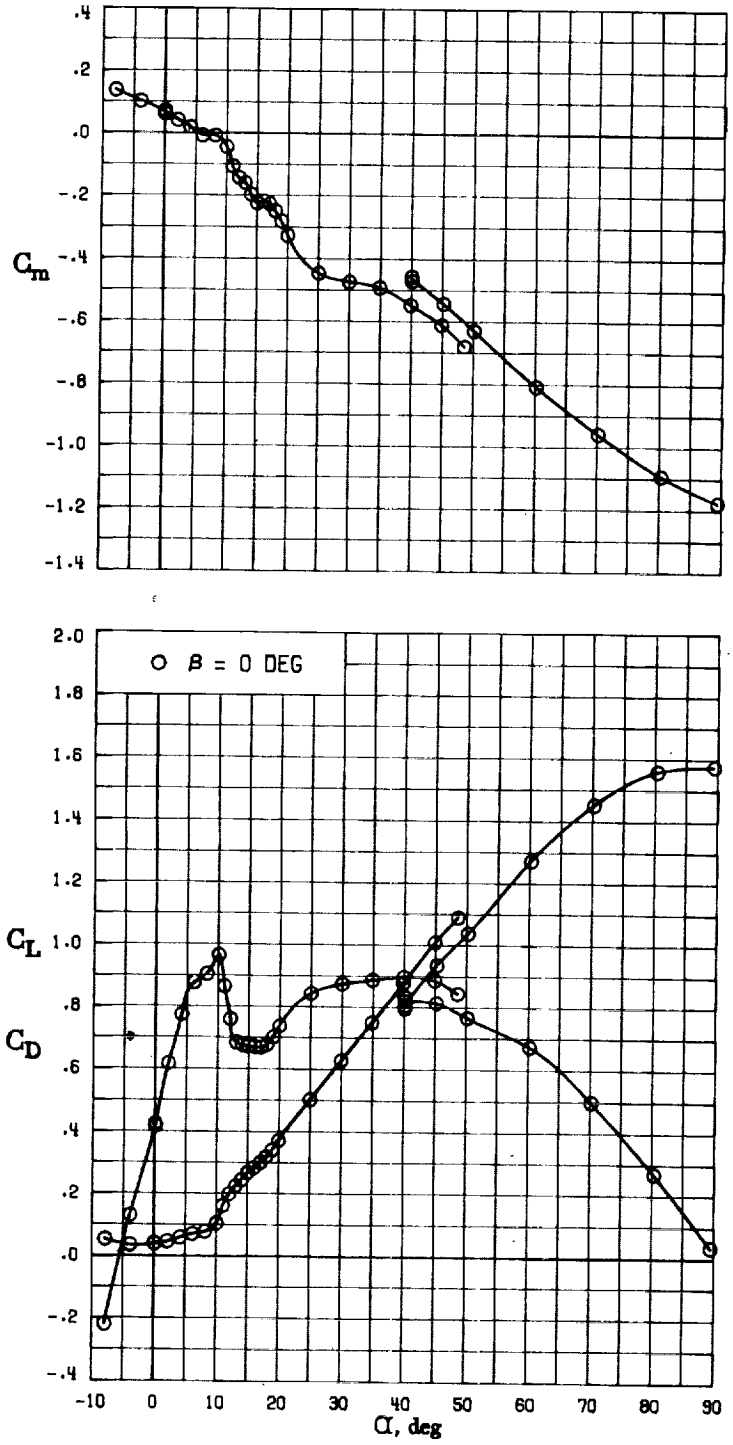

(A) LONGITUDINAL FORCE AND MOMENT COEFFICIENTS ABOUT STABILITY AXES.

FIGURE 64. - EFFECT OF ANGLE OF ATTACK AND SIDESLIP ANGLE ON AERODYNAMIC CHARACTERISTICS AT RE = .288 E+06 FOR CONFIGURATION B W1 H4 V D. $\delta_E = 0°$, $\delta_A = 0°$, $\delta_R = 0°$.

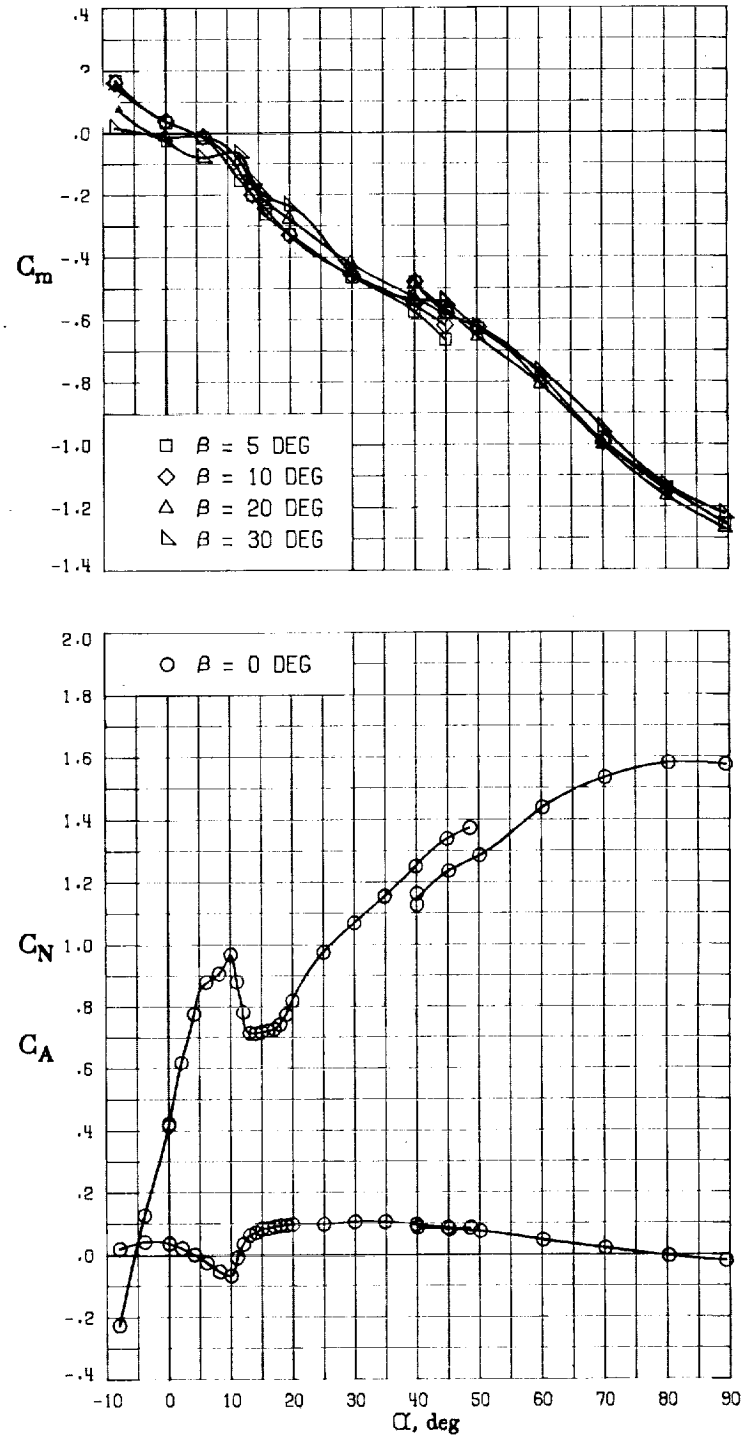

(B) LONGITUDINAL FORCE AND MOMENT COEFFICIENTS ABOUT BODY AXES.

FIGURE 64. - CONTINUED.

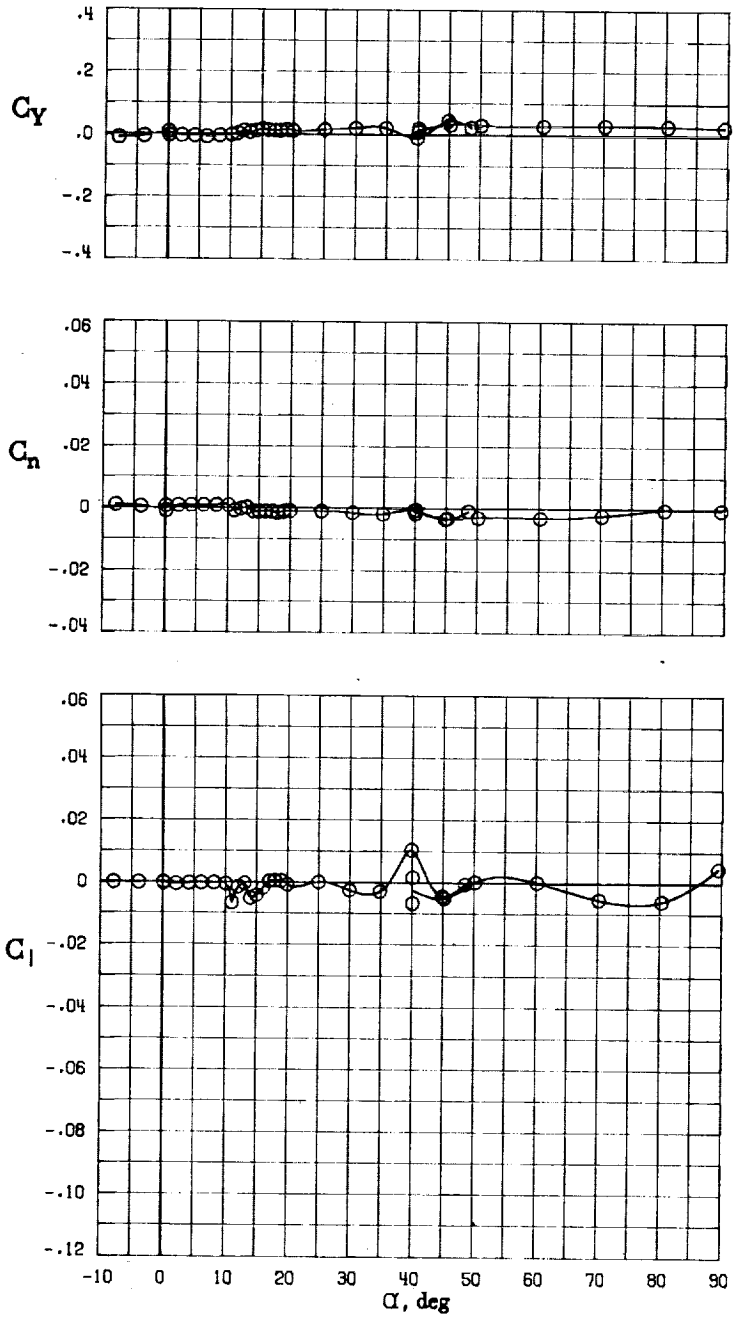

(C) LATERAL - DIRECTIONAL FORCE AND MOMENT COEFFICIENTS ABOUT BODY AXES. AT ZERO SIDESLIP.

FIGURE 64. - CONTINUED.

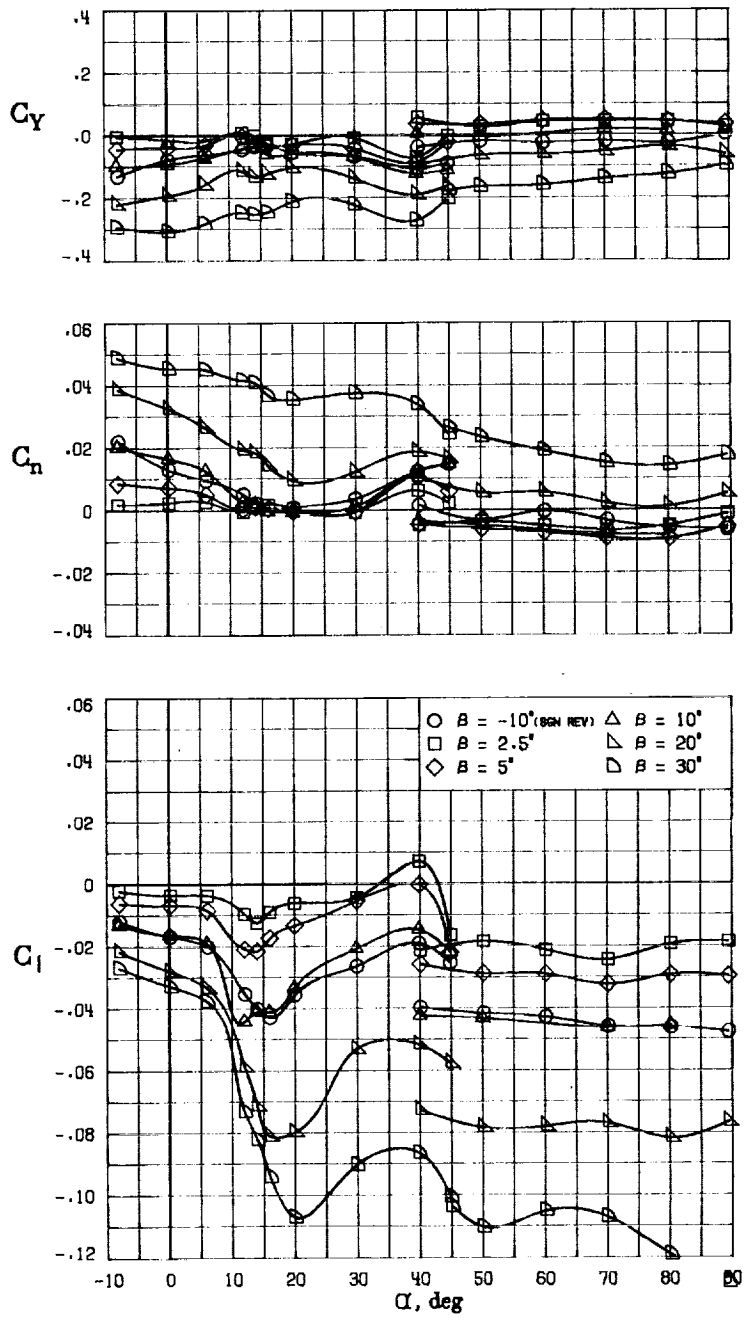

(D) LATERAL - DIRECTIONAL FORCE AND MOMENT COEFFICIENTS ABOUT BODY AXES.

FIGURE 64. - CONTINUED.

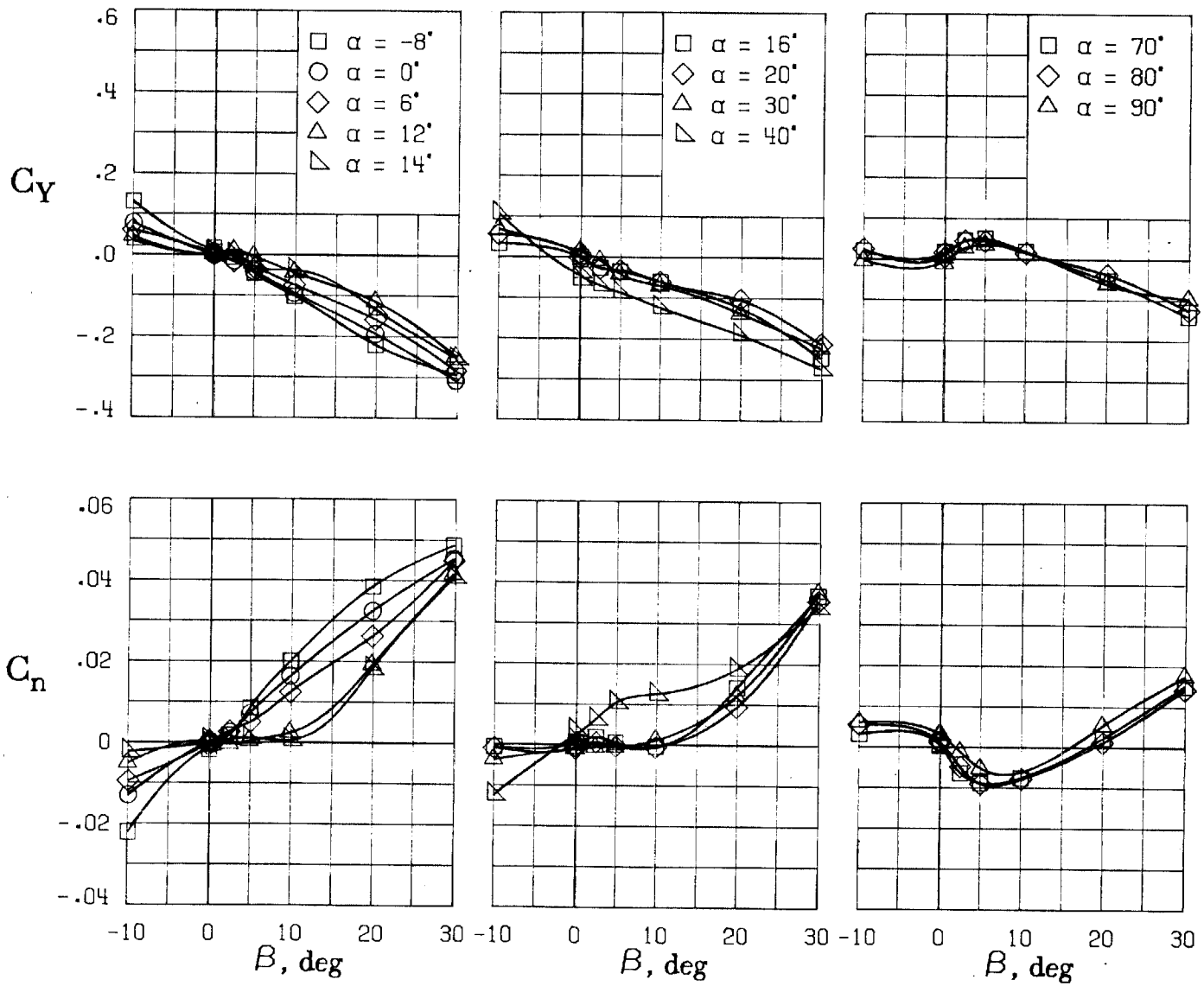

(E) DIRECTIONAL - STABILITY CHARACTERISTICS ABOUT BODY AXES AT VARIOUS ANGLES OF ATTACK.

FIGURE 64. - CONTINUED.

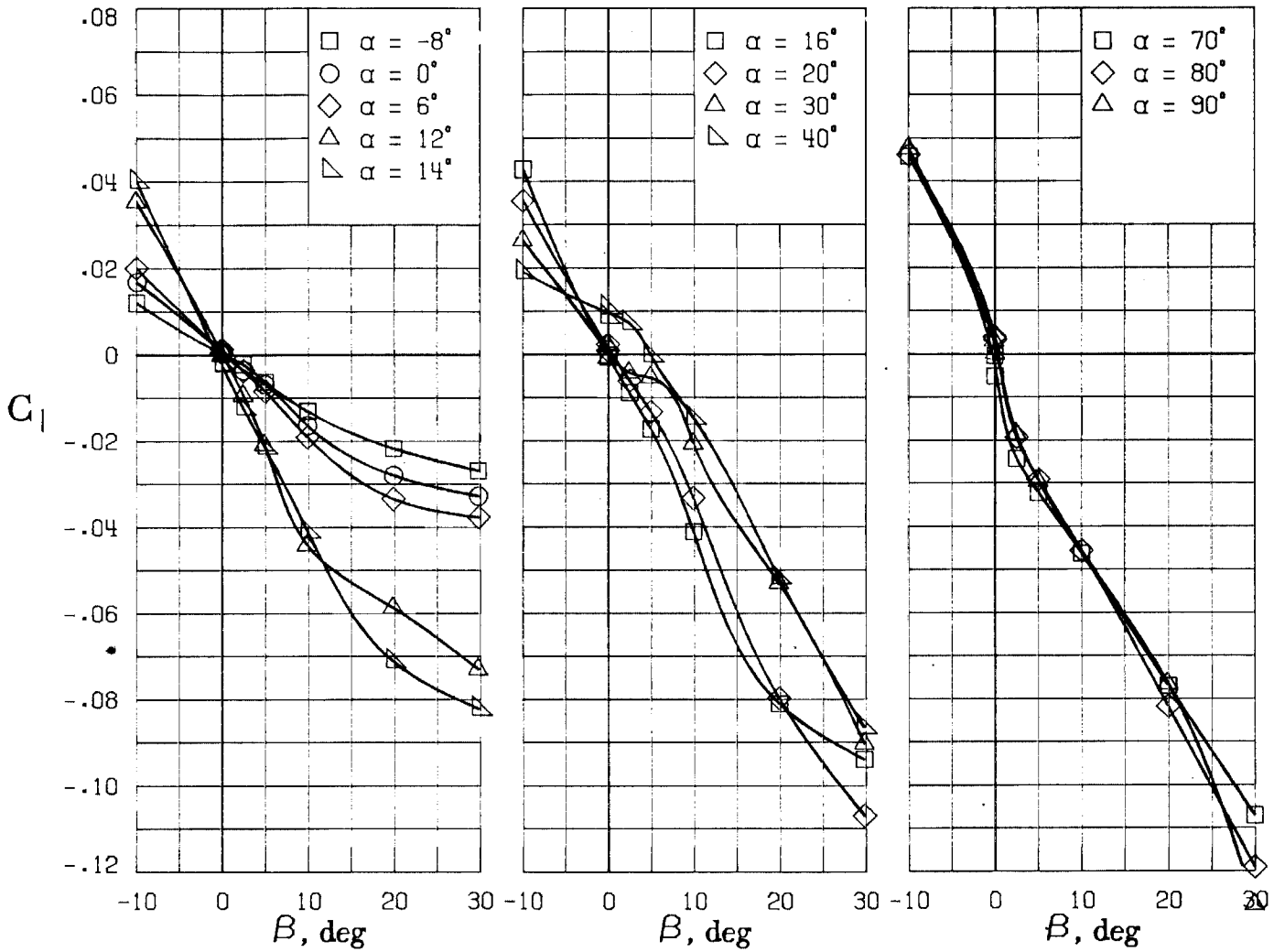

(F) LATERAL - STABILITY CHARACTERISTICS ABOUT BODY AXES AT VARIOUS ANGLES OF ATTACK.

FIGURE 64. - CONCLUDED.

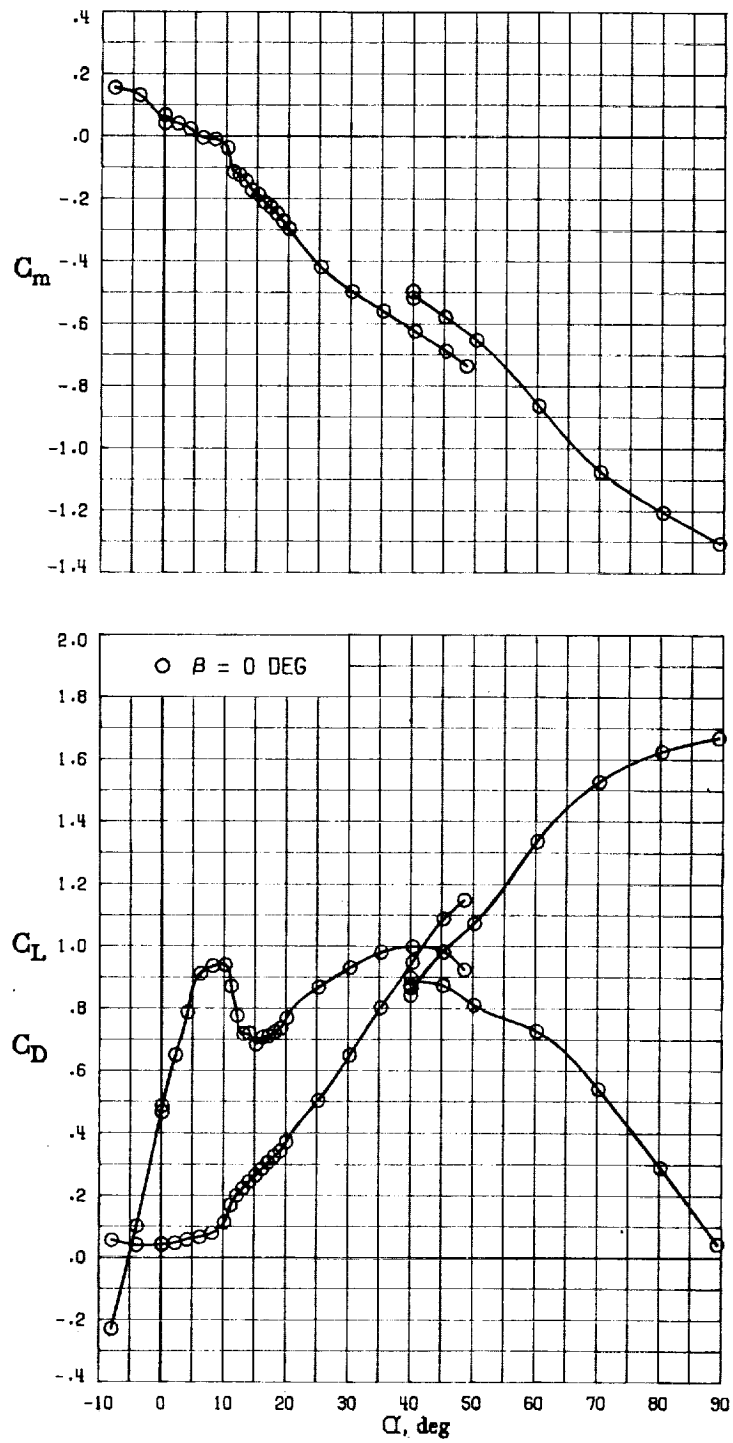

(A) LONGITUDINAL FORCE AND MOMENT COEFFICIENTS ABOUT STABILITY AXES.

FIGURE 65. - EFFECT OF ANGLE OF ATTACK AND SIDESLIP ANGLE ON AERODYNAMIC CHARACTERISTICS AT RE = .288 E+06 FOR CONFIGURATION B W1 H4 V FM. $\delta_E = 0°$, $\delta_A = 0°$, $\delta_R = 0°$.

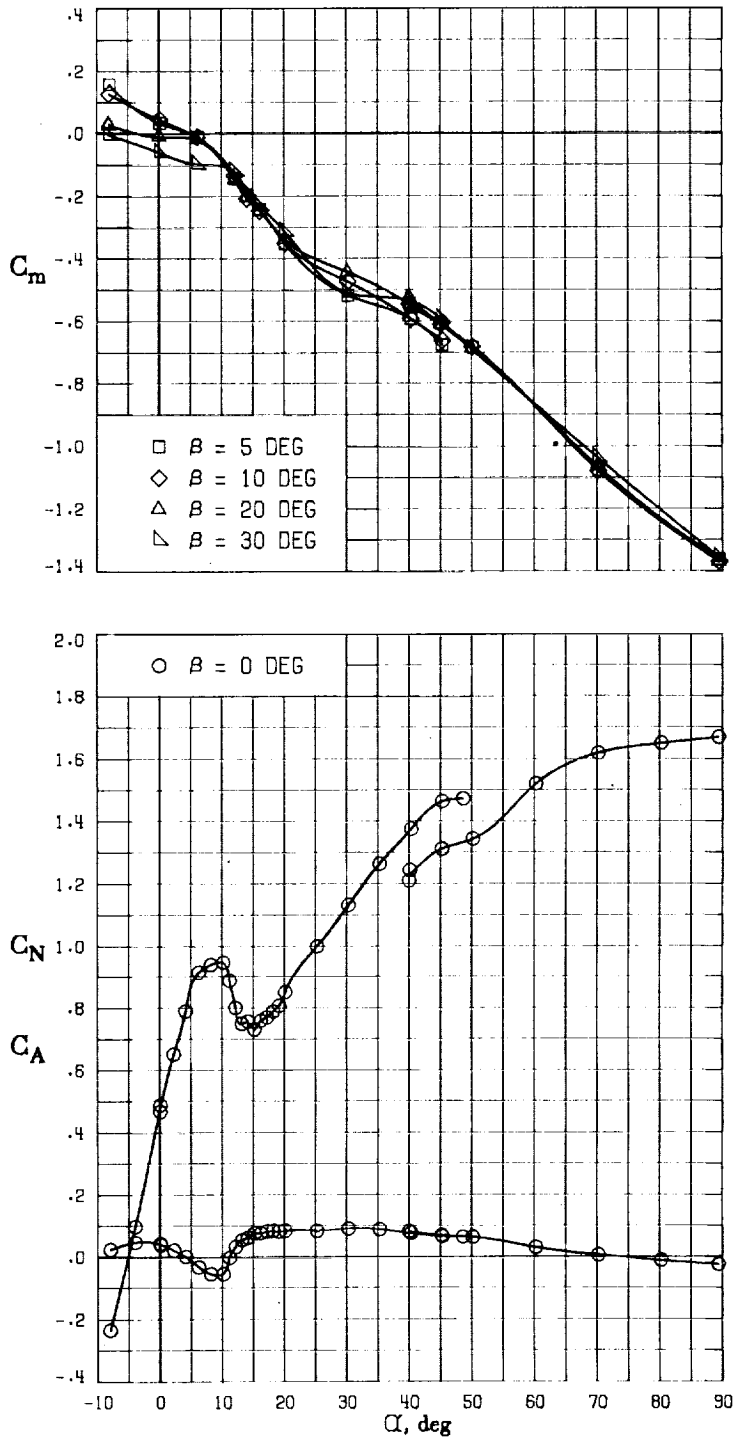

(B) LONGITUDINAL FORCE AND MOMENT COEFFICIENTS ABOUT BODY AXES.

FIGURE 65. - CONTINUED.

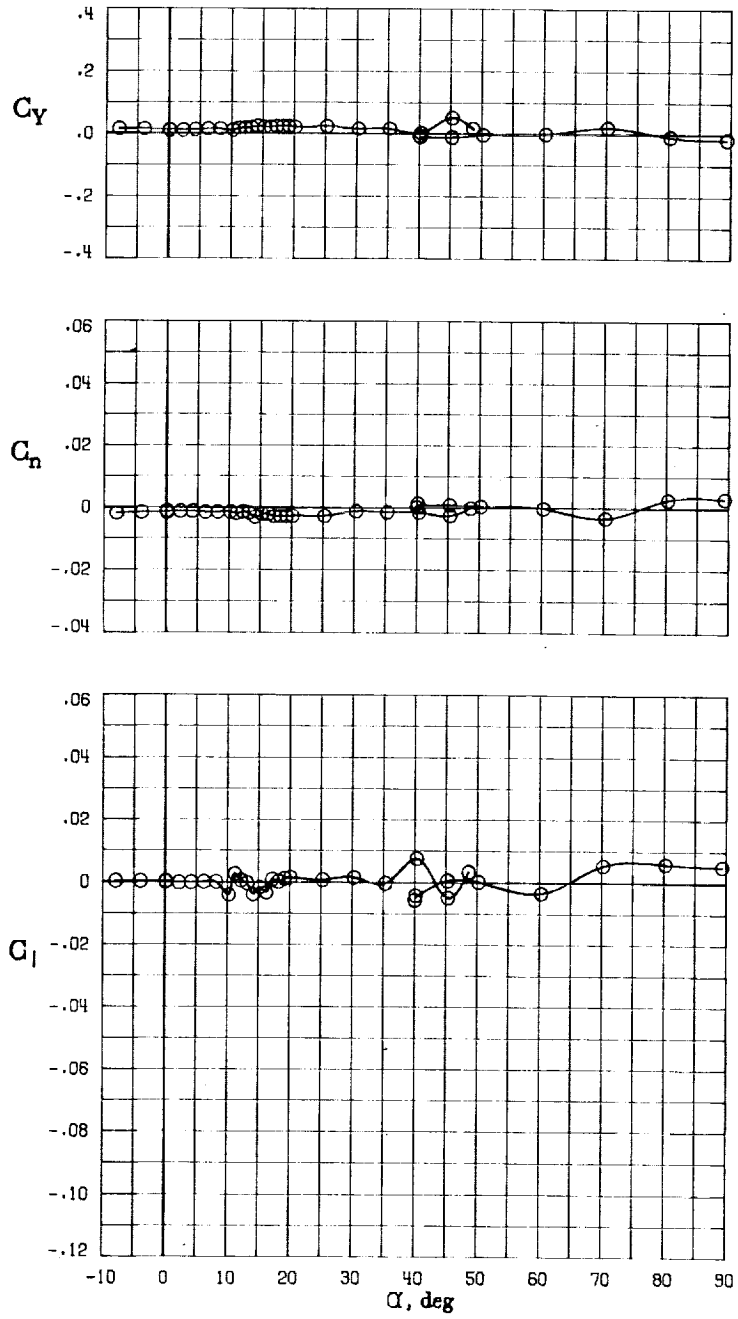

(C) LATERAL - DIRECTIONAL FORCE AND MOMENT COEFFICIENTS ABOUT BODY AXES AT ZERO SIDESLIP.

FIGURE 65. - CONTINUED.

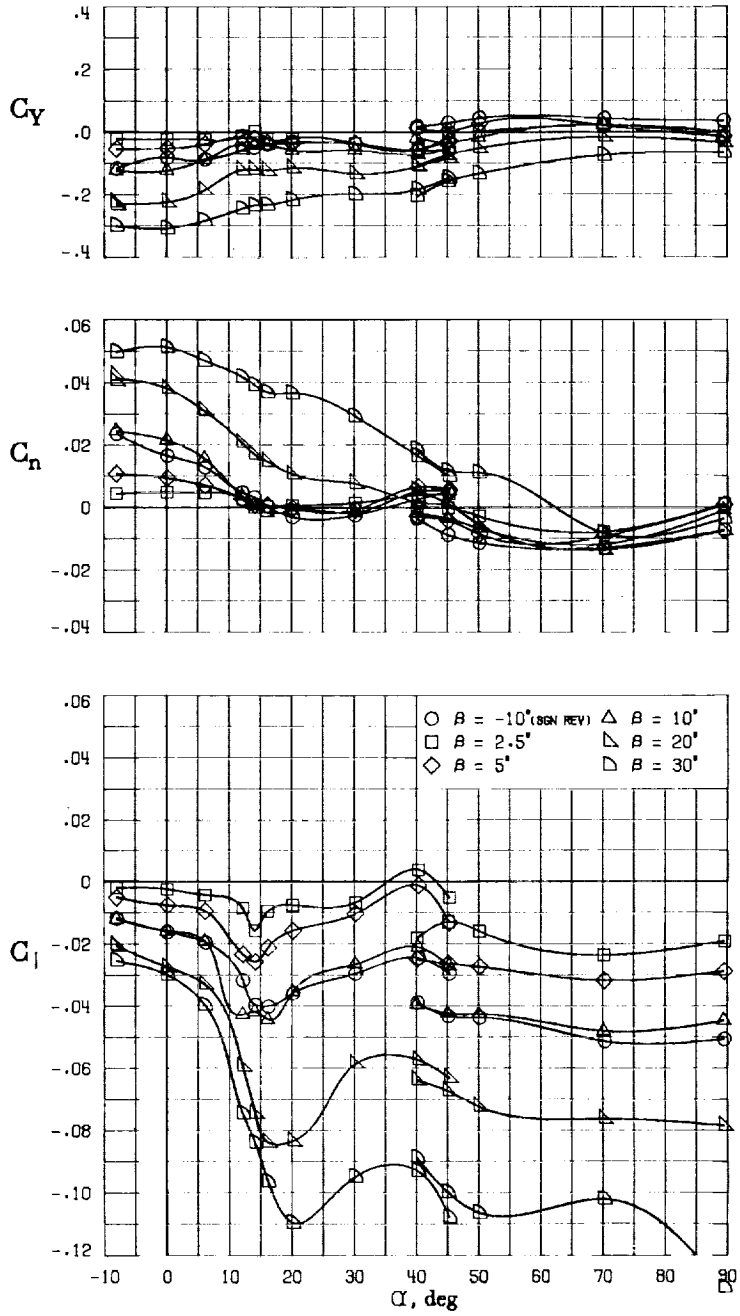

(D) LATERAL - DIRECTIONAL FORCE AND MOMENT COEFFICIENTS ABOUT BODY AXES.

FIGURE 65. - CONTINUED.

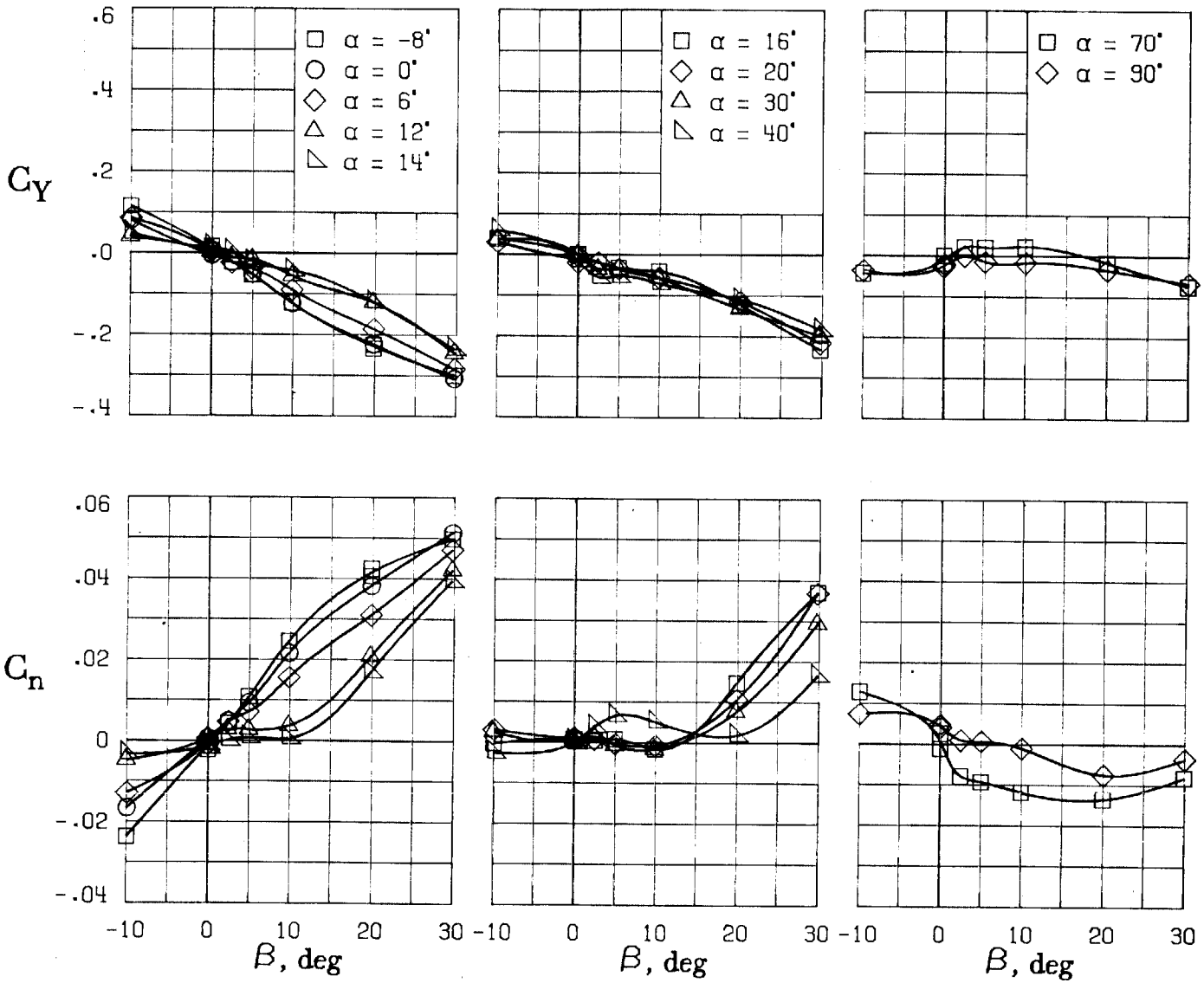

(E) DIRECTIONAL - STABILITY CHARACTERISTICS ABOUT BODY AXES AT VARIOUS ANGLES OF ATTACK.

FIGURE 65. - CONTINUED.

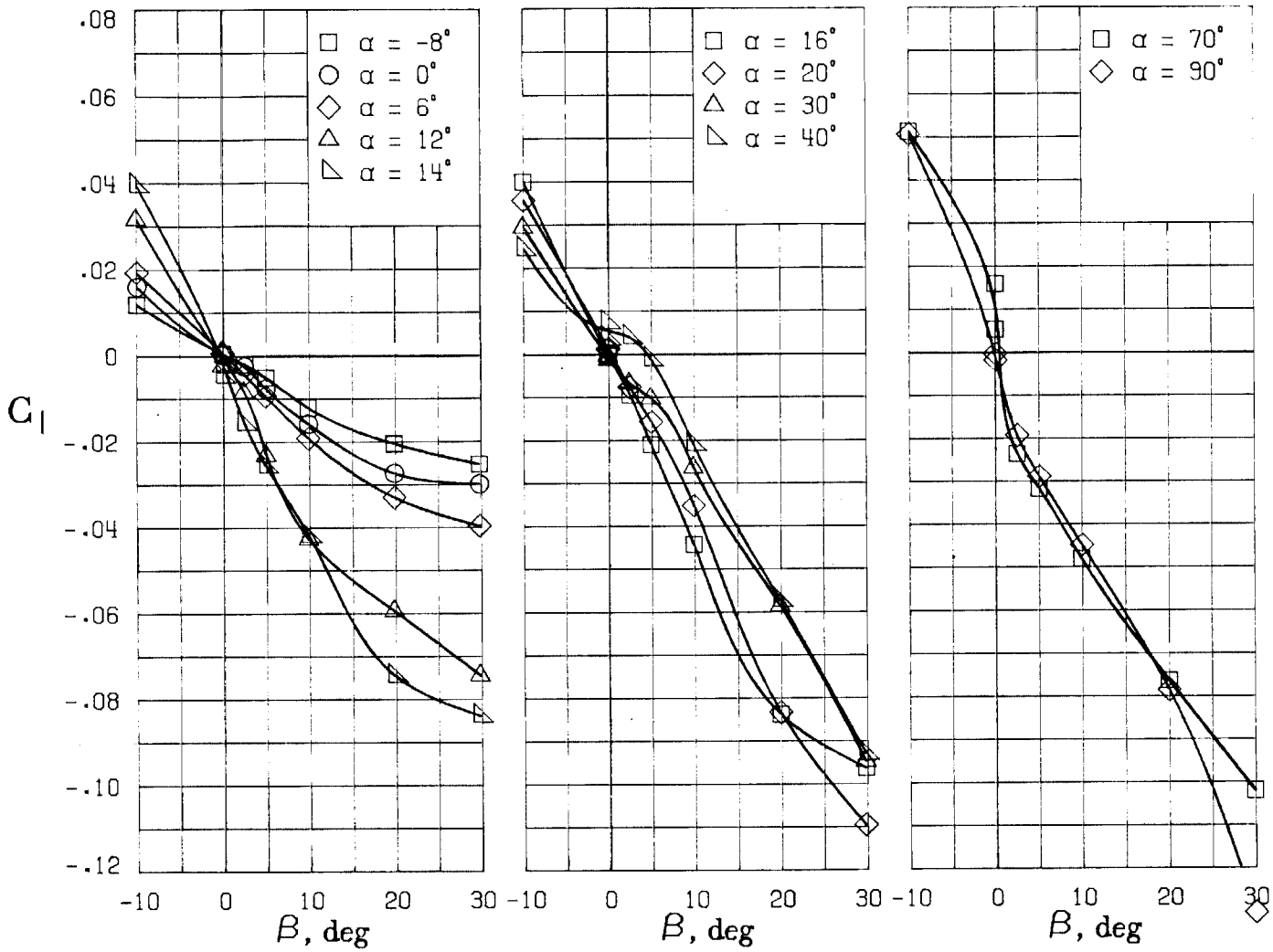

(F) LATERAL - STABILITY CHARACTERISTICS ABOUT BODY AXES AT VARIOUS ANGLES OF ATTACK.

FIGURE 65. - CONCLUDED.

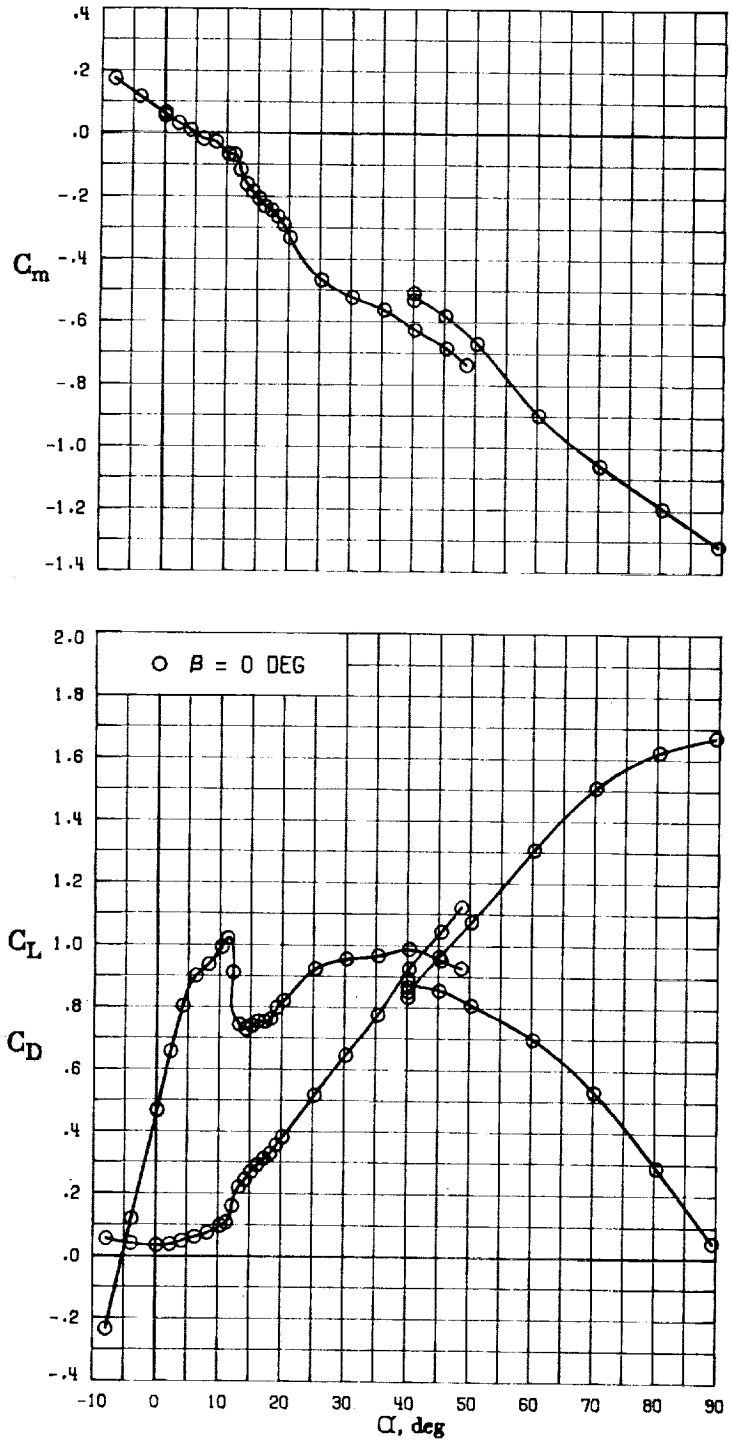

(A) LONGITUDINAL FORCE AND MOMENT COEFFICIENTS ABOUT STABILITY AXES.

FIGURE 66. - EFFECT OF ANGLE OF ATTACK AND SIDESLIP ANGLE ON AERODYNAMIC CHARACTERISTICS AT RE = .288 E+06 FOR CONFIGURATION B W1 H4 V -F. $\delta_E = 0°$, $\delta_A = 0°$, $\delta_R = 0°$.

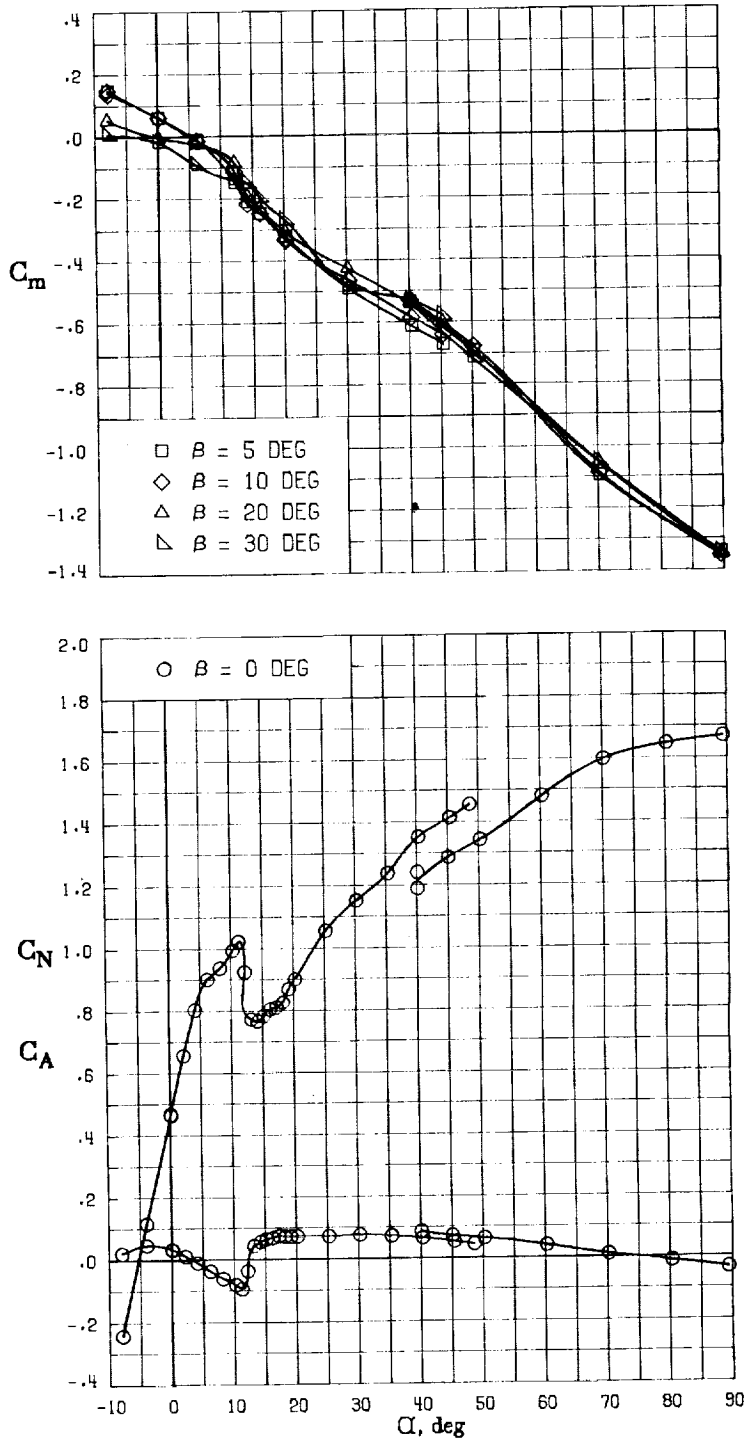

(B) LONGITUDINAL FORCE AND MOMENT COEFFICIENTS ABOUT BODY AXES.

FIGURE 66. - CONTINUED.

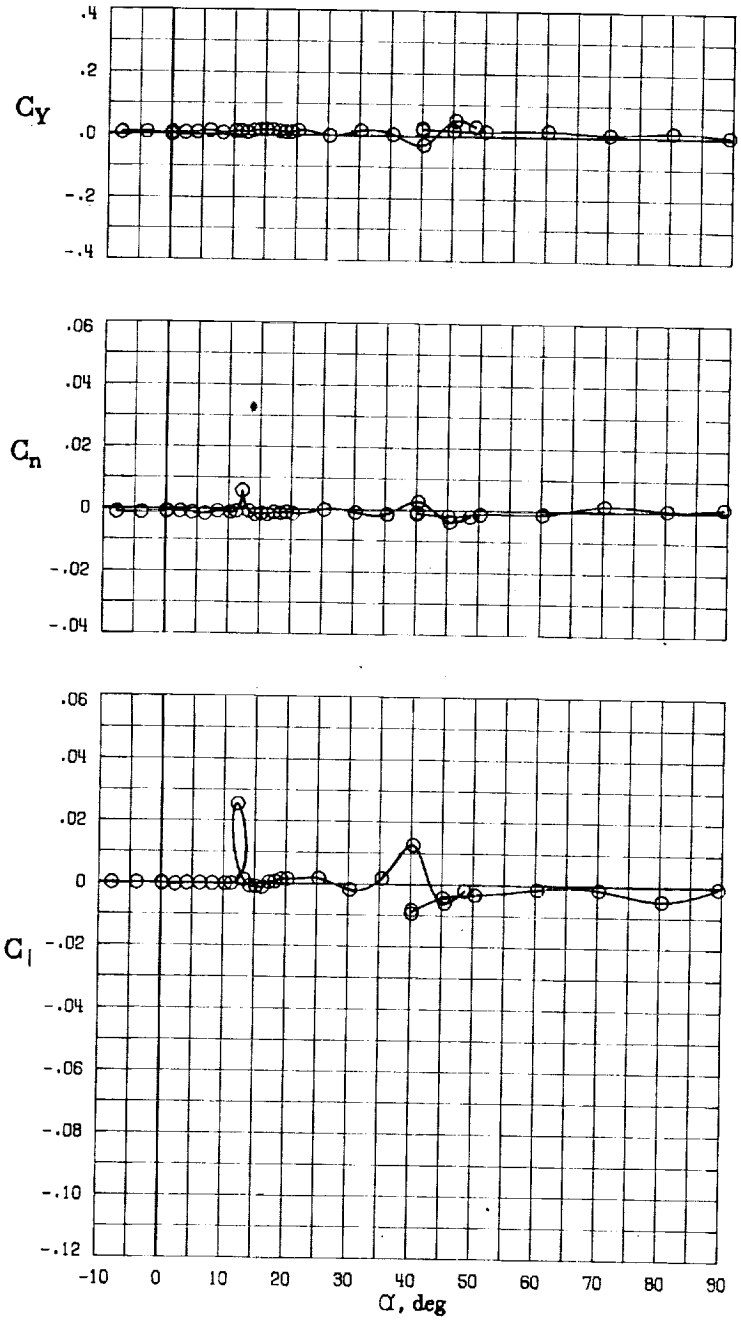

(C) LATERAL - DIRECTIONAL FORCE AND MOMENT COEFFICIENTS ABOUT BODY AXES AT ZERO SIDESLIP.

FIGURE 66. - CONTINUED.

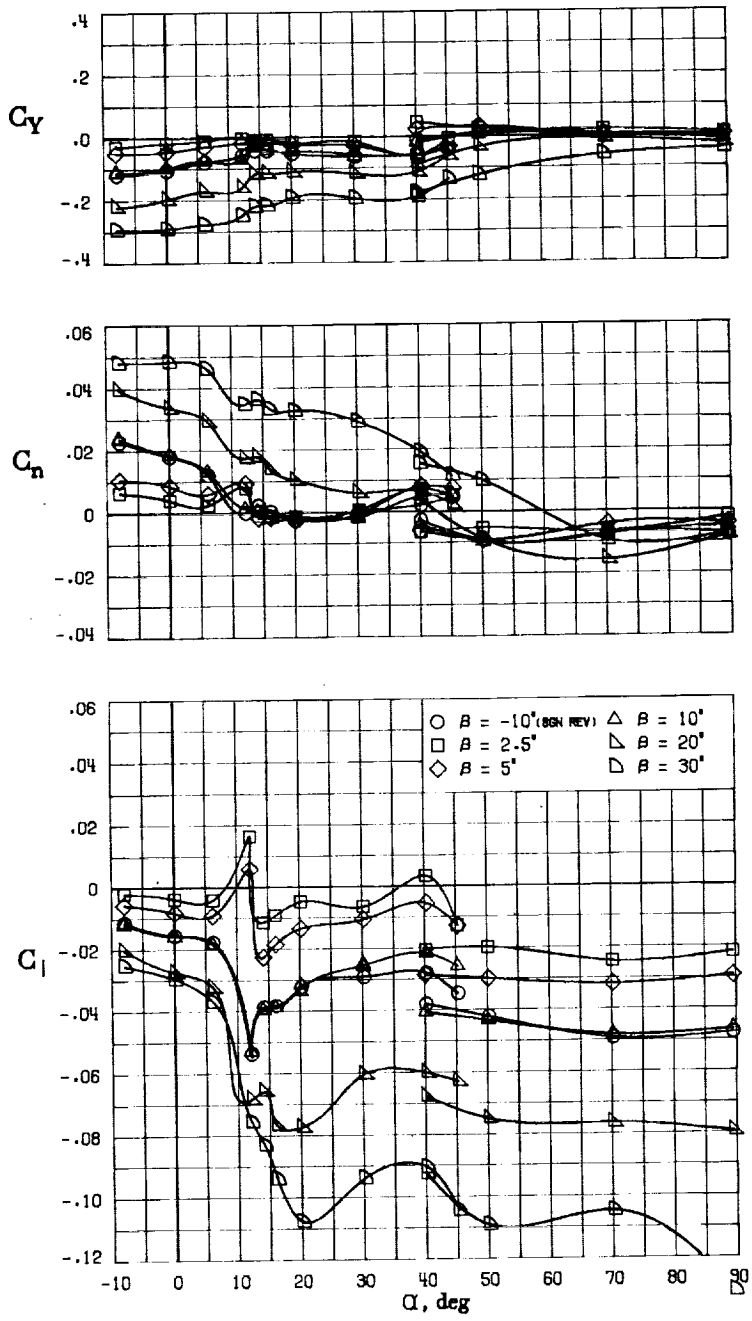

(D) LATERAL - DIRECTIONAL FORCE AND MOMENT COEFFICIENTS ABOUT BODY AXES.

FIGURE 66. - CONTINUED.

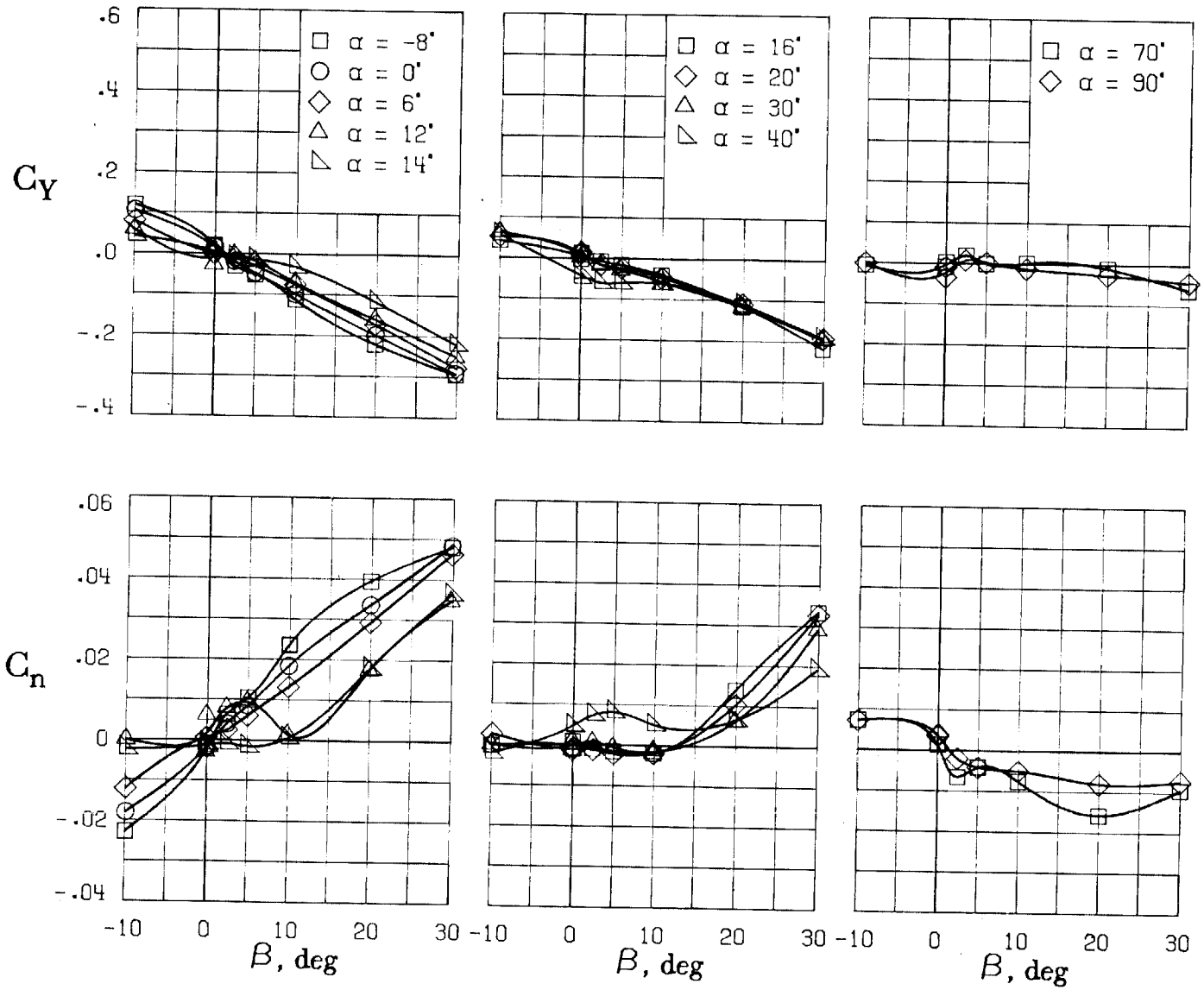

(E) DIRECTIONAL - STABILITY CHARACTERISTICS ABOUT BODY AXES AT VARIOUS ANGLES OF ATTACK.

FIGURE 66. - CONTINUED.

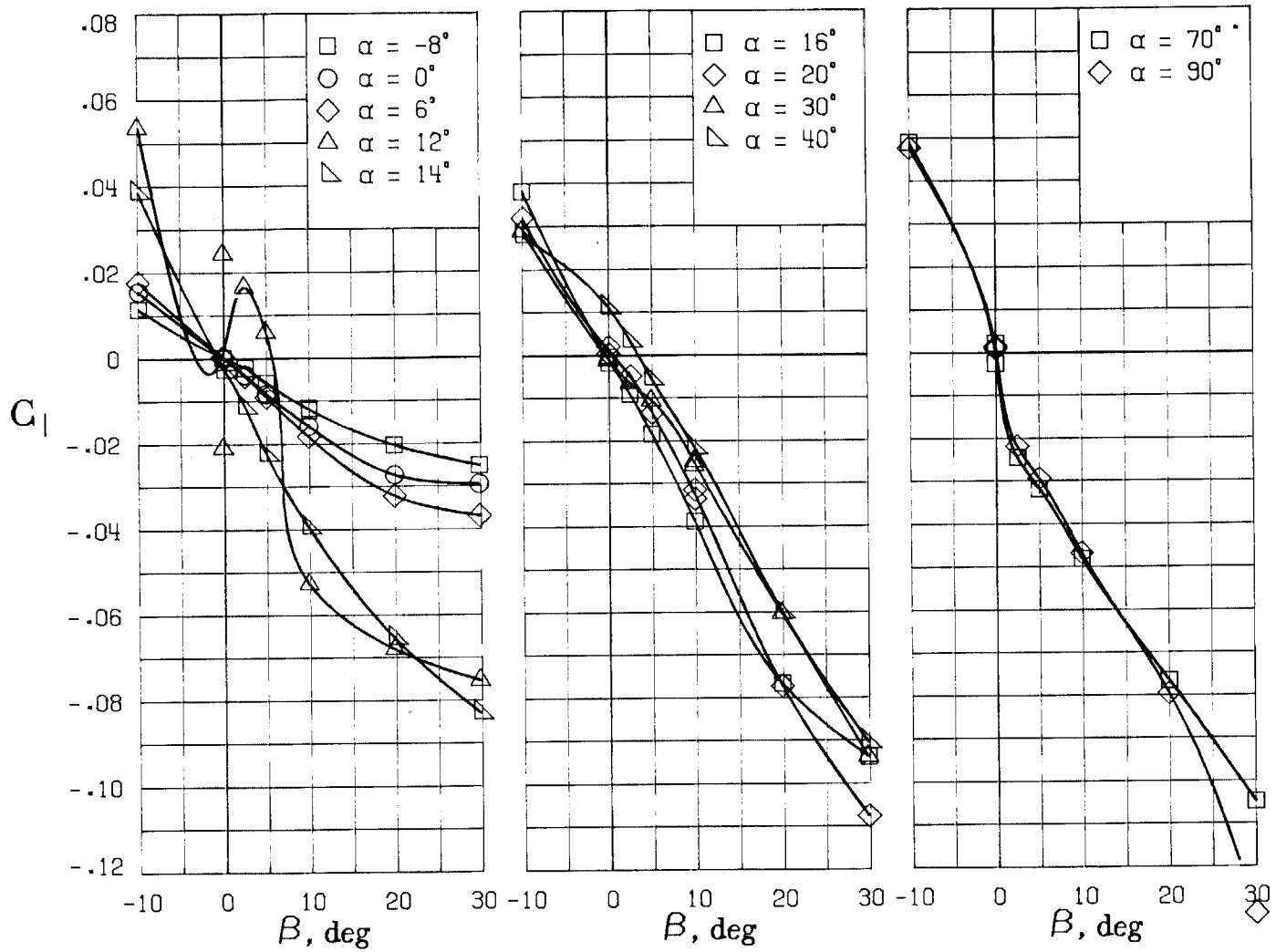

(F) LATERAL - STABILITY CHARACTERISTICS ABOUT BODY AXES AT VARIOUS ANGLES OF ATTACK.

FIGURE 66. - CONCLUDED.

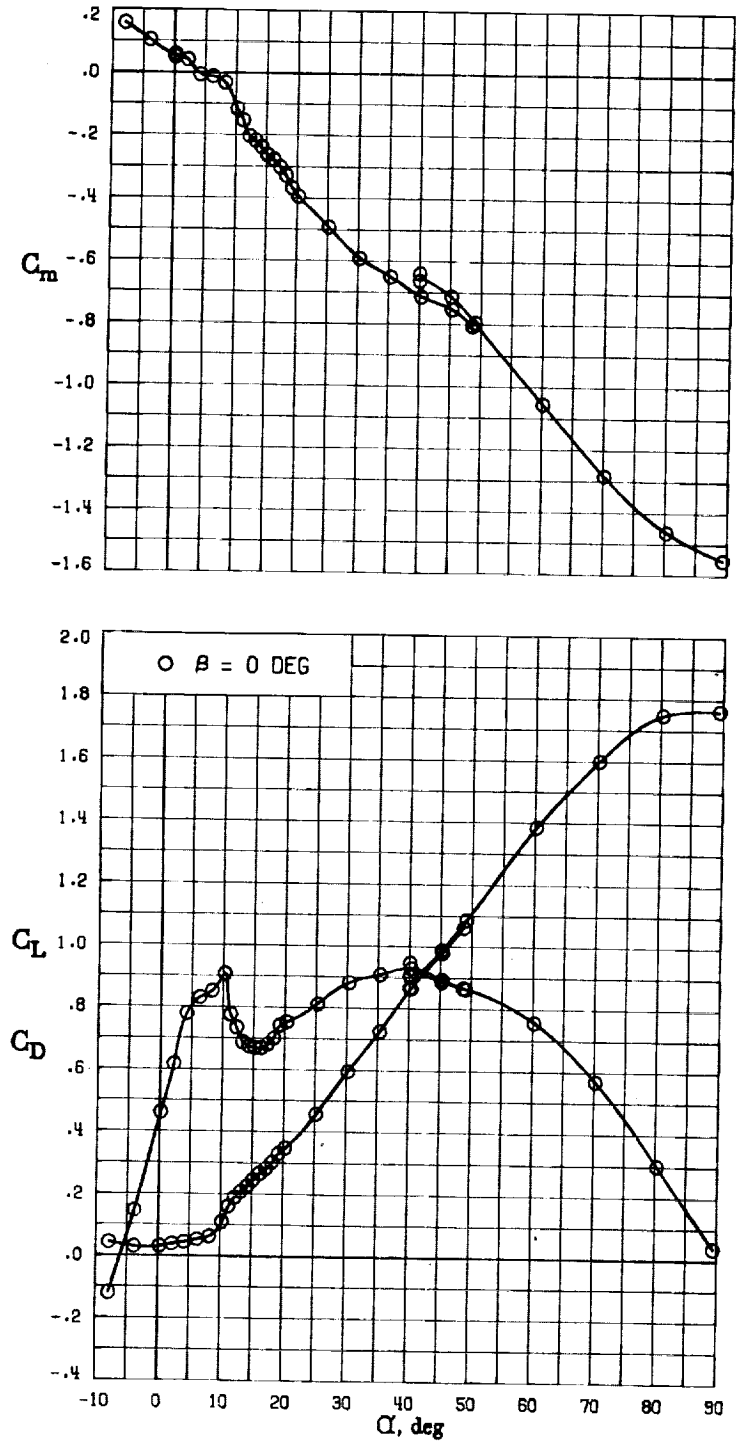

(A) LONGITUDINAL FORCE AND MOMENT COEFFICIENTS ABOUT STABILITY AXES.

FIGURE 67. - EFFECT OF ANGLE OF ATTACK AND SIDESLIP ANGLE ON AERODYNAMIC CHARACTERISTICS AT RE = .288 E+06 FOR CONFIGURATION B W1 H4 V E. $\delta_E = 0°$, $\delta_A = 0°$, $\delta_R = 0°$.

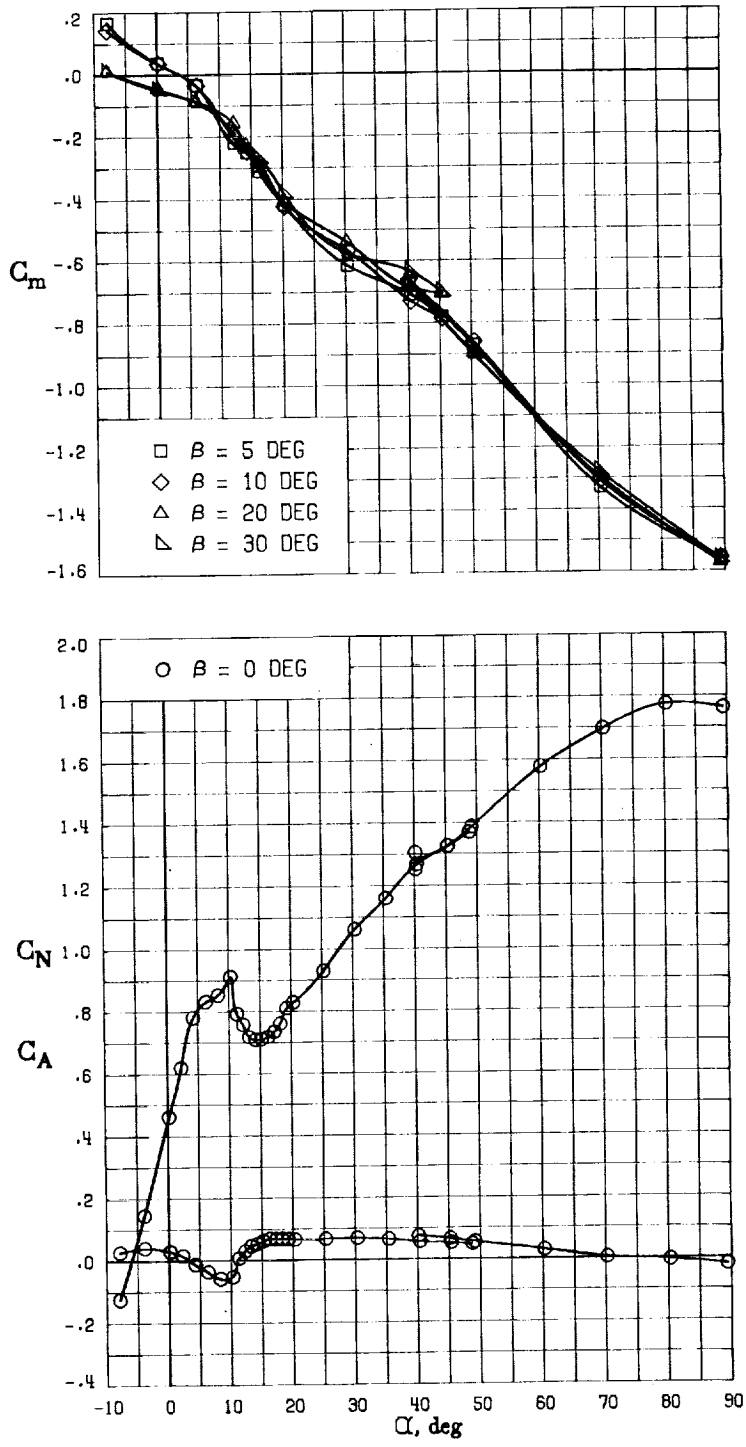

(B) LONGITUDINAL FORCE AND MOMENT COEFFICIENTS ABOUT BODY AXES.

FIGURE 67. - CONTINUED.

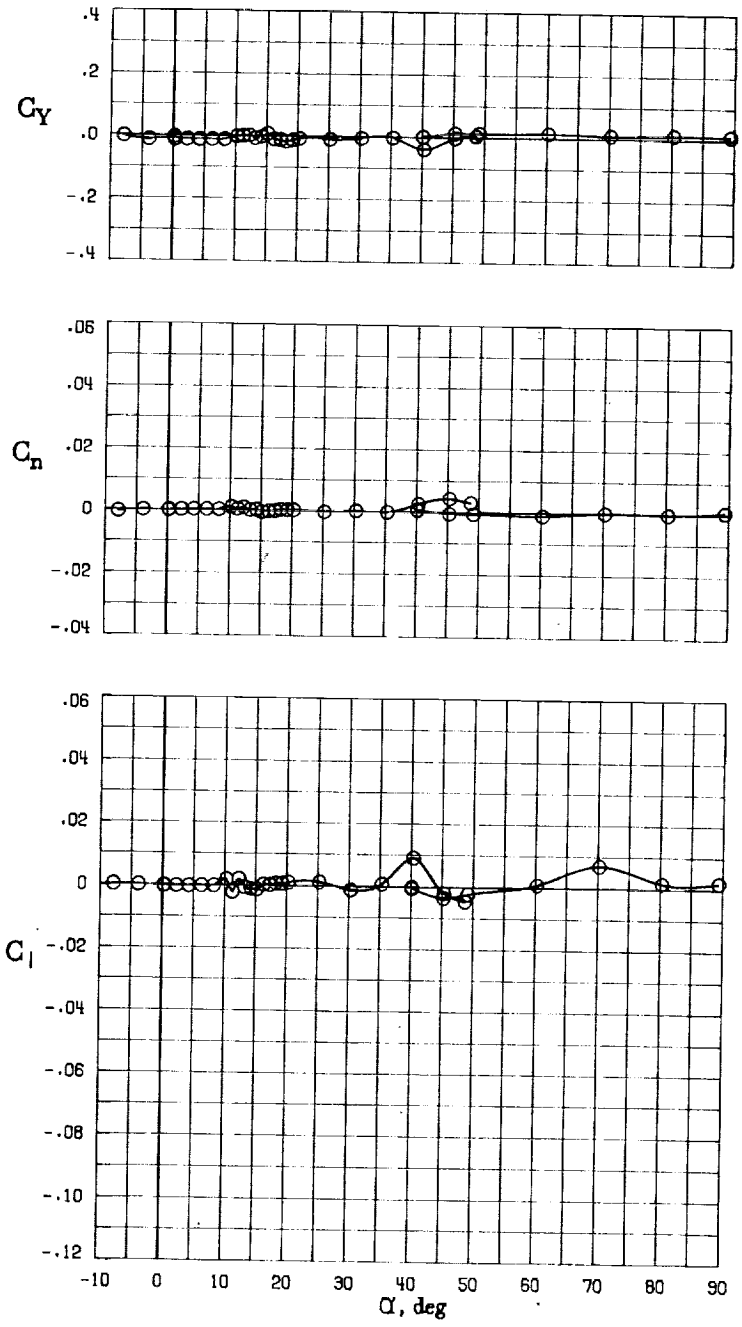

(C) LATERAL - DIRECTIONAL FORCE AND MOMENT COEFFICIENTS ABOUT BODY AXES AT ZERO SIDESLIP.

FIGURE 67. - CONTINUED.

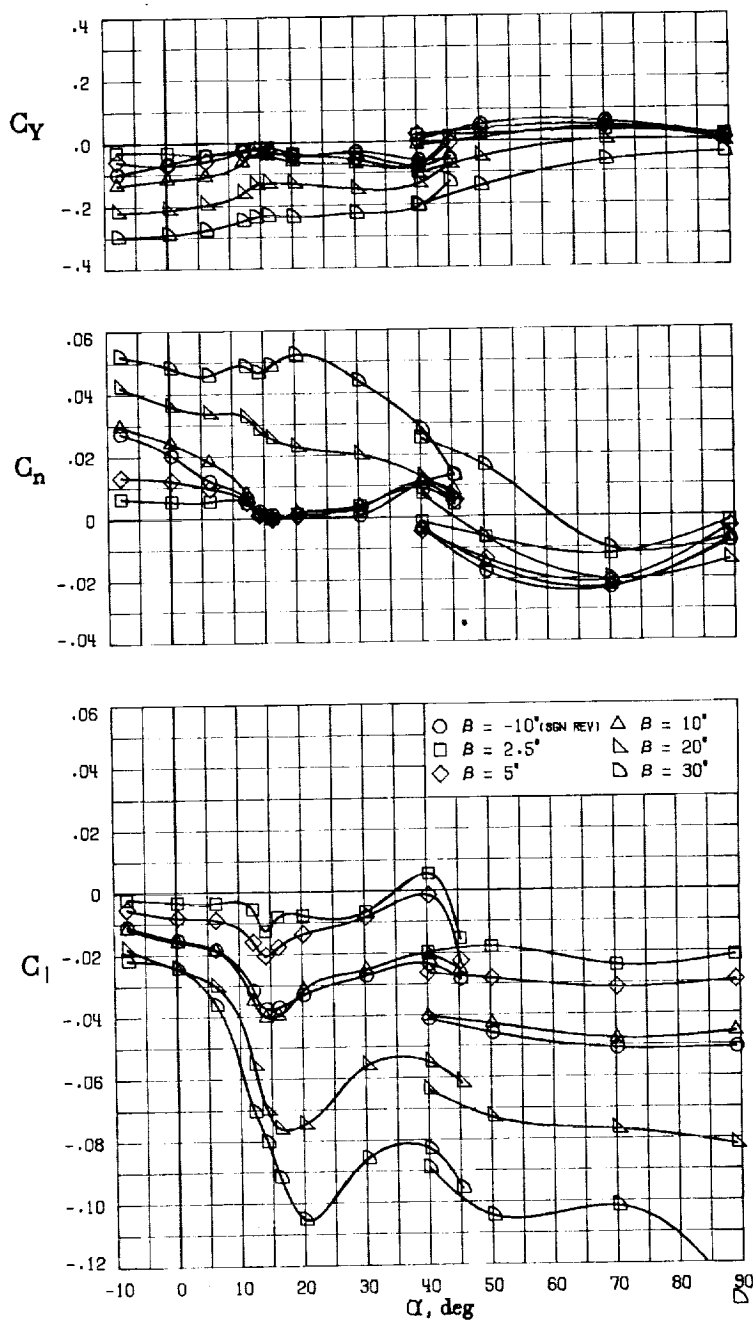

(D) LATERAL - DIRECTIONAL FORCE AND MOMENT COEFFICIENTS ABOUT BODY AXES.

FIGURE 67. - CONTINUED.

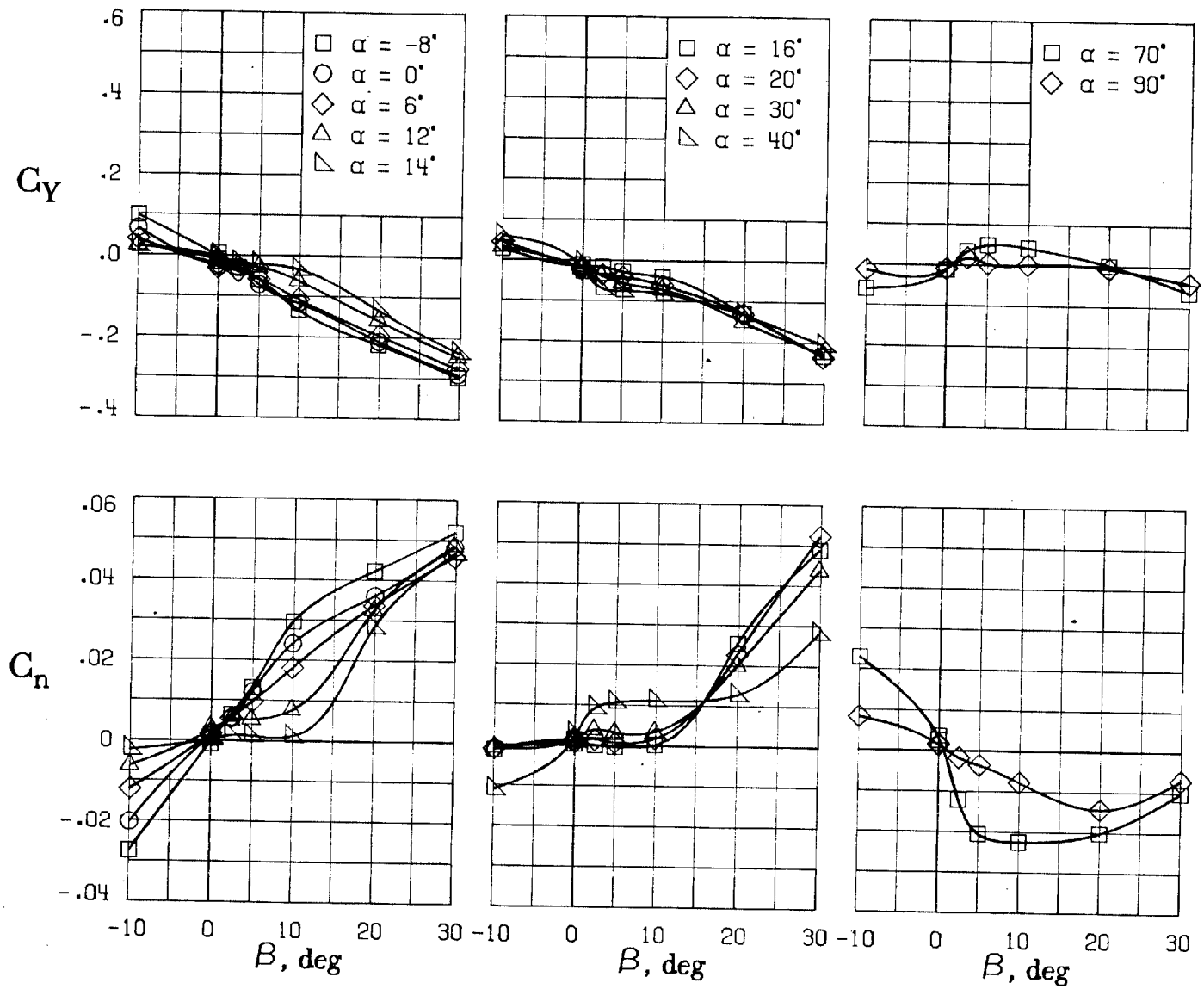

(E) DIRECTIONAL - STABILITY CHARACTERISTICS ABOUT BODY AXES AT VARIOUS ANGLES OF ATTACK.

FIGURE 67. - CONTINUED.

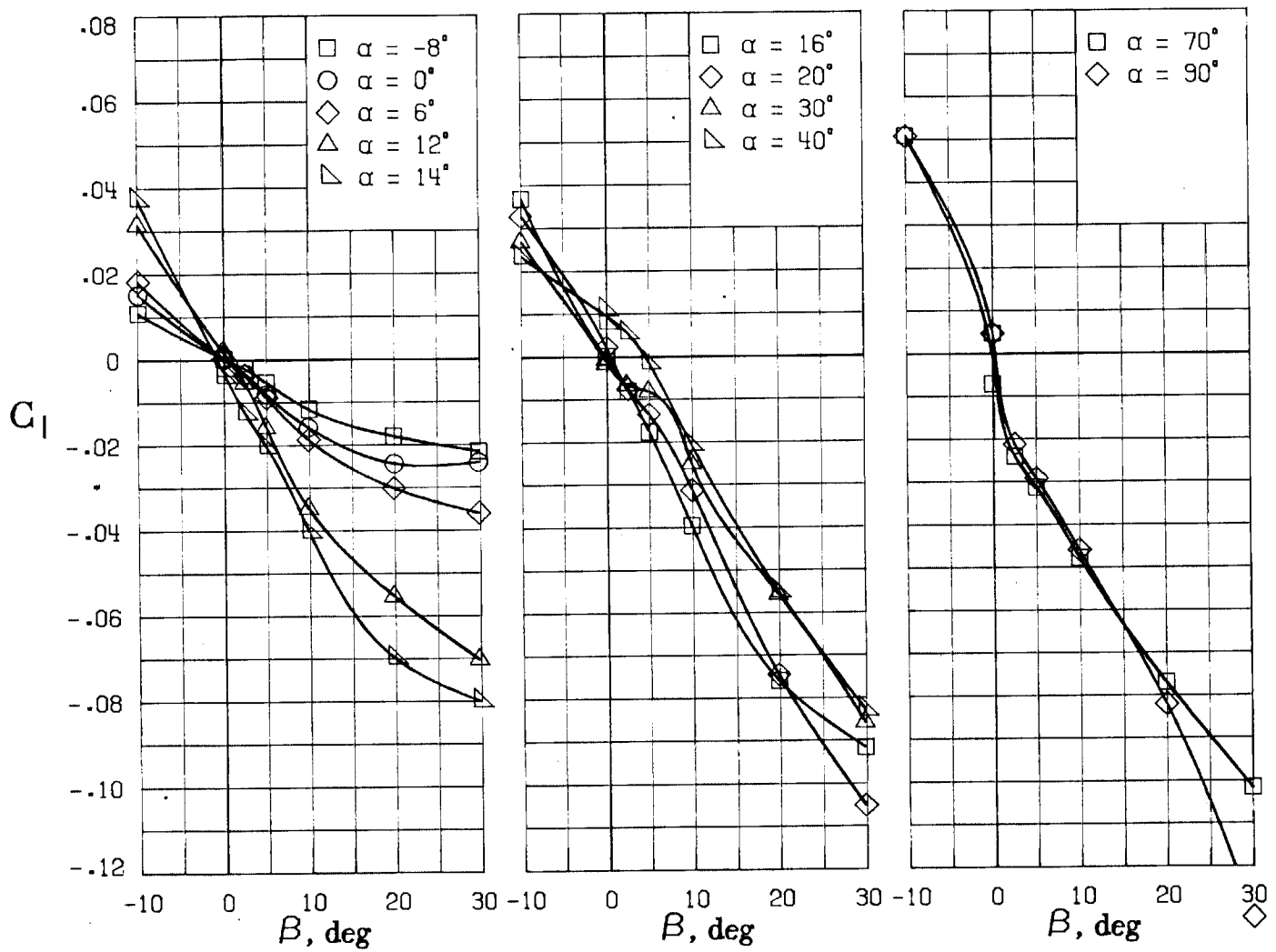

(F) LATERAL - STABILITY CHARACTERISTICS ABOUT BODY AXES AT VARIOUS ANGLES OF ATTACK.

FIGURE 67. - CONCLUDED.

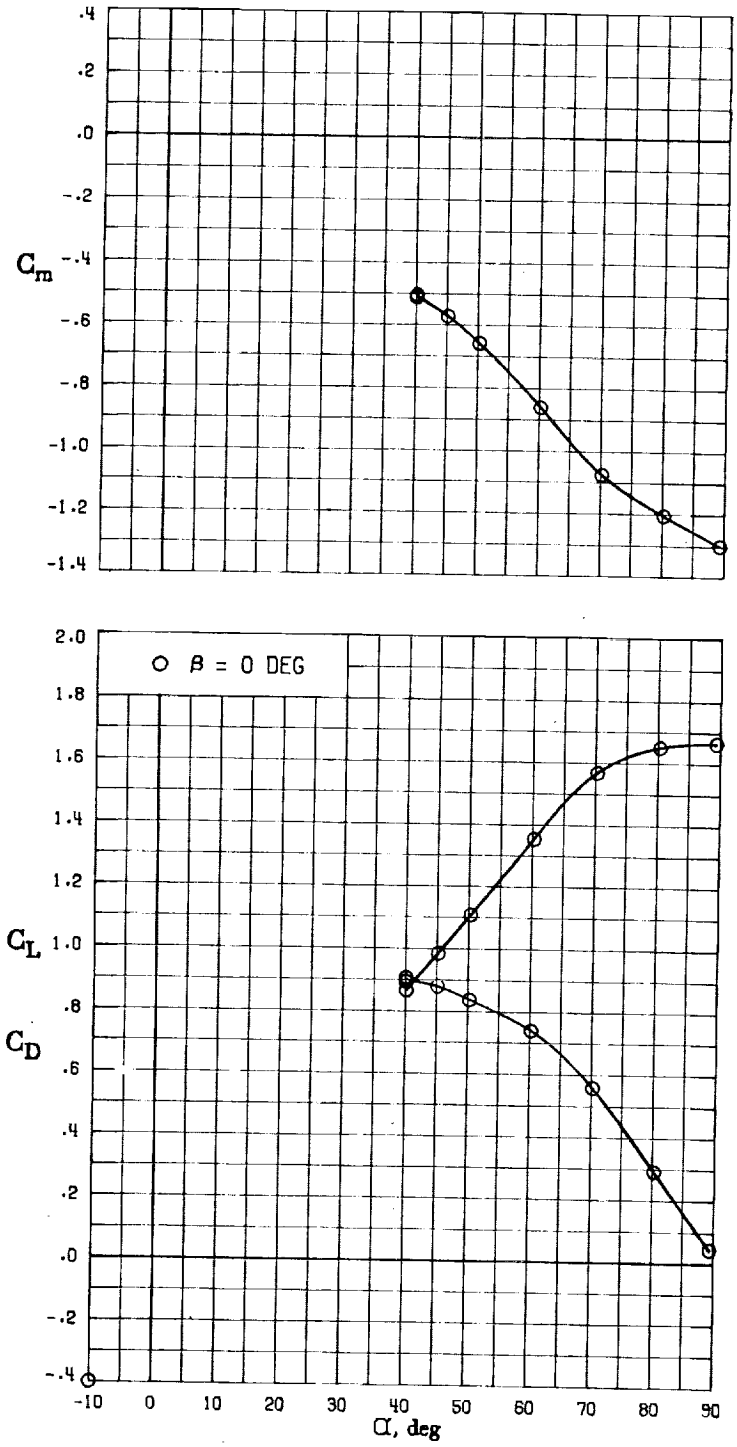

(A) LONGITUDINAL FORCE AND MOMENT COEFFICIENTS ABOUT STABILITY AXES.

FIGURE 68. - EFFECT OF ANGLE OF ATTACK AND SIDESLIP ANGLE ON AERODYNAMIC CHARACTERISTICS AT RE = .288 E+06 FOR CONFIGURATION B W1 H4 V. $\delta_E = 0°$, $\delta_A = 0°$, $\delta_R = -25°$.

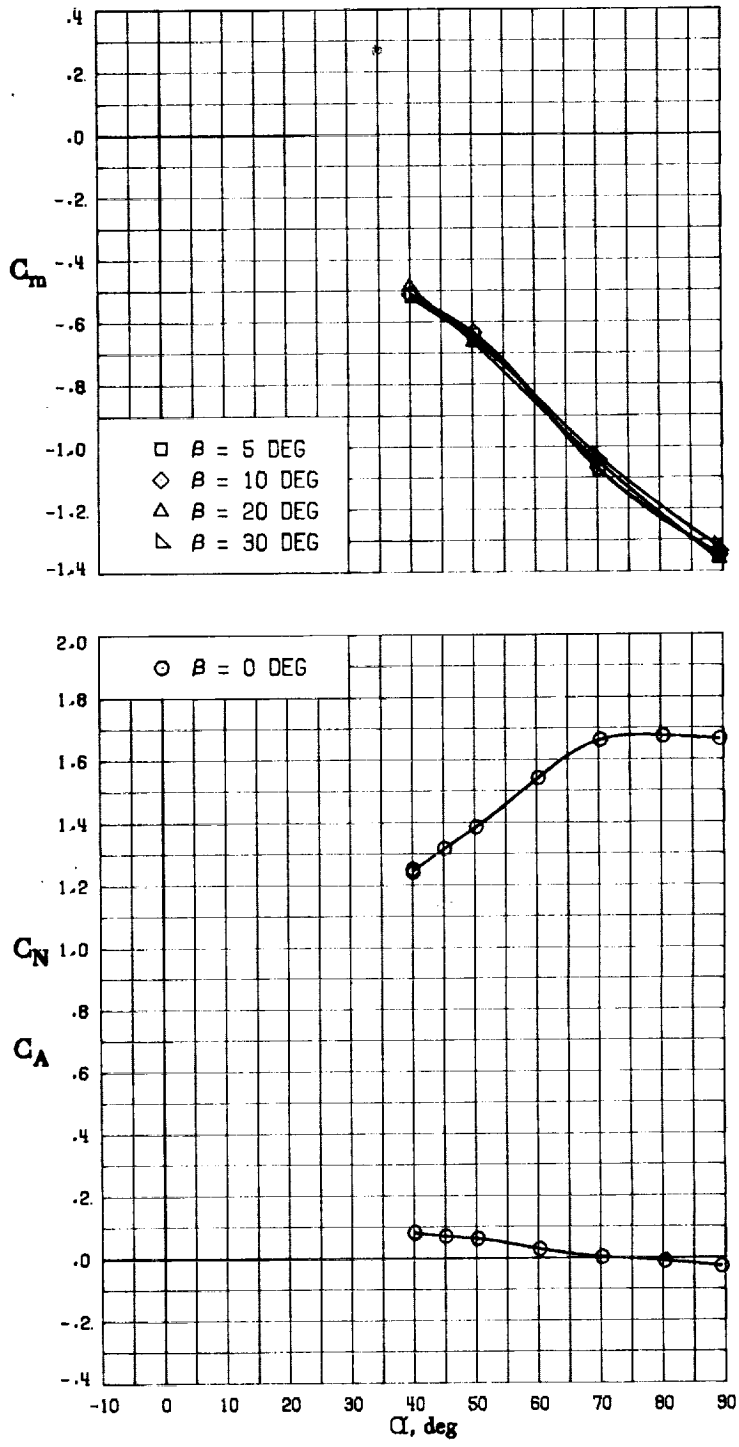

(B) LONGITUDINAL FORCE AND MOMENT COEFFICIENTS ABOUT BODY AXES.

FIGURE 68. - CONTINUED.

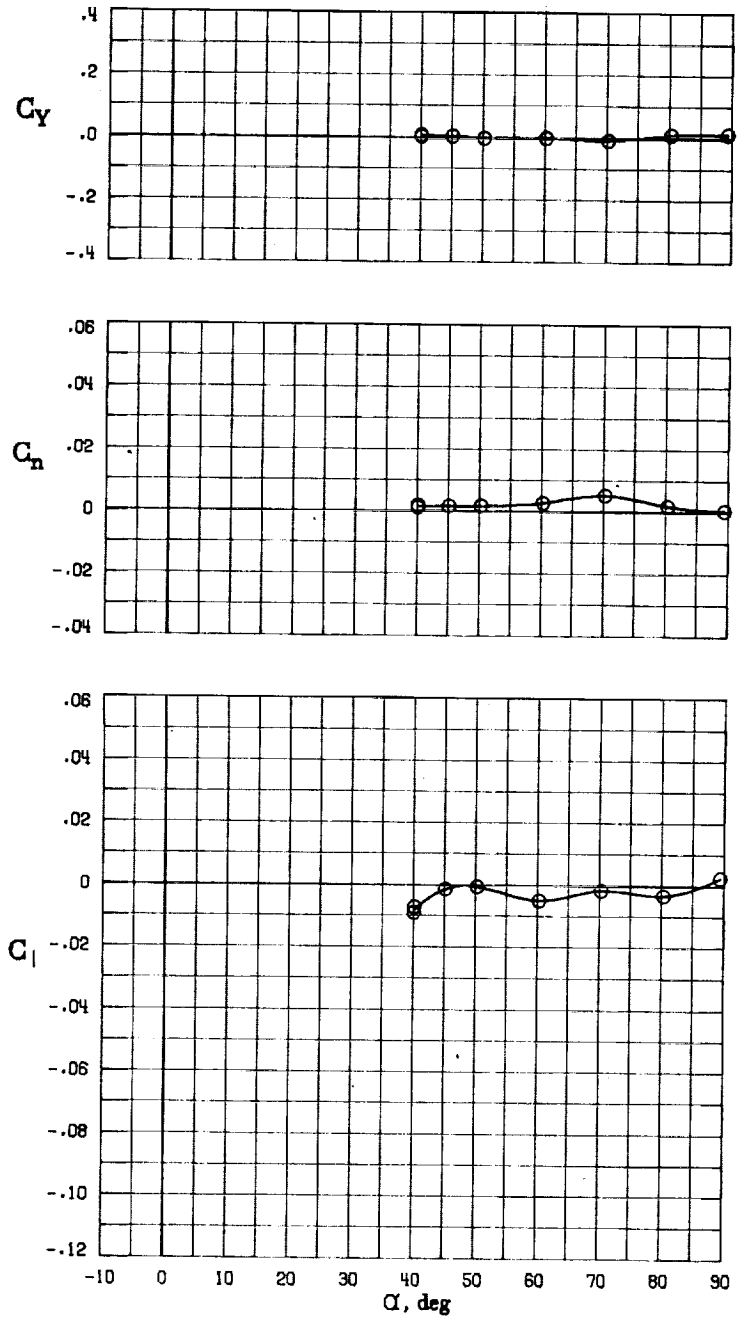

(C) LATERAL - DIRECTIONAL FORCE AND MOMENT COEFFICIENTS ABOUT BODY AXES AT ZERO SIDESLIP.

FIGURE 68. - CONTINUED.

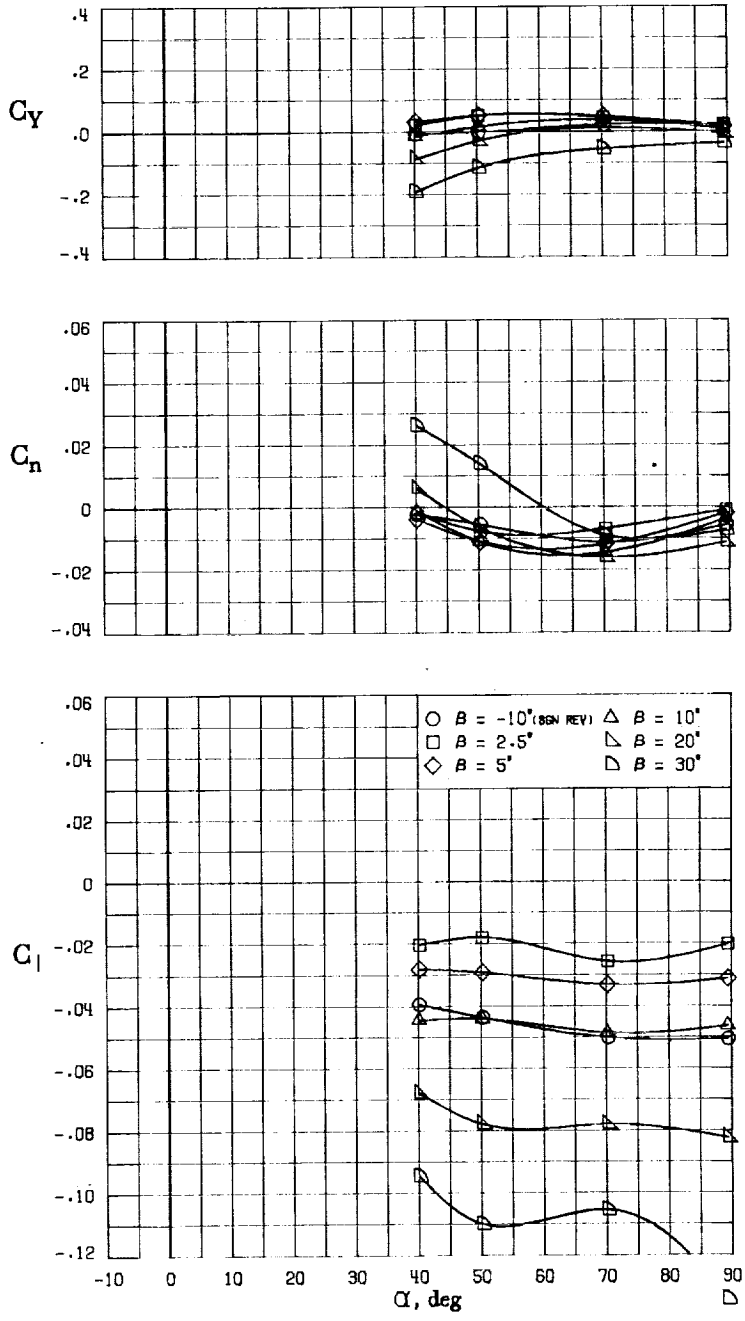

(D) LATERAL - DIRECTIONAL FORCE AND MOMENT COEFFICIENTS ABOUT BODY AXES.

FIGURE 68. - CONTINUED.

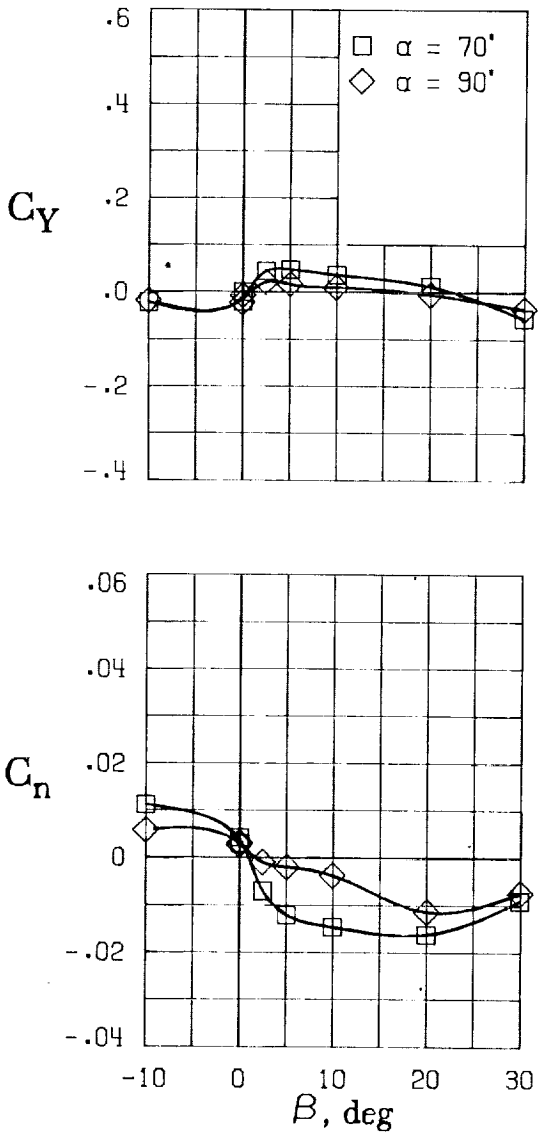

(E) DIRECTIONAL - STABILITY CHARACTERISTICS ABOUT BODY AXES AT VARIOUS ANGLES OF ATTACK.

FIGURE 68. - CONTINUED.

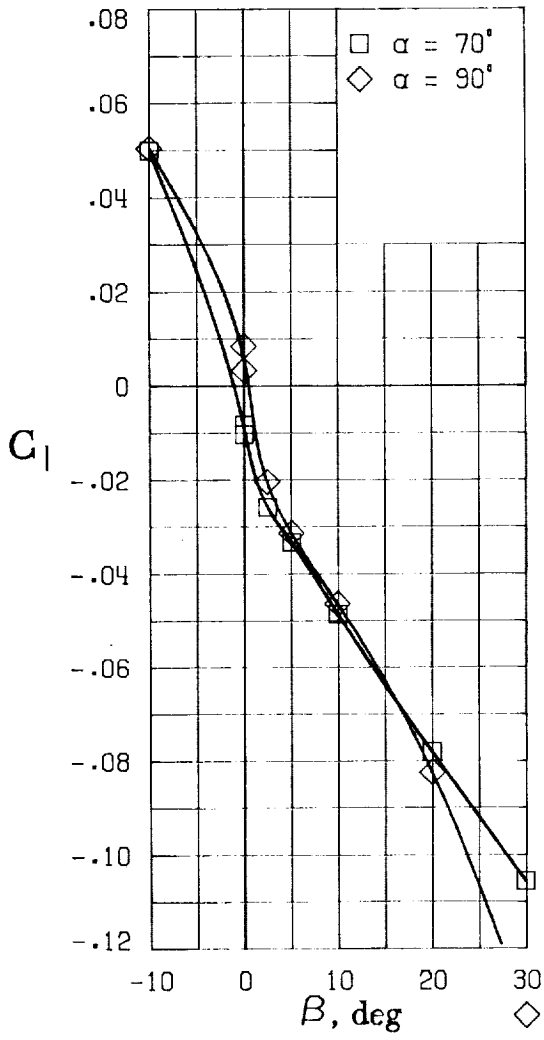

(F) LATERAL - STABILITY CHARACTERISTICS ABOUT BODY AXES AT VARIOUS ANGLES OF ATTACK.

FIGURE 68. - CONCLUDED.

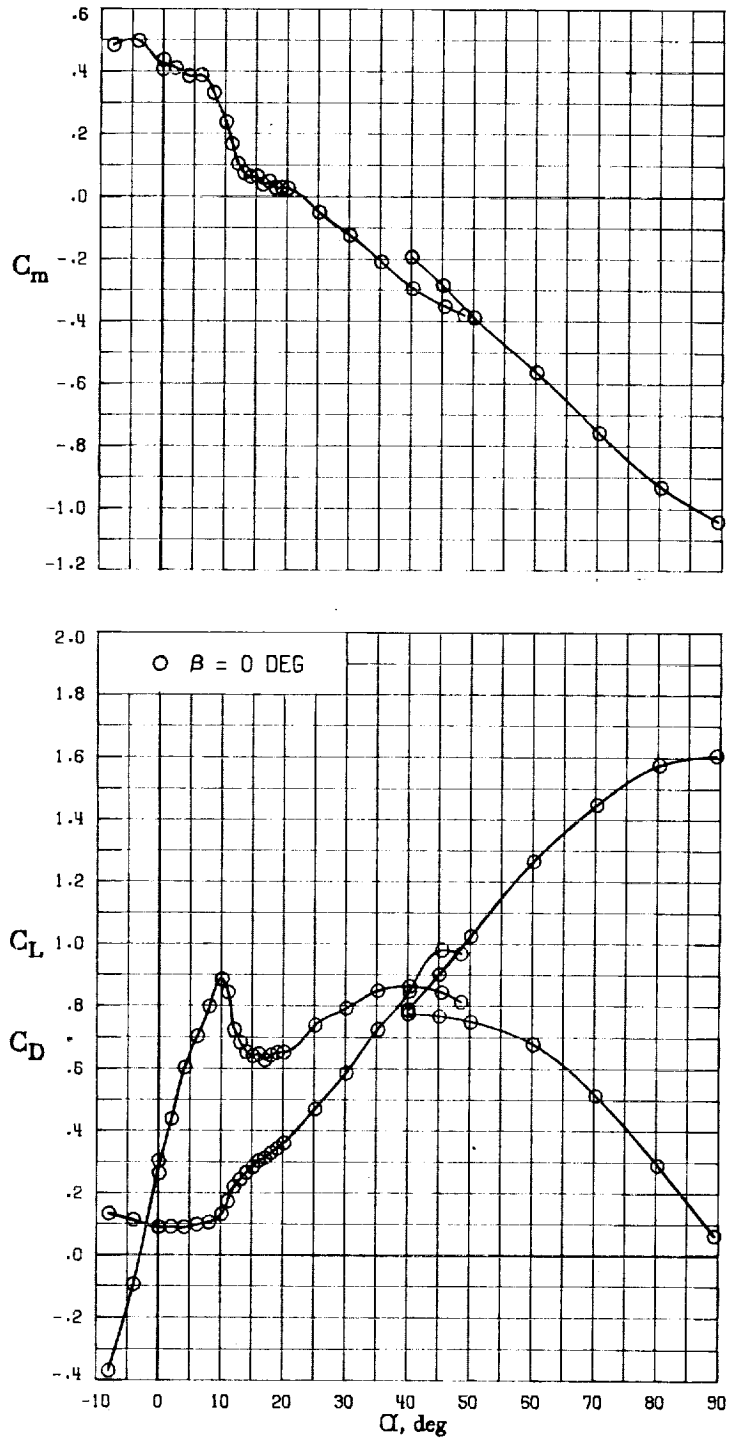

(A) LONGITUDINAL FORCE AND MOMENT COEFFICIENTS ABOUT STABILITY AXES.

FIGURE 69. - EFFECT OF ANGLE OF ATTACK AND SIDESLIP ANGLE ON AERODYNAMIC CHARACTERISTICS AT RE = .288 E+06 FOR CONFIGURATION B W1 H3 V. $\delta_E = -25°$, $\delta_A = 22°$, $\delta_R = -25°$.

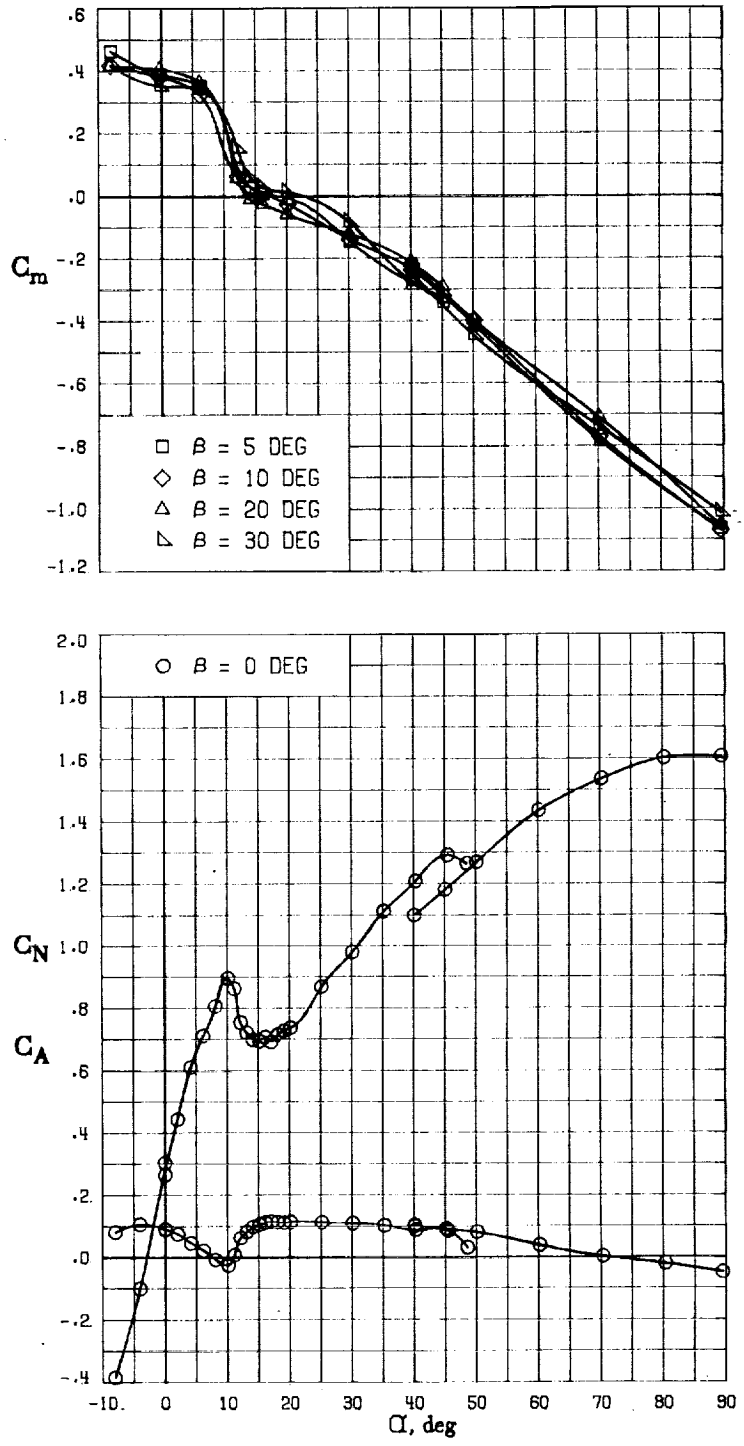

(B) LONGITUDINAL FORCE AND MOMENT COEFFICIENTS ABOUT BODY AXES.

FIGURE 69. - CONTINUED.

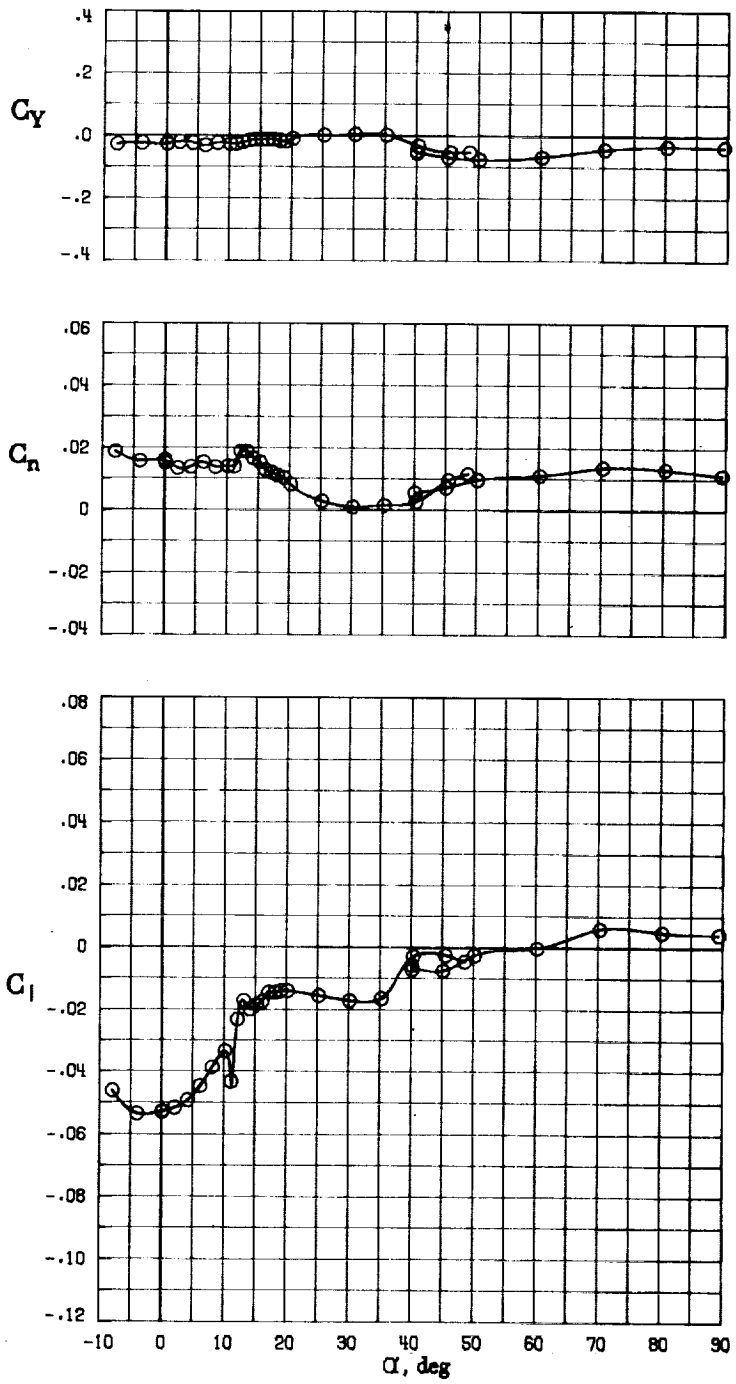

(C) LATERAL - DIRECTIONAL FORCE AND MOMENT COEFFICIENTS ABOUT BODY AXES AT ZERO SIDESLIP.

FIGURE 69. - CONTINUED.

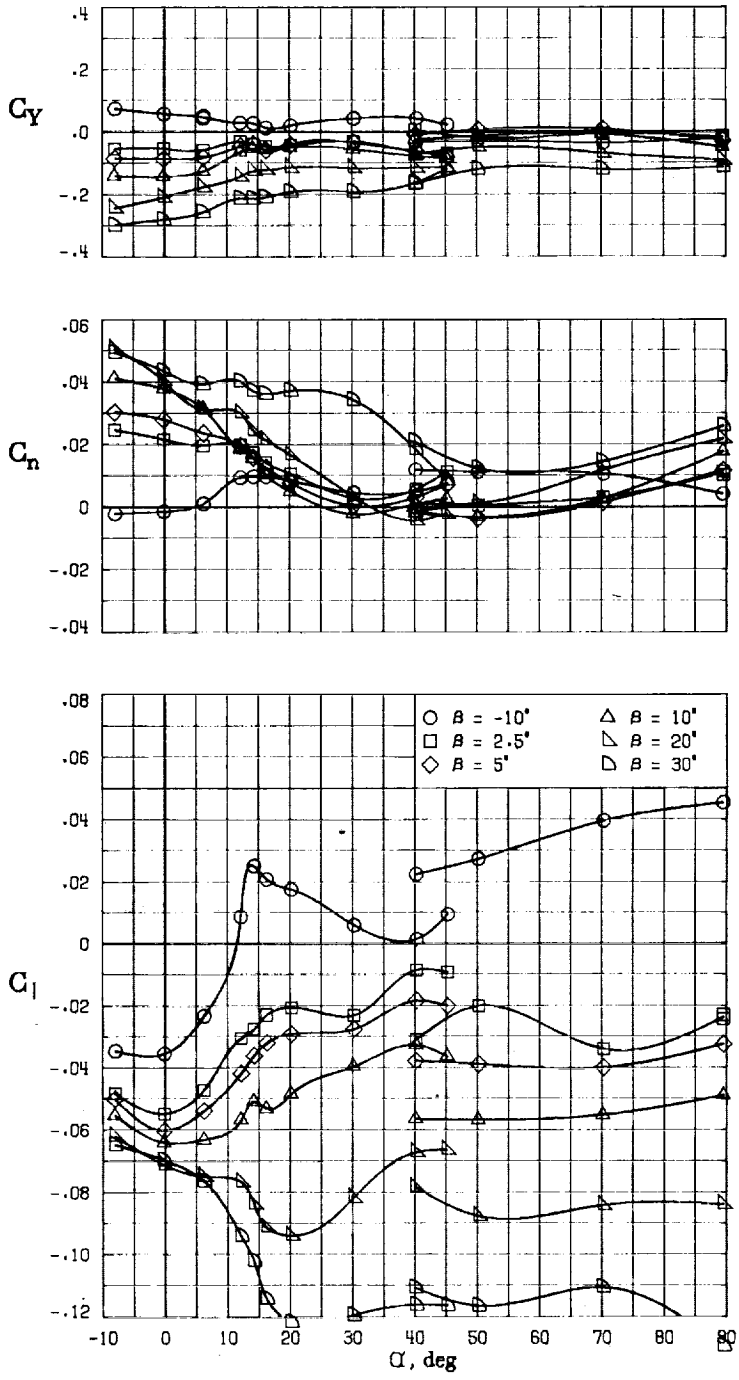

(D) LATERAL - DIRECTIONAL FORCE AND MOMENT COEFFICIENTS ABOUT BODY AXES.

FIGURE 69. - CONTINUED.

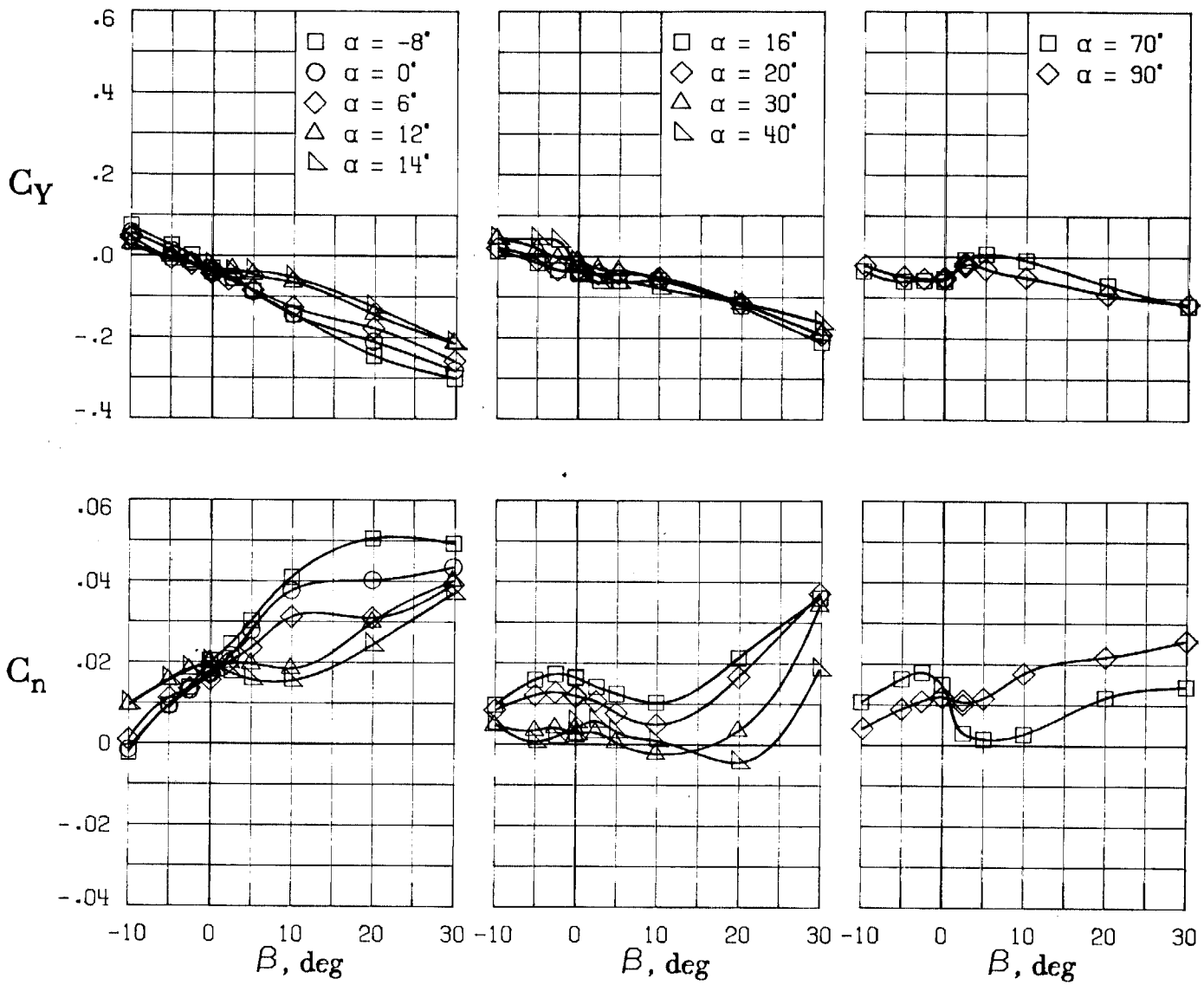

(E) DIRECTIONAL - STABILITY CHARACTERISTICS ABOUT BODY AXES AT VARIOUS ANGLES OF ATTACK.

FIGURE 69. - CONTINUED.

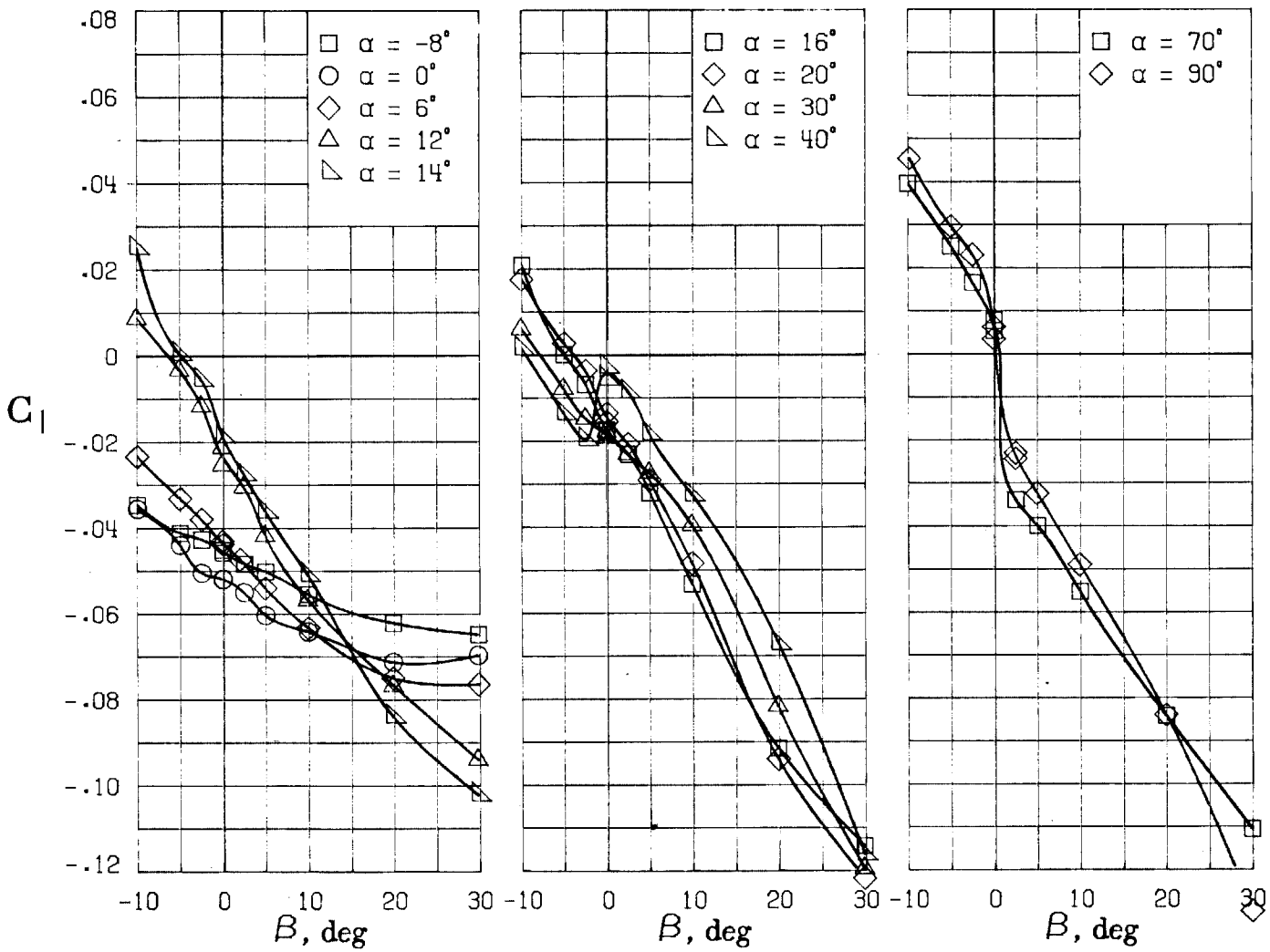

(F) LATERAL - STABILITY CHARACTERISTICS ABOUT BODY AXES AT VARIOUS ANGLES OF ATTACK.

FIGURE 69. - CONCLUDED.

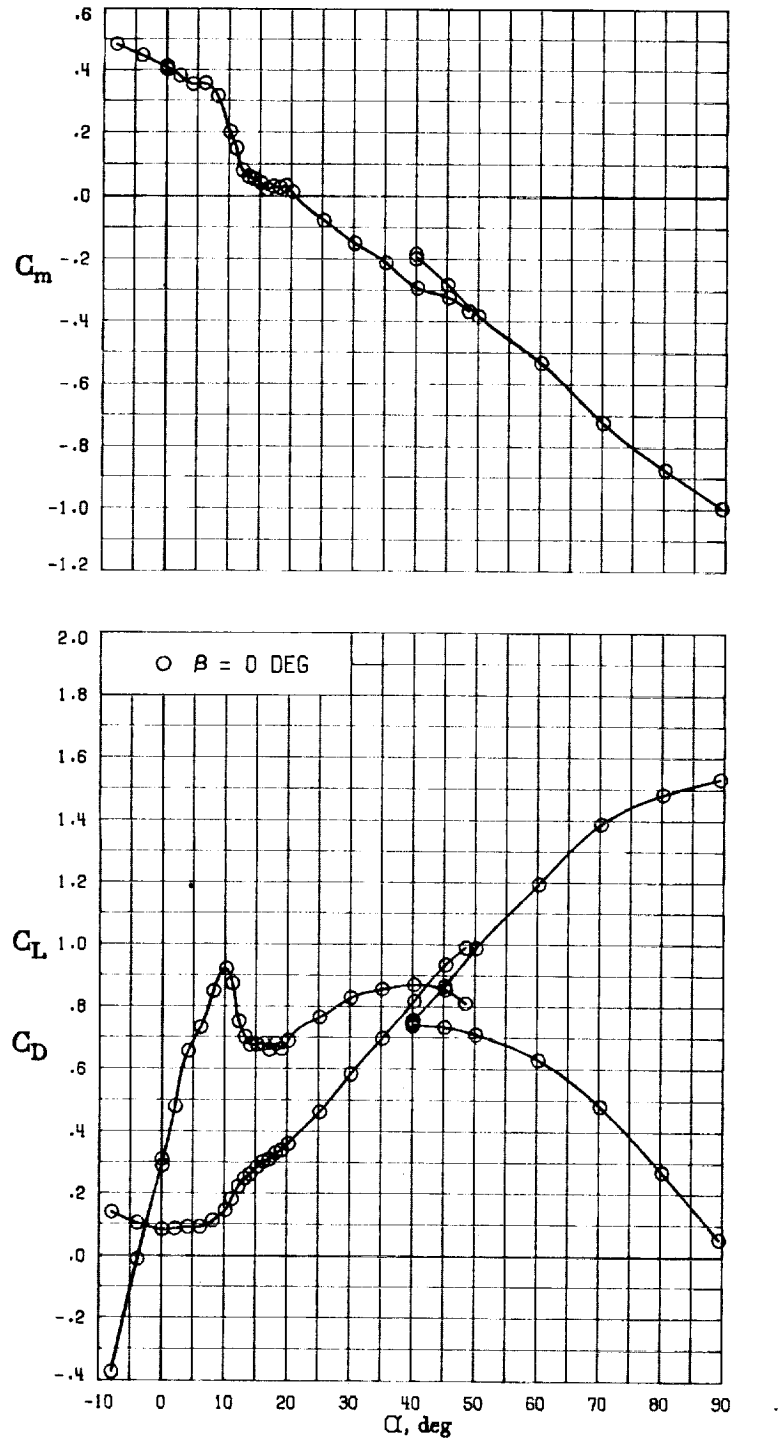

(A) LONGITUDINAL FORCE AND MOMENT COEFFICIENTS ABOUT STABILITY AXES.

FIGURE 70. - EFFECT OF ANGLE OF ATTACK AND SIDESLIP ANGLE ON AERODYNAMIC CHARACTERISTICS AT RE = .288 E+06 FOR CONFIGURATION B W1 H3 V. δ_E = -25°, δ_A = -22°, δ_R = -25°.

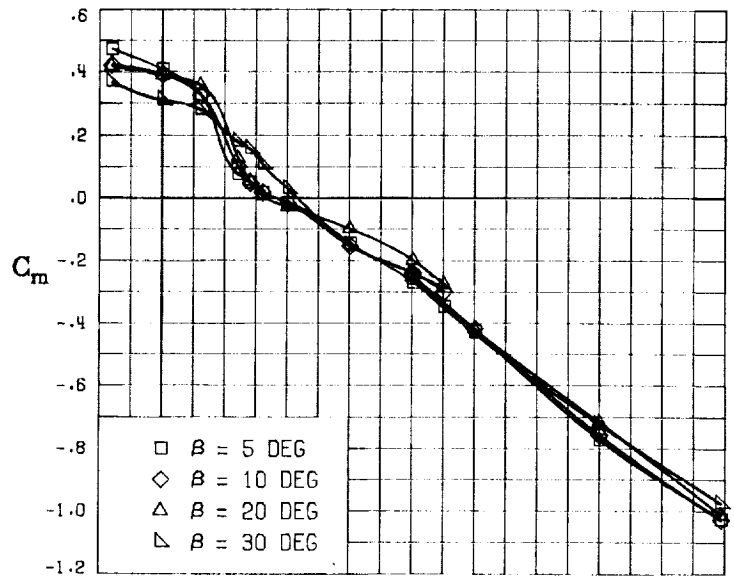

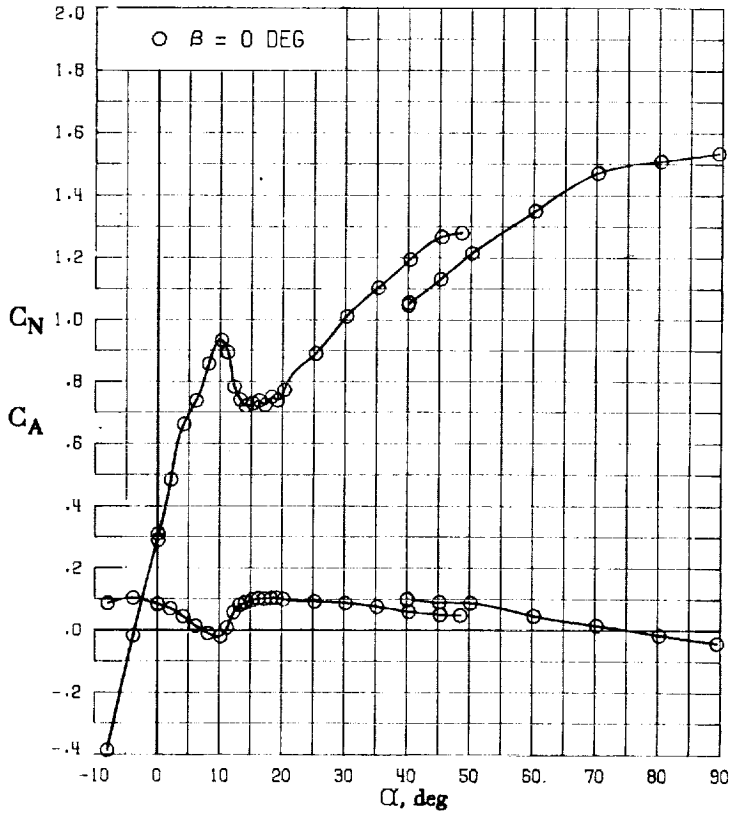

(B) LONGITUDINAL FORCE AND MOMENT COEFFICIENTS ABOUT BODY AXES.

FIGURE 70. - CONTINUED.

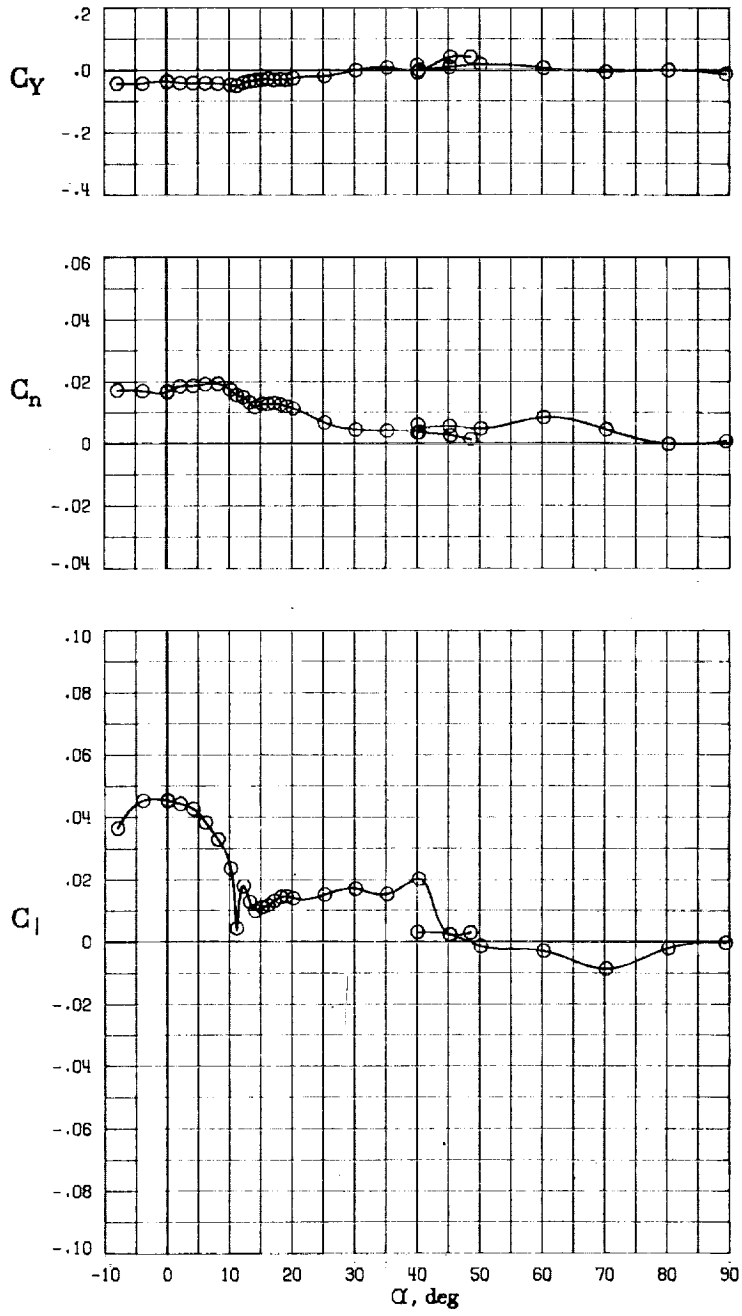

(C) LATERAL - DIRECTIONAL FORCE AND MOMENT COEFFICIENTS ABOUT BODY AXES AT ZERO SIDESLIP.

FIGURE 70. - CONTINUED.

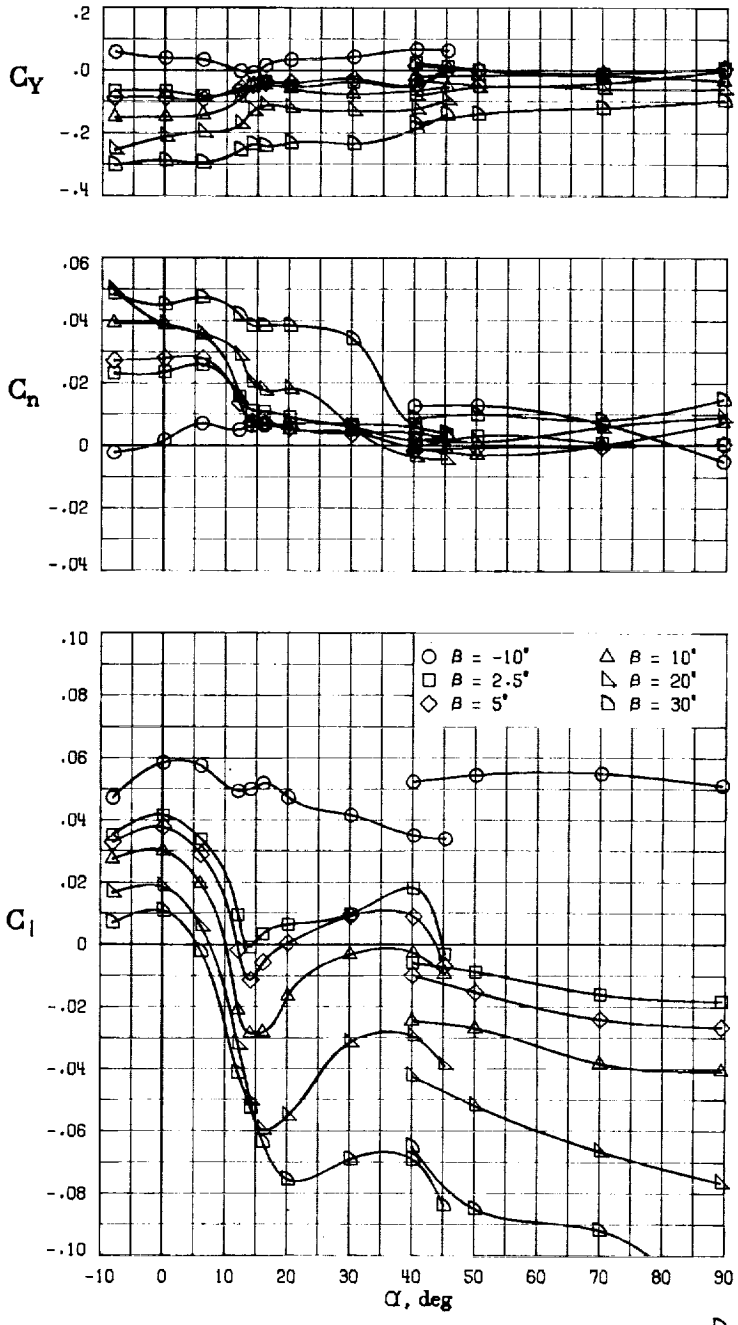

(D) LATERAL - DIRECTIONAL FORCE AND MOMENT COEFFICIENTS ABOUT BODY AXES.

FIGURE 70. - CONTINUED.

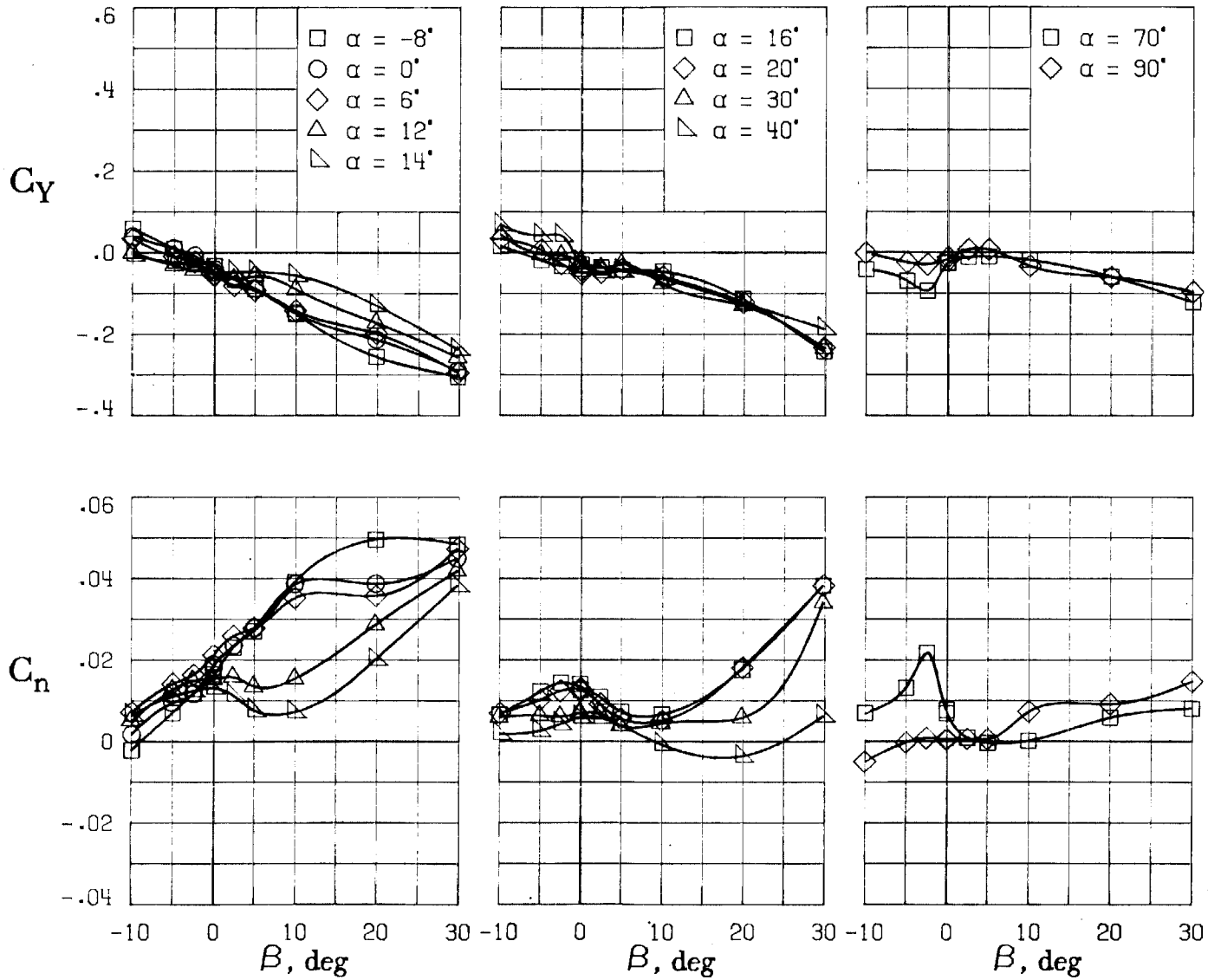

(E) DIRECTIONAL - STABILITY CHARACTERISTICS ABOUT BODY AXES AT VARIOUS ANGLES OF ATTACK.

FIGURE 20 CONTINUED

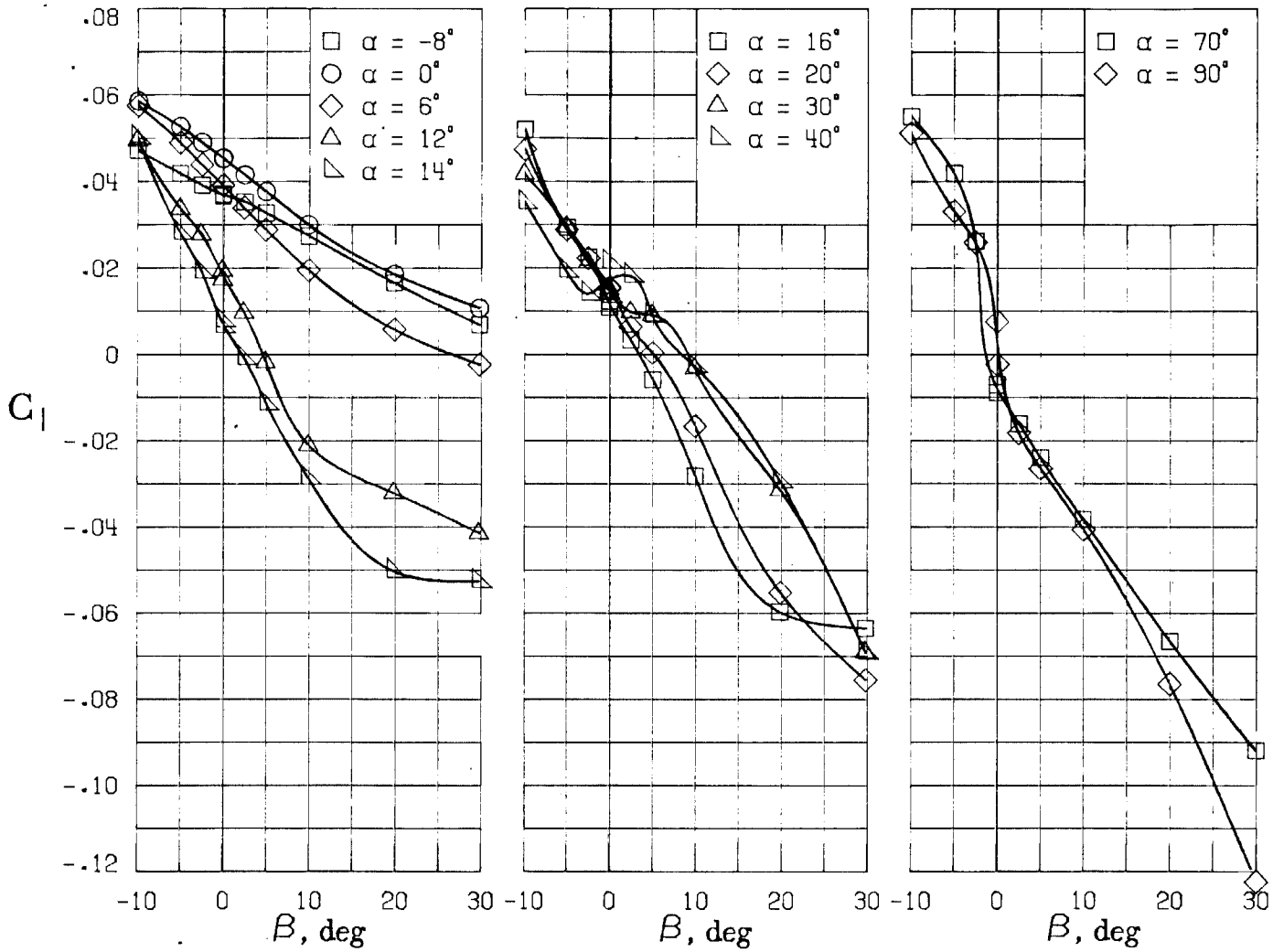

(F) LATERAL - STABILITY CHARACTERISTICS ABOUT BODY AXES AT VARIOUS ANGLES OF ATTACK.

FIGURE 70. - CONCLUDED.

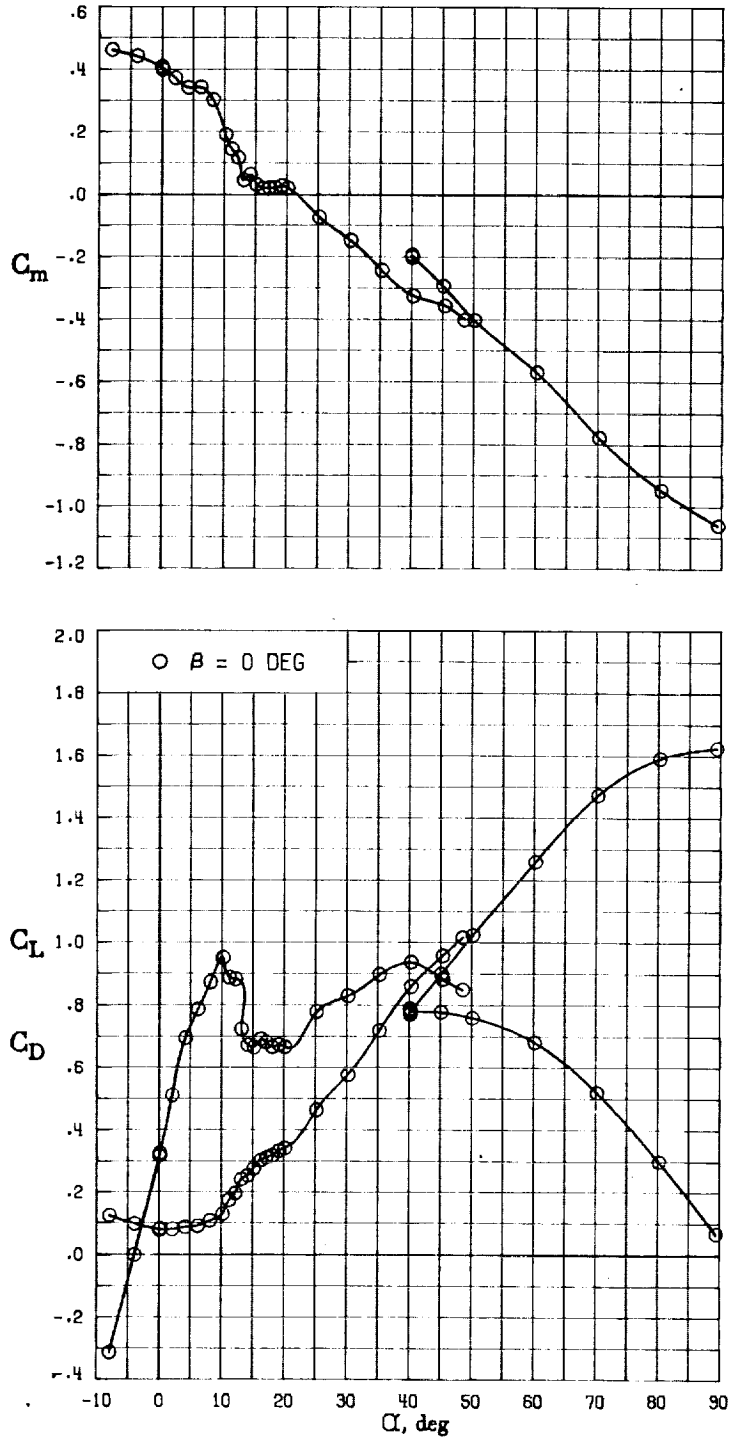

(A) LONGITUDINAL FORCE AND MOMENT COEFFICIENTS ABOUT STABILITY AXES.

FIGURE 71. - EFFECT OF ANGLE OF ATTACK AND SIDESLIP ANGLE ON AERODYNAMIC CHARACTERISTICS AT RE = .288 E+06 FOR CONFIGURATION B W1 H3 V. $\delta_E = -25°$; $\delta_A = 0°$, $\delta_R = -25°$.

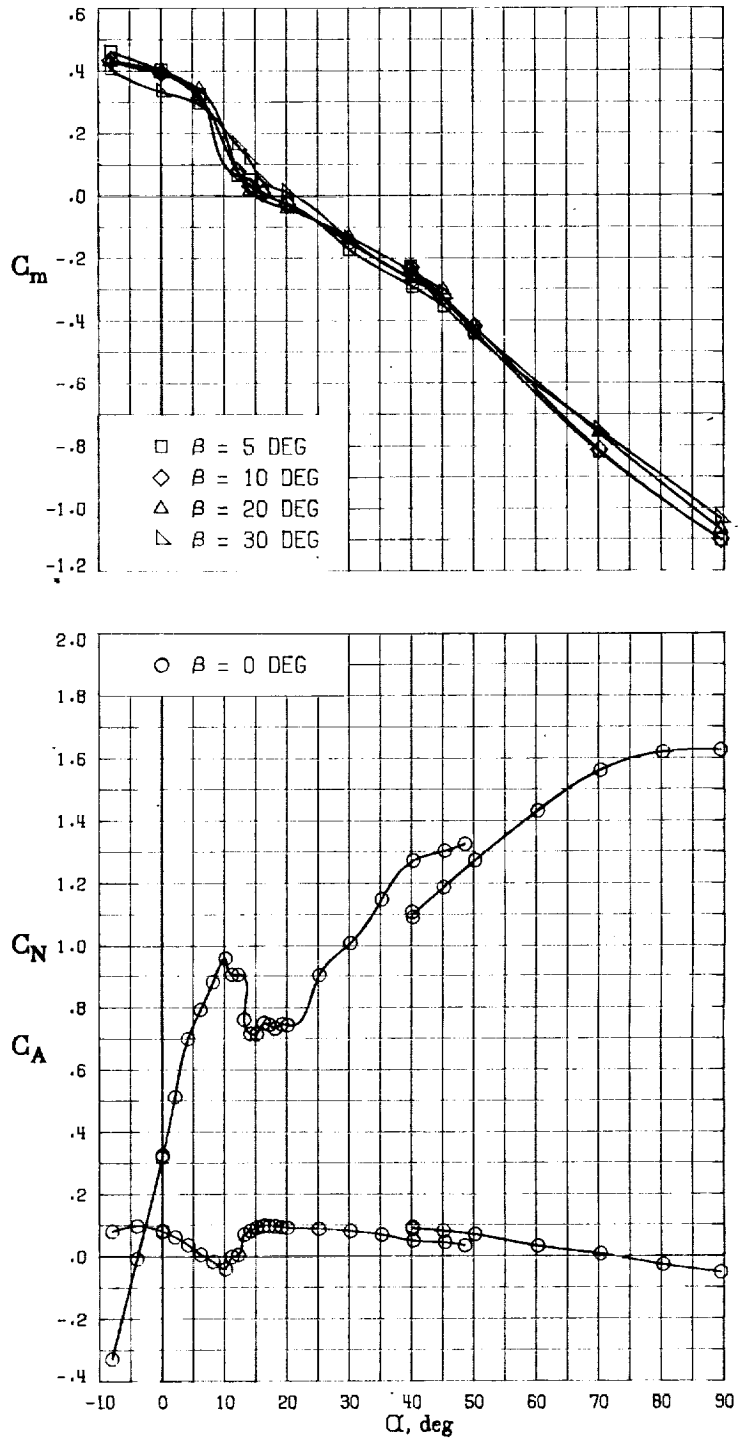

(B) LONGITUDINAL FORCE AND MOMENT COEFFICIENTS ABOUT BODY AXES.

FIGURE 71. - CONTINUED.

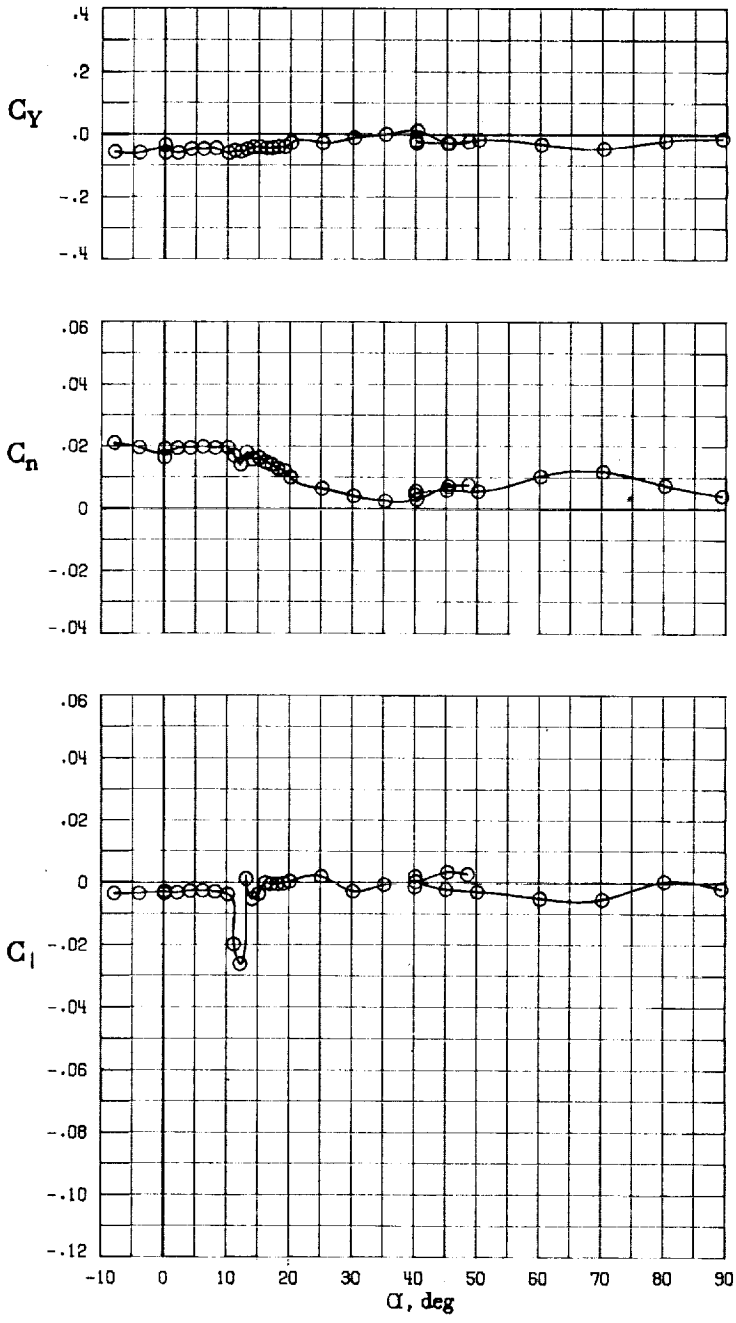

(C) LATERAL - DIRECTIONAL FORCE AND MOMENT COEFFICIENTS ABOUT BODY AXES AT ZERO SIDESLIP.

FIGURE 71. - CONTINUED.

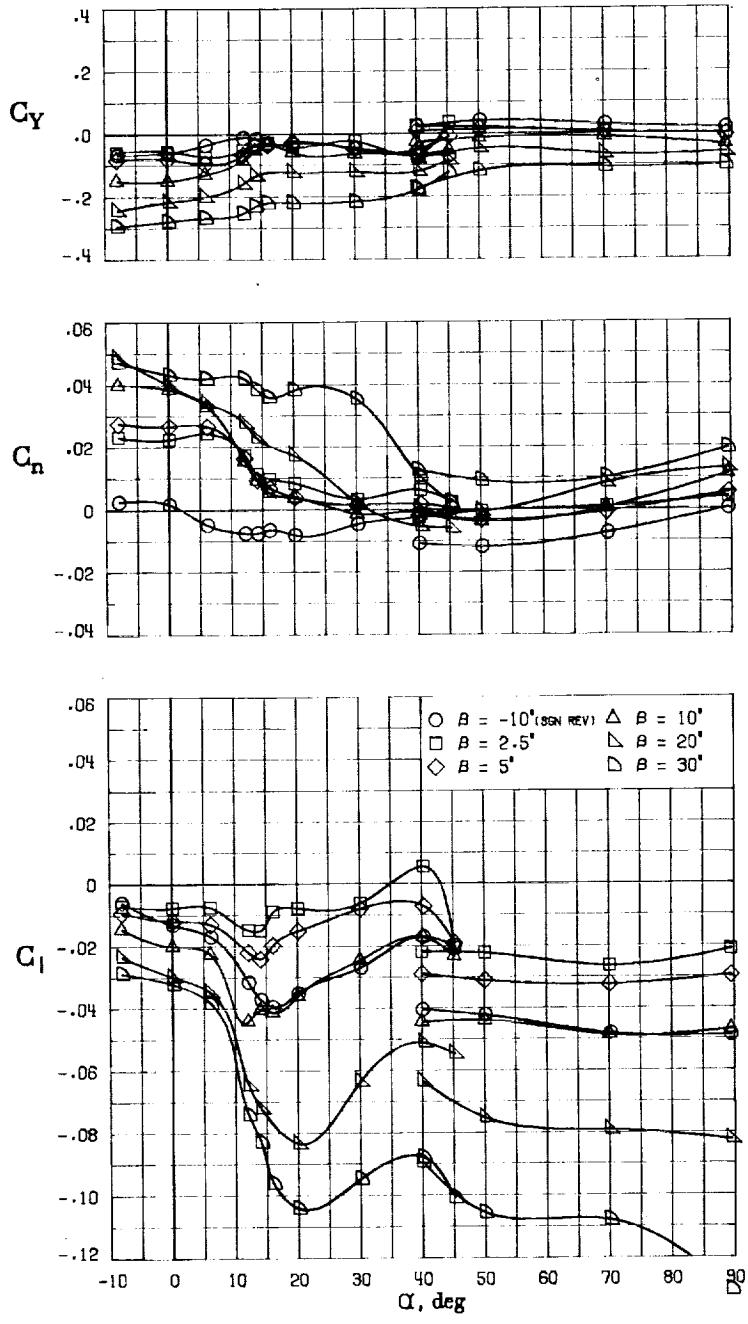

(D) LATERAL - DIRECTIONAL FORCE AND MOMENT COEFFICIENTS ABOUT BODY AXES.

FIGURE 71. - CONTINUED.

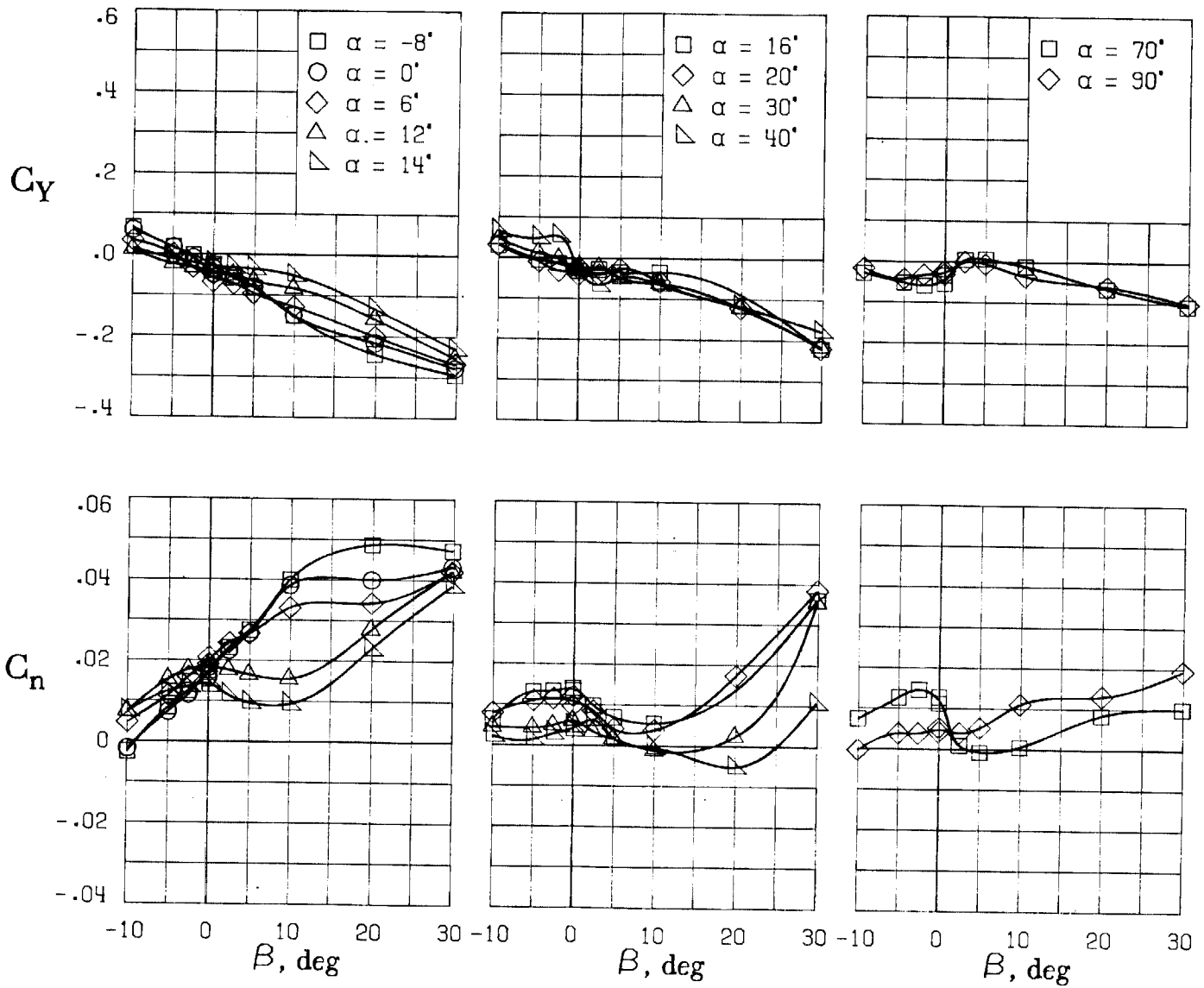

(E) DIRECTIONAL - STABILITY CHARACTERISTICS ABOUT BODY AXES AT VARIOUS ANGLES OF ATTACK.

FIGURE 71. - CONTINUED.

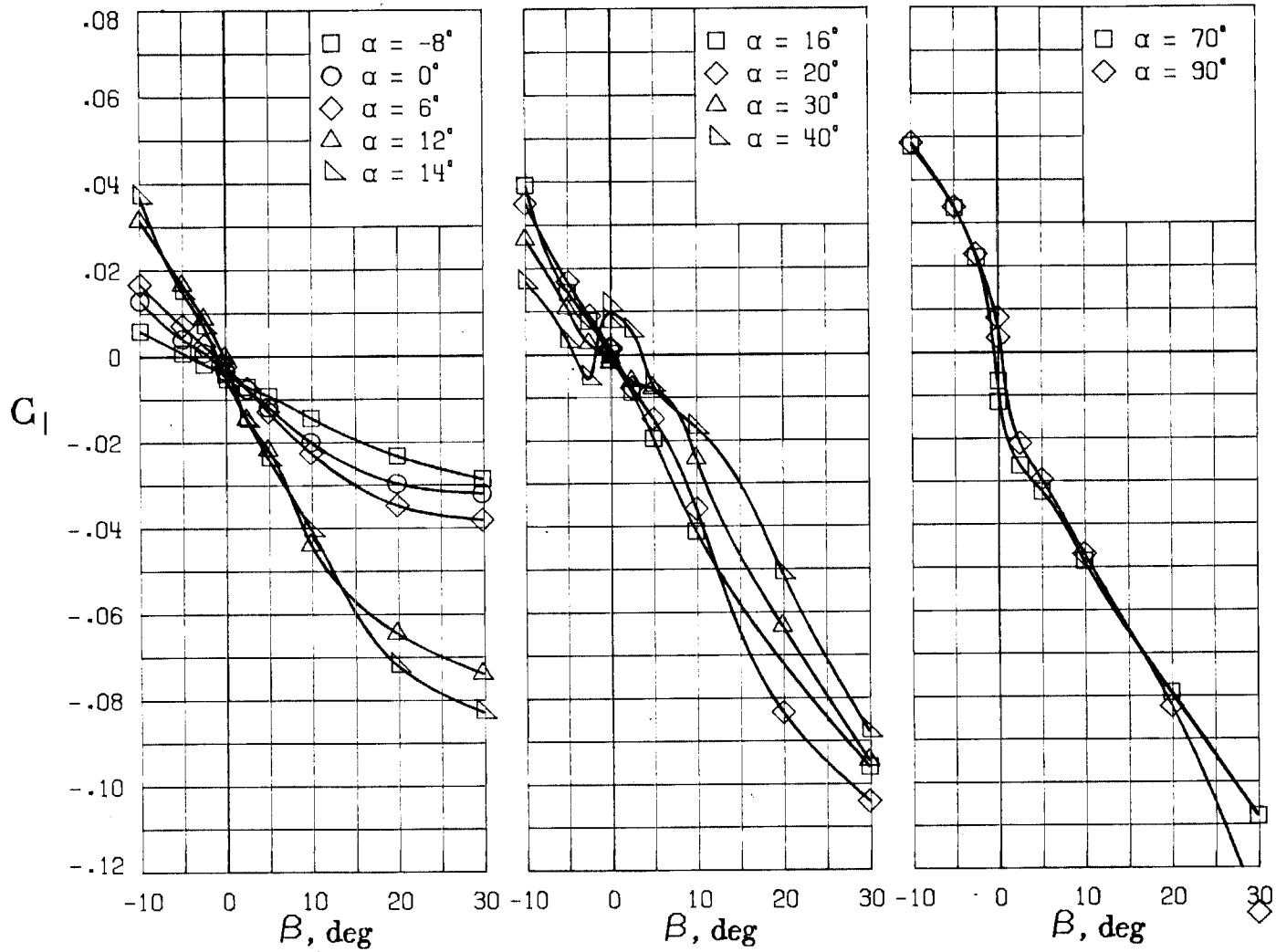

(F) LATERAL - STABILITY CHARACTERISTICS ABOUT BODY AXES AT VARIOUS ANGLES OF ATTACK.

FIGURE 71. - CONCLUDED.

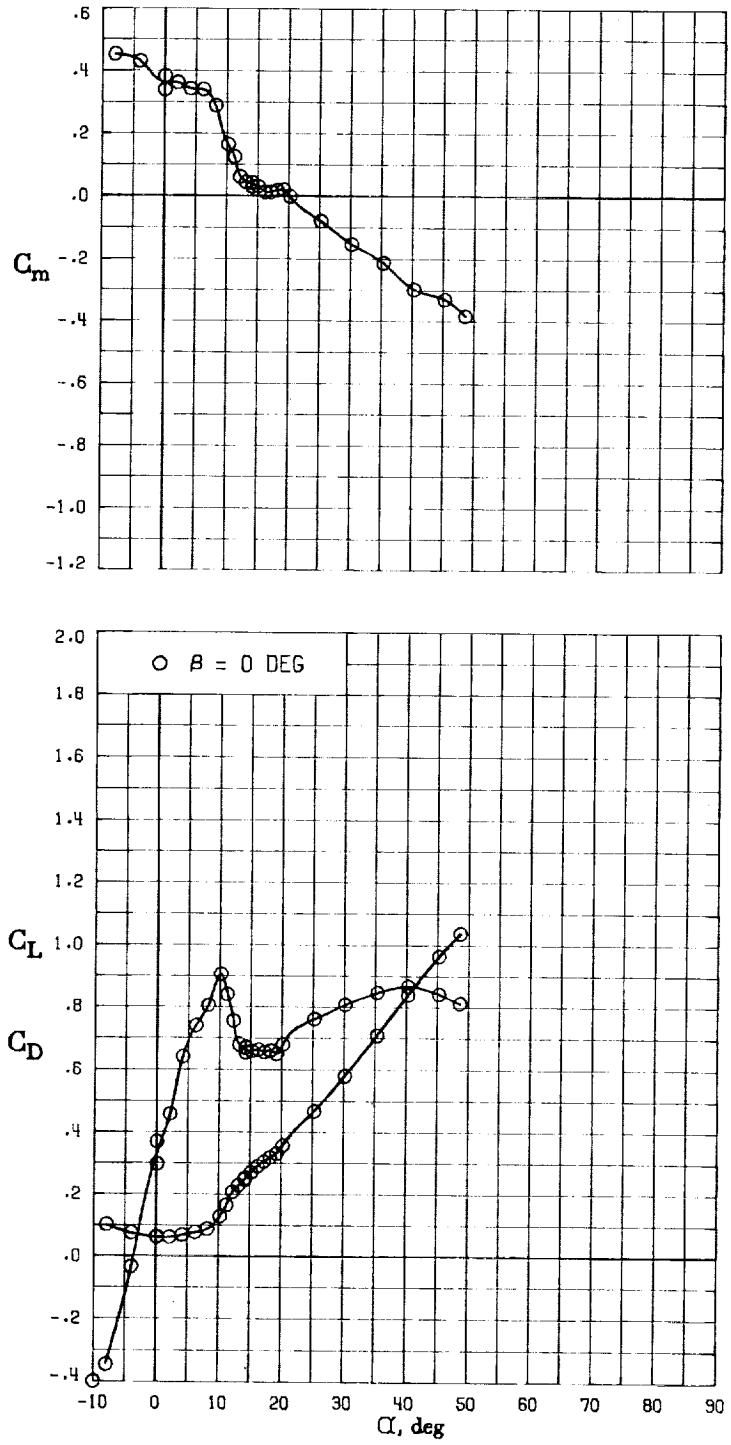

(A) LONGITUDINAL FORCE AND MOMENT COEFFICIENTS ABOUT STABILITY AXES.

FIGURE 72. - EFFECT OF ANGLE OF ATTACK AND SIDESLIP ANGLE ON AERODYNAMIC CHARACTERISTICS AT RE = .288 E+06 FOR CONFIGURATION B W1 H3 V. $\delta_E = -25°$, $\delta_A = -22°$, $\delta_R = 0°$.

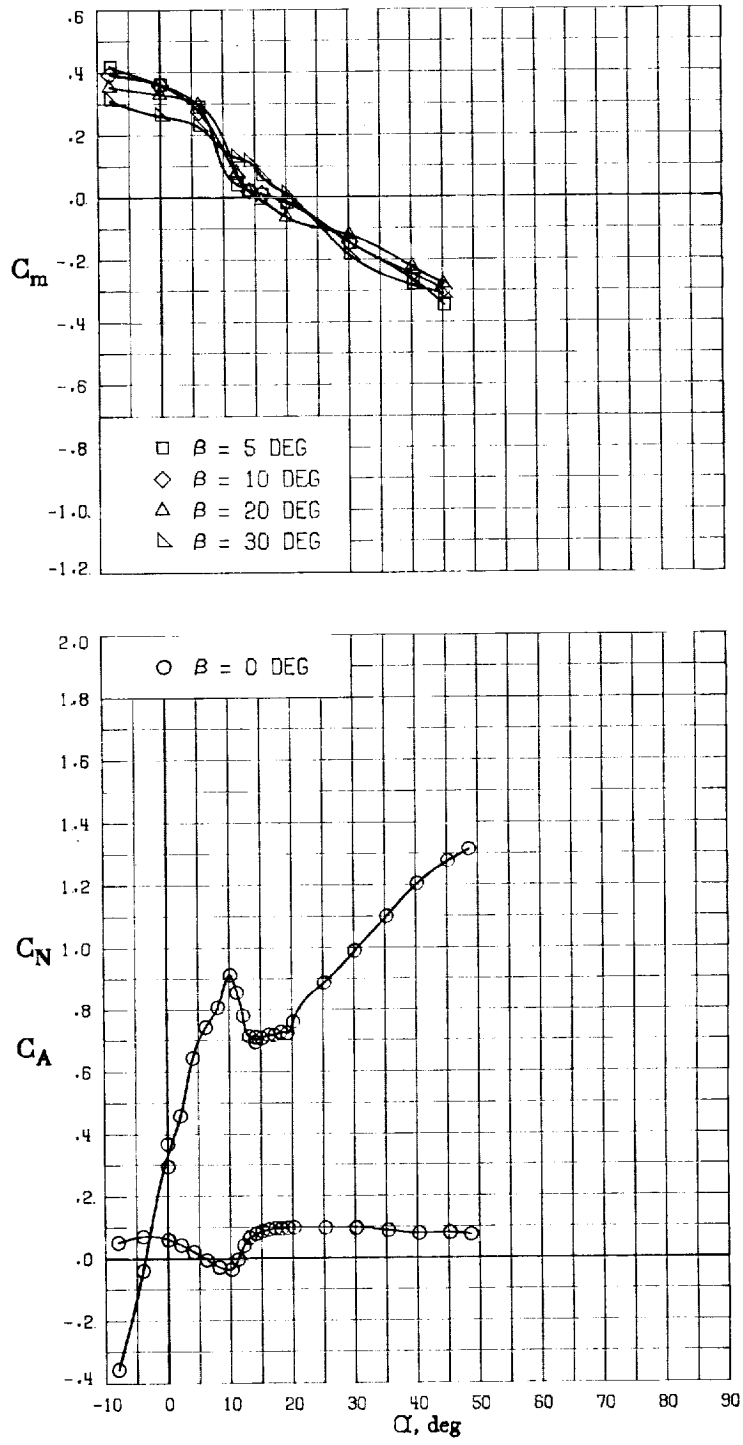

(B) LONGITUDINAL FORCE AND MOMENT COEFFICIENTS ABOUT BODY AXES.

FIGURE 72. - CONTINUED.

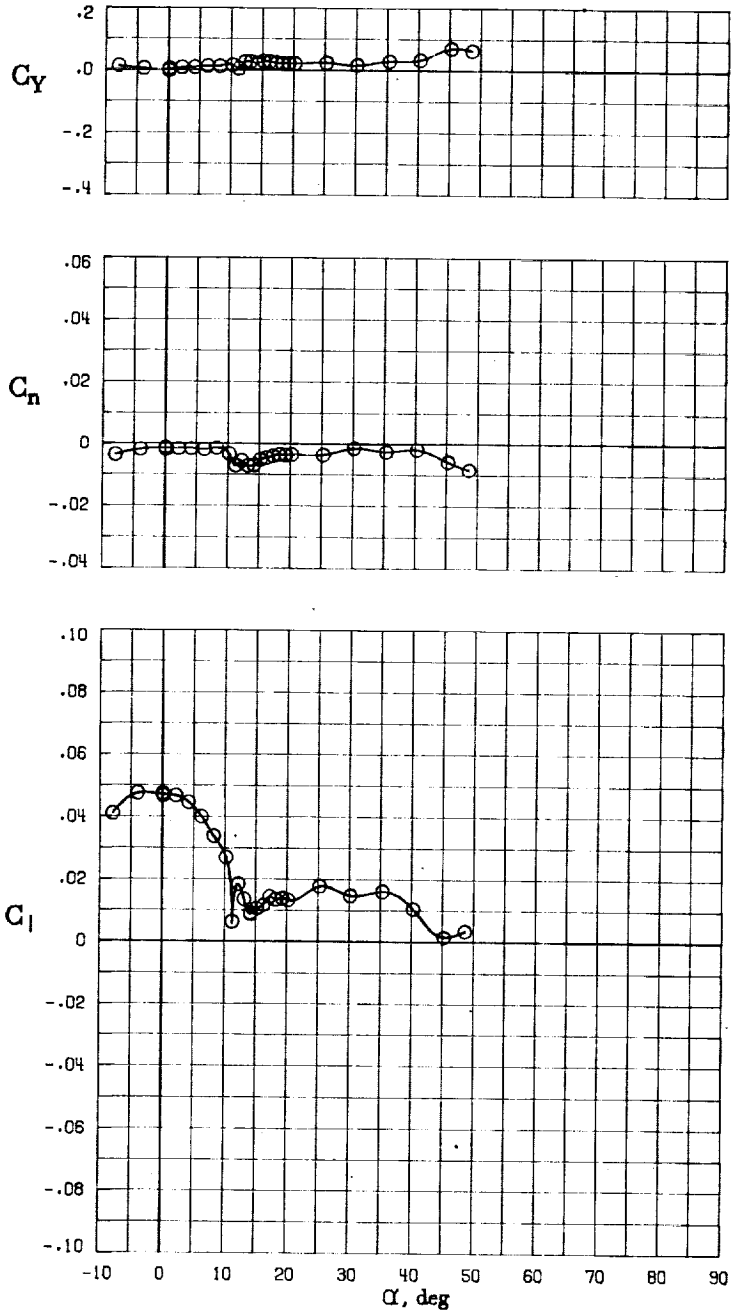

(C) LATERAL - DIRECTIONAL FORCE AND MOMENT COEFFICIENTS ABOUT BODY AXES AT ZERO SIDESLIP.

FIGURE 72. - CONTINUED.

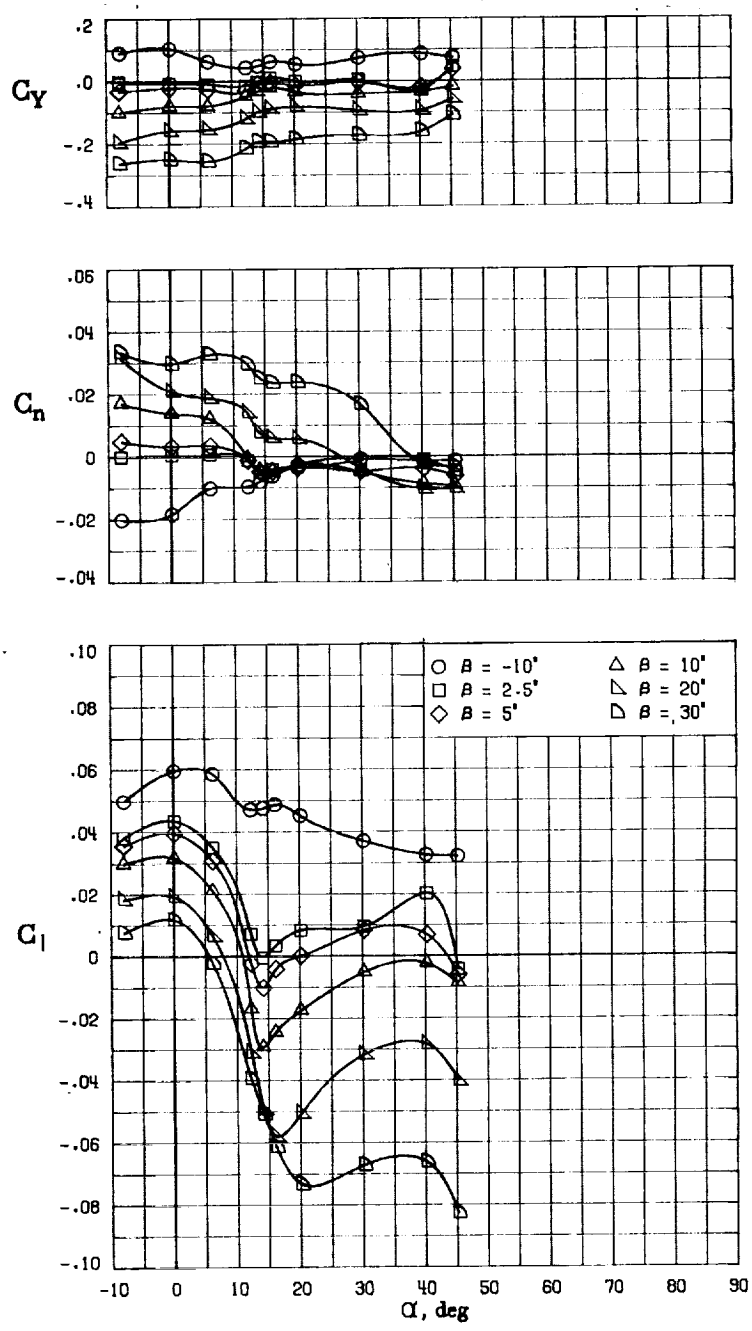

(D) LATERAL - DIRECTIONAL FORCE AND MOMENT COEFFICIENTS ABOUT BODY AXES.

FIGURE 72. - CONTINUED.

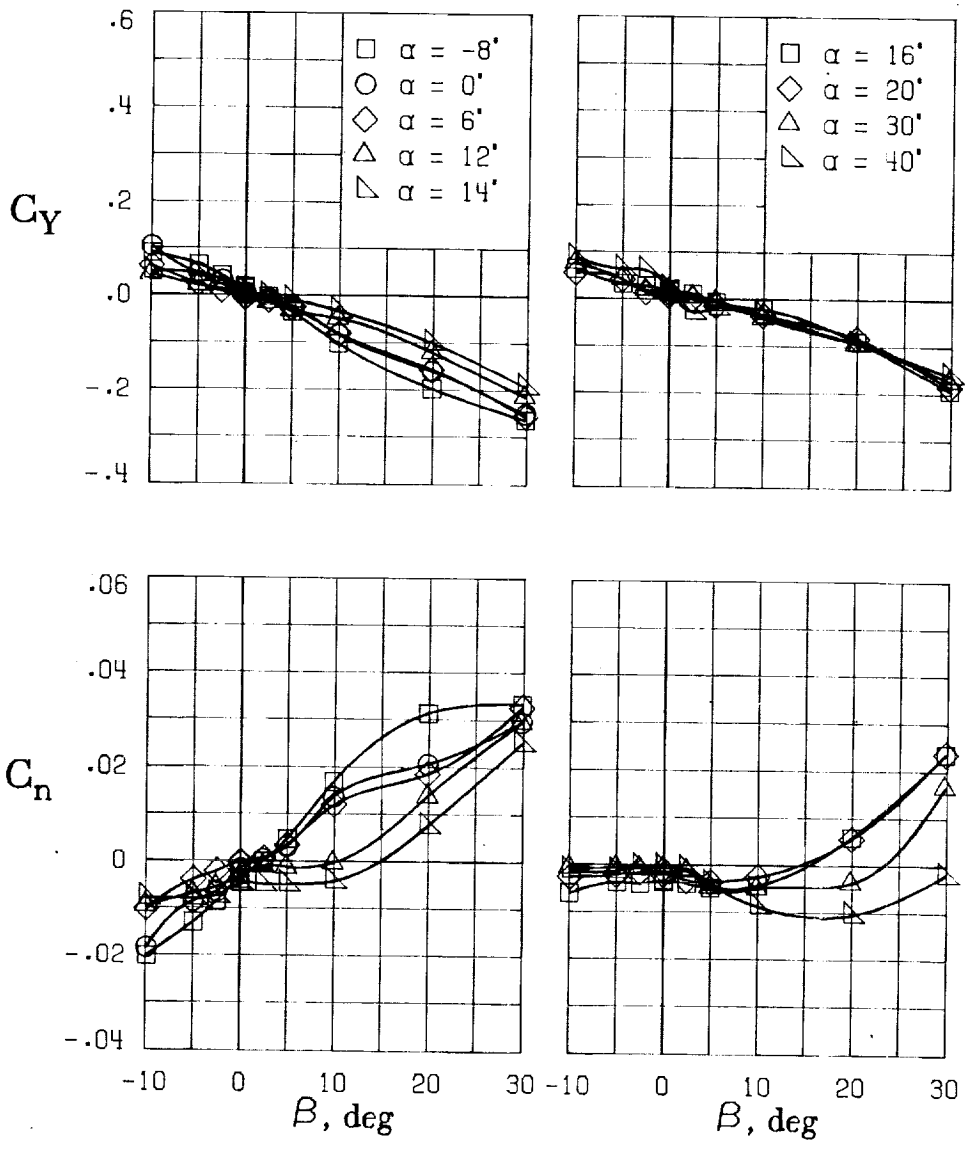

(E) DIRECTIONAL - STABILITY CHARACTERISTICS ABOUT BODY AXES AT VARIOUS ANGLES OF ATTACK.

FIGURE 72. - CONTINUED.

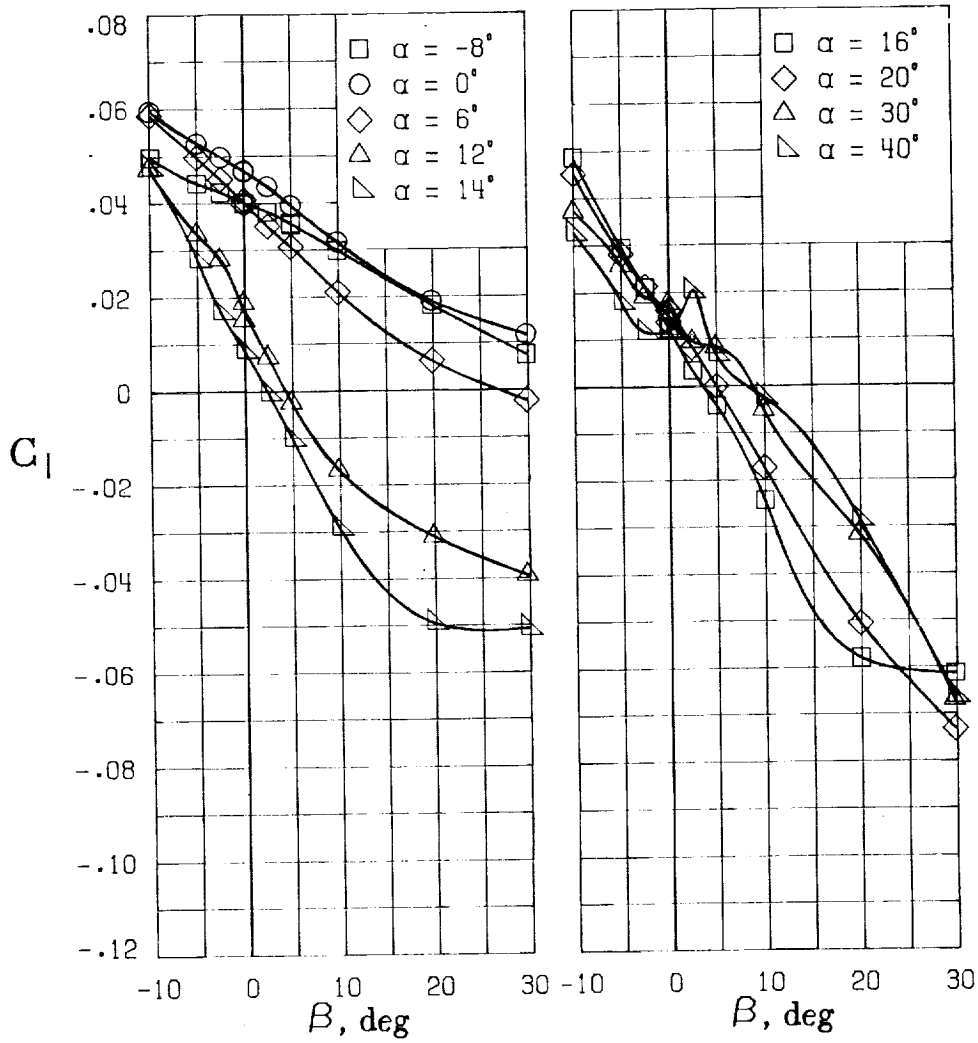

(F) LATERAL - STABILITY CHARACTERISTICS ABOUT BODY AXES AT VARIOUS ANGLES OF ATTACK.

FIGURE 72. - CONCLUDED.

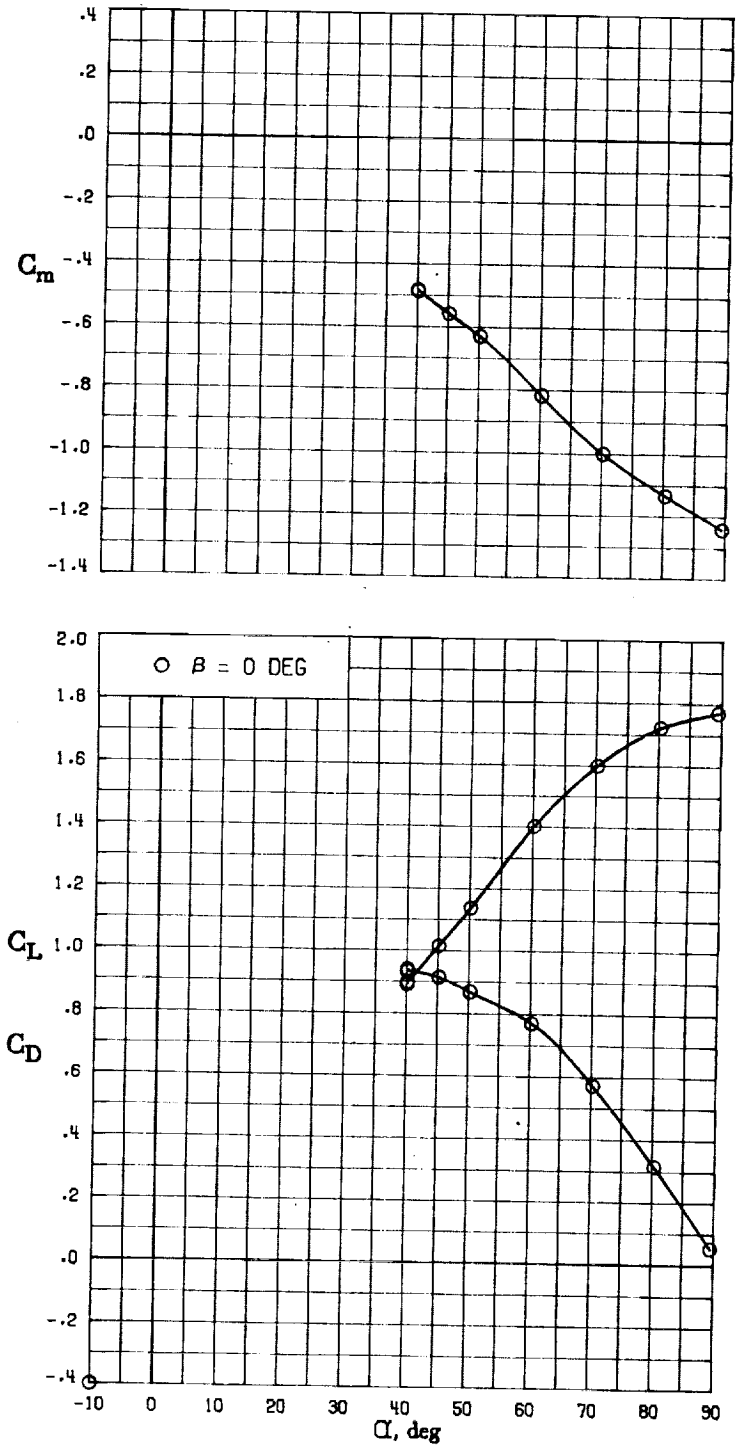

(A) LONGITUDINAL FORCE AND MOMENT COEFFICIENTS ABOUT STABILITY AXES.

FIGURE 73. - EFFECT OF ANGLE OF ATTACK AND SIDESLIP ANGLE ON AERODYNAMIC CHARACTERISTICS AT RE = .288 E+06 FOR CONFIGURATION B W1 H3 V. δ_E = 0°, δ_A = 0°, δ_R = -25°.

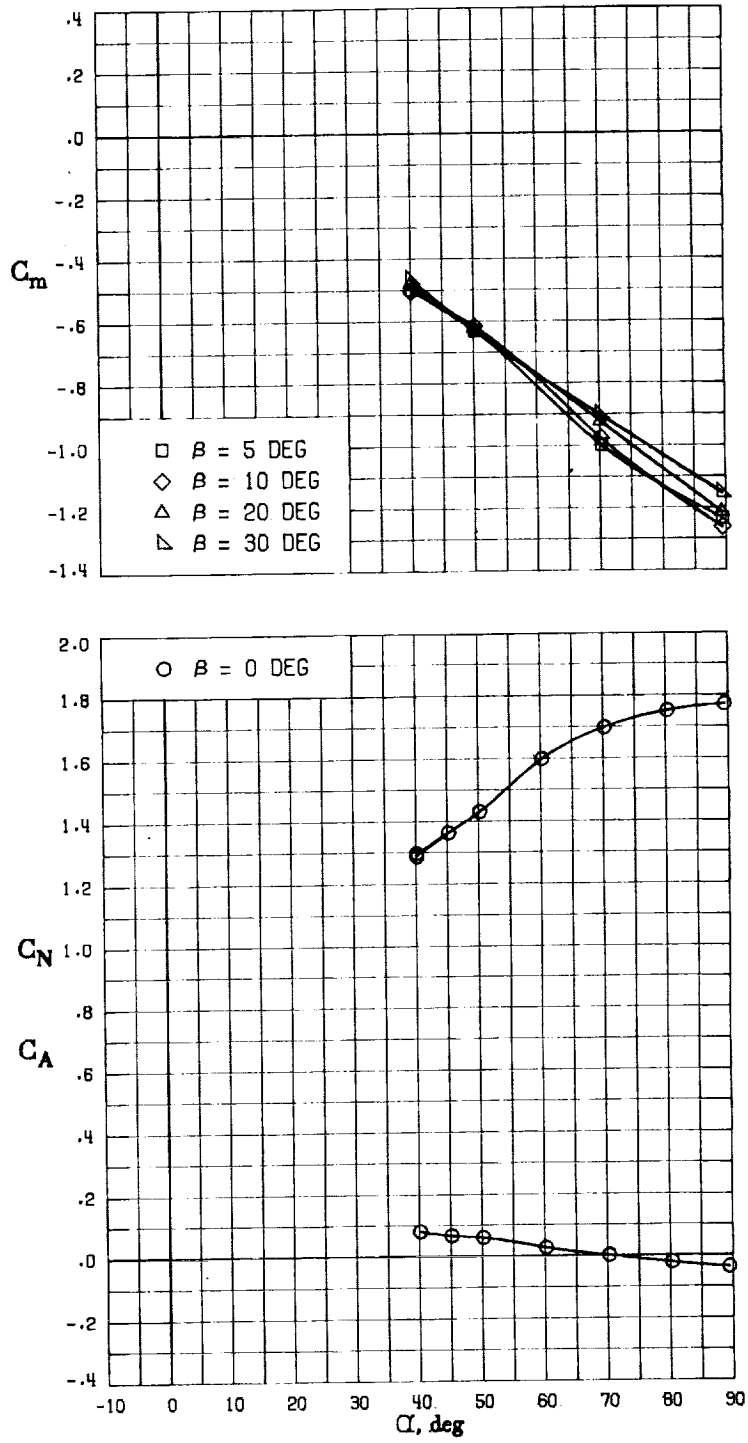

(B) LONGITUDINAL FORCE AND MOMENT COEFFICIENTS ABOUT BODY AXES.

FIGURE 73. - CONTINUED.

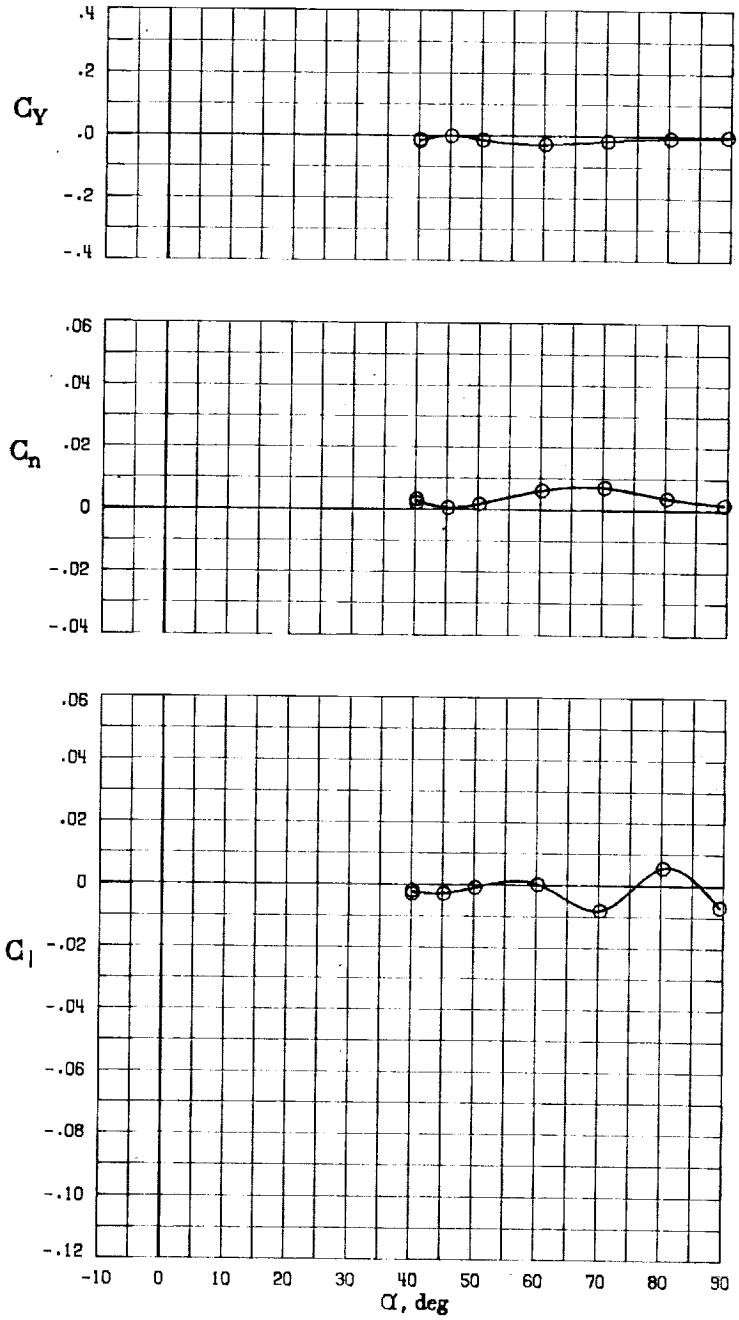

(C) LATERAL - DIRECTIONAL FORCE AND MOMENT COEFFICIENTS ABOUT BODY AXES AT ZERO SIDESLIP.

FIGURE 73. - CONTINUED.

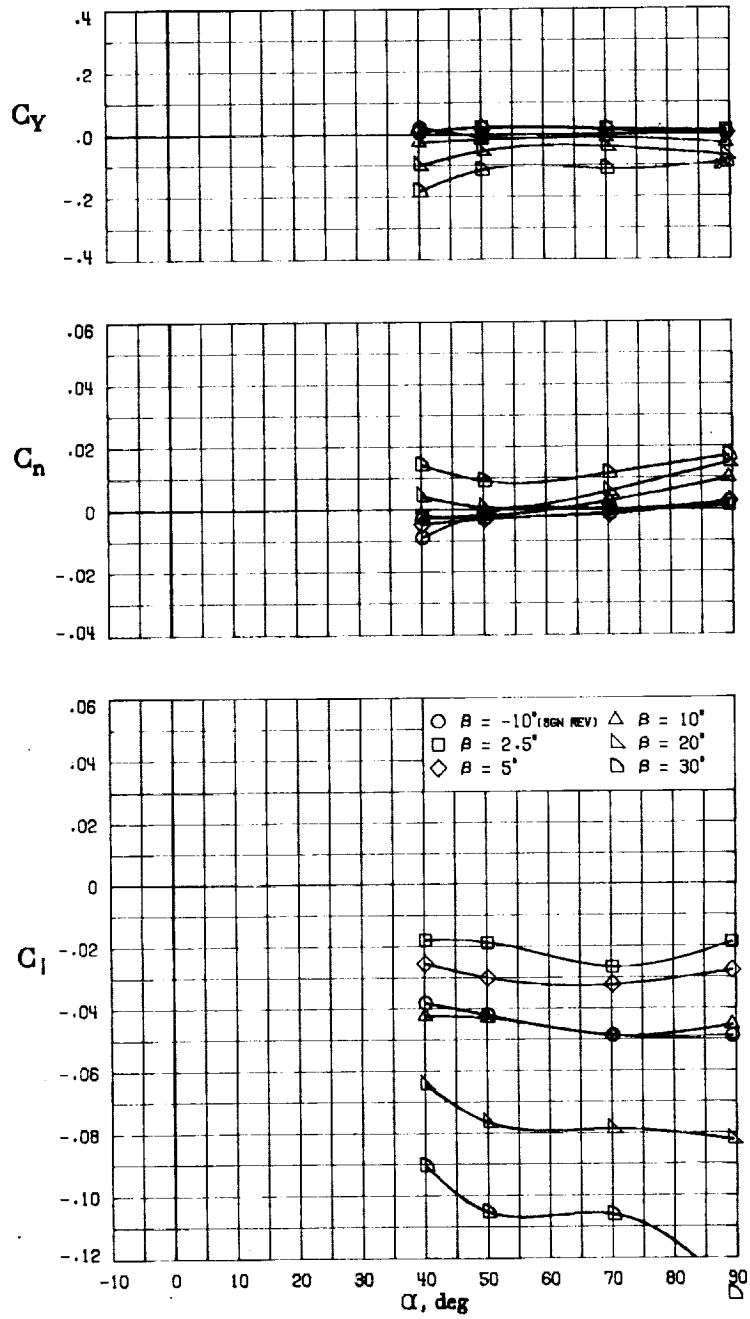

(D) LATERAL - DIRECTIONAL FORCE AND MOMENT COEFFICIENTS ABOUT BODY AXES.

FIGURE 73. - CONTINUED.

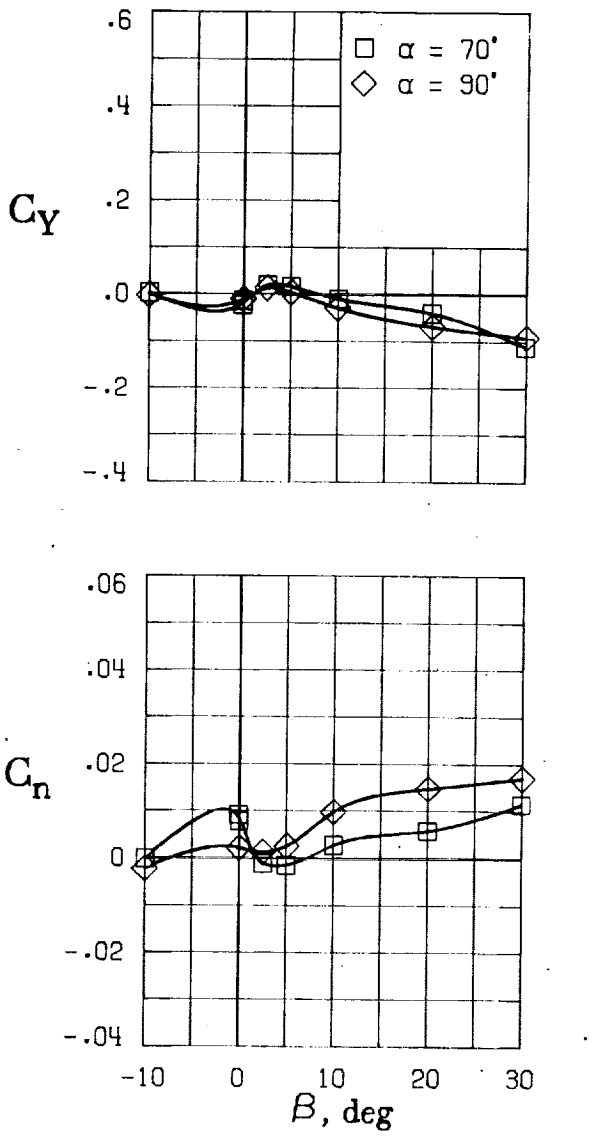

(E) DIRECTIONAL - STABILITY CHARACTERISTICS ABOUT BODY AXES AT VARIOUS ANGLES OF ATTACK.

FIGURE 73. - CONTINUED.

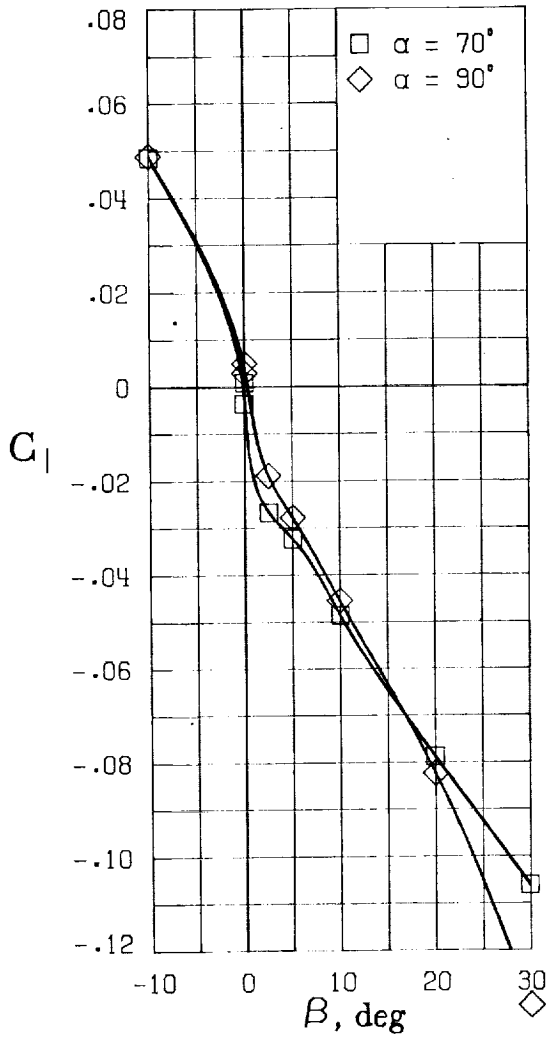

(F) LATERAL - STABILITY CHARACTERISTICS ABOUT BODY AXES AT VARIOUS ANGLES OF ATTACK.

FIGURE 73. - CONCLUDED.

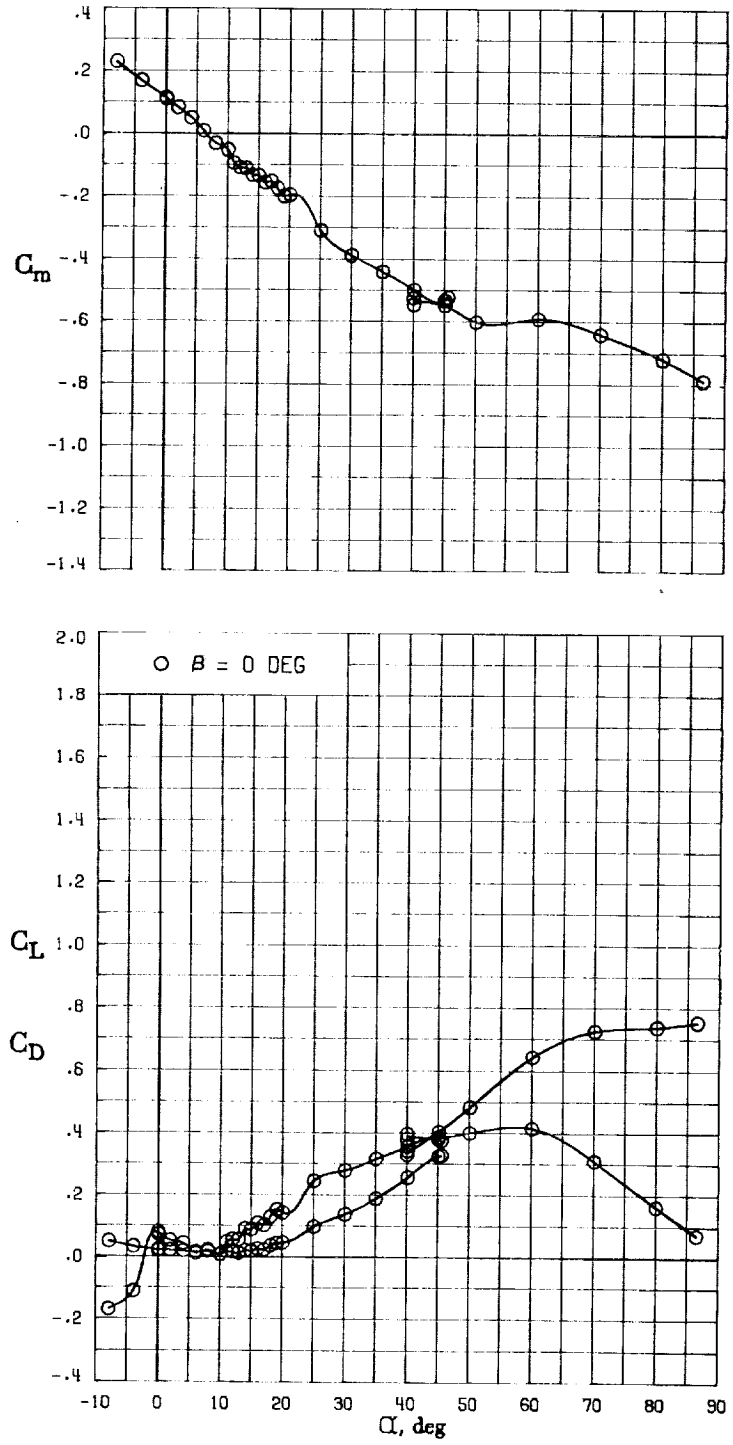

(A) LONGITUDINAL FORCE AND MOMENT COEFFICIENTS ABOUT STABILITY AXES.

FIGURE 74. - EFFECT OF ANGLE OF ATTACK AND SIDESLIP ANGLE ON AERODYNAMIC CHARACTERISTICS AT RE = .288 E+06 FOR CONFIGURATION B H3 V. δ_E = 0°, δ_A = 0°, δ_R = 0°.

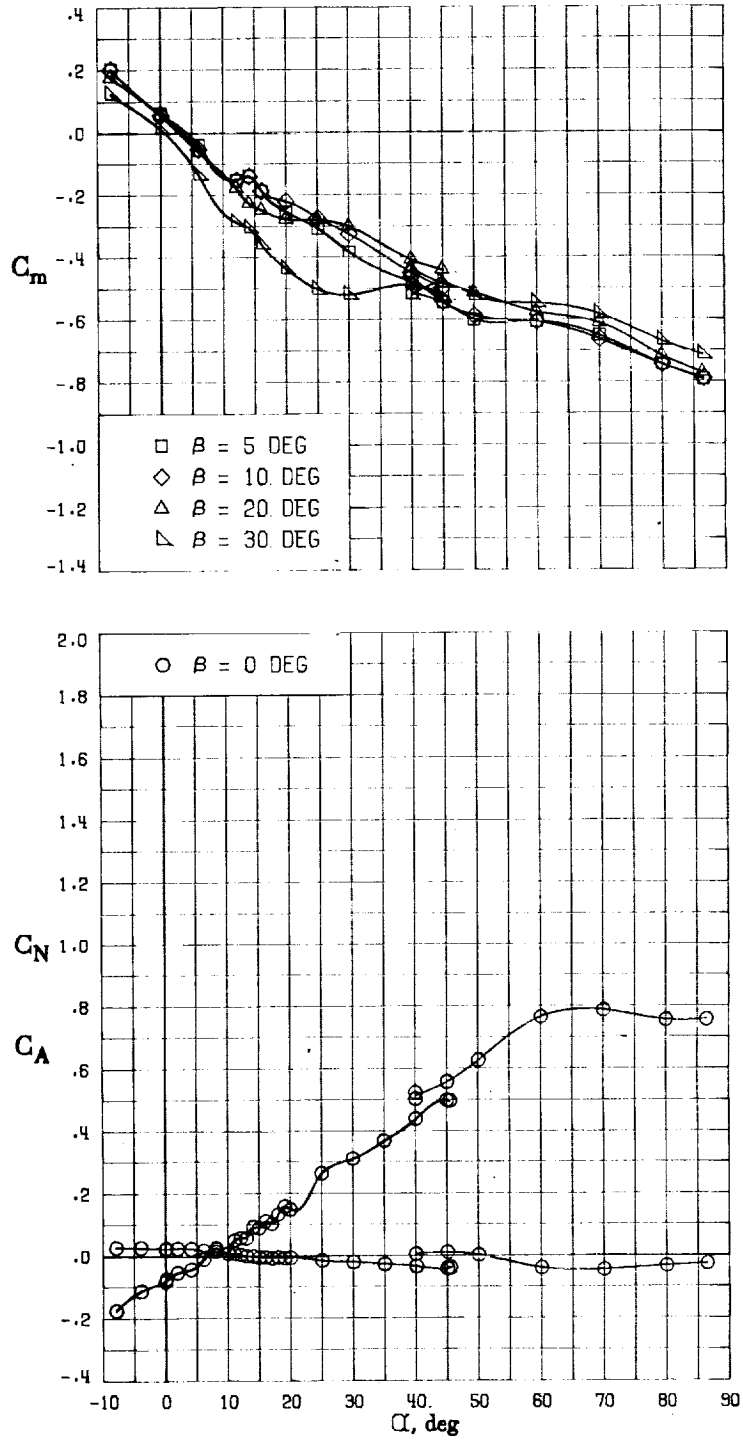

(B) LONGITUDINAL FORCE AND MOMENT COEFFICIENTS ABOUT BODY AXES.

FIGURE 74. - CONTINUED.

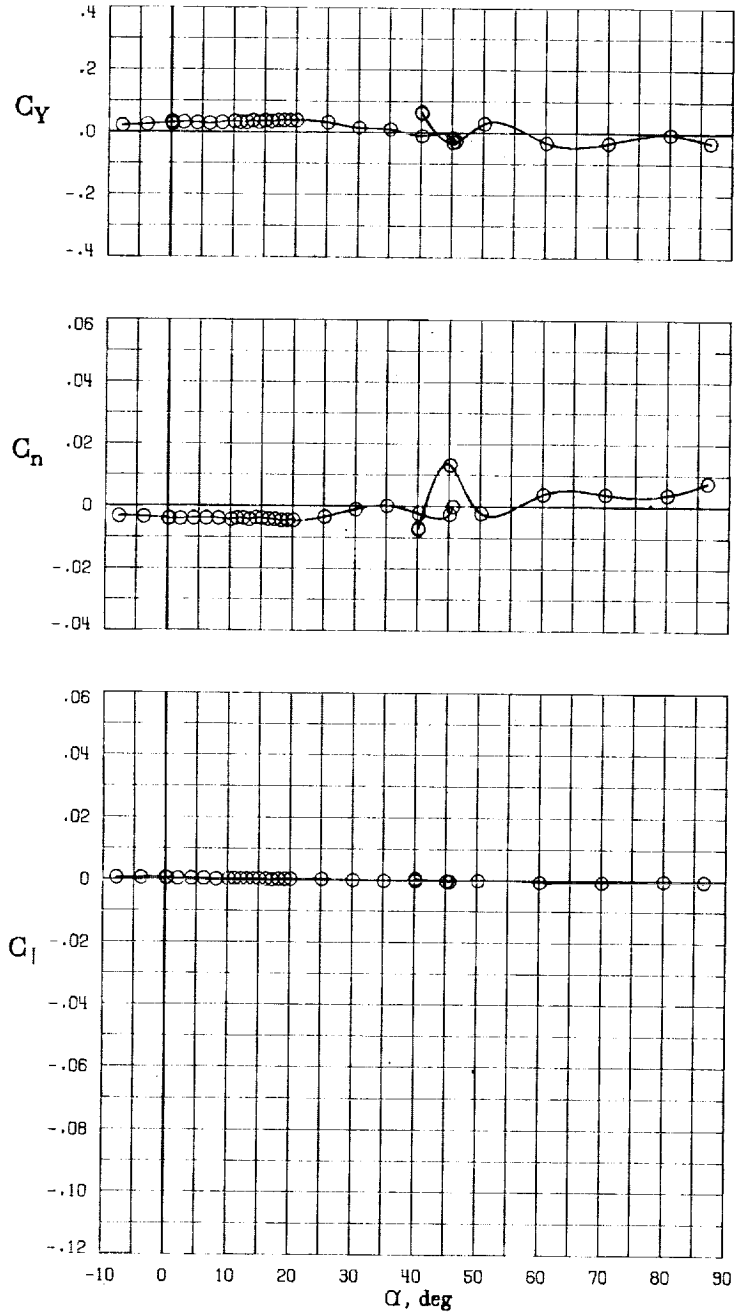

(C) LATERAL - DIRECTIONAL FORCE AND MOMENT COEFFICIENTS ABOUT BODY AXES AT ZERO SIDESLIP.

FIGURE 74. - CONTINUED.

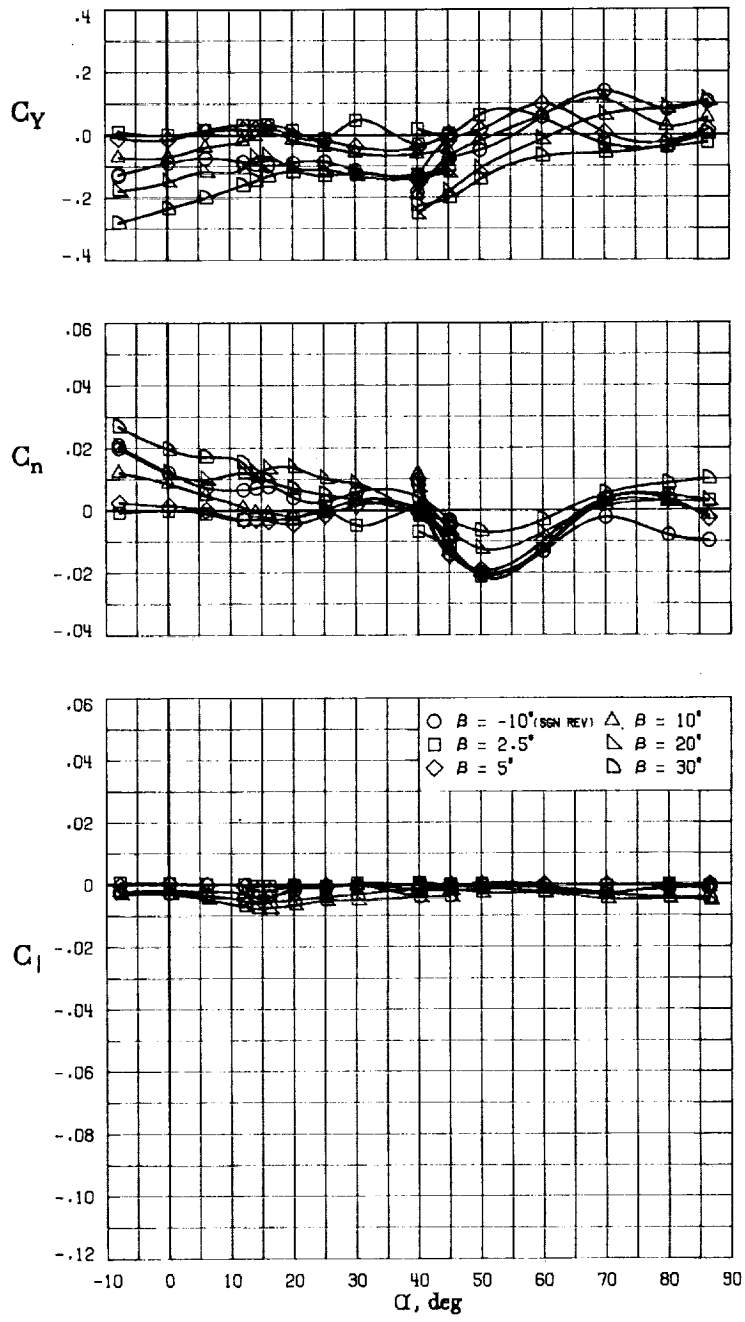

(D) LATERAL - DIRECTIONAL FORCE AND MOMENT COEFFICIENTS ABOUT BODY AXES.

FIGURE 74. - CONTINUED.

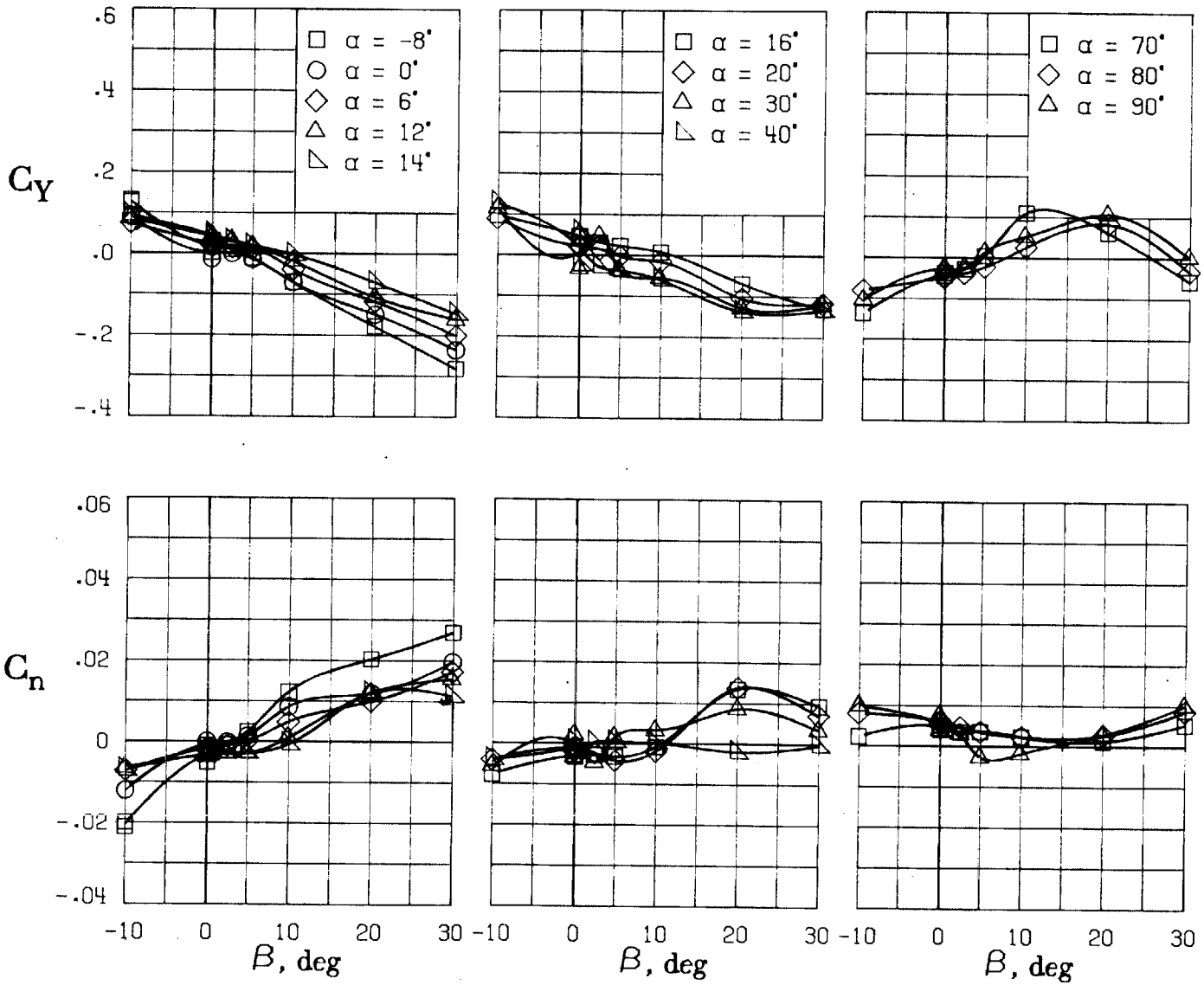

(E) DIRECTIONAL - STABILITY CHARACTERISTICS ABOUT BODY AXES AT VARIOUS ANGLES OF ATTACK.

FIGURE 74. - CONTINUED.

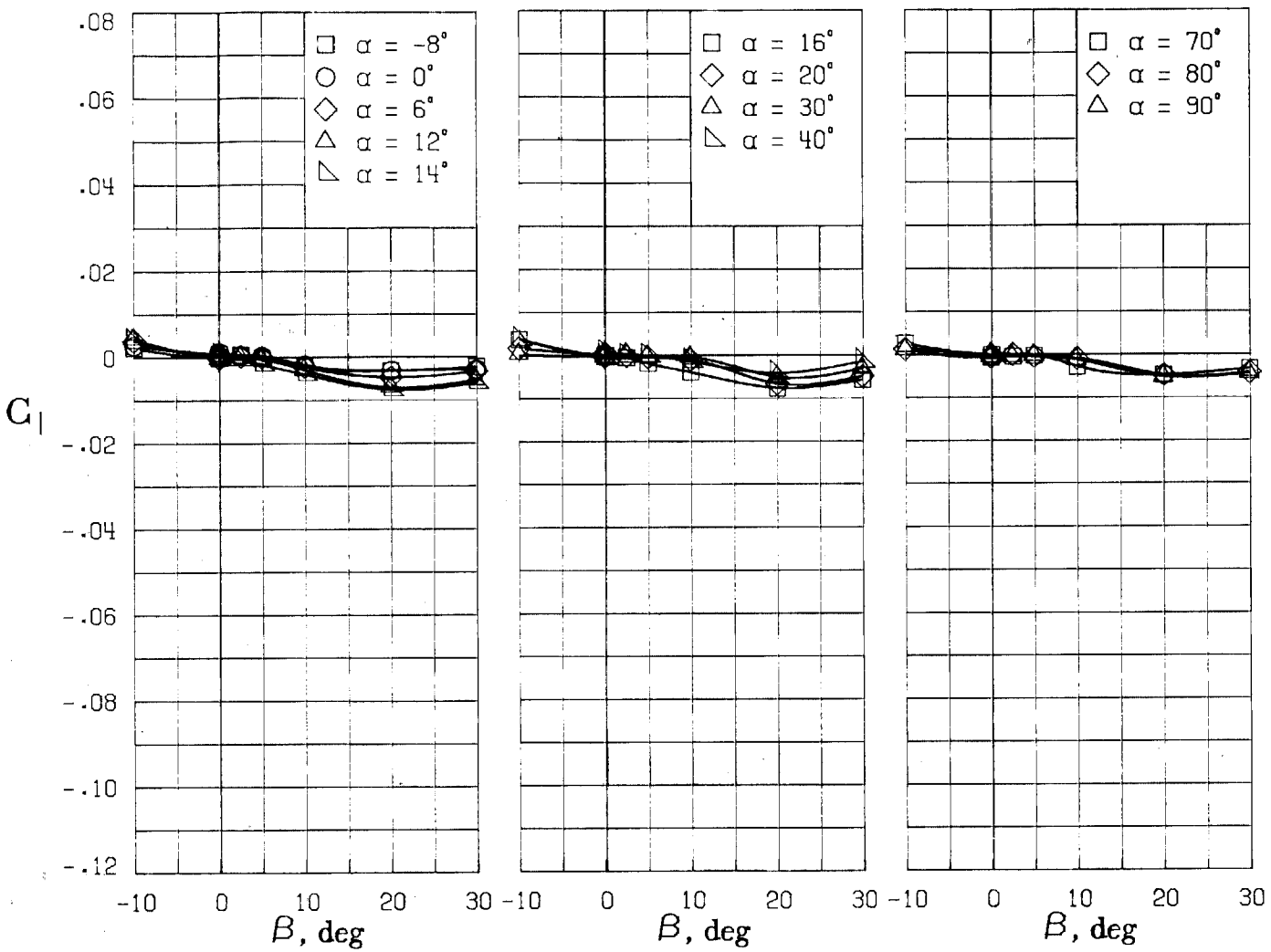

(F) LATERAL - STABILITY CHARACTERISTICS ABOUT BODY AXES AT VARIOUS ANGLES OF ATTACK.

FIGURE 74. - CONCLUDED.

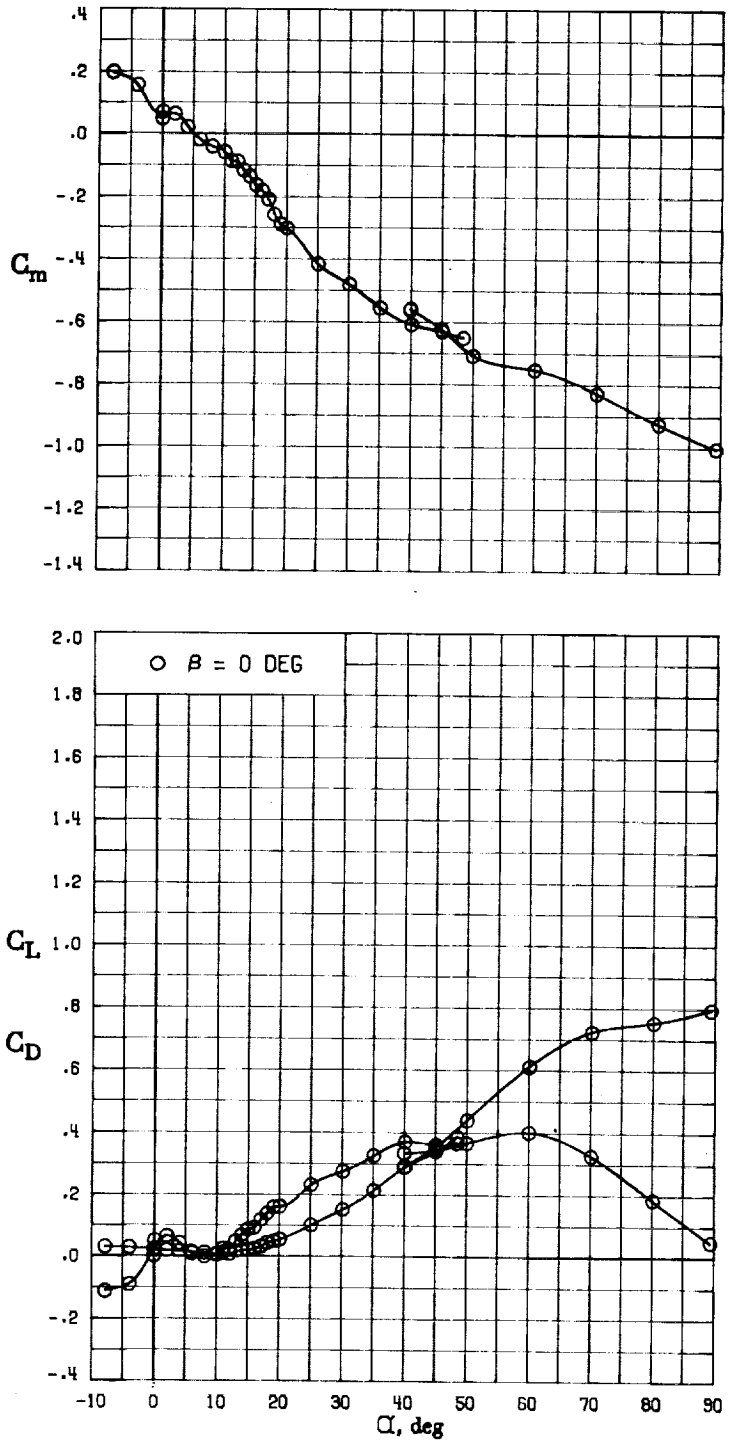

(A) LONGITUDINAL FORCE AND MOMENT COEFFICIENTS ABOUT STABILITY AXES.

FIGURE 75. - EFFECT OF ANGLE OF ATTACK AND SIDESLIP ANGLE ON AERODYNAMIC CHARACTERISTICS AT RE = .288 E+06 FOR CONFIGURATION B H4 V. $\delta_E = 0°$, $\delta_A = 0°$, $\delta_R = 0°$.

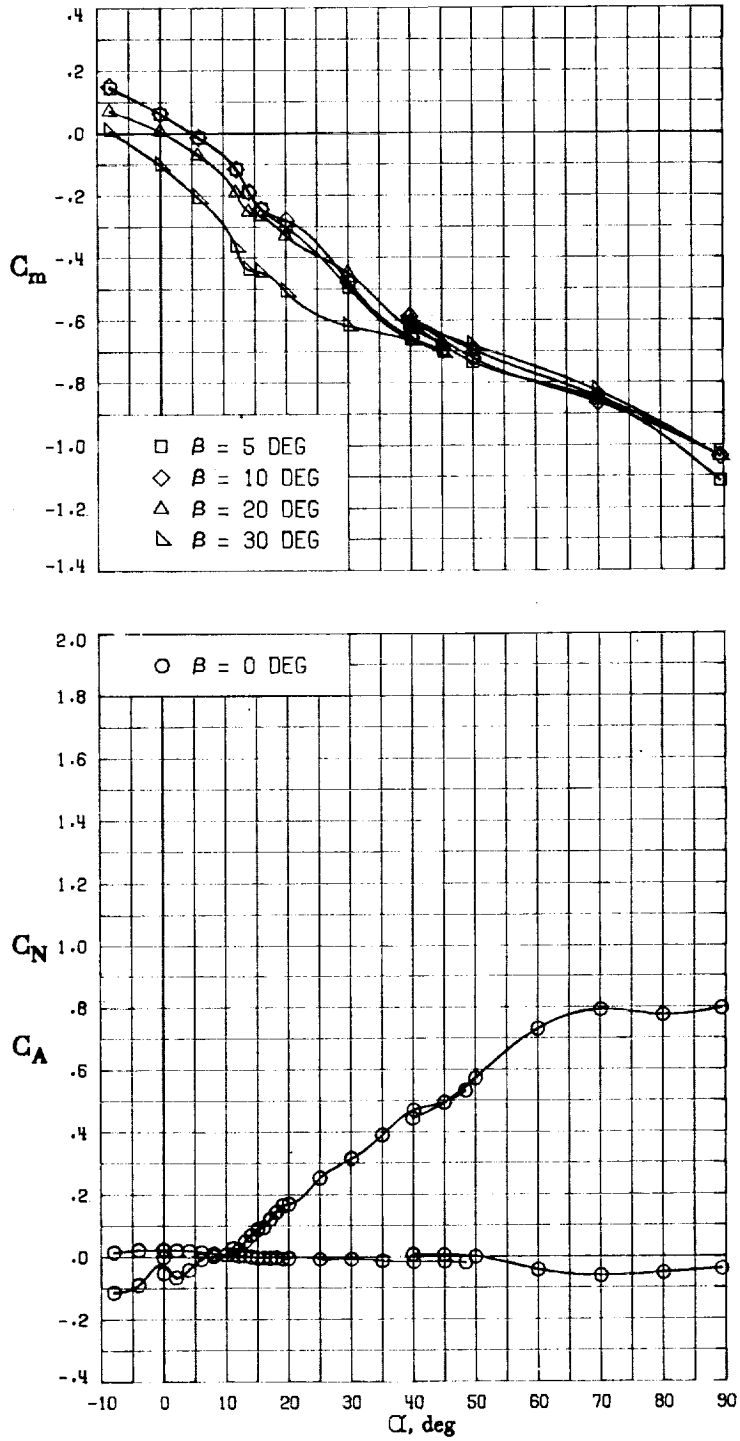

(B) LONGITUDINAL FORCE AND MOMENT COEFFICIENTS ABOUT BODY AXES.

FIGURE 75. - CONTINUED.

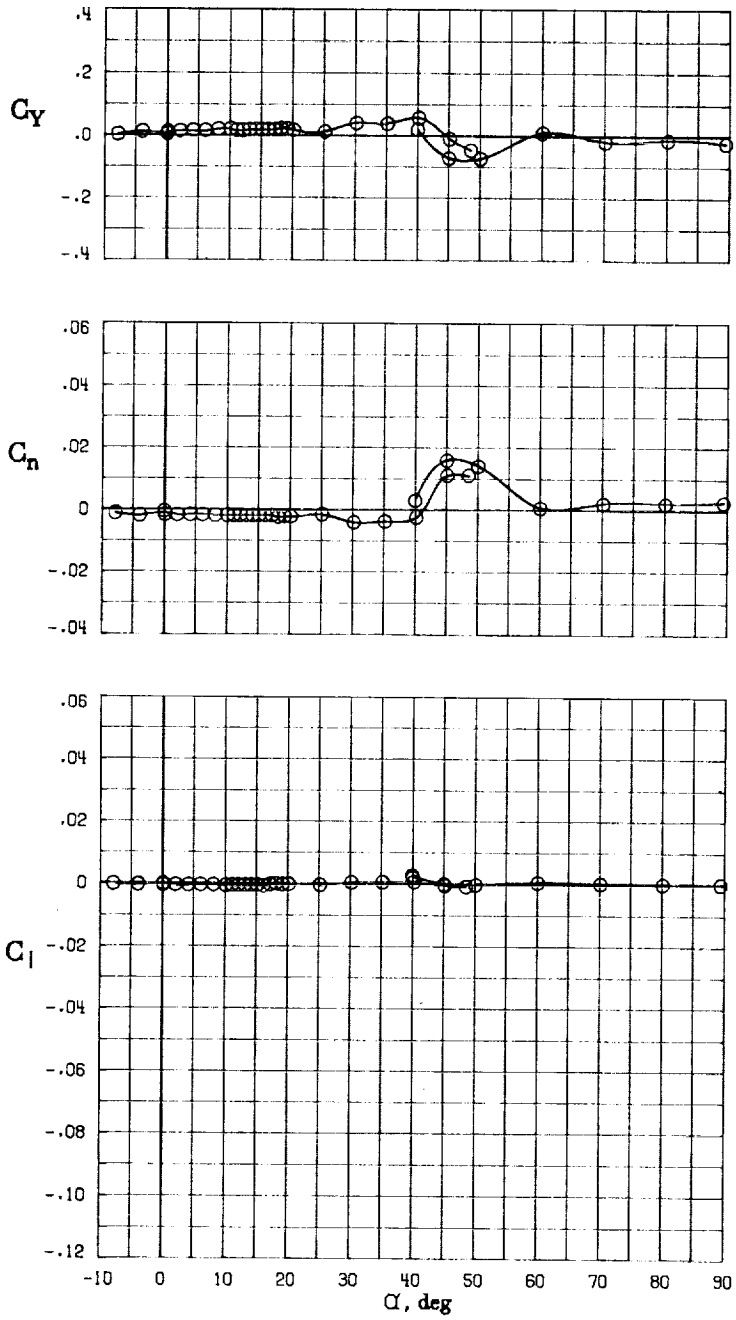

(C) LATERAL - DIRECTIONAL FORCE AND MOMENT COEFFICIENTS ABOUT BODY AXES AT ZERO SIDESLIP.

FIGURE 75. - CONTINUED.

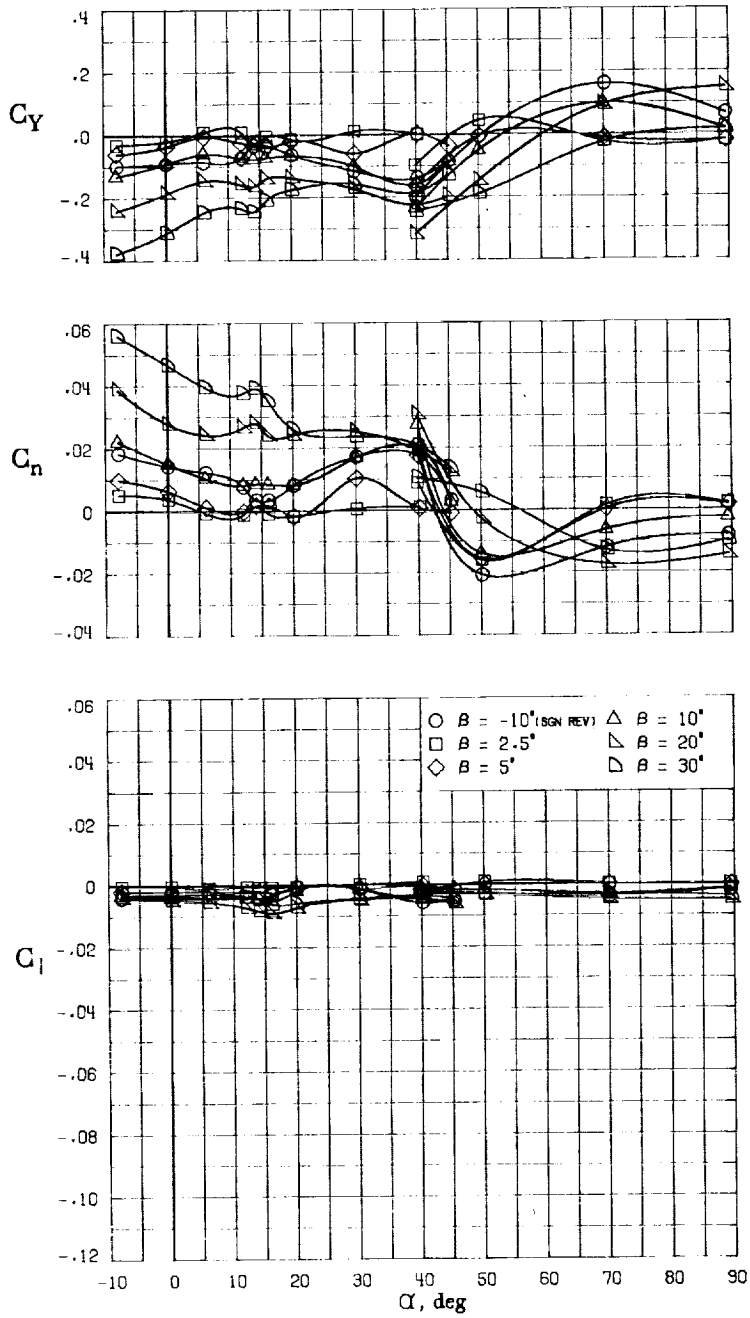

(D) LATERAL - DIRECTIONAL FORCE AND MOMENT COEFFICIENTS ABOUT BODY AXES.

FIGURE 75. - CONTINUED.

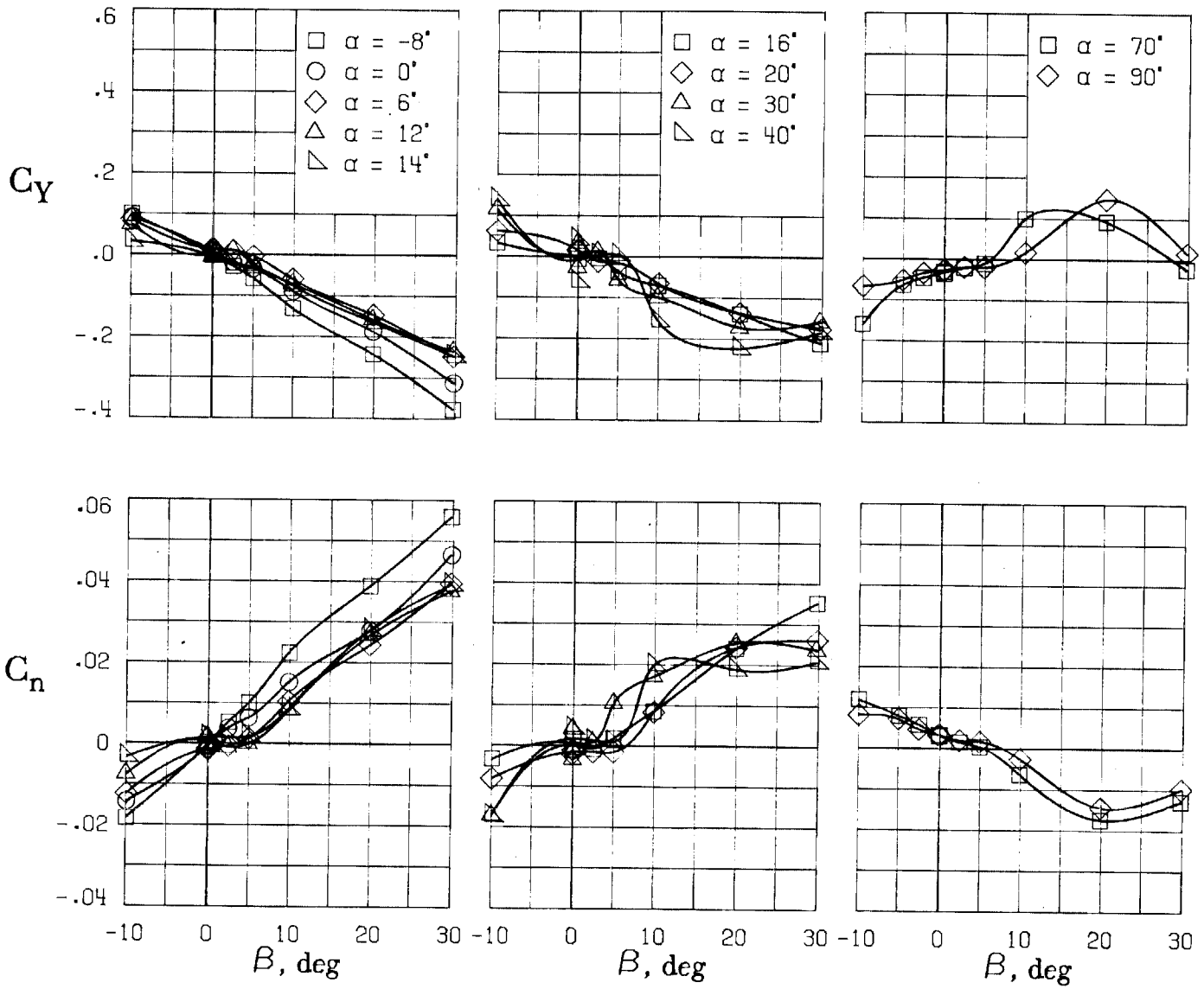

(E) DIRECTIONAL - STABILITY CHARACTERISTICS ABOUT BODY AXES AT VARIOUS ANGLES OF ATTACK.

FIGURE 75. - CONTINUED.

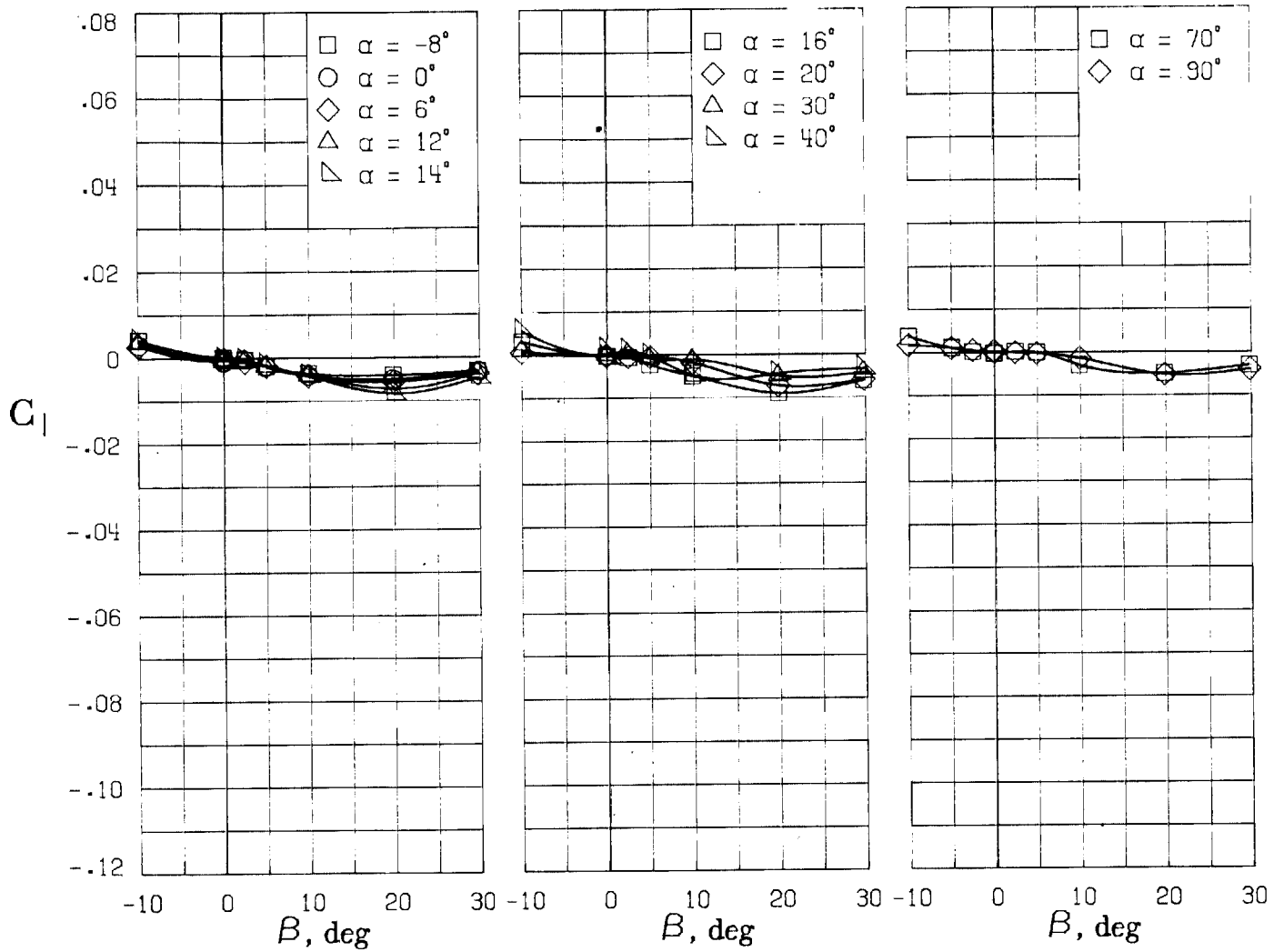

(F) LATERAL - STABILITY CHARACTERISTICS ABOUT BODY AXES AT VARIOUS ANGLES OF ATTACK.

FIGURE 75. - CONCLUDED.

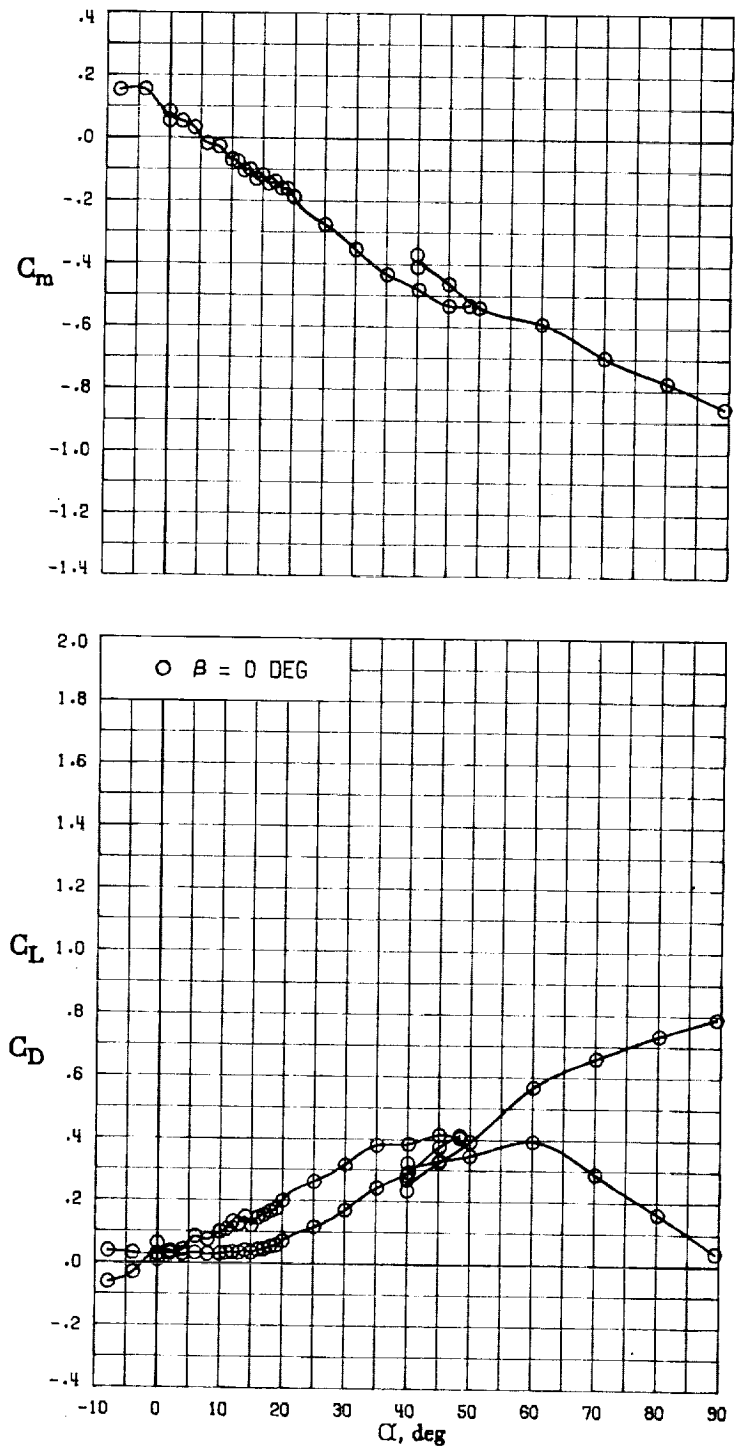

(A) LONGITUDINAL FORCE AND MOMENT COEFFICIENTS ABOUT STABILITY AXES.

FIGURE 76. - EFFECT OF ANGLE OF ATTACK AND SIDESLIP ANGLE ON AERODYNAMIC CHARACTERISTICS AT RE = .288 E+06 FOR CONFIGURATION B H6 V. $\delta_E = 0°$, $\delta_A = 0°$, $\delta_R = 0°$.

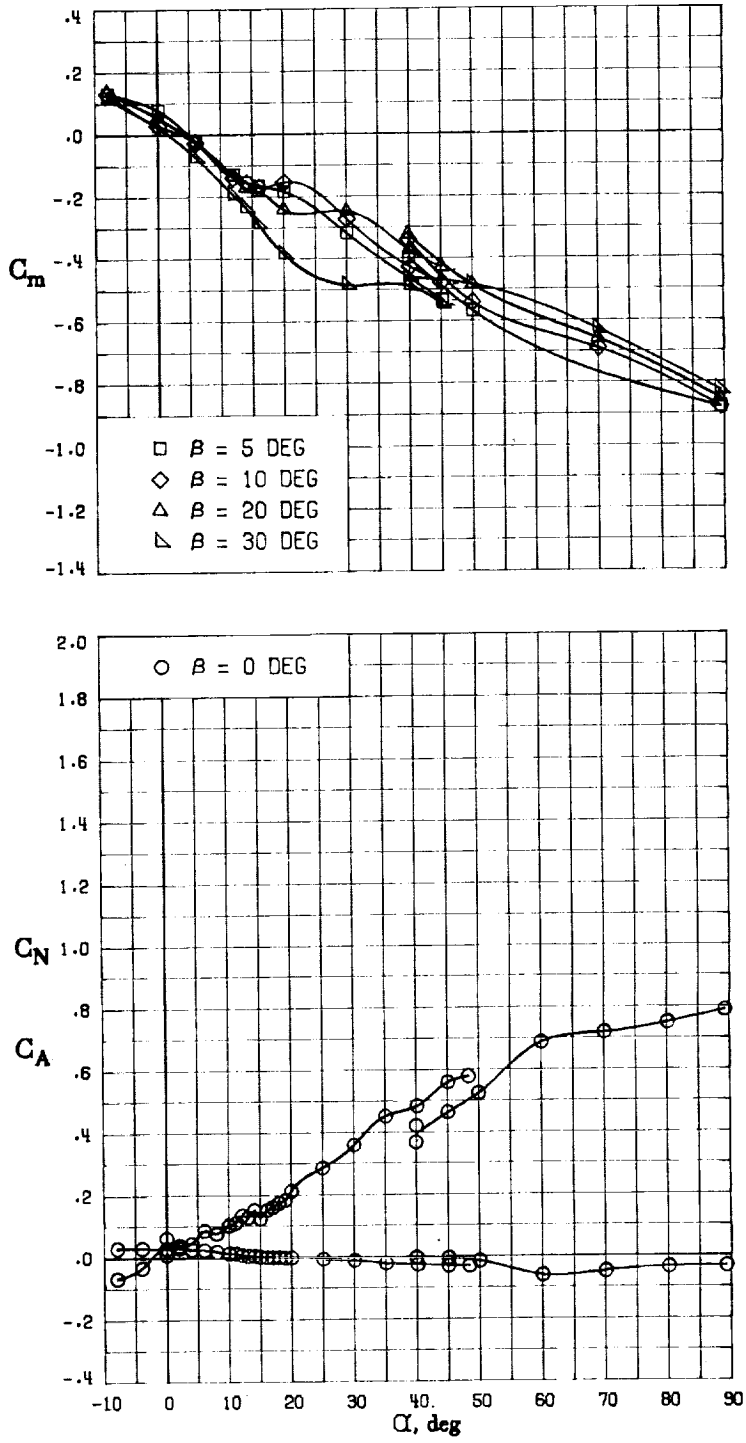

(B) LONGITUDINAL FORCE AND MOMENT COEFFICIENTS ABOUT BODY AXES.

FIGURE 76. - CONTINUED.

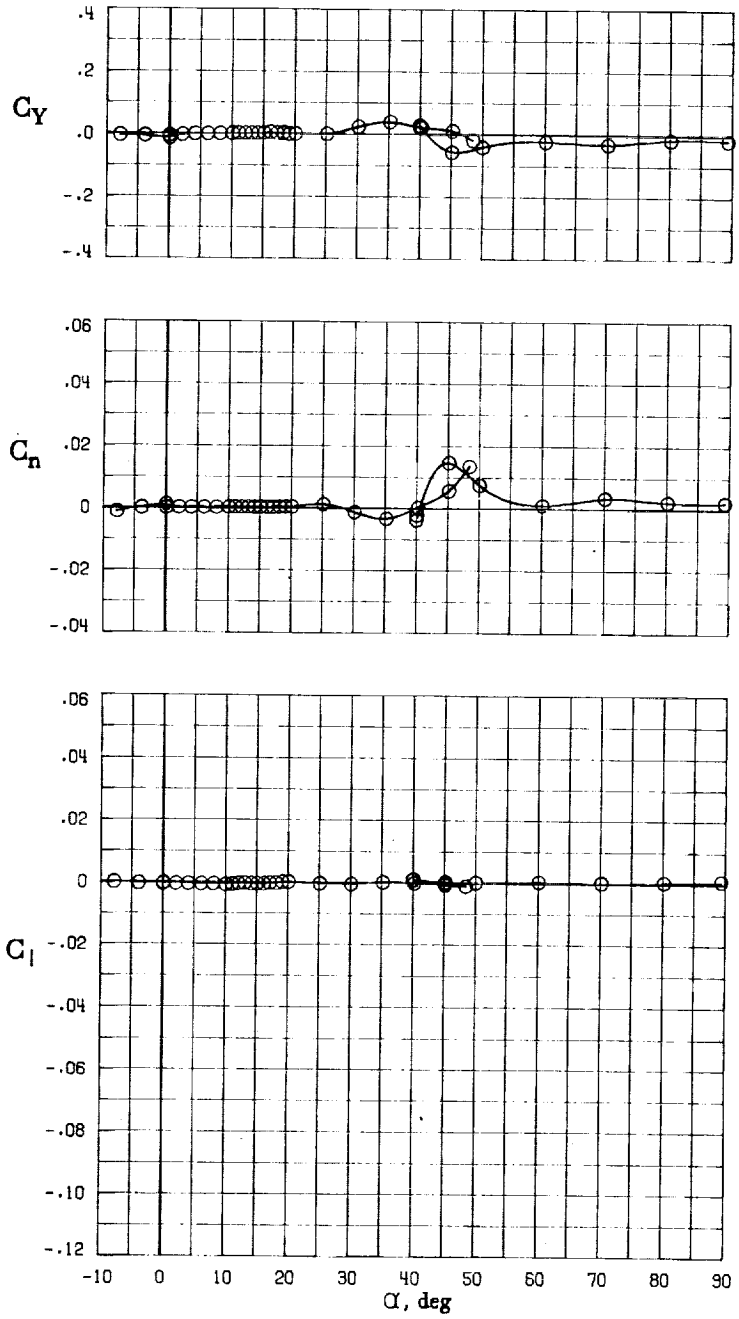

(C) LATERAL - DIRECTIONAL FORCE AND MOMENT COEFFICIENTS ABOUT BODY AXES AT ZERO SIDESLIP.

FIGURE 76. - CONTINUED.

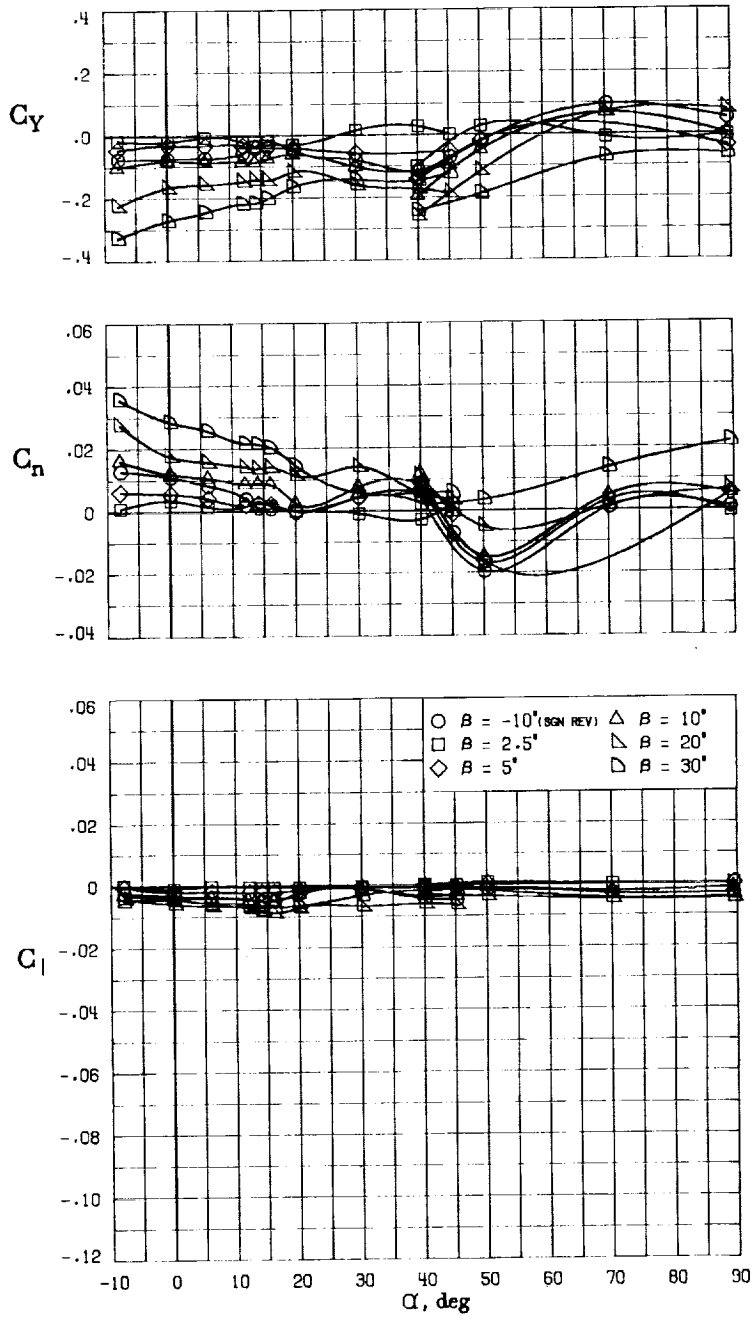

(D) LATERAL - DIRECTIONAL FORCE AND MOMENT COEFFICIENTS ABOUT BODY AXES.

FIGURE 76. - CONTINUED.

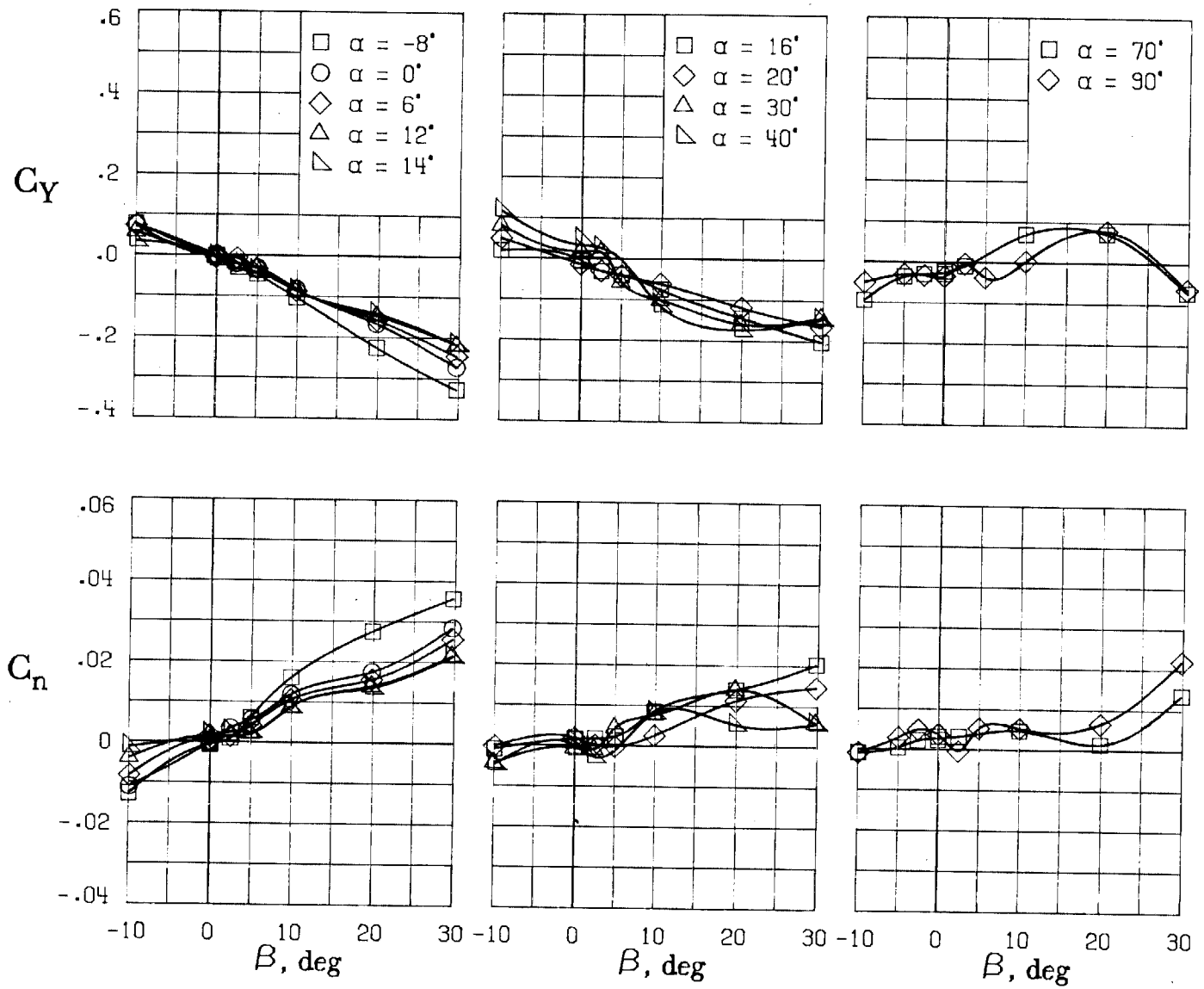

(E) DIRECTIONAL - STABILITY CHARACTERISTICS ABOUT BODY AXES AT VARIOUS ANGLES OF ATTACK.

FIGURE 76. - CONTINUED.

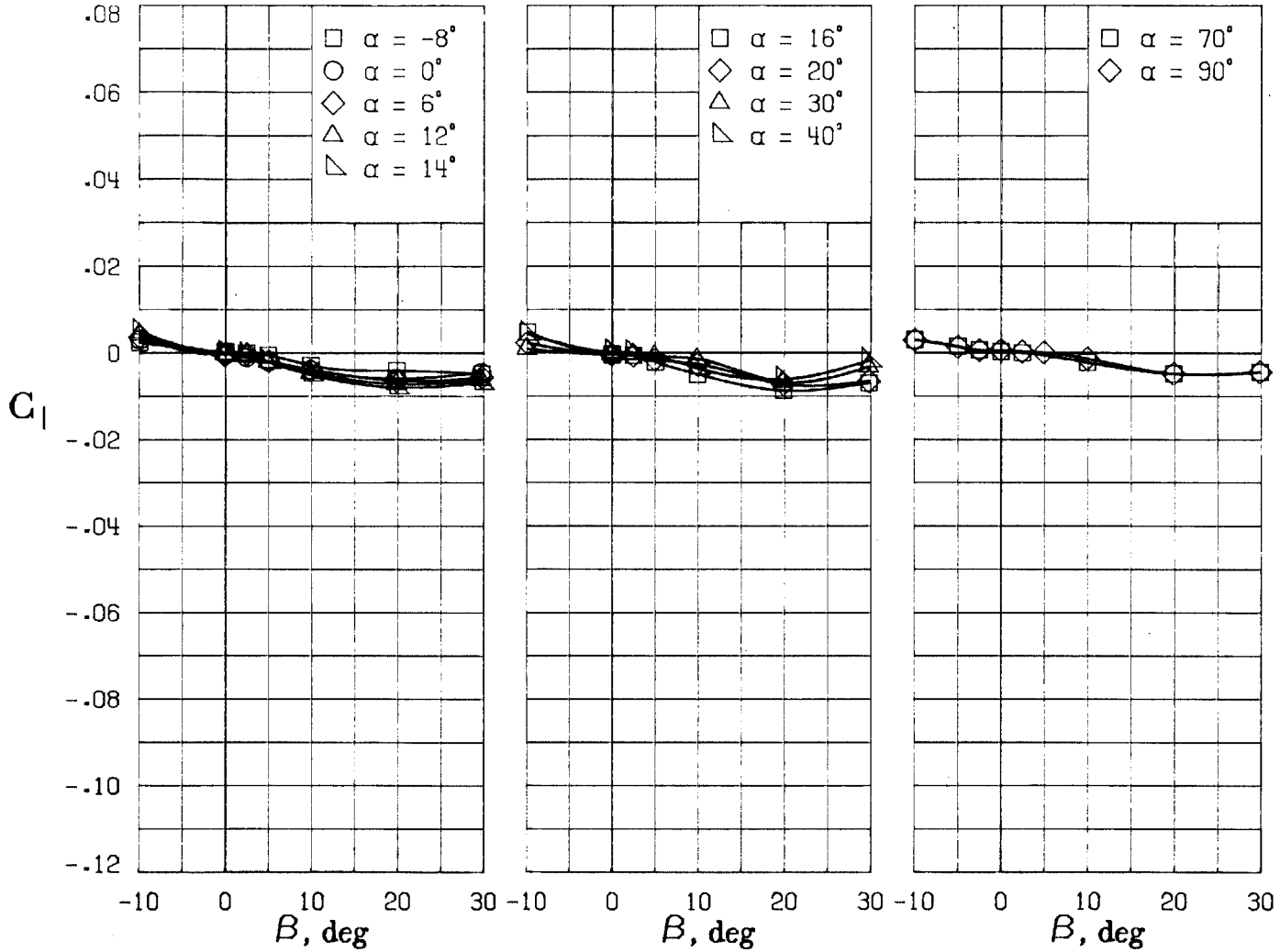

(F) LATERAL - STABILITY CHARACTERISTICS ABOUT BODY AXES AT VARIOUS ANGLES OF ATTACK.

FIGURE 76. - CONCLUDED.

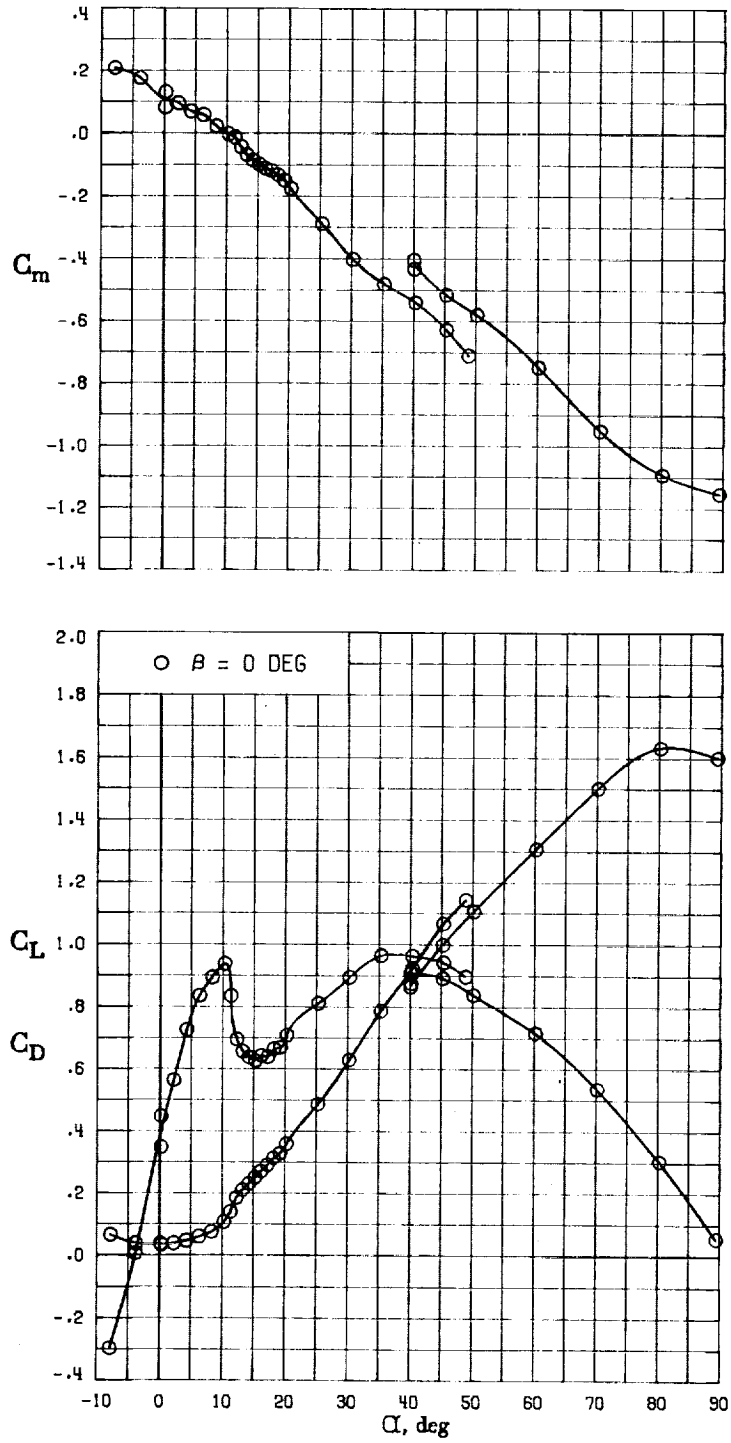

(A) LONGITUDINAL FORCE AND MOMENT COEFFICIENTS ABOUT STABILITY AXES.

FIGURE 77. - EFFECT OF ANGLE OF ATTACK AND SIDESLIP ANGLE ON AERODYNAMIC CHARACTERISTICS AT RE = .288 E+06 FOR CONFIGURATION B W1 H3. $\delta_E = 0°$, $\delta_A = 0°$, $\delta_R = 0°$.

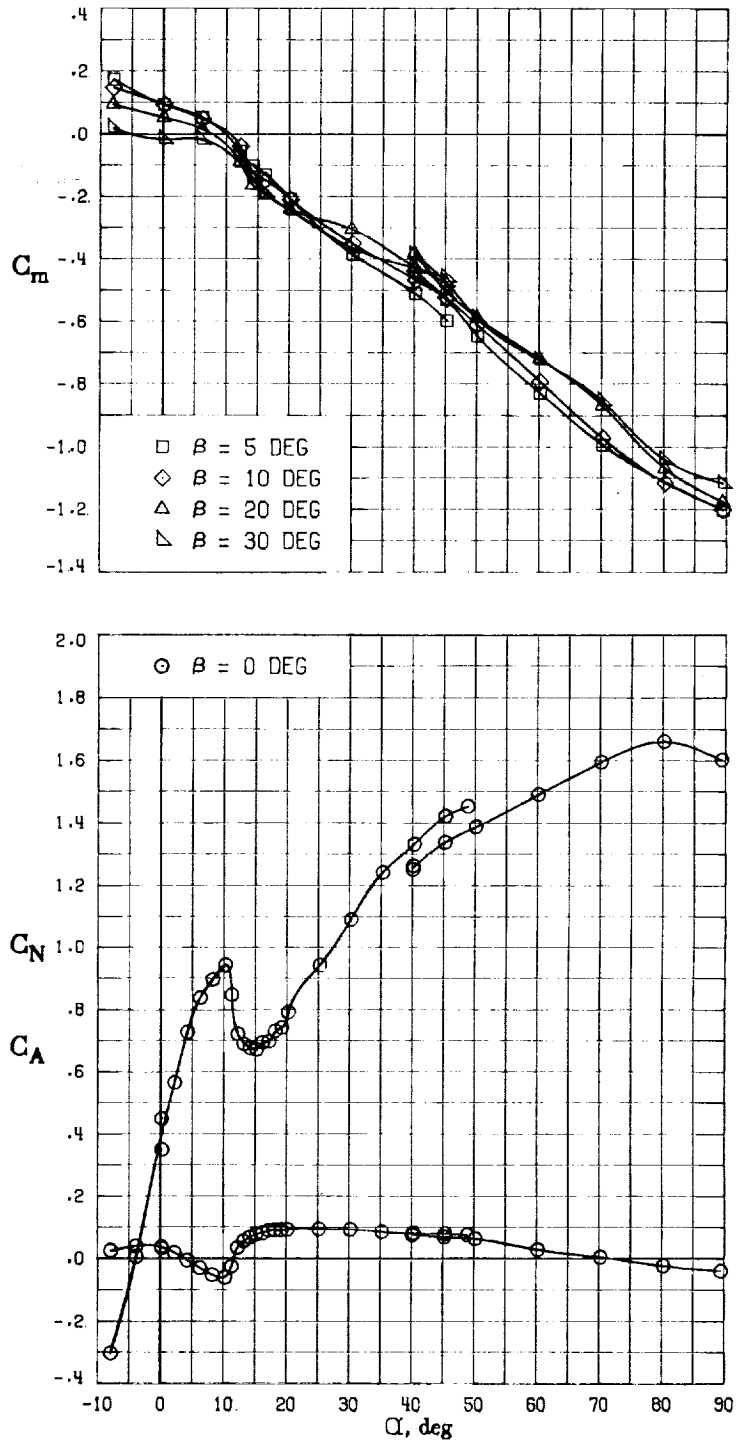

(B) LONGITUDINAL FORCE AND MOMENT COEFFICIENTS ABOUT BODY AXES.

FIGURE 77. - CONTINUED.

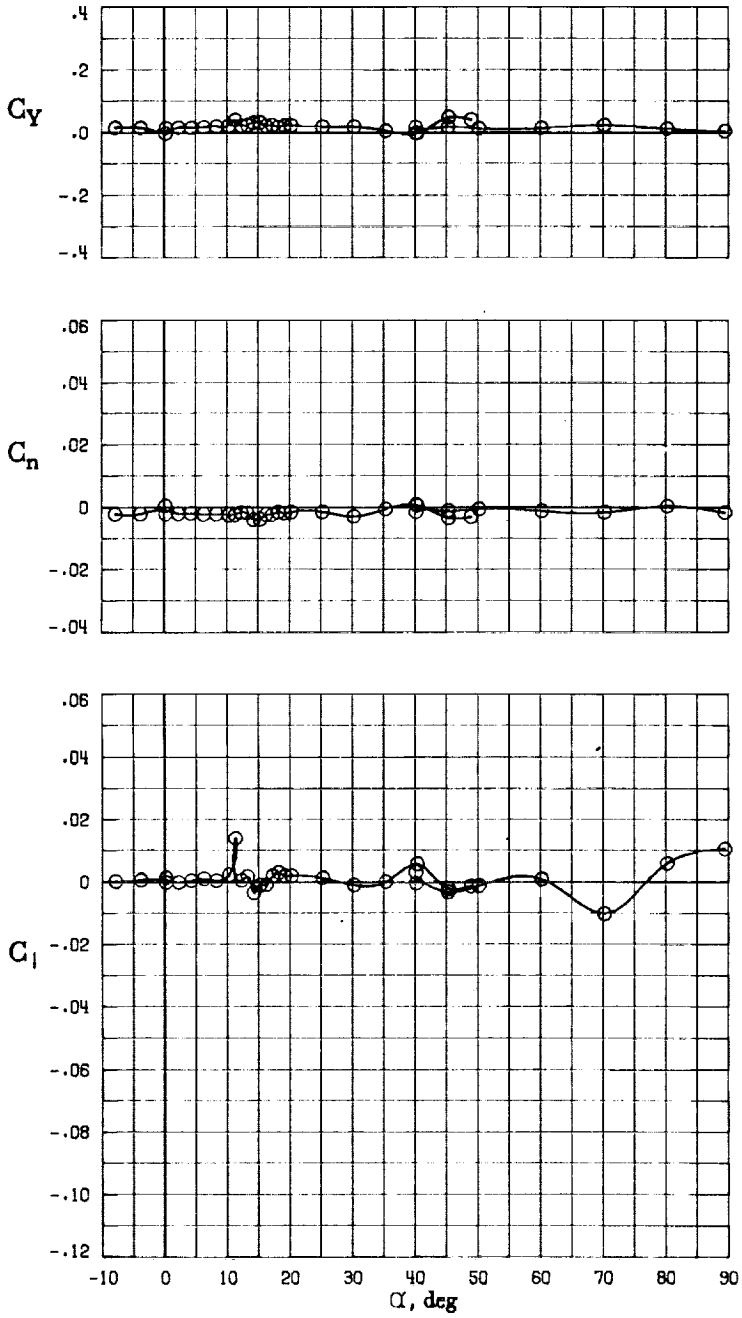

(C) LATERAL - DIRECTIONAL FORCE AND MOMENT COEFFICIENTS ABOUT BODY AXES AT ZERO SIDESLIP.

FIGURE 77. - CONTINUED.

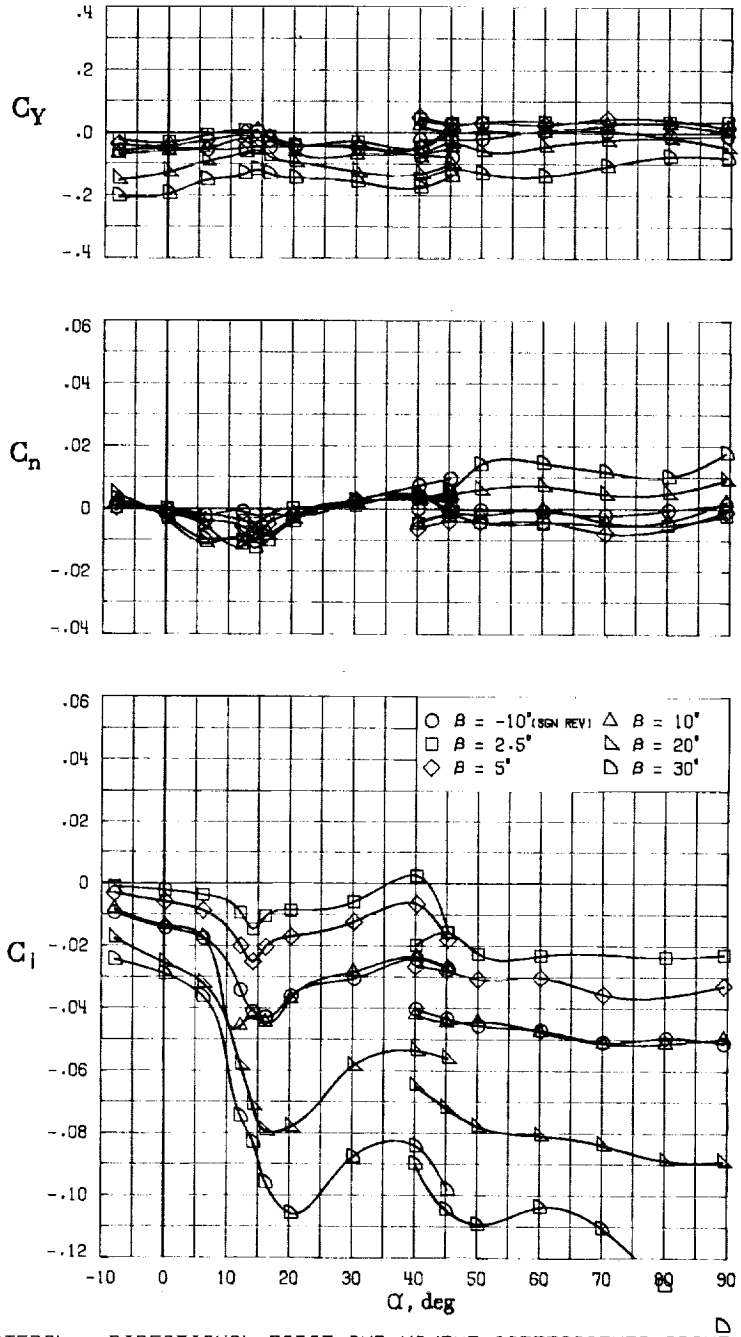

(D) LATERAL - DIRECTIONAL FORCE AND MOMENT COEFFICIENTS ABOUT BODY AXES.

FIGURE 77. - CONTINUED.

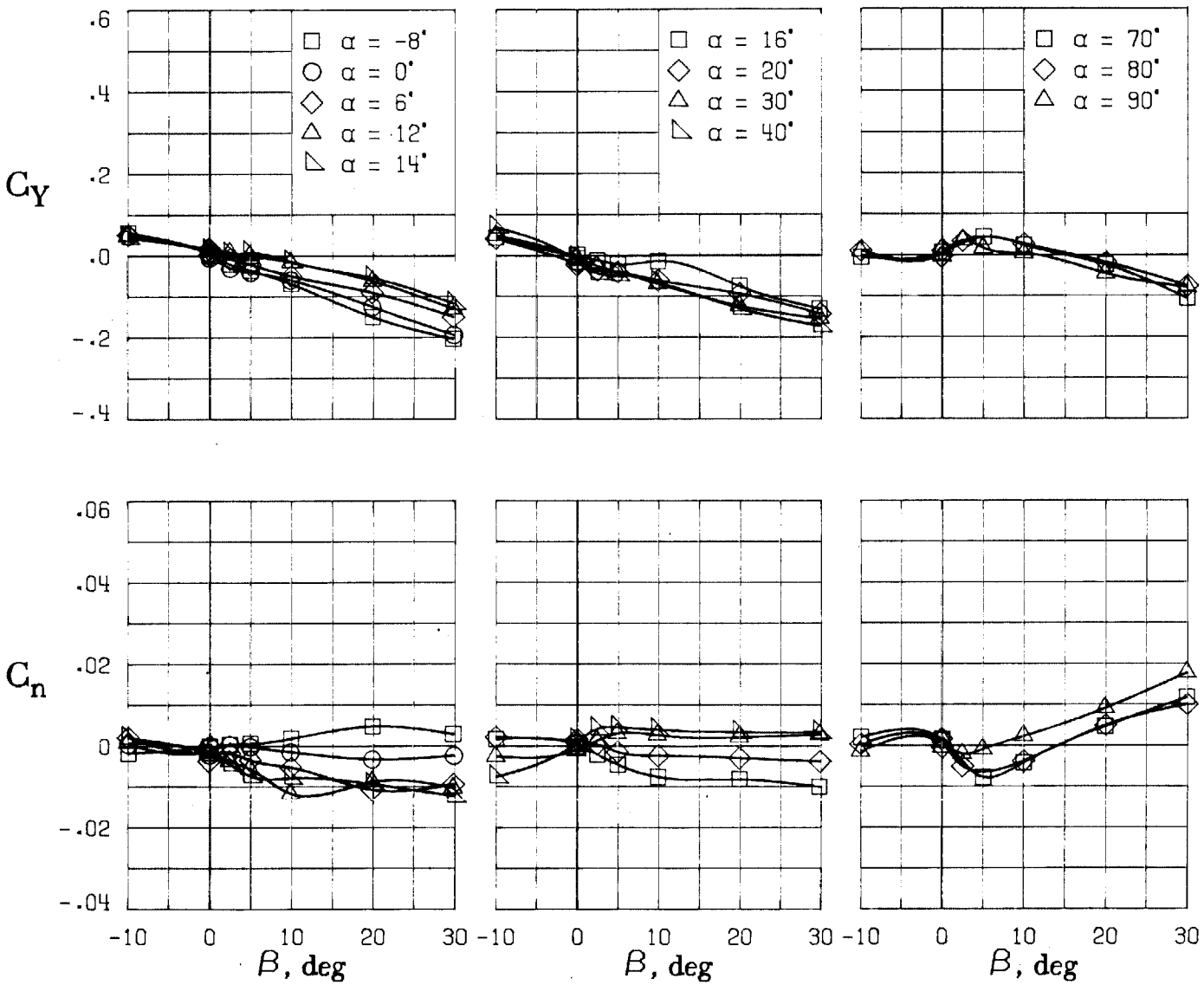

(E) DIRECTIONAL - STABILITY CHARACTERISTICS ABOUT BODY AXES AT VARIOUS ANGLES OF ATTACK.

FIGURE 77. - CONTINUED.

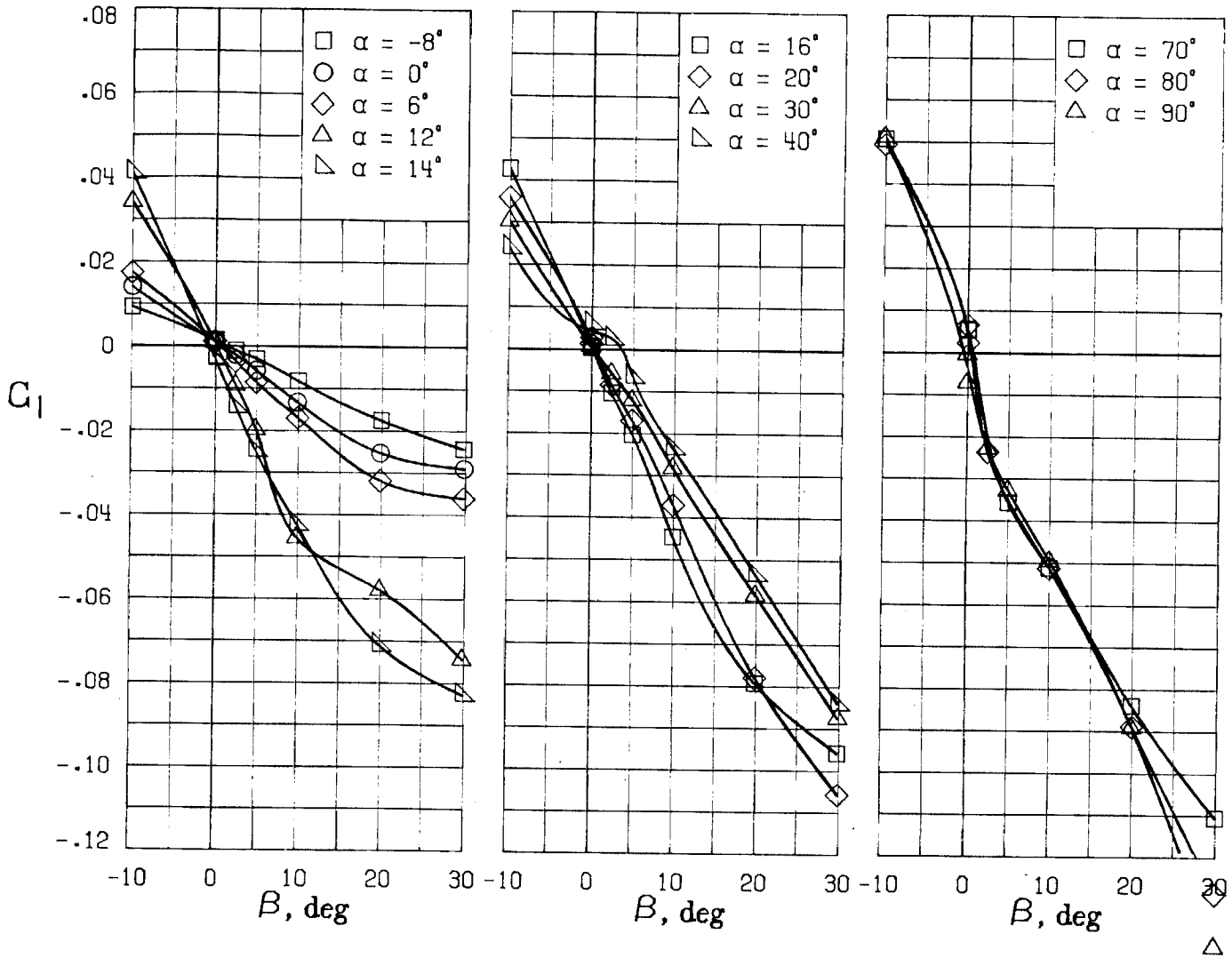

(F) LATERAL - STABILITY CHARACTERISTICS ABOUT BODY AXES AT VARIOUS ANGLES OF ATTACK.

FIGURE 77. - CONCLUDED.

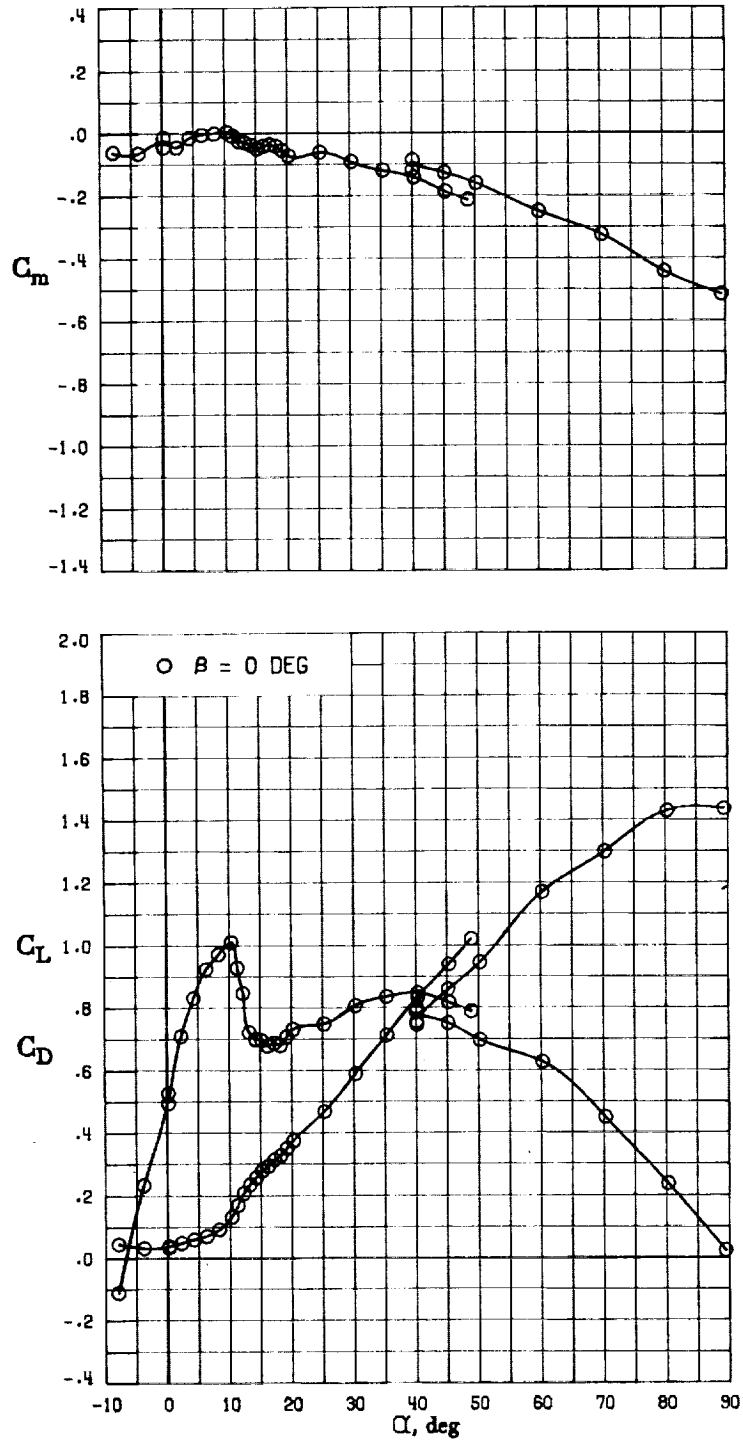

(A) LONGITUDINAL FORCE AND MOMENT COEFFICIENTS ABOUT STABILITY AXES.

FIGURE 78. - EFFECT OF ANGLE OF ATTACK AND SIDESLIP ANGLE ON AERODYNAMIC CHARACTERISTICS AT RE = .288 E+06 FOR CONFIGURATION B W1 V. $\delta_E = 0°$, $\delta_A = 0°$, $\delta_R = 0°$.

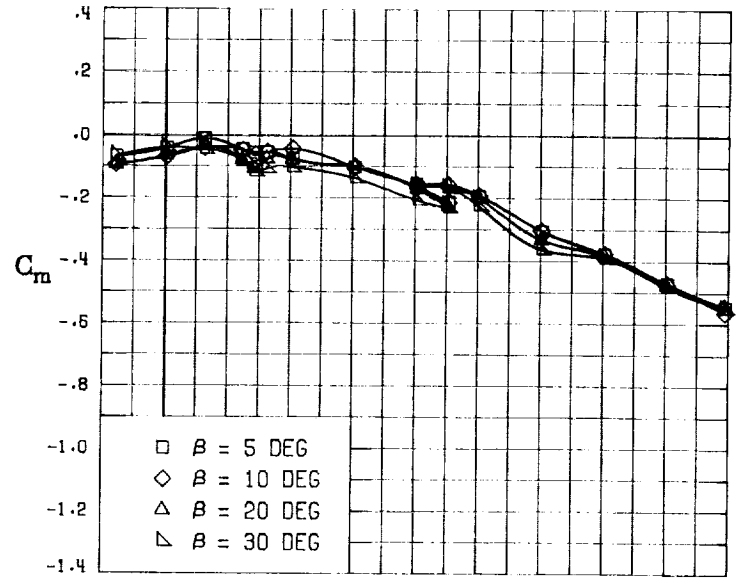

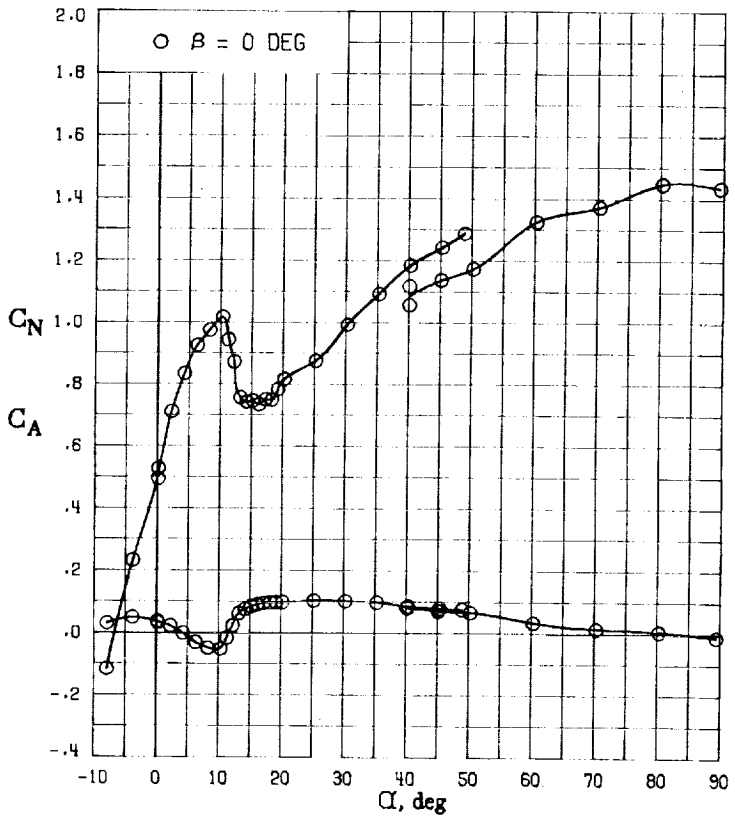

(B) LONGITUDINAL FORCE AND MOMENT COEFFICIENTS ABOUT BODY AXES.

FIGURE 78. - CONTINUED.

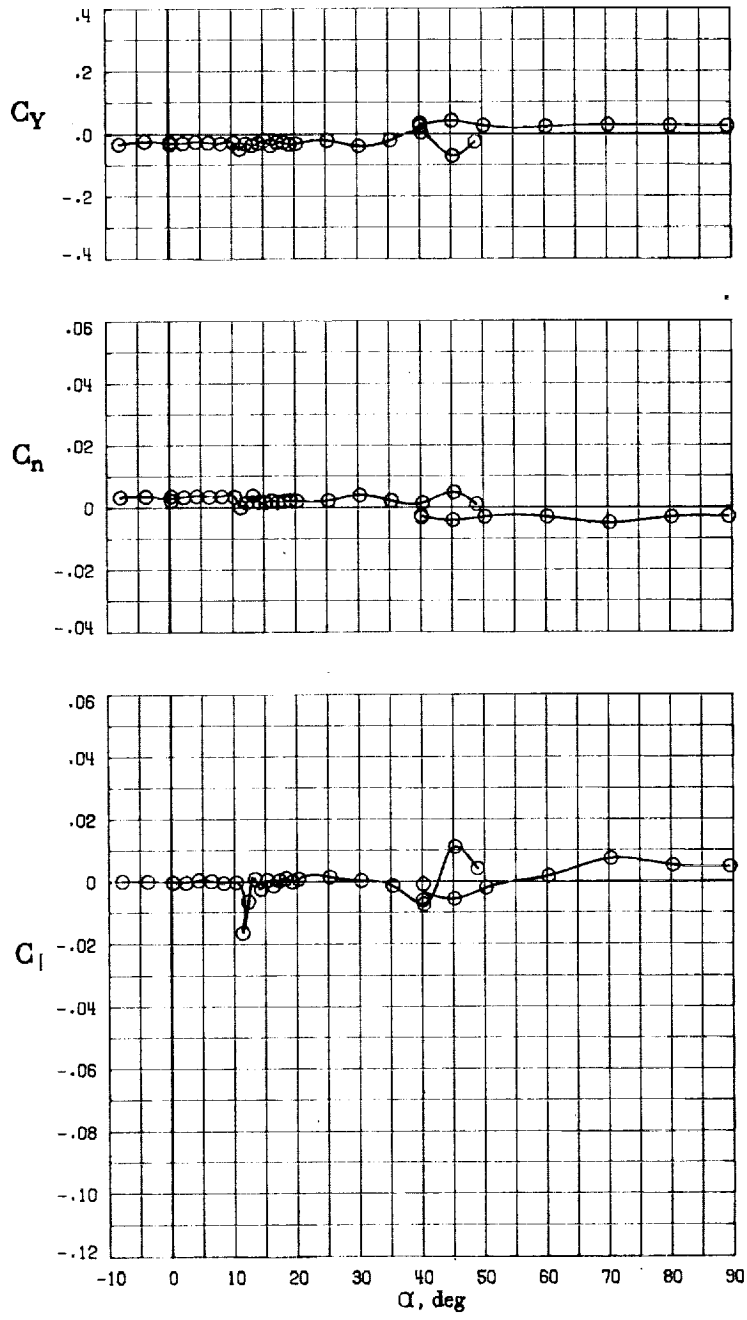

(C) LATERAL - DIRECTIONAL FORCE AND MOMENT COEFFICIENTS ABOUT BODY AXES AT ZERO SIDESLIP.

FIGURE 78. - CONTINUED.

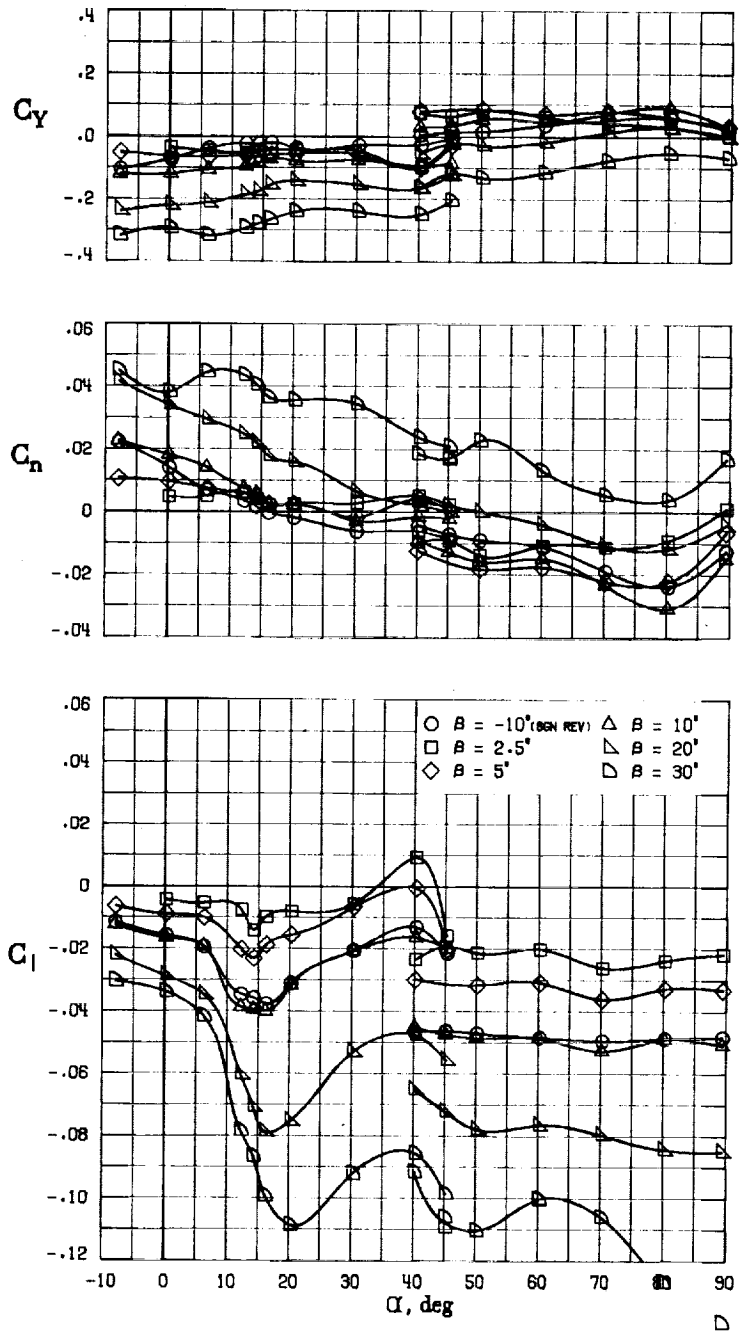

(D) LATERAL - DIRECTIONAL FORCE AND MOMENT COEFFICIENTS ABOUT BODY AXES.

FIGURE 78. - CONTINUED.

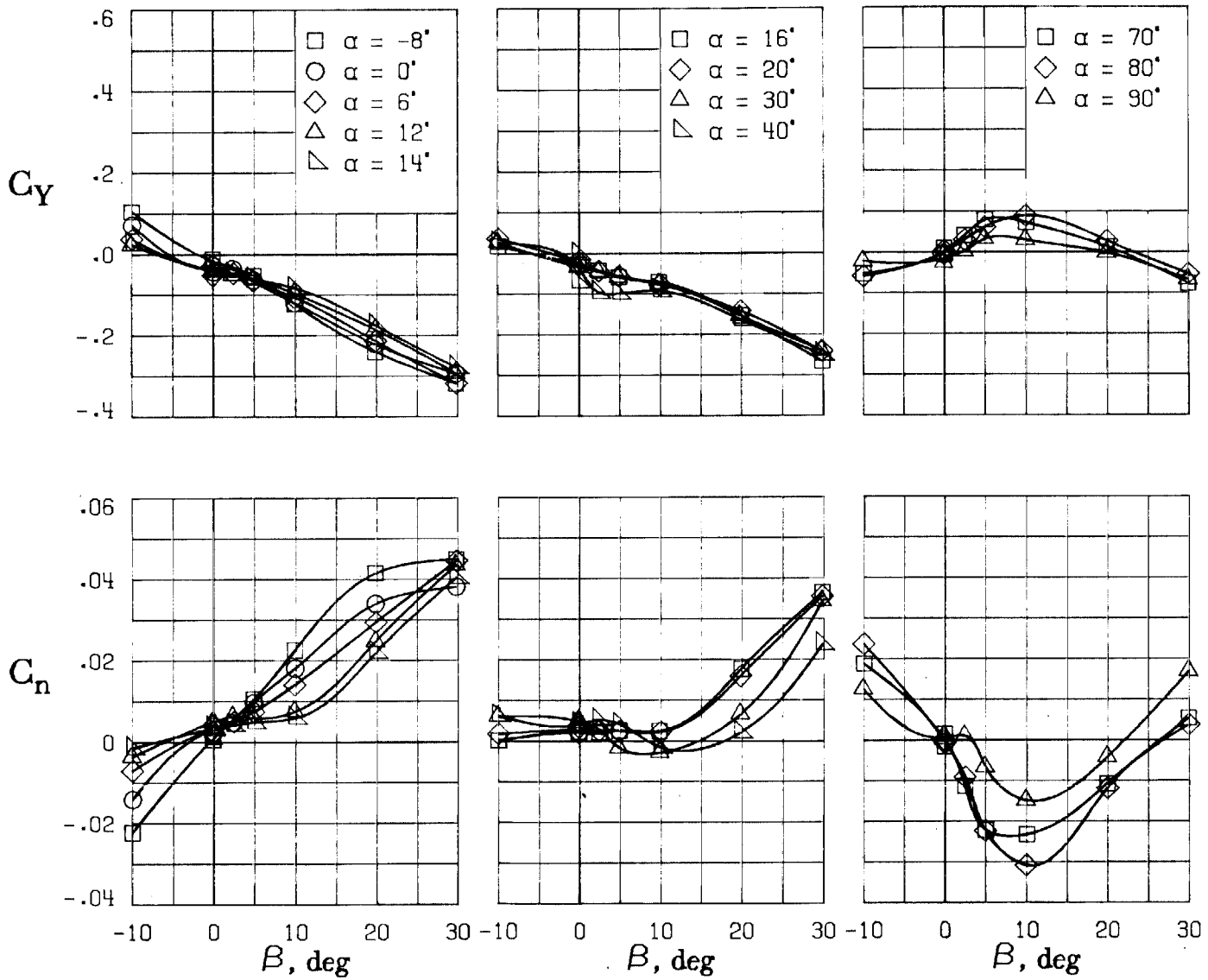

(E) DIRECTIONAL - STABILITY CHARACTERISTICS ABOUT BODY AXES AT VARIOUS ANGLES OF ATTACK.

FIGURE 78. - CONTINUED.

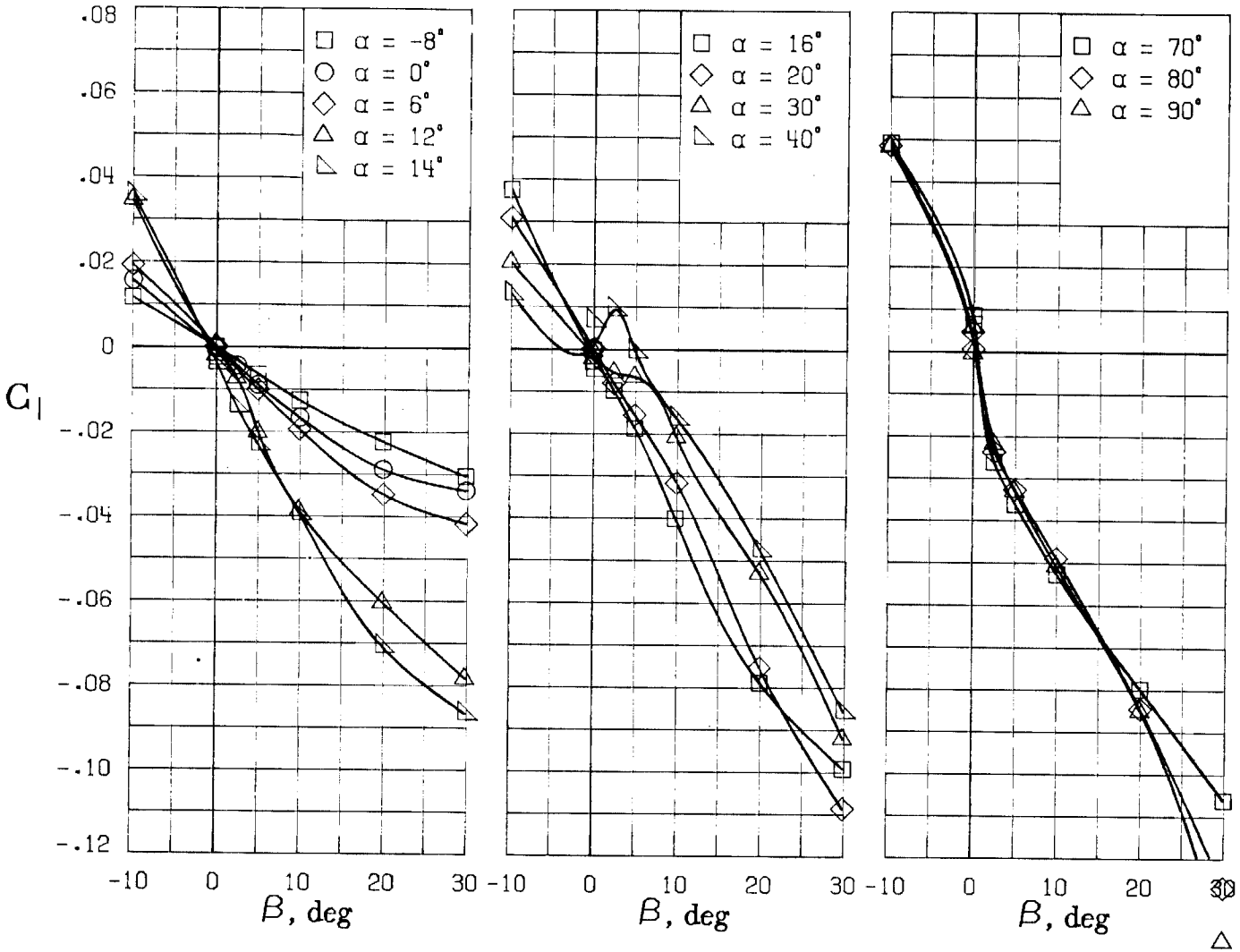

(F) LATERAL - STABILITY CHARACTERISTICS ABOUT BODY AXES AT VARIOUS ANGLES OF ATTACK.

FIGURE 78. - CONCLUDED.

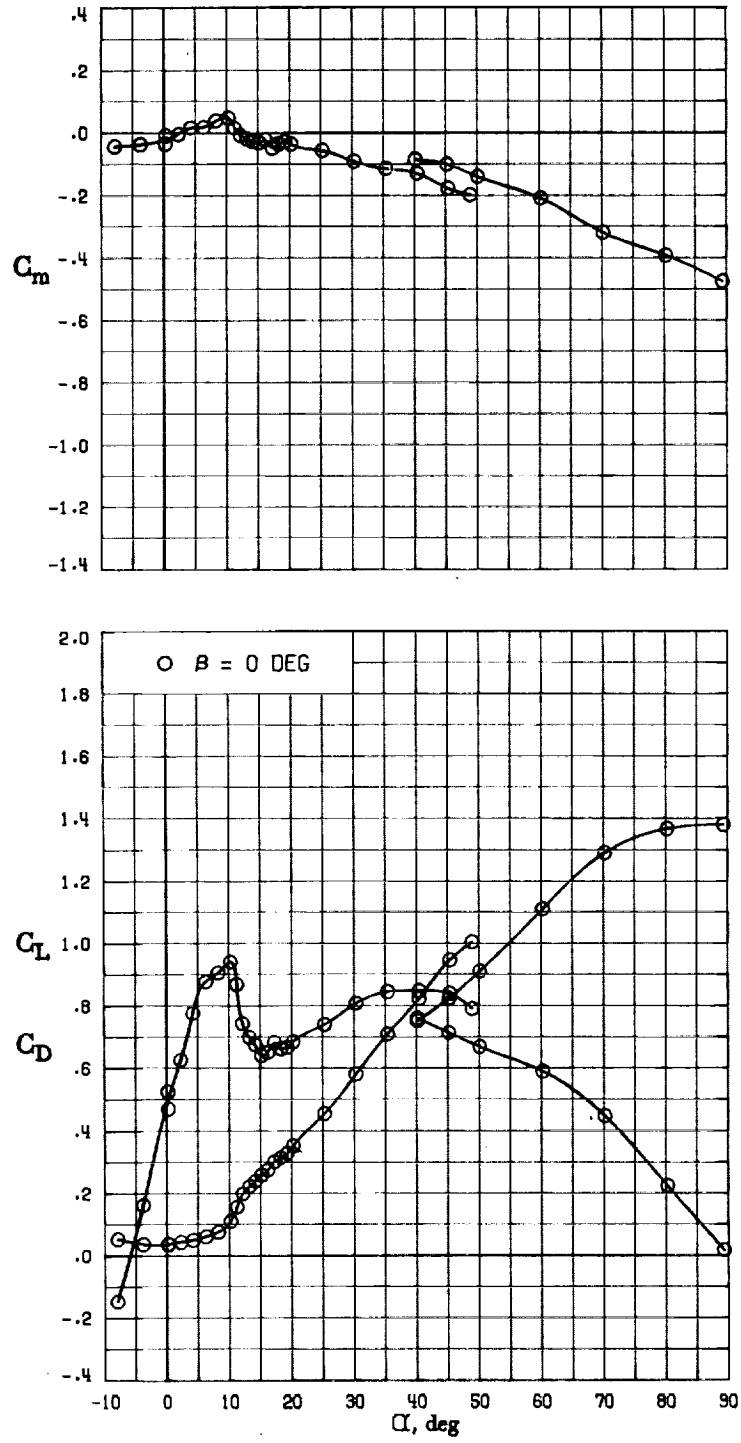

(A) LONGITUDINAL FORCE AND MOMENT COEFFICIENTS ABOUT STABILITY AXES.

FIGURE 79. - EFFECT OF ANGLE OF ATTACK AND SIDESLIP ANGLE ON AERODYNAMIC CHARACTERISTICS AT RE = .288 E+06 FOR CONFIGURATION B W1. $\delta_E = 0°$, $\delta_A = 0°$, $\delta_R = 0°$.

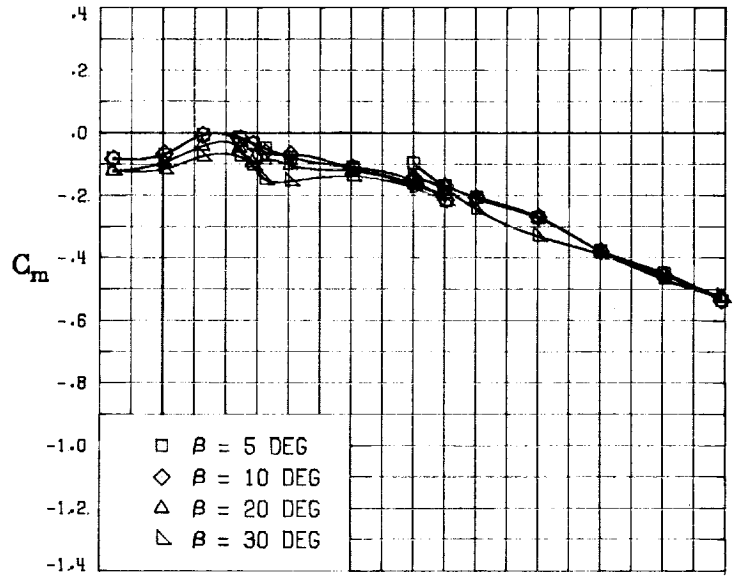

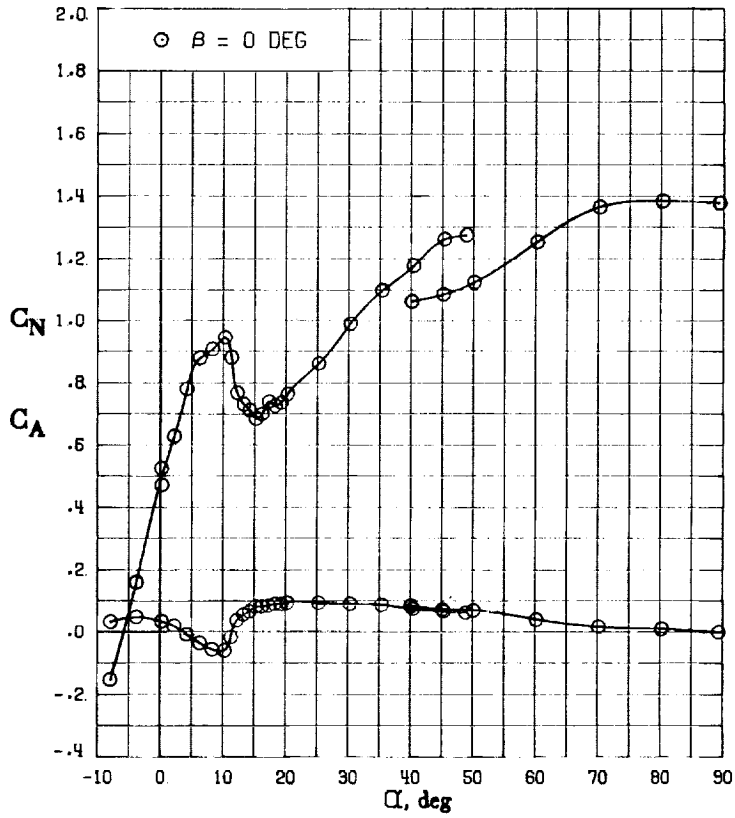

(B) LONGITUDINAL FORCE AND MOMENT COEFFICIENTS ABOUT BODY AXES.

FIGURE 79. - CONTINUED.

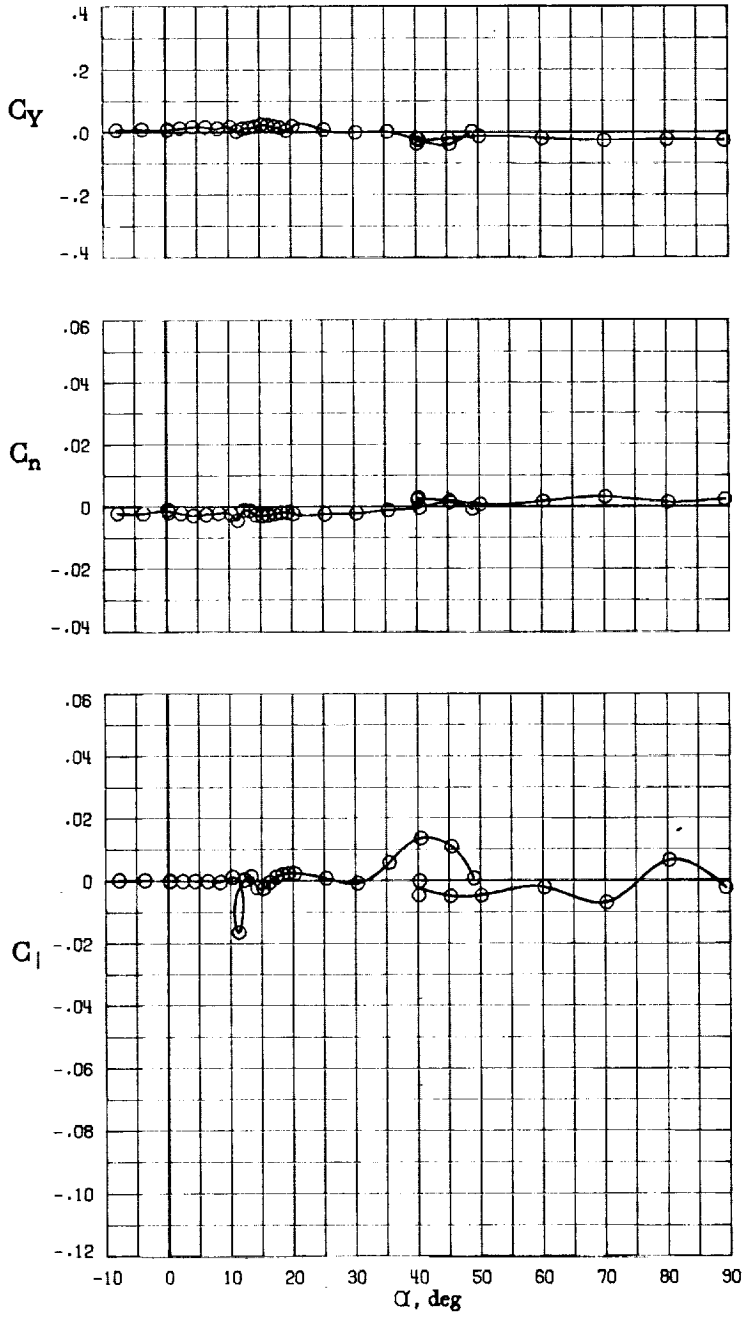

(C) LATERAL - DIRECTIONAL FORCE AND MOMENT COEFFICIENTS ABOUT BODY AXES AT ZERO SIDESLIP.

FIGURE 79. - CONTINUED.

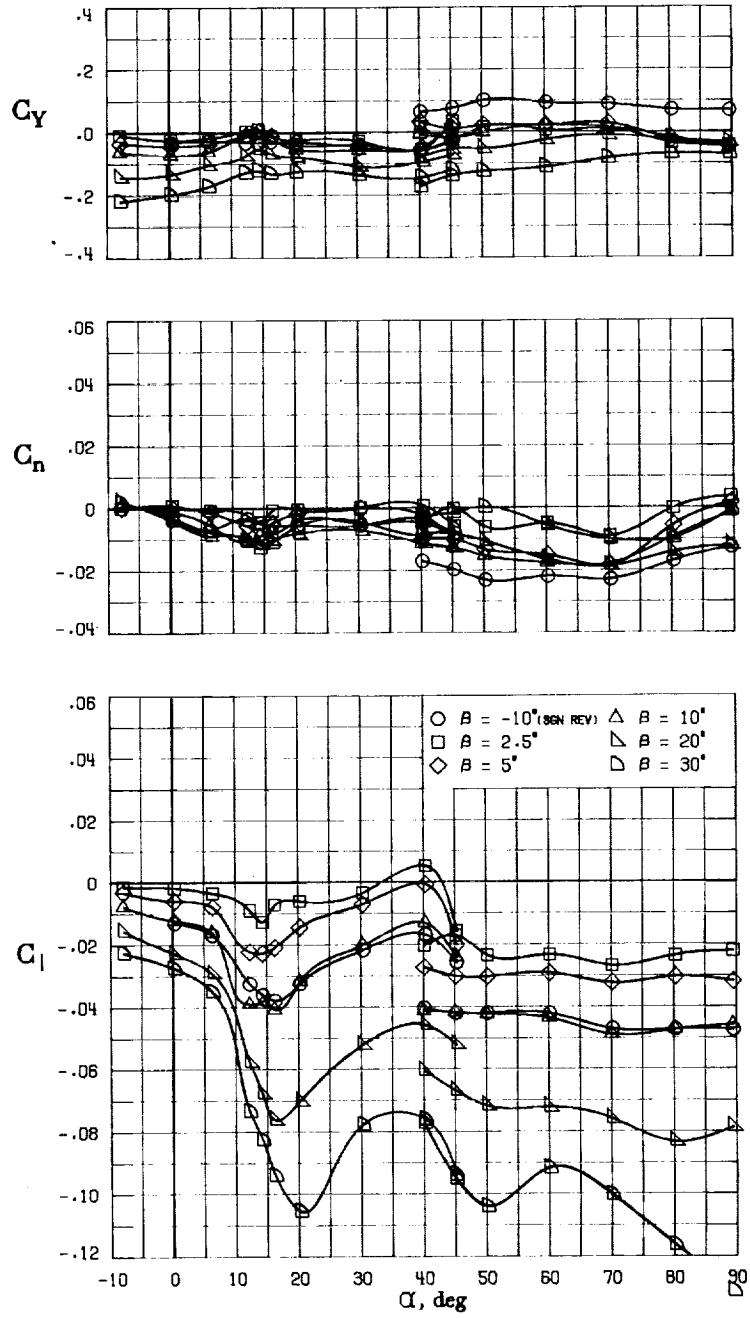

(D) LATERAL - DIRECTIONAL FORCE AND MOMENT COEFFICIENTS ABOUT BODY AXES.

FIGURE 79. - CONTINUED.

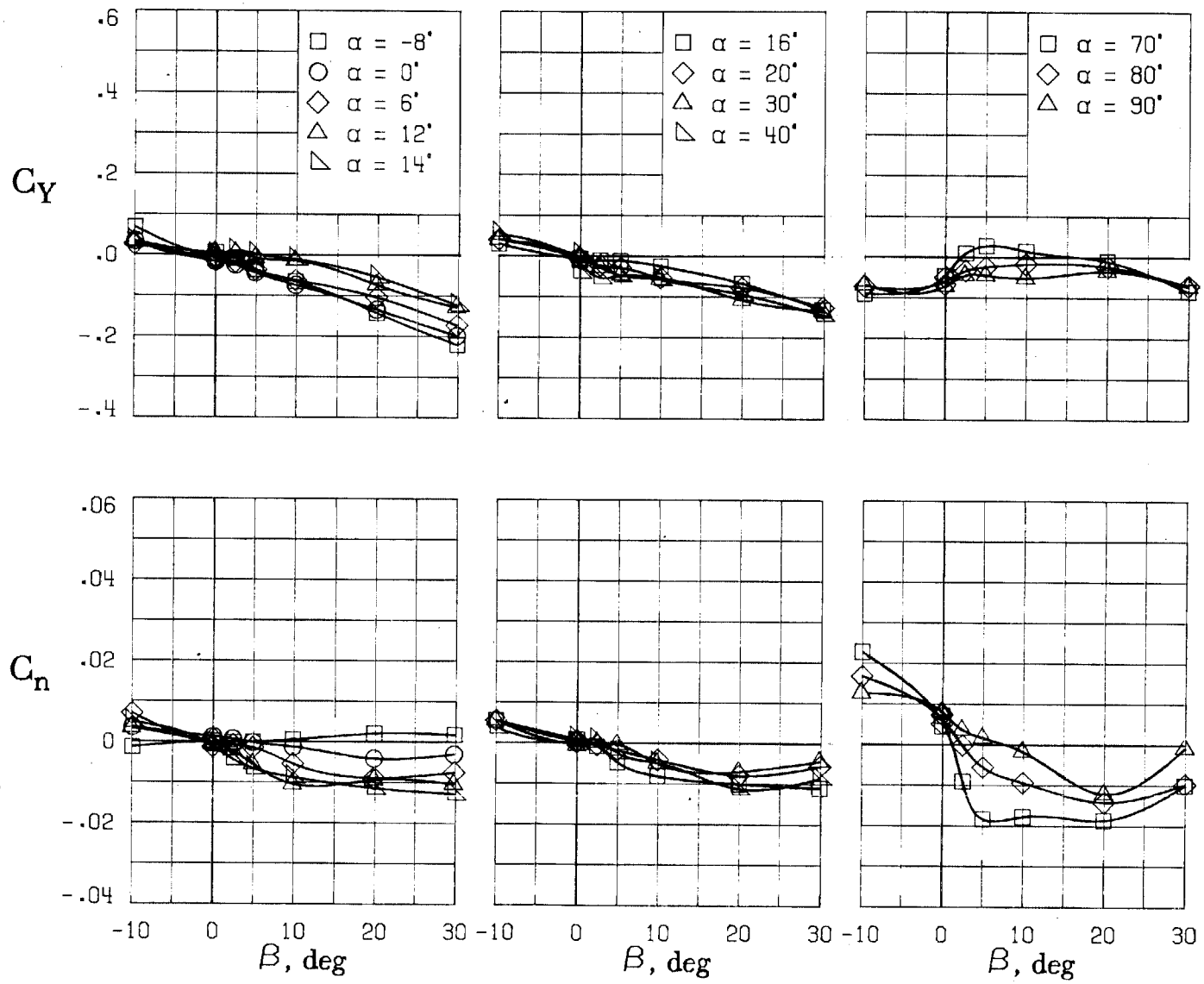

(E) DIRECTIONAL - STABILITY CHARACTERISTICS ABOUT BODY AXES AT VARIOUS ANGLES OF ATTACK.

FIGURE 79. - CONTINUED.

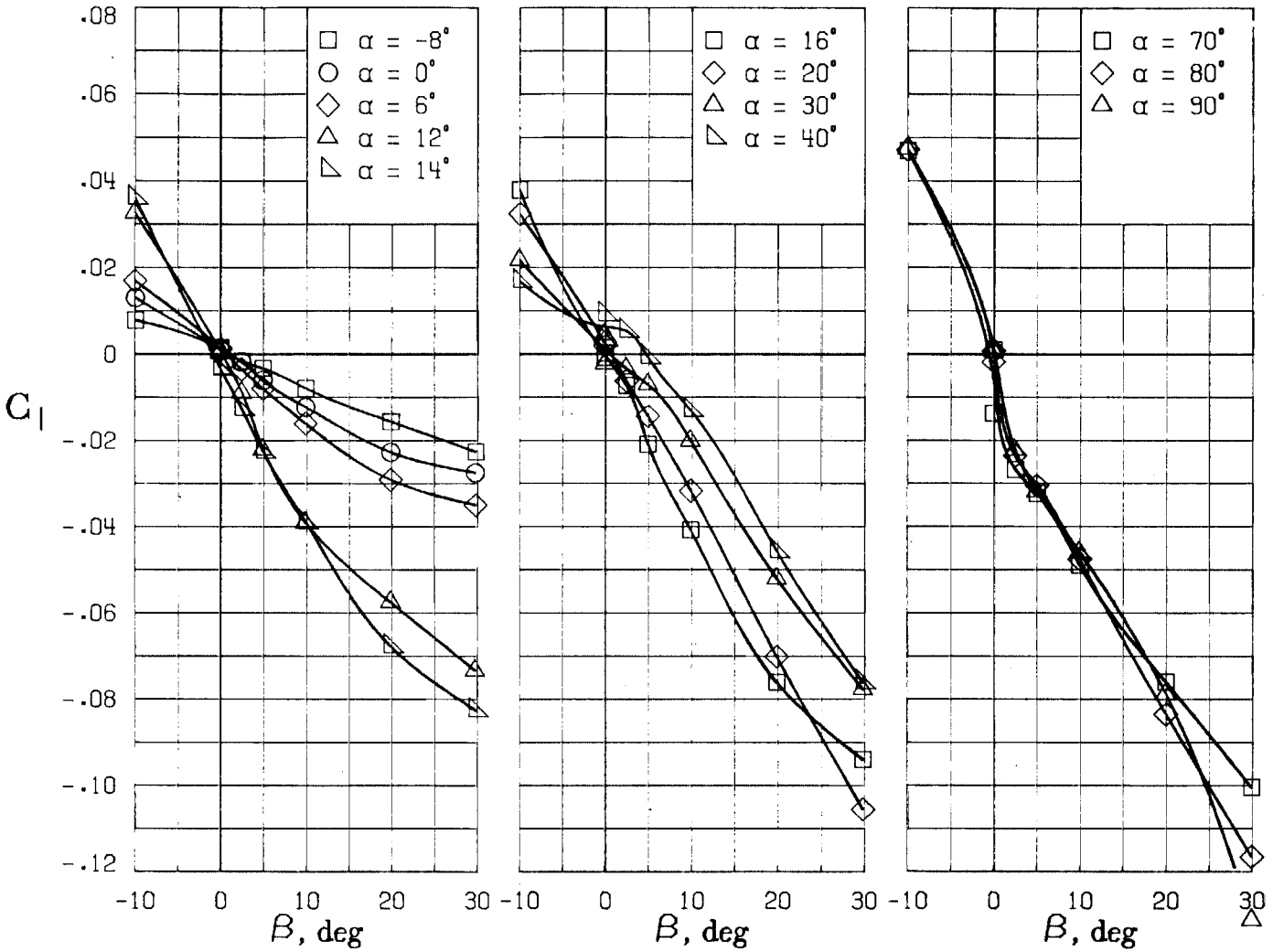

(F) LATERAL - STABILITY CHARACTERISTICS ABOUT BODY AXES AT VARIOUS ANGLES OF ATTACK.

FIGURE 79. - CONCLUDED.

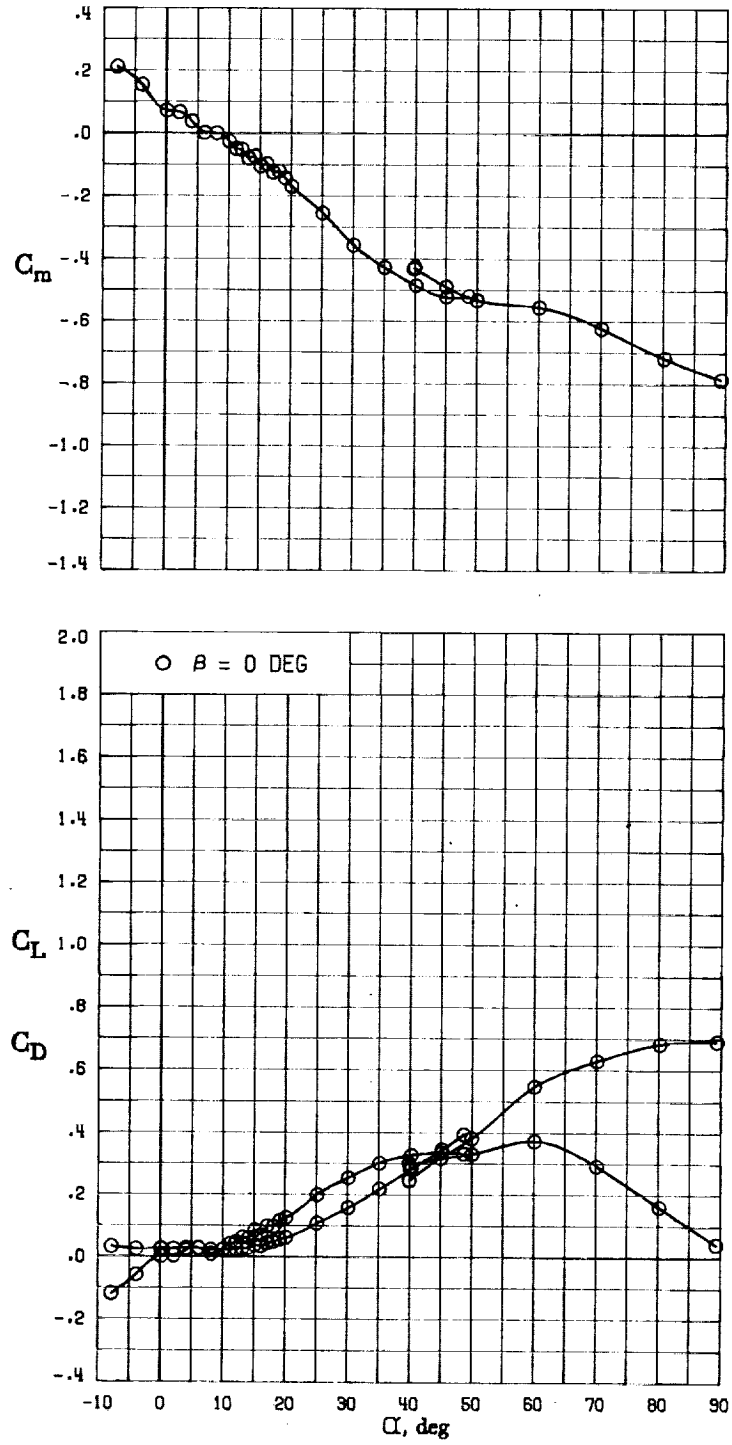

(A) LONGITUDINAL FORCE AND MOMENT COEFFICIENTS ABOUT STABILITY AXES.

FIGURE 80. - EFFECT OF ANGLE OF ATTACK AND SIDESLIP ANGLE ON AERODYNAMIC CHARACTERISTICS AT RE = .288 E+06 FOR CONFIGURATION B H3. $\delta_E = 0°$, $\delta_A = 0°$, $\delta_R = 0°$.

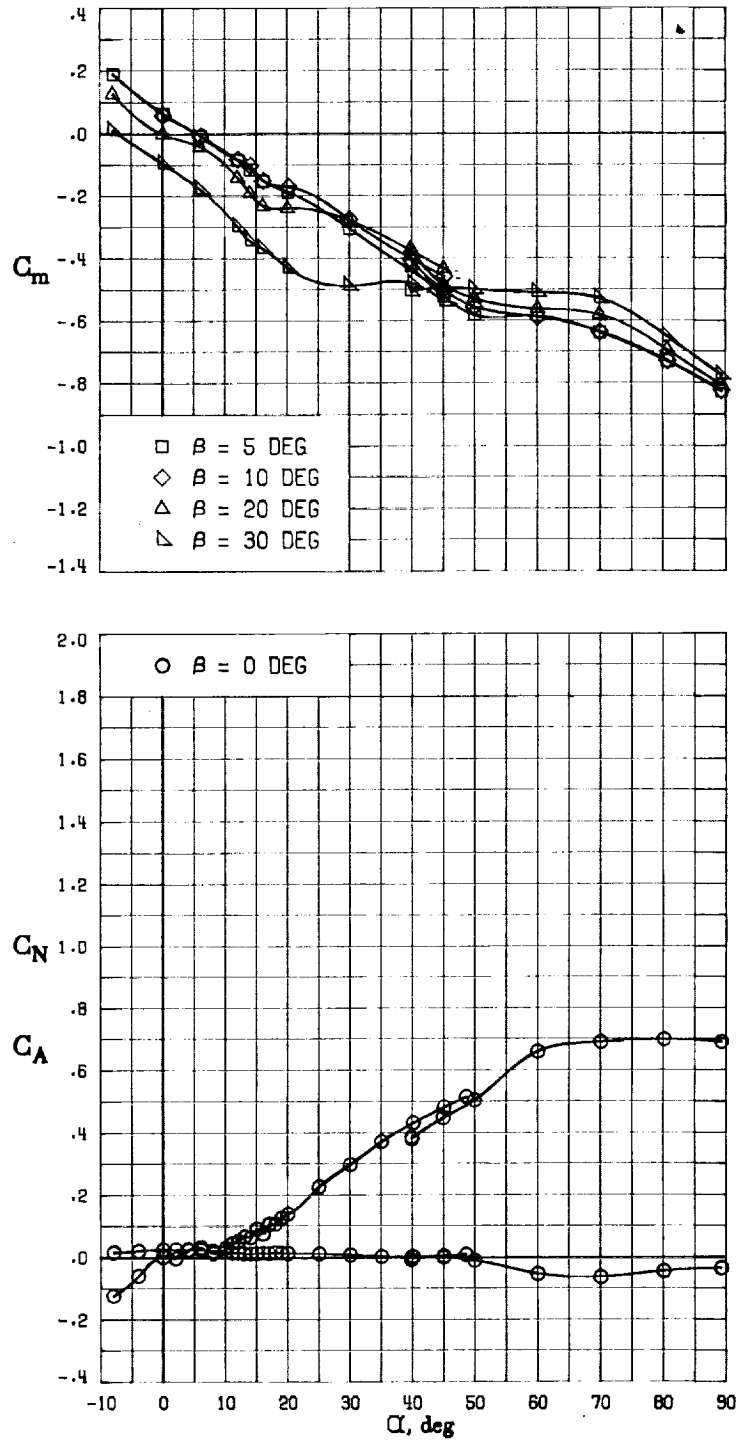

(B) LONGITUDINAL FORCE AND MOMENT COEFFICIENTS ABOUT BODY AXES.

FIGURE 80. - CONTINUED.

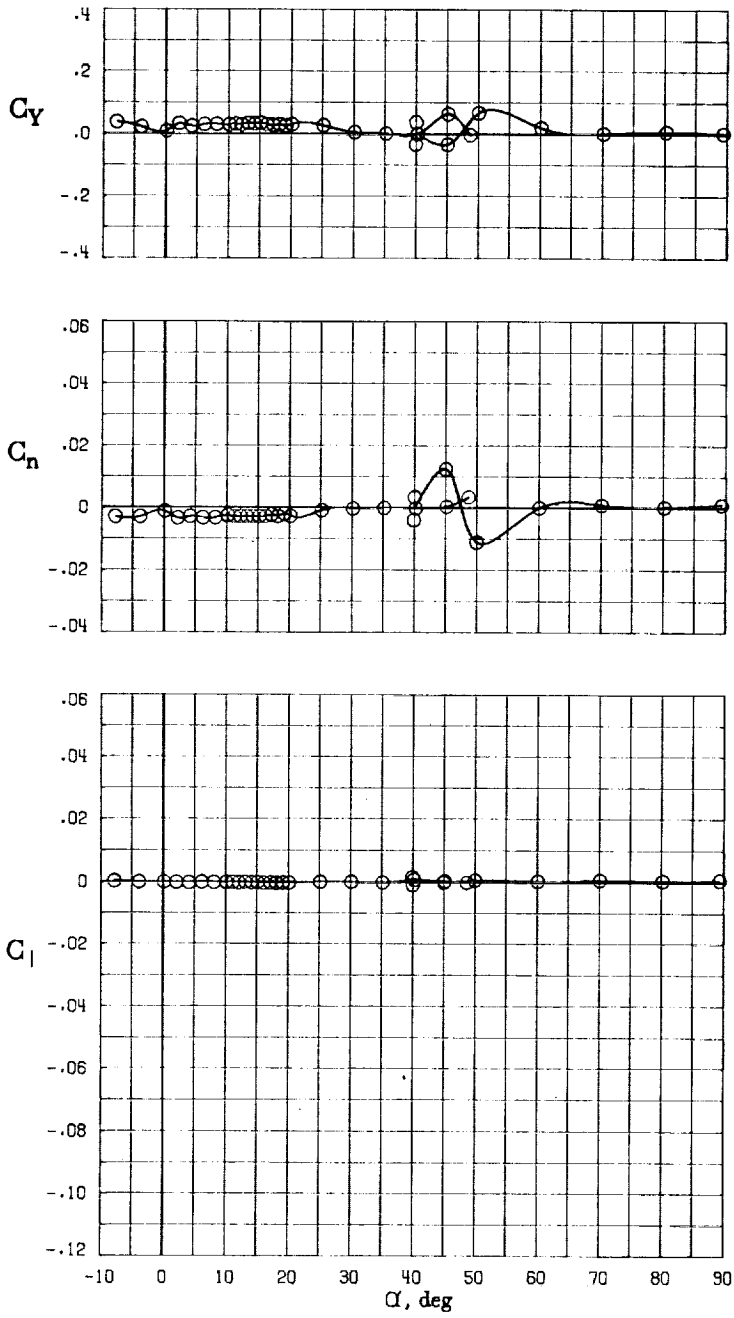

(C) LATERAL - DIRECTIONAL FORCE AND MOMENT COEFFICIENTS ABOUT BODY AXES AT ZERO SIDESLIP.

FIGURE 80. - CONTINUED.

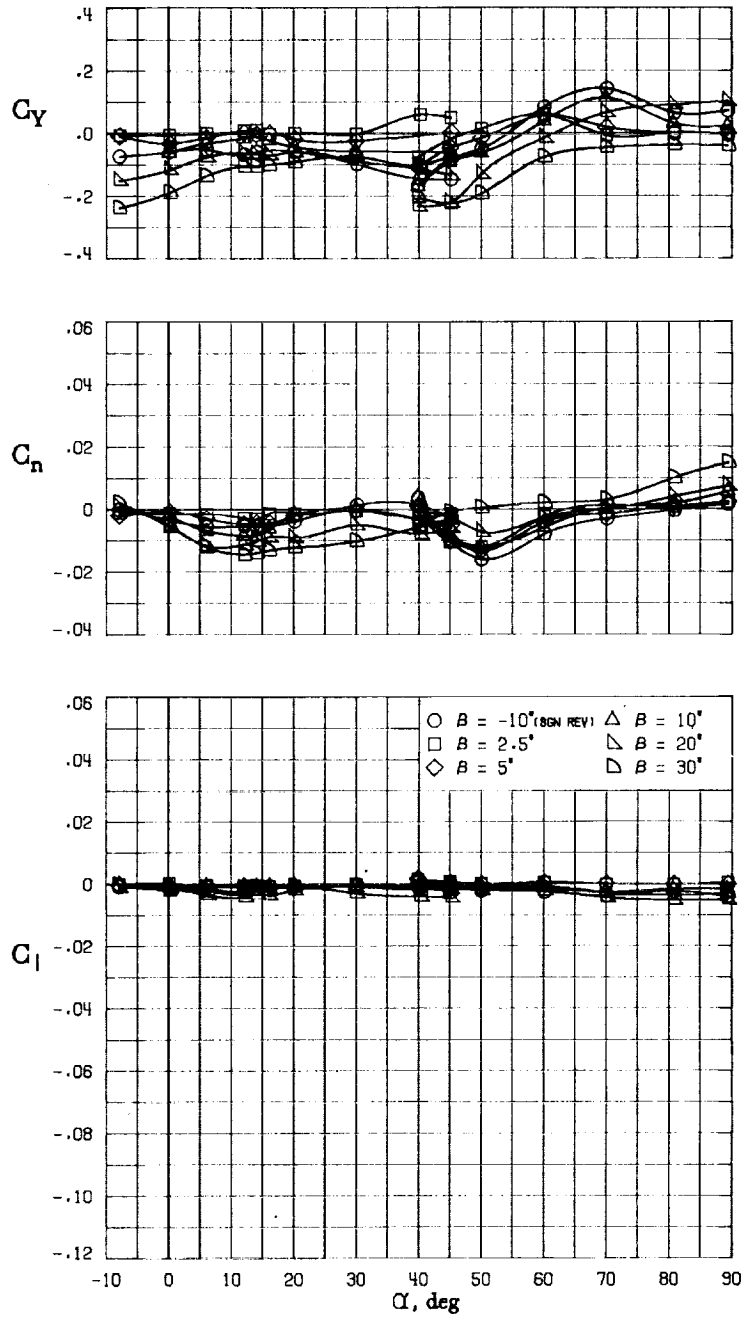

(D) LATERAL - DIRECTIONAL FORCE AND MOMENT COEFFICIENTS ABOUT BODY AXES.

FIGURE 80. - CONTINUED.

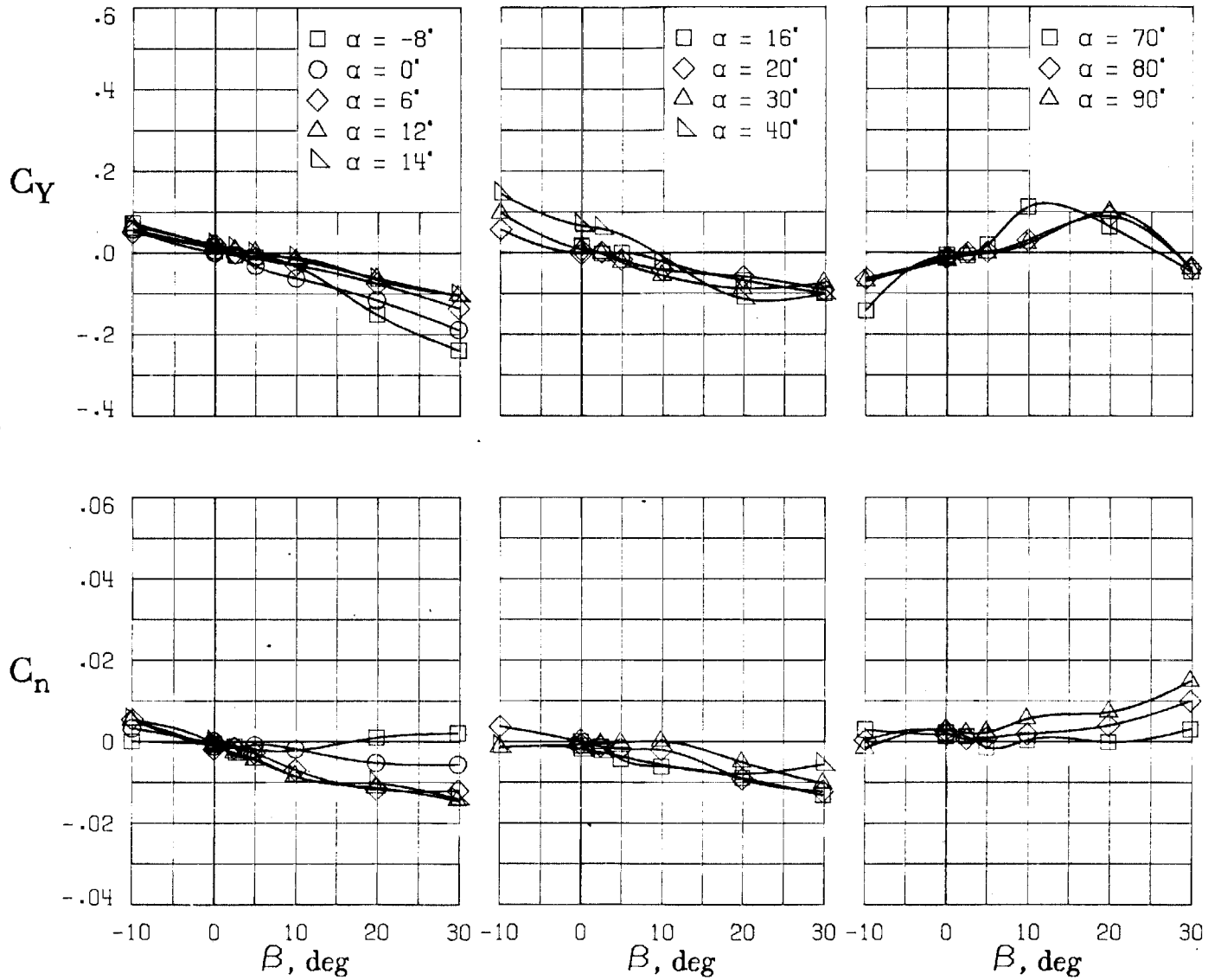

(E) DIRECTIONAL - STABILITY CHARACTERISTICS ABOUT BODY AXES AT VARIOUS ANGLES OF ATTACK.

FIGURE 80. - CONTINUED.

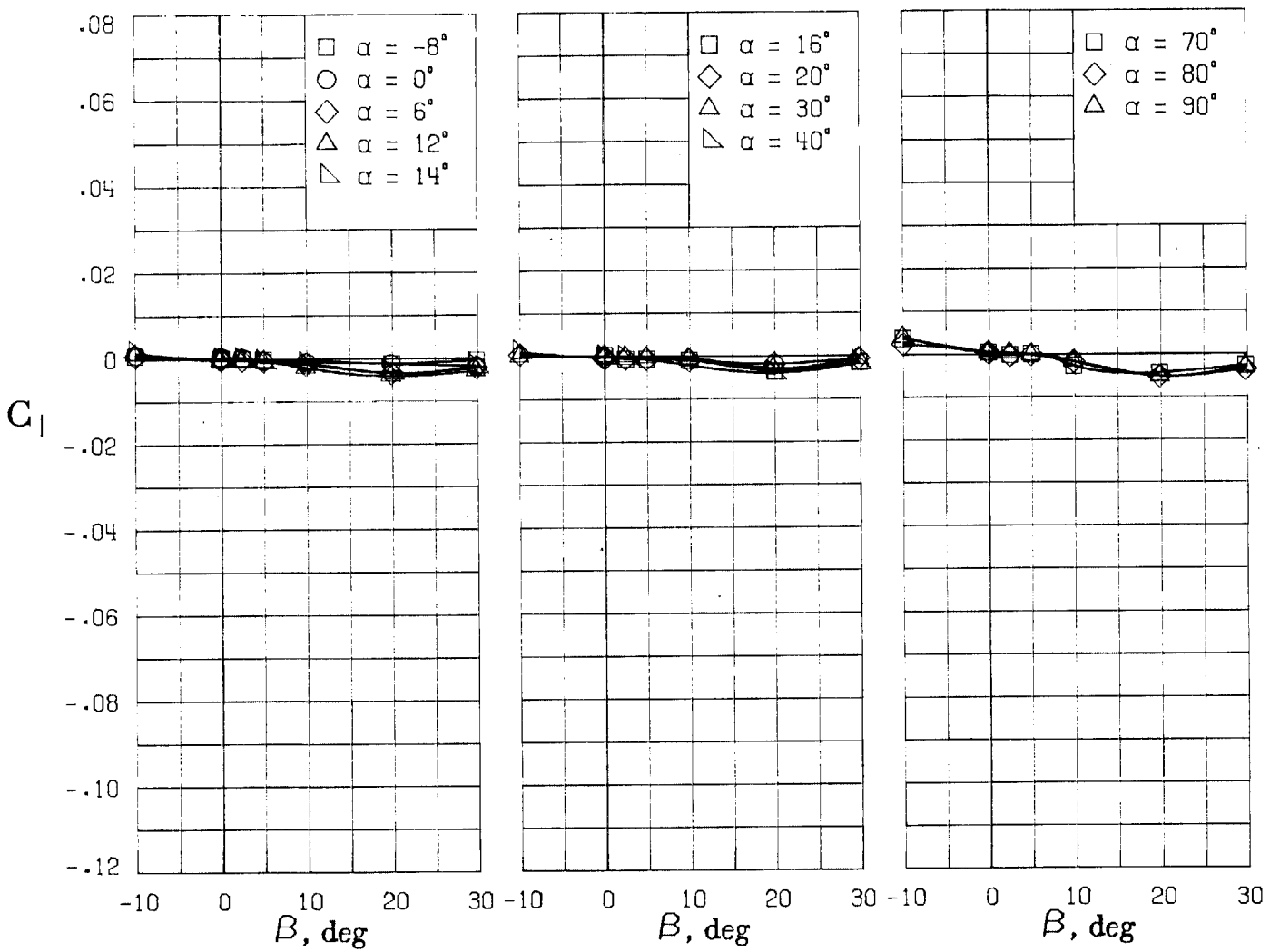

(F) LATERAL - STABILITY CHARACTERISTICS ABOUT BODY AXES AT VARIOUS ANGLES OF ATTACK.

FIGURE 80. - CONCLUDED.

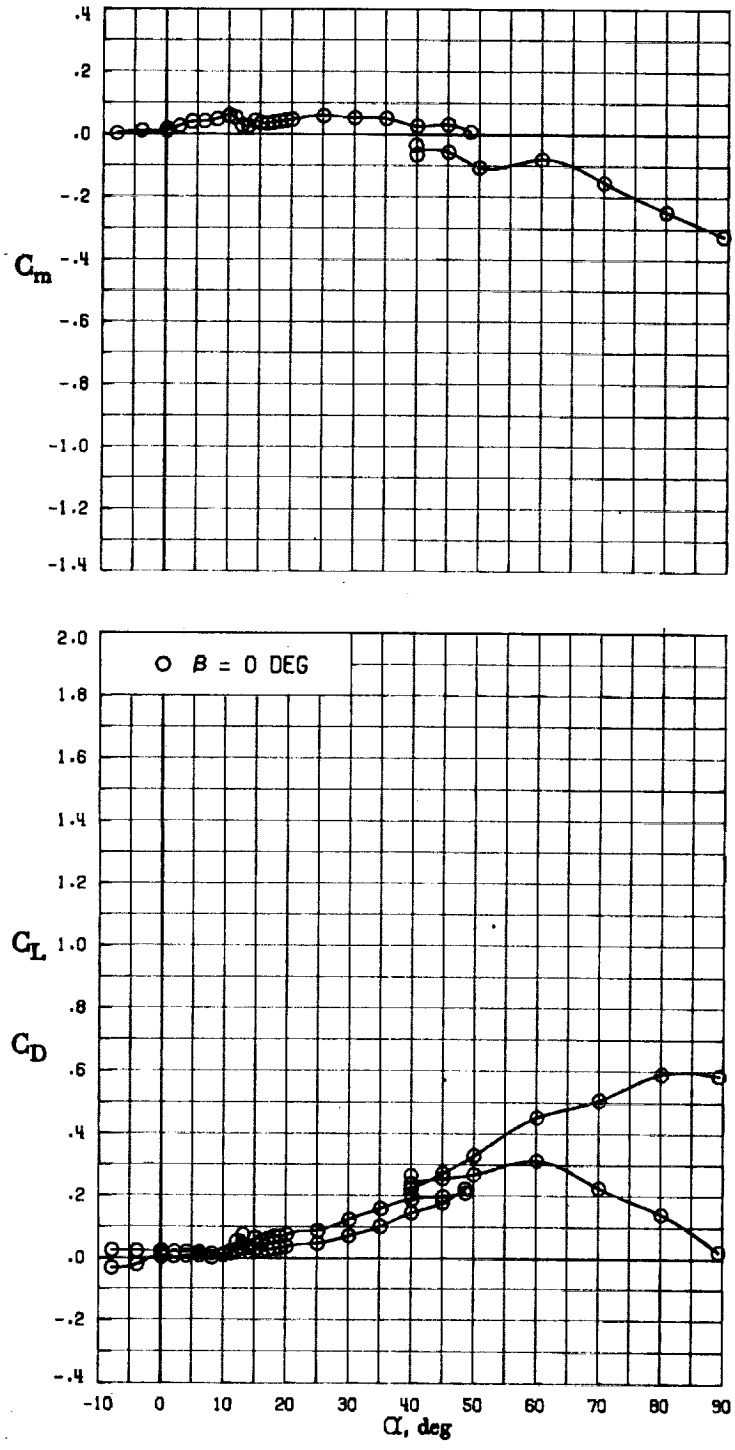

(A) LONGITUDINAL FORCE AND MOMENT COEFFICIENTS ABOUT STABILITY AXES.

FIGURE 81. - EFFECT OF ANGLE OF ATTACK AND SIDESLIP ANGLE ON AERODYNAMIC CHARACTERISTICS AT RE = .288 E+06 FOR CONFIGURATION B V. δ_E = 0°, δ_A = 0°, δ_R = 0°.

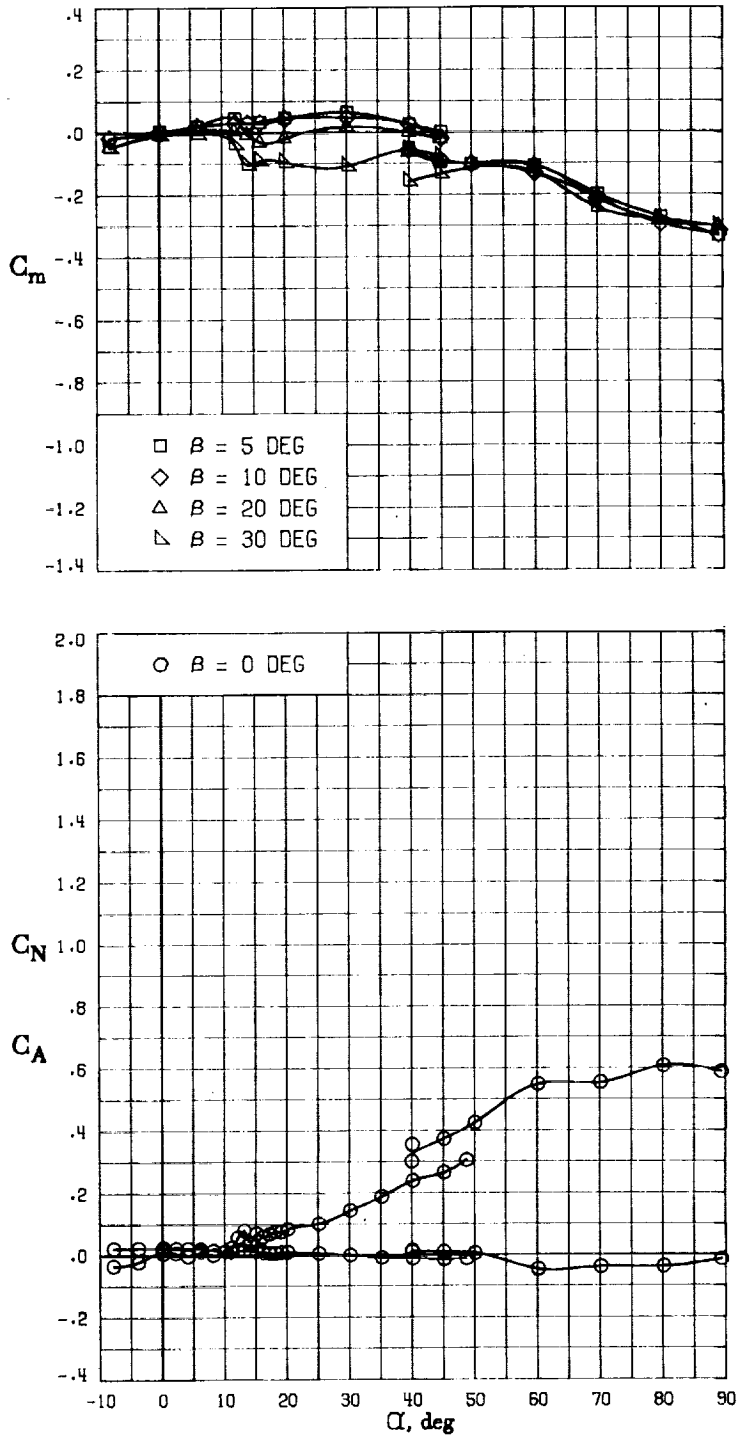

(B) LONGITUDINAL FORCE AND MOMENT COEFFICIENTS ABOUT BODY AXES.

FIGURE 81. - CONTINUED.

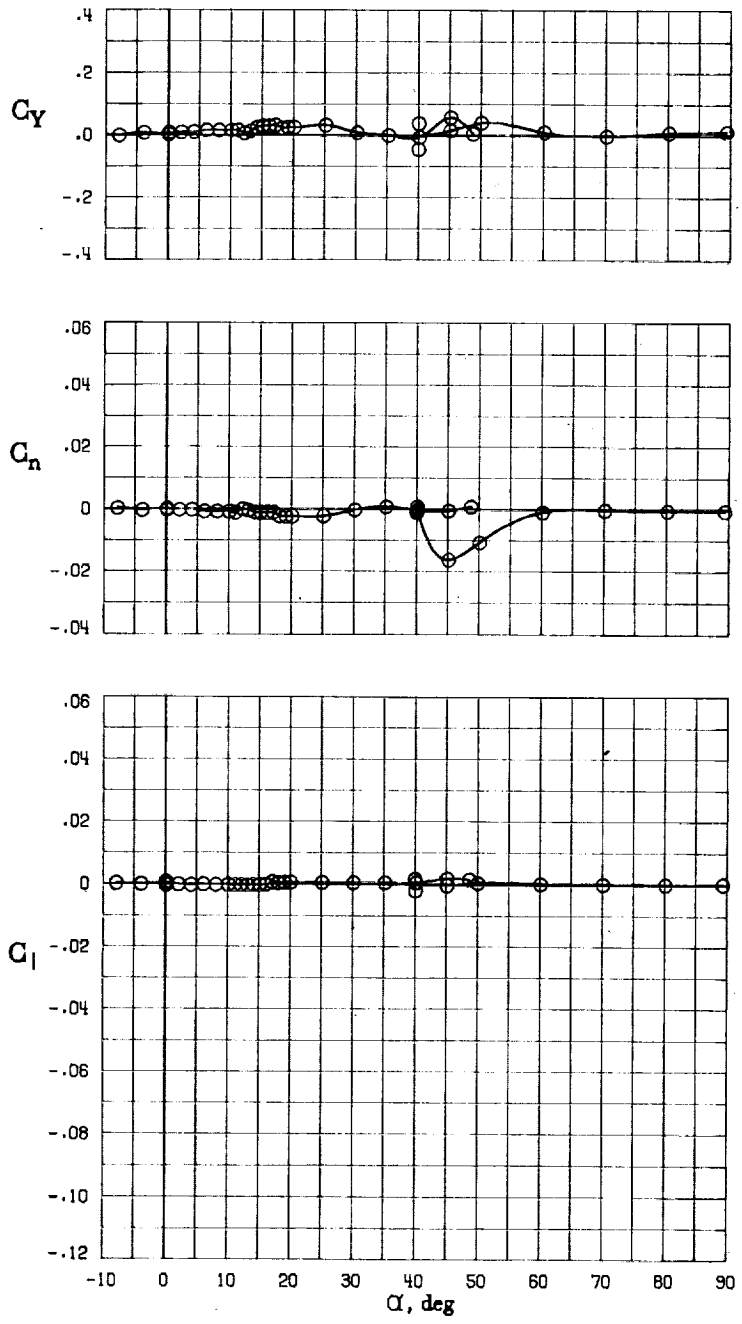

(C) LATERAL - DIRECTIONAL FORCE AND MOMENT COEFFICIENTS ABOUT BODY AXES AT ZERO SIDESLIP.

FIGURE 81. - CONTINUED.

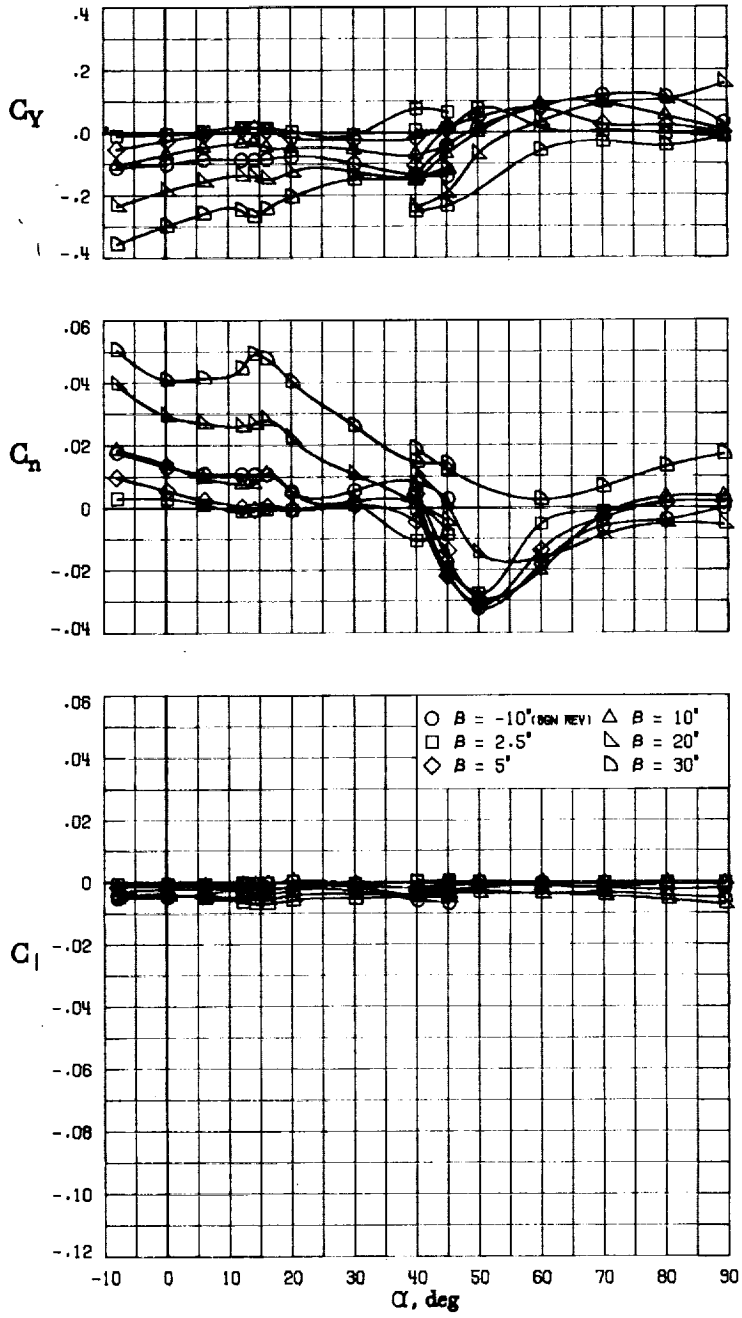

(D) LATERAL - DIRECTIONAL FORCE AND MOMENT COEFFICIENTS ABOUT BODY AXES.

FIGURE 81. - CONTINUED.

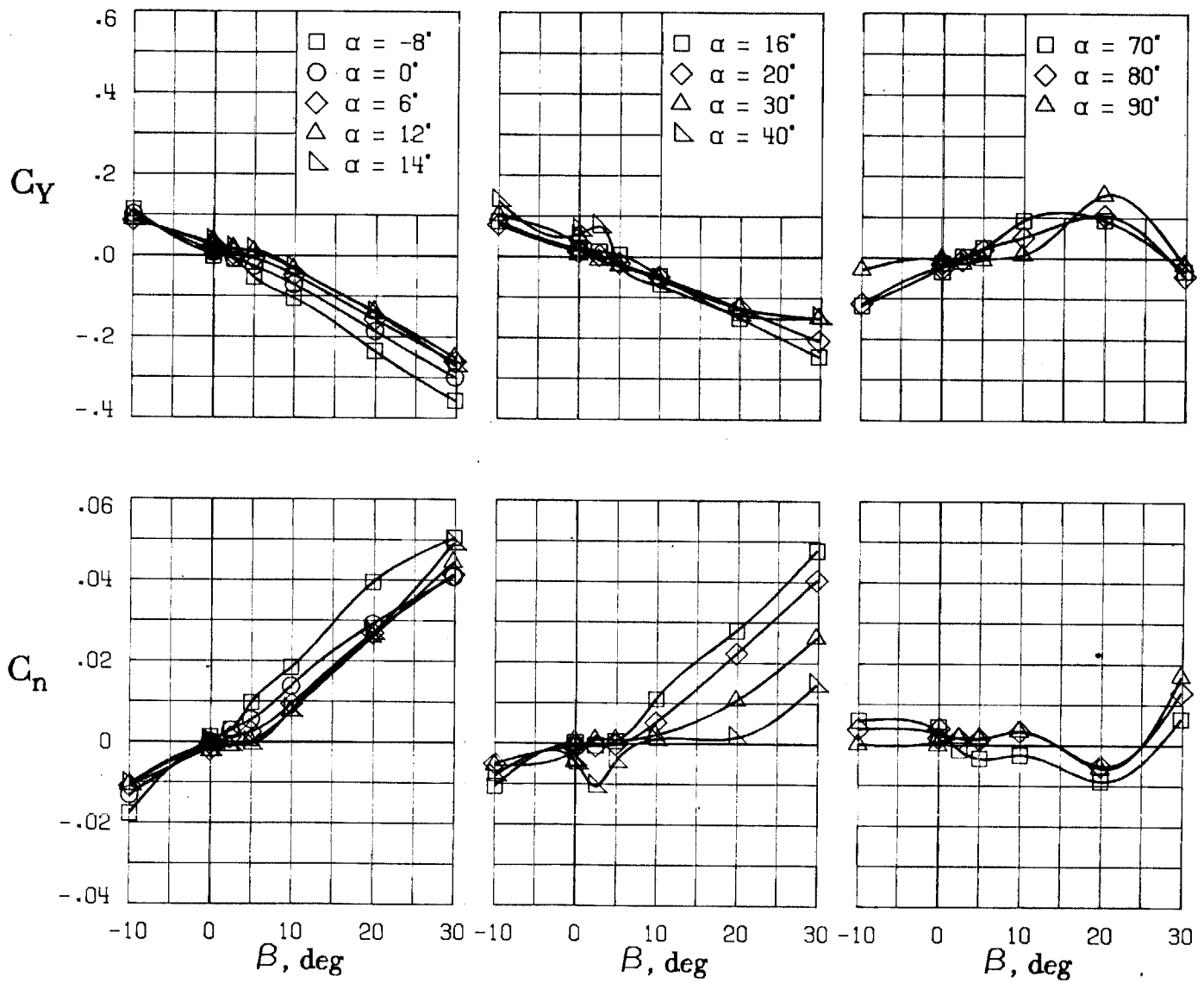

(E) DIRECTIONAL - STABILITY CHARACTERISTICS ABOUT BODY AXES AT VARIOUS ANGLES OF ATTACK.

FIGURE 81. - CONTINUED.

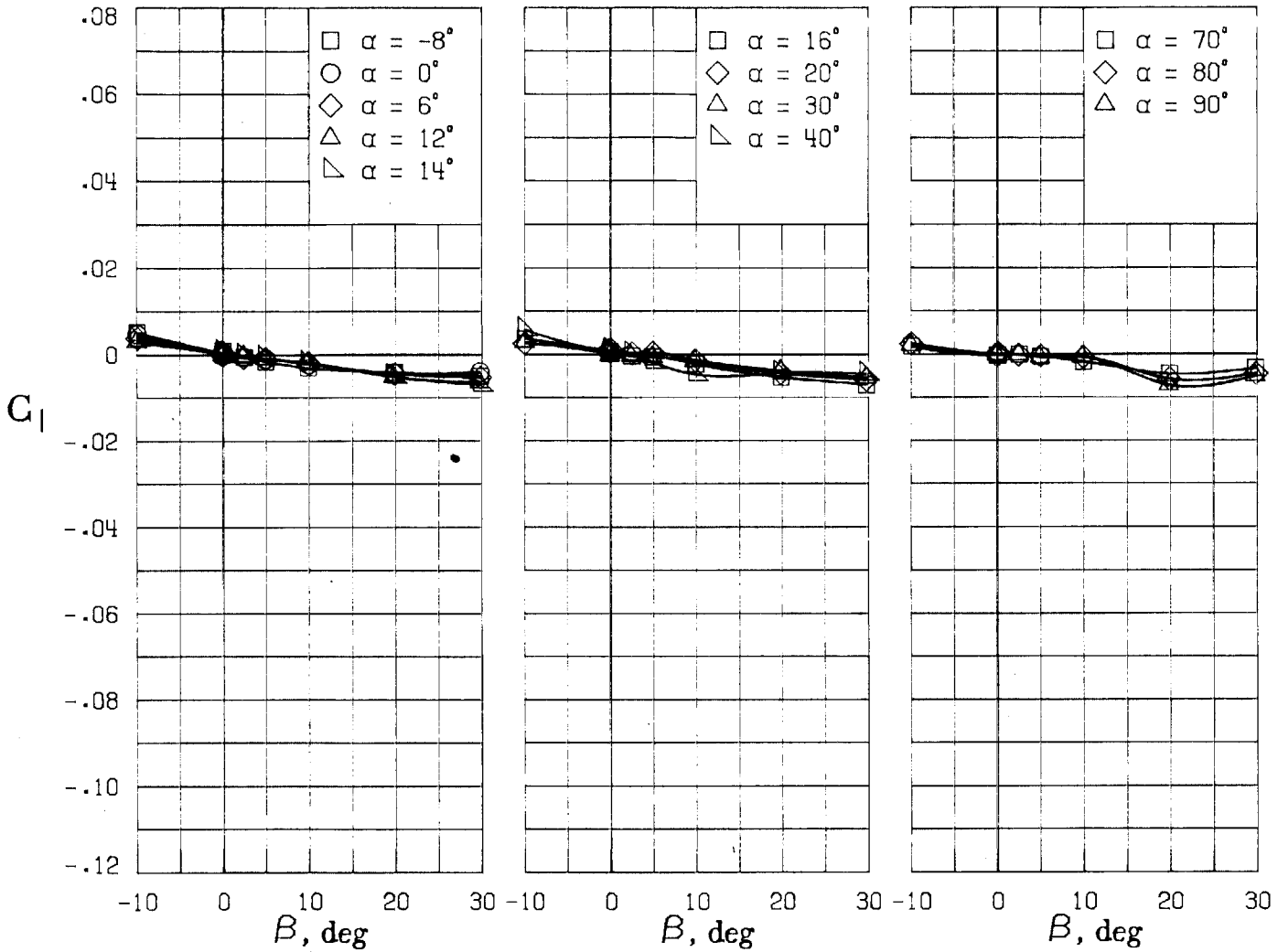

(F) LATERAL - STABILITY CHARACTERISTICS ABOUT BODY AXES AT VARIOUS ANGLES OF ATTACK.

FIGURE 81. - CONCLUDED.

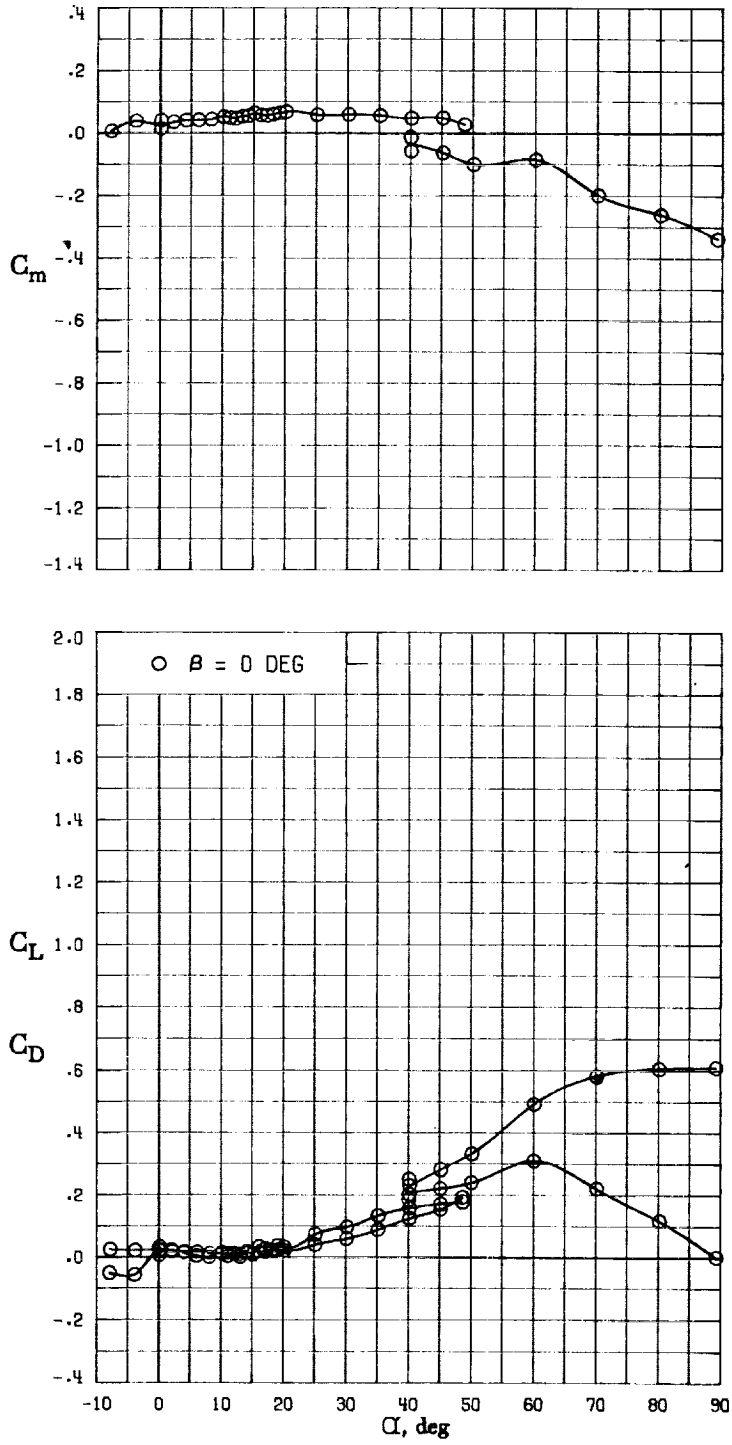

(A) LONGITUDINAL FORCE AND MOMENT COEFFICIENTS ABOUT STABILITY AXES.

FIGURE 82. - EFFECT OF ANGLE OF ATTACK AND SIDESLIP ANGLE ON AERODYNAMIC CHARACTERISTICS AT RE = .288 E+06 FOR CONFIGURATION B.
$\delta_E = 0°$, $\delta_A = 0°$, $\delta_R = 0°$.

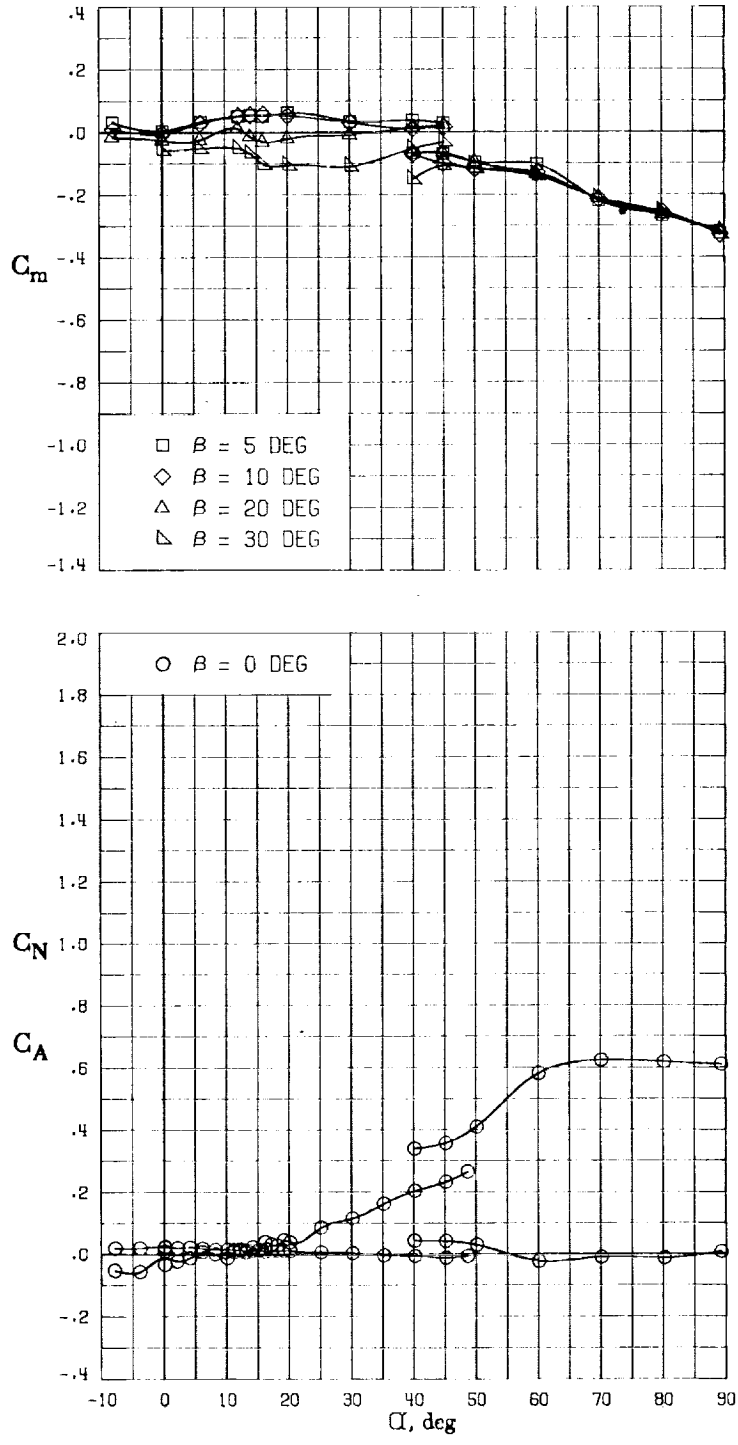

(B) LONGITUDINAL FORCE AND MOMENT COEFFICIENTS ABOUT BODY AXES.

FIGURE 82. - CONTINUED.

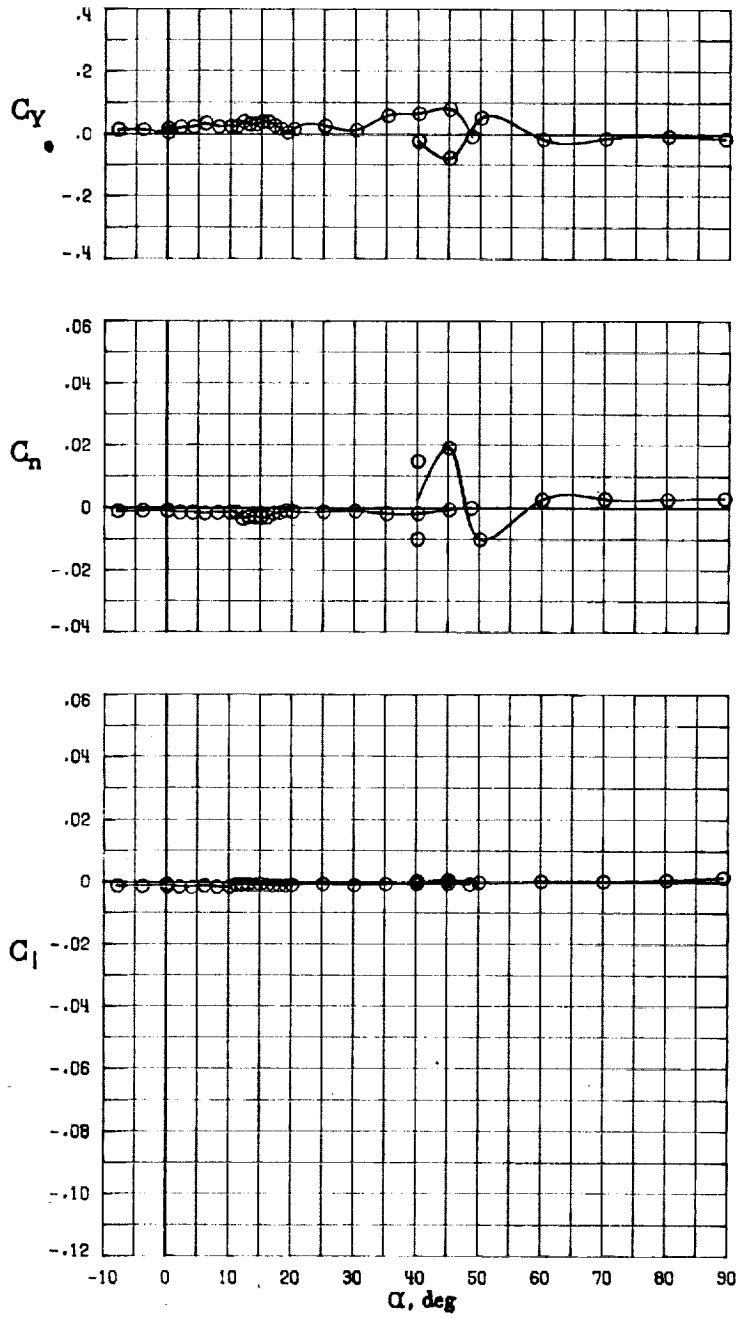

(C) LATERAL - DIRECTIONAL FORCE AND MOMENT COEFFICIENTS ABOUT BODY AXES AT ZERO SIDESLIP.

FIGURE 82. - CONTINUED.

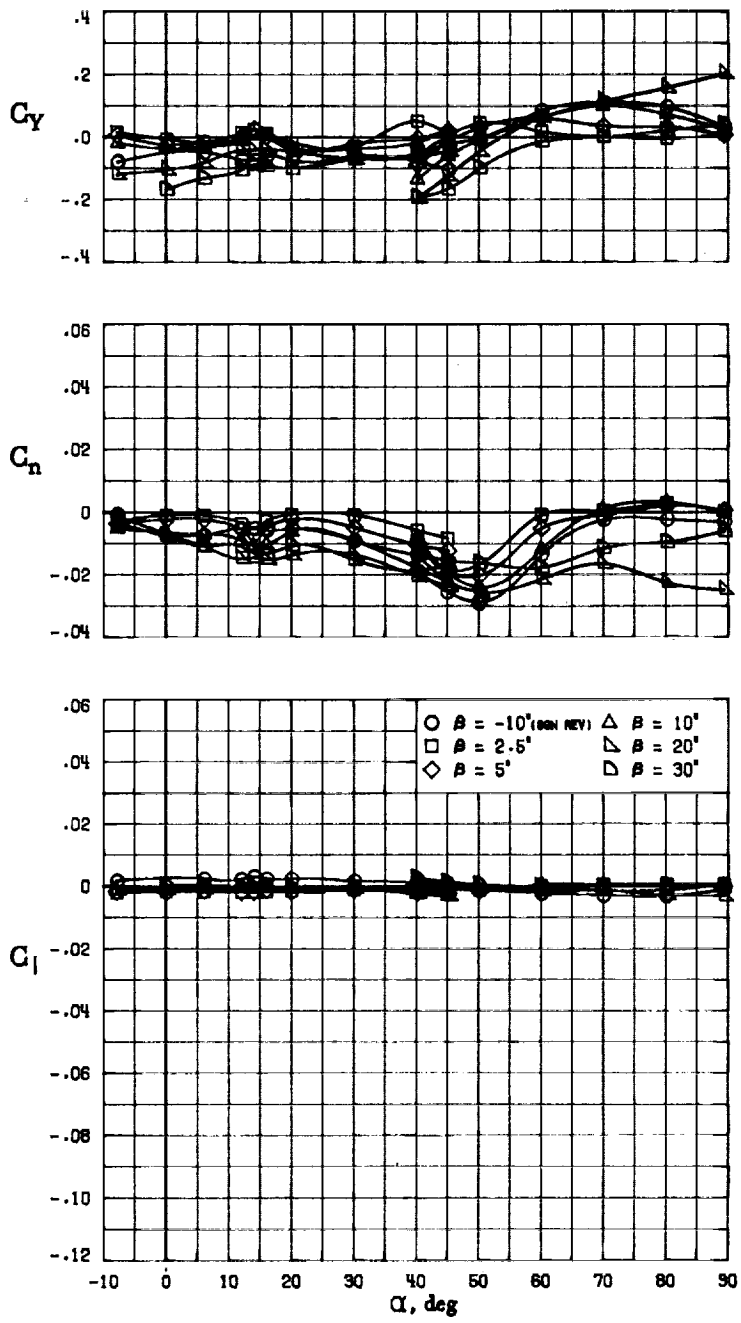

(D) LATERAL - DIRECTIONAL FORCE AND MOMENT COEFFICIENTS ABOUT BODY AXES.

FIGURE 82. - CONTINUED.

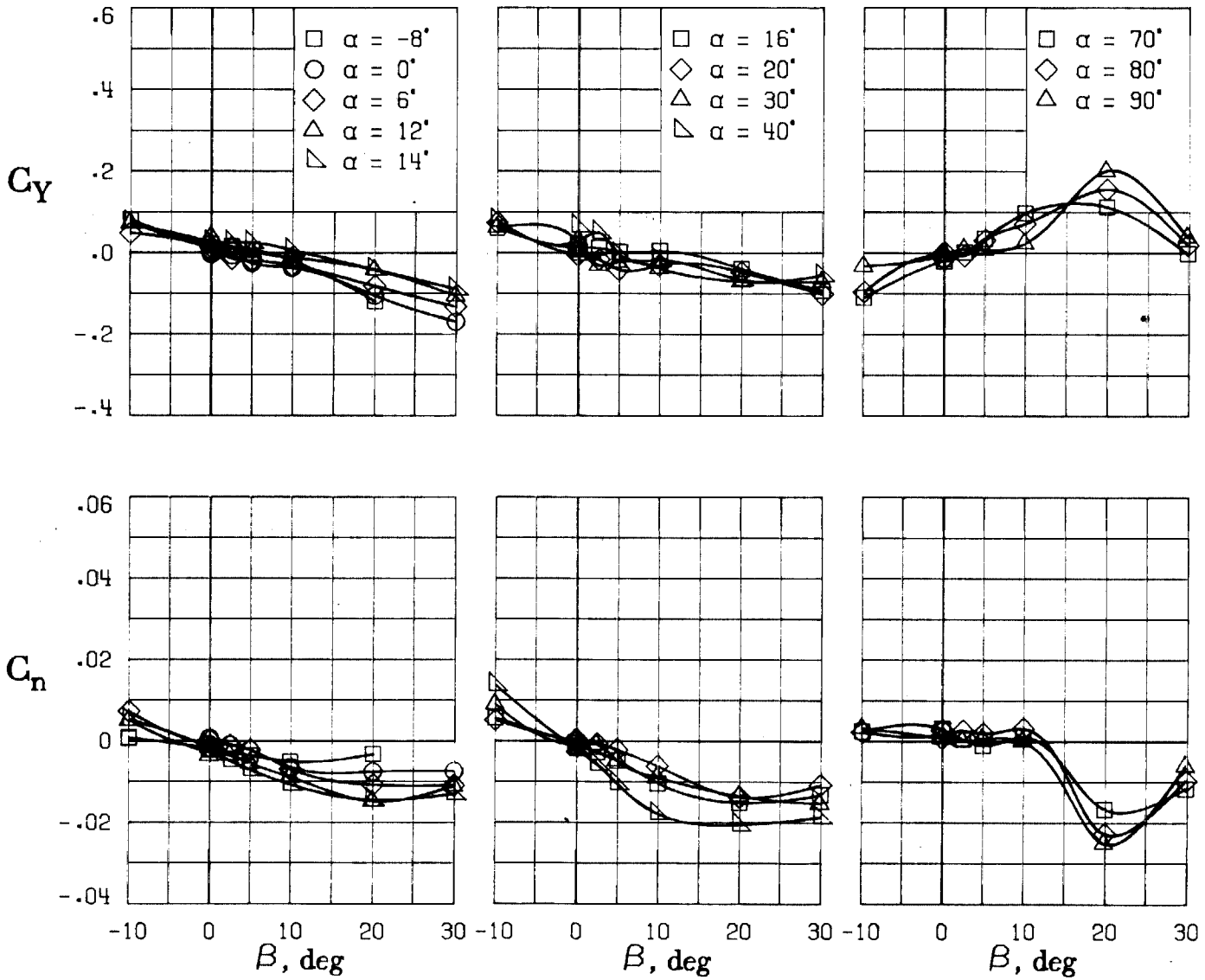

(E) DIRECTIONAL - STABILITY CHARACTERISTICS ABOUT BODY AXES AT VARIOUS ANGLES OF ATTACK.

FIGURE 82. - CONTINUED.

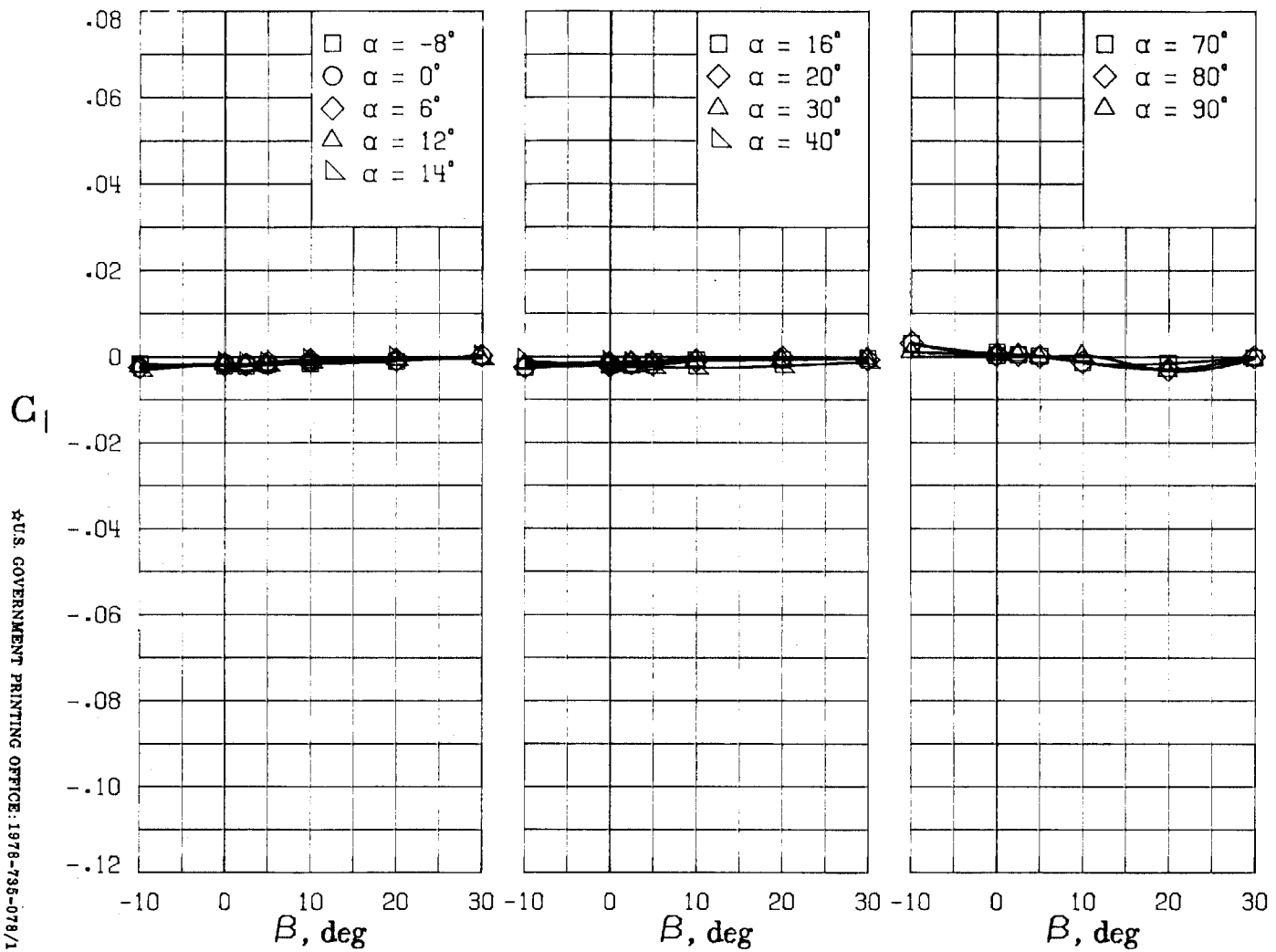

(F) LATERAL - STABILITY CHARACTERISTICS ABOUT BODY AXES AT VARIOUS ANGLES OF ATTACK.

FIGURE 82. - CONCLUDED.

☆U.S. GOVERNMENT PRINTING OFFICE:1978-735-078/12

1. Report No.	2. Government Accession No.	3. Recipient's Catalog No.
NASA CR-2971		

4. Title and Subtitle	5. Report Date
STATIC AERODYNAMIC CHARACTERISTICS OF A TYPICAL SINGLE-ENGINE LOW-WING GENERAL AVIATION DESIGN FOR AN ANGLE-OF-ATTACK RANGE OF -8° to 90°	July 1978
	6. Performing Organization Code

7. Author(s)	8. Performing Organization Report No.
WILLIAM BIHRLE, JR. BILLY BARNHART PAUL PANTASON	

9. Performing Organization Name and Address	10. Work Unit No.
BIHRLE APPLIED RESEARCH, INC. 400 JERICHO TURNPIKE JERICHO, NEW YORK 11753	505 10 1307
	11. Contract or Grant No.
	NAS1-14849, TASK 2
	13. Type of Report and Period Covered
	Contractor Report

12. Sponsoring Agency Name and Address	14. Sponsoring Agency Code
NATIONAL AERONAUTICS AND SPACE ADMINISTRATION LANGLEY RESEARCH CENTER HAMPTON, VIRGINIA 23665	

15. Supplementary Notes

Langley Technical Monitor: James S. Bowman, Jr.

Topical Report

16. Abstract

Static force data obtained at the NASA Ames Research Center 12-foot Pressure Tunnel are presented in plotted form for a 1/7-scale, single-engine, low-wing general aviation airplane model. The configurations tested included the basic airplane, various airfoil shapes, tail designs, fuselage strakes and fuselage modifications as well as airplane components. The test conditions included an angle-of-attack and sideslip range of -8 to 90 and -10 to 30 degrees, respectively, at a Mach number of 0.2 for Reynolds numbers of 0.288×10^6 and 3.45×10^6. The data are presented without analysis.

17. Key Words (Suggested by Author(s))	18. Distribution Statement
GENERAL AVIATION SPINNING REYNOLDS NUMBER HIGH ANGLE OF ATTACK WIND TUNNEL DATA	UNLIMITED DISTRIBUTION Subject Category 02

19. Security Classif. (of this report)	20. Security Classif. (of this page)	21. No. of Pages	22. Price*
UNCLASSIFIED	UNCLASSIFIED	463	$14.50

*For sale by the National Technical Information Service, Springfield, Virginia 22161